

EPA - 908/1 - 77 - 001

JUNE 1977

THE DEVELOPMENT OF A REGIONAL AIR POLLUTION MODEL AND ITS APPLICATION TO THE NORTHERN GREAT PLAINS



U.S. ENVIRONMENTAL PROTECTION AGENCY

REGION VIII

DENVER, COLORADO 80295

15127746

EPA-908/1-77-001

Final Report

THE DEVELOPMENT OF A REGIONAL AIR POLLUTION
MODEL AND ITS APPLICATION TO THE
NORTHERN GREAT PLAINS

by

Mei-Kao Liu
Dale R. Durran

(With Contributions from Mark J. Meldgin)

Systems Applications, Incorporated
950 Northgate Drive
San Rafael, California 94903

Contract No. 68-01-3591

SAI No. EF77-48

Project Officer

Donald Henderson

Environmental Protection Agency, Region VIII
Office of Energy Activities
1860 Lincoln Street
Denver, Colorado 80203

July 1977

DISCLAIMER

This report has been reviewed by the U.S. Environmental Protection Agency, Region VIII and approved for publication. Mention of trade names or commercial products does not constitute endorsement or recommendation for use.

This document is available to the public through the National Technical Information Service, Springfield, Virginia 22151.

ABSTRACT

This report describes a regional scale air pollution model and its application to existing and proposed energy developments in the Northern Great Plains. The objective of this study was to examine the air quality impacts roughly 100 to 1000 kilometers from these point sources of emissions.

The regional model is composed of two interconnected submodels: a mixing-layer model and a surface-layer model. The mixing-layer model is designed to treat transport and diffusion above the surface. The major feature of this model is the assumption that the pollutant distribution is nearly uniform in the vertical direction. This assumption permits adoption of a simplified form of the general atmospheric diffusion equation. The compelling reason for this choice is that the vertical diffusion term in that equation is shown by dimensional analysis to be about 100 times greater than the transport term. The model for the surface layer (which is embedded in the mixing layer) is designed to calculate pollutant fluxes to the ground. For emissions from elevated sources or distant ground-level sources, most of the pollutant mass is contained in the mixing layer. The removal processes thus consist of the diffusion of the pollutants through the surface layer to the ground and absorption or adsorption at the ground. A unique feature of the surface-layer model is its ability to incorporate the diurnal variation in surface temperature resulting from daytime heating and nighttime cooling of the ground. This variation affects the vertical pollutant distribution through atmospheric stabilities, and consequently, affects the rate of surface uptake of pollutants.

The regional model was designed to predict concentrations of primary and secondary pollutants averaged over areas of approximately 100 km²

with a temporal resolution on the order of 3 hours. This model was thoroughly tested via sensitivity analysis. The responses of the model were consistent with expectations based on physical reasoning. This model was exercised for all combinations of two emissions inventories (for 1976 and 1986) and three meteorological scenarios (a strong-wind winter case, a stagnation spring case, and a moderate-wind summer case). The predicted SO_2 and sulfate concentrations are generally greatest in spring, intermediate in winter, and lowest in summer. From these preliminary results it appears that neither the 1976 nor the 1986 emissions as estimated in this study will cause SO_2 or sulfate concentrations significantly higher than background values at locations far from emissions sources.

ACKNOWLEDGMENTS

We would like to sincerely thank a number of individuals whose kind and able assistance has been indispensable in carrying out this project. Terry Thoem, George Boulter, and Dave Maxwell in the Office of Energy Activities of the Environmental Protection Agency (Region VIII) provided the necessary emissions data, and David Joseph, also from the EPA Region VIII, furnished all of the pertinent air quality and meteorological measurements. The analysis of the meteorological data was performed, under a sub-contract with us, by Loren Crow.

We would also like to take this opportunity to express our appreciation to several of our colleagues: Shep Burton, Terry Jerskey, and Phil Roth for many stimulating discussions and constant encouragement; Tom Myers and Gary Lundberg for their help on computations; and Eric Mathre, Ron Rice, and Bob Frost in the preparation of the data base.

CONTENTS

| | |
|---|-----|
| DISCLAIMER | ii |
| ABSTRACT | iii |
| ACKNOWLEDGMENTS | v |
| LIST OF ILLUSTRATIONS | ix |
| LIST OF TABLES | xi |
| I INTRODUCTION | 1 |
| II COAL DEVELOPMENT IN THE NORTHERN GREAT PLAINS | 5 |
| A. Potential Sources of Energy | 6 |
| B. Coal Mining Methods | 7 |
| C. U.S. Coal Reserves | 8 |
| D. Possible Uses of NGP Coal | 14 |
| E. Scenarios for Use of NGP Coal | 16 |
| F. Air Quality Impacts from the Use of NGP Coal | 18 |
| PART A DEVELOPMENT OF A REGIONAL AIR POLLUTION MODEL FOR THE SIMULATION OF POLLUTANT TRANSPORT AND DIFFUSION OVER LONG DISTANCES | 23 |
| III OVERVIEW | 24 |
| IV REVIEW OF PREVIOUS STUDIES | 26 |
| A. Swedish Studies | 26 |
| B. Norwegian Studies | 27 |
| C. Finnish Studies | 28 |
| D. Danish Studies | 29 |
| E. British Studies | 30 |
| F. Studies in the United States | 32 |
| V MAJOR ATTRIBUTES OF LONG-RANGE DISPERSION MODELING | 36 |
| A. Transport and Diffusion | 36 |
| B. Removal Processes | 42 |
| 1. Dry Deposition | 43 |
| 2. Wet Deposition | 44 |

| | | |
|--------|--|-----|
| V | MAJOR ATTRIBUTES OF LONG-RANGE DISPERSION MODELING (continued) | |
| | C. Chemical Transformation | 46 |
| | D. Subgrid-Scale Problems | 47 |
| VI | DEVELOPMENT OF A REGIONAL AIR POLLUTION MODEL | 52 |
| | A. The Mixing Layer Model | 56 |
| | 1. The Model Equations | 56 |
| | 2. The Numerical Method | 61 |
| | B. The Surface Layer Model | 64 |
| | 1. Dry Deposition on Surfaces | 64 |
| | 2. The Formulation of a Surface Deposition Model | 66 |
| VII | SENSITIVITY OF THE REGIONAL AIR POLLUTION MODEL | 74 |
| | A. Horizontal Eddy Diffusivity | 75 |
| | B. Mixing Depth | 81 |
| | C. Prescription of Dry Deposition | 81 |
| | D. Surface Reaction Rate | 88 |
| | E. SO ₂ /Sulfate Conversion Rate | 88 |
| VIII | SUMMARY AND CONCLUSIONS FOR PART A | 96 |
| PART B | APPLICATION OF A REGIONAL AIR POLLUTION MODEL TO THE COAL DEVELOPMENT AREAS IN THE NORTHERN GREAT PLAINS | 97 |
| IX | OVERVIEW | 98 |
| X | COMPILATION OF THE DATA BASE | 102 |
| | A. Emissions Data | 102 |
| | B. Meteorological Data | 107 |
| | C. Surface Data | 110 |
| | D. Air Quality Data | 116 |
| XI | AIR QUALITY ANALYSIS | 119 |
| | A. Winter | 121 |
| | B. Spring | 121 |
| | C. Summer | 146 |
| | D. Air Quality Impacts | 146 |

| | | |
|------------|--|-----|
| XII | SUMMARY AND CONCLUSIONS FOR PART B | 159 |
| APPENDICES | | |
| A | AN ANALYSIS OF NUMERICAL METHODS | 160 |
| B | COMPILATION OF SIMULATION RESULTS | 174 |
| REFERENCES | | 272 |

ILLUSTRATIONS

| | | |
|----|--|-----|
| 1 | The Northern Great Plains | 4 |
| 2 | Schematic Illustration of Scales of Motion in the Atmosphere. . | 37 |
| 3 | Schematic Illustration of the Modeling Region in the Regional Air Pollution Model Developed in This Study | 54 |
| 4 | Vertical Distribution of SO_2 and $\text{SO}_4^{=}$ Over Central Germany . . . | 58 |
| 5 | Schematic Illustration of Diurnal Variations in Surface Deposition. | 68 |
| 6 | Schematic Illustration of the Surface Layer | 70 |
| 7 | Horizontal Eddy Diffusivity as a Function of Traveling Time and Plume Spread. | 76 |
| 8 | Predicted SO_2 Concentrations for the Base Case. | 77 |
| 9 | Predicted SO_2 Concentrations for Reduced Horizontal Diffusivity. | 79 |
| 10 | Predicted SO_2 Concentrations for Reduced Mixing Depths. | 82 |
| 11 | SO_2 Deposition Velocities (in mm/sec) Calculated with β as Prescribed by the Algorithm of Owen and Thompson | 84 |
| 12 | SO_2 Deposition Velocities (in mm/sec) Calculated with β as Prescribed by the Algorithm of Thom | 86 |
| 13 | Predicted SO_2 Concentrations for Reduced Surface Reaction Rate | 89 |
| 14 | Predicted SO_2 Concentrations for Increased SO_2 /Sulfate Conversion Rate | 92 |
| 15 | Predicted Sulfate Concentrations for Increased SO_2 /Sulfate Conversion Rate | 94 |
| 16 | Energy Conversion Facilities Scheduled for Completion before 1986 | 99 |
| 17 | Point Sources in the Northern Great Plains in 1976. | 105 |
| 18 | Point Sources in the Northern Great Plains in 1986. | 106 |

| | | |
|----|--|-----|
| 19 | Wind Measurement Networks in the Northern Great Plains | 108 |
| 20 | Temperature Gradients and Exposure Classes at Idaho Falls, Idaho. | 111 |
| 21 | Vertical Thickness of the Modeling Region (in Meters) | 112 |
| 22 | Vegetation in the Northern Great Plains | 115 |
| 23 | EPA SO ₂ Monitors in the Northern Great Plains | 117 |
| 24 | Winds at 850 Millibars Altitude During 27-31 January 1976 | 122 |
| 25 | Predicted SO ₂ Concentrations for Winter Case | 132 |
| 26 | Winds at 850 Millibars Altitude During 4-7 April 1976 | 135 |
| 27 | Predicted SO ₂ Concentrations for Spring Case | 143 |
| 28 | Winds at 850 Millibars Altitude During 9-12 July 1975 | 147 |
| 29 | Predicted SO ₂ Concentrations for Summer Case | 153 |
| 30 | 24-Hour-Average SO ₂ Measurements (in $\mu\text{g}/\text{m}^3$) in the Northern Great Plains | 155 |
| 31 | Predicted Concentration Distributions Using the Upstream Difference Scheme | 163 |
| 32 | Predicted Concentration Distributions Using the SHASTA Method. | 164 |
| 33 | Predicted Concentration Distributions Using the Egan and Mahoney Method. | 167 |
| 34 | Variation of Amplification Factor $ r $ as a Function of α for $\epsilon = 0.6$ | 172 |

TABLES

| | | |
|----|---|-----|
| 1 | Mineral Resource Terminology Adopted by the Interior Department. | 9 |
| 2 | Reserve Base of Coals in the Western United States by Sulfur Content | 11 |
| 3 | Characteristics of Three Northern Great Plains Coals and Illinois Basin Coal | 13 |
| 4 | Projected Production and Use of Northern Great Plains Coal in 1985 | 17 |
| 5 | Estimated Emission Rates of Various Trace Elements from Coal Combustion | 19 |
| 6 | Projected Increases in Statewide Emissions from Power Plants and Coal Gasification Plants, 1974-1985, for Various Development Scenarios | 20 |
| 7 | Hydrocarbon and Oxide of Nitrogen Emissions in the Los Angeles Basin and the Northern Great Plains | 21 |
| 8 | Mean Seasonal and Annual Morning and Afternoon Mixing Heights and Wind Speeds for the Northern Great Plains | 40 |
| 9 | Comparison of Physical Processes Pertinent to Long-Range Pollutant Transport | 41 |
| 10 | SO ₂ Removal Processes | 42 |
| 11 | Deposition of SO ₂ onto Vegetation | 44 |
| 12 | Downwind Distance Traveled by a Puff as a Function of Atmospheric Stability | 60 |
| 13 | Ps do-Diffusivity in Advective Transport for a 10 Kilometer Grid and $v\Delta t/\Delta x = 1/2$ | 63 |
| 14 | Surface Resistance Measurements for SO ₂ | 100 |
| 15 | Point Sources Emitting More than 10,000 Tons of SO _x per Year in 1976 | 103 |

| | | |
|----|---|-----|
| 16 | Point Sources Emitting More than 10,000 Tons of SO_x per Year in 1986 | 104 |
| 17 | Surface Roughnesses for Various Vegetation Types | 116 |
| 18 | Periods Chosen for Air Quality Analysis | 120 |
| 19 | SO_2 Emissions and Areas of Ohio and the Northern Great Plains. | 120 |
| 20 | Significant Deterioration Increments for SO_2 | 158 |
| 21 | Effective Diffusion Coefficients in the x-Direction for the First Test Problem. | 166 |
| 22 | Estimated Computation Time Required To Follow a Plume for 750 km. | 168 |

I INTRODUCTION

The energy crisis, dramatically thrust into the national and international scenes by the oil embargoes of 1973, has probably become one of the most challenging problems facing our society. In the search for solutions to the problem, a variety of energy sources have been proposed--nuclear and solar energy, coal and oil shale, and many others. However, it is only in the course of resolving the myriad of problems associated with the development or application of these new sources of energy that a painful realization has emerged: the shortage of energy is neither a short-term nor a isolated problem. The raw materials required in the development of new energy sources, including renewable sources, will become increasingly scarce. Obviously, concerns about resource availability, as well as a wide range of social, economic, and environmental problems, will have to be carefully analyzed before a rational approach for solving the long-range energy problem can be formulated.

For the near future, the vast amount of accessible coal reserves in the U.S. and the serious problems currently plaguing alternative energy sources easily make coal one of the more attractive candidates for coping with the energy problem. In addition to simply being a source of energy, coal is also an ideal substitute source of petrochemical feedstocks. It is thus interesting to note that of the seven goals set by President Carter in his April, 1977 address to the nation on energy, increasing coal production by about two-thirds to more than one billion tons per year by 1985 is the only goal that is not directly related to energy conservation.

Clearly the use of coal, particularly on a large scale, will pose problems. The most severe one appears to be the degradation of our air environment. Direct combustion of coal will undoubtedly produce

enormous amounts of air pollutants. For example, a large power plant without pollution control equipment typically emits several hundred tons of sulfur dioxide per day, as much as the entire Los Angeles metropolitan area. Uses of coal other than direct combustion, by new energy technologies such as coal gasification for example, may also generate large amounts of air pollutants. Furthermore, coal mining, transport of coal to power-demand population centers (an alternative to alleviate local environmental problems), and other activities related to various modes of coal development can all generate appreciable amounts of air pollutants. As a result of these emissions, significant deterioration of air quality in the vicinity of major coal users is an immediate problem. The short-range air quality impact in adverse meteorological conditions is generally characterized by extremely high pollutant concentrations of short duration within several kilometers from a major emission source. This problem has been studied extensively. For pollutants with relatively long half-lives that are emitted from tall stacks, a different air pollution problem arises because of long-range transport of these pollutants and their derivatives. On a time scale of the order of several days and a spatial scale of several hundred kilometers, the conversion of sulfur dioxide to sulfates, for example, becomes important. Elevated sulfur dioxide and sulfate levels may lead to a variety of environmental problems such as impacts on ecological systems, reductions in visibility, and acid rain. In view of the severity of these problems, characterizing the long-range transport of air pollutants has recently attracted considerable attention.

The Northern Great Plains contains one of the world's largest known coal reserves. Immense deposits of coal* exist in northeastern

* Coal can be basically classified into four types: lignite, sometimes referred to as brown coal; bituminous and subbituminous, known as soft coals; and anthracite, or hard coal. Each type of coal has a different range of carbon and hydrogen content. Eastern bituminous coal, from states such as West Virginia and Pennsylvania, generally has a higher sulfur content by weight than Western coals from states such as Montana and Wyoming, which are primarily subbituminous with some lignite.

Wyoming, eastern Montana, and western North Dakota (Figure 1). As part of an effort to achieve energy independence, many large coal-fired power plants using locally mined coal have already been built in this area. Many more power plants and coal gasification plants are being built or planned. (This development is reviewed in Chapter II.) The Northern Great Plains is largely undeveloped at present, and current ambient concentrations of air pollutants are low. Consequently, the stringent Federal regulations for preventing significant deterioration (Federal Register, 1974, 1975) apply to the area. It is clear that a careful study of the impact of coal developments on air quality is urgently needed.

Under the sponsorship of Environmental Protection Agency, this project has been initiated to address the general problem of maintenance of air quality in the Northern Great Plains. The primary emphasis of this project is to study the impact of SO_2 emissions from multiple point sources at large distances (on the order of several hundred kilometers). According to the original plan, an existing dispersion model suitable for assessing air quality impacts at large distances was to be selected and adapted for the Northern Great Plains. A careful review of the various models currently available revealed, however, that none of those models was adequate for handling multiple sources and chemical reactions on the temporal and spatial scales of interest to the present project. Instead a new long-range transport model was developed. A detailed discussion of the development of this model can be found in Part A of this report. Subsequently, this model was applied to the Northern Great Plains to examine the impact of coal developments. The result of this application is described in Part B of this report.

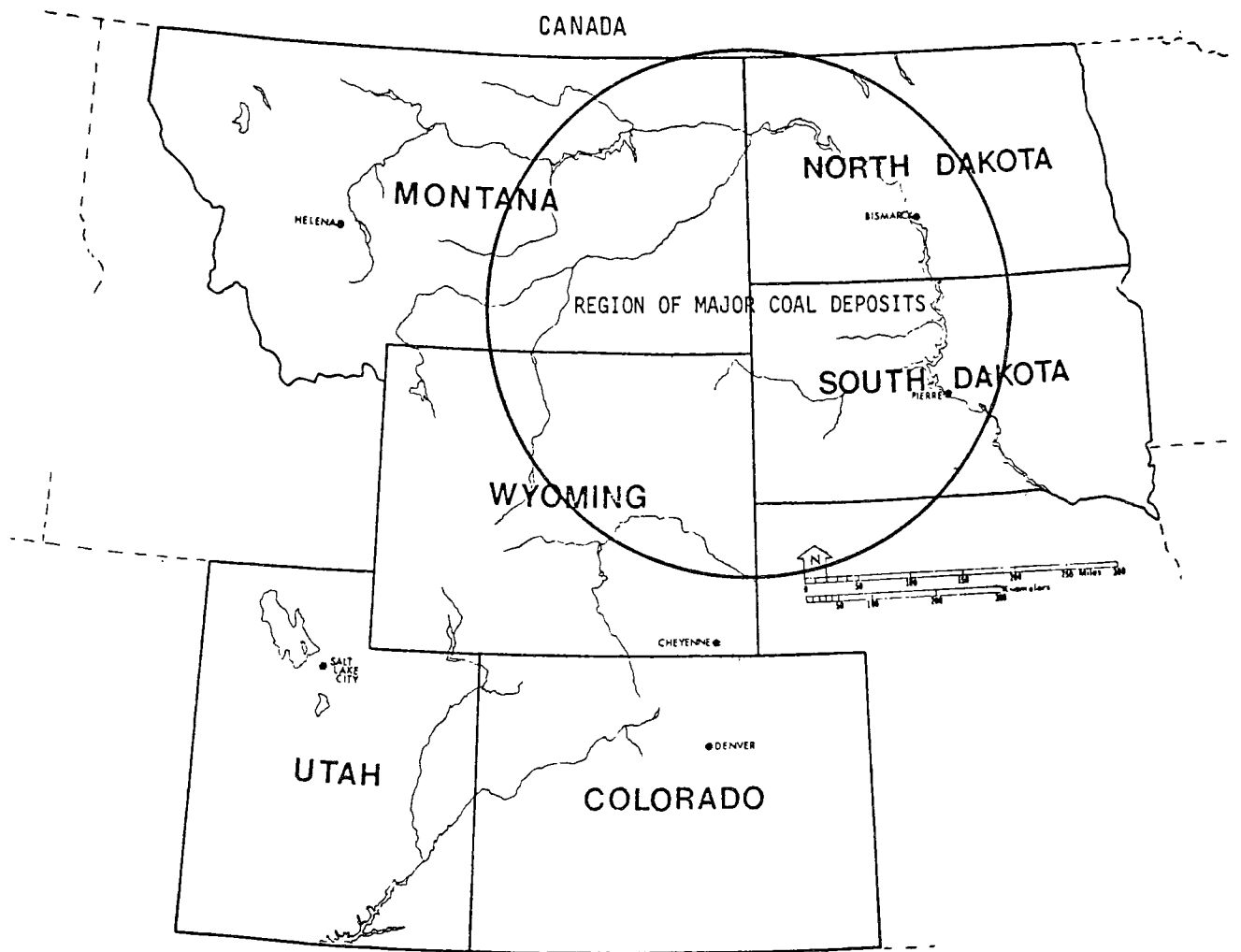


FIGURE 1. THE NORTHERN GREAT PLAINS

II COAL DEVELOPMENT IN THE NORTHERN GREAT PLAINS

Vast amounts of coal underlie the Northern Great Plains of the United States. This coal is being mined and will continue to be mined because its energy is needed. The main issues concerning the use of this coal are how it should be used and what level of environmental impact is acceptable. This chapter is intended to provide perspective on these issues, particularly with respect to air quality.

There is no question that coal is needed. In 1974 the total U.S. consumption of energy* was 7.31×10^{16} BTU. Petroleum liquids and natural gas produced in the U.S.A. accounted for about 60 percent of the total. At current rates of production, U.S. reserves of natural gas and petroleum would be depleted in four to eight decades. These estimates are highly uncertain because of the possibility of new discoveries and the difficulty of quantifying known reserves. In addition, current rates are unlikely to persist. Larger and more easily accessible deposits are generally extracted first, so further production will become more difficult and costly. Production of natural gas in the United States has declined since 1972, and production of petroleum will probably begin to decline after 1985 (Benedict, 1976). These declines may be reversed temporarily by deregulation of the price of natural gas, extensive drilling in Alaska and on the continental shelf, and by new production techniques such as CO_2 injection, but the conclusion is clear--the United States must look elsewhere for energy.

* By the First Law of Thermodynamics, energy is conserved, not consumed. "Energy consumption," as used here, means degradation of energy from concentrated forms into waste heat at near-ambient temperatures.

A. POTENTIAL SOURCES OF ENERGY

To satisfy its demand for energy, the United States has placed greater reliance on energy sources other than domestic fossil fuels. For example, in 1950 only 12 percent of the U.S. consumption of petroleum liquids was imported, but by 1974 39 percent was. The first nuclear power plant in the United States was opened in 1957, and by 1974 nuclear power supplied roughly 3 percent of the total energy consumption. Both of these sources have disadvantages. Petroleum imports cause a balance of payments problem and are not politically controlled by the United States. The safety of conventional nuclear power plants and the storage of nuclear wastes are matters of controversy. Aside from the safety issues, the planned and operating plants would consume the estimated U.S. reserves of natural uranium concentrates in less than 100 years (Hubbert, 1971; Benedict, 1976). Fast breeder reactors (cooled by liquid sodium) are much more efficient; they could probably meet the present demand for electricity for many years. However, development of most types of breeders in the United States has been halted by President Carter because their wastes can be reprocessed into atomic weapons.

Other potential domestic sources of energy include hydroelectric power, direct solar radiation, geothermal, wind, and tidal power, oil shale and tar sands, and fusion. If any of these sources were as economical as petroleum and natural gas, they would already have been developed. Such is the case for water power; most of the suitable sites in the U.S. are either in use or reserved for recreation and wilderness preservation. Direct solar radiation provides an enormous amount of power, but the costs of gathering and concentrating it with present technology are too high. Geothermal, wind, and tidal power are being used on a small scale in favorable locations, but these resources are not of sufficient magnitude to solve the U.S. energy problem. Oil shale and tar sands contain enormous amounts of oil; proven U.S. reserves of oil in oil shale are estimated at 2.3×10^{12} barrels, (InterTechnology Corp. 1971), or 12 times U.S. petroleum reserves. Separating the hydrocarbons from the shale or sand is expensive, however. In addition, current techniques for producing oil from

shale use 1 barrel of fresh water for each barrel of oil produced, and the material left after the oil is extracted takes up a greater volume than the original oil shale. The energy available from fusion is enormous. The fusion of the estimated world reserves of minable lithium-6 with deuterium, which appears to be the most practical fusion reaction, would provide roughly as much energy as the total world supply of all fossil fuels (Hubbert, 1971). But fusion is not expected to be a commercial energy source before the next century. In summary, none of these energy sources is expected to reduce our dependence on petroleum and natural gas in the next few decades.

The remaining energy source is coal. Coal is versatile--it can be converted to gaseous or liquid fuels or petrochemical feedstocks, or it can be burned directly to generate electricity. (Note that nuclear power is efficient only for generating electricity.) The technology to mine coal is well developed, and promising new technologies are being investigated. Finally, the United States has very large coal resources. The "identified resources" of the U.S. are 1.7×10^{12} short tons (Averitt, 1974), or roughly 3.4×10^{19} BTU.

B. COAL MINING METHODS

Before discussing coal resources, it is helpful to consider how coal is mined. Coal generally occurs in layers or seams. These seams may be 25 feet thick or more. Coal is mined by both subsurface and surface techniques. In subsurface mining, the roof of the mine must be supported (at least temporarily). In some techniques, such as the traditional room-and-pillar method, the roof is supported by leaving 30 to 50 percent of the coal in place. In longwall mining, coal is sheared and removed from a long face underground, and the roof is supported by hydraulic jacks. As coal is removed the hydraulic jacks are advanced, and the roof behind is allowed to collapse. Longwall mining recovers more of the coal in a seam than most subsurface techniques, but at present it is applicable only to certain types of rock strata. In the United States the average recovery factor for coal from all types of subsurface mines is 57 percent (Nephew, 1973).

Surface mining techniques include strip mining and augering. In strip mining the material above the coal seam, or the overburden, is cleared by heavy excavating equipment and the coal is removed. Then the overburden from an adjacent area is moved into the cleared area, exposing more coal. This process is repeated until the overburden is too thick to be handled economically. After mining (and before reclamation), a surface-mined area is generally covered with piles of broken overburden, or spoils, and at one end of the area is a nearly vertical wall where the stripping was stopped. The recovery factor for coal is typically 80 percent for strip mining and 50 percent for augering (Nephew, 1973). Surface mines are generally safer and more productive (in tons of coal per day per employee) than subsurface mines, and they have steadily increased in importance. The percentage of total U.S. coal production obtained from surface mines increased from 22 percent in 1950 to 50 percent in 1974 (Nephew, 1973; Nehring and Zycher, 1976).

C. U.S. COAL RESERVES

Estimate of coal reserves vary widely. In some studies the minimum thickness of subbituminous coal that is considered economically minable is 3 meters, in other studies it is 1.5 meters, and in some studies minability is ignored. Some studies include all coal within 90 meters of the surface, others include all coal within 1800 meters. All estimates are based on extrapolation from limited geologic data. Finally, what is being estimated differs. Coal deposits that are or may be minable are generally termed reserves; resources commonly include all coal, whether presently minable or not. Reserves, however, are divided differently in different estimates and sometimes reserves are called resources. The terminology adopted by the U.S. Department of the Interior is given in Table I (EPA, 1976a, p. 143).

The distribution of coal in the western United States is given in Table 2. In this table "total reserve base" is equivalent to

TABLE 1. MINERAL RESOURCE TERMINOLOGY ADOPTED BY THE INTERIOR DEPARTMENT

DEFINITIONS:

Resource - A concentration of naturally occurring solid, liquid, or gaseous materials in or on the earth's crust in such form that economic extraction of a commodity is currently or potentially feasible.

Identified Resources - Specific bodies of mineral-bearing material whose location, quality, and quantity are known from geologic evidence supported by engineering measurements with respect to the demonstrated category.

[illegible]

Undiscovered Resources - Unspecified bodies of mineral-bearing material surmised to exist on the basis of broad geologic knowledge and theory.

Reserve - That portion of the identified resource from which a usable mineral and energy commodity can be economically and legally extracted at the time of determination. The term ore is also used for reserves of some minerals.

TABLE 1 (Concluded)

The following definitions for measured, indicated, and inferred are applicable to both the Reserve and Identified-Subeconomic resource components (see chart).

Measured - Material for which estimates of the quality and quantity have been computed, within a margin of error of less than 20 percent, from analyses and measurements from closely spaced and geologically well-known sample sites.

Indicated - Material for which estimates of the quality and quantity have been computed partly from sample analyses and measurements and partly from reasonable geologic projections.

Demonstrated - A collective term for the sum of materials in both measured and indicated resources.

Inferred - Material in unexplored but identified deposits for which estimates of the quality and size are based on geologic evidence and projection.

Identified-Subeconomic Resources - Known deposits not now minable economically.

Paramarginal - The portion of subeconomic resources that (a) borders on being economically producible or (b) is not commercially available solely because of legal or political circumstances.

Submarginal - The portion of subeconomic resources which would require a substantially higher price (more than 1.5 times the price at the time of determination) or a major cost-reducing advance in technology.

Hypothetical Resources - Undiscovered materials that may reasonably be expected to exist in a known mining district under known geologic conditions. Exploration that confirms their existence and reveals quantity and quality will permit their reclassification as a Reserve or identified-subeconomic resource.

Speculative Resources - Undiscovered materials that may occur either in known types of deposits in a favorable geologic setting where no discoveries have been made, or in as yet unknown types of deposits that remain to be recognized. Exploration that confirms their existence and reveals quantity and quality will permit their reclassification as reserves of identified-subeconomic resources.

Source: EPA (1976a).

TABLE 2. RESERVE BASE OF COALS IN THE WESTERN UNITED STATES BY SULFUR CONTENT

(in 10^6 short tons)

| State | Less than 1.0 percent | 1.1 to 3 percent | Greater than 3 percent | Unknown Content | Total* Reserve Base |
|--------------|--------------------------|------------------|---------------------------|--------------------|------------------------|
| Alaska | 11,457.0 | 184.0 | 0 | 0 | 11,645.0 |
| Arizona | 173.0 | 177.0 | 0 | 0 | 350.0 |
| Arkansas | 81.0 | 463.0 | 46.0 | 74.0 | 665.7 |
| Colorado | 7,476.0 | 786.2 | 47.3 | 0 | 14,869.2 |
| Iowa | 1.6 | 226.7 | 2,105.9 | 549.2 | 2,884.9 |
| Kansas | 0 | 309.3 | 695.6 | 383.2 | 1,388.1 |
| Missouri | 0 | 182.0 | 5,226.0 | 4,080.5 | 9,487.3 |
| Montana | 101,646.9 | 4,115.3 | 502.6 | 2,166.7 | 108,396.3 |
| New Mexico | 3,575.5 | 793.5 | .8 | 27.5 | 4,394.8 |
| North Dakota | 5,389.0 | 10,325.5 | 268.7 | 15.0 | 16,003.0 |
| Oklahoma | 275.0 | 326.6 | 241.4 | 450.5 | 1,294.2 |
| Oregon | 1.5 | .3 | 0 | 0 | 1.9 |
| South Dakota | 103.1 | 287.9 | 35.9 | 1.0 | 428.0 |
| Texas | 659.8 | 1,884.7 | 284.1 | 444.0 | 3,271.9 |
| Utah | 1,968.5 | 1,546.8 | 49.4 | 478.3 | 4,042.5 |
| Washington | 603.5 | 1,265.4 | 39.0 | 45.1 | 1,954.0 |
| Wyoming | 33,912.0 | 14,657.4 | 1,701.1 | 3,060.3 | 53,336.1 |
| *Total* | 167,324.5 | 37,531.5 | 11,244.1 | 18,323.0 | 234,412.4 |

* Totals may not add due to rounding.

Note: Total reserve base for the entire U.S. is 4.37×10^{11} tons, 2.00×10^{11} tons of which have less than 1 percent sulfur.

Source: Bureau of Mines (1975).

"demonstrated reserves" as shown in Table 1; that is, coal believed to exist in thicknesses and at depths similar to that being mined on the basis of preliminary geologic and engineering evaluations. No allowance is made for recoverability factors of roughly 50 percent for subsurface mining and 80 to 90 percent for surface mining. Montana, North Dakota, and Wyoming account for 41 percent of the demonstrated reserves and 70 percent of the demonstrated reserves having less than 1 percent sulfur in the entire U.S. (The importance of the sulfur content is discussed in Section F.) These figures include the Wasatch and Fort Union formations, which are generally considered the Northern Great Plains coal field, and minor coal fields in western Montana and Wyoming.

Regardless of how it is estimated or labeled, the coal in the Northern Great Plains can provide an enormous amount of energy. According to Nehring and Zycher (1976, p. 20), the "most probable estimate of ultimate strippable resources [in the Northern Great Plains] is equal to 26 times U.S. energy consumption in 1974." By "strippable resources" they mean coal in seams more than 1.5 meters thick lying under less than 90 meters of overburden. The known strippable resource in Montana, North Dakota, and Wyoming is 7.89×10^{10} tons*, or 45 percent of the total U.S. strippable resource, and its average heat content is estimated to be 7.9×10^3 BTU/lb, which corresponds to lignite or sub-bituminous coal. Almost three-fourths of the coal contains less than 0.6 lbs sulfur/ 10^6 BTU. The deposits in Montana and Wyoming generally have a higher heat content and lower sulfur content than the North Dakota deposits (Nehring and Zycher, 1976).

The coal in the Northern Great Plains differs from eastern coal in many respects. Table 3 gives some properties of three coals from the Northern Great Plains and an average coal from the Illinois Basin, which is typical of many Eastern bituminous coals. Note that

* For comparison, the total U.S. production of coal in 1972 was 5.97×10^8 tons, which was valued at almost 4.5 billion dollars.

TABLE 3. CHARACTERISTICS OF THREE NORTHERN GREAT PLAINS
COALS AND ILLINOIS BASIN COAL

| | <u>Heat Content</u> <u>[BTU/lb (dry)]</u> | <u>Sulfur</u> | | <u>Ash</u> | | <u>Moisture</u> <u>(percent)</u> |
|------------------------|--|-------------------------------|-----------------------------------|-------------------------------|-----------------------------------|-------------------------------------|
| | | <u>lbs/10⁶ BTU</u> | <u>Percentage</u> <u>(dry)</u> | <u>lbs/10⁶ BTU</u> | <u>Percentage</u> <u>(dry)</u> | |
| Northern Great Plains | | | | | | |
| Coal I | 9511 | 0.76 | 0.72% | 21.7 | 20.6% | 27.0% |
| Coal II | 11708 | 0.42 | 0.49 | 6.15 | 7.2 | 29.2 |
| Coal III | 9838 | 1.46 | 1.44 | 12.6 | 12.4 | 36.8 |
| Illinois Basin | | | | | | |
| Average of 82 coals | 12750 | 2.75 | 3.51 | 8.85 | 11.28 | 10.02 |

Source: EPA (1976a).

these NGP coals are lower in heat content and sulfur content and higher in moisture content than Illinois Basin coal. Even on a heat equivalent basis, NGP coal has much less sulfur than Illinois Basin coal. For reasons discussed below, this low sulfur content is the main reason for development of NGP coal.

D. POSSIBLE USES OF NGP COAL

One of the main issues in the use of Northern Great Plains coal is how it should be used. As mentioned above, coal is a versatile fuel; it can be used in the following ways:

- > Burning to generate electricity
- > Conversion to low- or medium-BTU gas
- > Conversion to synthetic natural gas
- > Conversion to liquid fuels or petrochemical feedstocks.

These uses are discussed in turn below. Note that each use can take place either near the mine or at a distance.

Burning coal to generate electricity is its most common use. For example, 63 percent of the coal mined in the U.S. in 1973 was burned in coal-fired steam electric generating plants (FEA, 1975). When coal is burned, about 95 percent of the sulfur in it is converted to gaseous sulfur oxides (Smith, 1966). Federal and state limits on sulfur emissions are one of the major forces behind the development of coal gasification and liquefaction processes.

Coal gasification and liquefaction involve unavoidable energy losses, but they remove much of the sulfur and ash, converting coal into clean-burning forms. Dried coal typically has a hydrogen to carbon ratio of about 0.8. For comparison, crude oil has a ratio of about 1.1 and natural gas has a ratio of about 4.0, so coal conversion requires a source of hydrogen, usually steam.

Coal gasification is not new; it was widely used in the United States until the 1930s, when natural gas became available, and is used at present in many foreign countries. In modern coal gasification processes, pulverized coal and steam are heated together under pressure. Heat is produced in part by adding to the steam some air or oxygen, so the coal can burn slightly. The product is a gas consisting of CO , H_2 , CH_4 , CO_2 , H_2O , H_2S , other organic gases, and N_2 . H_2S can be removed efficiently, so the product gas is low in sulfur. The heat content of such gas is low, perhaps 100 to 200 BTU/scf if air is used and 250 to 500 BTU/scf if oxygen is used, compared to 1000 BTU/scf for natural gas. At this stage the synthesized gas cannot be piped long distances economically, so it may be either burned near the plant for electricity generation, or converted to high-BTU gas by "shift conversion" (i.e., $\text{CO} + \text{H}_2\text{O} \rightarrow \text{CO}_2 + \text{H}_2$) and catalytic methanation. Commercial coal gasification processes have efficiencies of 80 to 90 percent in producing low- or medium-BTU gas and 60 to 70 percent in producing high-BTU gas (Tillman, 1976).

Coal liquefaction processes are less well developed than coal gasification. Liquefaction is carried out for a variety of reasons: to remove sulfur and inorganics before combustion, to produce petrochemical feedstocks or substitutes for crude oil, or to produce fuel-grade methanol. The processes currently proposed include pyrolysis, solvent refining, and catalytic hydrogenation at high temperatures and pressures. A great deal of research in coal liquefaction is being carried out in this and other countries, some pilot plants have been built, and one plant operating in South Africa, but gasification is generally expected to be more important than liquefaction in the short term.

Coal from the Northern Great Plains could be transported economically by either rail or slurry pipeline. So-called "unit trains," which often contain 100 hopper cars, travel as units from mine to point of use and back, and seldom uncouple. Unit trains are commonly used at present in the Northern Great Plains. In slurry pipelines, finely pulverized coal is mixed with approximately an equal weight of water and pumped. Slurry

pipelines are claimed to transport coal at roughly one-half the cost of transport by unit trains, but none has yet been built in the Northern Great Plains because railroad companies have not granted permission to let pipelines cross their rights-of-way (C&EN, 1977).

E. SCENARIOS FOR USE OF NGP COAL

Future development of the coal in the Northern Great Plains depends on many factors, including leasing policies for public and Indian lands, environmental regulations, and the price of imported crude oil. Consequently, forecasting coal production and use is complex. The Northern Great Plains Resource Program (1974) assembled two forecasts of interest here, based on scenarios of most probable development and extensive development. The mining and use of coal in these scenarios is summarized in Table 4. Nehring and Zycher (1976) suggest that the projections of the most probable scenario will be exceeded because coal production under contracts already signed nearly equals these projections, and few contracts are signed more than five years before initial delivery.

The present report deals primarily with atmospheric sulfur dioxide and sulfates in the Northern Great Plains, but to provide a broader perspective we briefly discuss other impacts of projected large-scale use of coal. A major hindrance to development of NGP coal is scarcity of water. A coal-fired power plant with evaporative cooling requires roughly 4 tons of water for each ton of coal burned. (Dry cooling is much less efficient.) High- and low-BTU coal gasification require roughly 1.0 and 0.1 tons of H_2O per ton of coal if air cooling is used extensively (NGPRP, 1974, pp. 129-130; Radian Corp., 1975, p. B-19). The extensive development forecast of the NGPRP thus calls for use of 3.1×10^8 tons of water per year, or 2.3×10^5 acre-feet. For comparison, the mean annual flows of the two major rivers in southeastern Montana and northeastern Wyoming, the Tongue River and the Powder River, are 3.0×10^5 and 3.3×10^5 acre-feet, respectively (Nehring and Zycher, 1976). Coal development will therefore require extensive use of groundwater, or pipelines on the order of 100 miles in length to transport

TABLE 4. PROJECTED PRODUCTION AND USE OF NORTHERN
GREAT PLAINS COAL IN 1985(10⁶ short tons per year)

(a) Most Probable

| <u>State</u> | <u>Production</u> | <u>HCI</u> | <u>EG-M</u> | <u>EG-O</u> | <u>CG</u> |
|--------------|-------------------|------------|-------------|-------------|-----------|
| Montana | 74.2 | <0.05 | 11.0 | 41.0 | 22.2 |
| North Dakota | 49.1 | 1.0 | 19.1 | 9.0 | 20.1 |
| Wyoming | 60.5 | <0.05 | 4.2 | 40.8 | 15.5 |
| Total | 183.8 | 1.0 | 34.2 | 90.8 | 57.8 |

(b) Extensive Development

| <u>State</u> | <u>Production</u> | <u>HCI</u> | <u>EG-M</u> | <u>EG-O</u> | <u>CG</u> |
|--------------|-------------------|------------|-------------|-------------|-----------|
| Montana | 150.9 | <0.05 | 11.0 | 77.0 | 62.9 |
| North Dakota | 89.9 | 1.0 | 19.0 | 10.0 | 59.9 |
| Wyoming | 133.4 | <0.05 | 4.2 | 78.8 | 50.4 |
| Total | 374.2 | 1.0 | 34.2 | 165.8 | 173.2 |

Key: HCI = household, commercial, and industrial
 EG-M = electricity generation near mine
 EG-O = electricity generation out of state
 CG = coal gasification to produce high-BTU gas.

Source: NGPRP (1974); Nehring and Zycher (1976).

water to coalfields from larger rivers in nearby drainage basins, such as the Yellowstone, Big Horn, and Missouri Rivers. Water availability is only one phase of the problem; water rights, interstate water compacts, and other legal requirements must also be dealt with.

The land area to be used for coal development activities is extensive. For example, known strippable coal deposits in Montana and Wyoming occupy an area equal to the combined areas of Delaware and Rhode Island (Nehring and Zycher, 1976). The area disturbed by a single coal mine in the Northern Great Plains producing 3×10^7 tons of coal per year for 30 years is 15 to 178 square miles, depending on the thickness of the coal seam(s) being mined (Edwards, Broderson, and Hauser, 1976). Unless reclaimed, mined areas may become large sources of fugitive dust. Various types of reclamation are currently being carried out at coal mines in the Northern Great Plains (EPA, 1976a), but they are hindered by the low average rainfall in the region.

F. AIR QUALITY IMPACTS FROM THE USE OF NGP COAL

Air pollutants emitted from coal mining, transportation, burning, and conversion include various trace compounds, nitrogen oxides, particulates, hydrocarbons, carbon monoxide, and sulfur oxides. Trace compounds include both chemical elements present in small amounts and complex hydrocarbons that are formed or released during coal burning and gasification. Trace elements found in coal that are hazardous in excessive (though small) amounts include arsenic, beryllium, cadmium, fluorine, lead, mercury, and selenium (Magee, Hall, and Varga, 1973; Kaakinen, Jorden, and West, 1974). Except for selenium, which is enriched in coal by a factor of ten, these elements are contained in coal in roughly the same concentrations as in the earth's crust. A portion of these elements may enter the atmosphere after being subjected to a hot oxidizing atmosphere in a coal burner (see Table 5), or they may enter the water supply by leaching from ash, mines, or spoils. Trace compounds may also cause environmental problems. Many carcinogenic organic compounds have been identified in emissions from industrial boilers and output from coal gasification plants. At

TABLE 5. ESTIMATED EMISSION RATES OF VARIOUS TRACE ELEMENTS FROM COAL COMBUSTION

| <u>Trace Element</u> | <u>Emissions rate (lbs/10³ ton)</u> |
|----------------------|--|
| Arsenic | 2.9 |
| Beryllium | 3.7 |
| Cadmium | 1.0 |
| Manganese | 1.0 |
| Mercury | 0.4 |
| Nickel | 3.0 |
| Vanadium | 0.5 |

Source: EPA (1973).

present the potential degree of hazard of these compounds in the environment is unknown. A thorough review of both trace elements and trace compounds is given by Radian Corp. (1975, Vol. III, App. D).

The major air pollutants from coal utilization, namely nitrogen oxides, hydrocarbons, particulates, carbon monoxide, and sulfur oxides, have been studied far more extensively than trace compounds. Forecasts of the emissions of these pollutants from coal-fired power plants and coal gasification plants in the Northern Great Plains are presented by NGPRP for the two scenarios mentioned above (most probable and extensive development), and a scenario based on information derived from state agencies, utility companies, newspaper articles, and so on, which we will term "planned development." These estimates, listed in Table 6, are based on many assumptions, including the attainment of Federal New Source Performance Standards; in general they indicate maximum or worst-case emissions (NGPRP, 1974, p. 122). Table 6 also lists these emissions as percent increases over total statewide emissions in 1972.

Estimated increases in emissions of particulates and carbon monoxide from coal utilization are small fractions of current statewide emissions. Since these emissions come from point sources, it is possible that they

TABLE 6. PROJECTED INCREASES IN EMISSIONS FROM POWER PLANTS AND COAL GASIFICATION PLANTS, 1974-1985, FOR VARIOUS DEVELOPMENT SCENARIOS

| Pollutant | State | Emissions Increase for Given Scenario (in 10 ³ tons/year)* | | | | | | | | |
|-----------------|--------------|---|-------------------|-------------------|-----------------------|-------------------|-------------------|---------------------|-------------------|-------------------|
| | | Most Probable | | | Extensive Development | | | Planned Development | | |
| | | Power Plants | Coal Gasification | Percent Increase† | Power Plants | Coal Gasification | Percent Increase† | Power Plants | Coal Gasification | Percent Increase† |
| Particulates | Montana | 9.5 | 5.7 | 6 | 9.5 | 15.3 | 9 | 7.1 | 0 | 3 |
| | North Dakota | 11.2 | 3.8 | 13 | 11.2 | 11.5 | 20 | 24.5 | 1.9 | 23 |
| | Wyoming | <u>9.3</u> | <u>3.8</u> | 9 | <u>9.3</u> | <u>11.5</u> | 14 | <u>11.0</u> | <u>1.0</u> | 8 |
| | Total | 31.0 | 13.3 | | 31.0 | 38.3 | | 42.6 | 3.8 | |
| Sulfur Oxides | Montana | 114.1 | 64.6 | 43 | 114.1 | 172.2 | 69 | 85.3 | 0 | 21 |
| | North Dakota | 135.1 | 43.1 | 202 | 135.1 | 129.2 | 300 | 294.4 | 21.5 | 359 |
| | Wyoming | <u>111.3</u> | <u>43.1</u> | 212 | <u>111.3</u> | <u>129.2</u> | 329 | <u>132.0</u> | <u>21.5</u> | 210 |
| | Total | 360.5 | 150.8 | | 360.5 | 430.6 | | 511.7 | 43.0 | |
| Nitrogen Oxides | Montana | 66.5 | 31.1 | 89 | 66.5 | 82.9 | 135 | 49.7 | 0 | 45 |
| | North Dakota | 78.7 | 20.7 | 69 | 78.7 | 62.2 | 98 | 171.7 | 10.4 | 126 |
| | Wyoming | <u>64.9</u> | <u>20.7</u> | 81 | <u>64.9</u> | <u>62.2</u> | 120 | <u>77.0</u> | <u>10.4</u> | 82 |
| | Total | 210.1 | 72.5 | | 210.1 | 207.3 | | 298.4 | 20.8 | |
| Hydrocarbons | Montana | 2.0 | 261.2 | 147 | 2.0 | 696.6 | 390 | 1.5 | 0 | 1 |
| | North Dakota | 2.4 | 174.1 | 156 | 2.4 | 522.4 | 465 | 5.2 | 87.1 | 82 |
| | Wyoming | <u>2.0</u> | <u>174.1</u> | 173 | <u>2.0</u> | <u>522.4</u> | 514 | <u>2.3</u> | <u>87.1</u> | 87 |
| | Total | 6.4 | 609.4 | | 6.4 | 1741.4 | | 9.0 | 174.2 | |
| Carbon Monoxide | Montana | 6.8 | 2.3 | 1 | 6.8 | 6.1 | 1 | 5.0 | 0 | 1 |
| | North Dakota | 8.0 | 1.5 | 2 | 8.0 | 4.6 | 2 | 17.4 | 0.8 | 3 |
| | Wyoming | <u>6.6</u> | <u>1.5</u> | 2 | <u>6.6</u> | <u>4.6</u> | 3 | <u>7.8</u> | <u>0.8</u> | 2 |
| | Total | 21.4 | 5.3 | | 21.4 | 15.3 | | 30.2 | 1.6 | |

* Emissions associated with coal mining are not included.

† Percent increase over total emissions in state in 1972.

Source: NGPRP (1974).

may degrade air quality near the sources. (Note that these emissions estimates do not include the impacts of mining, which may be a large source of particulates.)

For hydrocarbons and nitrogen oxides, the precursors of photochemical oxidant, emissions from coal utilization substantially increase the total statewide emissions. Note that in all three scenarios coal gasification produces 90 percent or more of the hydrocarbon emissions from coal utilization. Some perspective on these emissions may be gained by comparing them with emissions in the Los Angeles Basin, as given in Table 7. The Los Angeles Basin is roughly 2,000 sq. mil. in area; eastern Montana, North Dakota, and Wyoming encompass 267,000 sq. mi. The NGPRP report provides information on the composition of hydrocarbon emissions from gasification plants. In view of the end product, it is possible that these emissions are largely methane, which is relatively unreactive in photochemical oxidant production.

TABLE 7. HYDROCARBON AND OXIDE OF NITROGEN EMISSIONS IN THE LOS ANGELES BASIN AND THE NORTHERN GREAT PLAINS

(10^3 tons/year)

| Species | Los Angeles Basin | Northern Great Plains (1985) | |
|-----------------|-------------------|------------------------------|-----------------------|
| | | Most Probable Development | Extensive Development |
| Hydrocarbons | 950* | 615 | 1750 |
| Nitrogen Oxides | 400† | 280 | 420 |

* Data for 1972 from Trijonis and Arledge (1975).

† Data for 1973 from LAAPCD (1974).

Perhaps the most serious air pollution problem from coal utilization is emission of sulfur oxides. Table 6 shows that coal utilization in the Northern Great Plains will substantially increase statewide emissions of sulfur oxides. This is ironic because the low sulfur content of NGP coal is the prime motivation for mining it. Sulfur

oxides cause damage to vegetation and the respiratory system. In addition, it is believed that they can cause acid rain as much as 1000 km downwind from sources. Because of these effects, the EPA and individual states have established strict controls on SO_x emissions from power plants. The EPA standard is $1.2 \text{ lbs } \text{SO}_x / 10^6 \text{ BTU input}$, or $0.6 \text{ lbs S} / 10^6 \text{ BTU}$. Thus subbituminous coal with a heat content of 8000 BTU/lb and a sulfur content greater than approximately 0.5 percent can be burned only if some method is employed to recover sulfur compounds. Much NGP coal meets the EPA standard, but most coal from the eastern U.S. does not. Sulfur recovery methods include flue gas desulfurization (FGD), or scrubbing, after burning and coal gasification, liquefaction, solvent refining, and washing before burning. The feasibility and costs of using these methods are matters of controversy (ES&T, 1976).

PART A

DEVELOPMENT OF A REGIONAL
AIR POLLUTION MODEL FOR THE SIMULATION
OF POLLUTANT TRANSPORT AND DIFFUSION
OVER LONG DISTANCES

III OVERVIEW

At present, emissions from new coal-fired electric generating plants are regulated by the New Source Performance Standards promulgated by the Environmental Protection Agency (EPA, 1975). Allowable ambient concentrations of many pollutants are also specified in various Federal and state standards. Furthermore, since most of the coal reserves are located in largely undeveloped areas where current ambient concentrations are low, more stringent Federal regulations for prevention of significant deterioration of air quality apply (Federal Register, 1974, 1975). In order to meet these statutes, different air pollution control techniques, ranging from direct clean-up at the stack to indirect methods such as tall stacks and the Supplementary Control System,* will have to be considered. If indirect control strategies are adopted, they will relieve air quality problems in the immediate vicinity of pollutant sources, particularly under worst-case meteorology. These control strategies do not reduce the emissions of pollutants, however, they are just released at greater heights and probably more uniformly. Consequently, primary pollutants can be expected to have longer residence times, and a net degradation of air quality can be expected at large distances from the sources. Longer residence times for primary pollutants in the atmosphere also promote the formation of secondary pollutants. This effect can be seen in many critical environmental problems that have been discovered recently, such as the observation of high sulfate levels, the increase of acidity in rain, the reduction in visibility in many pristine regions, and the observation of elevated oxidant concentrations over rural or semi-rural areas. These imposing problems have led to research on air quality problems at large, regional scales.

* The Supplementary Control System (SCS) is a time-variable emissions control scheme based on load curtailment or fuel switching during meteorological conditions of low dispersion.

Considerable effort has been expended in the past few years in attempts to obtain a quantitative understanding of long-range transport and to develop mathematical models for predicting air quality impacts. A review of previous studies pertinent to modeling of long-range air pollutant transport is presented in Chapter IV. A close examination of these models revealed that none of the models is adequate for handling multiple sources and chemical reactions on the temporal and spatial scales of interest in this project. It was thus decided that, instead of adapting an existing model as originally planned in this project, a new regional air quality model would be developed. Part A of this report is devoted to the description and discussion of this model. To provide a general background for modeling, various physical processes pertaining to the long-range transport of air pollutants are delineated in Chapter V. The model developed in this project adopts a grid modeling approach and is composed of a mixing layer model and a surface layer model. The development of this model and its components is described in Chapter VI. The model results appear to be affected by a number of physical parameters. To explore the effects of varying these parameters on the model predictions, a sensitivity test of the model was carried out as discussed in Chapter VII. Part A closes with a brief chapter of summary and conclusions on the development of the model.

The regional air quality model developed in this project was applied to the Northern Great Plains to examine the impact of coal development in that area. A detailed description of this application is given in Part B of this report.

IV REVIEW OF PREVIOUS STUDIES

A variety of mathematical models have become available for predicting the spread of air pollutants from point, line, or areal sources. Most of these models were developed to address problems characterized by spatial scales on the order of 100 km or less. Only a few modeling studies have focused on the simulation of pollutant transport over long distances (approximately 1000 km); these are discussed below.

A. SWEDISH STUDIES

Following an early study by Reiquam (1970), Rodhe (1971, 1972) appears to have been the first to suggest a model that considers the variation of surface deposition with travel distance from elevated industrial sources. The model was used to compute the atmospheric sulfur budget for northern Europe. Rodhe found that the anthropogenic sulfur emissions in this area outweigh natural emissions. His results also show that the dispersion of sulfur has a continental character; i.e., sulfur is transported, on the average, more than 1000 km before it is removed at the surface. His model yields an estimated atmospheric residence time for anthropogenic sulfur of two to four days. On the basis of this study, Rodhe dramatically concluded that about half of the sulfur measured in Sweden originates from foreign industrial emissions, and the other half is caused by Swedish emissions and a natural background.

To clarify the relative roles played by different physical processes in determining the residence time of atmospheric pollutants, Bolin and Granat (1973) and Bolin, Aspling, and Persson (1974) used a one-dimensional model describing the balance of vertical diffusion, sources, and sinks. Particular emphasis was given to assessing the importance of rainout, washout,*

* Washout, often referred to as precipitation scavenging, designates the process whereby pollutants are collected by falling raindrops. Rainout designates the process whereby pollutants are first absorbed by a cloud and then brought to the ground by rain.

and dry deposition. The results of the model calculations show that the residence time is strongly dependent on the deposition velocity, surface roughness, and turbulent intensity near the surface. For low-level emissions (≈ 20 meters), the height of emission also has an important effect on residence time, but it becomes less important as the height of emission increases.

B. NORWEGIAN STUDIES

In Norway, a modeling effort for the long-range transport of air pollutants was undertaken by Nordö and his associates (Nordö, 1973; Nordö, Eliassen, and Saltbones, 1974) in connection with the OECD* project, "Long Range Transport of Airborne Pollutants" (Ottar, 1973). Nordö's model is based on the two-dimensional, time-dependent, atmospheric diffusion equation that includes sources, sinks, and chemical transformations. Only two pollutant species, SO_2 and H_2SO_4 , were considered in that study. Both surface depositions and chemical transformations were parameterized; the former were characterized by linear decay, and the latter by both a linear and a quadratic term. The distribution of pollutants in the vertical direction was assumed to be homogeneous between the surface and the inversion layer, which was taken to be 2000 m in the model calculations. The observed winds on the 850 mb surface were used to estimate the horizontal wind distributions in this layer. The modeling region was divided into two-dimensional cells, and the governing equations were cast into finite difference form and were solved numerically. Two grid systems were tested in this study: A Cartesian coordinate and a polar coordinate consisting of eight sectors. Nordö found that numerical diffusion caused by the truncation error of the finite difference scheme is very pronounced in the Cartesian approach, so he selected the sector approach for computing the concentration fields.

*Organization for Economic Cooperation and Development. In 1973, the member countries included the United States, Canada, Australia, New Zealand, and 19 Western European countries.

The predictions of the sector approach were compared with those obtained from the moment method developed by Egan and Mahoney (1972a,b). The latter method was found to be more suitable for reducing numerical diffusion. In addition to the above numerical transport model, Nordo, Eliassen, and Saltbones (1974) also developed a trajectory model for analysis purposes. In the trajectory model, pollutants are uniformly distributed in the vertical direction, but the thickness of the mixing layer may change with position and time. The trajectories were used to follow the location of an air mass bounded by a triangle or a polygon in the horizontal plane. During the transport process the deformation of the polygon, which may shrink or expand, was compensated for by vertical displacement so that the mass continuity requirement was satisfied.

This trajectory model was further developed by Eliassen and Saltbones (1975). They used their model to estimate the rate of decay and transformation of SO_2 and SO_4 by comparing observed and predicted concentrations. In the model calculations, 48-hour isobaric trajectories were computed from analyzed wind fields on the 850 mb surface. The computed trajectories arrived at the sampling sites four times a day, and positions along a trajectory were given every half-hour. The results of this study show that the SO_2 decay rate due to dry deposition is on the order of $2 \times 10^{-5} \text{ sec}^{-1}$, corresponding to an atmospheric residence time of approximately 12 hours. The rate of SO_2 transformation to sulfate was found to be an order of magnitude smaller than the decay rate for dry deposition.

C. FINNISH STUDIES

An alternative approach for modeling long-range pollutant transport was taken by Nordlund (1973, 1975) of Finland. His model, also of the trajectory type, consists of an array of air columns (or cells) that flow into the emissions area. A cell is allowed to shrink in a convergent flow

and to expand in a divergent flow. At the same time, the height of the cell also changes so that its volume remains unchanged. The transport of the cells was calculated using the advective scheme based on the moment method (Egan and Mahoney, 1972a, b). Although lateral diffusion was also considered following the method of Smagorinsky (1963), it was noted that the effect is only marginal. However, the model predictions were found to be most sensitive to the following four parameters:

- > Emissions rate
- > Height of the mixing layer
- > Rate of pollutant removal
- > Wind velocity.

Nordlund applied this model to northwestern Europe for two different three-day periods; the calculated concentrations agreed relatively well with measurements.

D. DANISH STUDIES

In Denmark, Prahm and his colleagues (Prahm, Buch, and Torp, 1974; Prahm, Torp, and Stern, 1976) have studied the problem of long-range transport of atmospheric pollutants. On the basis of sulfate measurements and trajectory analysis, they showed that sulfur pollutants can be transported more than 500 to 1000 km over the Atlantic. The uncertainties in the trajectory analysis, however, made it difficult to trace the air masses. Consequently, they examined various numerical techniques suitable for long-range air quality modeling (Christensen and Prahm, 1976). Nineteen different numerical methods were examined including the Egan-Mahoney method (1972a,b) and the pseudo-spectral method (Fox and Orszag, 1973). They concluded that the pseudo-spectral method is the most accurate solution procedure for Eulerian models.

E. BRITISH STUDIES

Smith (1970) was credited with formulating a trajectory model using surface wind data to compute the distribution of pollutants emitted from Great Britain. His work was followed by an extensive effort by Scriven and Fisher (1975a,b), who developed a variety of models to address questions related to the long-range transport of air pollutants. Adopting a trajectory approach, they first showed that the two-dimensional steady-state diffusion equation can be used to derive an integral equation for the concentration distribution as a function of the transverse and vertical distance from the source. They then developed a box model that accounts for pollutant removal by washout and dry deposition in a linearly expanding plume. The effect of variable inversion height was also considered in this simple approach (Scriven and Fisher, 1975a). The following general conclusions were reached from an analysis of the model results:

- > Decay distances of several hundred kilometers are possible when rain is absent and when the inversion height is on the order of 1 km, assuming that the ratio of mean wind speed, u , to deposition velocity, v_g , is 500 or more. This is in qualitative agreement with the results obtained by Scandinavian investigators (Rodhe, 1971, 1972; Nordö, 1973; Nordö, Eliassen, and Saltbones, 1974; Eliassen and Saltbones, 1975).
- > For a fixed velocity ratio, u/v_g , the travel distance is proportional to the inversion height. Thus low-level inversions cause short travel distances unless the major part of the emissions rises above the inversion.
- > At a fixed distance from a large area source emitting at a constant rate, there is a maximum received concentration in the absence of rain as other meteorological conditions vary. This maximum concentration corresponds to a maximum rate of deposition that is independent of deposition velocity and falls off inversely with the distance.

Moderate rainfall (1 mm per hour) reduces travel distances considerably. Washout dominates deposition while it is raining, but not on a long-term basis (e.g., annual average).

In the absence of rain, sulfate aerosol travels much greater distances than SO_2 because the aerosols are removed from the atmosphere principally by washout and rainout rather than deposition. Thus their half-life is much longer. Annual average ambient concentrations and deposition rates are orders of magnitude smaller than "in-plume" values. Typically, large industrial areas emitting SO_2 at rates of hundreds of tons of SO_2 per hour give rise to dry deposition rates hundreds of kilometers away that are at most a small fraction of one gram of sulfur per square meter per year.

A more sophisticated model was also developed by Scriven and Fisher (1975b) to assess the accuracy of the simple box model discussed above and to investigate the buffering effect of diminishing atmospheric turbulence as an emissions plume approaches the earth's surface. The model is based on the time-dependent, one-dimensional diffusion equation, which follows a wind trajectory. The solution was written in terms of Green's function. The results of the model calculations show that, at most distances of interest, the predicted ground-level concentrations are lower than those computed from the simple box model. Consequently, the mean travel distance (or average residence time) is greater. Fisher (1975) subsequently applied this model to study the deposition of sulfur over Great Britain, Sweden, and the rest of Europe. His conclusion, based on model calculations, was that only approximately 6 percent of the total annual deposition of sulfur over rural Sweden can be attributed to high-level sources in the United Kingdom.

F. STUDIES IN THE UNITED STATES

Dickerson, Crawford, and Crandall (1972) carried out a study in the United States concerning the modeling of long-range transport of pollutants. This study, motivated by two previous Russian works (Petrov, 1971; Izrael, 1971), was concerned with the long-range transport, diffusion, and deposition of radioactive substances from a Russian nuclear cratering experiment. An interesting feature of this study is the inclusion of a method for computing wet deposition of tritium as a function of precipitation rate, storm cloud depth, and absolute humidity. Computed plume centerline concentrations, surface concentrations, and tritium deposition were reported to be in good agreement with airborne and surface measurements over Japan. The need for further understanding of the transport, diffusion, and deposition processes and for developing predictive capability over regional and extended scales was also discussed by Knox (1974).

Recently, a model similar to Nordo's (1973) was developed by Miller, Galloway, and Likens (1975) of the Air Resources Laboratories, National Oceanic and Atmospheric Administration, for the study of common air pollutants. Heffter, Taylor, and Ferber (1975) also developed a regional-scale transport model, based on the trajectory approach, that incorporates both dry and wet deposition. This model is a part of a global model for computing long-term pollutant concentrations. This model was applied by Lamb and Whitten (1975) to assess the impact of SO_2 emissions from Illinois on the air quality of the northeastern United States. More recently, a box model, similar to that of Machta (1966), was developed by Draxler and Elliott (1977) of the Air Resources Laboratories.

As part of an investigation to provide more data on atmospheric pollutant loadings over the Upper Great Lakes, McMahon, Denison, and Fleming (1976) developed a long-range air pollution model operating on a daily time scale. This simple model was adopted from a circular box approach proposed by Slade (1967), but modified to operate on a daily

basis and to account for wet and dry deposition. Their analysis showed that model predictions were very sensitive to the deposition velocity and the washout coefficient. They also concluded that background levels resulting from natural sources can be significant in the overall balance of the pollutant budget.

To assess the transport and deposition of sulfur dioxide over the continental United States, Fox (1975) adopted a trajectory model similar to that of Scriven and Fisher (1975a). He reported gross estimates for the SO_2 concentration levels of the ambient air in the United States that he deemed to be reasonable.

Under the sponsorship of Federal Republic of Germany, Johnson, Wolf, and Mancuso (1975) of the Stanford Research Institute demonstrated the feasibility of developing an air quality budget model for central Europe. The model tracks many "puffs" of SO_2 , which are released at 12-hour intervals from each grid cell containing areal sources. These puffs are transported according to the 850 mb wind field and are tracked every three hours. SO_2 emissions were assumed to be uniformly mixed in the vertical direction and a simple Fickian diffusion, with a diffusivity increasing linearly with time, was invoked for the lateral direction. Moreover, exponential decay relationships were used to account for both dry and wet deposition. The authors stated that the results from preliminary model calculations provided rough but reasonable estimates for sulfur dioxide fluxes across international boundaries and amounts of sulfur dioxide removed by deposition processes within individual countries.

More recently, several field measurement programs were initiated to examine the long-range transport of air pollutants. A few of the more well-known ones are

- > MISTT--Midwest Interstate Sulfur Transformation and Transport Project (White et al., 1976).

- > SURE--Sulfate Regional Experiment (Hidy, Tong, and Mueller, 1976).
- > MAP³S--Multistate Atmospheric Power Production Pollution Study (MacCracken, 1976).
- > Northeast Oxidant Transport Study (Bufalini and Lonneman, 1977).

In conjunction with these studies, many regional airshed models were also proposed. For example, as part of the Sulfate Regional Experiment a three-dimensional grid model was developed (Rao, Thomson, and Egan, 1976). The Egan-Mahoney moment method (Egan and Mahoney, 1972a,b) was adopted for solving the atmospheric diffusion equations for sulfur dioxide and sulfate. The effect of surface deposition was parameterized in terms of a simple boundary condition at the ground surface, and chemical transformations between SO₂ and sulfate were grossly represented by a first-order reaction. This model was applied to an air pollution episode (October 3, 1974) over northeastern United States. The results appear to compare favorably with the measurements collected at the AIRMAP Network of Environmental Research and Technology, Inc. In another study, Rao, Lague, and Egan (1976) developed a one-dimensional Lagrangian model. The pollutant mass in each box was assumed to be well-mixed in the vertical direction. From their sensitivity analyses they concluded that more accurate estimates of chemical reaction rates relative to surface removal rates are clearly important.

Another regional airshed model (Wendell, Powell, and Drake, 1976) is being developed by the Battelle Pacific Northwest Laboratories for the Multistate Atmospheric Power Production Pollution Study (MAP³S) (MacCracken, 1976). This model is based on a trajectory approach, and utilizes a scheme proposed by Wendell (1972). A power law is used to prescribe the horizontal diffusion as a function of distance from the source. Pollutant removal by dry deposition, precipitation scavenging, and chemical reactions is included via simple linear relationships. As part of a continuing program, the effect of the precipitation pattern on pollutant removal and the effect of

wind shear on the regional air pollution distribution are also being examined.

The cursory review presented above is intended only as an overview of previous work in the modeling of pollutant transport over long distances. In the next chapter, we delineate what we view to be the major attributes of long-range transport models.

V MAJOR ATTRIBUTES OF LONG-RANGE DISPERSION MODELING

A variety of long-range air quality models were discussed in Chapter IV. These models differ in data requirements and model objectives, and use various modeling approaches or formulations. Moreover, they place different degrees of emphasis on the treatment of the many physical processes pertinent to the long-range transport of air pollutants. It thus seems important at this juncture to delineate the major attributes of long-range dispersion modeling.

Some atmospheric processes play an important role in the dispersion of air pollutants on large spatial scales, and others are important on small spatial scales. The interactions among these processes, and the overlapping influences of them on the eventual pollutant distributions, are very complex (Fortak, 1974). A classical example, shown in Figure 2, is the effect of atmospheric turbulence of different scales on pollutant transport and dispersion. The following sections discuss physical and chemical phenomena that are unique to long-range air pollution modeling.

A. TRANSPORT AND DIFFUSION

The spatial and temporal scales of interest to the present study are on the order of several hundred kilometers and several days. As shown in Figure 2, the atmospheric motions important on these scales range from mesoscale convection to synoptic-scale cyclonic waves.

Changes of wind speed and direction in the lowest layer of the atmosphere are the result of many competing physical processes. The

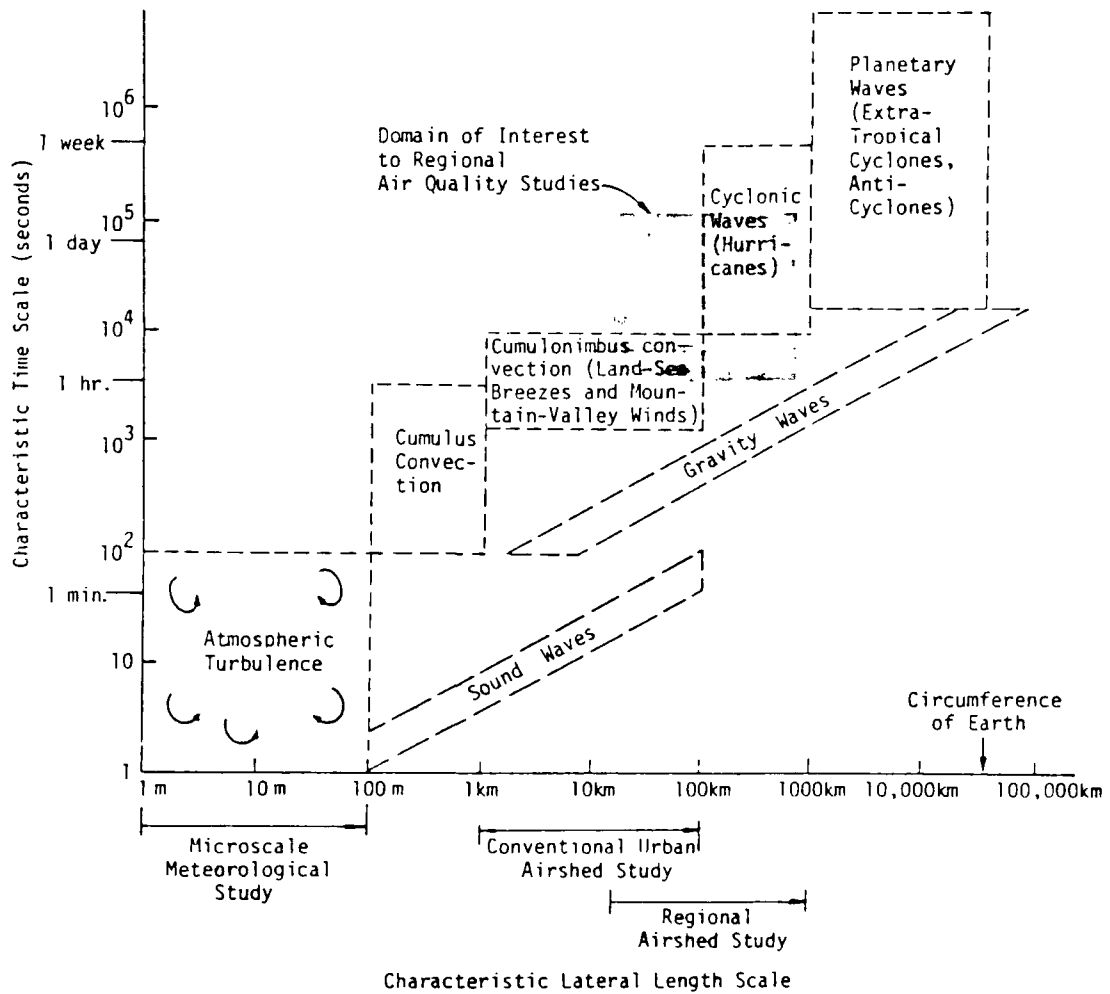


FIGURE 2. SCHEMATIC ILLUSTRATION OF SCALES OF MOTION IN THE ATMOSPHERE

interaction between the synoptic-scale air motion and the surface boundary layer usually produces complex flow patterns. These patterns change diurnally and seasonally. They also vary spatially if nonuniform terrain or inhomogeneous heating is present. The terrain of the Northern Great Plains, with the exception of the Black Hills in western South Dakota, can be characterized as flat. This condition simplifies air quality modeling because it eliminates complicated flow patterns such as valley winds and drainage flows. More interesting to the long-range transport models, as pointed out by Pasquill (1974), is the fact that the prevailing wind flow on this scale will have a characteristic frequency which coincides with or is larger than that of the "spectral gap" in the longitudinal velocity spectrum of the atmosphere (Van der Hoven, 1957). Minor topographic features can sometimes lead to high surface concentrations under special flow situations. For example, according to a tracer study carried out by Heimbach, Super and McPartland (1975), the highest SO_2 concentration in the vicinity of the Colstrip Power Plant near Billings, Montana, is observed at a hill about 350 meters higher than the plant and 20 kilometers downwind. Obviously, this result is due to the impingement of the plant's emissions plume upon the hill. Clearly, both mesoscale and microscale flow patterns are important in determining ground-level concentrations of pollutants.

Aside from the dominant atmospheric motions, divergence in the synoptic and mesoscale horizontal wind regimes leads to vertical air motions. Vertical currents, which give rise to the phenomenon known as Ekman pumping, are also generated by viscous forces in the boundary layer and can be particularly large in regions of complex terrain. Although the vertical velocities generated by these processes have a magnitude of only 1 to 10 cm/sec, they can have significant effects on the net transport of air pollutants (Liu and Seinfeld, 1975). Accurate estimates of the vertical components of the wind vectors on this scale are extremely difficult to obtain. Thus, in all of the long-range dispersion models discussed above, horizontal wind fields were prescribed

from upper air pressure distributions^{*}, and no vertical velocity components were specified.

Over the Northern Great Plains, wind fields are often strongly influenced by the high pressure system west of the Rocky Mountains. The magnitude of the prevailing westerlies is governed by the location and strength of the Pacific High. Holzworth (1972) calculated the average wind speed and the mixing-layer depth within the mixing layer from a five-year record of upper air observations at National Weather Service stations. The portion of that data pertinent to this study is reproduced in Table 8. We note that in the Northern Great Plains wind speeds and mixing depths are generally lower in winter than in other seasons, and thus it is expected that the greatest potential for air pollution episodes in this region should occur in winter.

Relative to horizontal transport by wind, vertical diffusion plays a completely different role than lateral diffusion in determining the fate of air pollutants at large distances. This can be seen from a simple analysis. According to Table 9, the following two ratios can be formed:

$$\frac{\text{Lateral Diffusion}}{\text{Horizontal Transport}} = \frac{K_H}{U\Delta x}$$

$$\frac{\text{Vertical Diffusion}}{\text{Horizontal Transport}} = \frac{K_V}{U\Delta x} \left(\frac{\Delta x}{\Delta z} \right)^2$$

where

U = characteristic wind speed,

Δx = characteristic length in the lateral direction,

Δz = characteristic length in the vertical direction,

^{*} These are typically derived from the 850 mb pressure surfaces.

TABLE 8. MEAN SEASONAL AND ANNUAL MORNING AND AFTERNOON MIXING HEIGHTS AND WIND SPEEDS FOR THE NORTHERN GREAT PLAINS*

| Station | Time | Winter | | Spring | | Summer | | Autumn | | Annual | |
|--------------------------|-----------|-------------------|-----------------------------------|-------------------|-----------------------------------|-------------------|-----------------------------------|-------------------|-----------------------------------|-------------------|-----------------------------------|
| | | Mixing Height (m) | Wind Speed (m sec ⁻¹) | Mixing Height (m) | Wind Speed (m sec ⁻¹) | Mixing Height (m) | Wind Speed (m sec ⁻¹) | Mixing Height (m) | Wind Speed (m sec ⁻¹) | Mixing Height (m) | Wind Speed (m sec ⁻¹) |
| Lander, Wyoming | Morning | 188 | 2.5 | 427 | 3.3 | 326 | 2.7 | 265 | 2.6 | 301 | 2.8 |
| | Afternoon | 808 | 3.6 | 2629 | 6.4 | 3406 | 6.3 | 1907 | 4.6 | 2187 | 5.2 |
| Glasgow, Montana | Morning | 220 | 4.7 | 347 | 5.9 | 277 | 5.4 | 232 | 5.0 | 269 | 5.3 |
| | Afternoon | 428 | 6.2 | 1855 | 7.7 | 2409 | 7.1 | 1257 | 7.5 | 1487 | 7.1 |
| Great Falls, Montana | Morning | 447 | 8.8 | 527 | 6.5 | 359 | 4.4 | 422 | 7.0 | 438 | 6.7 |
| | Afternoon | 874 | 9.9 | 2318 | 8.4 | 2984 | 6.9 | 1641 | 9.0 | 1954 | 8.6 |
| Bismarck, North Dakota | Morning | 272 | 5.0 | 378 | 5.5 | 239 | 3.9 | 255 | 4.4 | 286 | 4.7 |
| | Afternoon | 528 | 7.0 | 1756 | 8.7 | 2015 | 7.0 | 1299 | 7.9 | 1399 | 7.6 |
| Rapid City, South Dakota | Morning | 226 | 4.7 | 362 | 5.8 | 298 | 4.5 | 264 | 5.0 | 287 | 5.0 |
| | Afternoon | 848 | 7.2 | 2032 | 8.4 | 2419 | 6.7 | 1559 | 7.6 | 1714 | 7.5 |

* Data excluding precipitation and no-inversion cases.

Source: Adapted from Holzworth (1972).

TABLE 9. COMPARISON OF PHYSICAL PROCESSES PERTINENT TO LONG-RANGE POLLUTANT TRANSPORT

| <u>Physical Process</u> | <u>Mathematical Representation</u> | <u>Characteristic Value</u> |
|-------------------------|--|-------------------------------------|
| Horizontal Transport | $U \frac{\partial C}{\partial x}$ | $U \frac{\Delta C}{\Delta x}$ |
| Lateral Diffusion | $\frac{\partial}{\partial x} \left(K_H \frac{\partial C}{\partial x} \right)$ | $K_H \frac{\Delta C}{(\Delta x)^2}$ |
| Vertical Diffusion | $\frac{\partial}{\partial z} \left(K_V \frac{\partial C}{\partial z} \right)$ | $K_V \frac{\Delta C}{(\Delta z)^2}$ |

K_H = horizontal eddy diffusivity,

K_V = vertical eddy diffusivity.

Eddy diffusivity in the horizontal direction is known to vary not only with lateral scale and altitude, but also with latitude (Czeplak and Junge, 1974). Furthermore, the zonal and meridional components of the large-scale eddy diffusivity can be shown to be different in magnitude (Kao, 1974). According to Heffter (1965) and Randerson (1972), a value of $10^4 \text{ m}^2/\text{s}$ appears to be the median horizontal diffusivity for the spatial and temporal scale of interest. Vertical eddy diffusivity is a strong function of height and atmospheric stability. For the present analysis, a value of $10^2 \text{ m}^2/\text{s}$ can be viewed as representative (Pasquill, 1974). Thus, using a 10 m/s average wind, and $\Delta x = 100 \text{ km}$, $\Delta z = 100 \text{ m}$, the above two ratios become

$$\frac{\text{Lateral Diffusion}}{\text{Horizontal Transport}} \sim 10^{-2} ,$$

$$\frac{\text{Vertical Diffusion}}{\text{Horizontal Transport}} \sim 10^2 .$$

The implication of this analysis is that while vertical diffusion is overwhelmingly dominant, lateral (or horizontal) diffusion is also marginally important in pollutant transport over large distances.

B. REMOVAL PROCESSES

Over a travel distance of, say, 1000 km, more than half of the total mass of most pollutants is removed by various removal processes. For sulfur dioxide, the rough estimates in Table 10 provide a ranking of the importance of each removal process.

It is thus clear that the following three processes should be included in models of long-range SO_2 transport:

- > Dry deposition
- > Rainout and washout
- > Photochemical reactions (if significant NO_x and HC are present)

The first two processes are discussed below and the third in the next section.

TABLE 10. SO_2 REMOVAL PROCESSES

| Process | Rate of Removal of SO_2 (Percent per Hour) ² |
|--|---|
| Photochemical Reaction (SO_2 /Clean Air) | 0.03 |
| Fog | 2 |
| Photochemical Reaction (SO_2 / NO_x /HC) | 1-10 |
| Dry Deposition | 1-10 |
| Rainout and washout | 12 |

1. Dry Deposition

The most extensive outdoor areas available for the deposition of SO_2 are the oceans, vegetation, and soil. In towns and cities, building materials must also be added to this list. In his study of the atmospheric sulfur cycle, Junge (1963) estimated that the direct uptake of SO_2 and hydrogen sulfide (H_2S) by soil and plants is 7×10^7 tons per year, with a similar amount being absorbed by the sea. Junge compared this with an industrial release of 4×10^7 tons of SO_2 per year and a biological release of H_2S from the soil, sea, and coast of 16×10^7 tons per year. Most H_2S is thought to be oxidized to SO_2 , so that the residence time of H_2S in the atmosphere is only a few days. These estimates show that, of the total sulfur emitted in gaseous form, 35 percent could be deposited on plants and soil, and 35 percent in the oceans. The remainder is probably oxidized in the atmosphere and removed as sulfate either in rainwater or on particulates.

A number of measurements have been made of the rate of deposition of SO_2 onto vegetation. These data have been converted to velocities of deposition and are summarized in Table 11. A value of 1.8 cm sec^{-1} has been derived for the total deposition of SO_2 over the ground area of Great Britain (Chamberlain, 1960). Such a value suggests that deposition onto vegetation could account for most, if not all, of SO_2 deposition on the ground in Great Britain. Hill (1971) has commented that 90 percent of the United States is covered with vegetation, and that vegetation may significantly reduce atmospheric SO_2 concentrations. The data in Table 11 adequately support this view.

It is important to note that the rate of uptake of SO_2 by leaves is controlled largely by the stomata (Spedding, 1969). When the stomata are closed the uptake rate drops by at least a power of 10; hence, SO_2 removal from the atmosphere is dependent upon factors influencing stomatal opening. In general, stomata are open in the daylight at times when

TABLE 11. DEPOSITION OF SO_2 ONTO VEGETATION

| <u>Plant Examined</u> | <u>Velocity of Deposition (cm sec⁻¹)</u> | <u>Method Used To Obtain Velocity</u> | <u>Reference</u> |
|---------------------------|---|--|------------------|
| Alfalfa | 2.5 | Rate of removal of SO_2 by leaves | Hill (1971) |
| Mustard | 0.7 | Analysis of S in leaves | Spedding (1969) |
| Barley | 1.5 | Analysis of S in leaves | Spedding (1969) |
| Several | 2.0 | -- | Eriksson (1966) |

plant roots have an adequate supply of water and when the relative humidity of the atmosphere is high. Under conditions that wilt leaves the stomata are closed. A further factor influencing the opening or closing of stomata is the concentration of atmospheric SO_2 . At SO_2 concentrations greater than about 0.4 ppm, the closing of the stomata is increased (Katz, 1949; Mansfield and Heath, 1963). Field observations of this effect were reported by Martin and Barber (1971).

2. Wet Deposition

Rainout and washout have long been considered to be major sinks for atmospheric SO_2 . It has been speculated that these physical mechanisms are responsible for the occurrence of "acid rain." The efficiency of rainout and washout in removing SO_2 from the atmosphere generally depends on three factors:

- > The amount of clouds.
- > The efficiency of the consumption mechanisms of clouds and raindrops.
- > The frequency of rains.

The absorption of gases by cloud droplets, known as rainout, depends on the chemical composition of the droplets. Much further work is needed to provide a quantitative understanding of this process, but there is evidence of a rather rapid transformation of sulfur dioxide into sulfuric acid in clouds as long as the pH of the cloud droplets is significantly greater than 4 (Brosset, 1973). But clearly the most important factor in the overall efficiency of rainout in removing SO_2 from the atmosphere is the frequency of rains (Rodhe and Grandell, 1973). On the basis of rain statistics from Stockholm, Rodhe and Grandell showed that even with very effective transfer of SO_2 into cloud droplets--and ultimately into rain drops--the average residence time for SO_2 in the atmosphere would be about 40 hours in winter and 90 hours in summer if rainout were the only removal mechanism. These values are approximate, of course, and would certainly be different in another climatic region. Rodhe and Grandell (1973) derived the distribution function for the probability of rainout of a pollutant released at an arbitrary instant (see also Bolin and Rodhe, 1973). Although a more precise characterization of rainout might well be important, it has been generally assumed that removal of pollutants by precipitation can be described adequately by a characteristic mean residence time, and that the amount of pollutant removed by rainout at any one place is proportional to the concentration of that pollutant in the air.

The capture of gases and particles by falling raindrops is called washout. Typically, the duration of washout is relatively short compared with that of rainout. However, pollutant concentrations at the cloud level are generally much lower than those near the ground in the presence of an emissions plume. Thus, rainout and washout can be of similar importance in the acidification of rain. The uptake of SO_2 by rain depends on physical

parameters, such as rainfall intensities and raindrop size distributions, and on chemical characteristics, such as the presence of oxidizing agents in the atmosphere and the chemical composition of the raindrops. Other factors may also be influential. For example, Li and Landsberg (1975) found that the extent of acidic washout from a plume has a notable dependence on wind speed. Models of washout generally reduce asymptotically to two limiting cases. These cases are mass-transfer-limited (i.e., irreversible washout) and chemical-reaction-limited (i.e., equilibrium washout). A recent study by Dana, Hales, and Wolf (1972) suggests that under typical atmospheric conditions washout is often mass-transfer-limited.

C. CHEMICAL TRANSFORMATION

Most pollutants undergo a variety of chemical changes in the atmosphere. The chemical reaction of most interest to this study is the oxidation of sulfur dioxide to sulfate. Sulfate is found in particulate matter primarily as sulfuric acid (H_2SO_4), ammonium bisulfate (NH_4HSO_4), and ammonium sulfate [$(\text{NH}_4)_2\text{SO}_4$]. Atmospheric sulfur dioxide (SO_2) is both reactive and soluble. It can thus participate in many homogeneous and heterogeneous chemical reactions, and many mechanisms have been proposed for its oxidation to sulfate. Although these complex reactions are not currently well understood, it is generally thought that near a source sulfur dioxide inhibits the production of ozone and the formation of photochemical smog. Downwind of a source, on the other hand, photochemically initiated free-radical interactions of sulfur dioxide and nitrogen oxides are thought to produce secondary pollutants such as ozone and sulfuric acid.

Basically, SO_2 can be converted to other pollutants in two ways:

- > Gas phase reactions lead to the formation of sulfur trioxide (SO_3), which rapidly combines with water to give sulfuric acid (H_2SO_4). The H_2SO_4 molecules formed in the gas phase can

then dissolve in existing droplets or serve as nuclei for clusters of water molecules. In the presence of hydrocarbons and nitrogen oxides, SO_2 can be oxidized in the atmosphere at appreciable rates (on the order of 5 percent per hour), forming SO_3 . Reactions of SO_2 with oxygen-containing free radicals, principally OH, and with oxidized products of ozone-olefin reactions generally account for most of the gas phase conversion of SO_2 to SO_3 .

- > Sulfur dioxide dissolves in aerosol droplets where it is subsequently oxidized to sulfate (SO_4). The oxidation requires a catalyst. Two types of catalysts have been identified and studied--dissolved NH_3 and metal salts. The catalytic oxidation of SO_2 in solution is known to be promoted by ammonium ions (NH_4^+) and by metal ions, such as Fe^{+3} and Mn^{+2} . NH_4^+ is essential to the oxidation of SO_2 in solution because it buffers the solution, permitting effective absorption of SO_2 from the gas phase. The absorbed SO_2 then forms sulfurous acid and sulfite ions. The solution chemistry of this system seems to be reasonably well understood (Scott and Hobbs, 1967; Miller and de Pena, 1972).

The above discussion is largely qualitative. Quantitatively the chemistry of SO_2 , particularly in complex systems, is not well understood, although some advances have been made recently. For example, Liu et al. (1976) developed a kinetic mechanism for the chemistry of the hydrocarbon-nitrogen oxides- SO_2 system. This kinetic mechanism, based in part on data from smog chamber experiments, has been used in studying the chemical reactions occurring in power plant plumes.

D. SUBGRID-SCALE PROBLEMS

On the subgrid scale, modeling of large point sources at long distances presents certain unique problems. Compared to emissions of pollutants from areal sources (generally related to transportation or

residential use of fossil fuels), emissions from point sources such as power plants, refineries, and other industrial facilities possess several distinct physical characteristics. The most obvious ones can be stated as follows:

- > The emissions from point sources are generally more concentrated.
- > The emissions from point sources are almost invariably released at greater heights.
- > The emissions from point sources are most often buoyant.

These characteristics distinguish the point source air pollution problem from that associated with areal emissions. Perhaps the most prominent difference between point and areal source models is the question of spatial resolution. Due to the disparity in spatial scales appropriate to each, conventional grid models--even the most sophisticated ones--have difficulty in properly treating the transport and dispersion of point source emissions in the immediate vicinity of the stack. This is probably the reason why the Gaussian formula has been used so extensively for point sources in the past, despite its many known deficiencies. Because the emissions from a point source are buoyant and are released into the atmosphere at great heights, an accurate prediction of the impact--in particular, the impact on ground-level concentrations--will require knowledge of not only the height to which the plume will eventually rise (the effective plume height), but also the effects of plume interaction with the ground surface, particularly if the terrain is not flat.

The special characteristics of point sources pose a variety of problems in modeling. Foremost of these, perhaps, is the problem of predicting plume rise. Although there is no lack of plume rise formulas (Liu et al., 1976), they are generally empirically based.

Because of the different terrain, meteorological, and emission conditions under which data were collected to derive these formulas, it is not uncommon for the predictions of plume rise formulas to vary by more than a factor of two.

To compound the problem of estimating plume rise, plume behavior is critically affected by the vertical structure of the atmosphere. In the case of a surface layer capped by an elevated temperature inversion, which is generally associated with the worst air pollution episodes, a number of possible plume configurations may take place. A buoyant plume can penetrate an elevated inversion if the plume is "strong" and the inversion is "weak", but the plume can be entirely trapped underneath the temperature inversion if the opposite is true. During transient conditions, such as those associated with the daily heating of the surface layer or the development of a diurnally varying land-sea breeze along coastal areas, the gradual entrainment of a plume into the surface layer gives rise to plume fumigation, which typically produces the greatest ground-level concentrations. All of the phenomena described above are intimately connected with the prediction of plume rise.

Other problems related to the effective plume height can be equally important. One of these is concerned with wind shear. Ideally, to minimize the error in model predictions, one should use the measured wind speed at the height of the pollutant cloud. This does not pose a major problem in the modeling of ground-based areal sources because surface wind data can generally be considered as representative and are readily available. In the case of a buoyant plume, however, the effective plume height is not always known a priori. Furthermore, to measure the wind speed at that height is not a trivial matter. The current practice is to use the measured wind speed at the stack height. Any attempt to correct this deficiency clearly requires knowledge of the vertical profile of the horizontal wind. Many Gaussian models

have achieved this by simply adopting a power-law wind profile for the conversion of the measured wind speeds at the stack height to those at the effective plume height.

The importance of other, more complex aspects of the plume-wind shear interaction should not be disguised by the simple discussion presented above. For example, under the conditions of a local surface wind--such as the drainage flow or sea breeze--imbedded in a synoptic-scale flow of the opposite direction, a drastic change in wind profiles may be responsible for the occurrence of such anomalies as bifurcation of the plume (Liu et al., 1976).

Also related to the elevated nature of point sources is the problem of the impact of the plume on the topography. Depending upon the relative heights of the plume and the ground surface and the vertical structure of the atmosphere, it is conceivable that the plume can either be lifted above or impinge upon the surface. The occurrence of either should depend in general on whether the kinetic energy of the air stream approaching an obstacle is greater or smaller than the potential energy required to lift it over the obstacle, which is in turn dependent upon atmospheric stabilities. Thus, the conditions that are conducive to plume impingement are light winds and stable atmosphere. However, the physical processes governing the occurrence of impingement phenomena are extremely complex, and have only very recently received the attention of air pollution researchers.

For reactive pollutants, certain features are also unique to the point source problem. Because the emissions from power plants are rich in nitric oxide, ozone entrained from the ambient air is generally completely depleted within the plume in the vicinity of the stack. This phenomenon has been frequently observed and is well documented. At large downwind distances, depending upon the ambient hydrocarbon

and nitrogen oxide levels, secondary pollutants can be formed in some situations (Liu et al., 1976). Thus, in the modeling of reactive pollutants, it is important to assess the interactions of the plume with urban or rural background emissions.

VI DEVELOPMENT OF A REGIONAL AIR POLLUTION MODEL

It had been originally conceived that in this study a suitable regional air pollution model was to be selected and adapted for application to the Northern Great Plains. The selection of a model must of course be based on its ability to include the attributes discussed in the previous chapter, so that the effects of various sources on air quality can be predicted with reasonable accuracy. For the present study, the following model attributes appear to be particularly pertinent:

- > The ability to handle a multitude of emission sources.
- > An adequate treatment of pollutant transport over large distances.
- > An adequate treatment of pollutant depletion processes.
- > Provisions for including chemically reactive pollutants.

Other important considerations include computational requirements and availability and resolution of the data base.

As discussed in Chapter IV, a variety of regional models have been developed recently and are available for estimating concentrations of air pollutants at large distances from the sources. These models generally fall into the following four categories:

- > Box models (e.g., Johnson, Wolf, and Mancuso, 1975)
- > One-dimensional models (e.g., Bolin, Aspling, and Persson, 1974)
- > Gaussian models (e.g., Scriven and Fisher, 1975b)
- > Numerical models (e.g., Rao, Thomson, and Egan, 1976).

A careful examination of all these models revealed that the model developed by Rao, Thomson, and Egan (1976) appeared to be closest to satisfying

the model attributes listed above. This model, however, suffers from the following two deficiencies:

- > It does not contain a sufficiently detailed algorithm for the prescription of surface deposition. For the present application, which deals primarily with elevated emission sources, the diurnal variations in deposition rates are expected to be quite important.
- > This model has unfortunately retained the vertical dimension. As discussed in the previous chapter, the inclusion of this dimension is unnecessary and obviously imposes a severe computational burden.

In view of these deficiencies, it was decided during the course of this study that a new regional air pollution model be developed. As shown in Figure 3, this model is composed of two interconnected submodels:

- > A mixing layer model
- > A surface layer model.

The mixing layer model is designed to treat transport and diffusion above the surface. A grid approach is adopted in this project in order to facilitate the handling of multiple sources and complex chemistry. The major feature of this model is the assumption that pollutant distribution is nearly uniform in the vertical direction. With this assumption, a simplified form of the general atmospheric diffusion equation can be invoked.

The surface layer model is designed to calculate the pollutant fluxes lost to the ground. The surface layer, a shallow layer immediately above the terrain, is embedded within the mixing layer. For pollutants originating from either elevated sources or distant ground-level sources, most of the pollutant mass is contained in a layer aloft, i.e., in the mixing layer. The removal processes consist of the diffusion of the pollutants

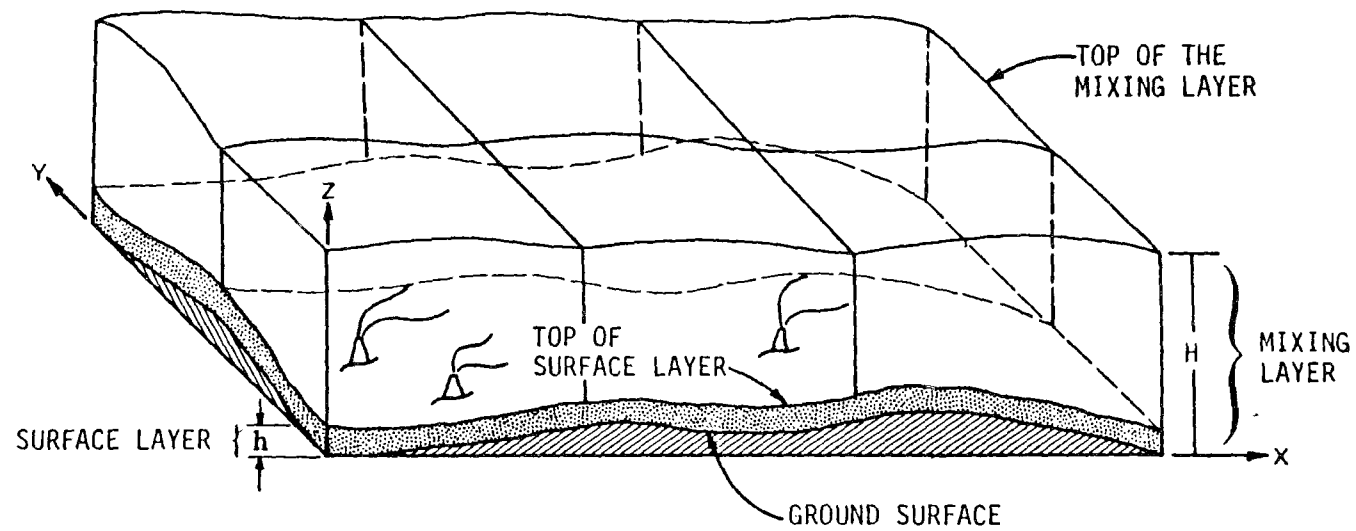


FIGURE 3. SCHEMATIC ILLUSTRATION OF THE MODELING REGION IN THE REGIONAL AIR POLLUTION MODEL DEVELOPED IN THIS STUDY

through the surface layer to the ground, followed by absorption or adsorption at the atmosphere-ground interface. A unique feature of the surface layer is its diurnal variation in surface temperature, which is a result of daytime heating and nighttime cooling. This variation affects the vertical pollutant distribution through atmospheric stabilities, and consequently, affects the rate of surface uptake of pollutants.

These submodels are discussed separately in the following sections. It should be emphasized, however, that because of the limited scope of this study, we attempted only to develop the basic and most desirable elements of an ideal regional air quality model. A number of important issues were not addressed, including:

- > Predictions from the regional air quality model in its present form are unlikely to be applicable within, say, a few kilometers downwind of a major emission source. Thus, subgrid-scale concentration distributions, as discussed in Chapter V must be dealt with on a different level. Models of this type have been discussed in a recent report by Liu et al. (1976).
- > The only pollutant removal process treated is dry deposition on the surface. Other important removal processes such as rainout and washout are not considered. Unless these processes are included, the present model is, strictly speaking, applicable only during periods of no precipitation.
- > The treatment of chemical reactions is limited to a first-order overall reaction between SO_2 and sulfate. Although no constraint except computational time imposes any problem, the inclusion of complex chemistry awaits the development of a kinetic model capable of simulating chemical transformations during nighttime and the effects of natural emissions of hydrocarbons.

A. THE MIXING LAYER MODEL

The mixing layer model is designed to treat the transport and diffusion of air pollutants over long distances. The model formulation is discussed in Section 1. As stated earlier, the grid approach was adopted in the present study. There are a number of significant advantages to the grid approach--it is very versatile, and it can easily handle time- and space-varying emissions and meteorological variables, complex chemistry, and surface sinks. But there is one major disadvantage associated with this approach; pseudo-diffusion associated with the numerical solution of the governing equation can be overwhelming. An accurate scheme must thus be found for the simulation of the advection term. The selection of an appropriate numerical method is discussed in Section 2.

1. The Model Equations

Within the framework of the so-called gradient-transport theory,* the concentration distributions of N reactive species can be described by the atmospheric diffusion equation of the following form (Monin and Yaglom, 1971):

$$\begin{aligned} \frac{\partial c_i}{\partial t} + u \frac{\partial c_i}{\partial x} + v \frac{\partial c_i}{\partial y} + w \frac{\partial c_i}{\partial z} = & \frac{\partial}{\partial x} \left(K_x \frac{\partial c_i}{\partial x} \right) + \frac{\partial}{\partial y} \left(K_y \frac{\partial c_i}{\partial y} \right) \\ & + \frac{\partial}{\partial z} \left(K_z \frac{\partial c_i}{\partial z} \right) + R_i(c_1, c_2, \dots, c_N) \\ & + S_i(c_i) \quad i = 1, 2, \dots, N \quad , \quad (1) \end{aligned}$$

* The gradient-transport theory, analogous to molecular diffusion theory, states that a pollutant flux in the direction of decreasing concentration is established as a result of turbulent fluctuations. The magnitude of this flux is assumed to be proportional to the gradient of the average concentration. The limitations of models based on the gradient-transport theory, also known as K-theory, were examined by Corrsin (1974).

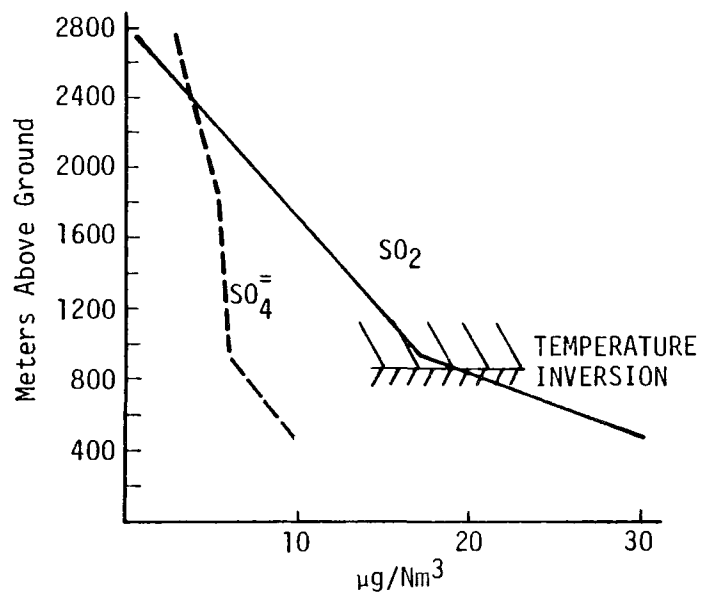
where c_i denotes concentration for pollutant species i , u , v , w , and K_x , K_y , K_z represent wind speeds and turbulent eddy diffusivities in the x , y , and z directions, respectively, and R and S are the chemical reaction and source (and/or sink) terms.

One of the major simplifications in the present model is the assumption of vertical homogeneity in the concentration distribution. One of the reasons for this choice is that the vertical diffusion term, based on the dimensional analysis shown above, is about 100 times greater than the transport term, and the horizontal diffusion term is only a fraction of the transport term. Thus retaining the vertical variation terms in the diffusion equation will compound difficulties in the numerical solution of the governing equation, without necessarily improving the accuracy of the model's predictions. As shown in Figure 4, measurements of the vertical distributions of sulfur compounds over central Germany (Georgii, 1970) show that in these remote areas the profiles are fairly uniform beneath the temperature inversion. Similar observations were also reported by Rodhe (1971) in southern Sweden. Thus it does not seem necessary to include the vertical dimension in the model.

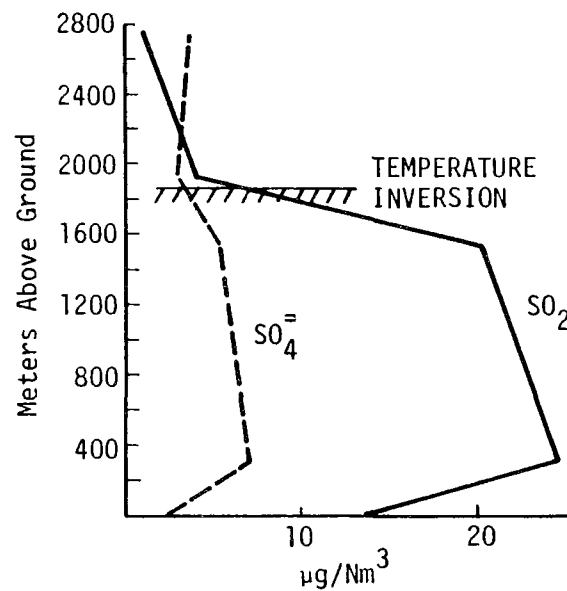
Assuming that the concentration distribution in the vertical is nearly uniform below the base of the temperature inversion, a vertically averaged concentration can be defined as

$$\bar{c}_i = \frac{1}{H} \int_0^H c_i dz \quad , \quad (2)$$

where H is the height of the inversion base. Performing the same operation on Eq. (1) and imposing the appropriate vertical boundary conditions, one obtains



(a) 25 February 1967



(b) 26 April 1967

Source: Georgii (1970).

FIGURE 4. VERTICAL DISTRIBUTION OF SO_2 AND SO_4 OVER CENTRAL GERMANY

$$\frac{\partial \bar{c}_i}{\partial t} + \bar{u} \frac{\partial \bar{c}_i}{\partial x} + \bar{v} \frac{\partial \bar{c}_i}{\partial y} = \frac{\partial}{\partial x} \left(K_x \frac{\partial \bar{c}_i}{\partial x} \right) + \frac{\partial}{\partial y} \left(K_y \frac{\partial \bar{c}_i}{\partial y} \right) + R_i(\bar{c}_1, \bar{c}_2, \dots, \bar{c}_N) + S_i(\bar{c}_i) + D \cdot \zeta(D) \quad i = 1, 2, \dots, N \quad (3)$$

where c_{0i} is the background concentration of species i , \bar{u} and \bar{v} are the vertically averaged horizontal wind components ($\bar{u} = \int_0^H u dz/H$, $\bar{v} = \int_0^H v dz/H$), D is the two-dimensional divergence [$D = (\partial \bar{u}/\partial x) + (\partial \bar{v}/\partial y)$], and $\zeta(D)$ is a step function defined by

$$\zeta(D) = \begin{cases} \bar{c}_{0i} & \text{for } D > 0 \\ \bar{c}_i & \text{for } D \leq 0 \end{cases} \quad (4)$$

In the derivation of Eq. (3), the following assumptions were made:

- > Deviations from the average concentration, \bar{c}_i , in the vertical direction are small.
- > The vertical velocity at the top boundary is approximately given by

$$w = - \int_0^H \left(\frac{\partial u}{\partial x} + \frac{\partial v}{\partial y} \right) dz \approx - H \left(\frac{\partial \bar{u}}{\partial x} + \frac{\partial \bar{v}}{\partial y} \right) \quad (5)$$

- > The diffusive flux of pollutants at the top boundary is negligible.
- > The following relationships hold for the reaction and source/sink terms:

$$\bar{R}_i(c_1, c_2, \dots, c_N) = R_i(\bar{c}_1, \bar{c}_2, \dots, \bar{c}_N) \quad (6)$$

$$\bar{S}_i(c_i) = S_i(\bar{c}_i) \quad (7)$$

One of the problems encountered in the present model formulation is the disparity of scales in the treatment of emission sources. Since the preponderance of sulfur dioxide emissions in the area of interest comes from isolated point sources, the spatial scales associated with these sources and the grid spacings adopted in the mixing layer model are certainly not commensurate. In order to resolve this subgrid-scale problem, a special algorithm was developed in which the emissions are first treated as puffs. These puffs are emitted from each major point source at regular time intervals and tracked downwind along their separate trajectories. The horizontal spread of each puff is calculated according to the Gaussian formula (Turner, 1969). When the width of a puff reaches that of one grid cell, the emissions contained in that puff are released into that cell. Table 12 lists typical downwind distances at which the width of the puff^{*} equals 10 km. It is apparent that, particularly under stable conditions, the puff can travel a few grid cells before it is picked up by the mixing layer model.

TABLE 12. DOWNWIND DISTANCE TRAVELED BY A PUFF
AS A FUNCTION OF ATMOSPHERIC STABILITY

| <u>Stability Category</u> | <u>Downwind Distance Where $4\sigma = 10 \text{ km}^\dagger$</u> |
|-------------------------------|---|
| A | 13.3 km |
| B | 17.7 km |
| C | 25.8 km |
| D | 42.8 km |
| E | 59.0 km |
| F | 88.5 km |

* The width has been chosen to be 4σ , within which the puff contains more than 95 percent of the pollutant mass.

† From Turner (1969); σ adjusted for a one-hour sampling time.

2. The Numerical Method

The solution of Eq. (3) with appropriate initial conditions and boundary conditions surrounding the modeling region requires a numerical method. Since the transport of pollutants on this scale is dominated, as demonstrated above, by horizontal advection, the problem of numerical diffusion arises in the discretization processes. That is, the numerical solution tends to smooth any sharp concentration profiles as the pollutants are advected downwind, even when the horizontal diffusivity is zero. We investigated and compared the accuracy and computing time requirements of three finite difference methods for solving simplified forms of Eq. (3):

- > The upstream difference method
- > The SHASTA method
- > The Egan-Mahoney method.

The upstream difference method is the simplest of the three. It is also well-known and widely used (Forsythe and Wasow, 1960). The SHASTA method (Sharp And Smooth Transport Algorithm) was developed by Boris and Book (1973). The method proposed by Egan and Mahoney (1972a,b) has the distinctive feature that the first and second moments of the mass distribution in each cell are also calculated. The performance of each method was examined using hypothetical situations. Based upon considerations of both accuracy and computing speed, the SHASTA method appeared to be most suitable to the needs of the present study and was thus selected for treating the horizontal advection terms. (Details of the numerical analysis and selection are given in Appendix A.) In the following paragraphs we present a brief description of the numerical method used in the mixing layer model.

Let the continuous variables be represented on a grid with mesh widths Δx and Δy so that $x_{ij} = x(i\Delta x, j\Delta y)$. Define the operators

$$D_{\pm}^{(1)} c_{ij} = \pm (c_{i\pm 1, j} - c_{ij}) \quad D_{\pm}^{(2)} c_{ij} = \pm (c_{i, j\pm 1} - c_{ij}) \quad (8)$$

$$D_0^{(1)} c_{ij} = c_{i+1, j} - c_{i-1, j} \quad D_0^{(2)} c_{ij} = c_{i, j+1} - c_{i, j-1}$$

$$Q_{\pm}^{(1)} u_{ij} = \frac{\frac{1}{2} \mp u_{ij} \left(\frac{\Delta t}{\Delta x} \right)}{1 \pm (u_{i\pm 1, j} - u_{ij}) \frac{\Delta t}{\Delta x}} \quad Q_{\pm}^{(2)} v_{ij} = \frac{\frac{1}{2} \mp v_{ij} \left(\frac{\Delta t}{\Delta x} \right)}{1 \pm (v_{i, j\pm 1} - v_{ij}) \frac{\Delta t}{\Delta x}} \quad (9)$$

Then our numerical method is given by the following three fractional steps (Yanenko, 1971):

Step 1--x-direction

$$\begin{aligned} c^* &= \left[\alpha_1 + \frac{1}{2} (Q_+^{(1)} u)^2 \right] D_+^{(1)} c^n - \left[\alpha_1 + \frac{1}{2} (Q_-^{(1)} u)^2 \right] D_-^{(1)} c^n \\ &\quad + \left[Q_+^{(1)} u + Q_-^{(1)} u + (r - d) \Delta t \right] c^n \\ \tilde{c} &= \frac{1}{2} \left(Q_+^{(1)} u \right)^2 D_+^{(1)} c^n - \frac{1}{2} \left(Q_-^{(1)} u \right)^2 D_-^{(1)} c^n + \left(Q_+^{(1)} u + Q_-^{(1)} u \right) c^n \\ c^{**} &= c^* - \frac{1}{8} D_+^{(1)} D_-^{(1)} \tilde{c} \quad , \end{aligned} \quad (10)$$

Step 2--y-direction

$$\begin{aligned} c^{***} &= \left[\alpha_2 + \frac{1}{2} (Q_+^{(2)} v)^2 \right] D_+^{(2)} c^{**} - \left[\alpha_2 + \frac{1}{2} (Q_-^{(2)} v)^2 \right] D_-^{(2)} c^{**} \\ &\quad + \left(Q_+^{(2)} v + Q_-^{(2)} v - \frac{w \Delta t}{\Delta H} \right) c^{**} \\ \tilde{c} &= \frac{1}{2} (Q_+^{(2)} v)^2 D_+^{(2)} c^{**} - \frac{1}{2} (Q_-^{(2)} v)^2 D_-^{(2)} c^{**} + (Q_+^{(2)} v + Q_-^{(2)} v) c^{**} \\ c^+ &= c^{***} - \frac{1}{8} D_+^{(2)} D_-^{(2)} \tilde{c} \end{aligned} \quad (11)$$

Step 3--point sources




$$c^{n+1} = c^+ + S \quad , \quad (12)$$

$$\text{where } \alpha_1 = \frac{K_x \Delta t}{\Delta x^2} \quad , \quad \alpha_2 = \frac{K_y \Delta t}{\Delta y^2} \quad ,$$

r is the chemical reaction rate, and d is the surface deposition rate. The stability and accuracy of the scheme are analyzed in detail for the constant velocity case in Appendix A. The advection terms are treated with at least second-order accuracy while the fractionalized scheme as a whole is accurate to the second order in space and to the first order in time.

In order to estimate the accuracy of the numerical method adopted, in Table 13 we give the effective psuedo-diffusivities produced by the model on the ten-kilometer grid with an optimum stepsize. For the present problem, the pseudo-diffusion generated appears to be small when compared with the physical diffusivity in the horizontal plane, which is estimated to be on the order of $10^4 \text{ m}^2/\text{sec}$ (Randerson, 1972). A more thorough analysis of the problem of psuedo-diffusion is presented in Appendix A.

TABLE 13. PSEUDO-DIFFUSIVITY IN ADVECTIVE TRANSPORT
FOR A 10 KILOMETER GRID AND $v\Delta t/\Delta x = 1/2$

| <u>Wave Type</u> | <u>Wave Number (m^{-1})</u> | <u>Pseudo-Diffusivity (m^2/sec)</u> |
|---|---|--|
|  | $60\pi/10^6$ | 2.5×10^3 |
|  | $30\pi/10^6$ | 1.6×10^2 |
|  | $15\pi/10^6$ | 40 |

On the other hand, computational stability is guaranteed when

$$\max \left(\frac{u\Delta t}{\Delta x}, \frac{v\Delta t}{\Delta y} \right) \leq 0.6 \quad (13)$$

$$\max \left(\frac{K_x \Delta t}{\Delta x^2}, \frac{K_y \Delta t}{\Delta y^2} \right) \leq 0.15 \quad . \quad (14)$$

With a ten-kilometer square grid cell, the most restrictive stability constraint derives from the advection terms [Eq. (13)] if K_x and K_y are less than $10^5 \text{ m}^2/\text{sec}$. For higher horizontal diffusivities, Eq. (14) becomes more stringent. The time step used in the mixing layer model has been chosen in such a way that these conditions are always satisfied. Thus accurate and stable solutions were obtained for the mixing layer model.

B. THE SURFACE LAYER MODEL

Pollutants are removed from the atmosphere via both dry and wet deposition. Only dry deposition at the earth's surface was considered because of the limited scope of this study. The importance of surface deposition on pollutant concentrations at large distances has been well established (e.g., Bolin et al., 1973, 1974; Scriven and Fisher, 1975a,b). Thus an indispensable element in the regional air pollution model is the treatment of pollutant depletion processes near the surface. In this section, we describe the surface layer model, beginning with a discussion of previous studies on surface deposition, followed by a description of the approach adopted in this study.

1. Dry Deposition on Surfaces

In most studies, removal of pollutants by the ground surface is generally characterized by

$$F = V_d c \quad , \quad (15)$$

where F is the mass flux to the surface, c is the concentration measured at an unspecified reference height, and V_d , having the units of velocity, is commonly referred to as the deposition velocity. In this expression, the deposition velocity is viewed as a proportionality constant whose magnitude is established empirically. The surface deposition is governed by many complex physical processes, which depend primarily upon:

- > The state of atmosphere near the ground
- > The types and configurations of the surface.

For example, Bolin, Aspling, and Persson (1974) noted that for a perfect sink of a particular gas, in which all molecules of that gas reaching the surface are absorbed, the ground-level concentration is zero and the deposition velocity is theoretically infinite. In this case the flux is diffusion-limited. Consequently, the simple concept of the deposition velocity is generalized.

In analogy with electrical circuits, surface deposition was treated in terms of resistance to mass transfer (Owen and Thompson, 1963; Chamberlain, 1966). The transfer of gases from the atmosphere to a surface is described by three resistances in parallel:

- > The resistance to momentum transfer, r_m .
- > The excess resistance to mass or heat transfer, r_h .
- > The resistance at the ground surface, r_s .

The total resistance, R , which is defined as the reciprocal of the deposition velocity, is then given by

$$V_d \equiv \frac{1}{R} = \frac{1}{r_m} + \frac{1}{r_h} + \frac{1}{r_s} \quad . \quad (16)$$

Within the framework of the surface boundary layer (Owen and Thompson, 1963)

$$r_m = \frac{u(z)}{u_*} \quad , \quad (17)$$

where $u(z)$ is the vertical wind profile and u_* is the friction velocity. The deviation between momentum and mass/heat transfer is characterized by

$$r_h = \frac{1}{\beta u_*} \quad , \quad (18)$$

where β is dependent on the surface roughness, a Reynolds number appropriate to the flow in the roughness layer, and the ratio of the kinematic viscosity of air to the molecular diffusion coefficient of the pollutant gas. This correction is necessary because the process of mass transfer is generally less efficient than that of momentum transfer, resulting in a nonzero concentration of the gas at the surface. Based upon a study of the heat transfer to roughened glass plates, Owen and Thompson (1963) suggested

$$\beta^{-1} = \alpha (u_* z_0 / \nu)^{0.45} \left(\frac{\nu}{D} \right)^{0.8} \quad , \quad (19)$$

where u_* , z_0 , ν , and D are the friction velocity, surface roughness, kinematic viscosity, and molecular diffusivity, respectively, and α is an empirical constant determined by the shape of the roughness elements. In further investigations by Chamberlain (1966) and Thom (1972), little functional relation was found between β and z_0 . Thus, Thom proposed

$$\beta^{-1} = \alpha_1 u_*^{1/3} \left[\alpha_2 \left(\frac{\nu}{D} \right)^{2/3} - 1 \right] \quad , \quad (20)$$

where α_1 and α_2 are empirical constants primarily determined by the surface roughness elements.

2. The Formulation of a Surface Deposition Model

For pollutants originating from either elevated sources or distant ground-level sources, most of the pollutant mass is contained in the mixing layer. The removal processes, as discussed above, consist of

diffusion of the pollutants through the surface layer to the ground and absorption or adsorption at the atmosphere-ground interface. As illustrated in Figure 5, the diurnal variation of temperature in the surface layer affects the vertical pollutant distribution through atmospheric stabilities, and consequently, affects the rate of surface uptake of pollutants (Hogstrom, 1975). As a result, an algorithm that can account for these variations must be included as part of the surface layer model.

The surface layer model developed in this study for the prescription of pollutant fluxes is similar to those discussed by Bolin and Granat (1973) and Galbally (1974), but has been extended to include:

- > Diabatic atmospheric conditions
- > Nonlinear surface reactions.

We favor this approach over the relatively simple resistance approach primarily because the latter is restricted to linear surface reactions, which may not fit all situations of interest. For example, Hill (1971) observed that the adsorption of ozone by leaves does not vary linearly with concentration at high concentration levels.

In the model, it is envisioned that the transfer of pollutant gases from the atmosphere to a surface is accomplished via three stages (Sehmel, Sutter, and Dana, 1973; Galbally, 1974):

- > The gases are transported to a laminar sublayer just above the surface primarily by turbulent diffusion.
- > The gases are transported through this laminar sublayer primarily by molecular diffusion.
- > The gases interact by adsorption or chemical reaction with the surface.

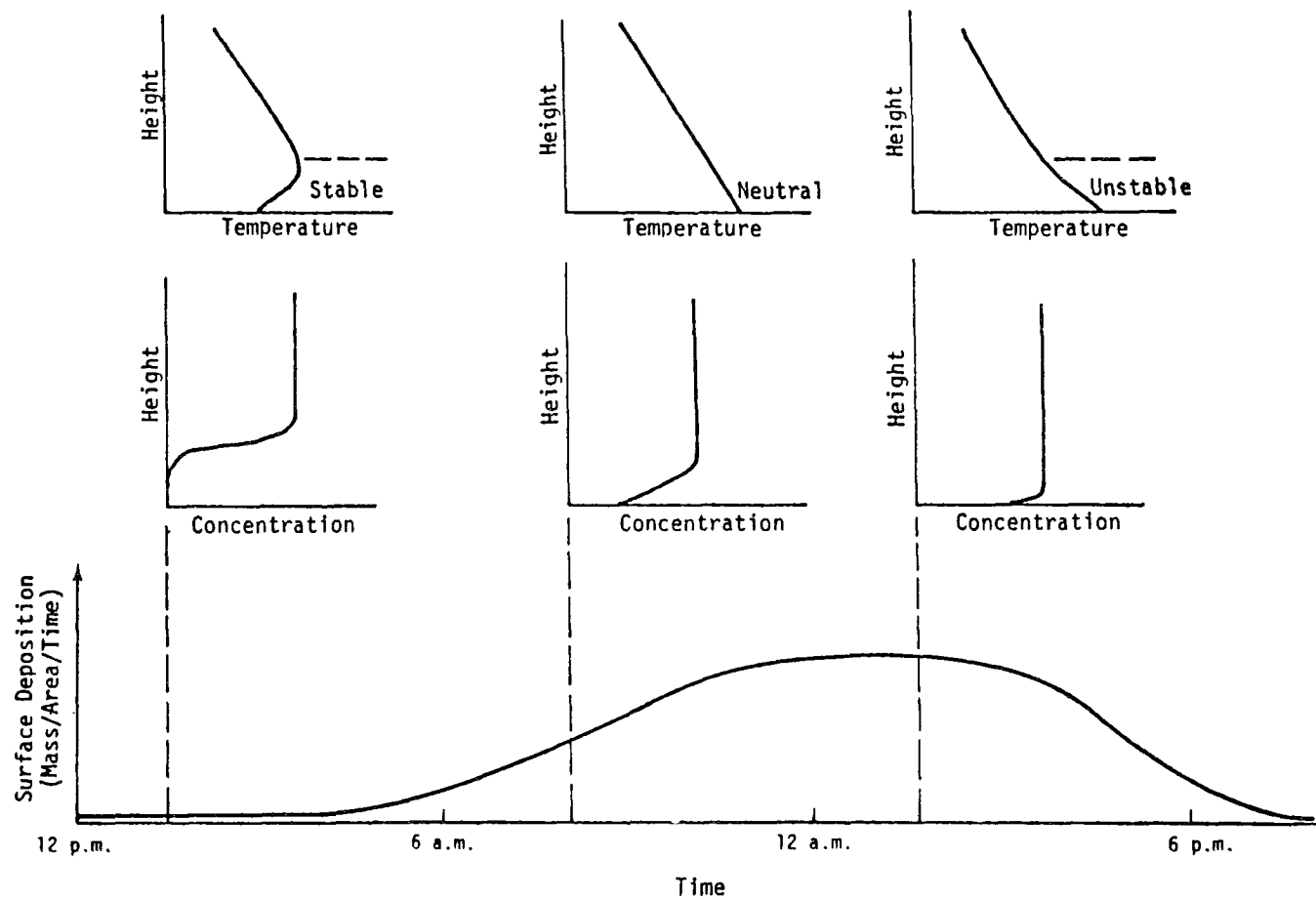


FIGURE 5. SCHEMATIC ILLUSTRATION OF DIURNAL VARIATIONS IN SURFACE DEPOSITION

Thus, as shown in Figure 6, the surface layer is divided into two parts: the turbulent layer and the laminar sublayer. In the turbulent layer, after the atmosphere reaches an equilibrium state, the atmospheric diffusion equation becomes

$$\frac{\partial}{\partial z} \left[K_V \left(\frac{\partial c}{\partial z} \right) \right] = 0 \quad , \quad (21)$$

with the following boundary conditions,

$$c = \bar{c} \quad \text{at } z = h \quad ,$$

$$K_V \left(\frac{\partial c}{\partial z} \right) = F \quad \text{at } z = z_0 \quad ,$$

where \bar{c} is the cell-averaged concentration in the mixing layer, F is the pollutant flux across the turbulent layer-laminar sublayer interface, and z_0 is the height of the surface roughness element. The vertical diffusivity K_V can be prescribed as

$$K_V = \frac{k u_* z}{\phi \left(\frac{z}{L} \right)} \quad , \quad (22)$$

where

- k = von Karman constant (= 0.35)
- u_* = friction velocity
- z = height
- L = Monin-Obukhov length.

This formula is the result of the similarity theory for the constant-flux surface layer (Businger et al., 1971). For the neutral case, the ϕ -function equals unity. For the stable and unstable cases, the ϕ -function is greater and less than one, respectively. The following empirical expressions for the ϕ -function were proposed by Businger et al. (1971) based on observational data:

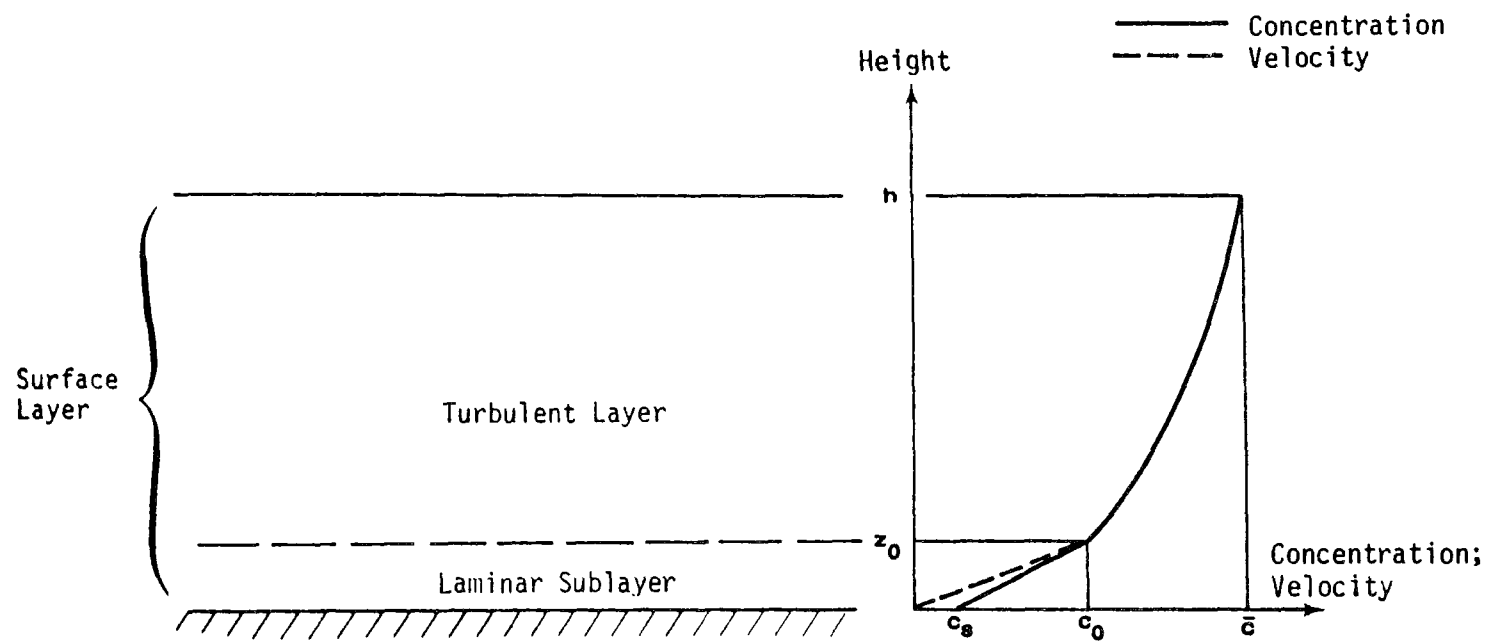


FIGURE 6. SCHEMATIC ILLUSTRATION OF THE SURFACE LAYER

For the stable case ($L > 0$)

$$\phi_s\left(\frac{z}{L}\right) = 1 + 4.7\left(\frac{z}{L}\right) \quad , \quad (23)$$

For the unstable case ($L < 0$)

$$\phi_u\left(\frac{z}{L}\right) = \left[1 - 15\left(\frac{z}{L}\right)\right]^{-1/4} \quad . \quad (24)$$

The friction velocity is determined by

$$u_* = \frac{ku_r}{f} \quad , \quad (25)$$

where u_r denotes a reference wind speed measured at a reference height, z_r , and

$$f = \ln\left(\frac{z_r}{z_0}\right) + 4.7\left(\frac{z_r - z_0}{L}\right) \quad (\text{stable}) \quad , \quad (26)$$

$$\begin{aligned} f = & \ln\left[\frac{1 - \phi_u\left(\frac{z_r}{L}\right)}{1 + \phi_u\left(\frac{z_r}{L}\right)}\right] - \ln\left[\frac{1 - \phi_u\left(\frac{z_0}{L}\right)}{1 + \phi_u\left(\frac{z_0}{L}\right)}\right] \\ & + 2 \tan^{-1}\left[\frac{1}{\phi_u\left(\frac{z_r}{L}\right)}\right] - 2 \tan^{-1}\left[\frac{1}{\phi_u\left(\frac{z_0}{L}\right)}\right] \quad (\text{unstable}) \quad . \end{aligned} \quad (27)$$

For either the stable or unstable case, the solution of Eq. (21) is simply

$$c = \bar{c} - F \cdot \int_z^h \frac{\phi(z)}{ku_* z} dz \quad . \quad (28)$$

Across the laminar sublayer, it is assumed that the pollutant flux can be written as

$$F = \beta u_* (c_0 - c_s) \quad , \quad (29)$$

where c_0 and c_s denote the concentrations at the interface and the surface, respectively, and β , analogous to the Stanton number in heat transfer, is the inverse of a dimensionless resistance for the laminar sublayer. If it is further assumed that mass and momentum are transferred in an identical manner in the turbulent layer, but differently through the laminar sublayer, then the relationships established by Owen and Thompson (1963) and Thom (1972) discussed above can be used:

$$\beta^{-1} = \alpha \left(u_* \frac{z_0}{\nu} \right)^{0.45} \left(\frac{\nu}{D} \right)^{0.8} \quad (\text{Owen-Thompson}) \quad , \quad (30)$$

$$\beta^{-1} = \alpha_1 u_*^{1/3} \left[\alpha_2 \left(\frac{\nu}{D} \right)^{2/3} - 1 \right] \quad (\text{Thom}) \quad . \quad (31)$$

To complete the description of the surface layer model, a boundary condition is required at the surface. Uptake of air pollutants occurs by chemical reaction with, or catalytic decomposition within either the soil or vegetation or by these processes at their surfaces. These processes are generally dependent on the gas concentration at the surface. A general equation for the gas loss per unit area per unit time can be written as (Benson, 1968),

$$F = \gamma c_s^a \quad , \quad (32)$$

where F is the pollutant flux, γ is a reaction rate constant, and c_s the concentration of the gas at the soil or vegetation surface. The exponent, a , denotes the reaction order. Eliminating c_0 and c_s from Eqs. (28), (29), and (32), the following transcendental equation is obtained for F ,

$$I \cdot F + \gamma^{-1/a} \cdot F^{1/a} - \bar{c} = 0 \quad , \quad (33)$$

where

$$I \equiv \frac{1}{\beta u_*} + \int_{z_0}^h \frac{\phi(z)}{k u_* z} dz \quad .$$

Although the reaction order is most likely to be 1, closed-form solutions can be found for the cases of $a = 1, 2$, and 3 ,

$$F = \begin{cases} \frac{\bar{c}}{I + \frac{1}{\gamma}} & a = 1 \\ -\frac{\frac{1}{\sqrt{\gamma}} + \left(\frac{1}{\gamma} + 4I\bar{c}\right)^{1/2}}{2I} & a = 2 \\ (A_+ + A_-)^3 & a = 3 \end{cases} \quad (34)$$

where

$$A_{\pm} = 3 \left\{ \frac{\bar{c}}{I} \pm \left[\left(\frac{\bar{c}}{2I} \right)^2 + \frac{1}{27\gamma I^3} \right]^{1/2} \right\}^{1/2} .$$

It is interesting to note that these formulas reduce to that of Chamberlain (1966) or Galbally (1974) for the special case of (1) a first-order surface reaction and (2) a neutrally stratified atmosphere.

VII SENSITIVITY OF THE REGIONAL AIR POLLUTION MODEL

In the process of model development, the study of the sensitivity of the model plays a vital role. Through systematic variation of input parameters within the range of physical reality, the sensitivity study serves as a vehicle for examining the responses of the model under controlled but realistic conditions. The purpose of carrying out such a study is to assess the relative importance of various physical parameters to the predictions of the model.

In order to test the sensitivity of the regional air pollution model developed in this study, we selected as a base case four typical days in Spring (as represented by the meteorological patterns of 4 April 1976 through 7 April 1976) with emissions projected for the year 1986. A detailed description of the meteorological and emissions data associated with this case can be found in Part B of this report. After the base case was chosen, parameters in the base case were varied one at a time and the regional air pollution model was exercised. The parameters studied in this project include:

- > Horizontal eddy diffusivity
- > Mixing depth
- > Prescription of dry-deposition algorithms
- > Surface reaction rate
- > SO₂/sulfate conversion rate.

A discussion of the sensitivity of model predictions to each of these parameters follows.

A. HORIZONTAL EDDY DIFFUSIVITY

Horizontal spreading of the plume by turbulent diffusion in the atmosphere is expected to play an important role in long-range transport of contaminants. Dispersion of air pollutants at the mesoscale depends upon a number of variables. For example, Kao and Henderson (1970) investigated the relative diffusion of particles in six different synoptic-scale flow configurations. It is, however, well known that for pollutants released at lower levels the plume spread is a function of travelling time. As shown in Figure 7, the range of equivalent horizontal diffusivities pertinent to the temporal and spatial scales of interest to the present study is

$$10^5 \text{ m}^2/\text{sec} > K_H > 10^3 \text{ m}^2/\text{sec} \quad (35)$$

with a median value of $10^4 \text{ m}^2/\text{sec}$, a number used in the base case.

To test the effect of horizontal diffusivity on air quality predictions, we lowered the base case value of $10^4 \text{ m}^2/\text{sec}$ to $10^3 \text{ m}^2/\text{sec}$. The results of the base case simulation are shown in Figure 8* for the morning hours (2:00-5:00) and afternoon hours (14:00-17:00) on the fourth day of the base case, 7 April 1976. The corresponding results of the simulation with the reduced diffusivity are shown in Figure 9. A comparison of these figures shows that, as expected, the maximum concentrations and the impact areas are significantly larger for the lower diffusivity. It is clear that this is one of the most important parameters in the determination of concentrations at long distances. Unfortunately, it is also one of the most uncertain ones. Thus a separate effort will be made to search for a better way to prescribe this parameter.

* In these figures isopleths are drawn for concentrations of 2^n , where $n = 0, 1, 2, \dots$

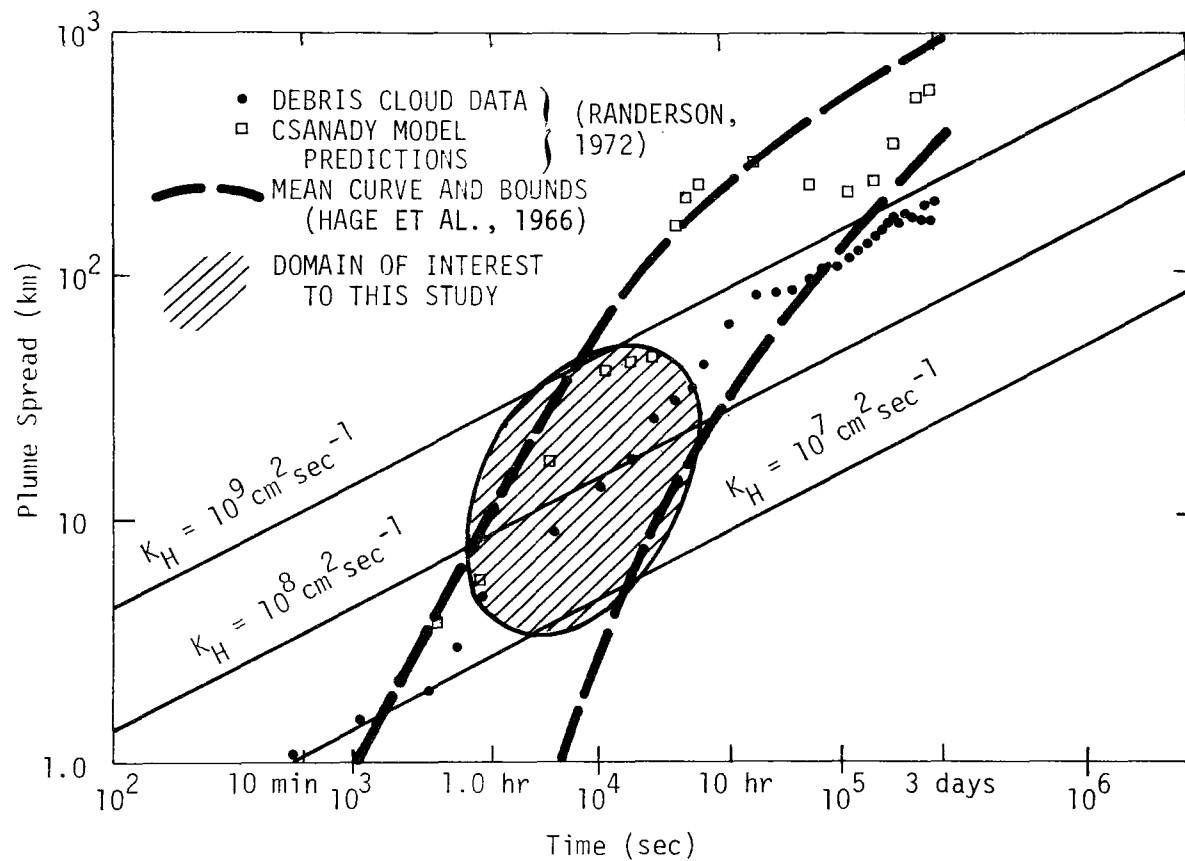
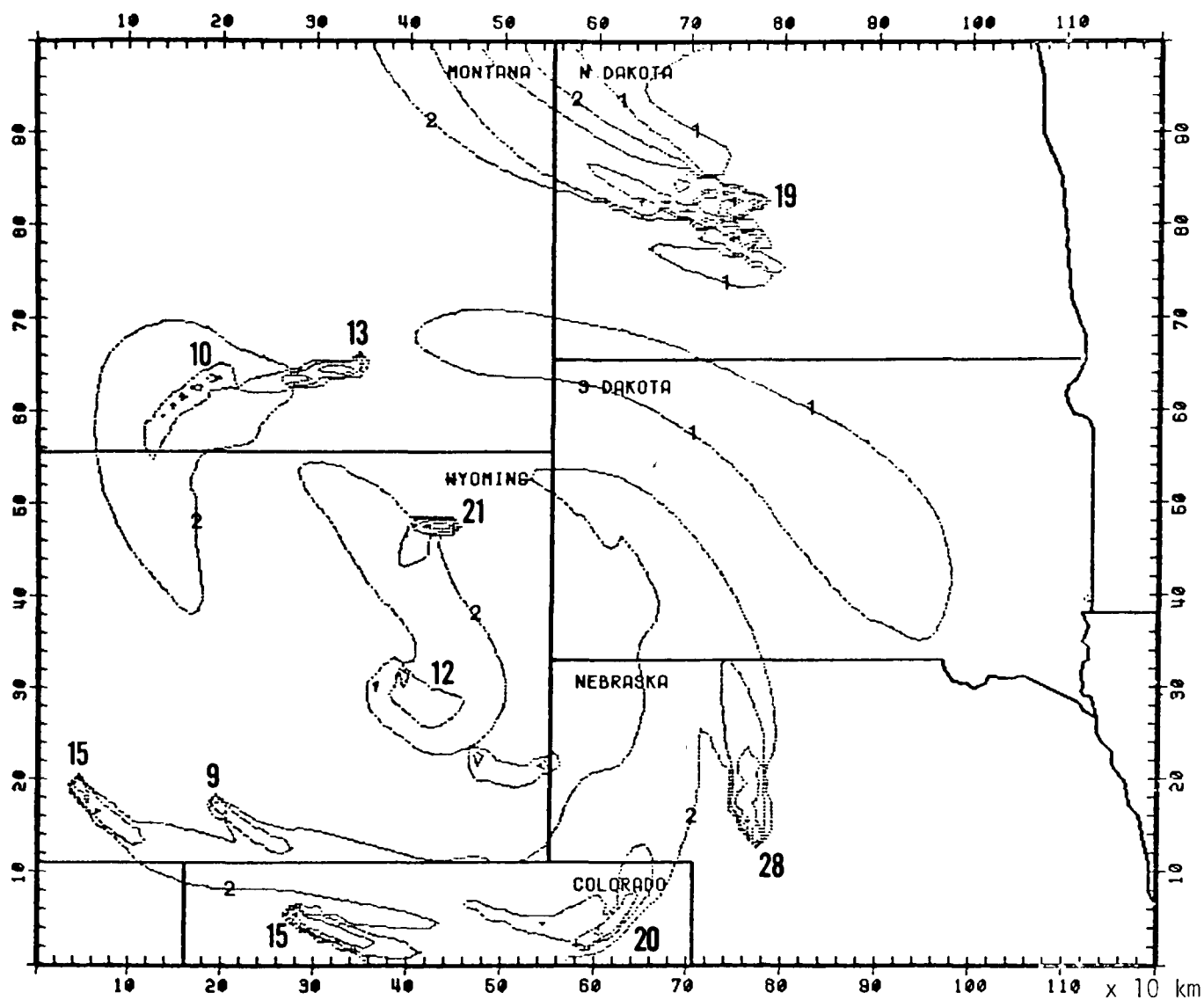


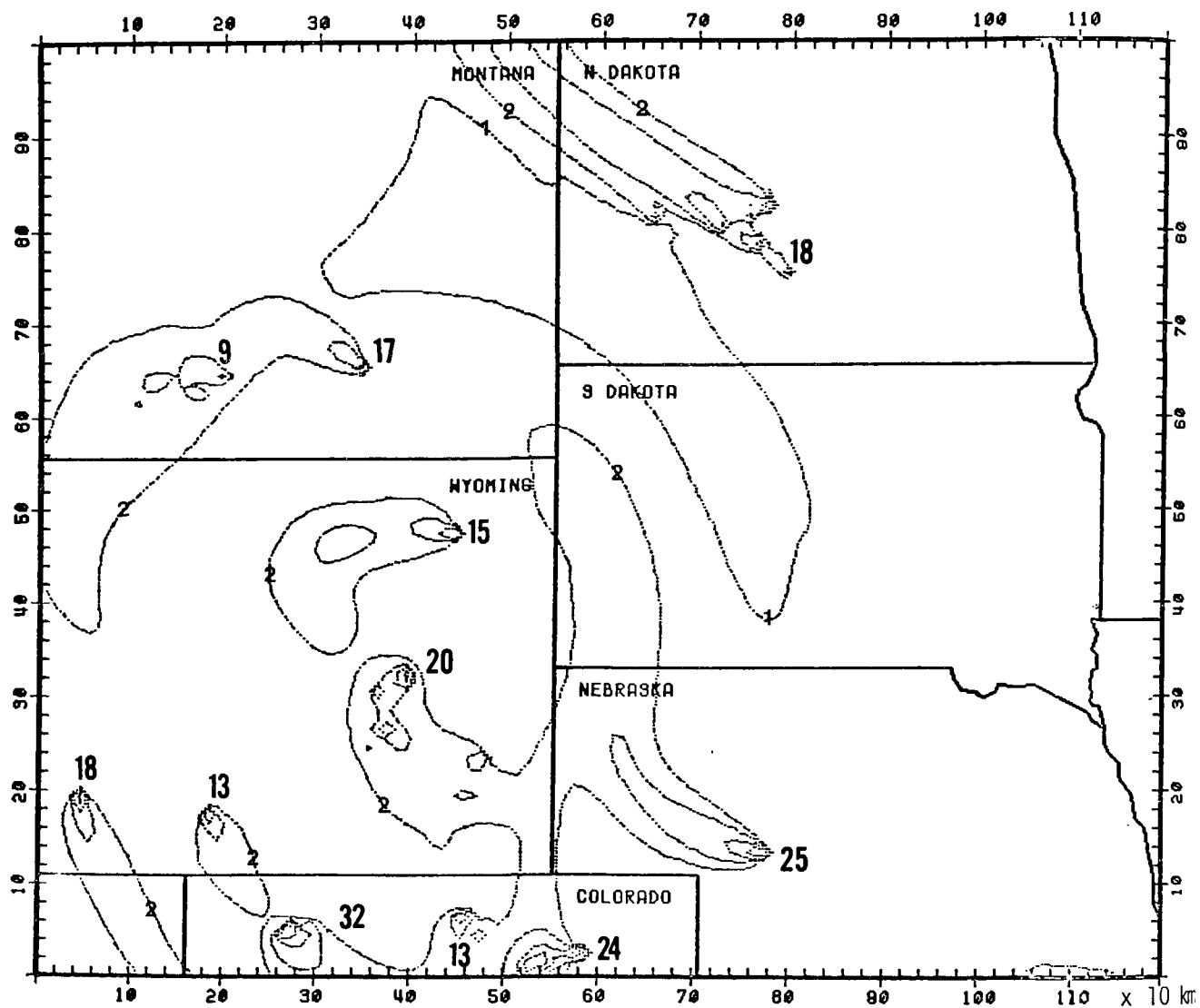
FIGURE 7. HORIZONTAL EDDY DIFFUSIVITY AS A FUNCTION OF TRAVELING TIME AND PLUME SPREAD



(a) 200-500 MST 7 April 1976

(1986 emissions)

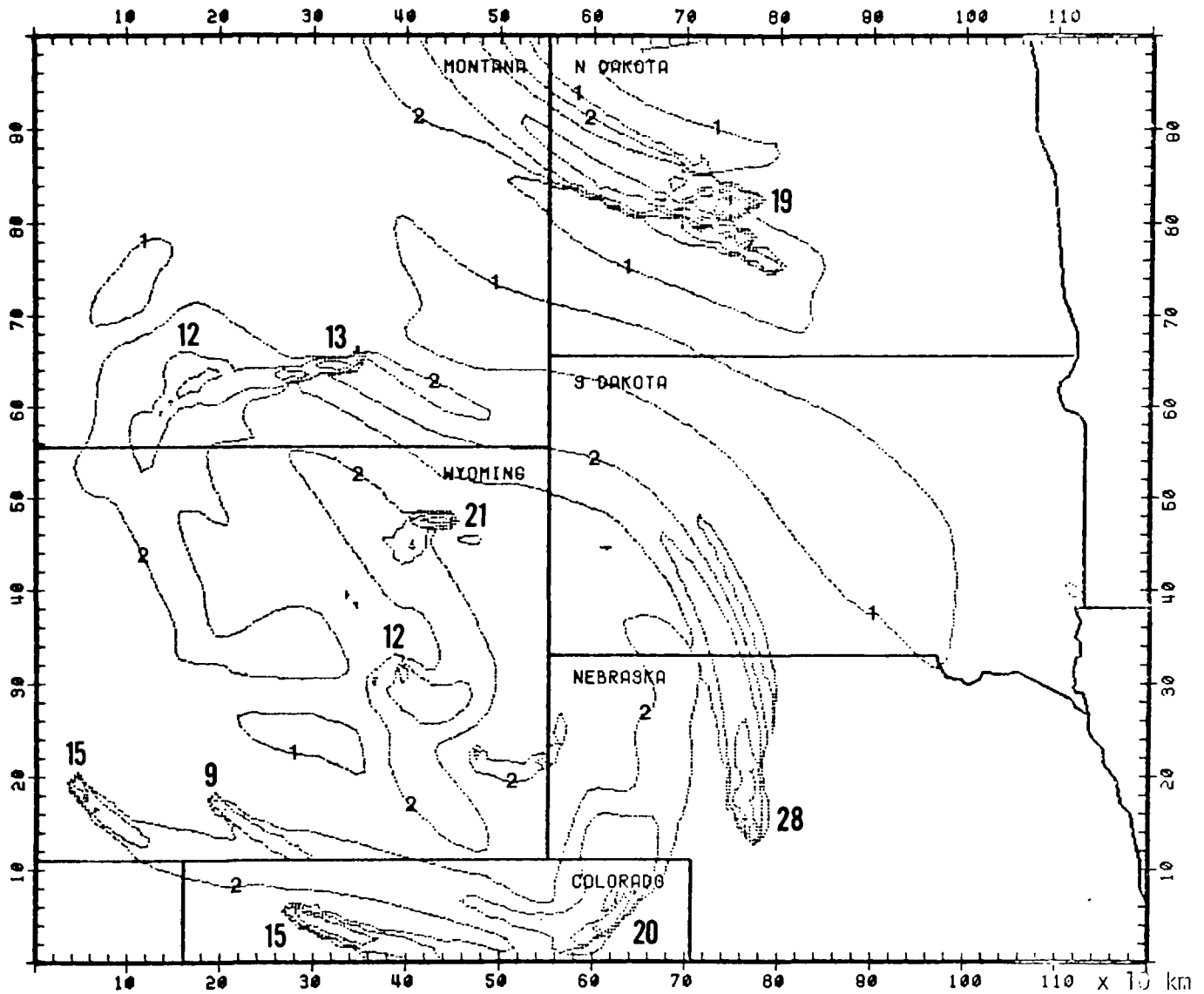
FIGURE 8. PREDICTED SO₂ CONCENTRATIONS FOR THE BASE CASE. Isopleths at 1, 2, 4, ..., $\mu\text{g}/\text{m}^3$; plume maxima in boldface.



(b) 1400-1700 MST 7 April 1976

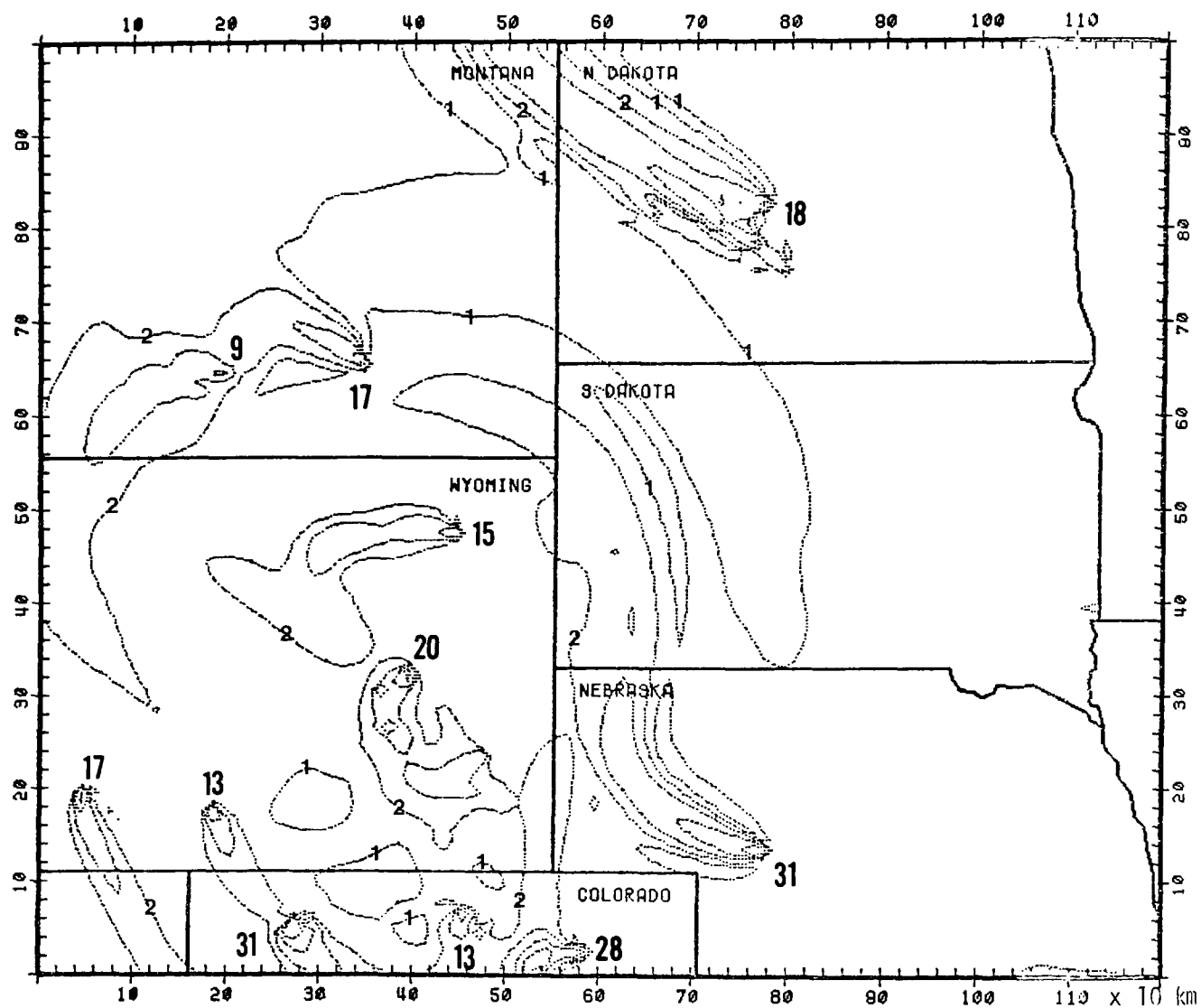
(1986 emissions)

FIGURE 8 (Concluded)



(a) 200-500 MST 7 April 1976;
 $K_H = 10^3 \text{ m}^2/\text{sec}.$

FIGURE 9. PREDICTED SO_2 CONCENTRATIONS FOR REDUCED HORIZONTAL DIFFUSIVITY. Isopleths at 1, 2, 4, ..., $\mu\text{g}/\text{m}^3$; plume maxima in boldface.



(b) 1400-1700 MST 7 April 1976;
 $K_H = 10^3 \text{ m}^2/\text{sec.}$

FIGURE 9 (Concluded)

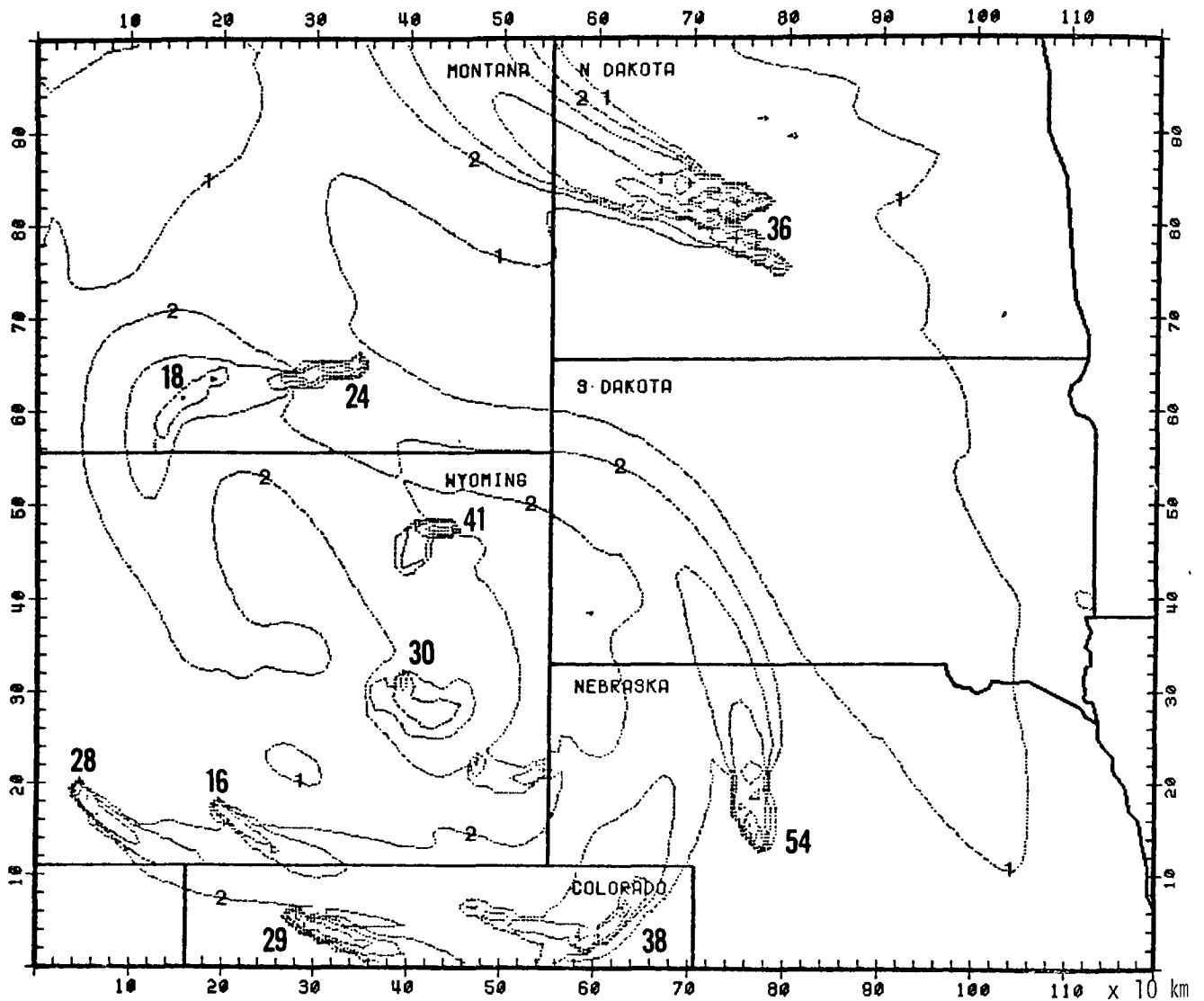
B. MIXING DEPTH

Vertical ventilation of air pollutants is restricted within the mixing layer, the top of which is generally defined by the base of inversion. As discussed in Part B, in the application of the regional air pollution model to the Northern Great Plains, the seasonal average mixing depths in the afternoon as estimated by Holzworth (1972) were used. For the base case, the afternoon mixing depth (for spring) varies from 1,500 meters to 2,800 meters in this region. These estimates are comparable with those measured in northern Europe (Georgii, 1970; Rodhe, 1971). In order to examine the effect of the mixing depth on predicted concentrations, the base case values were uniformly decreased by a factor of two. The results for the two three-hour periods are presented in Figure 10. It can be seen from a comparison with the base case results (Figures 8a and 8b) that the concentrations increase appreciably for lower mixing depths, particularly during the afternoon.

C. PRESCRIPTION OF DRY DEPOSITION

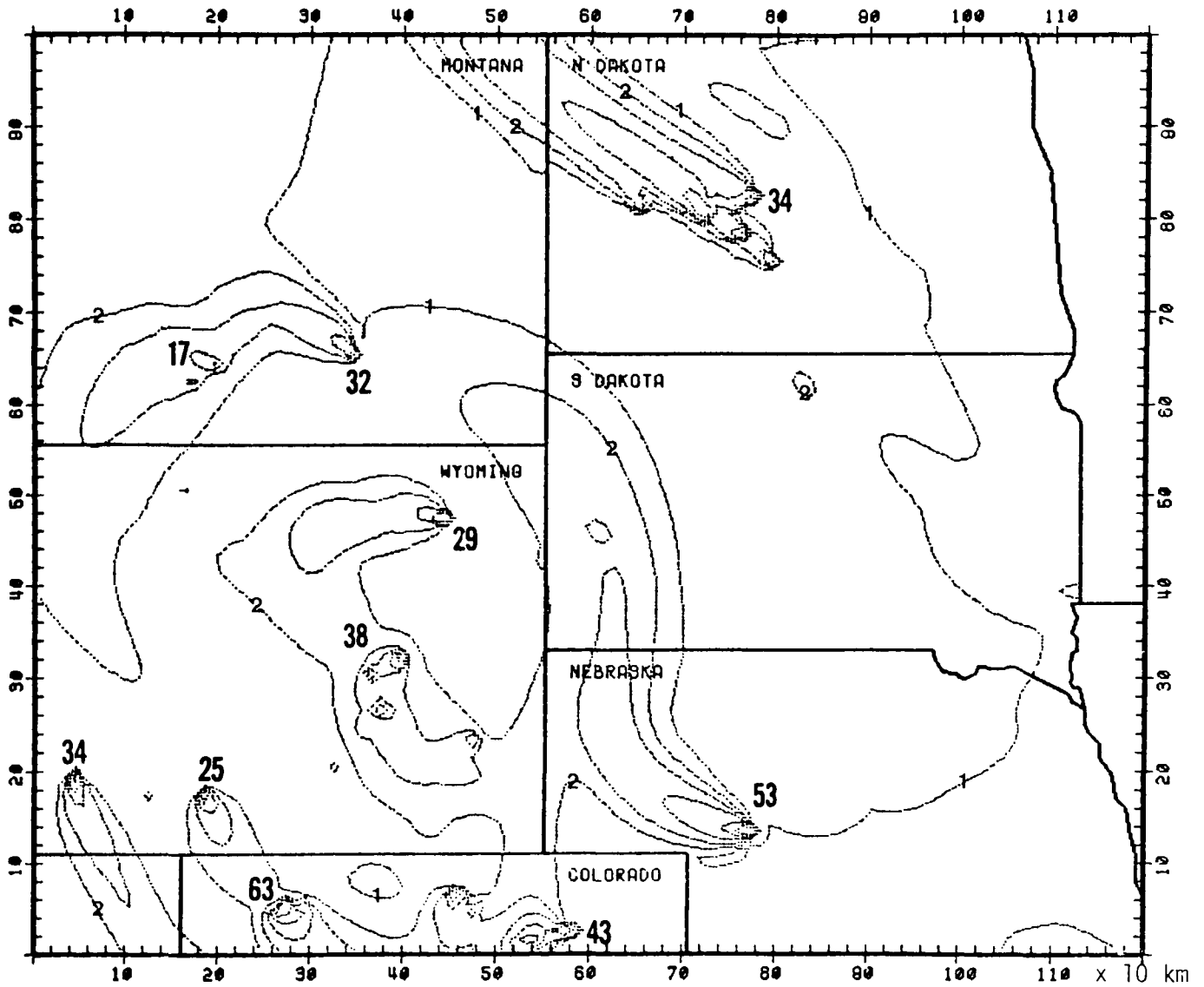
As discussed in the previous chapter, two prescriptions--one proposed by Owen and Thompson (1963), one by Thom (1972)--are available for prescribing the β factor in the surface deposition model. The two algorithms have different functional forms for the dependent variables.

Figures 11 and 12 show the predicted deposition velocities for 1400-1700 MST 4 April 1976 and 200-500 MST 5 April 1976 calculated using β as prescribed by Owen/Thompson and by Thom. Davis et al. (1976) reported that the Black Hills in South Dakota are a strong sink for atmospheric pollutants; Thom's prescription of β appears to produce deposition patterns consistent with these measurements. On the other hand, Shepherd (1974) observed that the process of SO_2 deposition onto vegetation is often surface-limited; the deposition



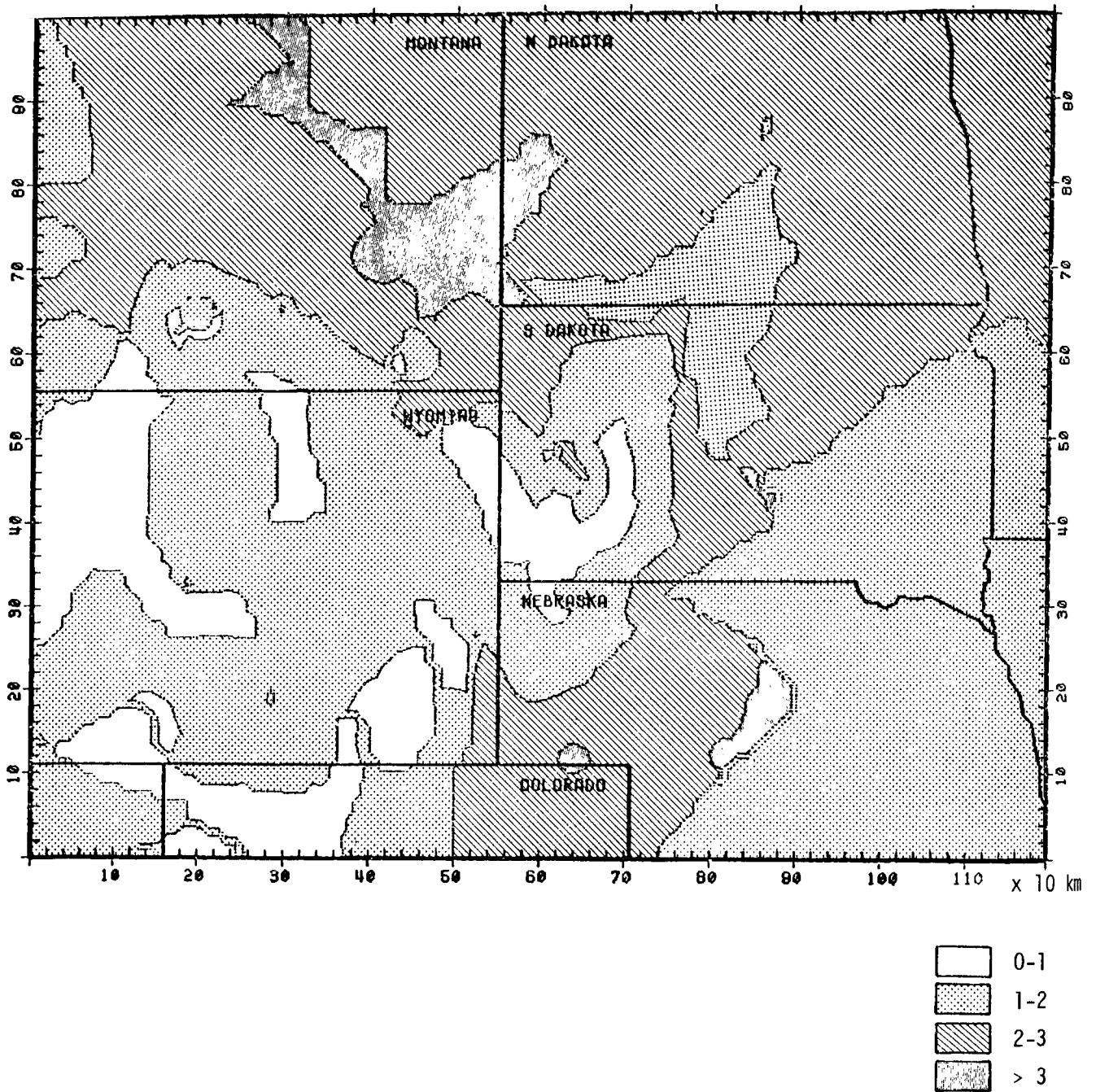
(a) 200-500 MST 7 April 1976; mixing depths
one-half of base case values

FIGURE 10. PREDICTED SO_2 CONCENTRATIONS FOR REDUCED MIXING DEPTHS.
Isopleths at 1, 2, 4, ..., $\mu\text{g}/\text{m}^3$; plume maxima in boldface.



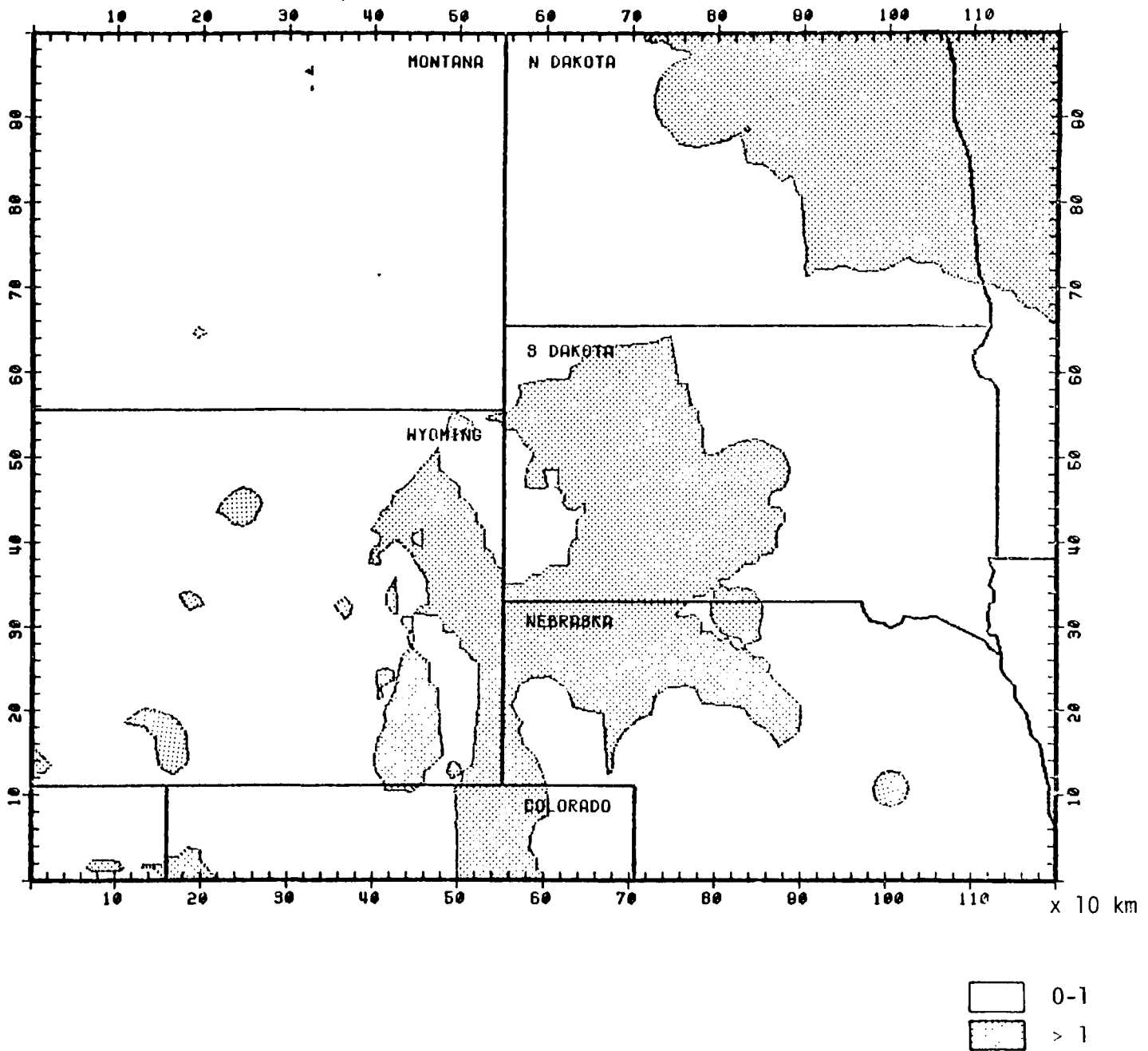
(b) 1400-1700 MST 7 April 1976; mixing depths
one-half of base case values

FIGURE 10 (Concluded)



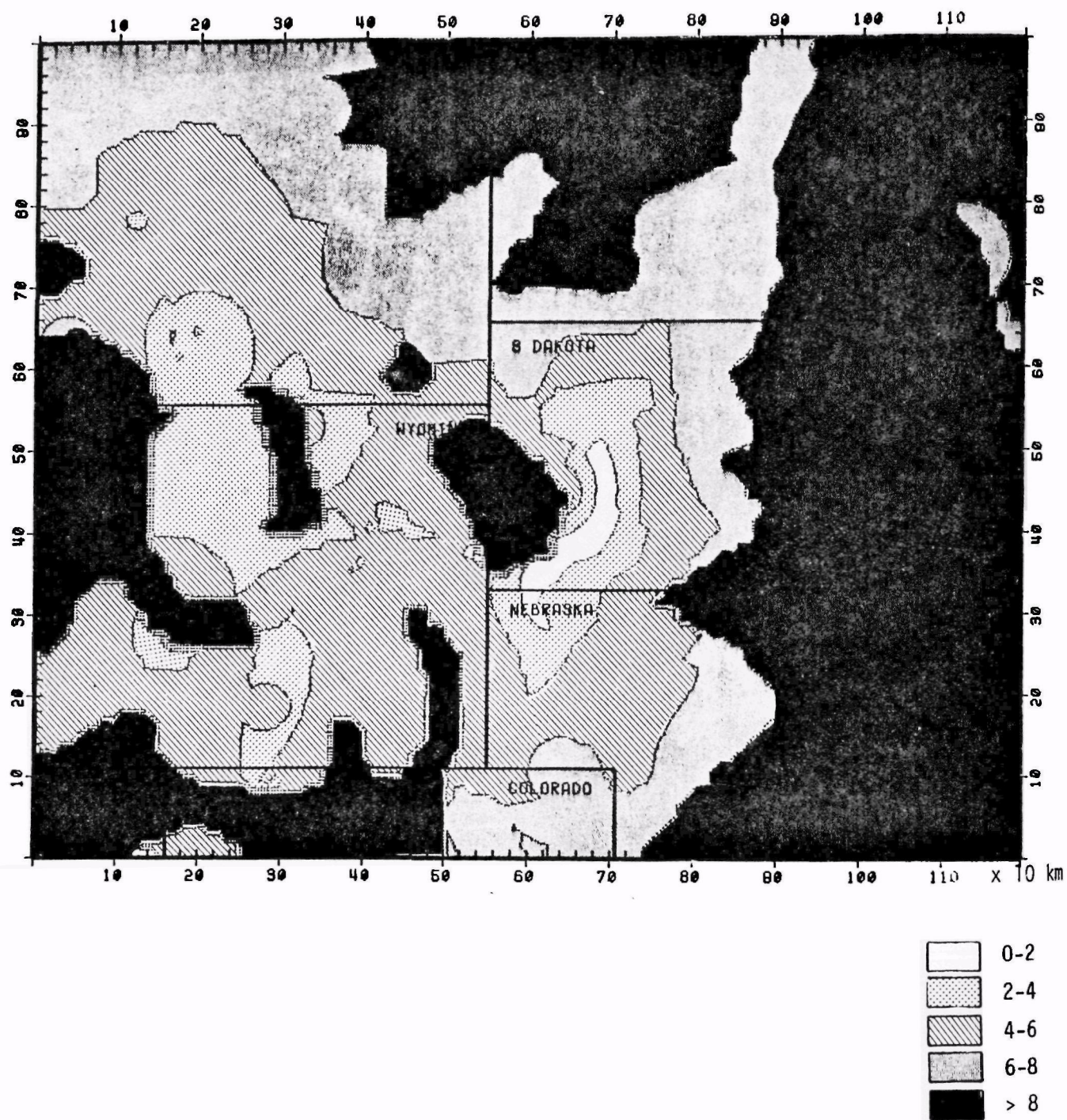
(a) 1400-1700 MST 4 April 1976

FIGURE 11. SO₂ DEPOSITION VELOCITIES (IN mm/sec) CALCULATED WITH β AS PRESCRIBED BY THE ALGORITHM OF OWEN AND THOMPSON



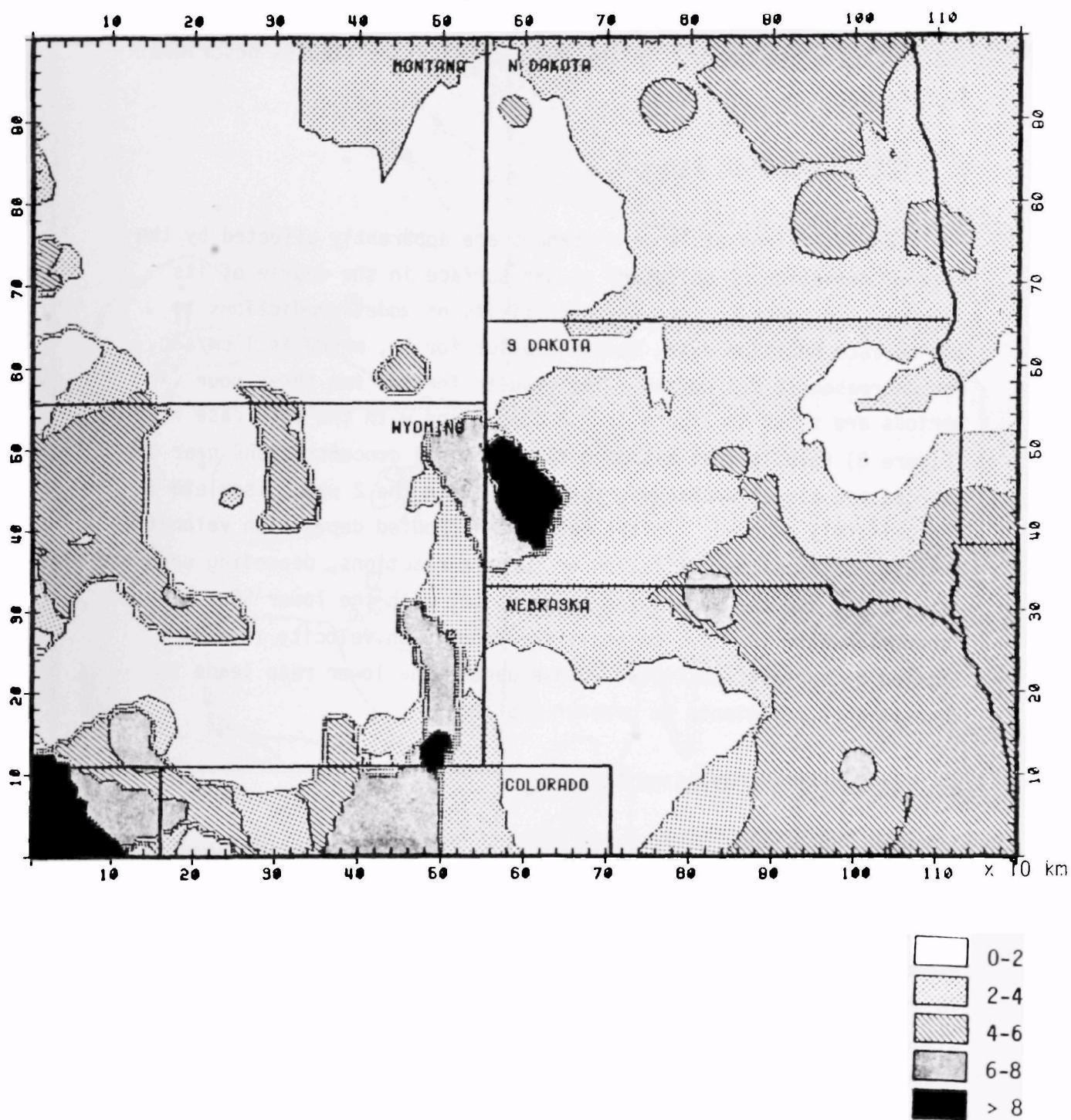
(b) 200-500 MST 5 April 1976

FIGURE 11 (Concluded)



(a) 1400-1700 MST 4 April 1976

FIGURE 12. SO₂ DEPOSITION VELOCITIES (IN mm/sec) CALCULATED WITH β AS PRESCRIBED BY THE ALGORITHM OF THOM



(b) 200-500 MST 5 April 1976

FIGURE 12 (Concluded)

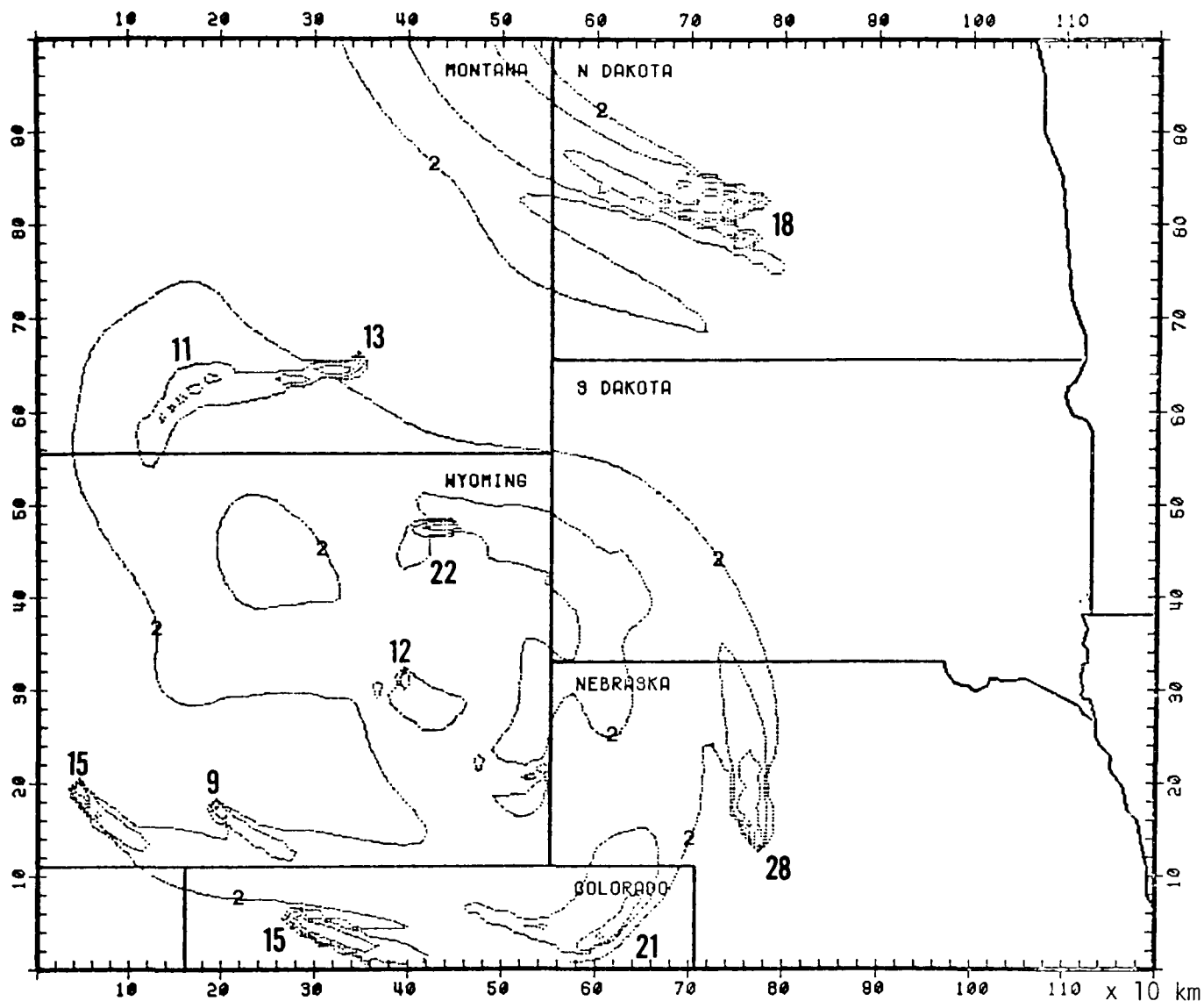
velocities generated by Thom's algorithm for prescribing β also seem to duplicate such behavior. Thus Thom's formulation was selected for the base case and for use in the model application studies described in Part B.

D. SURFACE REACTION RATE

Concentrations at large distances are apparently affected by the rate of depletion of pollutant at the surface in the course of its journey. In order to test the sensitivity of model predictions to the surface reaction rate, the base value for k_s , which is 1 cm/sec, was decreased to 0.1 cm/sec. The results for the two three-hour periods are shown in Figure 13. A comparison with the base case results (Figure 8) reveals that although the predicted concentrations near the sources are almost unchanged, the area within the $2 \mu\text{g}/\text{m}^3$ isopleth is approximately doubled. In the base case computed deposition velocities are limited by either diffusion or surface reactions, depending upon the time of day and the underlying terrain, but with the lower SO_2 /sulfate conversion rate ($R = 0.1$ cm/sec), the deposition velocity is always limited by surface reactions. Consequently the lower rate leads to transport of pollutants to greater distances.

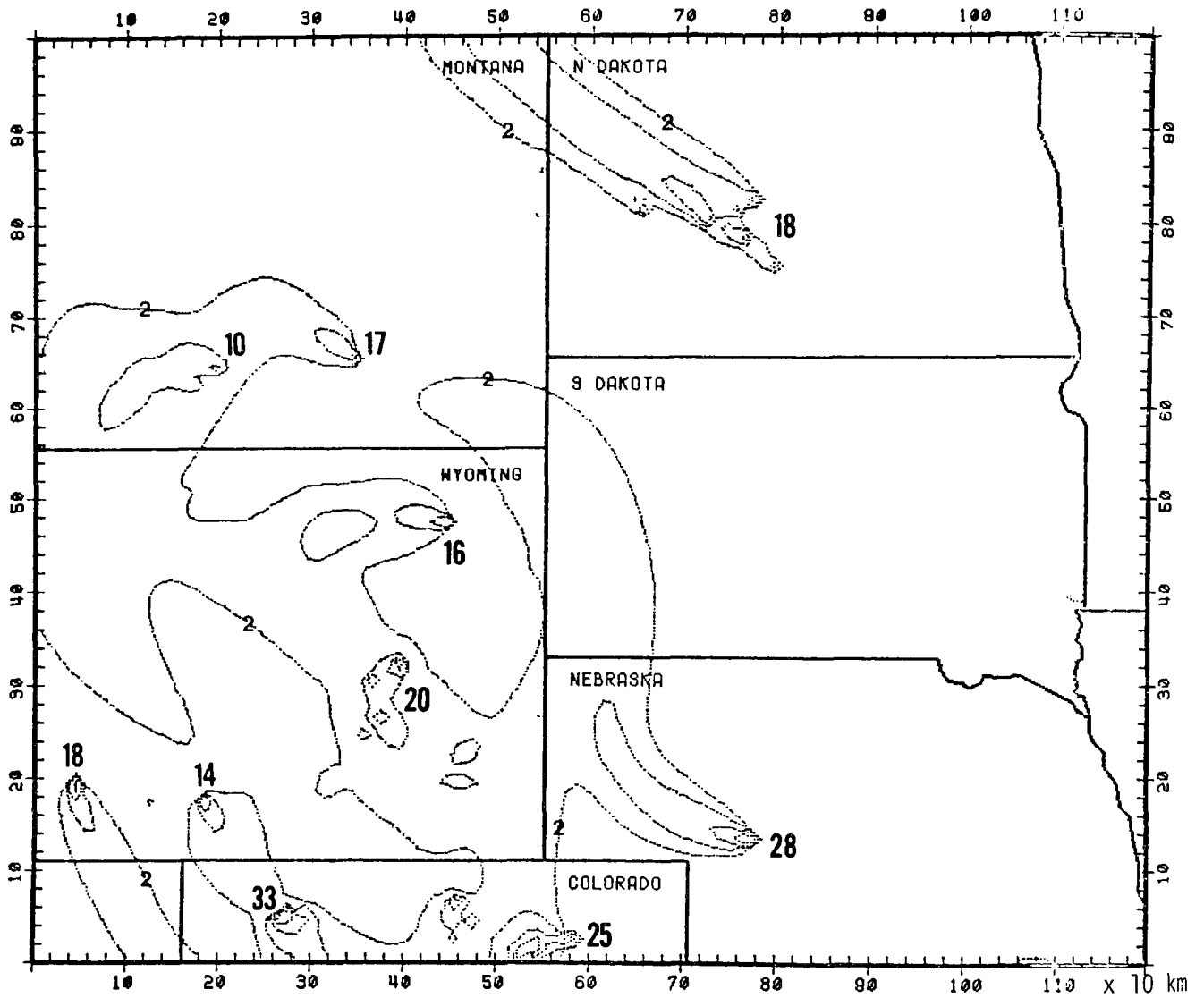
E. SO_2 /SULFATE CONVERSION RATE

It was stated earlier that one of the major concerns in the development of the present regional-scale model is the ability to predict sulfate distributions, because of the variety of problems apparently associated with high atmospheric sulfate concentrations. Reduction in visibility and increase of acid rain are only two examples. As discussed in Chapter V, the rate of conversion of gaseous SO_2 to sulfate depends upon a number of physical and chemical parameters. Humidity and the presence of other reactive pollutants are probably among the most influential ones. The SO_2 /sulfate conversion rate has been reported to be as low as 0.1 percent per hour and as high as 10 percent per hour. For a largely undeveloped area with relatively



(a) 200-500 MST 7 April 1976; surface reaction rate = 0.1 cm/sec

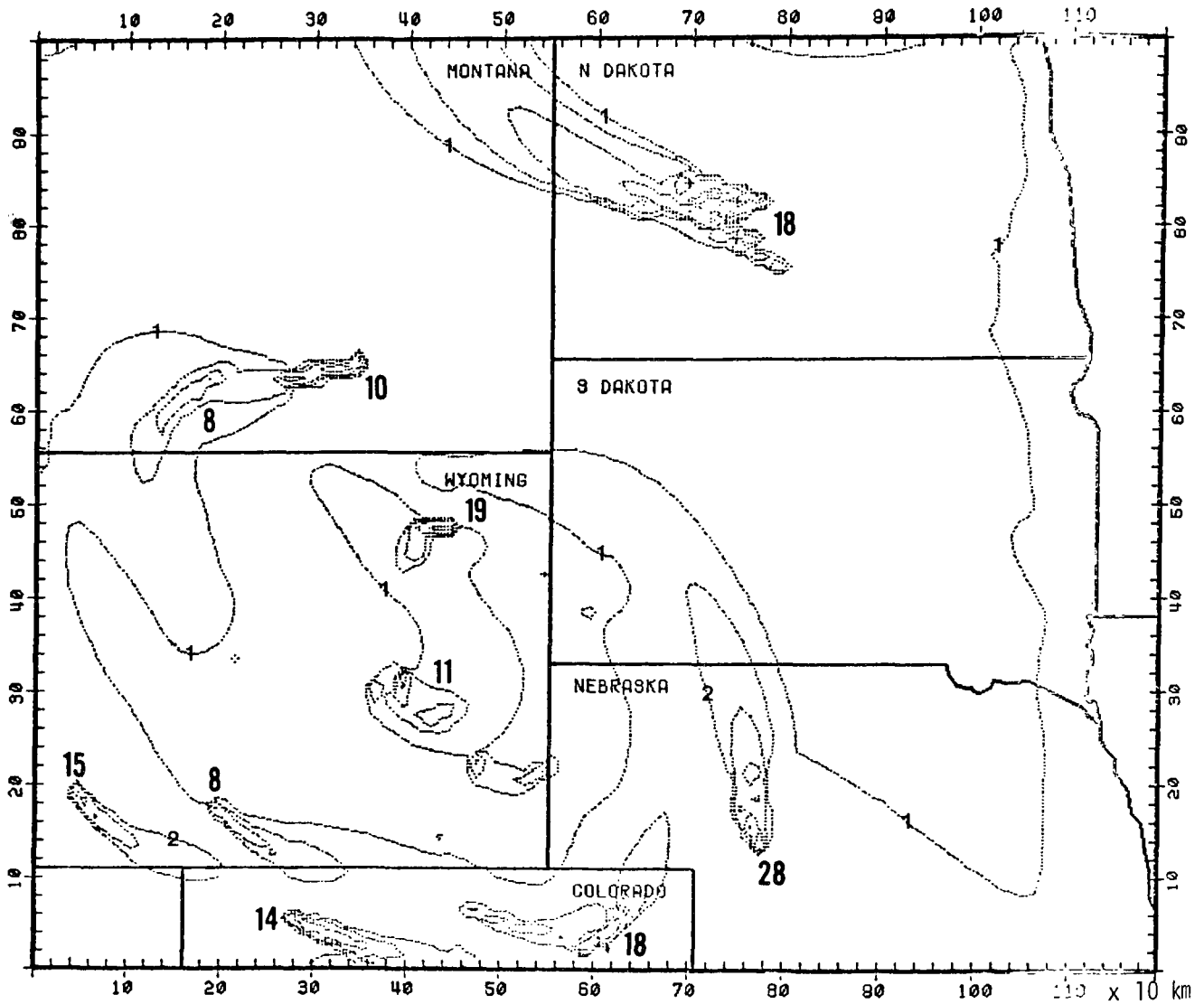
FIGURE 13. PREDICTED SO₂ CONCENTRATIONS FOR REDUCED SURFACE REACTION RATE. Isopleths at 1, 2, 4, ..., $\mu\text{g}/\text{m}^3$; plume maxima in boldface.



(b) 1400-1700 MST 7 April 1976; surface
reaction rate = 0.1 cm/sec

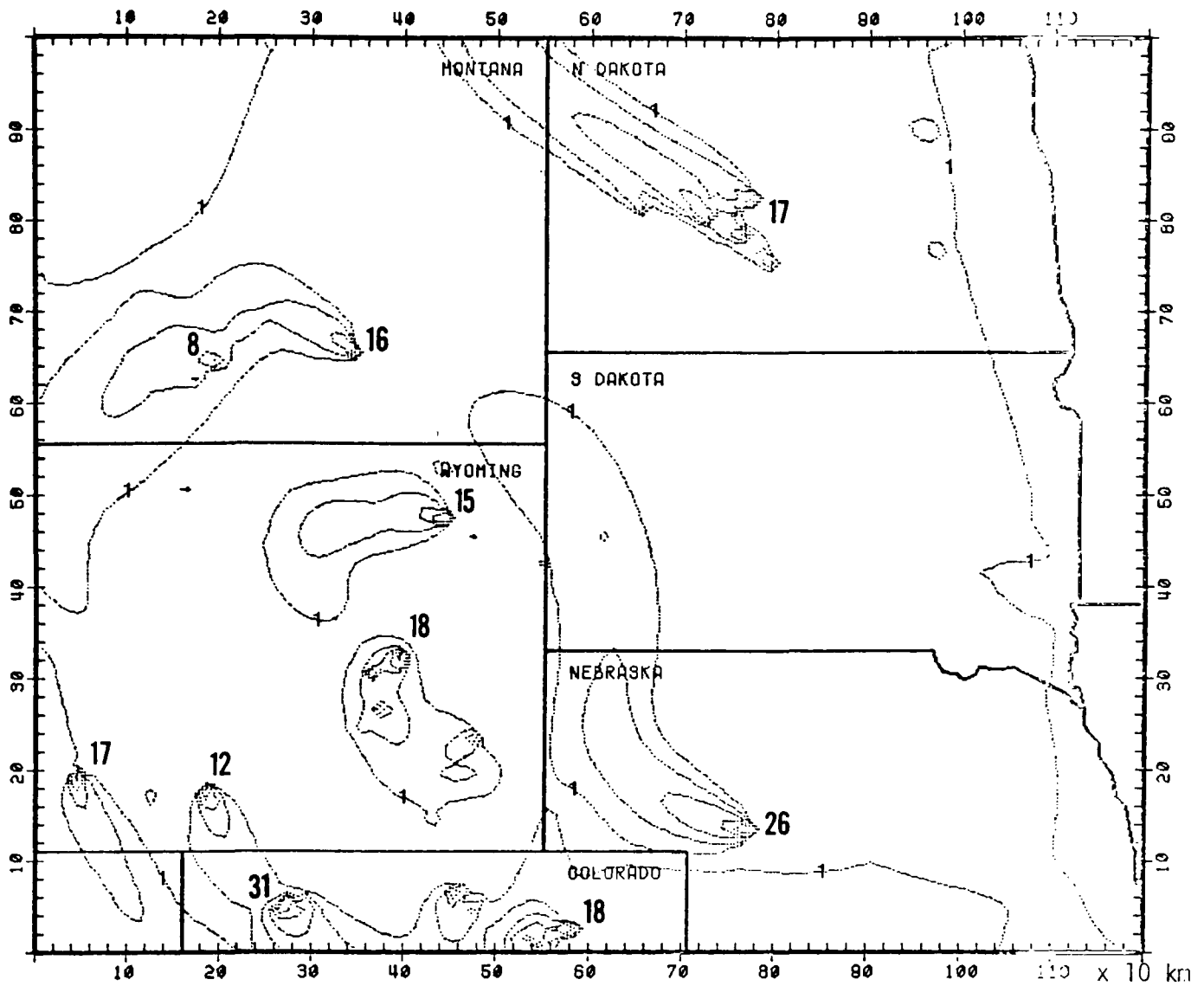
FIGURE 13 (Concluded)

clean air and generally low relative humidity, such as the Northern Great Plains, only a low conversion rate can be justified. Thus a conversion rate of 0.3 percent per hour was selected for the base case. The predicted sulfate concentrations were extremely low and are shown in Figure 14. In the sensitivity study, a higher value of 3 percent per hour was used. The calculated SO_2 and sulfate concentrations are presented in Figures 14 and 15. It is interesting to note that the distributions of SO_2 and sulfate are entirely different. SO_2 is a source-oriented pollutant and SO_2 emanating from a number of major emission sources is clearly visible. As a product of chemical reactions, sulfate is not easily linked to identifiable sources. The maximum predicted sulfate concentration, using a 3 percent per hour conversion rate, is approximately 20 ug/m^3 . This level would exceed the 10 ug/m^3 limit which is being considered by EPA for the standard. Also, it has been shown that as little as $1\text{-}2 \text{ ug/m}^3$ SO_4 concentration will reduce visibility significantly.



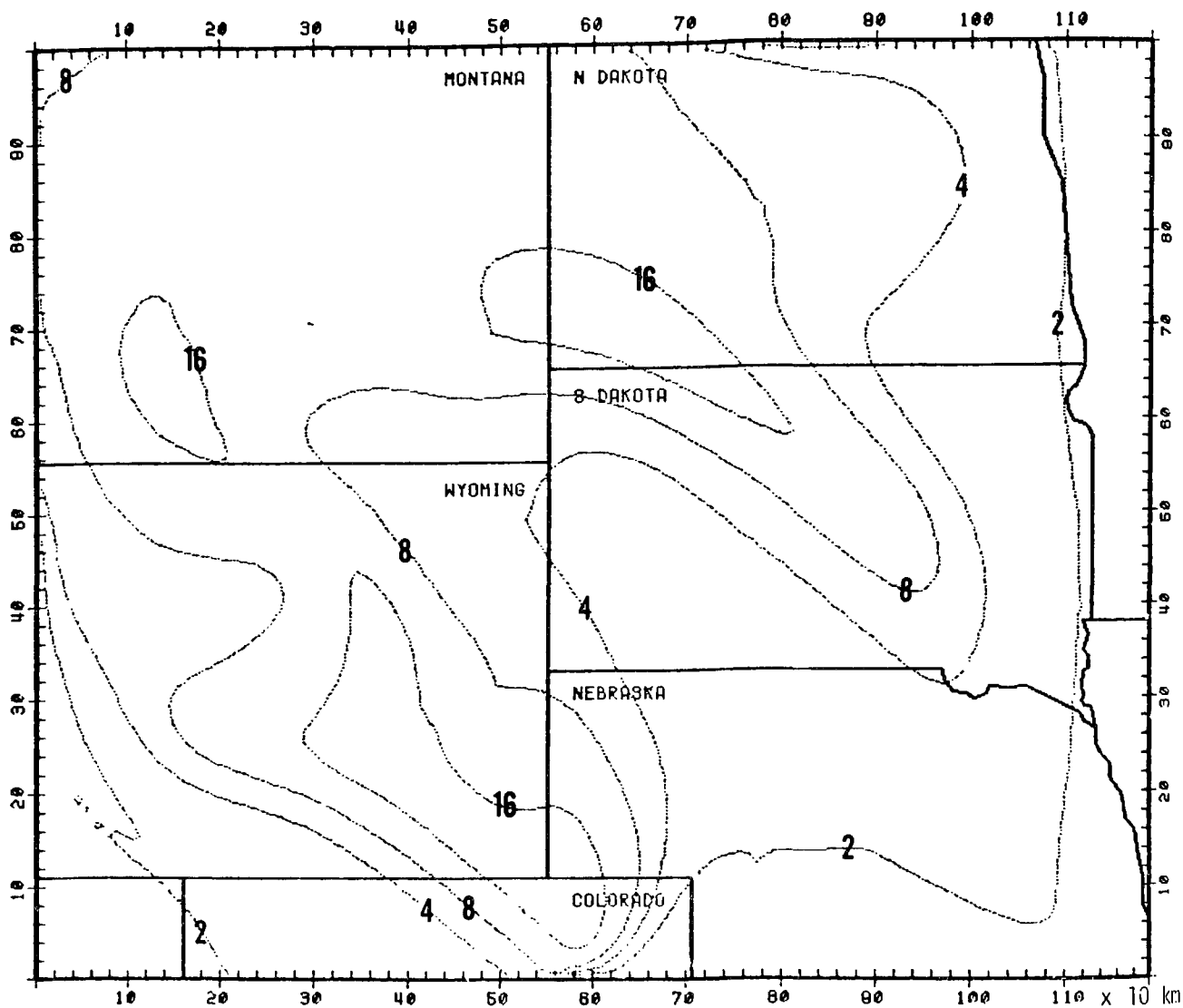
(a) 200-500 MST 7 April 1976; SO_2 /sulfate conversion rate = 3 percent per hour

FIGURE 14. PREDICTED SO_2 CONCENTRATIONS FOR INCREASED SO_2 /SULFATE CONVERSION RATE. Isopleths at 1, 2, 4, ..., $\mu\text{g}/\text{m}^3$; plume maxima in boldface.



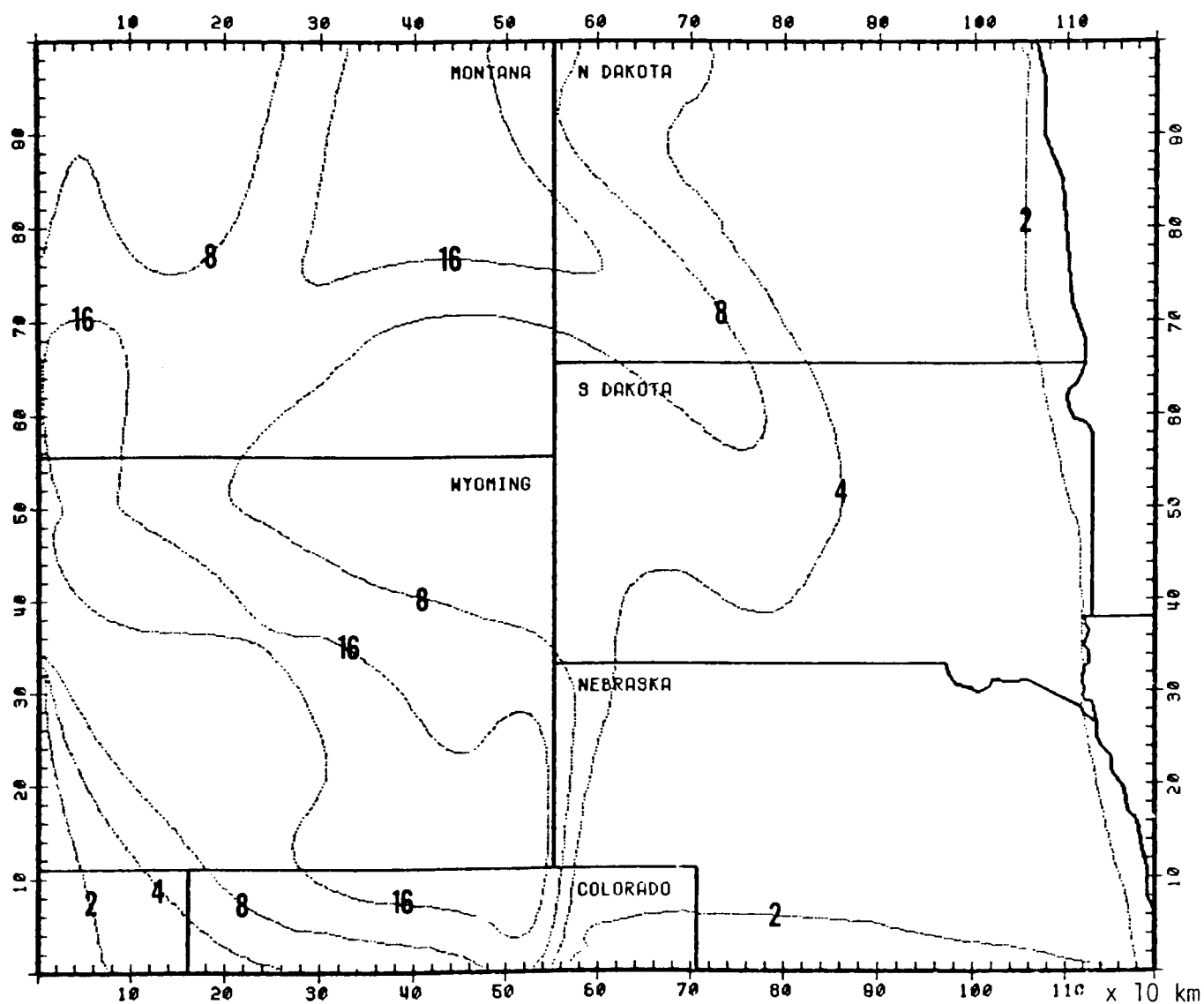
(b) 1400-1700 MST 7 April 1976; SO₂/sulfate conversion rate = 3 percent per hour.

FIGURE 14 (Concluded)



(a) 200-500 MST 7 April 1976; SO_2 /sulfate conversion rate = 3 percent per hour

FIGURE 15. PREDICTED SULFATE CONCENTRATIONS FOR INCREASED SO_2 /SULFATE CONVERSION RATE. Isopleths at 2, 4, 8, ... $\mu\text{g}/\text{m}^3$.



(b) 1400-1700 MST 7 April 1976; SO_2 /sulfate
conversion rate = 3 percent per hour

FIGURE 15 (Concluded)

VIII SUMMARY AND CONCLUSIONS FOR PART A

Part A contains a review of previous studies pertinent to the transport of air pollutants over large distances (ca. 100 to 1000 km), followed by a delineation of the major attributes governing the distribution of atmospheric pollutants on this scale. The development of a regional air pollution model accommodating these major attributes is then described. This model is primarily intended for the prediction of pollutant concentrations averaged over areas of approximately 100 km² with a temporal resolution on the order of 3 hours. Two unique features of this model are the assumption of homogeneous pollutant distributions in the vertical and the incorporation of a model of diurnally varying surface deposition. This model was thoroughly tested via sensitivity analysis. The responses of the model are consistent with expectations based on physical reasoning.

PART B

APPLICATION OF A REGIONAL AIR POLLUTION MODEL
TO THE COAL DEVELOPMENT AREAS
IN THE NORTHERN GREAT PLAINS

IX OVERVIEW

The Northern Great Plains currently enjoys some of the cleanest air and possesses some of the richest coal deposits in the United States. The U.S. energy program includes mining this coal and using it for electric power generation or synthetic fuel production. Such activities are certain to adversely affect air quality in the Northern Great Plains. In Part B of this report we examine this impact by applying the regional air pollution model discussed in Part A.

Figure 16 shows the locations of proposed energy conversion plants scheduled for completion before 1986. These plants are scattered over a large area containing many types of terrain. A few are located in the Rocky Mountains, where pollutant dispersion modeling would be more difficult, but fortunately most of the facilities of interest to the present study lie in the plains of Montana, Wyoming, Colorado, and North Dakota.

In Part A of this report, the development of a regional air pollution model was described. This model is composed of two interconnected sub-models, a mixing layer model and a surface layer model. The mixing layer model is designed to treat the transport, diffusion, and chemical reactions of pollutants by numerically solving the two-dimensional atmospheric diffusion equation

$$\begin{aligned} \frac{\partial c_i}{\partial t} + u \frac{\partial c_i}{\partial x} + v \frac{\partial c_i}{\partial y} = \frac{\partial}{\partial x} \left(K_H \frac{\partial c_i}{\partial x} \right) + \frac{\partial}{\partial y} \left(K_H \frac{\partial c_i}{\partial y} \right) \\ + R_i + S_i - (c_i - c) \cdot D \cdot \zeta(D) \end{aligned}$$

$i = 1, 2 \quad .$

(36)

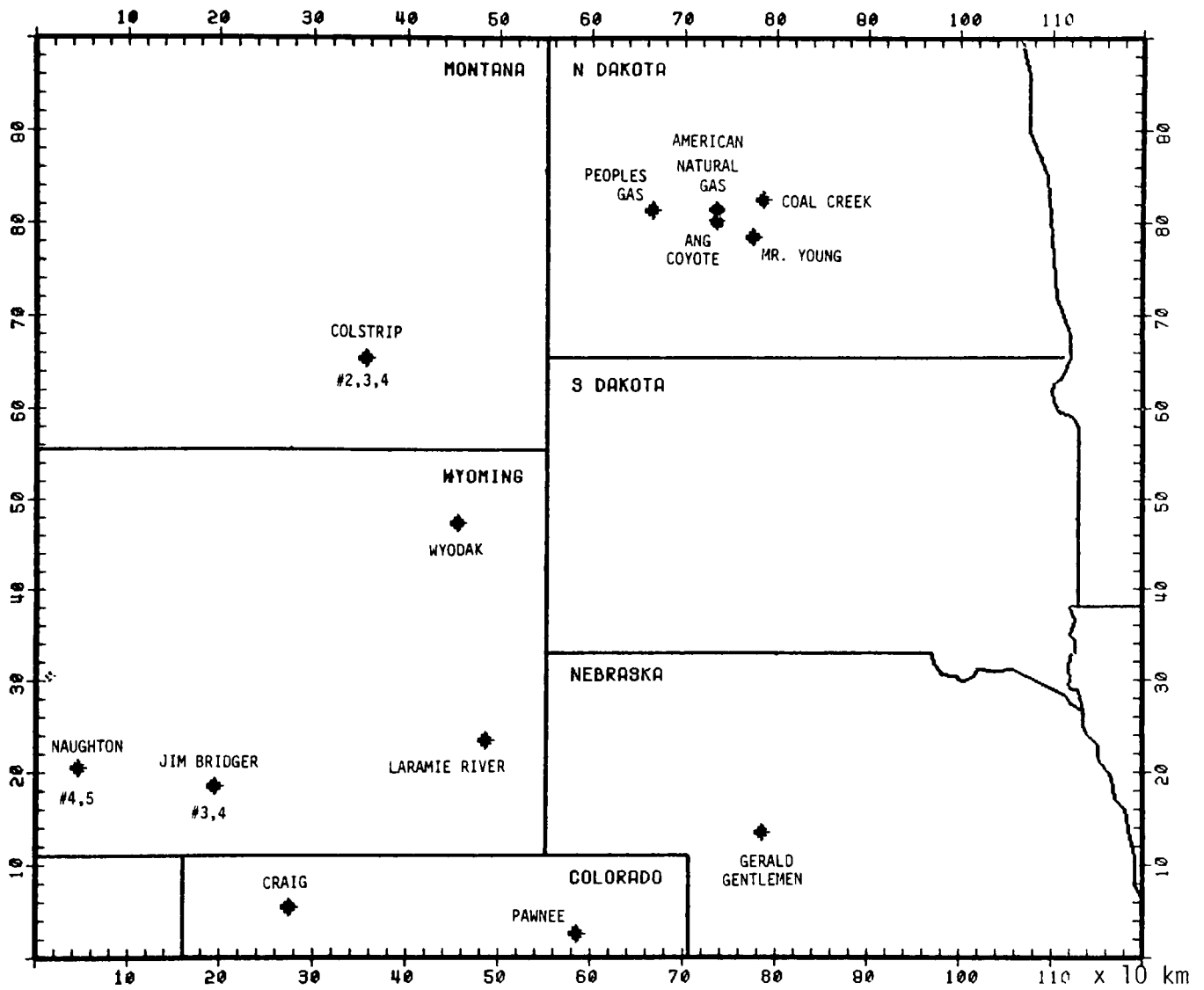


FIGURE 16. ENERGY CONVERSION FACILITIES SCHEDULED FOR COMPLETION BEFORE 1936

For this study $i = 1$ for SO_2 and $i = 2$ for sulfate, although the modeling approach can be extended to handle more complex chemistry.

The surface layer model, which is embedded in the mixing layer model, is designed to calculate the pollutant fluxes lost to the ground due to dry deposition. As shown in Part A of this report, for linear surface reaction the pollutant flux to the ground surface, or the surface removal rate, can be expressed as

$$F = c \left/ \left(\frac{1}{\beta u_*} + \int_{z_0}^h \frac{\phi(z)}{k u_* z} dz + \frac{1}{r_s} \right) \right. \quad (37)$$

where u_* is the friction velocity and $r_s \equiv 1/\gamma$ is the resistance to deposition at the ground surface. The surface removal rate generally varies linearly with concentration unless the concentration is so high that saturation effects take place (Hill, 1971). Measured values of r_s for deposition of SO_2 on grass appear in Table 14.

TABLE 14. SURFACE RESISTANCE MEASUREMENTS FOR SO_2

| Type of Surface | Surface Resistance (sec/m) | Reference |
|-------------------------|----------------------------------|-------------------------|
| Grass (3 cm)/summer | 80 | Shepherd (1974) |
| Grass (3 cm)/winter | 300 | Shepherd (1974) |
| Grass ($z_0 = 0.5$ cm) | 150 | Garland et al. (1974) |
| Grass (9-13 cm) | 75 | Owers and Powell (1974) |

As discussed in Part A, two different formulas, one by Owen and Thompson (1963) and one by Thom (1972), were examined for the prescription of β . A comparison of these formulas in the sensitivity analysis revealed that the formula proposed by Thom appears to yield more realistic results. As a result, this formula was adopted in this study.

In the next chapter (X), the compilation of emissions and meteorological data for the Northern Great Plains is described. The regional air pollution model was exercised for three different meteorological patterns and two emissions scenarios. Based upon these simulations, the impact of energy conversion plants on air quality is analyzed in Chapter XI. The application of the regional air pollution model to the Northern Great Plains is summarized in Chapter XII.

X COMPILATION OF THE DATA BASE

The application of the regional model requires extensive data, which can be divided into four general categories:

- > Emissions data
- > Meteorological data
- > Vegetation data
- > Air quality data.

Considerable effort was required to collect and analyze input data for the Northern Great Plains modeling exercise. This section is devoted to the discussion of this task.

A. EMISSIONS DATA

In the NGP 86 percent of the total SO_x emissions are attributable to point sources (EPA, 1976b). Future energy development should increase this figure, so only point source emissions were included in our model. The point source inventory was assembled by the EPA Region VIII office in Denver from the most recent complete base-year emissions data for each state, either 1973 or 1975. The emissions data were obtained from permit application data provided by plant engineers, or from data provided to an individual state by a hired contractor. Emissions estimates projected for future sources were drawn from the following: (1) "Existing and Proposed Fuel Conversion Facilities Summary" (EPA, 1976c), (2) Northern Great Plains Resource Program: Atmospheric Aspects Workgroup Report", (NGPRP, 1976), and (3) "FPC Form 67: Steam Electric Plant Air and Water Quality Control Data for the Year Ending December 31, 1975" (FPC, 1976).

Tables 15 and 16 and Figures 17 and 18 summarize the emissions data. The tables list point sources in the 1976 and 1986 inventories that emit

TABLE 15. POINT SOURCES EMITTING MORE THAN
10,000 TONS OF SO_x PER YEAR IN 1976

| <u>Source</u> | <u>MW</u> | <u>Grid Location</u> | <u>SO_x Emissions (tons/year)</u> | <u>% Control</u> |
|------------------------------|-----------|--------------------------|---|------------------|
| Dave Johnston, WY | 750 | (40,32) | 31,000 | 50% control #3 |
| Ideal Basic Industries CO | - | (46,7) | 25,800 | - |
| Naughton, WY | 710 | (4,20) | 21,700 | - |
| Exxon, MT | - | (20,64) | 17,300 | - |
| Milton R. Young, ND | 240 | (77,78) | 16,000 | - |
| Stanton, ND | 167 | (76,81) | 15,600 | - |
| Leland Olds, ND | 650 | (76,81) | 14,500 | - |
| Hayden, CO | 180 | (30,5) | 14,200 | - |

TABLE 16. POINT SOURCES EMITTING MORE THAN 10,000
TONS OF SO_x PER YEAR IN 1986

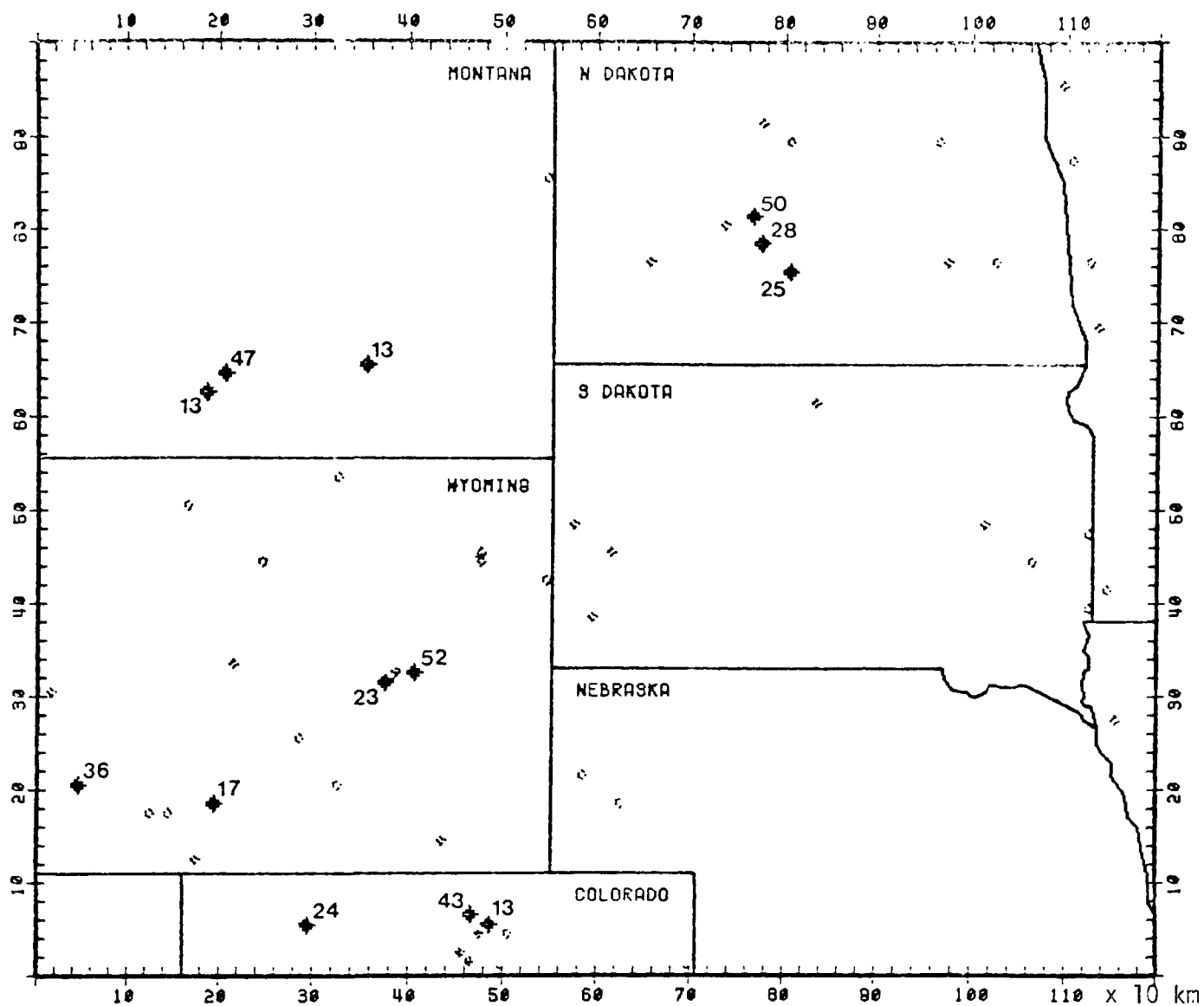
| Source | MW | Grid Location | SO _x Emissions (tons/year) | % Cont. |
|-------------------------------|-------------------|---------------|--|-----------------|
| Gerald Gentleman, NB | 1300 | (78,13) | 98,200 | NA |
| Craig, CO | 1520 | (28,6) | 87,900 | - |
| Naughton, WY | 1510 ¹ | (4,20) | 50,000 | - |
| Colstrip, MT | 2060 ² | (35,65) | 50,000 | 50 |
| Pawnee, CO | 1000 | (59,3) | 50,000 | - |
| Coal Creek, ND | 1000 | (78,82) | 42,500 | 38 |
| Wyodak, WY | 660 | (45,47) | 38,400 | - |
| ANG, ND Antelope Valley | 880 | (73,80) | 37,400 | - |
| Coyote, ND | 880 | (73,80) | 37,400 | 20 |
| Jim Bridger, WY | 2000 | (19,18) | 34,700 | 55 |
| Dave Johnston, WY | 750 | (40,32) | 31,000 | 50 ³ |
| Milton R. Young, ND | 688 | (77,78) | 31,000 | 40 ⁴ |
| Ideal Basic Industries, CO | - | (46,7) | 25,800 | NA |
| American Natural Gas, ND | - | (73,81) | 21,500 | NA |
| Peoples Gas, ND | - | (66,81) | 21,500 | NA |
| Exxon, MT | - | (20,64) | 17,300 | NA |
| Stanton, ND | 167 | (76,81) | 15,600 | - |
| Leland Olds, ND | 650 | (76,81) | 14,500 | - |
| Hayden, CO | 430 | (30,5) | 14,200 | - |
| Laramie River, WY | 1500 | (48,23) | 11,000 | 83% |

1 Unit 4 & 5 may not be built, equivalent units may be built in Utah

2 Units 3 & 4 (700 MW each) may not be constructed

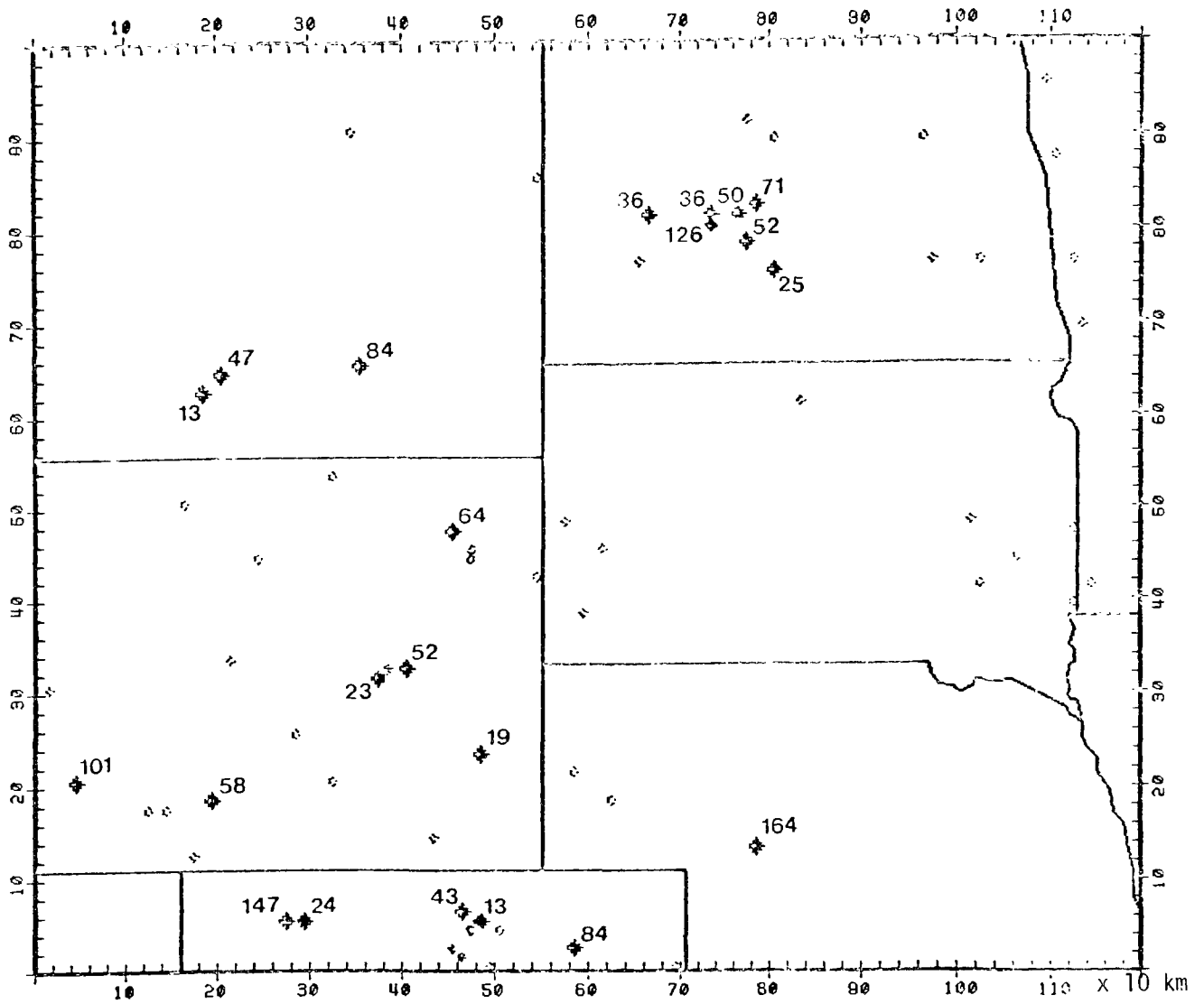
3 Control on Unit No. 4 only

4 Control on Unit No. 2 only



Source: EPA (1977).

FIGURE 17. POINT SOURCES IN THE NORTHERN GREAT PLAINS IN 1976. Numbers represent emissions in kg/min; small diamonds represent emissions of less than 10 kg/min or 6000 tons/year.



Source: EPA (1977).

FIGURE 18. POINT SOURCES IN THE NORTHERN GREAT PLAINS IN 1986. Numbers represent emissions in kg/min; small diamonds represent emissions of less than 10 kg/min or 6000 tons/year.

more than 10,000 tons of SO_x per year. The figures show the locations of all grid cells that contain sources in the 1976 and 1986 inventories. Cells where the sum of all point source emissions exceeds 6,000 tons per year are marked by dark diamonds and the strengths of emissions are noted. Of the total SO_x emitted by point sources, 97 percent was assumed to be SO_2 and 3 percent sulfate.

B. METEOROLOGICAL DATA

The long-range transport model requires several different meteorological inputs. These include: vertically averaged horizontal winds, surface wind speeds, afternoon mixing depths, and a measure of the thermal gradient near the ground. These data were compiled for three meteorological episodes:

- > Strong wind winter case based on data for 27-31 January 1976.
- > Stagnation spring case based on data for 4-7 April 1976.
- > Moderate wind summer case based on data for 9-11 July 1975.

The winds in the mixing layer determine how pollutants move after they are emitted, so characterization of these winds is crucial to the modeling exercise. The winds for the three test cases were calculated by Mr. Loren Crow, a consulting meteorologist, under subcontract from SAI. He computed a set of wind vectors for the 30-point coarse grid shown in Figure 19. These coarse grid wind fields were constructed at six-hour intervals to represent vertical averages through a layer 500 to 1500 feet above the terrain. The wind data were derived from:

- > The geostrophic winds associated with the 850 and 700 millibar maps available every 12 hours from the U.S. Weather Service.
- > Twice daily measurements from the eight U.S. Weather Service rawinsonde stations shown in Figure 19.
- > Twice daily pibal measurements taken on alternate days by the EPA monitoring network at the stations shown in Figure 19.

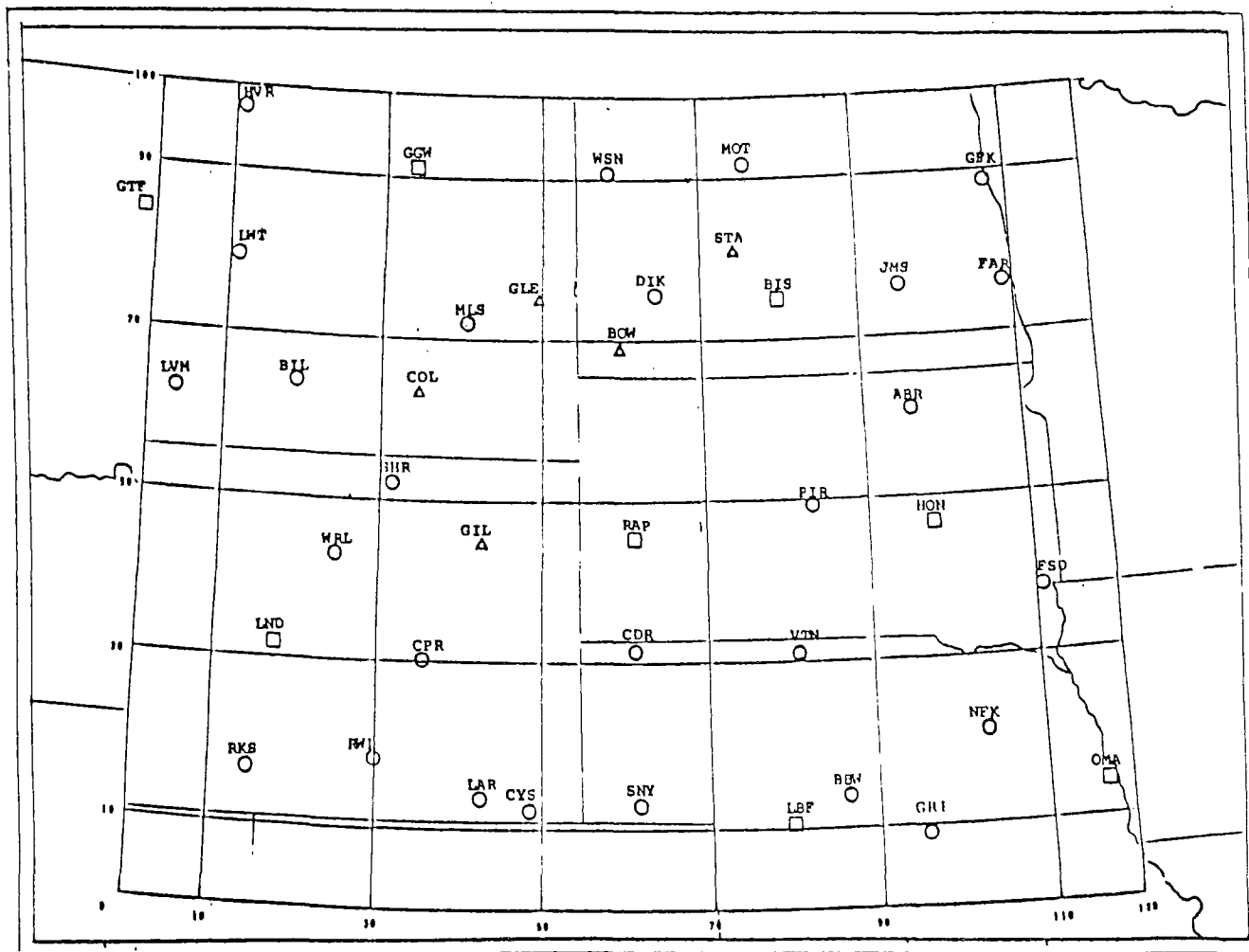


FIGURE 19. WIND MEASUREMENT NETWORKS IN THE NORTHERN GREAT PLAINS

After the 12-hour maps were completed additional maps at intermediate six-hour intervals were generated by consulting three-hour surface wind maps to estimate probable changes in the upper air flow. Finally, these six-hour coarse grid wind vectors were linearly interpolated in time and bilinearly interpolated in space to produce three-hour-averaged winds for the entire 120 x 100 grid.

Surface wind speeds are required for deposition calculations in the surface layer submodel. Mr. Loren Crow collected hourly surface wind data from the National Weather Service stations shown in Figure 19. The surface wind vectors were averaged over three-hour intervals and then a value for each grid cell was interpolated according to the following prescription:

$$\hat{v}_j = \frac{\sum_{r_{ij} < R} \left(\frac{\bar{v}_i}{r_{ij}} \right)}{\sum_{r_{ij} < R} \left(\frac{1}{r_{ij}} \right)}, \quad (38)$$

where

- \bar{v}_i = measured wind vector at monitoring station i
- r_{ij} = distance between grid point j and monitoring station i
- R = radius of influence; in our study it was 250 km.

Finally, the magnitude of each wind vector was calculated to produce three-hour-averaged surface wind speeds for the entire 120 x 100 grid.

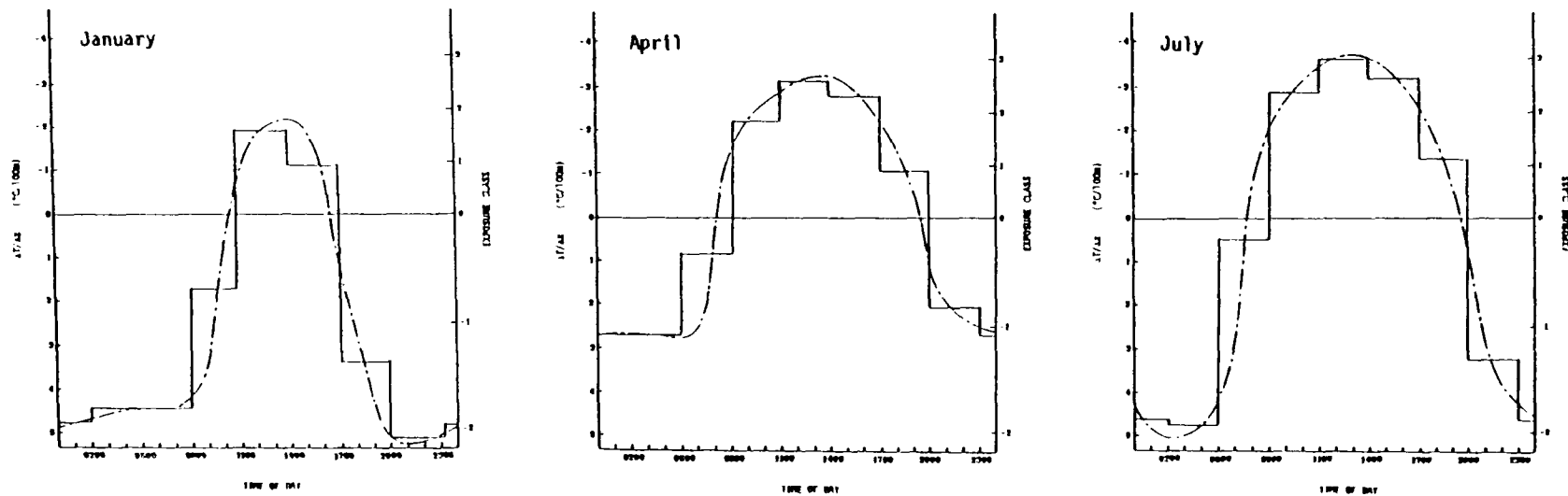
Thermal turbulence near the ground increases pollutant deposition by bringing material to absorbing surfaces more quickly. A complete characterization of this turbulence is extremely difficult. DeMarrais and Islitzer (1960) measured the vertical temperature gradient at

Idaho Falls from January 1955 through May 1958. These data, averaged for the months of January, April, and July, are plotted in Figure 20. As expected, the gradient is closely linked to the incoming solar radiation and shows both diurnal and seasonal variations. This information is incorporated in the regional model through the dimensionless variable, exposure class (Liu and Durran, 1977). The second set of vertical axes in Figure 20 gives exposure class as a function of the time of day.

The afternoon mixing heights determine the thickness of the modeling region, and hence the amount of dilution due to vertical diffusion. Mixing height data for the Northern Great Plains are virtually unobtainable. In the regional model we used the seasonally averaged afternoon mixing heights shown in Figure 21 (Holzworth, 1972). It is unfortunate that particular data for our three episodes are not available, but since the afternoon mixing depths only approximately represent the depth of the layer above the ground through which most mesoscale transport occurs, the seasonal averages are probably adequate.

C. SURFACE DATA

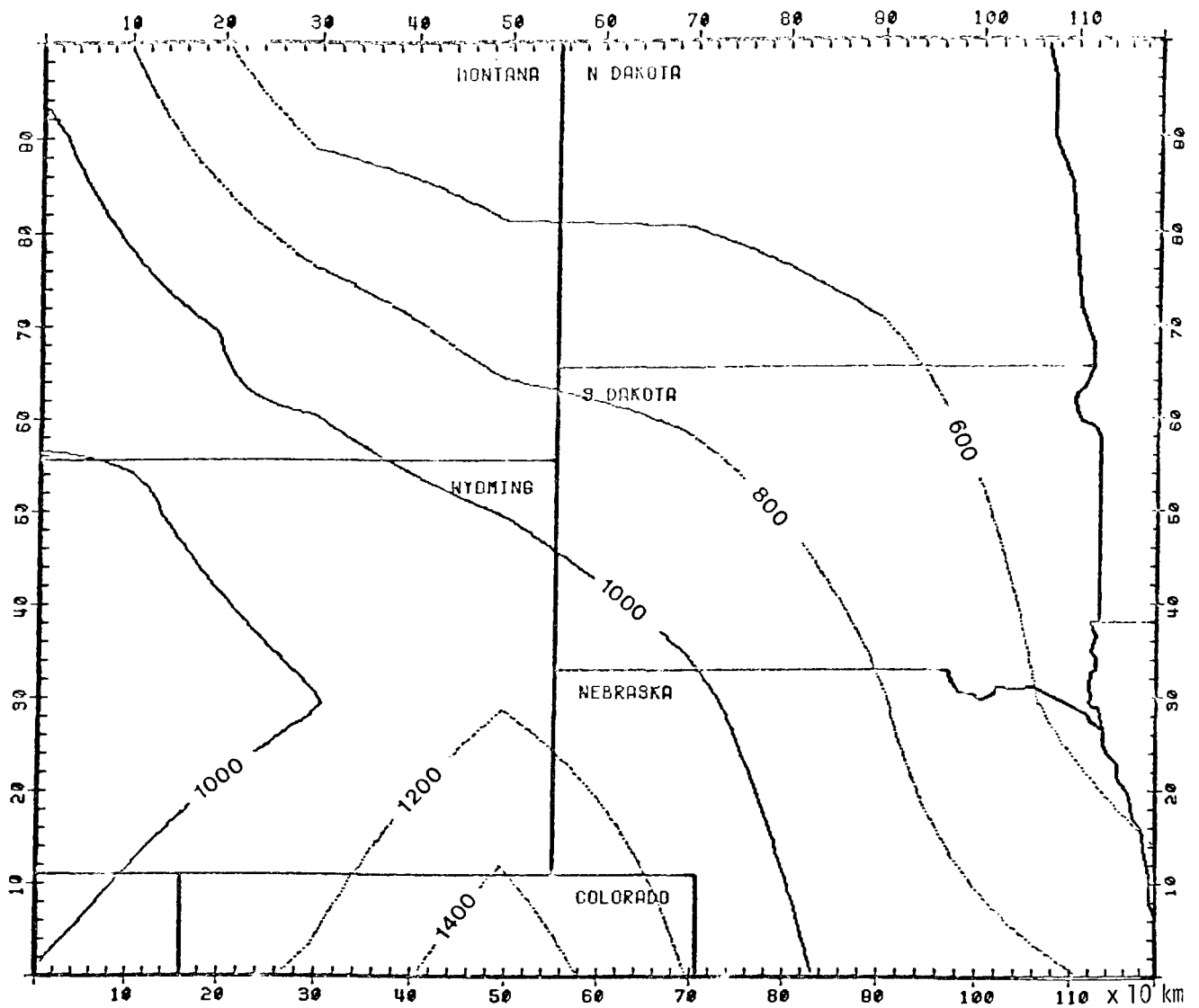
Surface deposition rates are influenced by vegetation and ground cover. We have already noted that available data are insufficient to distinguish the surface resistance of a pine needle from that of a blade of grass. Moreover, the different geometries of pine trees and grasses generate different amounts of mechanical turbulence, thereby promoting different rates of deposition. Figure 22 shows the modeling region divided into six different vegetation types. The divisions reflect differences in potential natural vegetation (Küchler, 1966) or current land use (Marschner, 1950). The surface roughnesses (without zero plane displacement) associated with each vegetation type appear in Table 17; they were estimated from a self-consistent summary of experimental data compiled by Sellers (1965).



111

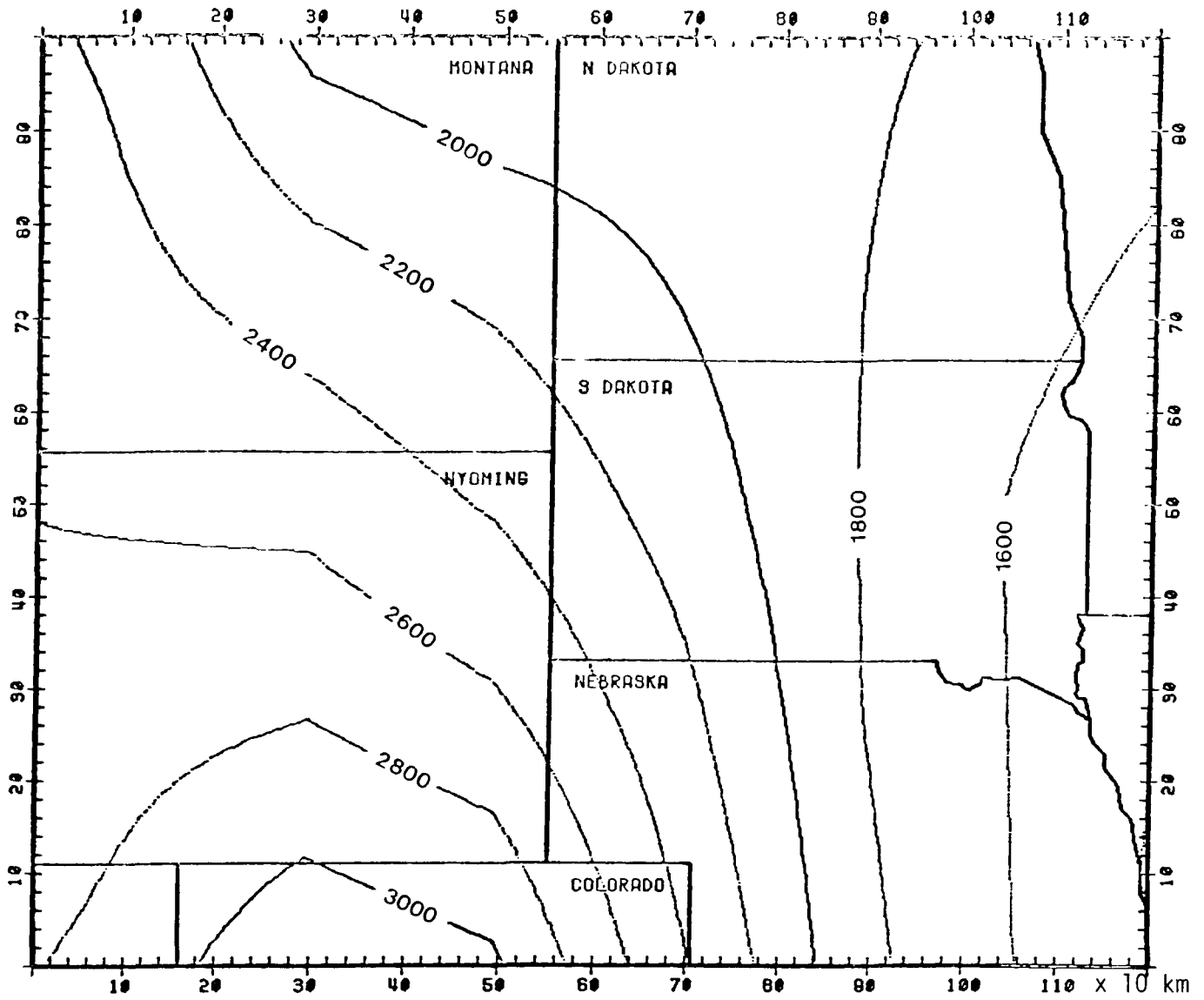
Source: DeMarrais and Islitzer (1960).

FIGURE 20. TEMPERATURE GRADIENTS AND EXPOSURE CLASSES AT IDAHO FALLS, IDAHO



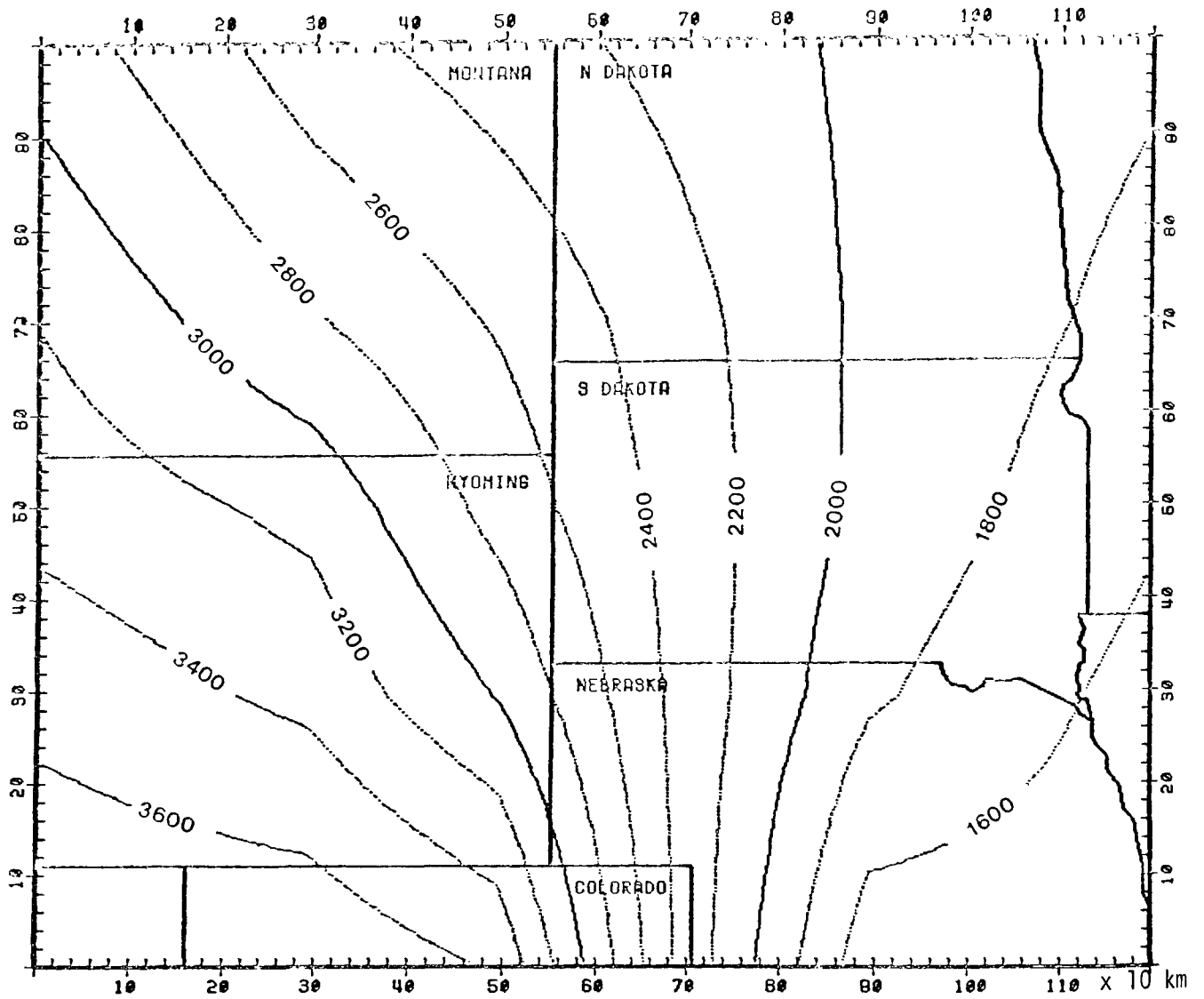
(a) January 1976

FIGURE 21. VERTICAL THICKNESS OF THE MODELING REGION (IN METERS)



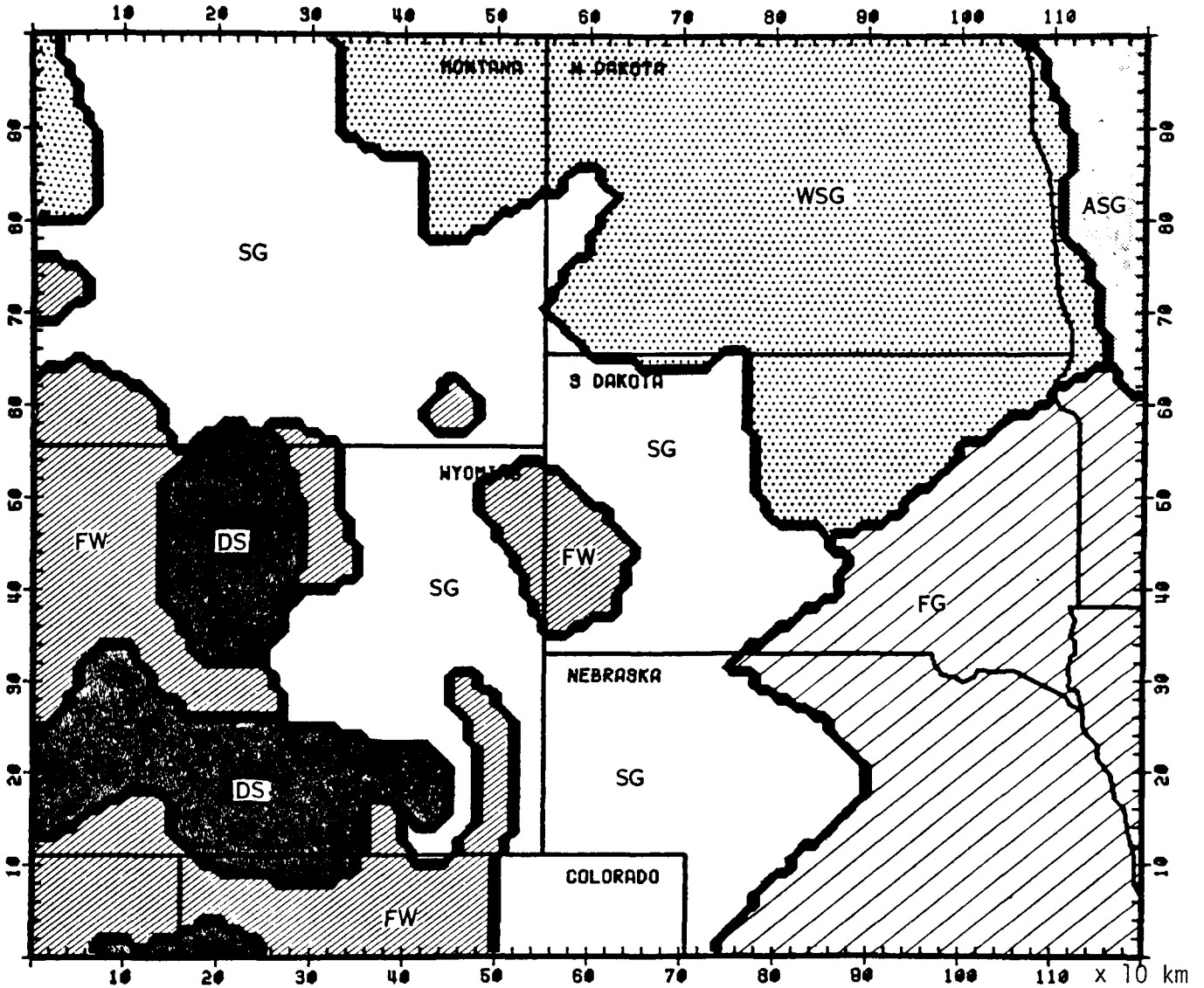
(b) April 1976

FIGURE 21 (Continued)



(c) July 1975

FIGURE 21 (Concluded)



Key:

ASG alfalfa, small grains
 DS sagebrush, steppe
 FG corn, soybeans, oats
 FW pine, fir, spruce
 SG alfalfa, hay
 WSG wheat, barley, flax

FIGURE 22. VEGETATION IN THE NORTHERN GREAT PLAINS

TABLE 17. SURFACE ROUGHNESSES FOR VARIOUS VEGETATION TYPES

| <u>Vegetation Code*</u> | | <u>Surface Roughness (cm)</u> |
|-------------------------|-----------------------|-----------------------------------|
| SG | alfalfa, hay | 2.4 |
| DS | sage brush, steppe | 2.6 |
| ASG | alfalfa, small grains | 15 |
| WSG | wheat, barley, flax | 22 |
| FG | corn, soybeans, oats | 75 |
| FW | pine, fir, spruce | 283 |

* Code used in Figure 22.

D. AIR QUALITY DATA

Initial and boundary pollutant concentrations are the remaining inputs required by the regional model. The ideal way to generate such inputs is from air quality measurements, but this requires a dense modeling network throughout the region and along its borders. Measurements taken at a point are not strictly equivalent to the volume-averaged concentrations used in grid modeling; the problem is especially serious in long-range modeling because the grid cells are large. Each cell in the regional model represents a layer 1000 to 3000 meters thick above a surface of 100 square kilometers. The pollutant concentration measured at a single location in such a cell could certainly be much different from the actual average concentration in that cell. In particular, measurements taken at urban locations in the Northern Great Plains are unsuitable for input to or validation of the regional model. The most useful measurements for regional modeling are those gathered at ten SO₂ monitoring sites established by the EPA at the rural locations shown in Figure 23. Two of these stations had continuous SO₂ monitors, and the rest took a 24-hour-averaged measurement every six days.

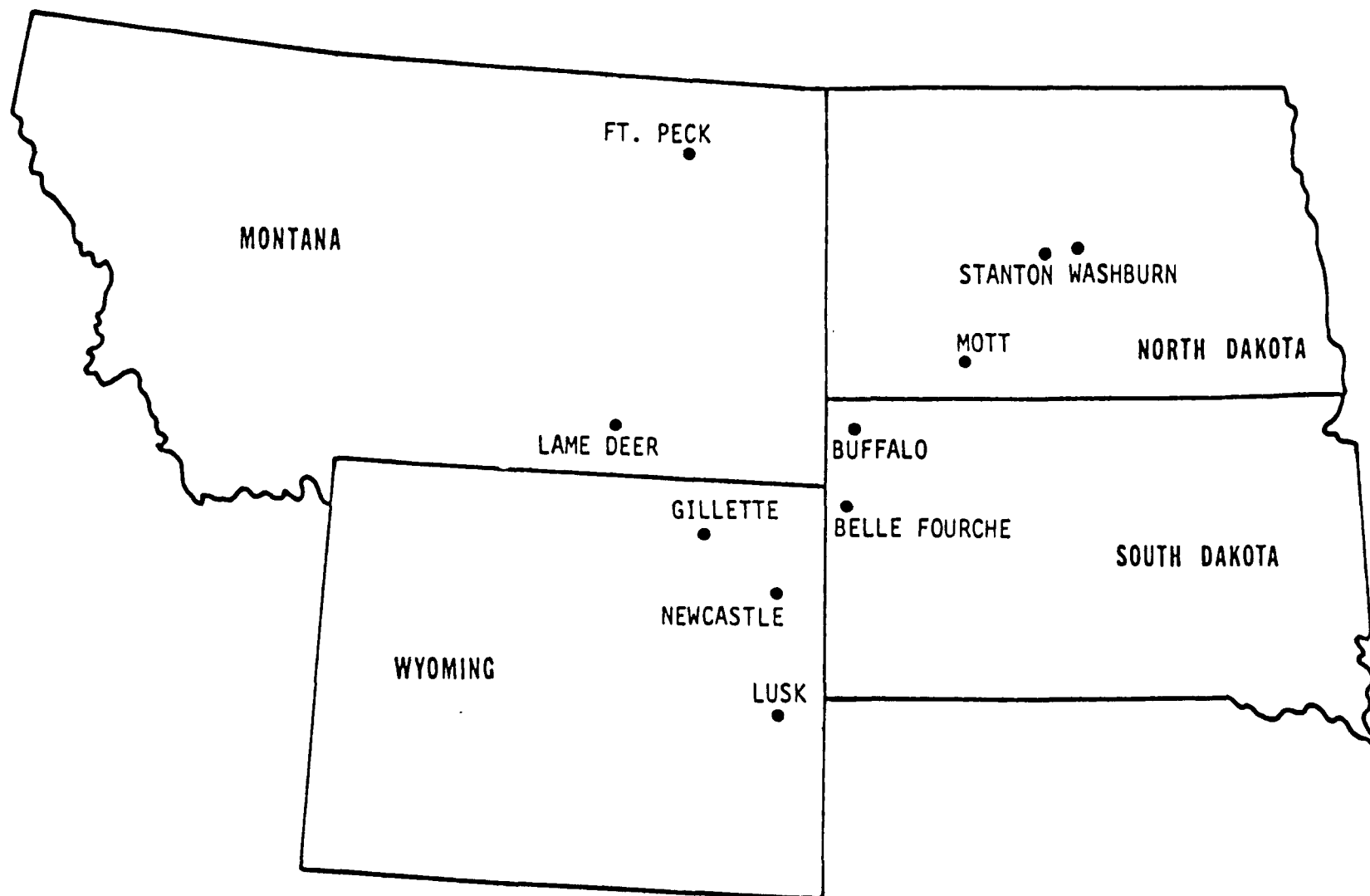


FIGURE 23. EPA SO₂ MONITORS IN THE NORTHERN GREAT PLAINS

These ten stations can be of some use when assessing the accuracy of model predictions, but they simply do not provide enough data to determine initial and boundary conditions. Rasmussen, Taheri, and Kabel (1974) estimated a general background SO_2 concentration of 1 to 4 $\mu\text{g}/\text{m}^3$ and Georgii (1970) measured 0.5 to 2 $\mu\text{g}/\text{m}^3$ over Colorado. In the regional model a background SO_2 concentration of 1.5 $\mu\text{g}/\text{m}^3$ was used for both initial and boundary conditions. McMullen, Faoro, and Morgan (1970) suggested an average nonurban sulfate concentration of 2.5 $\mu\text{g}/\text{m}^3$. A comparison of the estimates of Georgii and Rasmussen et al. suggests that background SO_2 concentrations in the Northern Great Plains are somewhat lower than many rural sites, so 1.5 $\mu\text{g}/\text{m}^3$ was also taken for initial and boundary sulfate concentrations.

XI AIR QUALITY ANALYSIS

For the assessment of the impact of coal development on air quality in the Northern Great Plains, three meteorological patterns were selected. The selection was based on considerations of meteorological and air quality conditions of interest and data availability. The three cases probably represent typical situations for winter, spring, and summer in this area, as shown in Table 18. For each meteorological pattern, the regional air pollution model was exercised for two emissions scenarios:

- > Scenario I--emissions in 1976
- > Scenario II--emissions in 1986.

A complete list of the SO_2 concentrations predicted for the three cases and two emission scenarios (a total of six simulations) is presented on isopleth contour maps in Appendix B. The isopleth contour intervals are $2^n \mu\text{g}/\text{m}^3$, where $n = 0, 1, 2 \dots$. The model is started from a constant initial concentration of $1.5 \mu\text{g}/\text{m}^3$ SO_2 , so the first several plots in each series show the concentration field building up to a quasi-equilibrium. Maps of point source locations in 1976 and 1986 are included as clear overlays in a pocket inside the back cover; they fit over the maps in Appendix B to show the locations of these sources relative to their plumes. Because the initial SO_2 concentration assumed in the model was $1.5 \mu\text{g}/\text{m}^3$, the outer isopleth around each plume is generally the $2 \mu\text{g}/\text{m}^3$ contour.

TABLE 18. PERIODS CHOSEN FOR AIR QUALITY ANALYSIS

| <u>Case</u> | <u>Season</u> | <u>Dates</u> |
|-------------|---------------|--------------------|
| 1 | Winter | 27-31 January 1976 |
| 2 | Spring | 4-7 April 1976 |
| 3 | Summer | 9-11 July 1975 |

The isopleth maps show that concentrations greater than $16 \mu\text{g}/\text{m}^3$ are rarely predicted over more than one cell by the 1976 emissions inventory; in the 1986 case predictions rarely exceed $32 \mu\text{g}/\text{m}^3$. Table 19 provides a comparison of total SO_x emissions within the study area with SO_x emissions in the State of Ohio. Ohio generates thirteen times the SO_x emissions in one-tenth of the study area of the Northern Great Plains. Twenty-four-hour-averaged concentrations exceeding $150 \mu\text{g}/\text{m}^3$ have been measured at many locations in Ohio (EPA, 1976b), so the 4 and $8 \mu\text{g}/\text{m}^3$ predictions shown in Appendix B seem reasonable. The three cases listed in Table 18 are analyzed in more detail in the following sections.

TABLE 19. SO_2 EMISSIONS AND AREAS OF OHIO AND THE NORTHERN GREAT PLAINS

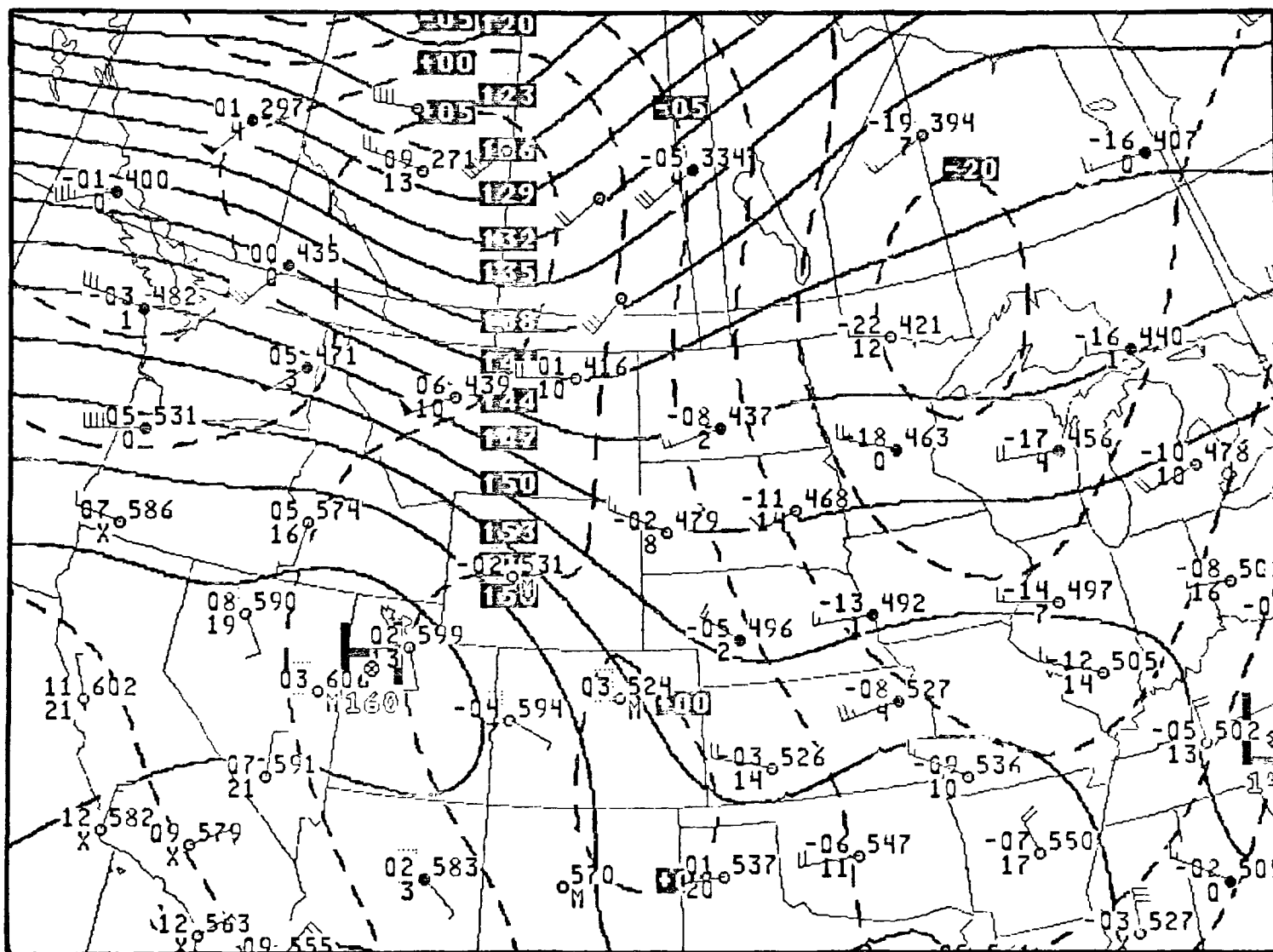
| <u>State</u> | <u>Total SO_x Emissions (tons/year)</u> | <u>Area (sq. miles)</u> |
|-----------------|---|-----------------------------|
| Eastern Montana | 43,000 | 98,000 |
| Nebraska | 55,000 | 77,000 |
| North Dakota | 80,000 | 71,000 |
| South Dakota | 3,000 | 77,000 |
| Wyoming | 70,000 | 98,000 |
| Total | 251,000 | 421,000 |
| Ohio | 3,347,000 | 41,000 |

A. WINTER

The winter case, characterized by low mixing depths and a strong, relatively constant wind from the northwest, provides favorable conditions for long-range transport. Selected 850 millibar maps for the winter case meteorology are shown in Figure 24. Figure 25 shows the predicted SO_2 concentrations for the 1976 and 1986 emissions inventories 33, 48, and 67 hours after the beginning of the simulation. The greatest cell-averaged concentration at the head of each plume is given in $\mu\text{g}/\text{m}^3$. The predicted SO_2 concentrations in the southeastern corner of the modeling region are less than $1 \mu\text{g}/\text{m}^3$ in Figures 25a, b, e, and f. This value is lower than the initial and boundary SO_2 conditions. Concentrations decrease below background when an air parcel moves extended distances without encountering significant emissions. The diagonal corridor from southeastern Nebraska through northwestern South Dakota to the Canadian border is free of major SO_2 emissions. Pollutant parcels blowing down this corridor experience surface deposition and chemical decay losses but no emissions loading, hence SO_2 concentrations may be depleted below the initial concentrations. A shift in the winds (Figures 25c and d) can eliminate such regions. The 1986 case (Figure 25d) reveals SO_2 transport to great distances. Plumes from Colstrip, Montana and Wyodak, Wyoming merge and travel into Sutherland, Nebraska to link with the Gerald Gentleman plume, and the $2 \mu\text{g}/\text{m}^3$ isopleth from the North Dakota developments extends well into Iowa.

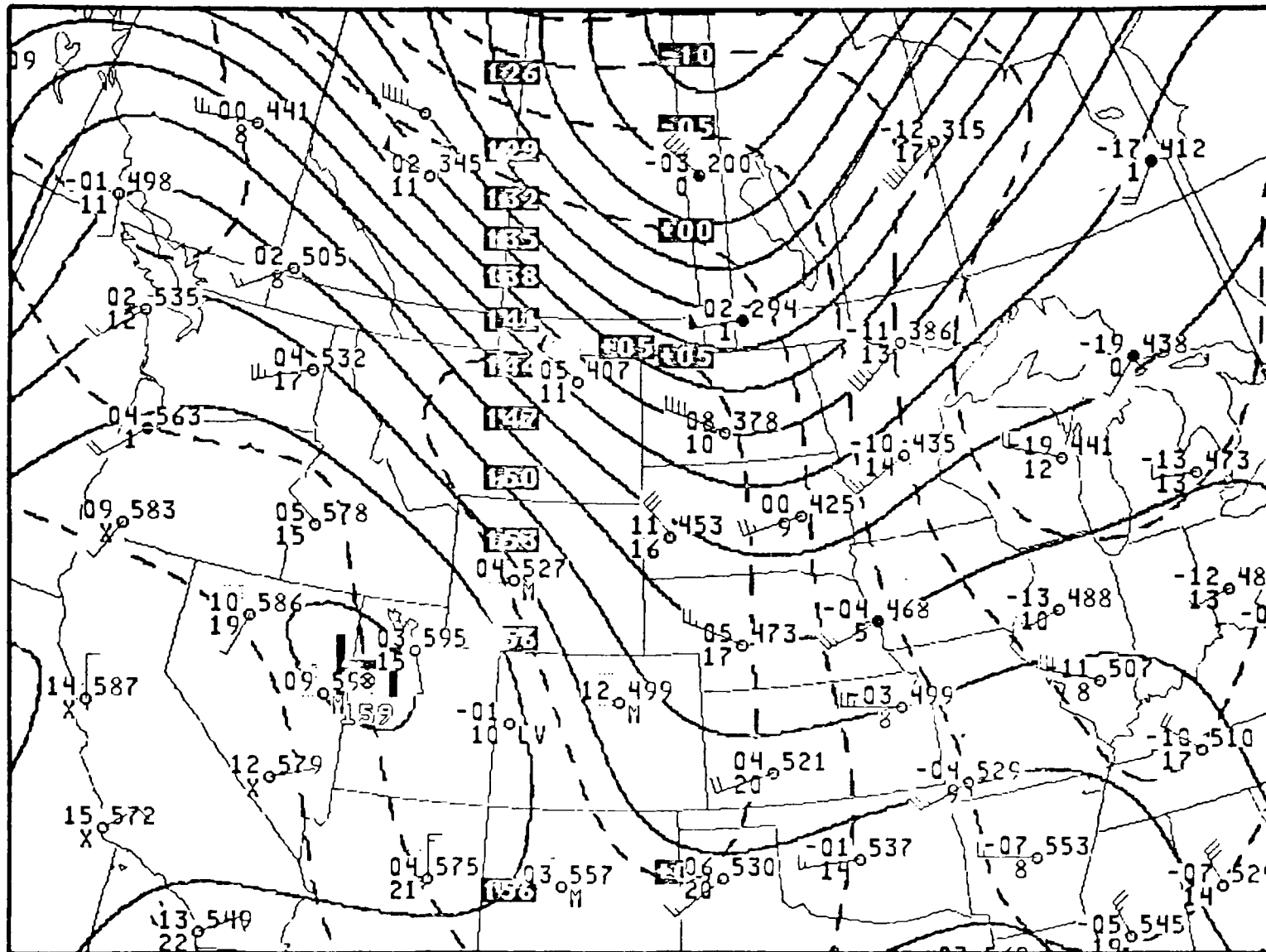
B. SPRING

Unlike the winter case, the spring case conditions are favorable for the retention of pollutants within the Northern Great Plains. The 850 millibar maps for the spring case, given in Figure 26, show a stagnant high pressure system lingering over the region. The resulting winds in the mixing layer are light and variable. Figure 27, which indicates pollutant concentrations 24, 33, and 51 hours after the start of the simulation, shows a reversal in the mixing layer



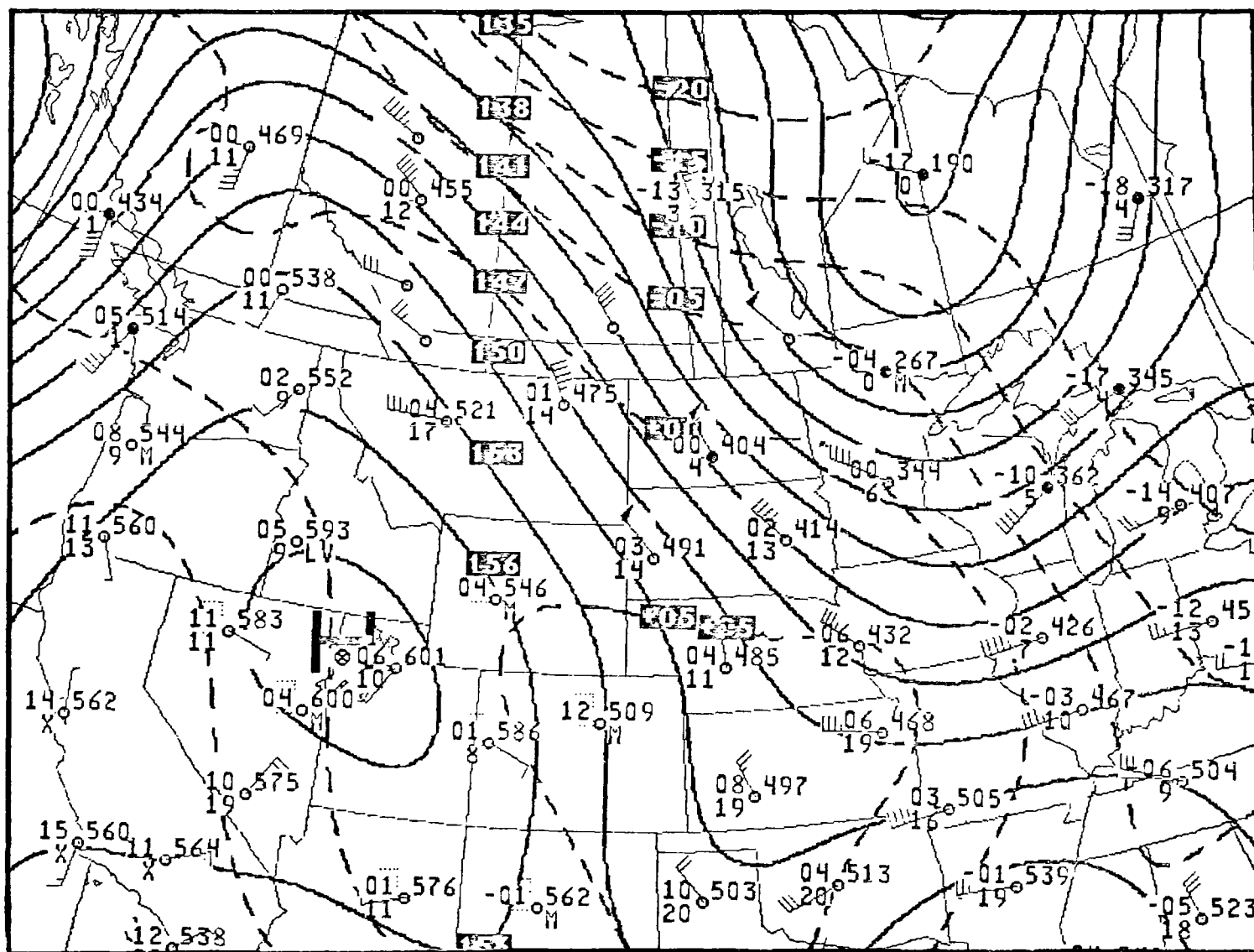
(a) 500 MST 27 January 1976

FIGURE 24. WINDS AT 850 MILLIBARS ALTITUDE DURING 27-31 JANUARY 1976



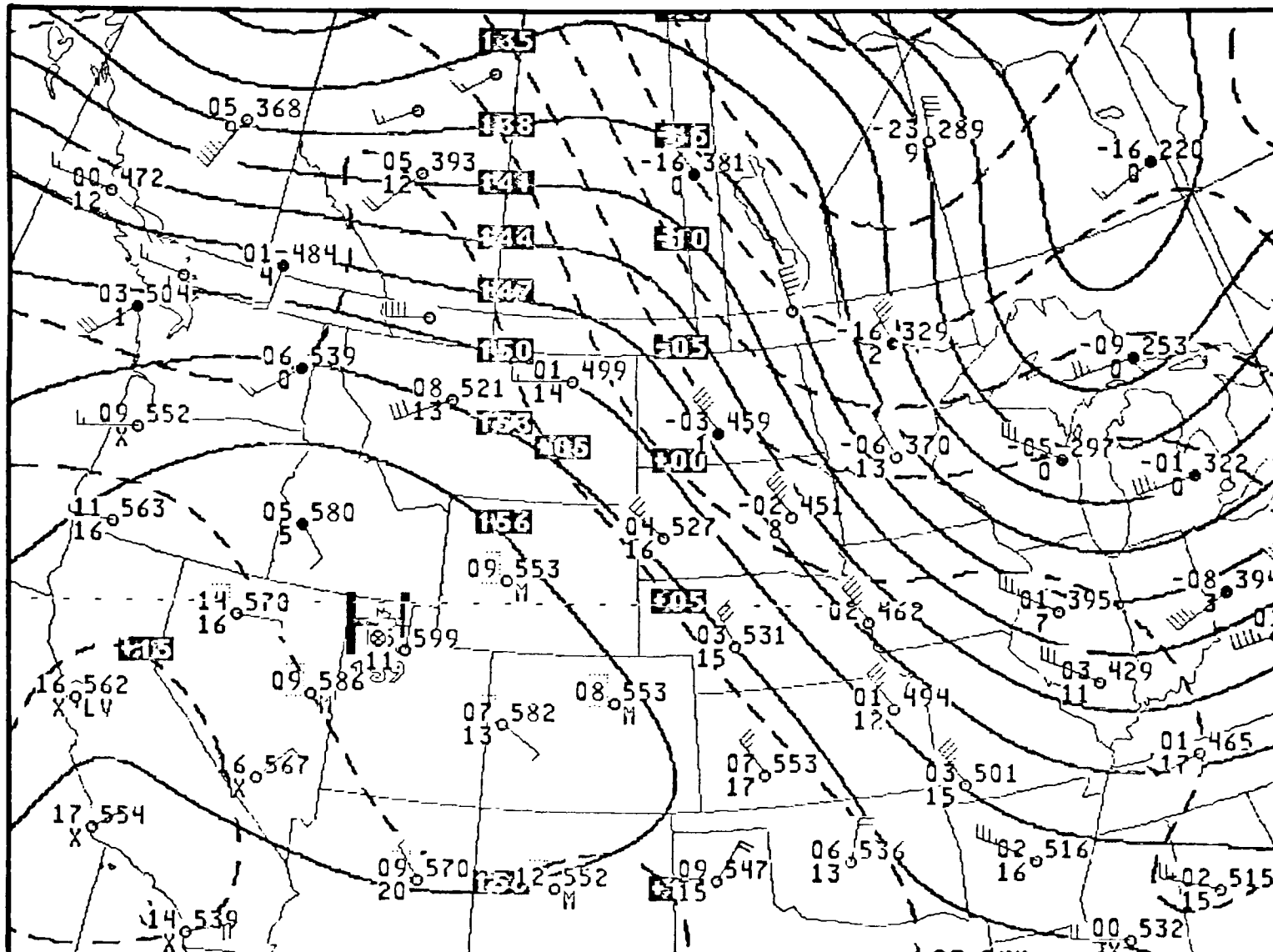
(b) 1700 MST 27 January 1976

FIGURE 24 (Continued)



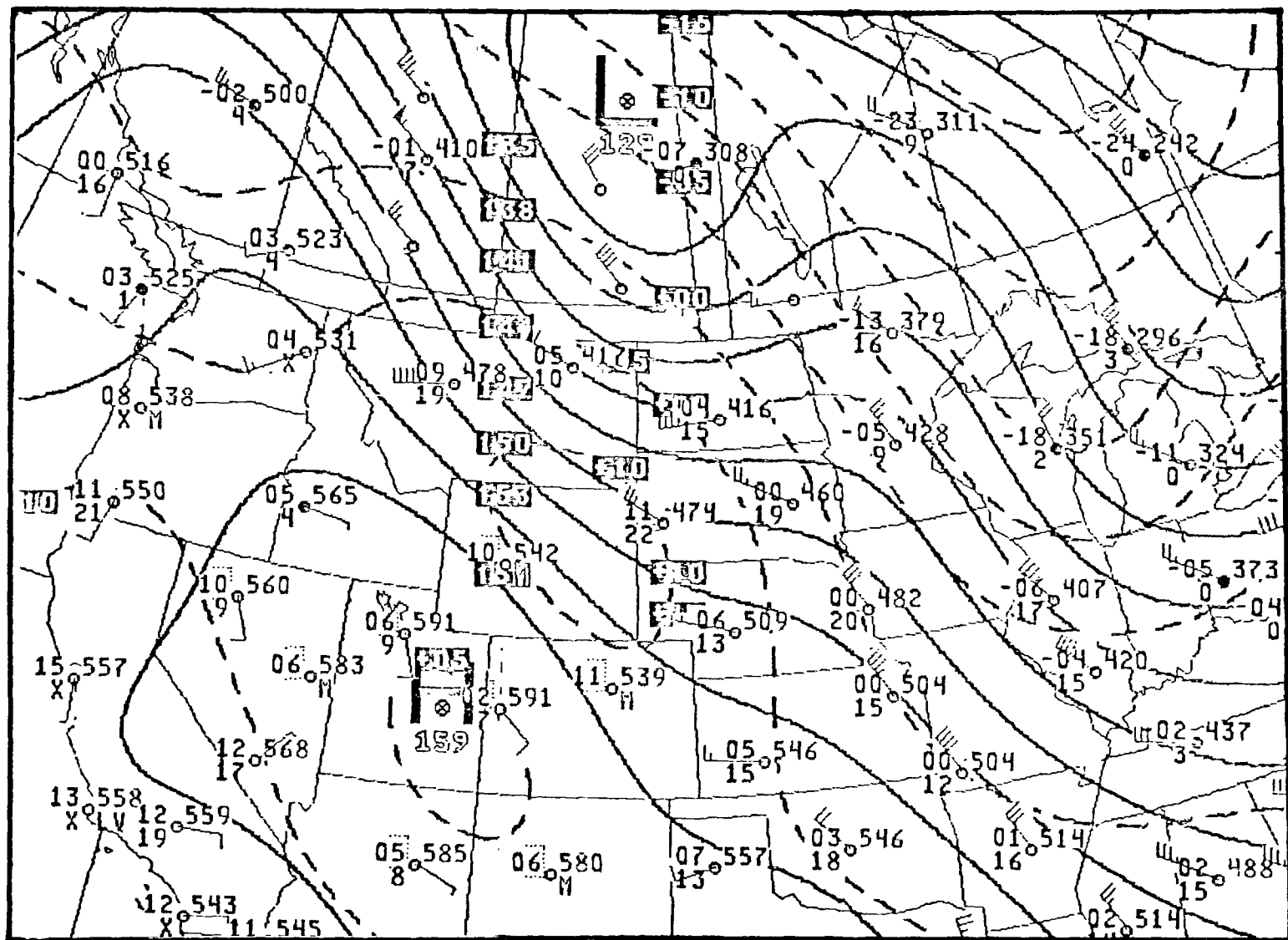
(c) 500 MST 28 January 1976

FIGURE 24 (Continued)



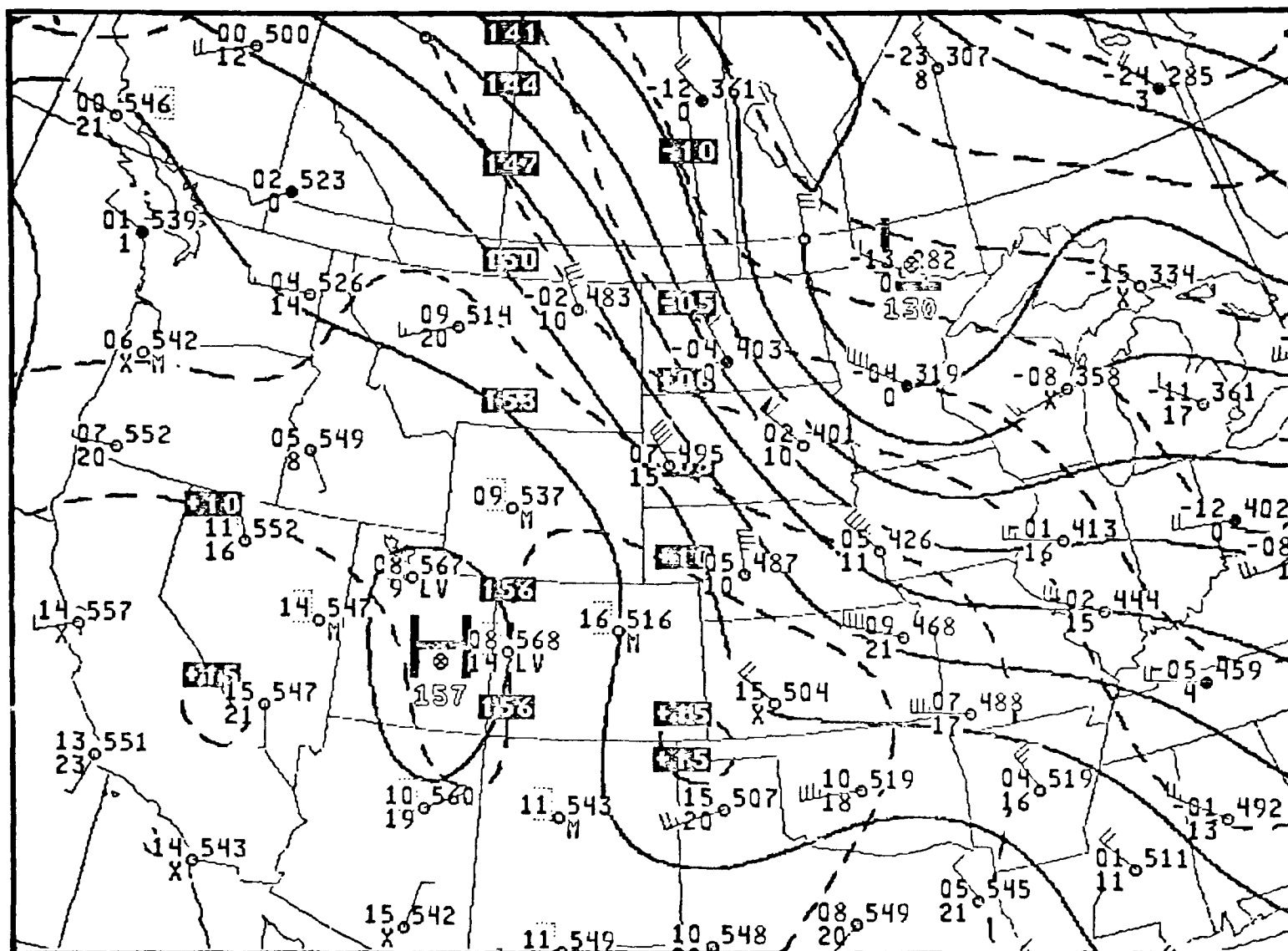
(d) 1700 MST 28 January 1976

FIGURE 24 (Continued)



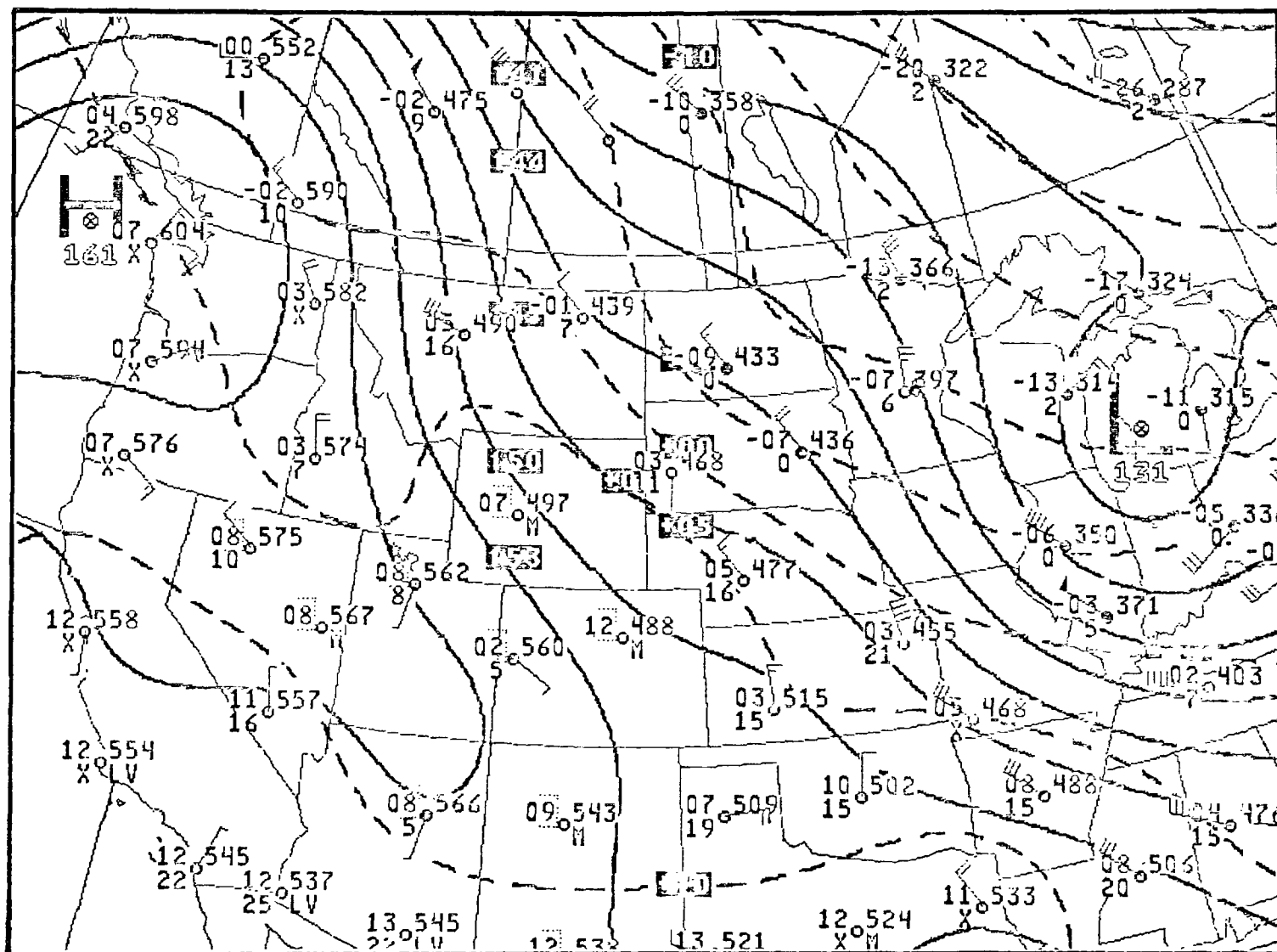
(e) 500 MST 29 January 1976

FIGURE 24 (Continued)



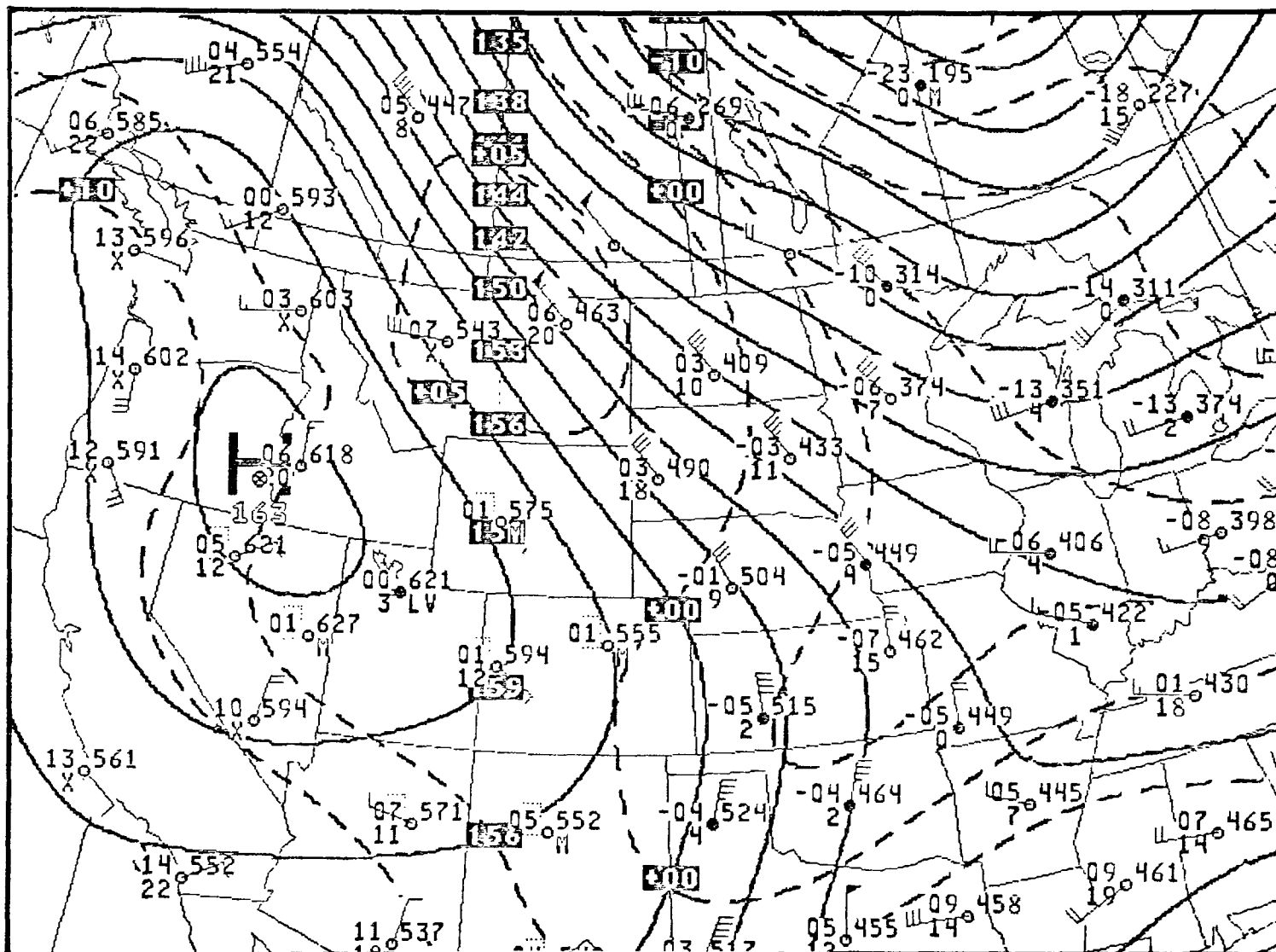
(f) 1700 MST 29 January 1976

FIGURE 24 (Continued)



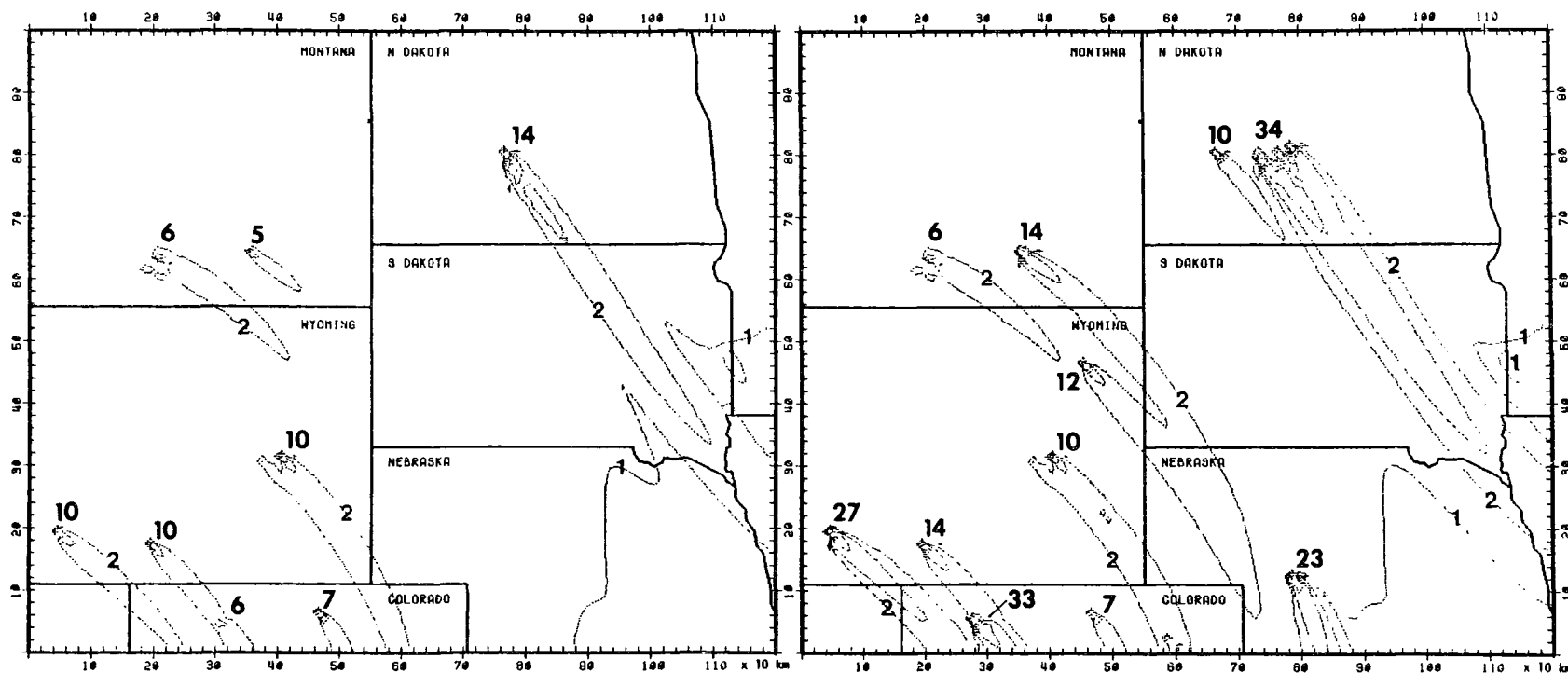
(g) 500 MST 30 January 1976

FIGURE 24 (Continued)



(i) 500 MST 31 January 1976

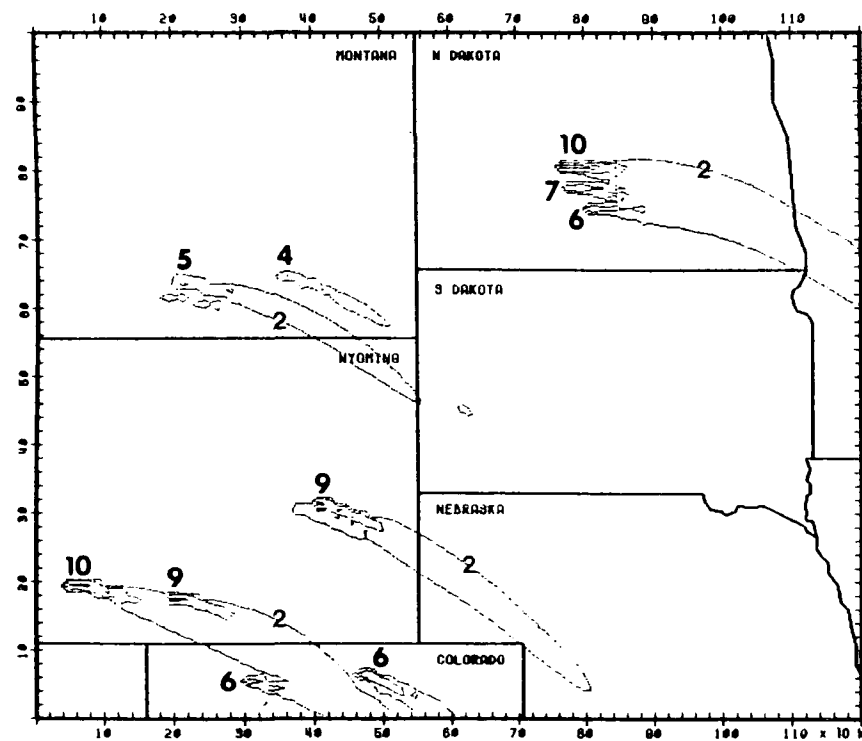
FIGURE 24 (Continued)



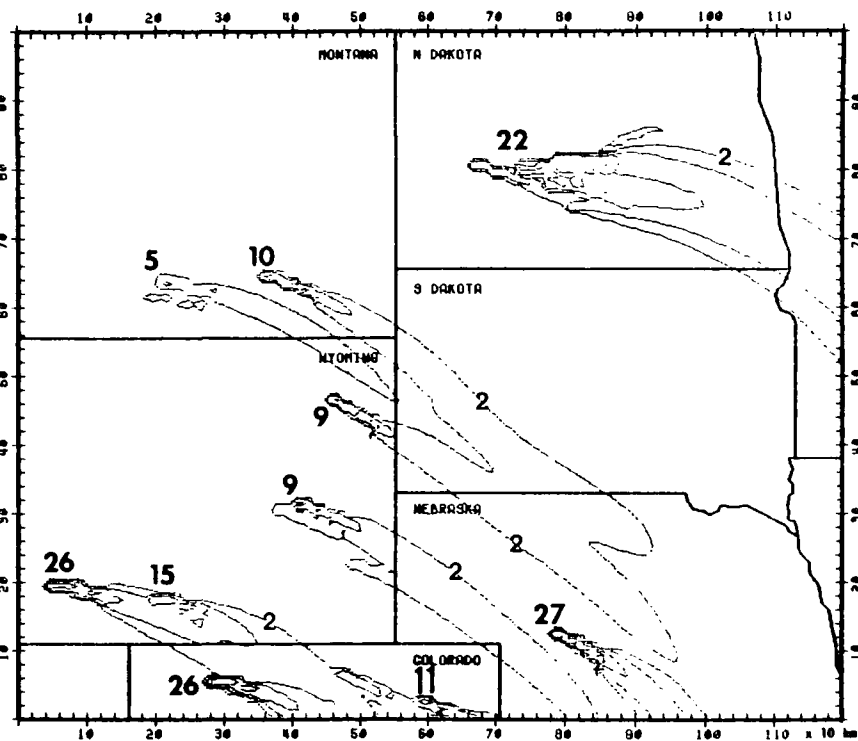
(a) 1400-1700 MST 28 January 1976; 1976 emissions

(b) 1400-1700 MST 28 January 1976; 1986 emissions

FIGURE 25. PREDICTED SO₂ CONCENTRATIONS FOR WINTER CASE. Isopleths at 1, 2, 4, ..., µg/m³; plume maxima in boldface.

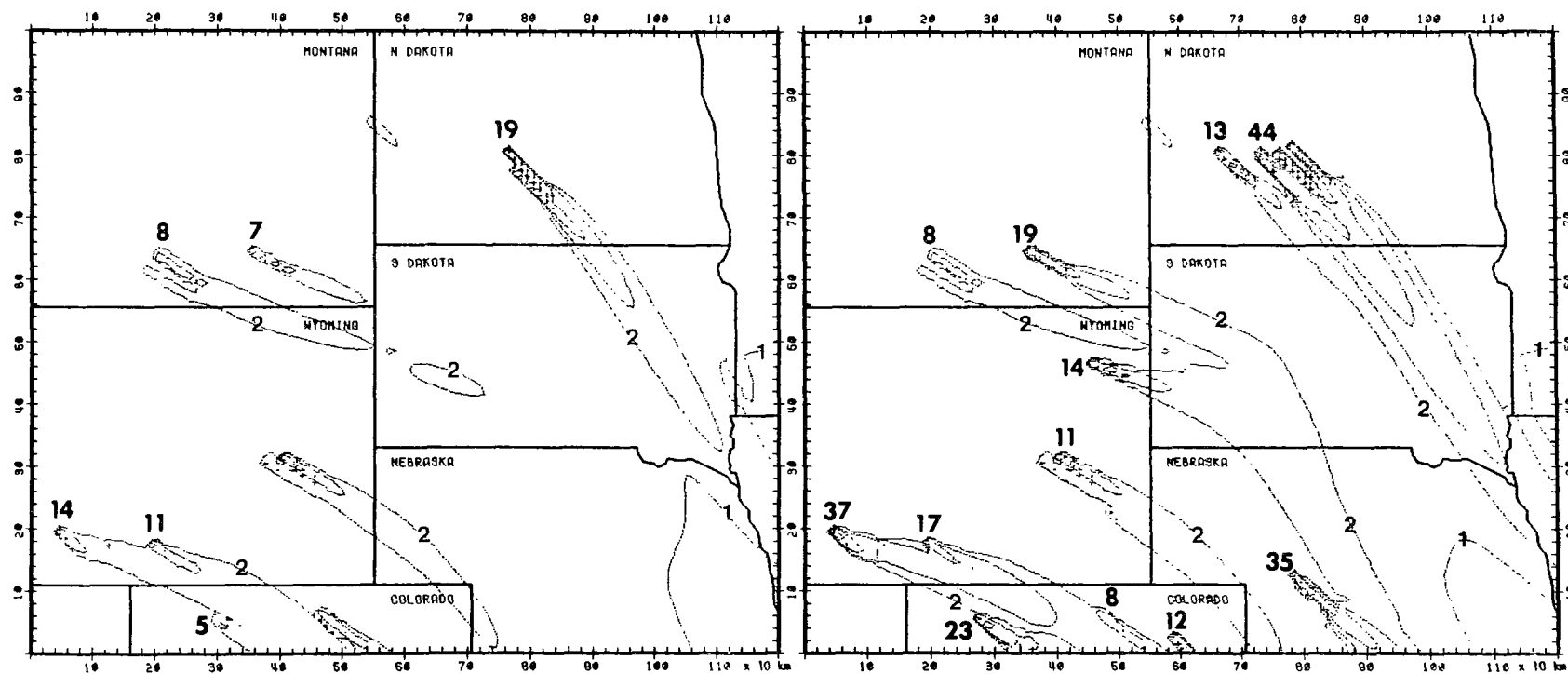


(c) 500-800 MST 29 January 1976; 1976 emissions



(d) 500-800 MST 29 January 1976; 1986 emissions

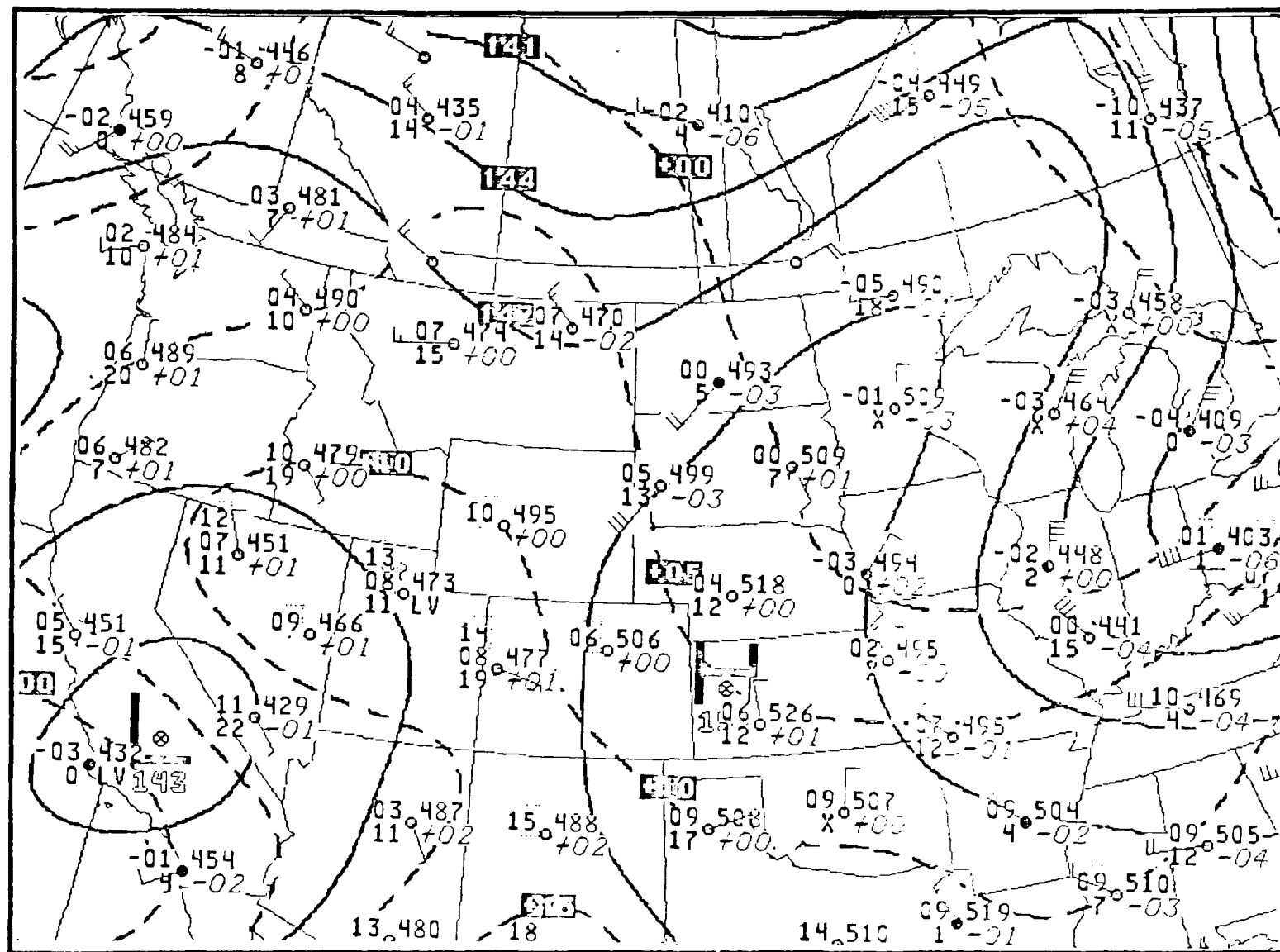
FIGURE 25 (Continued)



(e) 800-1100 MST 30 January 1976; 1976 emissions

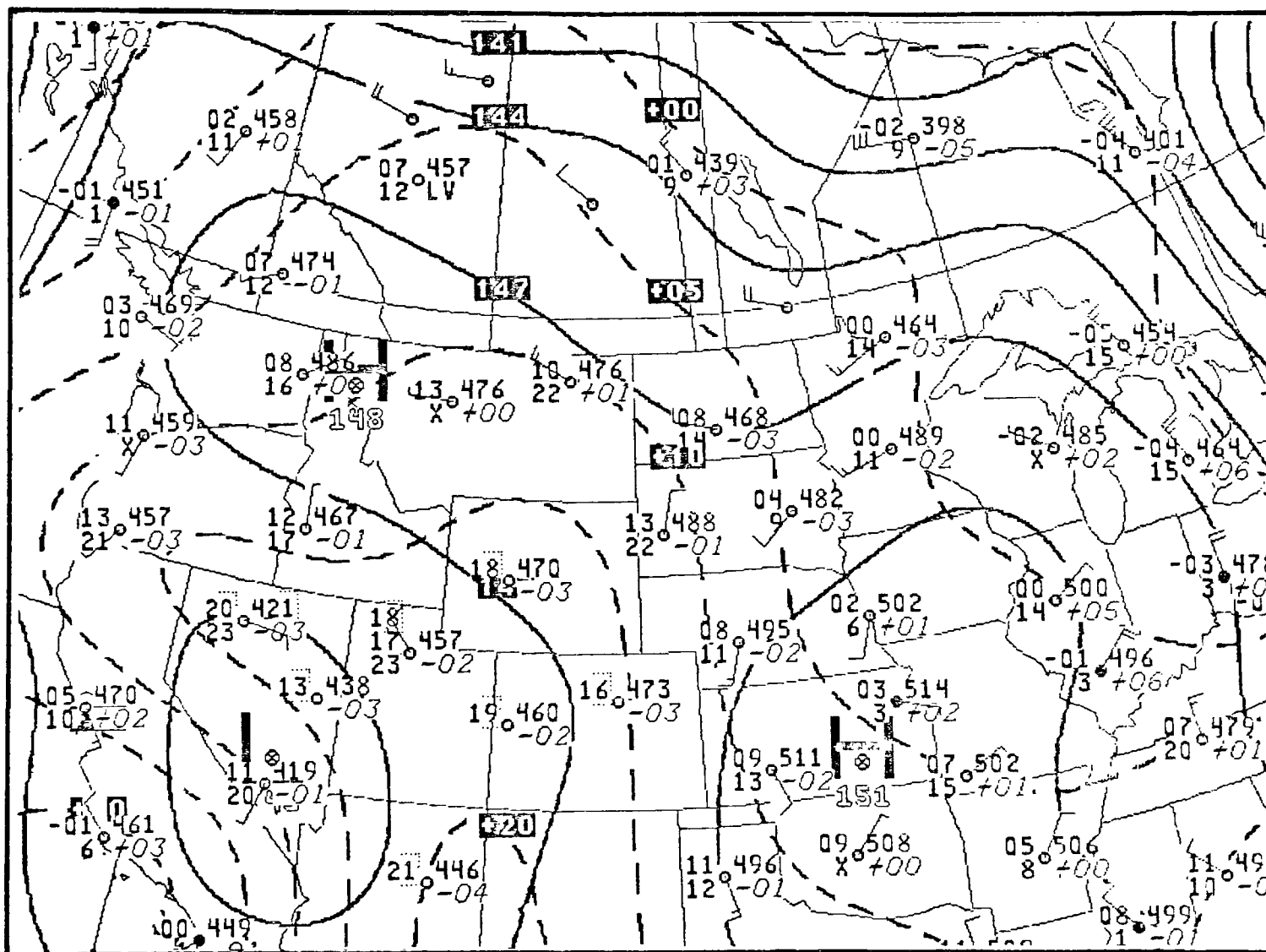
(f) 800-1100 MST 30 January 1976; 1986 emissions

FIGURE 25 (Concluded)



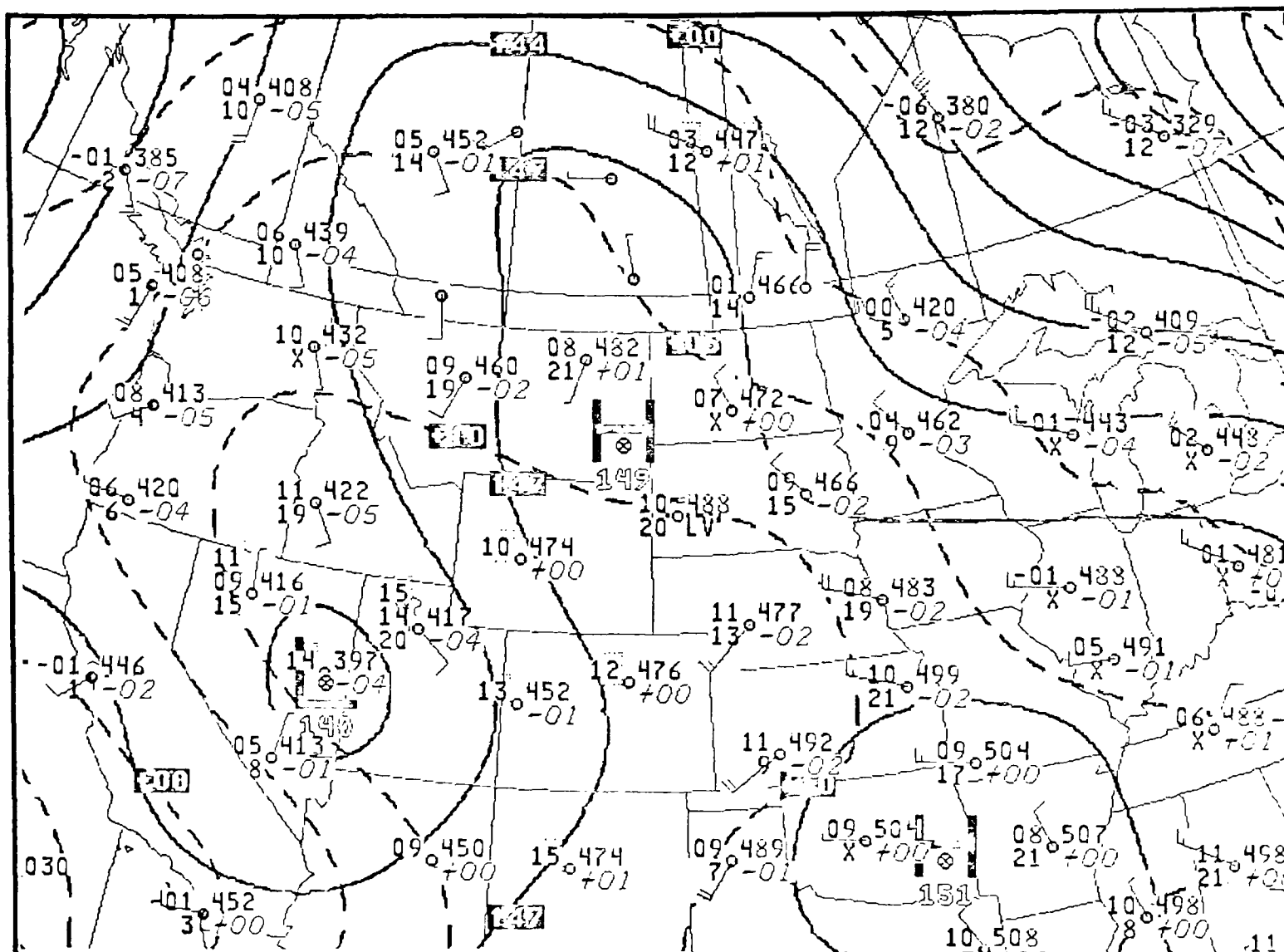
(a) 500 MST 4 April 1976

FIGURE 26. WINDS AT 350 MILLIBARS ALTITUDE DURING 4-7 APRIL 1976



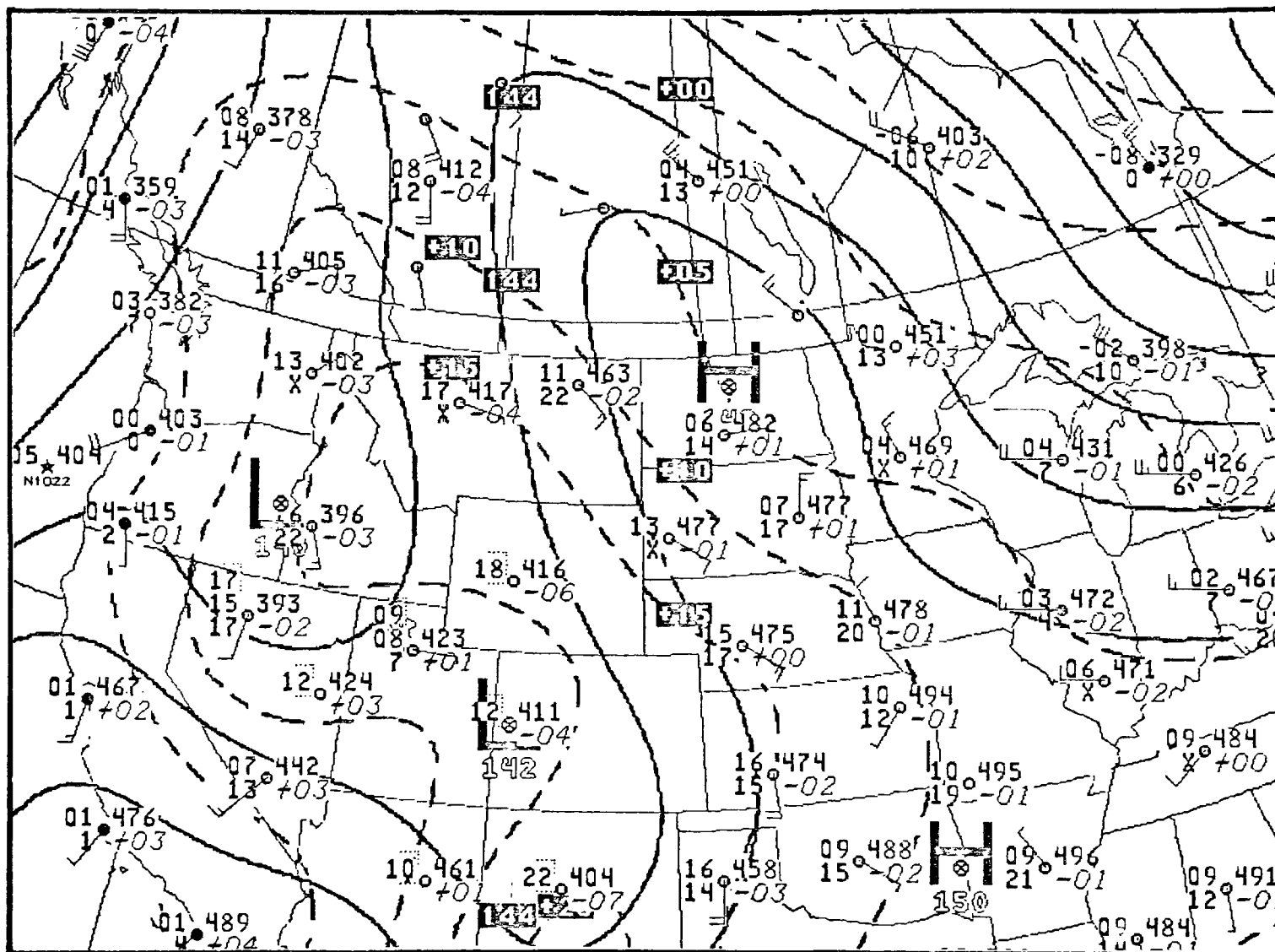
(b) 1700 MST 4 April 1976

FIGURE 26 (Continued)



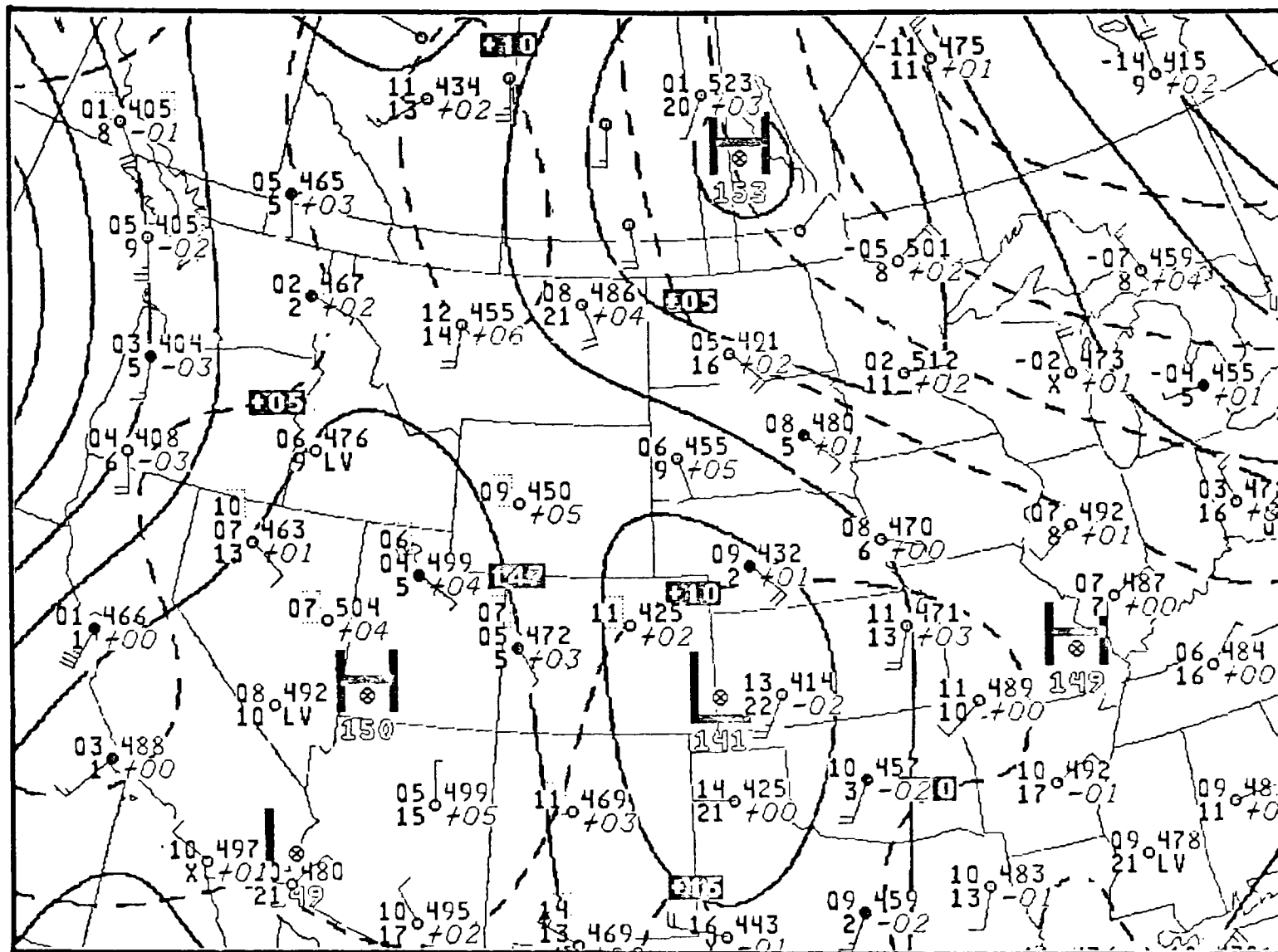
(c) 500 MST 5 April 1976

FIGURE 26 (Continued)



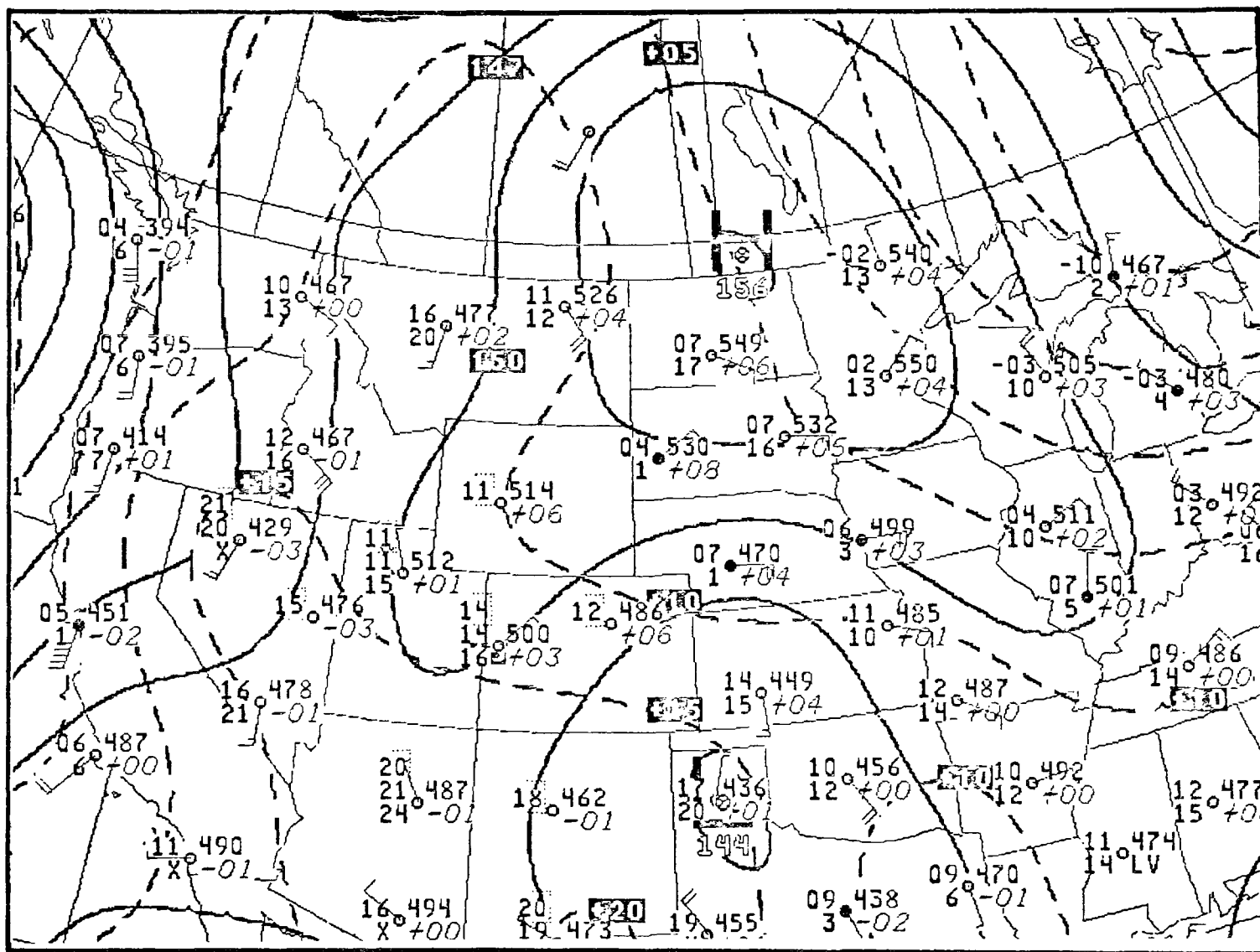
(d) 1700 MST 5 April 1976

FIGURE 26 (Continued)



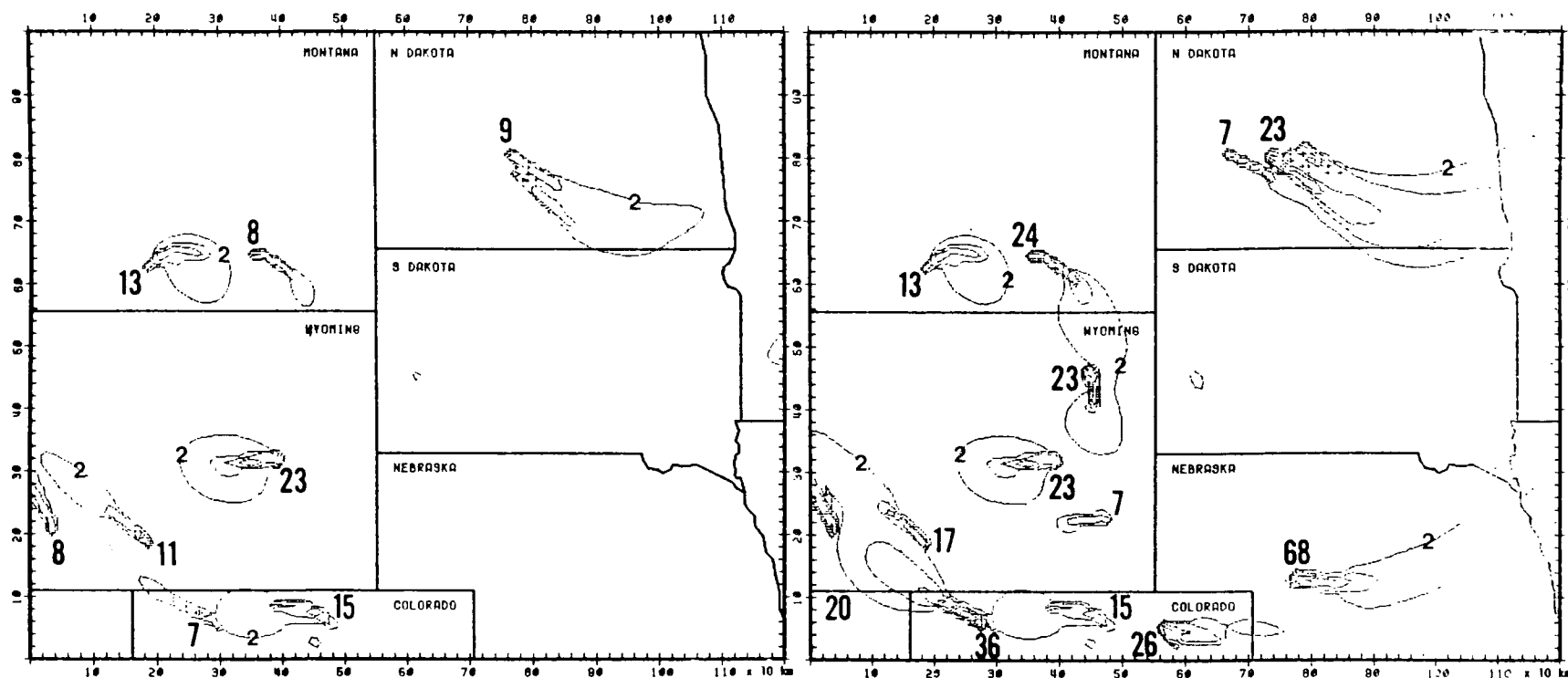
(g) 500 MST 7 April 1976

FIGURE 26 (Continued)



(h) 1700 MST 7 April 1976

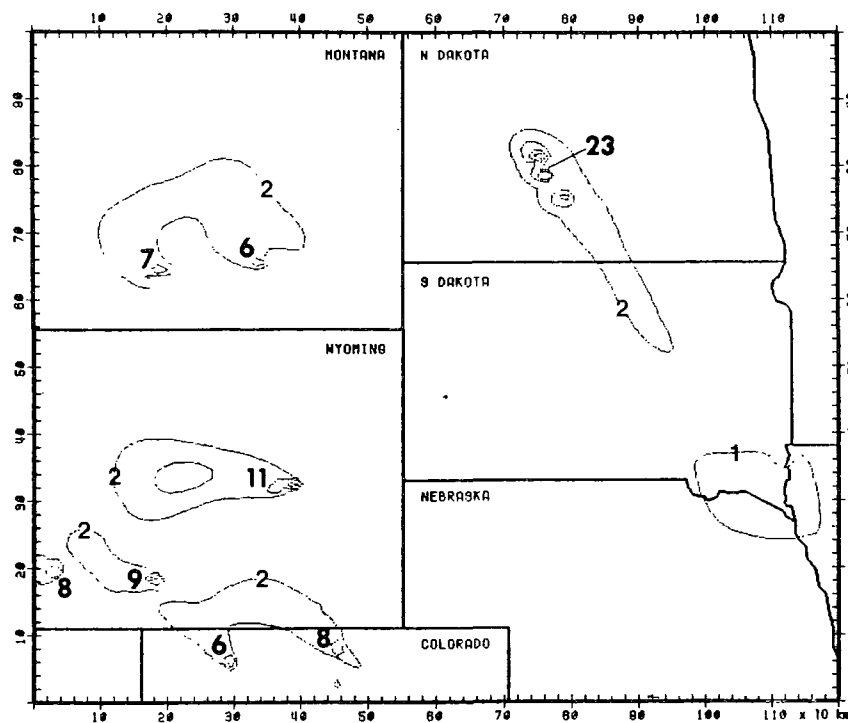
FIGURE 26 (Concluded)



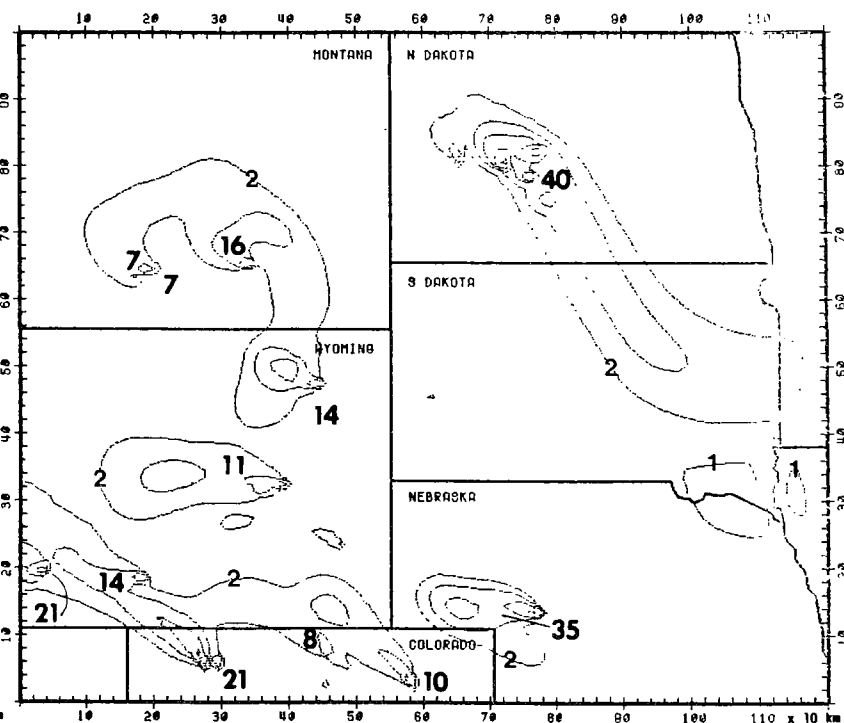
(a) 500-800 MST 5 April 1976; 1976 emissions

(b) 500-800 MST 5 April 1976; 1986 emissions

FIGURE 27. PREDICTED SO₂ CONCENTRATIONS FOR SPRING CASE. Isopleths at 1, 2, 4, ..., $\mu\text{g}/\text{m}^3$; plume maxima in boldface.

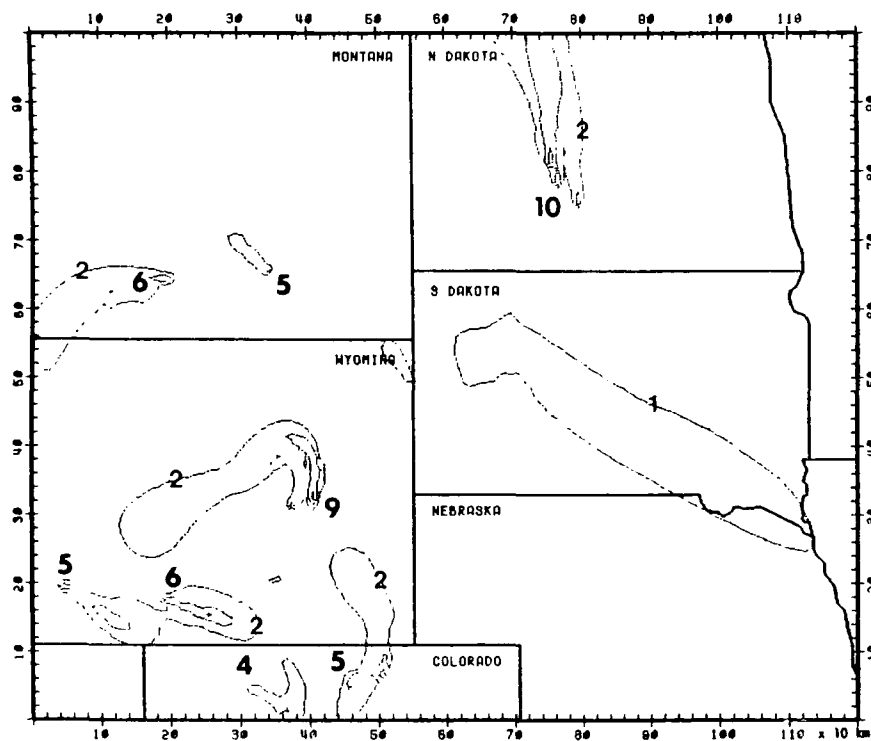


(c) 1700-2000 MST 5 April 1976; 1976 emissions

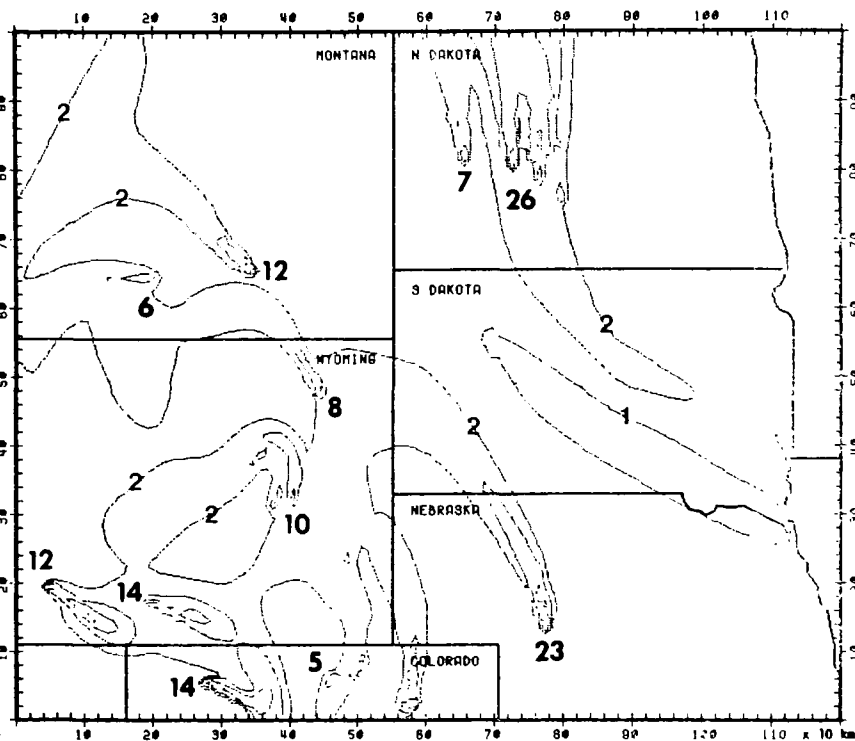


(d) 1700-2000 MST 5 April 1976; 1986 emissions

FIGURE 27 (Continued)



(e) 800-1100 MST 6 April 1976; 1976 emissions



(f) 800-1100 MST 6 April 1976; 1986 emissions

FIGURE 27 (Concluded)

wind pattern. Depleted areas (dotted regions) again appear in the emissions-free corridor.

C. SUMMER

The 850 millibar maps for the summer case appear in Figure 28. Figure 29 gives SO_2 concentrations 33 and 51 hours after the start of the simulation. It shows slow westerly flow in Wyoming and Colorado and a strong southerly flow through the Dakotas.

D. AIR QUALITY IMPACTS

Certain behavior is common to all three cases. The predicted 1986 SO_2 concentrations are seldom more than double the 1976 values, but the area impacted by the $2 \mu\text{g}/\text{m}^3$ isopleth increases dramatically (see especially Figures 27e, f and 29c, d). The deposition rate showed considerable temporal and spatial variation (see Figure 12); in all cases deposition rates were generally lowest in the early morning and highest in the late afternoon. Predicted SO_2 concentrations reflected this; they were generally highest at dawn and lowest at dusk.

Ten monitoring stations measured SO_2 at rural sites in the NGP. Most stations measured only one 24-hour-average concentration in each multi-day episode. These data are displayed in Figure 30; most of the measurements were less than the $4 \mu\text{g}/\text{m}^3$ noise limit of the instruments (as were most of the model predictions). These data agree qualitatively with the model predictions.

The EPA significant deterioration increments for Class I and Class II regions are given in Table 20. Currently the entire Northern Great Plains is a Class II region. However, it has been proposed that some areas be reclassified as Class I. In our simulations the Class I increments were exceeded by the 1986 energy developments only near plant stacks; Class II increments were never violated. It should be noted, however, that in view

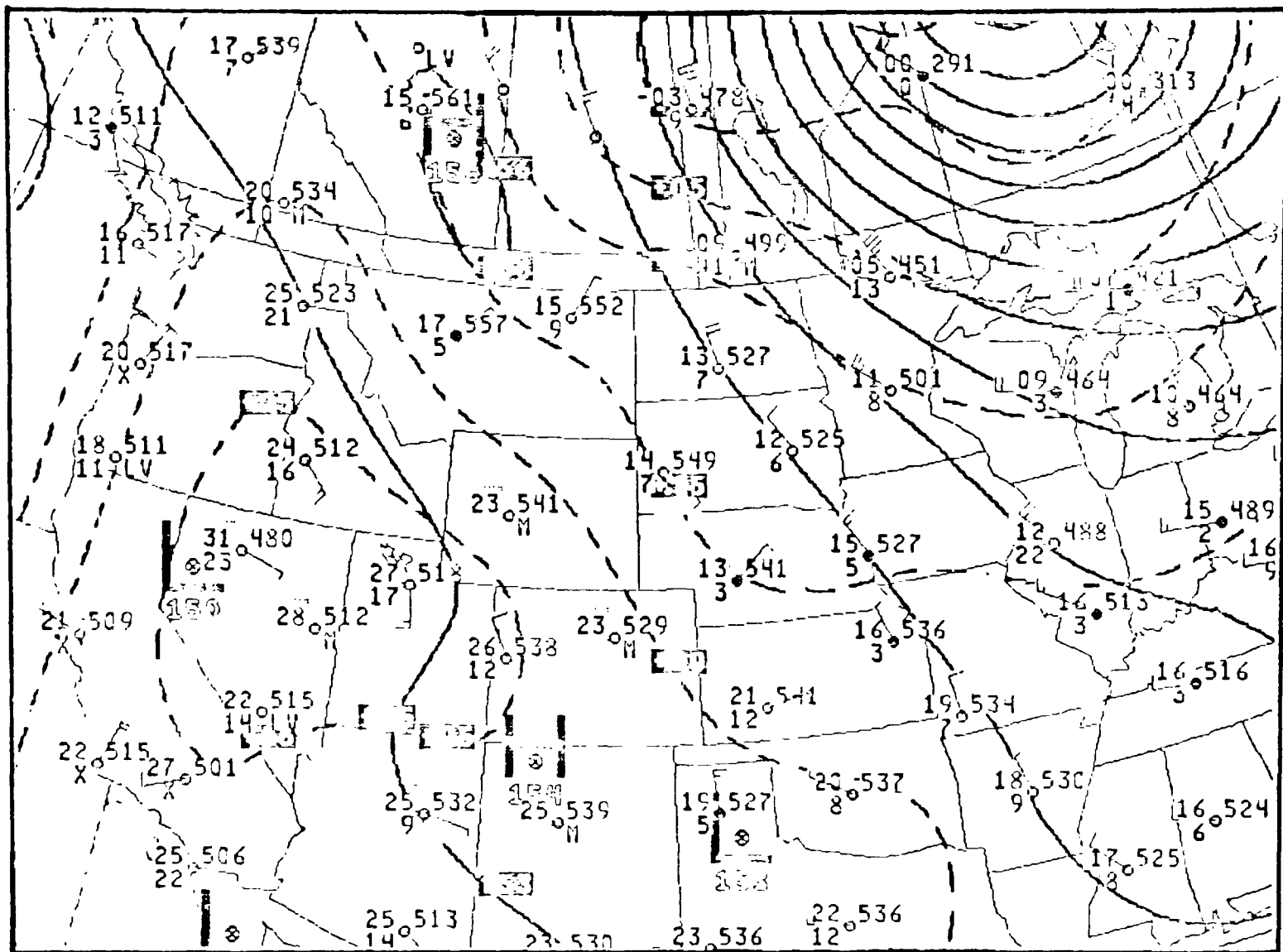
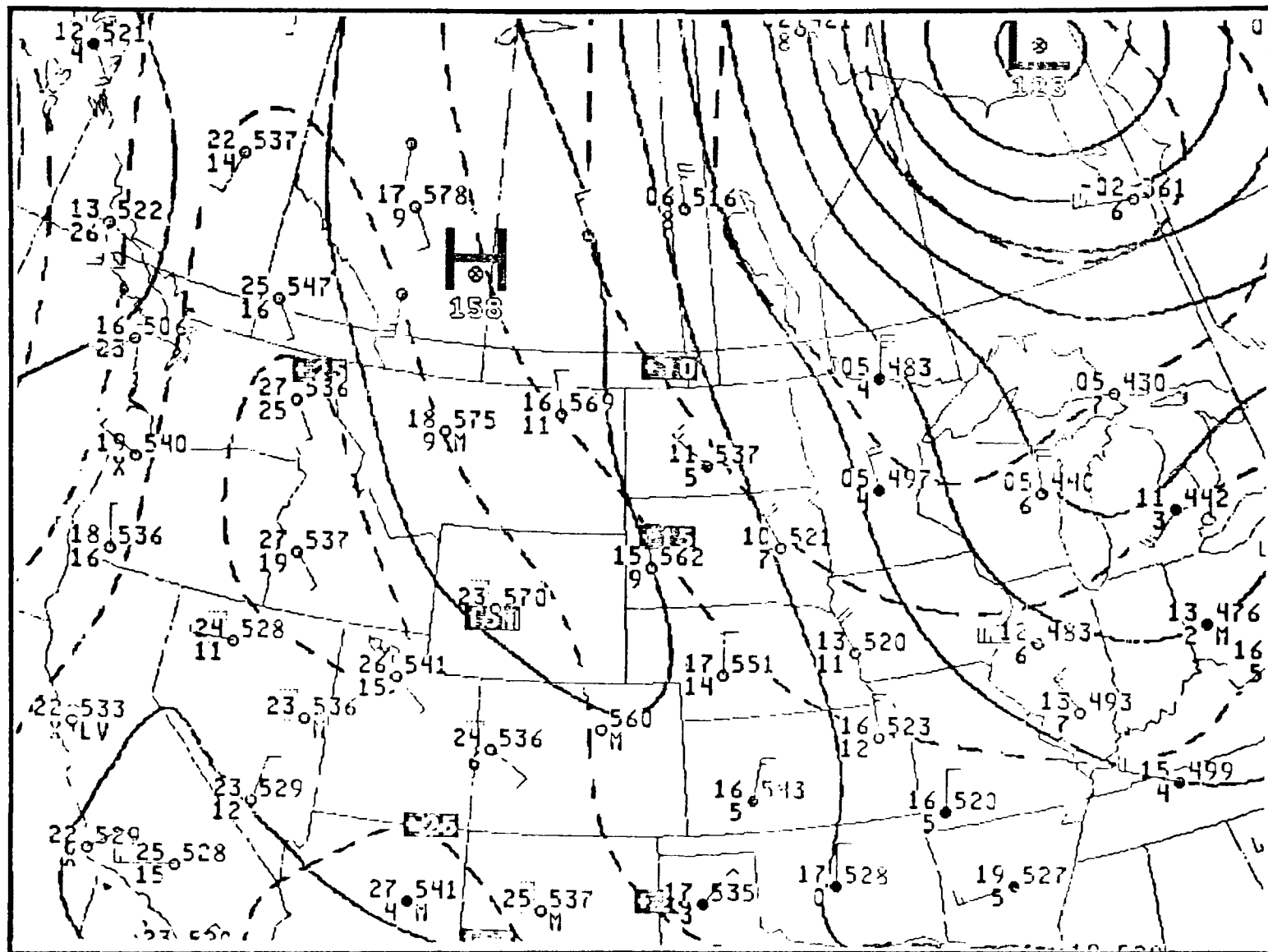
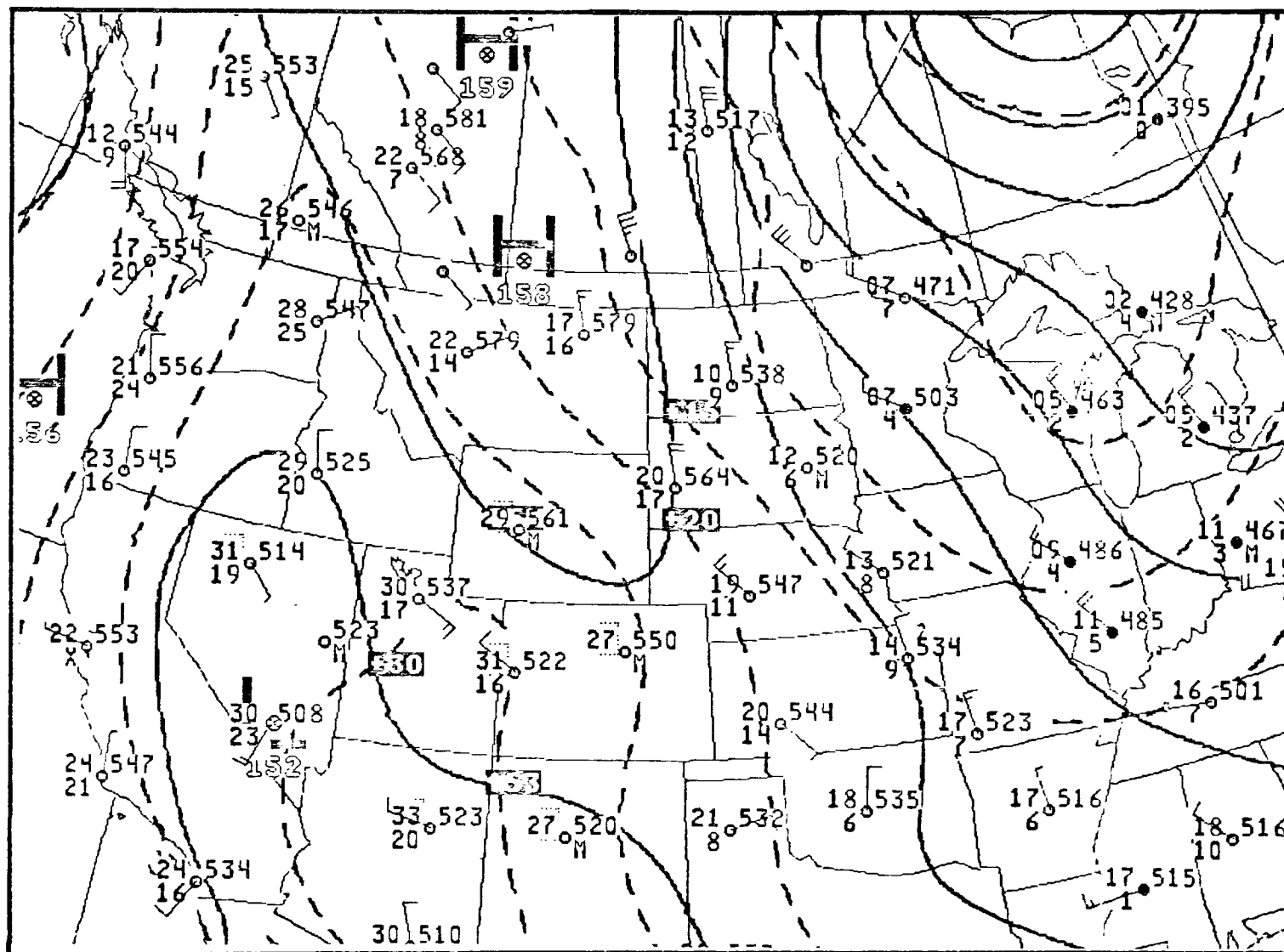


FIGURE 23. WINDS AT 850 MILLIBARS ALTITUDE DURING 9-12 JULY 1975



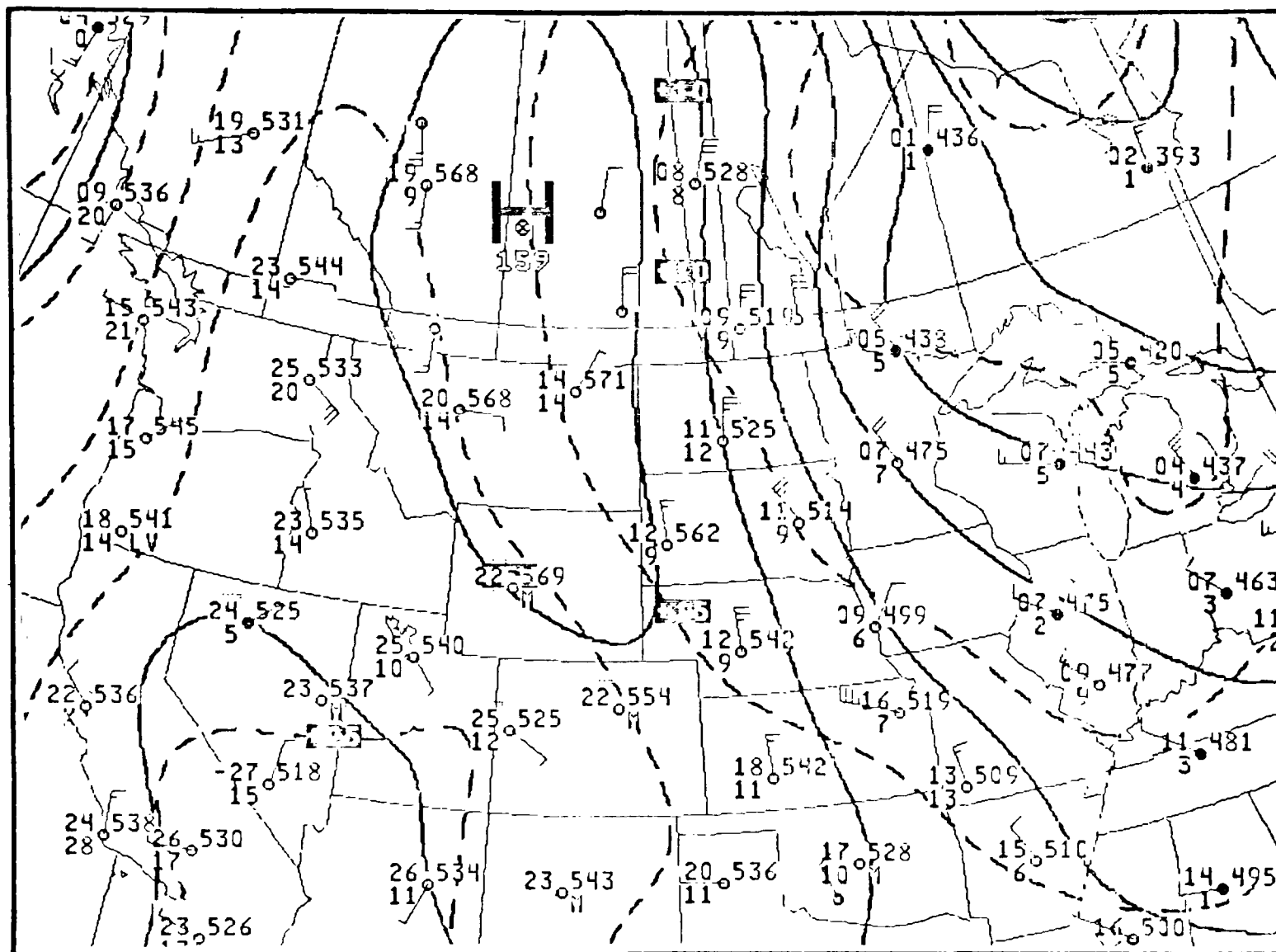
(c) 500 MST 10 July 1975

FIGURE 28 (Continued)



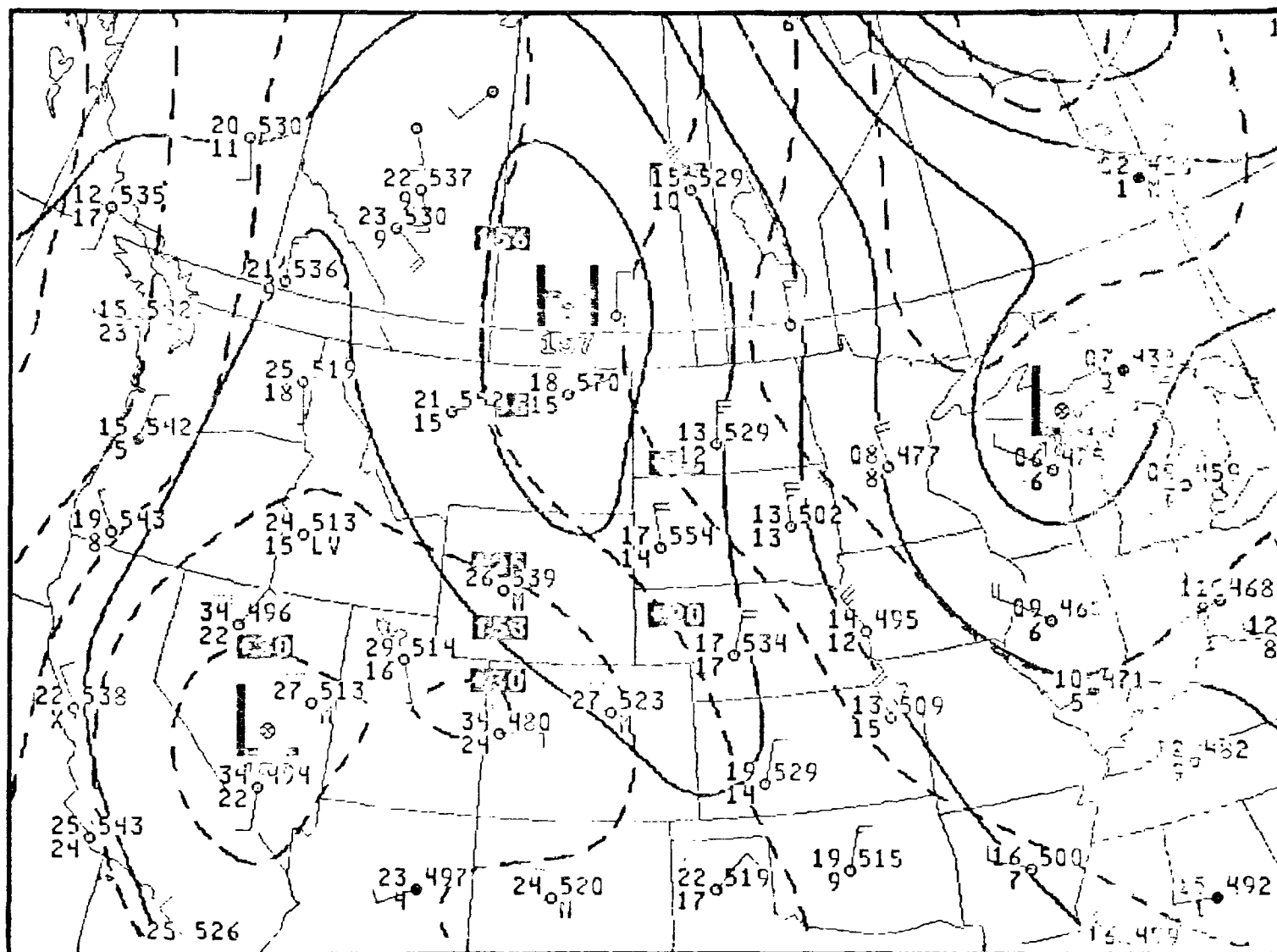
(d) 1700 MST 10 July 1975

FIGURE 28 (Continued)



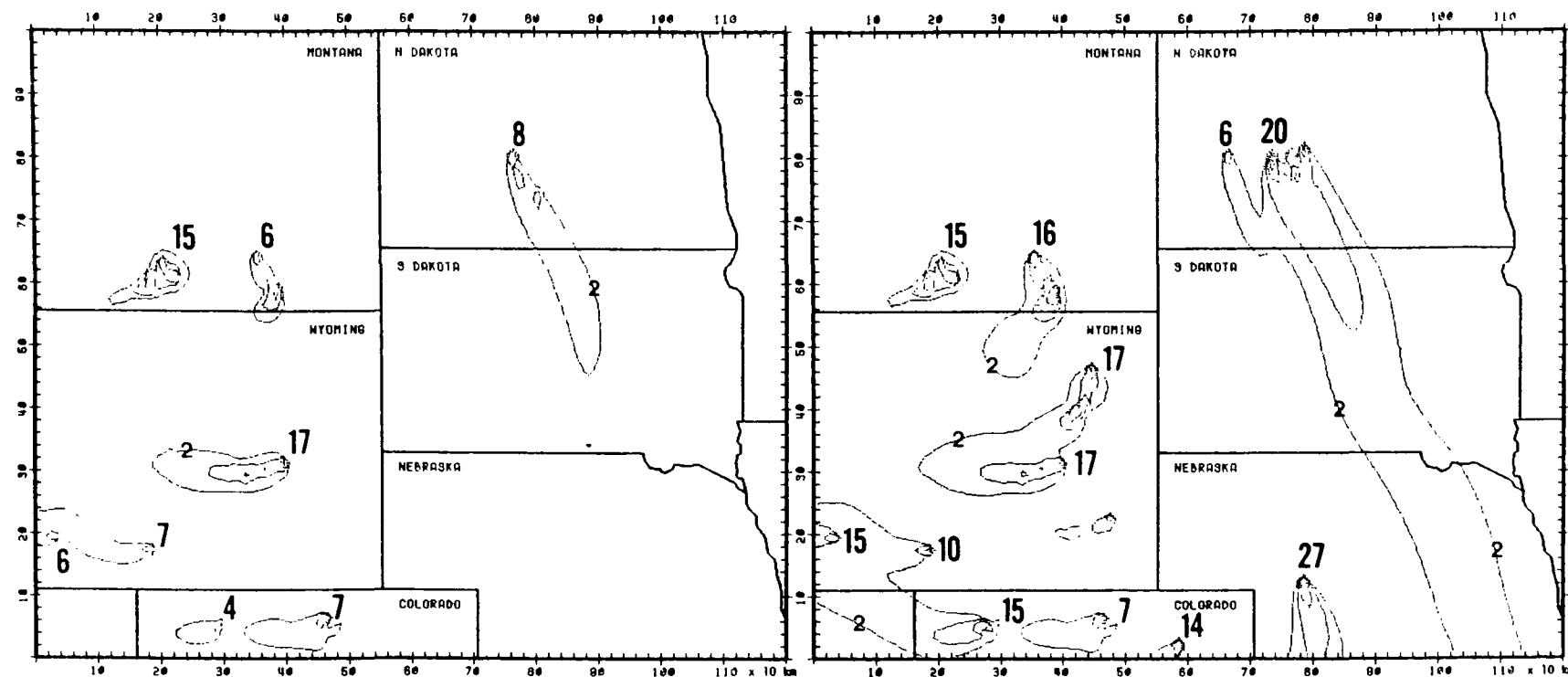
(e) 500 MST 11 July 1975

FIGURE 28 (Continued)



(f) 1700 MST 11 July 1975

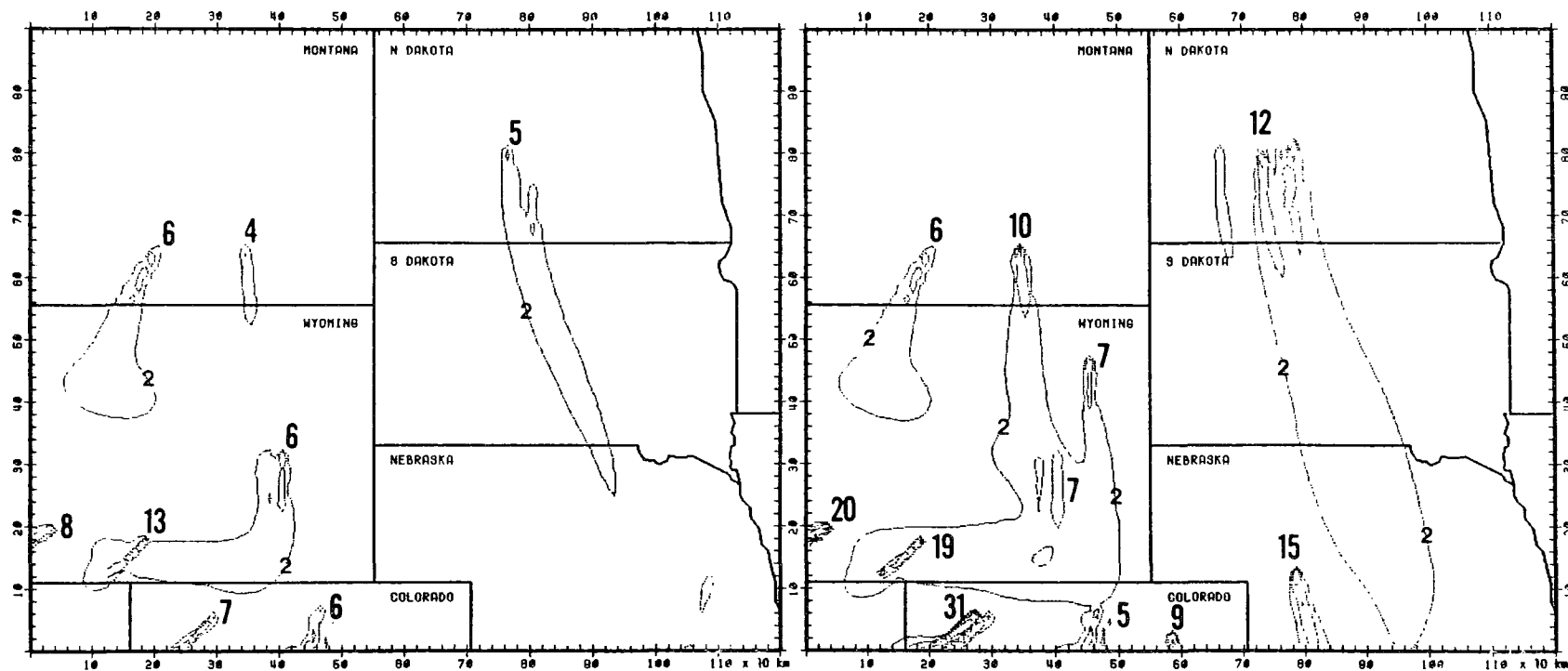
FIGURE 28 (Concluded)



(a) 1400-1700 MST 10 July 1975; 1976 emissions

(b) 1400-1700 MST 10 July 1975; 1986 emissions

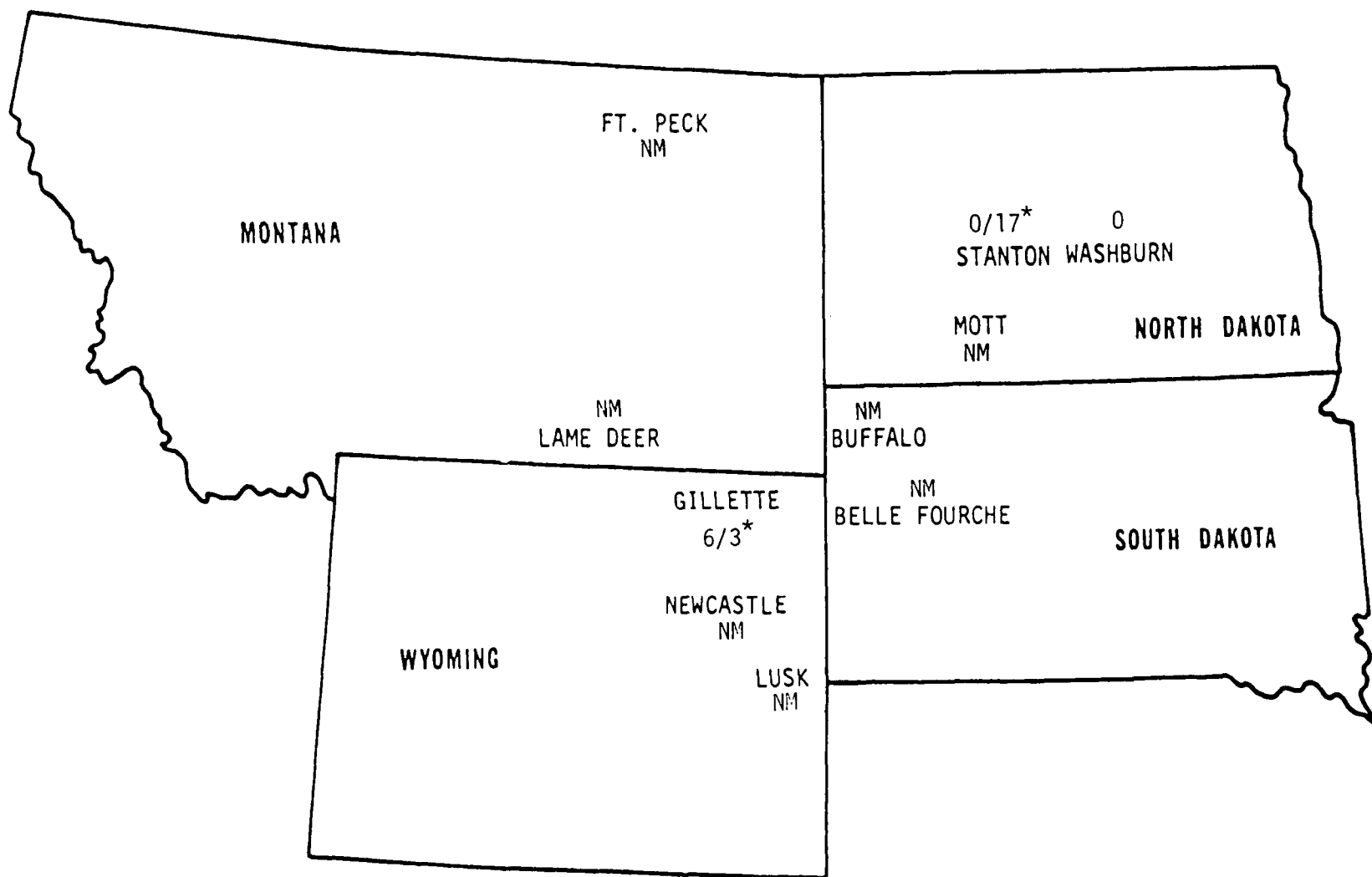
FIGURE 29. PREDICTED SO_2 CONCENTRATIONS FOR SUMMER CASE. Isopleths at 1, 2, 4, ..., $\mu\text{g}/\text{m}^3$; plume maxima in boldface.



(c) 800-1100 MST 11 July 1975; 1976 emissions

(d) 800-1100 MST 11 July 1975; 1986 emissions

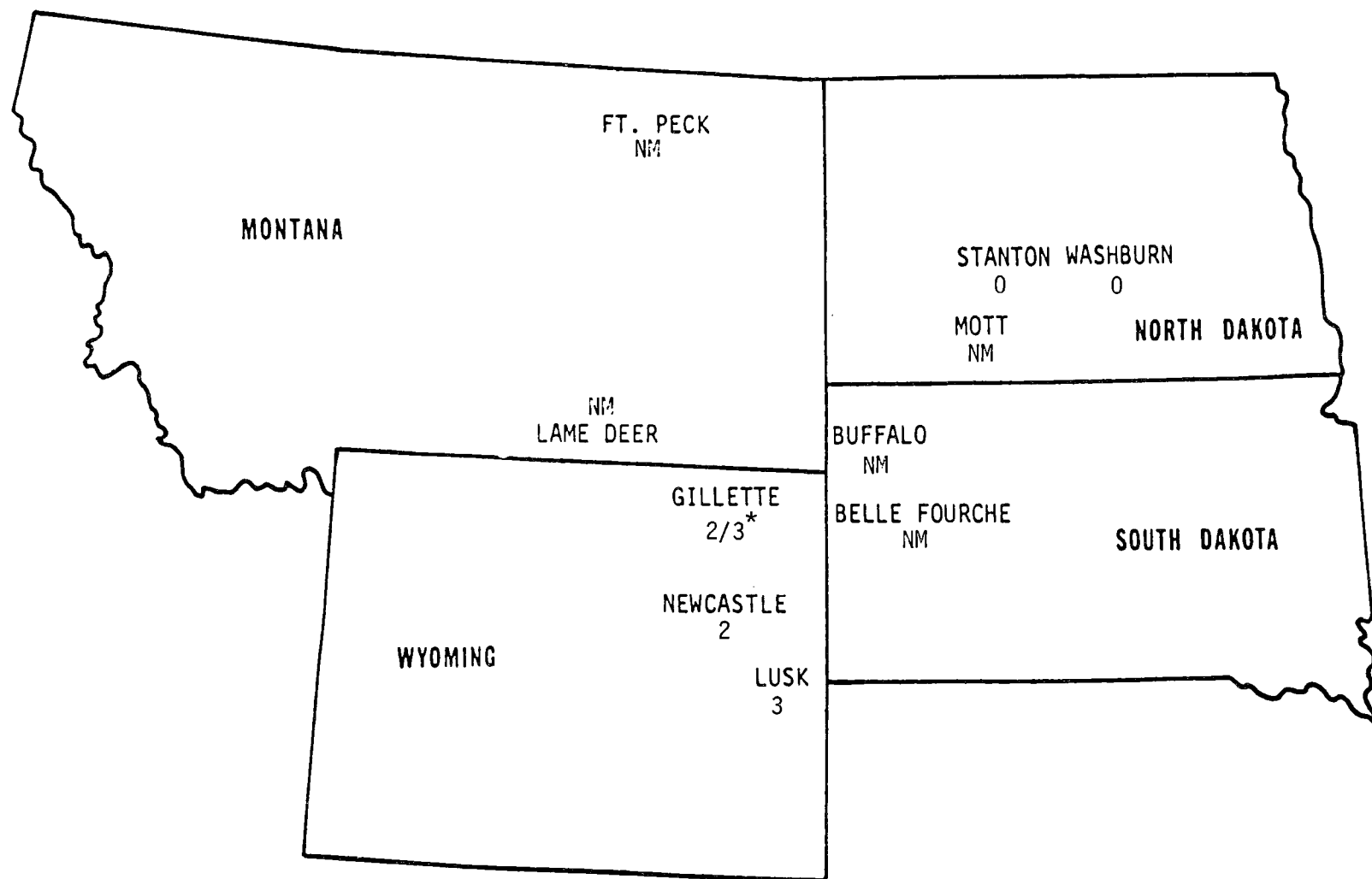
FIGURE 29 (Concluded)



* Second value is the maximum three-hour average obtained from a continuous SO₂ monitor at the same site; NM means no measurement was made.

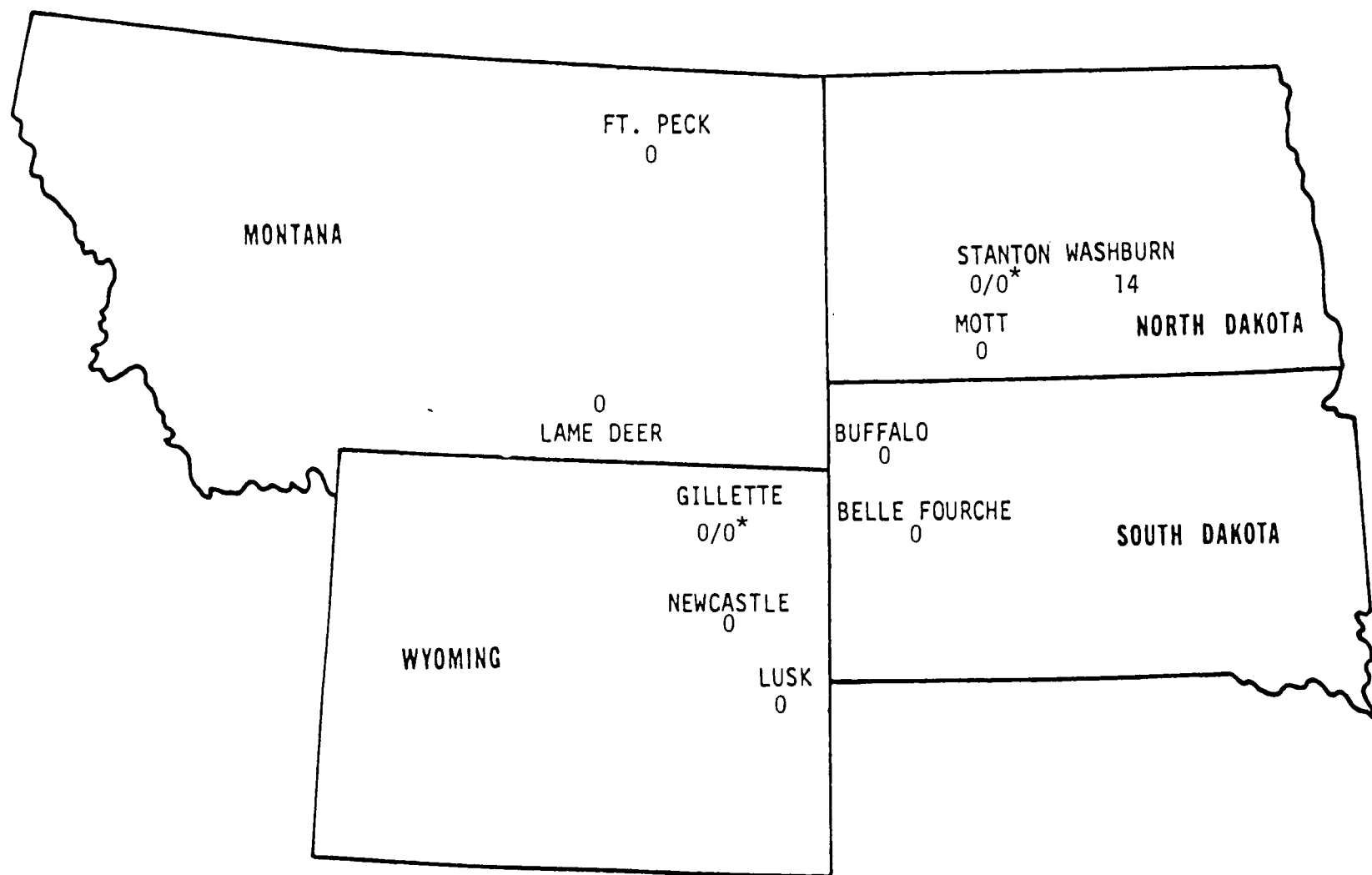
(a) 27-31 January 1976

FIGURE 30. 24-HOUR-AVERAGE SO₂ MEASUREMENTS (IN µg/m³) IN THE NORTHERN GREAT PLAINS



(b) 4-7 April 1976

FIGURE 30 (Continued)



(c) 9-11 July 1975

FIGURE 30 (Concluded)

of the approximations invoked in the present model formulation, higher uncertainties are associated with model predictions near major emissions sources.

The regional model also predicted sulfate concentrations for the same episodes. The 0.3 percent per hour conversion rate for SO_2 to sulfate selected for this investigation did not result in significant sulfate production in the Northern Great Plains. Consequently, sulfate concentrations were largely masked by the $1.5 \mu\text{g}/\text{m}^3$ initial and boundary concentrations. As noted in Chapter VII, sulfate concentrations are increased considerably by a faster conversion rate of 3 percent per hour.

TABLE 20. SIGNIFICANT DETERIORATION INCREMENTS FOR SO_2

| Averaging Period | SO ₂ Increment ($\mu\text{g}/\text{m}^3$) | |
|---------------------|---|----------|
| | Class I | Class II |
| One year | 2 | 15 |
| 24 hours | 5 | 100 |
| 3 hours | 25 | 700 |

Source: Federal Register (1974, 1975).

XII SUMMARY AND CONCLUSIONS FOR PART B

The regional air pollution model described in Part A was applied to the Northern Great Plains to assess the air quality impacts of existing and proposed energy developments utilizing coal resources in that area. Emissions inventories were prepared for the years 1976 and 1986. Three meteorological scenarios, a strong-wind winter case, a stagnation spring case, and a moderate-wind summer case, were selected for the impact analyses. Model simulations were carried out for each combination of emissions inventory and meteorological scenario. Sulfur dioxide and sulfates were considered. In general, the predicted impacts are greatest in spring, intermediate in winter, and lowest in summer. From the present preliminary results it appears that neither the 1976 nor the 1986 emissions as estimated in this study are likely to cause pollutant concentrations significantly higher than background values at locations far from the emissions sources. Also, in our simulations the Class I increments were exceeded by the 1986 energy developments only near plant stacks; Class II increments were never violated.

APPENDIX A
AN ANALYSIS OF NUMERICAL METHODS

APPENDIX A

AN ANALYSIS OF NUMERICAL METHODS

One of the major decisions in the development of the long-range dispersion model is the selection of a suitable numerical method for solving the model equations described in Chapter VI. Therefore, at the outset of this project, an effort was made to carry out a comparative study of different numerical methods with respect to accuracy and efficiency. Three methods were examined:

- > Upstream differencing
- > The SHASTA (Sharp and Smooth Transport Algorithm) method
- > The Egan-Mahoney method.

As discussed in Section 1, the SHASTA method appeared to be the best for the present application and was thus chosen. A detailed analysis of this method can be found in Section 2 of this appendix.

1. COMPARISON OF THREE NUMERICAL METHODS

Mesoscale atmospheric transport is dominated by advection, so in the horizontal direction the numerical method selected for the present project must be able to treat the pure advection case without generating excessive numerical diffusion. As a test we compared three numerical methods for the solution of a two-dimensional advection problem with a constant wind on a 40 x 40 grid of 25-kilometer squares:

$$c_t + (uc)_x + (vc)_y = 0 \quad . \quad (39)$$

The wind was a uniform 25 and 12.5 km/hr in the x and y directions, respectively. A point source yielding a cell-averaged concentration

of $20 \mu\text{g}/\text{m}^3$ was located on the upwind boundary. The background concentration was $2 \mu\text{g}/\text{m}^3$; physical diffusion was zero.

The first method tested was a fractional step upstream differencing method:

$$\begin{aligned} c_{ij}^* &= (1 - \sigma_x) c_{ij}^n + \sigma_x c_{i-1,j}^n \quad , \quad (\text{Step 1}) \\ c_{ij}^{n+1} &= (1 - \sigma_y) c_{ij}^* + \sigma_y c_{i,j-1}^* \quad , \quad (\text{Step 2}) \end{aligned} \quad (40)$$

where $\sigma_x = u\Delta t/\Delta x$ and $\sigma_y = v\Delta t/\Delta x$. As shown in Figure 31, this method is highly inaccurate. (Since physical diffusion is zero any plume spread is due to numerical diffusion.) The lowest-order error term in an individual fractional step is

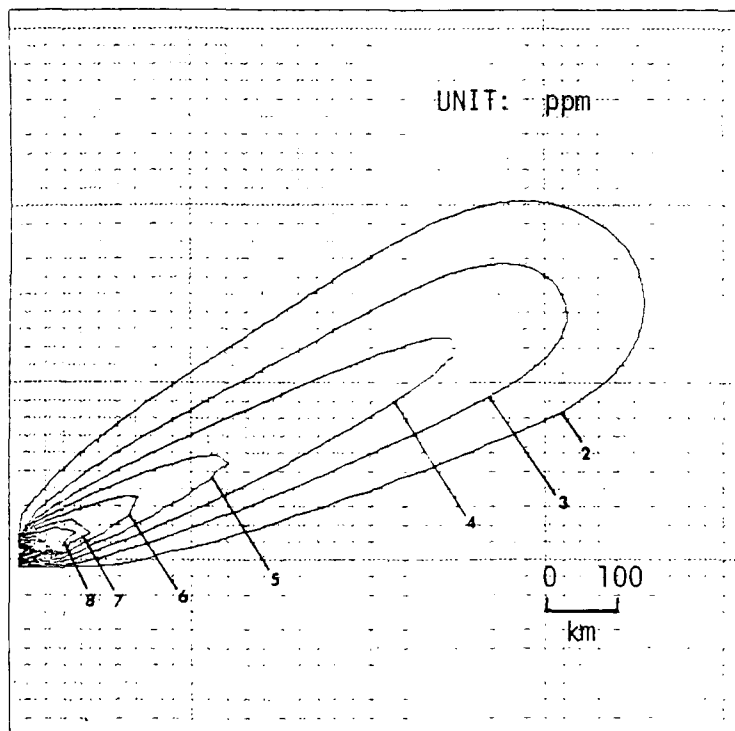
$$\frac{u}{2} (\Delta x - u\Delta t) \frac{\partial^2 c}{\partial x^2} \quad . \quad (41)$$

In the first test case [Figure 31(a)], $\sigma_x = 1$. Therefore this term in the first fractional step is always zero. In fact the transport in the x-direction is indeed exact, hence the plume appears to chop off abruptly as expected. Figure 31(b) shows the same simulation with $\sigma_x = 1/2$, for which the effective numerical diffusion in the x-direction is $4.3 \times 10^4 \text{ m}^2/\text{sec}$.

Figure 32 shows the performance of a fractional step version of the SHASTA method:

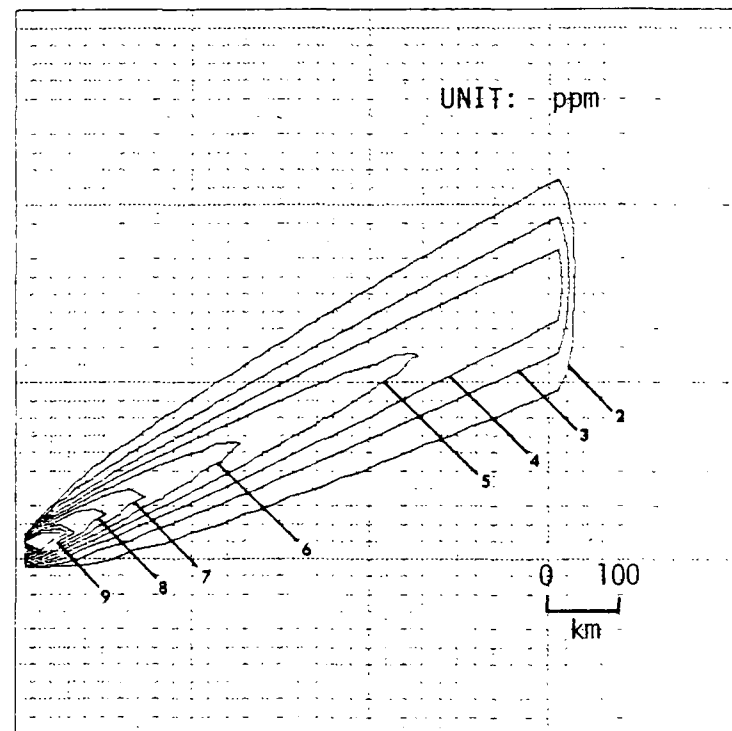
$$\begin{aligned} \tilde{c}_{ij} &= c_{ij}^n + \sigma_x D_0^{(1)} c_{ij}^n + \left(\frac{1}{8} + \frac{\sigma_x^2}{2} \right) D_+^{(1)} D_-^{(1)} c_{ij}^n \quad , \\ c_{ij}^* &= \tilde{c}_{ij} - \frac{1}{8} D_+^{(1)} D_-^{(1)} \tilde{c}_{ij} \quad , \quad (\text{Step 1}) \end{aligned}$$

DISPERSION OF A SINGLE PLUME



(a) $\sigma_x = 1/2, \sigma_y = 1/4$

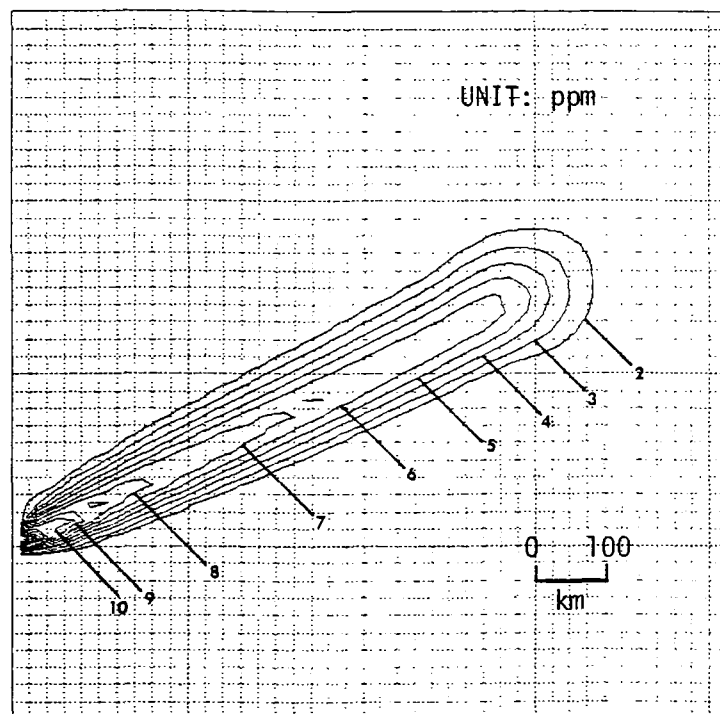
DISPERSION OF A SINGLE PLUME



(b) $\sigma_x = 1, \sigma_y = 1/2$

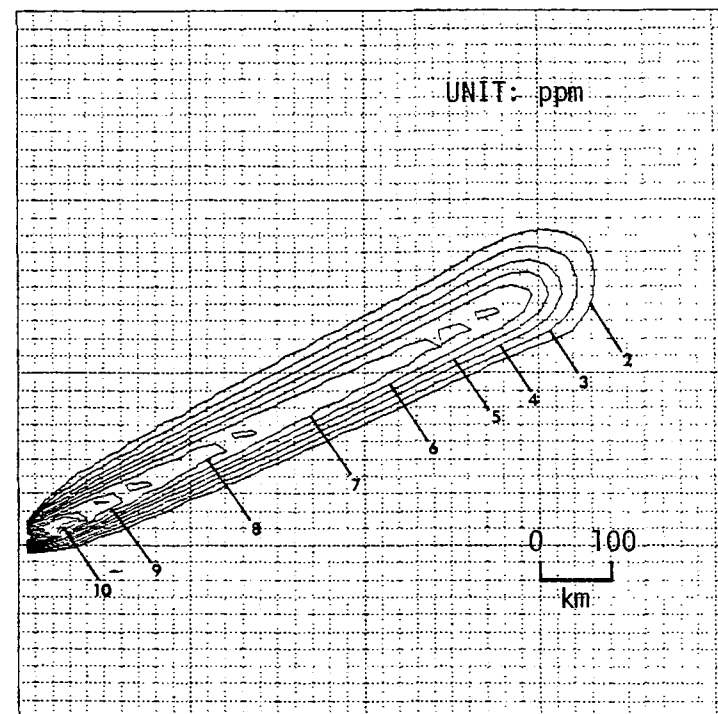
FIGURE 31. PREDICTED CONCENTRATION DISTRIBUTIONS USING THE UPSTREAM DIFFERENCE SCHEME

DISPERSION OF A SINGLE PLUME



(a) $\sigma_x = 1/4, \sigma_y = 1/8$

DISPERSION OF A SINGLE PLUME



(b) $\sigma_x = 1/2, \sigma_y = 1/4$

FIGURE 32. PREDICTED CONCENTRATION DISTRIBUTIONS USING THE SHASTA METHOD

$$\tilde{c}_{ij} = c_{ij}^* + \sigma_y D_0^{(2)} c_{ij}^* + \left(\frac{1}{8} + \frac{\sigma_y^2}{2} \right) D_+^{(2)} D_-^{(2)} c_{ij}^* ,$$

$$c_{ij}^{n+1} = \tilde{c}_{ij} - \frac{1}{8} D_+^{(2)} D_-^{(2)} \tilde{c}_{ij} . \quad (\text{Step 2}) \quad (42)$$

The computed plume profile is reasonably contained in a corridor with a constant width of six cells and is relatively independent of σ_x and σ_y . The lowest-order truncation errors in a single fractional step of the SHASTA method are

$$k_1 \frac{\partial^3 c}{\partial x^3} + k_2 \frac{\partial^4 c}{\partial x^4} , \quad (43)$$

where

$$k_1 = \frac{u}{6} \left(\Delta t^2 u^2 - \frac{\Delta x^2}{4} \right)$$

and

$$k_2 = \frac{u^4 \Delta t^3}{24} - \frac{u^2 \Delta t \Delta x^2}{48} - \frac{3 \Delta x^4}{192 \Delta t} .$$

Numerical error is generated by dispersive errors from the c_{xxx} term, and diffusive errors from the c_{xxxx} term, so we cannot characterize pseudo-diffusion by the simple coefficient in the c_{xx} term. When $\phi_x = 1/2$, the c_{xxx} term vanishes and the error becomes purely diffusive and thus easy to analyze.

Consider the two equations



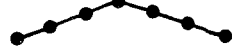
$$\begin{aligned} c_t &= k_0 c_{xx} & c(0) &= e^{i\omega x} \\ c_t &= -k_2 c_{xxxx} & c(0) &= e^{i\omega x} \end{aligned} \quad (44a)$$

which have the solutions

$$\begin{aligned} c(t) &= e^{i\omega x} e^{-k_0 \omega^2 t} \\ c(t) &= e^{i\omega x} e^{-k_2 \omega^4 t} . \end{aligned} \quad (44b)$$

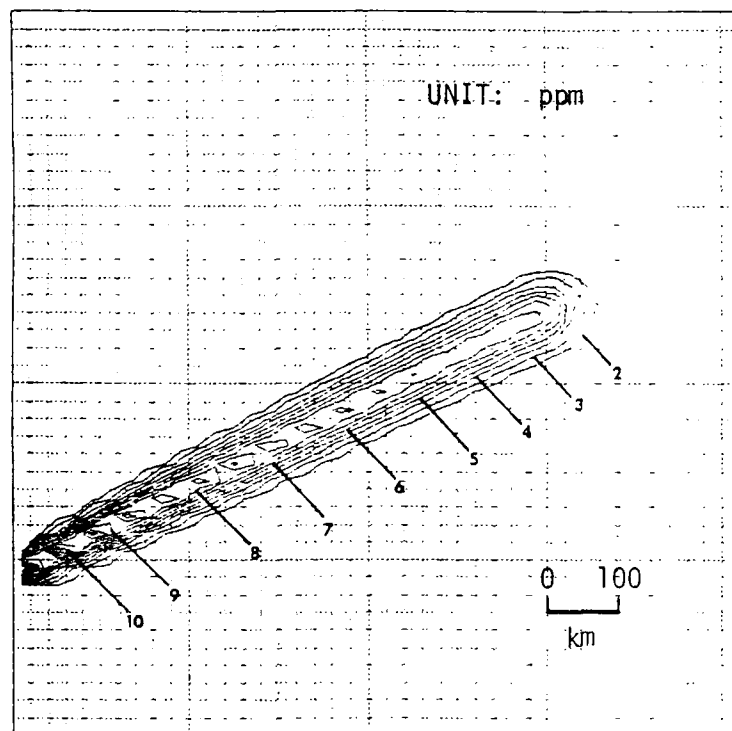
When $\sigma_x = 1/2$ the effective coefficient of pseudo-diffusion generated by SHASTA is thus $-k_2\omega^2$. This is wavenumber-dependent; in our test case the shortest wave has a wavelength of $20\pi/10^6$ (meters) $^{-1}$ and is affected by a numerical diffusion of 1.2×10^4 m²/sec. All other waves, being longer, diffuse more slowly. Table 21 compares the numerical diffusion associated with upstream differencing and the SHASTA method for various wavelengths in the first test problem. Note that these results are dependent on grid size, so decreasing the cell width will decrease the numerical diffusion. The computations for the SHASTA method are based on the assumption that $\sigma_x = 1/2$. Although Figures 31 through 33 indicate that SHASTA is less sensitive to σ_x and σ_y than the other methods, this is still an optimal condition; the entries in Table 21 are not worst case. Similarly, the estimates for the upstream differencing method are not upper bounds either; as σ_x decreases both methods generate greater errors.

TABLE 21. EFFECTIVE DIFFUSION COEFFICIENTS IN THE x-DIRECTION FOR THE FIRST TEST PROBLEM. $\sigma_x = 1/2$, $\Delta x = 25$ km.

| Wave | Wavenumber (m ⁻¹) | Effective Diffusion Coefficient (m ² /sec) | |
|---|----------------------------------|--|-------------------|
| | | Upstream Differencing | SHASTA |
|  | $20\pi/10^6$ | 4.3×10^4 | 1.2×10^4 |
|  | $10\pi/10^6$ | 4.3×10^4 | 3.0×10^3 |
|  | $5\pi/10^6$ | 4.3×10^4 | 7.5×10^2 |

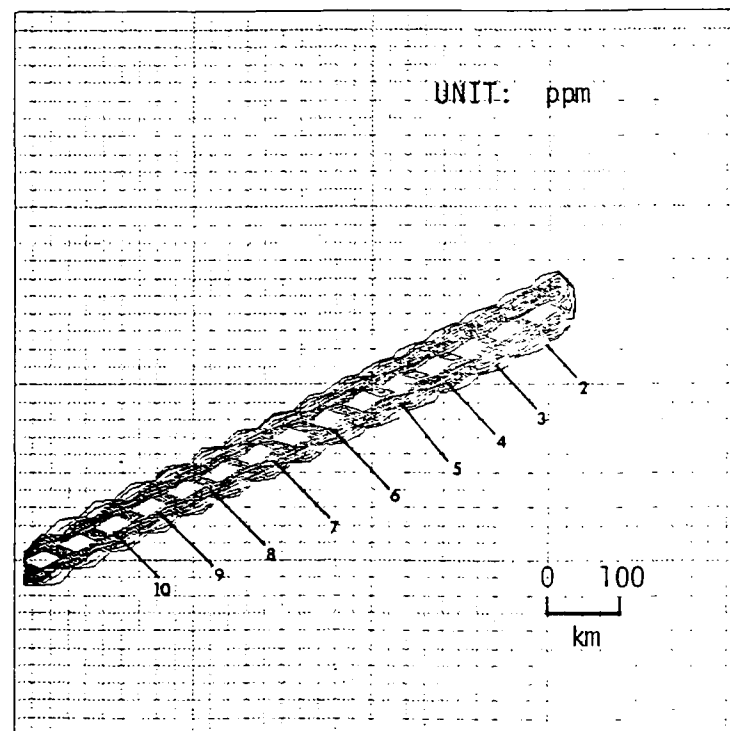
The third method tested in the present study was the two-dimensional Egan-Mahoney method, which computes the pollutant concentration and the first and second moments of that concentration in each grid cell. By calculating these subgrid-scale details the Egan-Mahoney

DISPERSION OF A SINGLE PLUME



(a) $\sigma_x = 1/2, \sigma_y = 1/4$

DISPERSION OF A SINGLE PLUME



(b) $\sigma_x = 1, \sigma_y = 1/2$

FIGURE 33. PREDICTED CONCENTRATION DISTRIBUTIONS USING THE EGAN AND MAHONEY METHOD

method achieves considerable accuracy. Details of the method can be found in Egan and Mahoney (1972a,b) and Pedersen and Prahm (1974). Figures 33(a) and 33(b) show that in the Egan-Mahoney solution with $\sigma_x = 1/2$ the plume corridor is 5 cells wide; with $\sigma_x = 1$ the width is just 3 cells. However, as with upstream differencing, the x-direction transport is essentially exact when $\sigma_x = 1$ so that the high quality solution shown in Figure 33(b) must be interpreted with care.

The authors are not aware of any estimates of the numerical diffusion associated with the Egan-Mahoney method. Unlike the methods discussed above, the numerical error in this method is dependent upon the concentration itself. The method will follow a $10 \mu\text{g}/\text{m}^3$ spike through a zero background concentration without generating any numerical diffusion, but a $110 \mu\text{g}/\text{m}^3$ spike cannot be followed through a $100 \mu\text{g}/\text{m}^3$ background concentration without considerable diffusive error. In our application background concentrations should be low, so that, as Figure 33 indicates, the Egan-Mahoney method should be suitably accurate for the present application.

Table 22 shows the relative speed of each method. The Egan-Mahoney method produces a better solution than SHASTA, but is an order of magnitude slower, and hence much more expensive. In terms of overall efficiency, it appears that the SHASTA method possess the blend of speed and accuracy most suited to our application.

TABLE 22. ESTIMATED COMPUTATION TIME REQUIRED
TO FOLLOW A PLUME FOR 750 km

| Numerical Method | σ_x^* | Number of Steps | Required Computing Time [†] |
|-----------------------|--------------|-----------------|--------------------------------------|
| Upstream differencing | 1 | 30 | 0.187 sec |
| SHASTA | 1/2 | 60 | 0.845 sec |
| Egan and Mahoney | 1 | 30 | 11.0 sec |

* $\sigma_x = u\Delta t/\Delta x$. The σ 's associated with each method are optimal for that method. Δx is 25 km.

† On a CDC 7600 computer.

2. ANALYSIS OF THE SHASTA METHOD

In Section 1 of this appendix we examined the psuedo-diffusion associated with three numerical methods. Based on considerations of accuracy and computation time, we selected the SHASTA method for use in our model. Now we will focus on an analysis of the stability and formal accuracy of SHASTA for the simplified constant wind case.

a. Accuracy

Under constant wind conditions the Step 1 difference scheme [see Chapter VI, Eq.(10)] may be written as the following one-step scheme:

$$\begin{aligned}
 c_{ij} = & \left(\frac{\epsilon}{16} - \frac{\epsilon^2}{16} - \frac{1}{64} \right) c_{i+2,j}^n + \left(\alpha + \frac{1}{16} - \frac{5\epsilon}{8} + \frac{3\epsilon^2}{4} \right) c_{i+1,j}^n \\
 & + \left(\frac{31}{32} + \lambda - 2\alpha - \frac{11\epsilon^2}{8} \right) c_{ij}^n + \left(\alpha + \frac{1}{16} + \frac{5\epsilon}{8} + \frac{3\epsilon^2}{4} \right) c_{i-1,j}^n \\
 & + \left(\frac{-\epsilon}{16} - \frac{\epsilon^2}{16} - \frac{1}{64} \right) c_{i-2,j}^n \quad , \quad (45)
 \end{aligned}$$

where

$$\begin{aligned}
 \epsilon &= u\Delta t/\Delta x \\
 \alpha &= k_x \Delta t/\Delta x^2 \\
 \lambda &= \left(k - \frac{w}{\Delta H} \right) \Delta t \quad .
 \end{aligned}$$

Substituting the true solution into Eq. (45), we obtain c_{ij}^{**} , $c_{i+2,j}^n$, $c_{i+1,j}^n$, $c_{i-1,j}^n$, and $c_{i-2,j}^n$ by Taylor series expansion about c_{ij}^n . {At the moment we are considering this fractional step individually, not the scheme as a whole, so we assume $c_{ij}^{**} = c_{ij}[(n+1)\Delta t]$. The result may be simplified and expressed:

$$\begin{aligned} \frac{\partial c}{\partial t} + u \frac{\partial c}{\partial x} = & k_x \frac{\partial^2 c}{\partial x^2} + \left(k - \frac{\omega}{\Delta H} \right) c + \Delta t \left(u^2 \frac{\partial^2 c}{\partial x^2} - \frac{\partial^2 c}{\partial t^2} \right) \\ & - \Delta x^2 \left(\frac{u}{24} \frac{\partial^3 c}{\partial x^3} \right) + O(\Delta t^2 + \Delta x^3) \quad . \end{aligned} \quad (46)$$

Evidently Step 1 (and Step 2) are accurate to first-order in time, second-order in space. But again, the problem is dominated by horizontal advection; if our Step 1 equation is reduced to:

$$\frac{\partial c}{\partial t} + u \frac{\partial c}{\partial x} = 0 \quad (47)$$

Equation (46) becomes

$$\frac{\partial c}{\partial t} + u \frac{\partial c}{\partial x} = \frac{u}{6} \left(\Delta t^2 u^2 - \frac{\Delta x^2}{4} \right) \frac{\partial^3 c}{\partial x^3} + \left(\frac{u^4 \Delta t^3}{24} - \frac{u^2 \Delta t \Delta x^2}{48} - \frac{3 \Delta x^4}{192 \Delta t} \right) \frac{\partial^4 c}{\partial x^4} \quad . \quad (48)$$

This is second-order in both space and time; in the special case where $\epsilon = 1/2$ it is third-order. Thus, the important advection terms in Eq. (1) of Chapter VI should be handled with acceptable accuracy.

The entire three-step method, being a fractional-step formulation, is inherently only accurate to the first order in time. Steps 1 and 2 are second-order in space; Step 3 has no spatial discretization errors, so the overall three-step spatial accuracy is second-order.

b. Computational Stability

Assume that the solution to Eq. (39) may be expanded in a Fourier series and that a separation of time and space variables is possible. A typical Fourier component may be written

$$\psi(t) e^{i\omega x} \quad , \quad (49)$$

where ω is called the wavenumber. We define the amplification factor as

$$r = \psi(t + \Delta t)/\psi(t) \quad . \quad (50)$$

When $\lambda = 0$ the solutions to fractional steps 1 and 2 should be nonincreasing; the stability requirement is thus $|r| \leq 1$ for all wavenumbers. Substituting Eq. (49) into Eq. (45), we find

$$\begin{aligned} r = & \frac{\epsilon i}{8} \sin 2\omega\Delta x - \left(\frac{\epsilon^2}{8} + \frac{1}{32} \right) \cos 2\omega\Delta x - \frac{5\epsilon i}{4} \sin \omega\Delta x \\ & + \left(2\alpha + \frac{1}{8} + \frac{3\epsilon^2}{2} \right) \cos \omega\Delta x + \left(\frac{29}{32} - 2\alpha - \frac{11\epsilon^2}{8} \right) \quad . \quad (51) \end{aligned}$$

Figure 34 shows $|r|$ as a function of $\omega\Delta x$ for $\epsilon = 0.6$ and various values of α . We are assured of stability whenever $\epsilon \leq 0.6$ and $\alpha \leq 0.15$. The condition on α may be relaxed by tightening that on ϵ , but there is no advantage to relaxing this condition. Advection dominates diffusion in the horizontal so that the most restrictive time-step constraint derives from the requirement that $\epsilon \leq 0.6$.

The chemistry and removal term, λ , can also affect the performance of the method. Formal stability will not be lost by adding this undifferentiated term (the Strang Perturbation Theorem), but more is required. When $\lambda\Delta t < 0$ the solution decays in time, and we would like to ensure that our numerical method has the same property. The addition of the chemistry term to Eq. (51) adds $\lambda\Delta t$ to the real part of r . This real part is at a minimum when $k\Delta x = \pi$. From Eq. (51) we calculate that $|r| < 1$ requires

$$-\lambda\Delta t < \frac{7}{4} - 3\epsilon^2 - 4\alpha \quad . \quad (52)$$

In the most restrictive case, $\epsilon = 0.6$ and $\alpha = 0.15$, we have $-\lambda\Delta t < 0.07$. This is easily satisfied in our model since surface deposition and chemical reactions occur at relatively slow rates when compared with atmospheric transport across a 10 km grid cell.

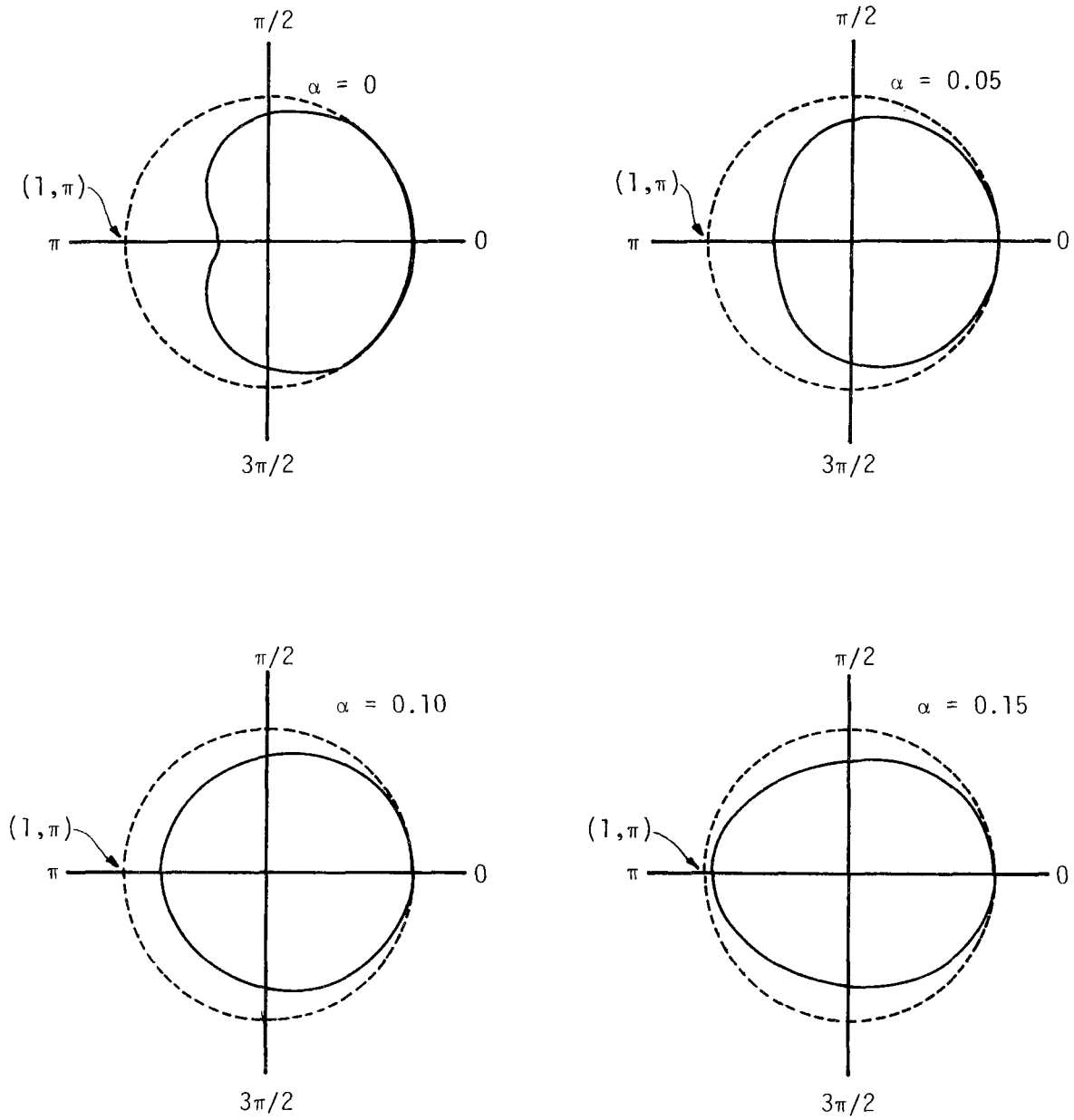


FIGURE 34. VARIATION OF AMPLIFICATION FACTOR $|r|$ AS A FUNCTION OF α FOR $\epsilon = 0.6$

In conclusion, it was shown that the SHASTA method as modified in the present study is stable and accurate, and is capable of producing acceptable results at reasonable cost.

APPENDIX B
COMPILATION OF SIMULATION RESULTS

APPENDIX B

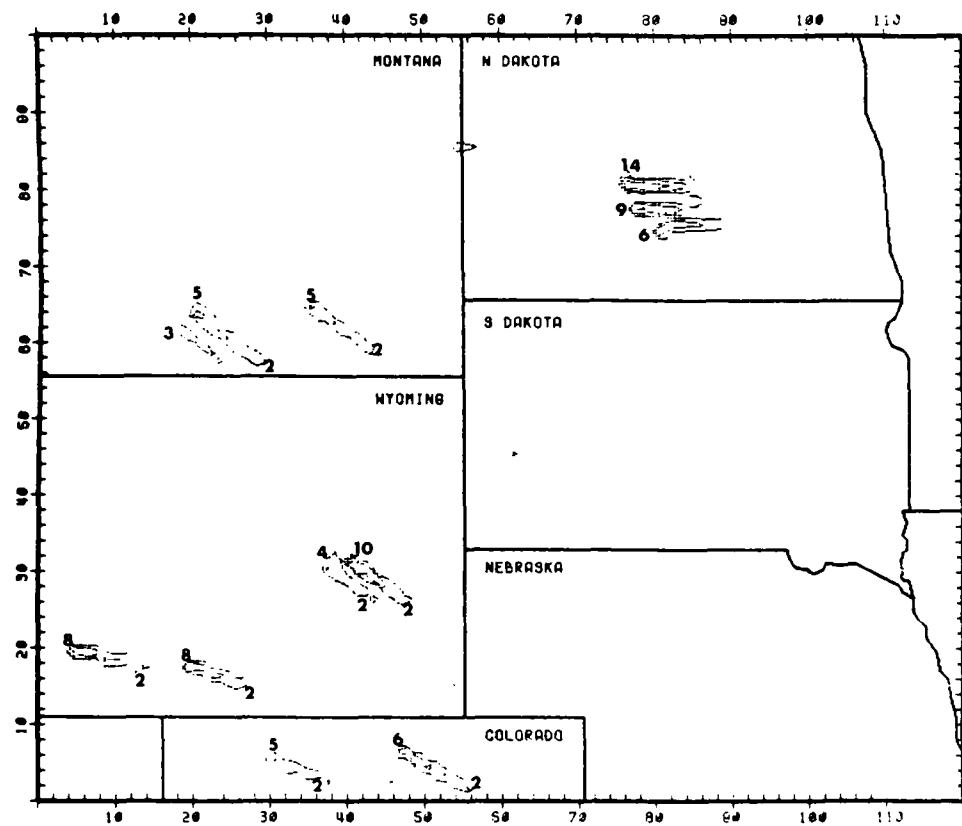
COMPILATION OF SIMULATION RESULTS

The long-range air pollution model developed in this project was used in six simulations:

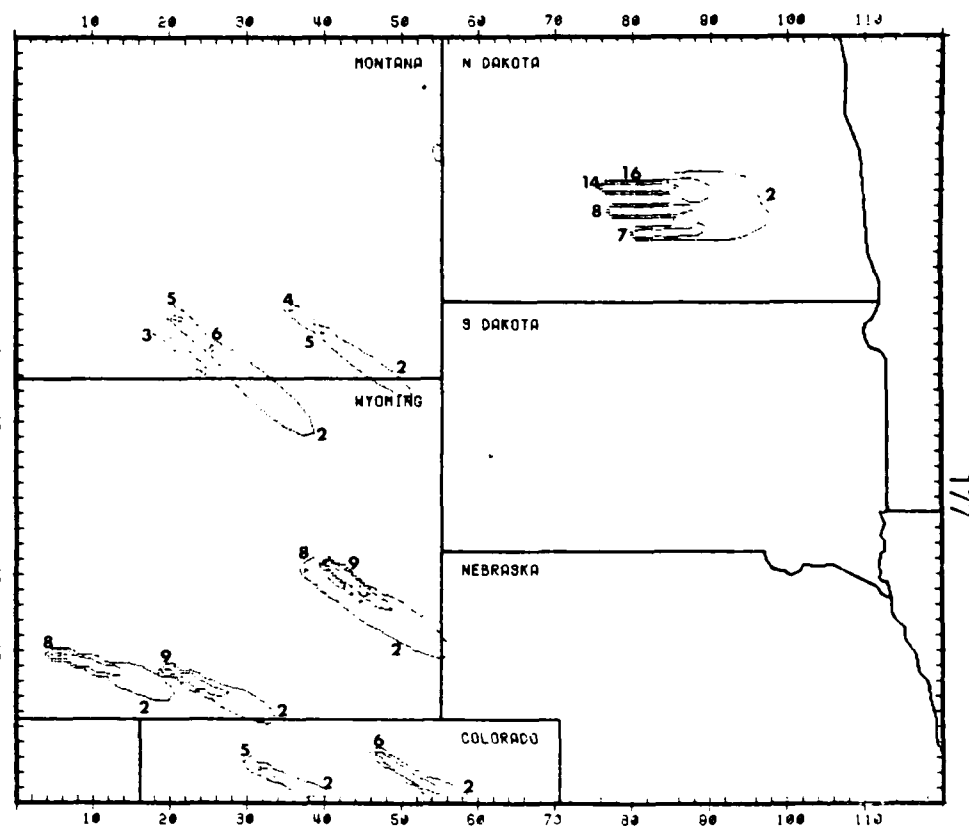
1. 27-31 January 1976 meteorology, 1976 emissions; pp. 176-195
2. 27-31 January 1976 meteorology, 1986 emissions; pp. 196-215
3. 4-7 April 1976 meteorology, 1976 emissions; pp. 216-232
4. 4-7 April 1976 meteorology, 1986 emissions; pp. 233-247
5. 9-11 July 1975 meteorology, 1976 emissions; pp. 248-259
6. 9-11 July 1975 meteorology, 1986 emissions; pp. 260-271.

Isopleth maps of predicted three-hour-average SO_2 concentrations from these simulations are presented in this appendix. Isopleths are drawn for concentrations of 1, 2, 4, 8, ..., $\mu\text{g}/\text{m}^3$. In the maps the axes are in units of 10 km; thus the region of 100 x 120 grid cells is 1000 x 1200 km.

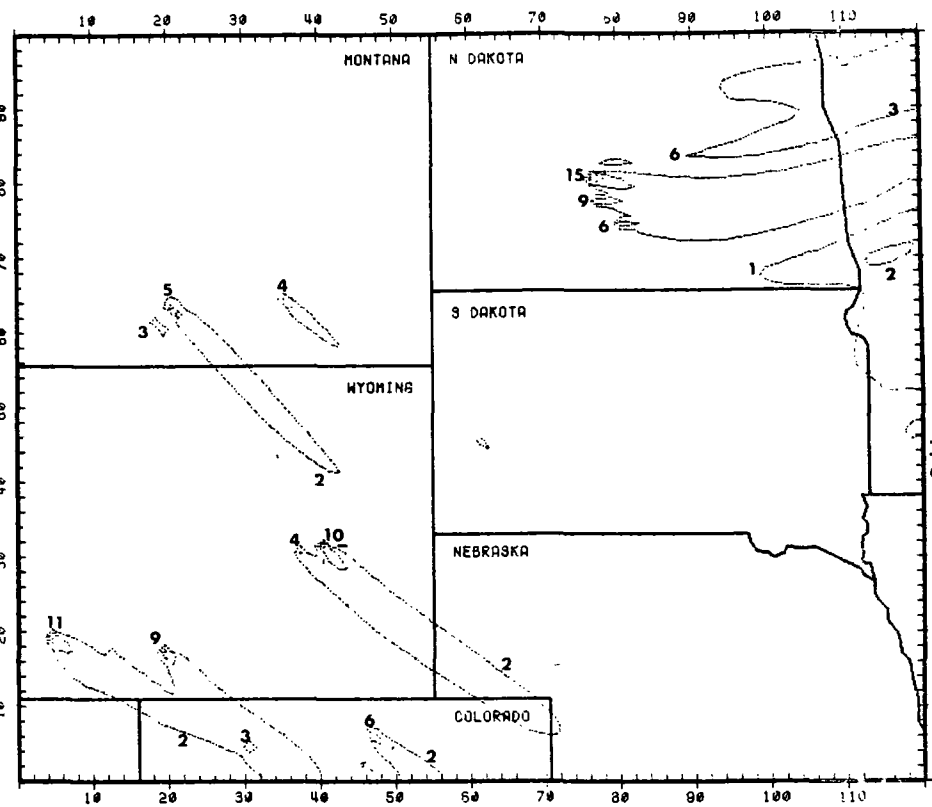
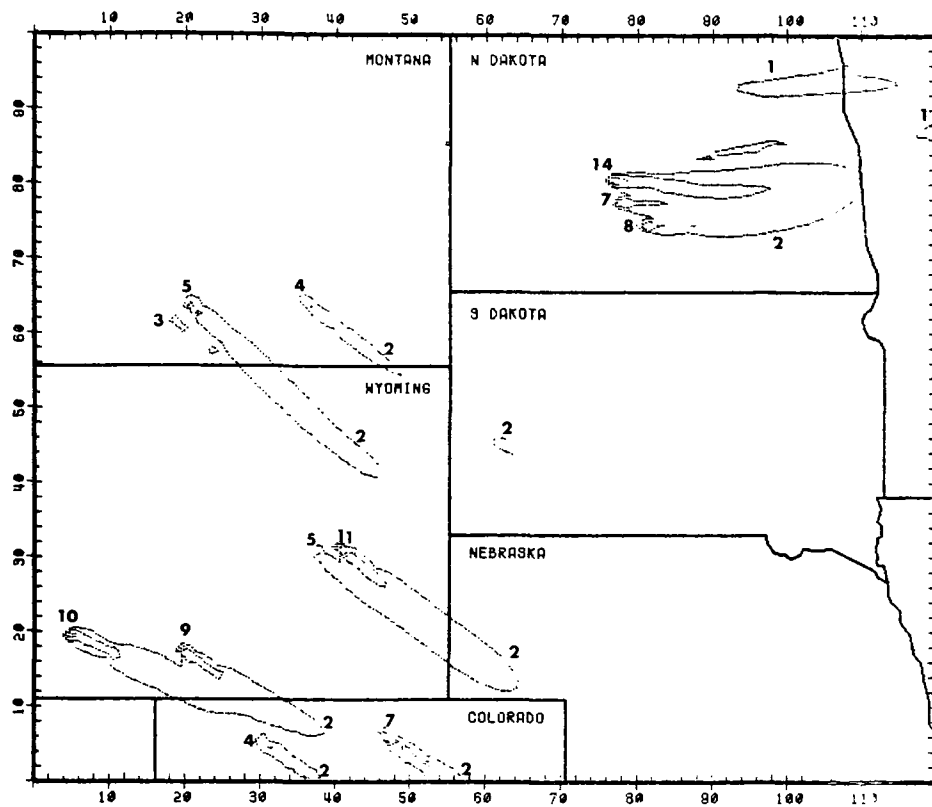
1. 27-31 JANUARY 1976 METEOROLOGY; 1976 EMISSIONS



SO₂ CONCENTRATIONS IN UG/M³ FOR THE HOUR 500-800 MST ON 760117

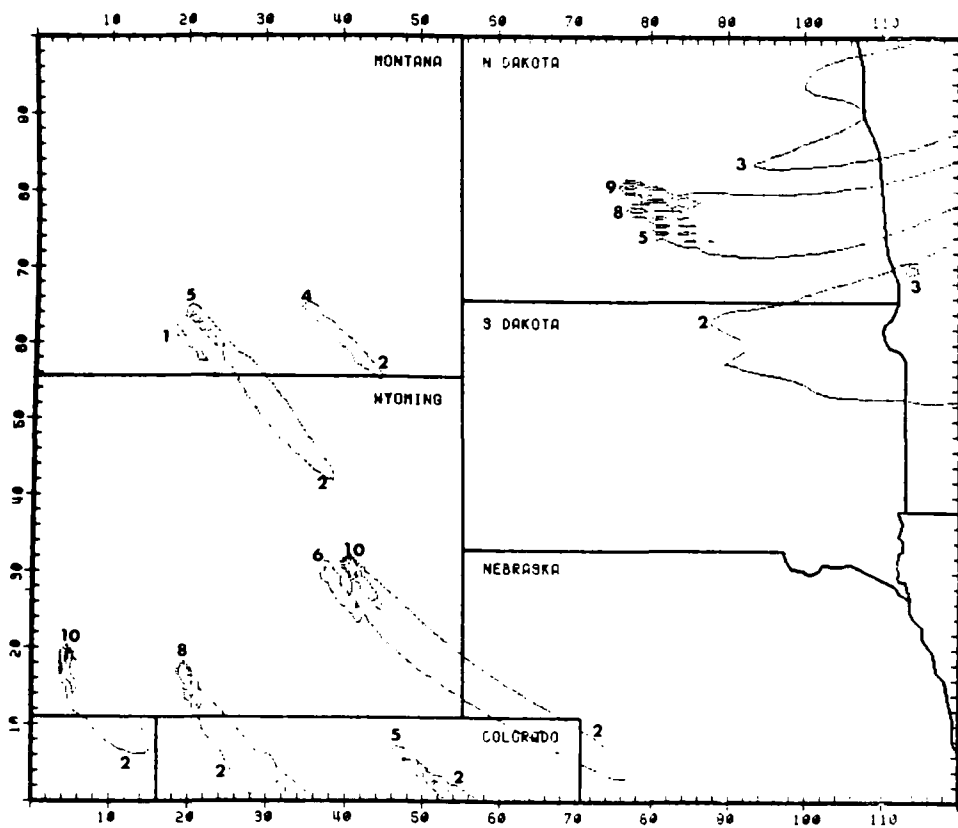


SO₂ CONCENTRATIONS IN UG/M³ FOR THE HOUR 800-1100 MST ON 760117

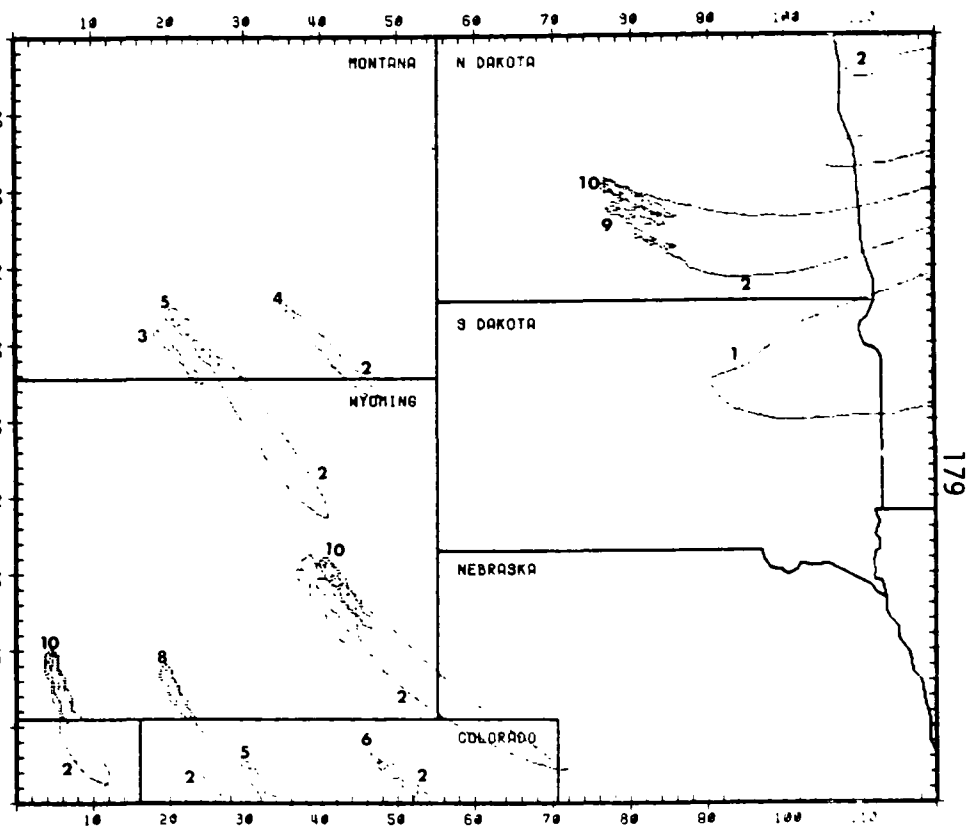


SO2 CONCENTRATIONS IN UG/M3 FOR THE HOUR 1100-1400 MST ON 7/30/17

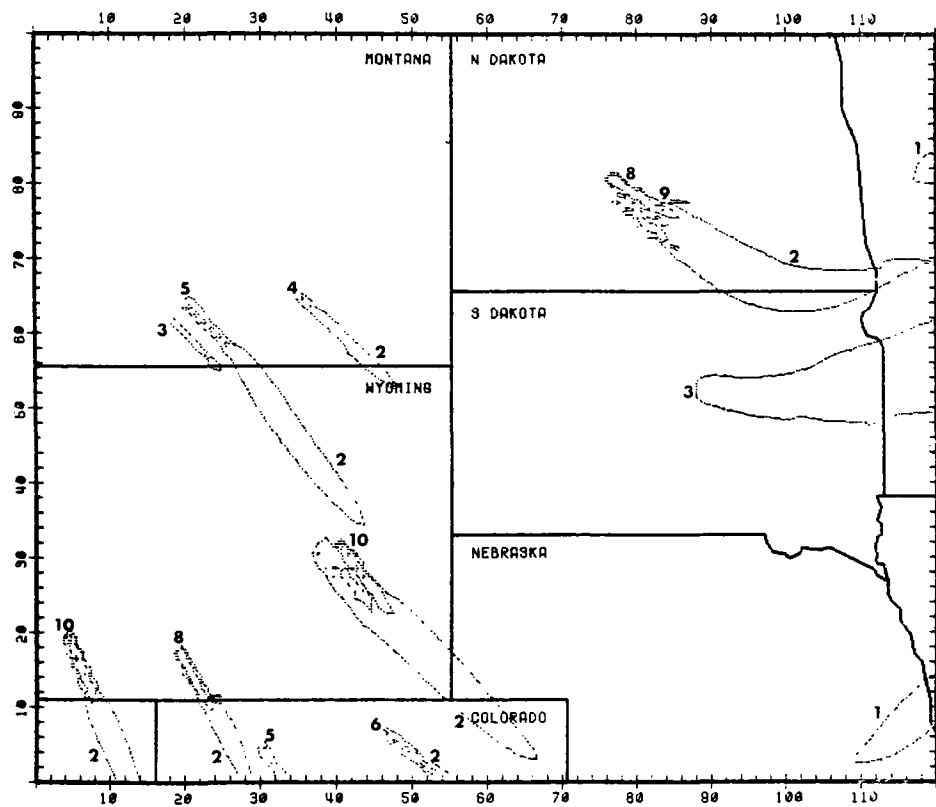
SO2 CONCENTRATIONS IN UG/M3 FOR THE HOUR 1400-1700 MST ON 7/30/17



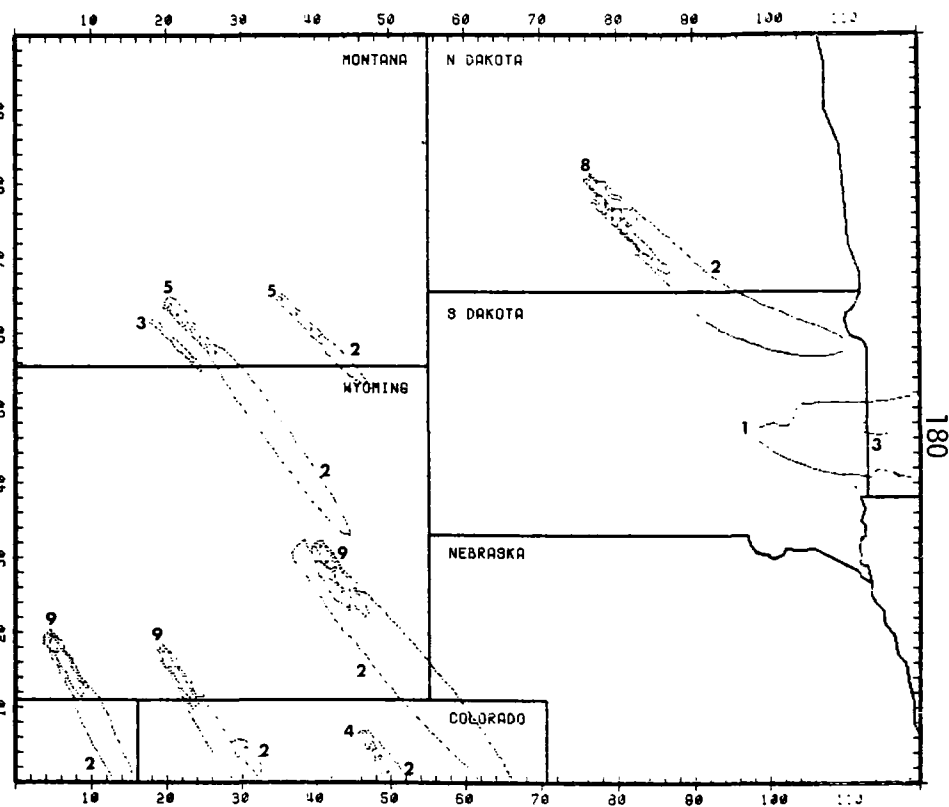
SO2 CONCENTRATIONS IN $\mu\text{G}/\text{M}^3$ FOR THE HOUR 1700-2000 MST ON 7/31/17



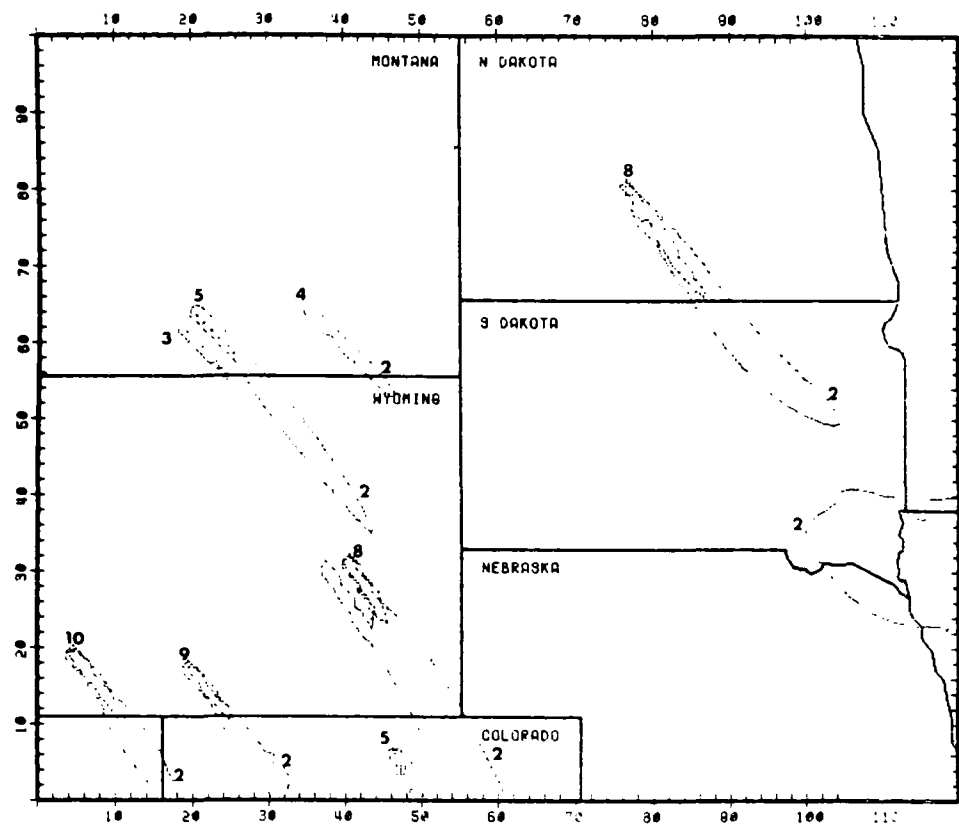
SO2 CONCENTRATIONS IN $\mu\text{G}/\text{M}^3$ FOR THE HOUR 2000-2300 MST ON 7/31/17



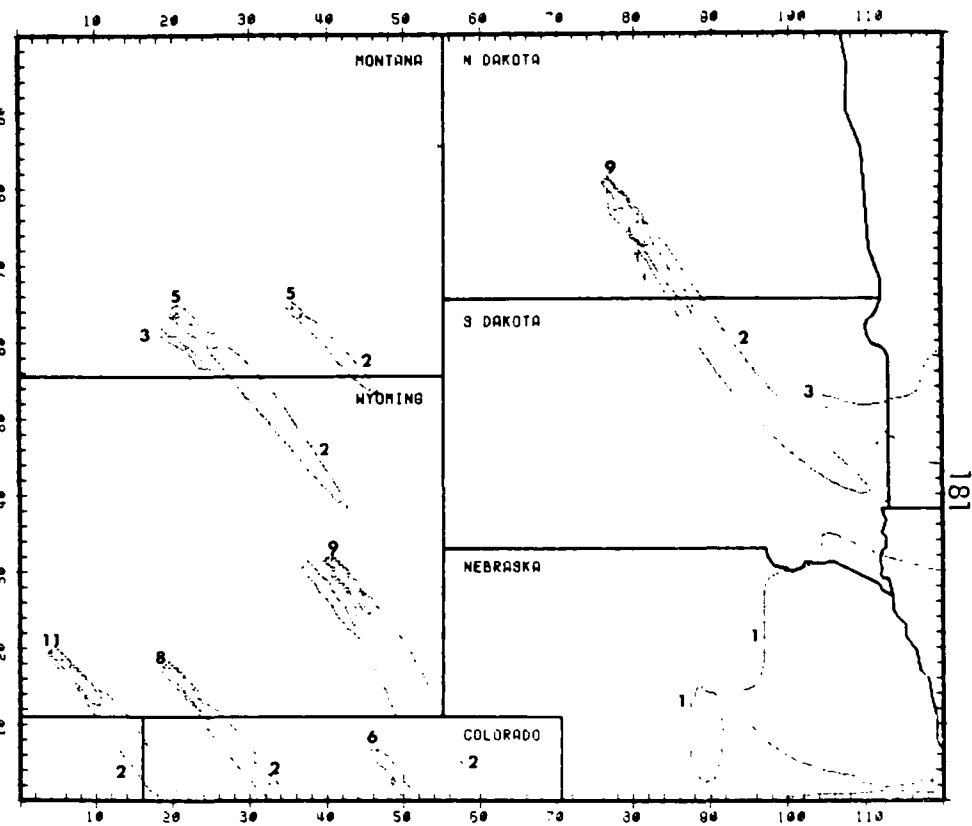
SO2 CONCENTRATIONS IN $\mu\text{G}/\text{M}^3$ FOR THE HOUR -100-200 MST ON 760128



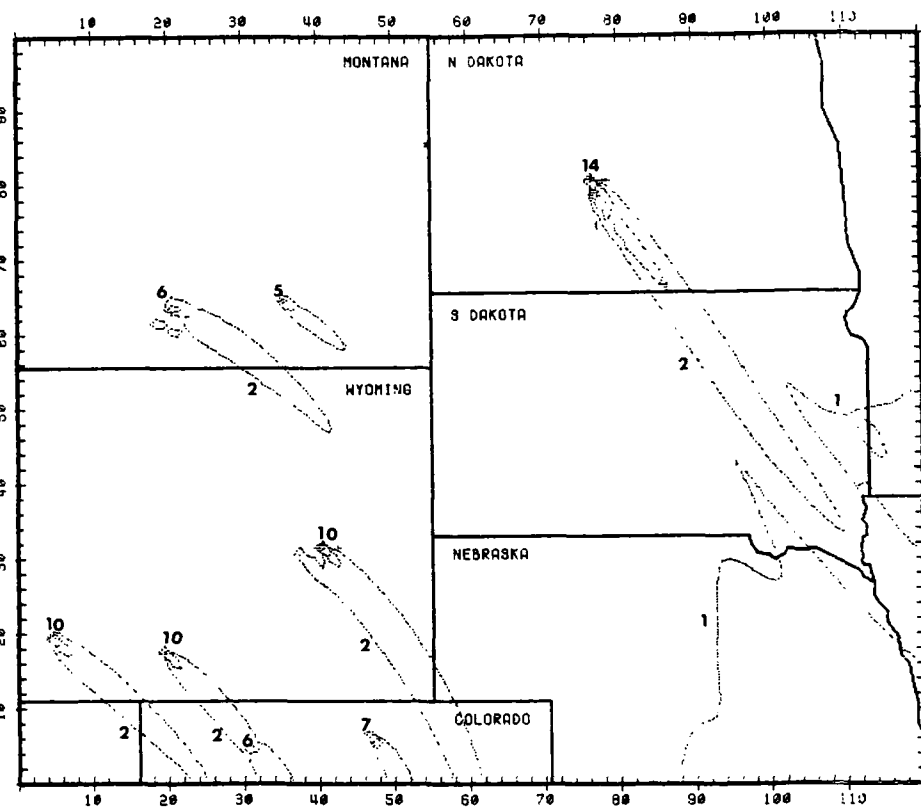
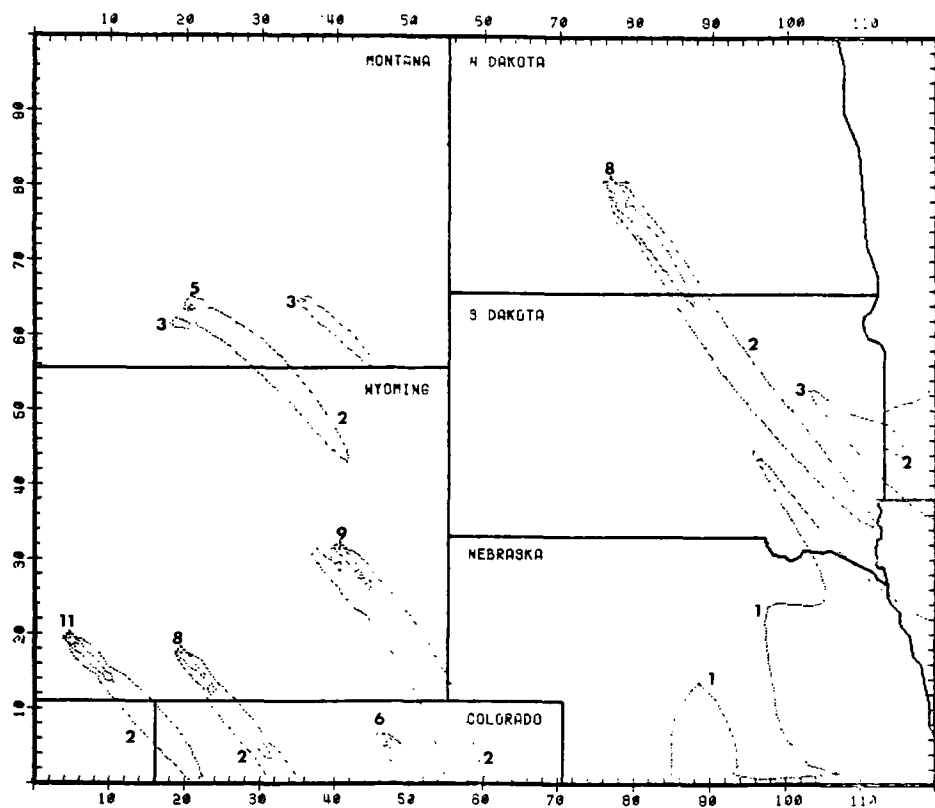
SO2 CONCENTRATIONS IN $\mu\text{G}/\text{M}^3$ FOR THE HOUR 200-500 MST ON 760128



SO2 CONCENTRATIONS IN UG/M3 FOR THE HOUR 500-800 MST ON 760113

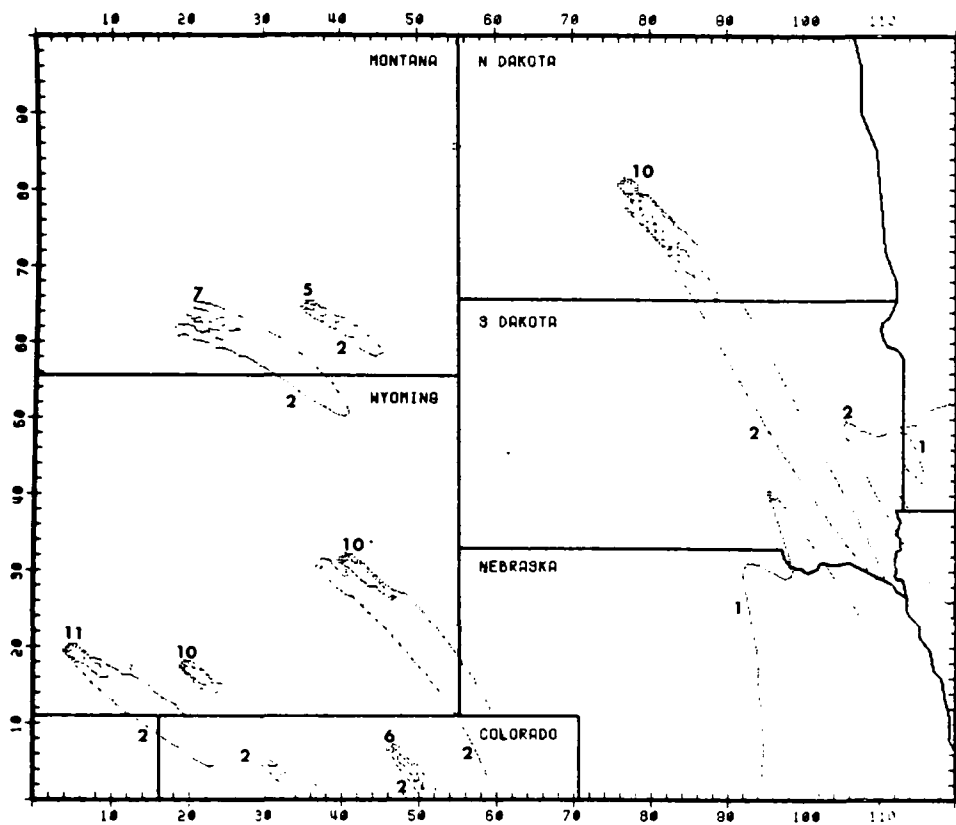


SO2 CONCENTRATIONS IN UG/M3 FOR THE HOUR 800-1100 MST ON 760123

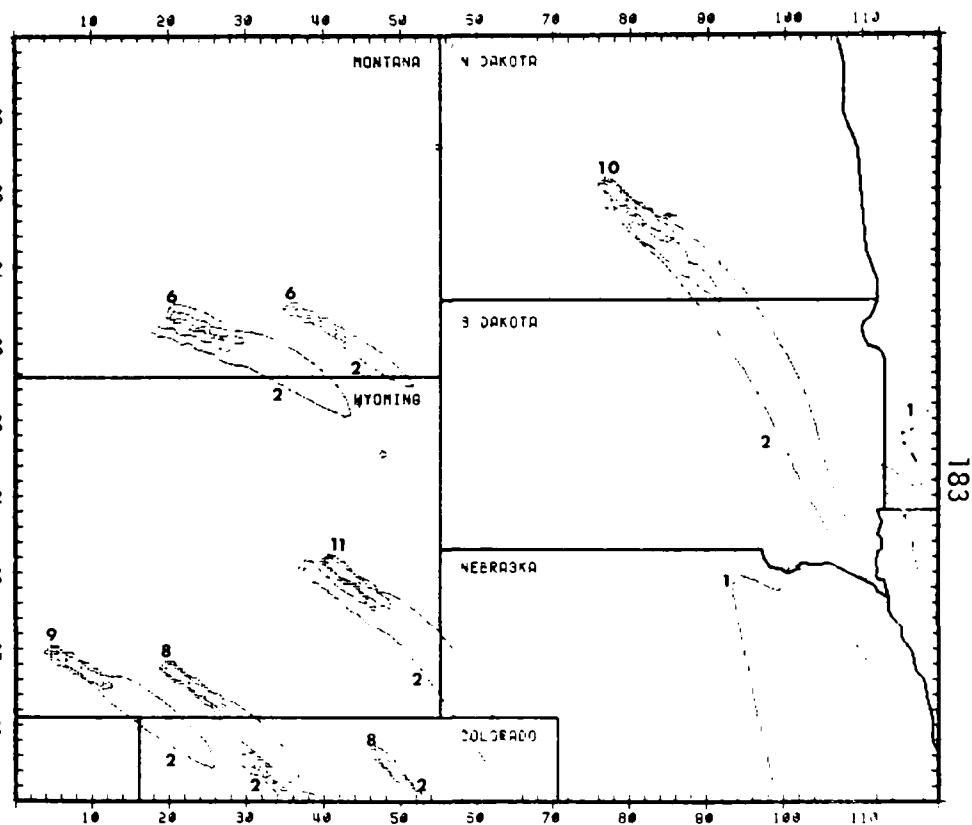


SO2 CONCENTRATIONS IN $\mu\text{g}/\text{m}^3$ FOR THE HOUR 1100-1400 MST ON 7/30/12

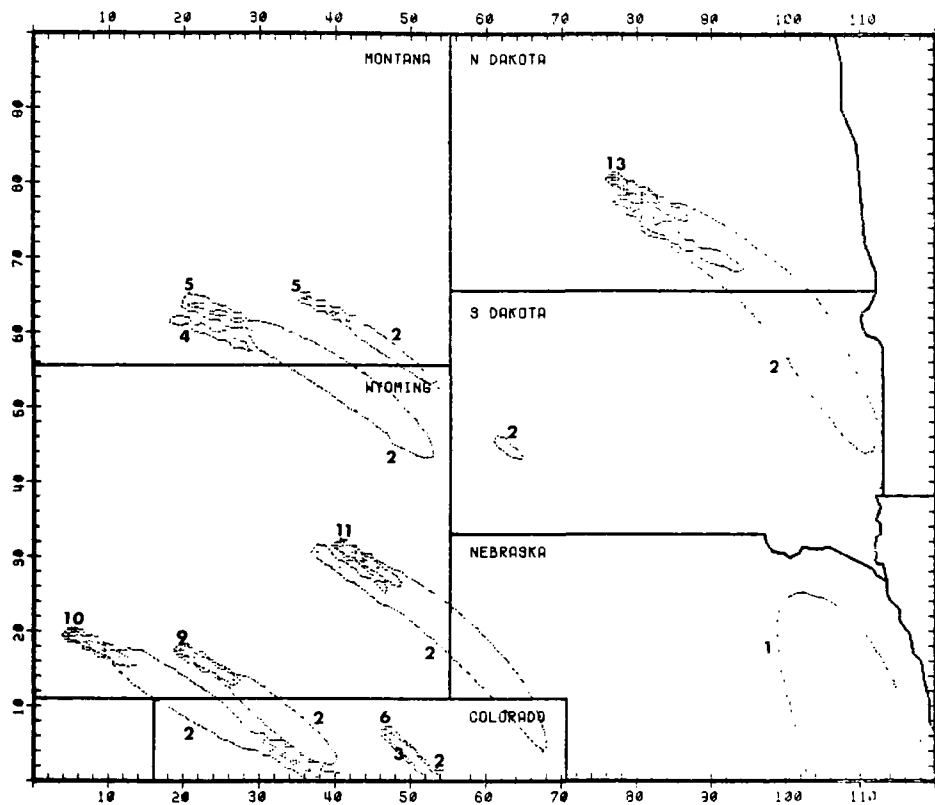
SO2 CONCENTRATIONS IN $\mu\text{g}/\text{m}^3$ FOR THE HOUR 1400-1700 MST ON 7/30/12



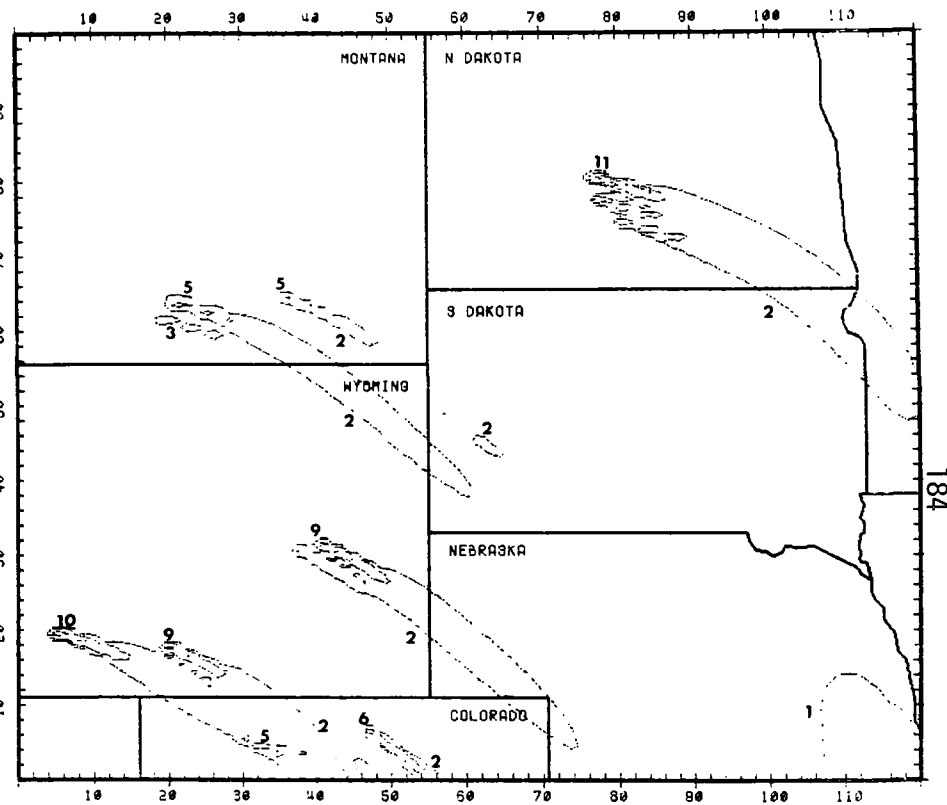
SO2 CONCENTRATIONS IN $\mu\text{g}/\text{m}^3$ FOR THE HOUR 1700-2000 MST ON 7/6/13



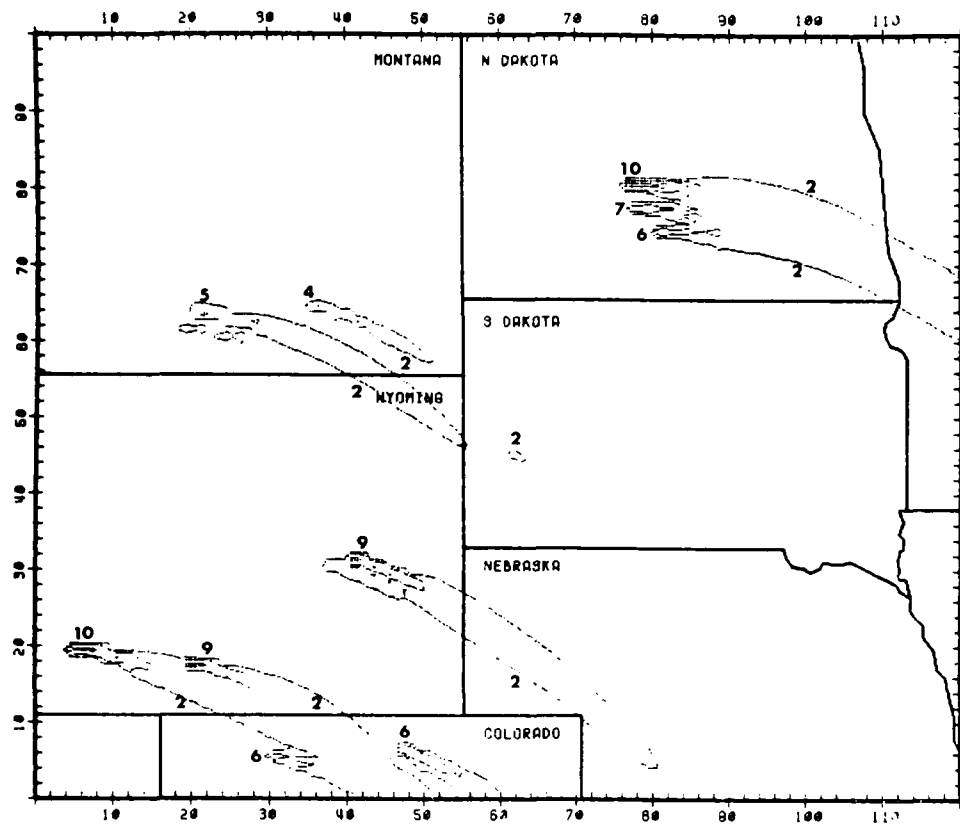
SO2 CONCENTRATIONS IN $\mu\text{g}/\text{m}^3$ FOR THE HOUR 2000-2300 MST ON 7/6/13



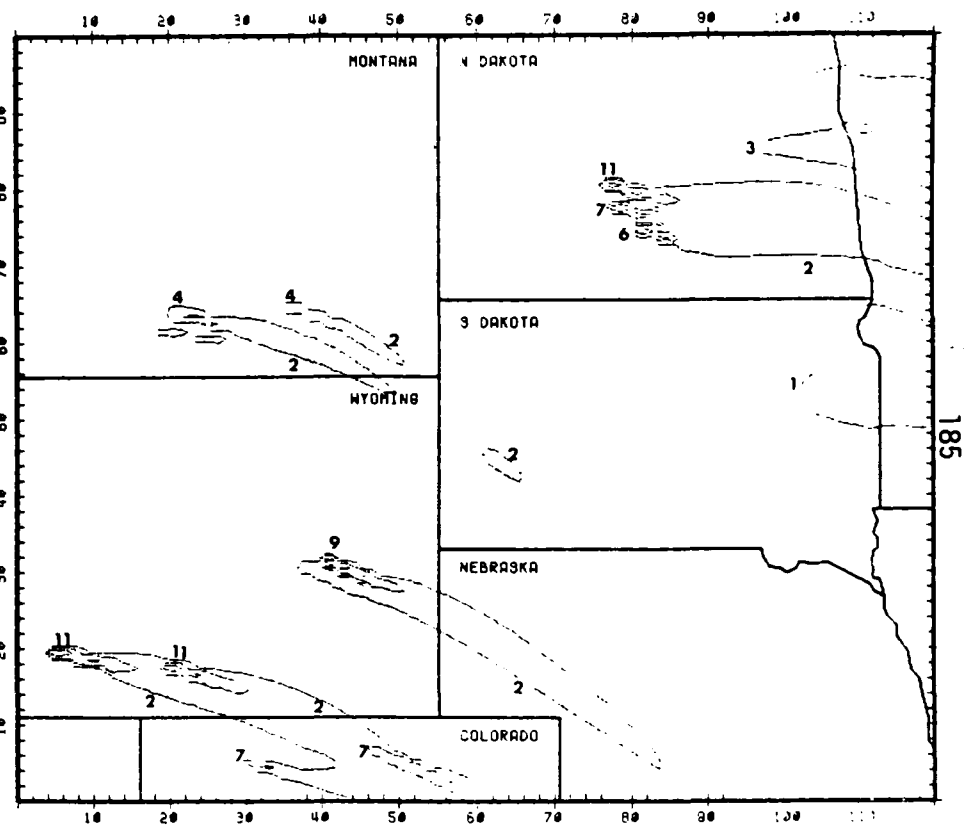
SO2 CONCENTRATIONS IN $\mu\text{G}/\text{M}^3$ FOR THE HOUR -100-200 MST ON 7/01/29



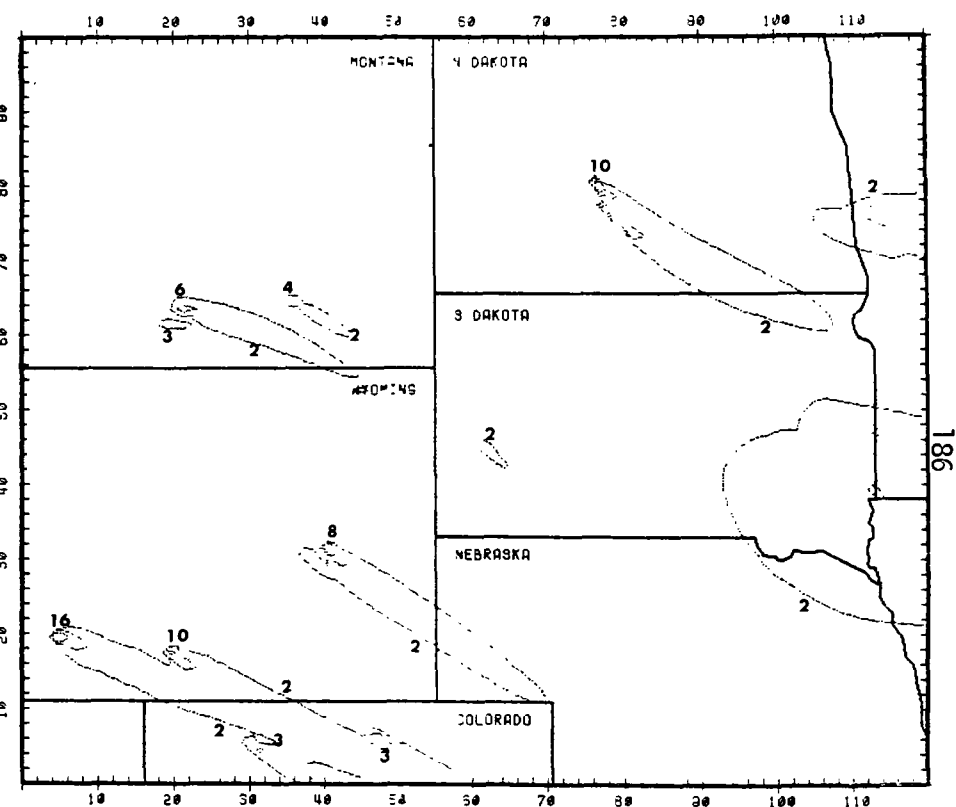
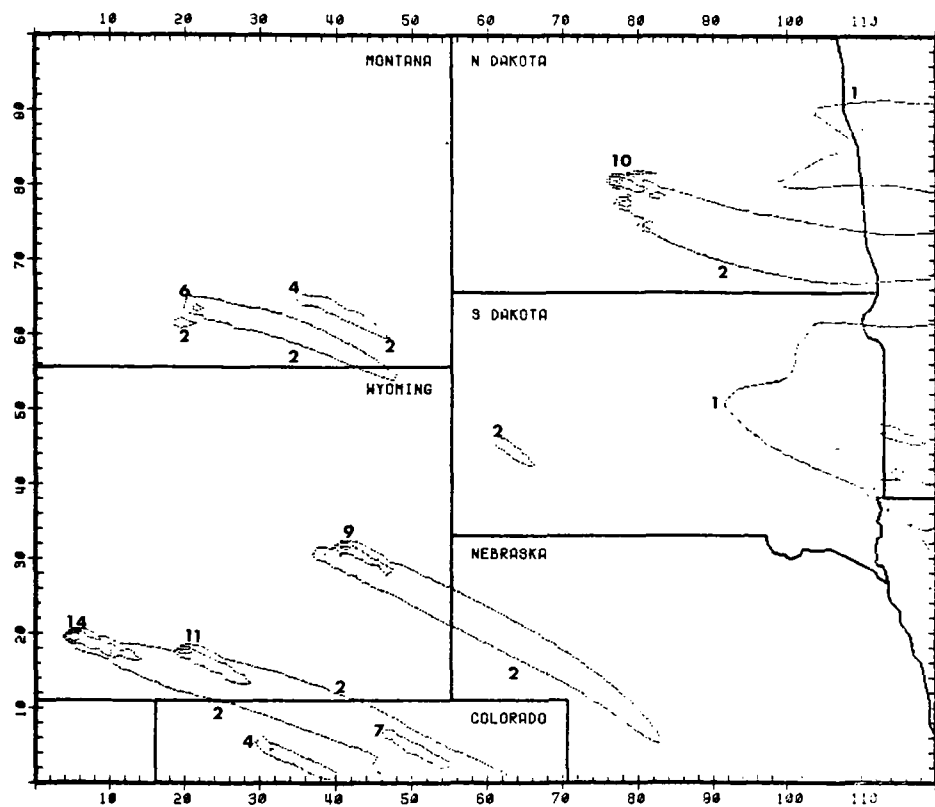
SO2 CONCENTRATIONS IN $\mu\text{G}/\text{M}^3$ FOR THE HOUR 200-500 MST ON 7/01/29



SO2 CONCENTRATIONS IN $\mu\text{G}/\text{M}^3$ FOR THE HOUR 500-300 MST ON 7/12/10

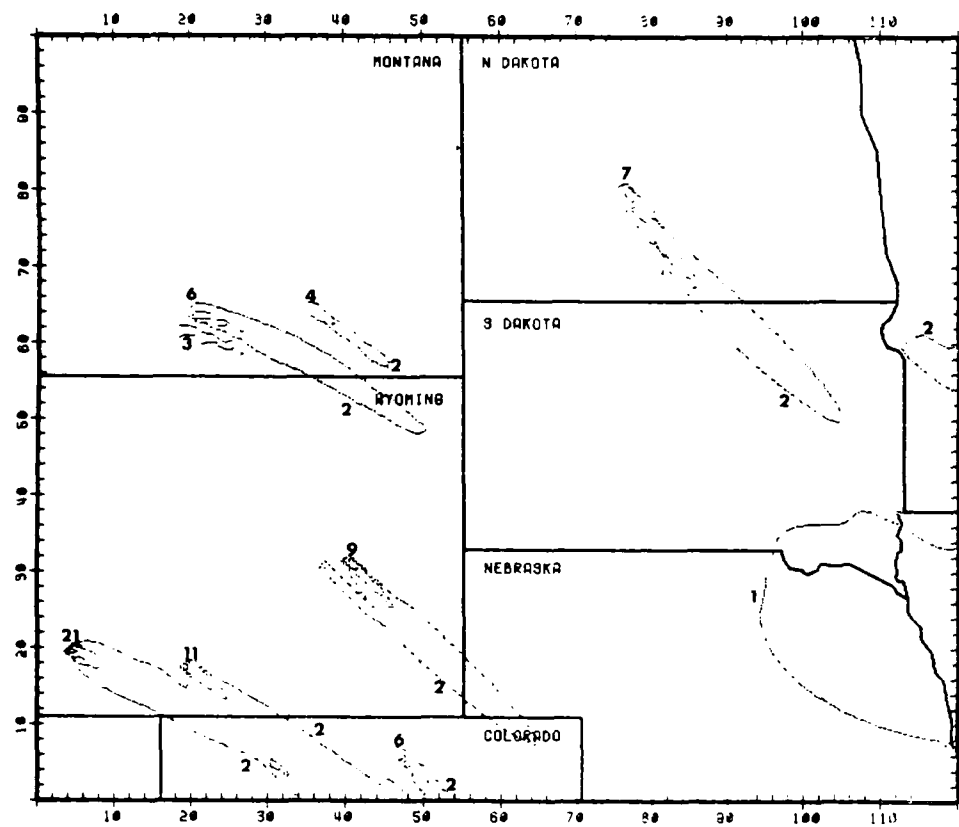


SO2 CONCENTRATIONS IN $\mu\text{G}/\text{M}^3$ FOR THE HOUR 800-1100 MST ON 7/12/10

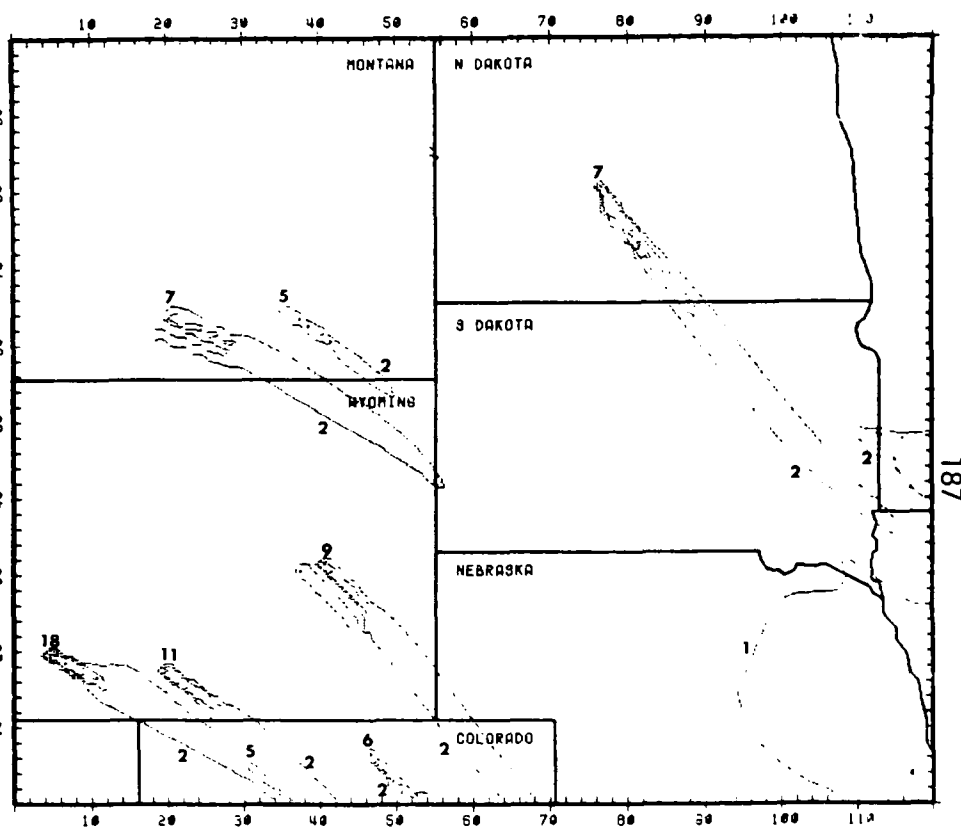


SO₂ CONCENTRATIONS IN UG/M3 FOR THE HOUR 1100-1400 MST ON 760129

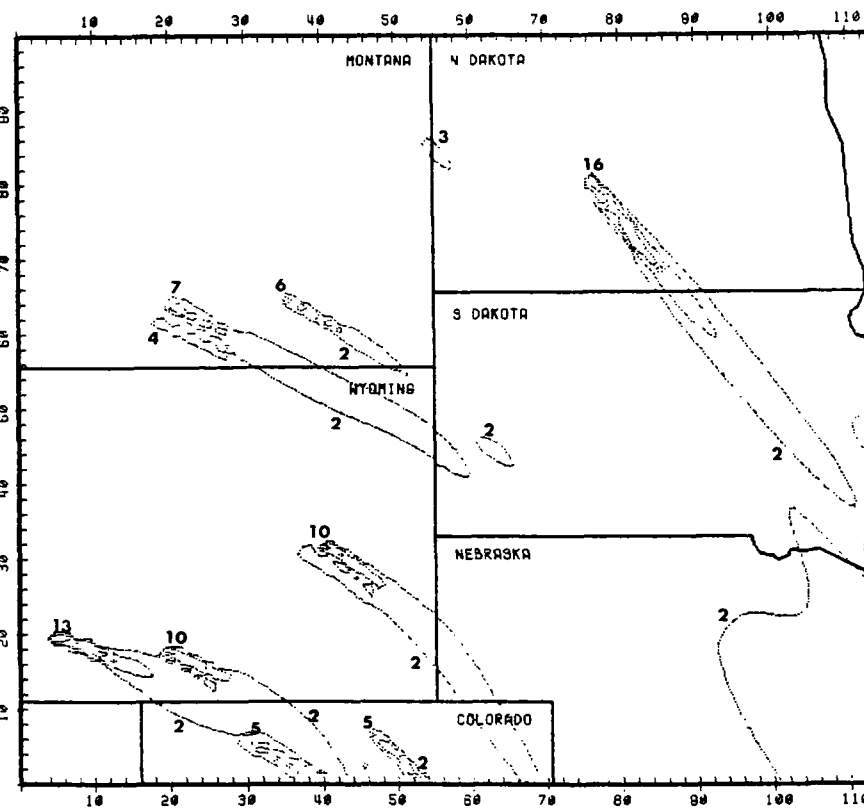
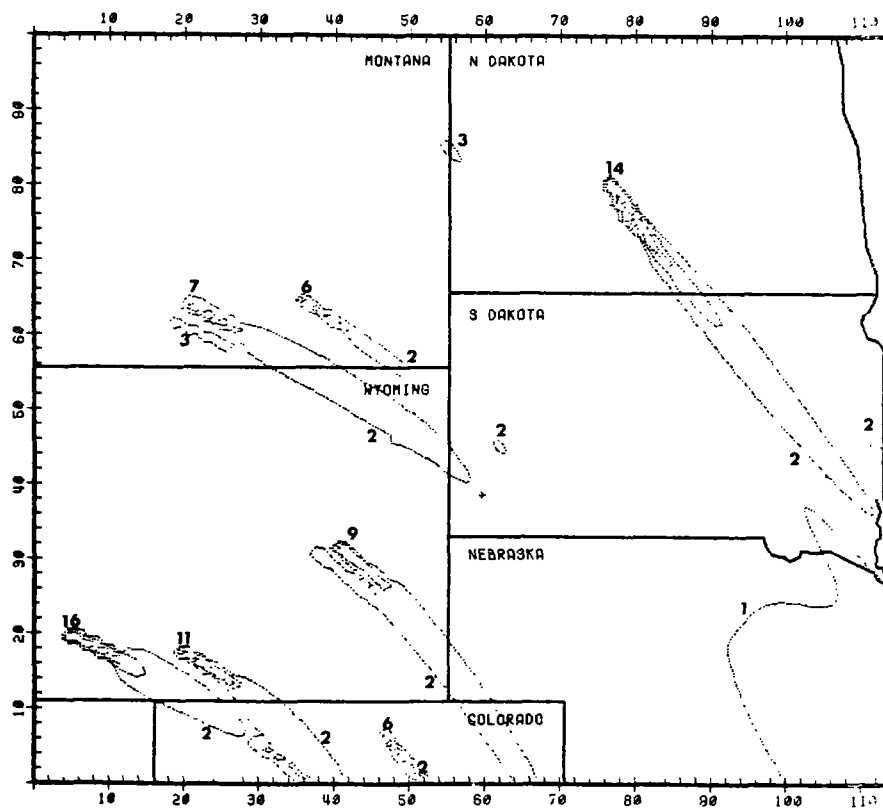
SO₂ CONCENTRATIONS IN UG/M3 FOR THE HOUR 1400-1700 MST ON 760129



SO₂ CONCENTRATIONS IN UG/M3 FOR THE HOUR 1700-2000 MST ON 760129

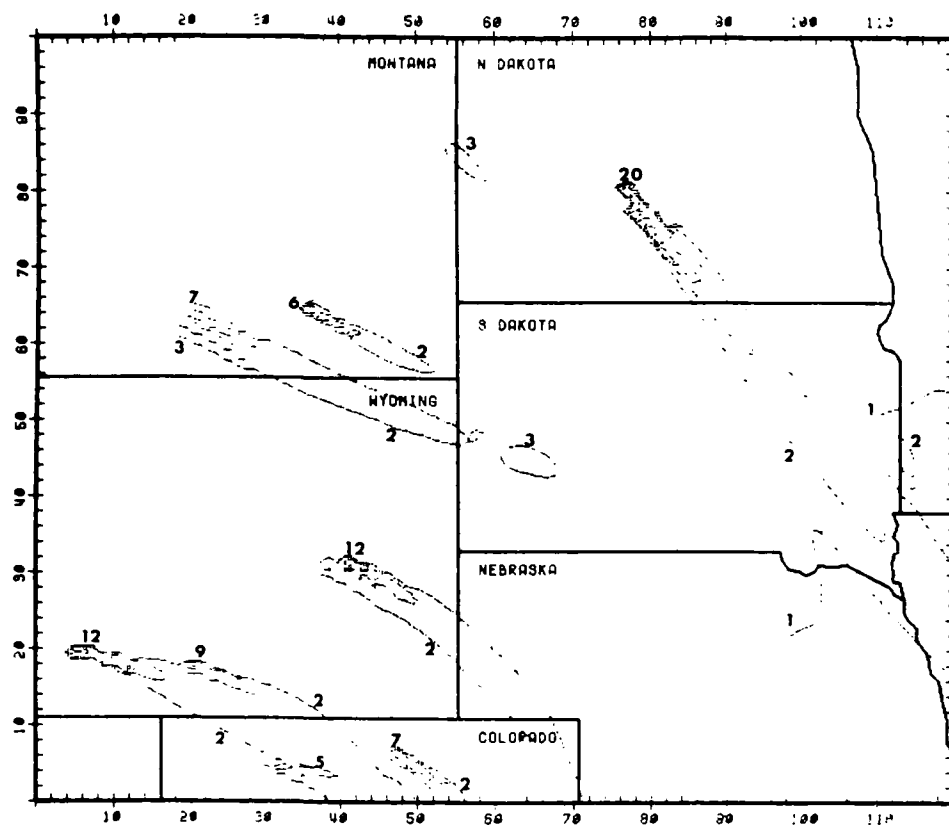


SO₂ CONCENTRATIONS IN UG/M3 FOR THE HOUR 2000-2300 MST ON 760129

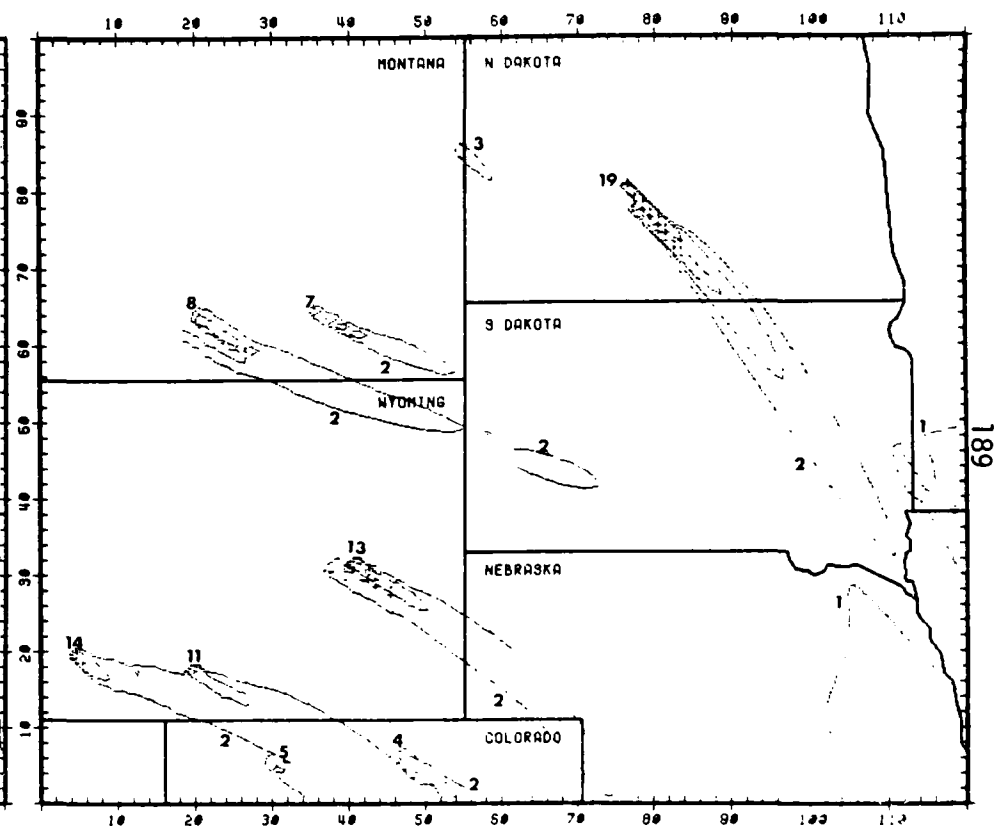


SO2 CONCENTRATIONS IN UG/M3 FOR THE HOUR -100-200 MST ON 760130

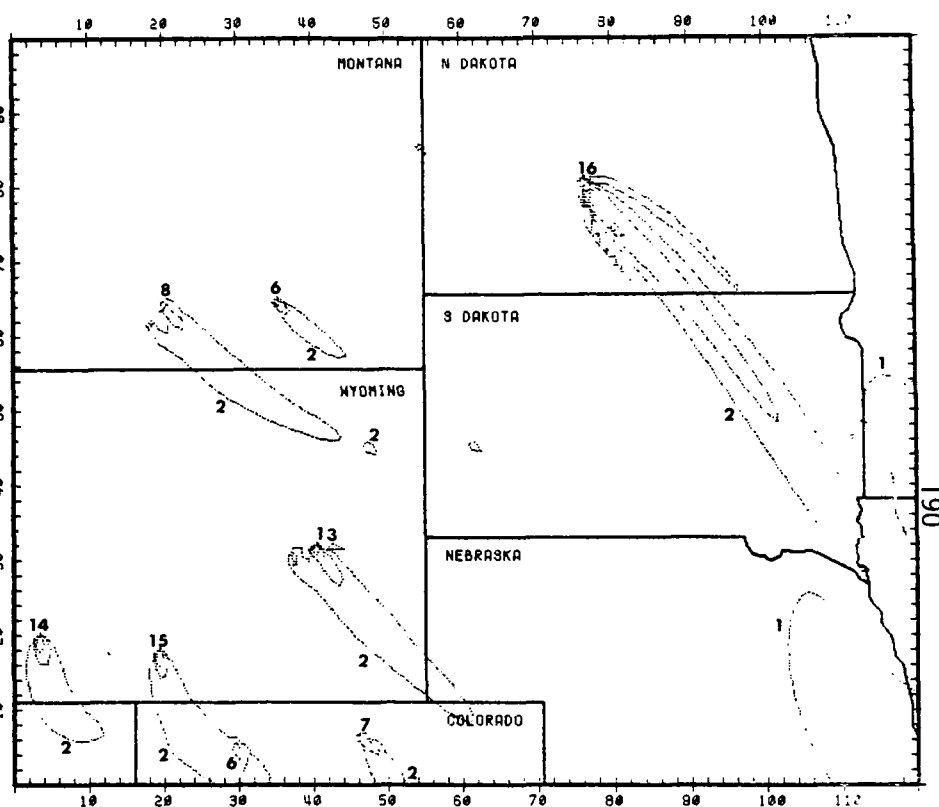
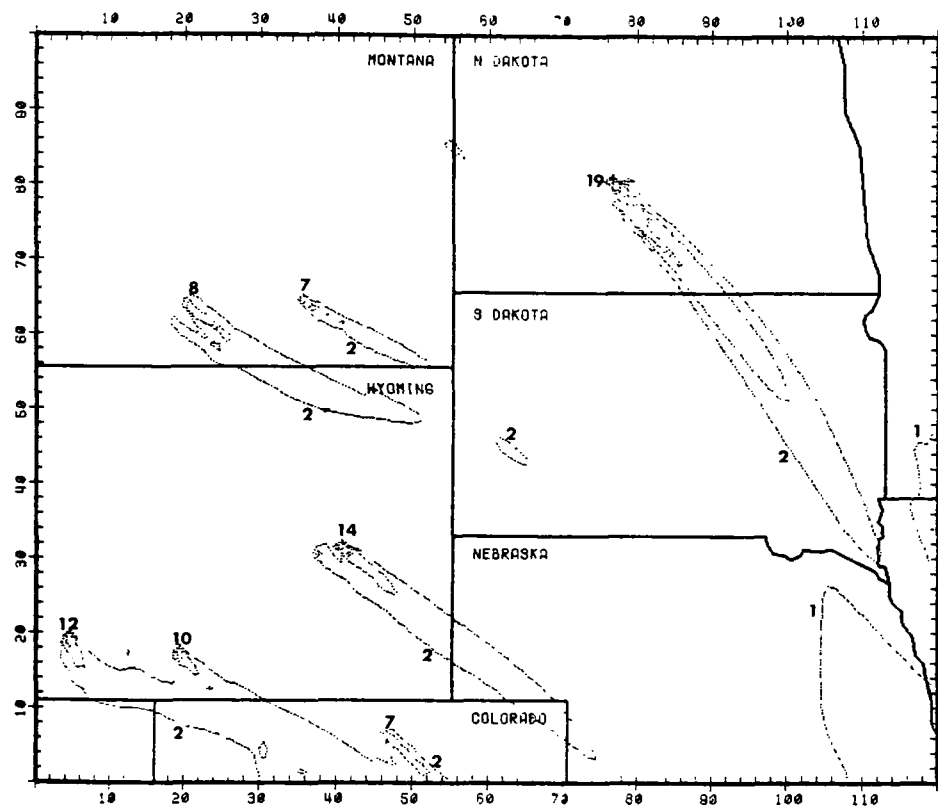
SO2 CONCENTRATIONS IN UG/M3 FOR THE HOUR 200-500 MST ON 760130



SO2 CONCENTRATIONS IN UG/M3 FOR THE HOUR 500-800 MST ON 7/20/1991

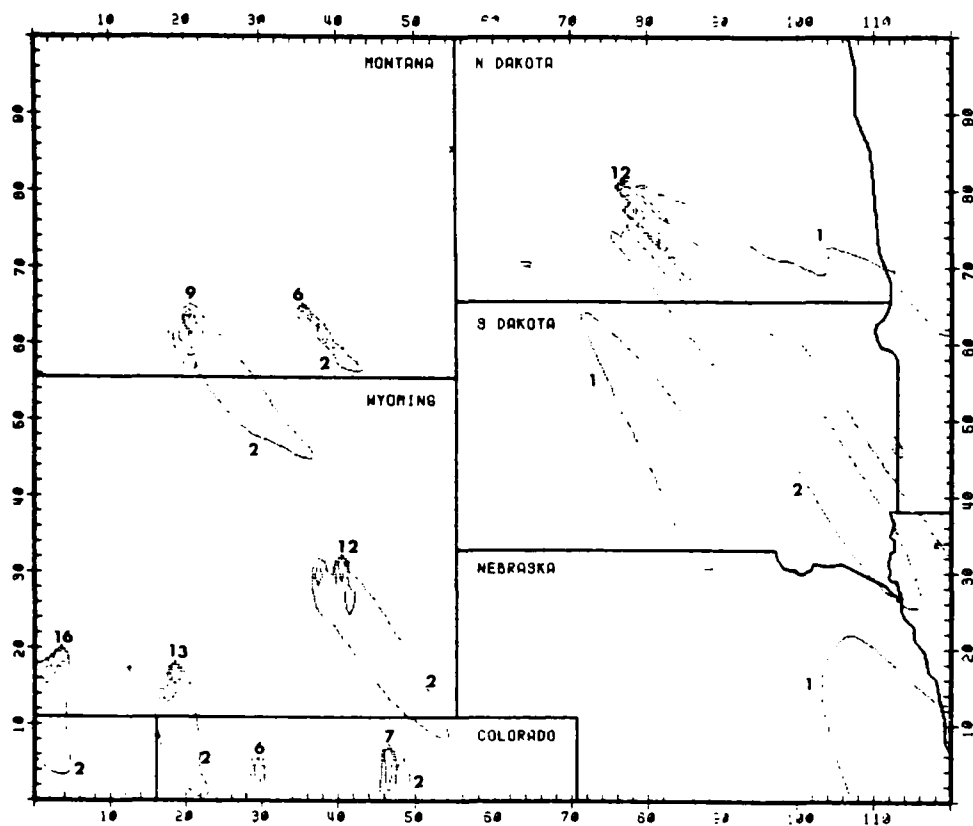


SO2 CONCENTRATIONS IN UG/M3 FOR THE HOUR 800-1100 MST ON 7/20/1991

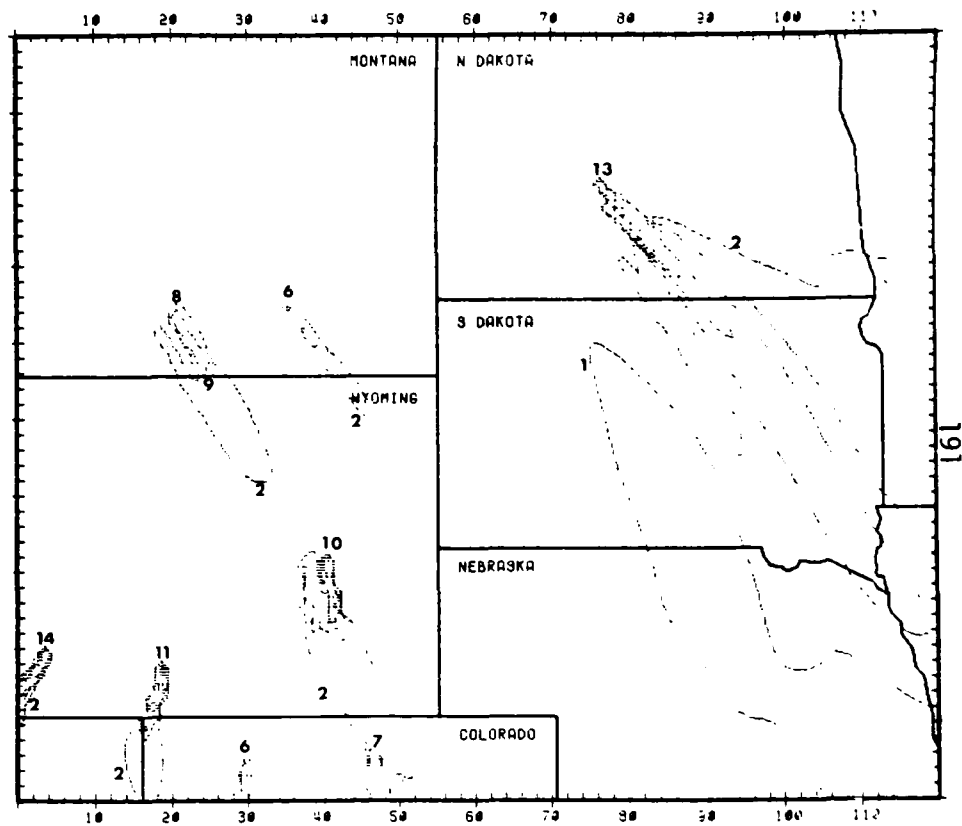


SO2 CONCENTRATIONS IN UG/M3 FOR THE HOUR 1100-1400 MST ON 760130

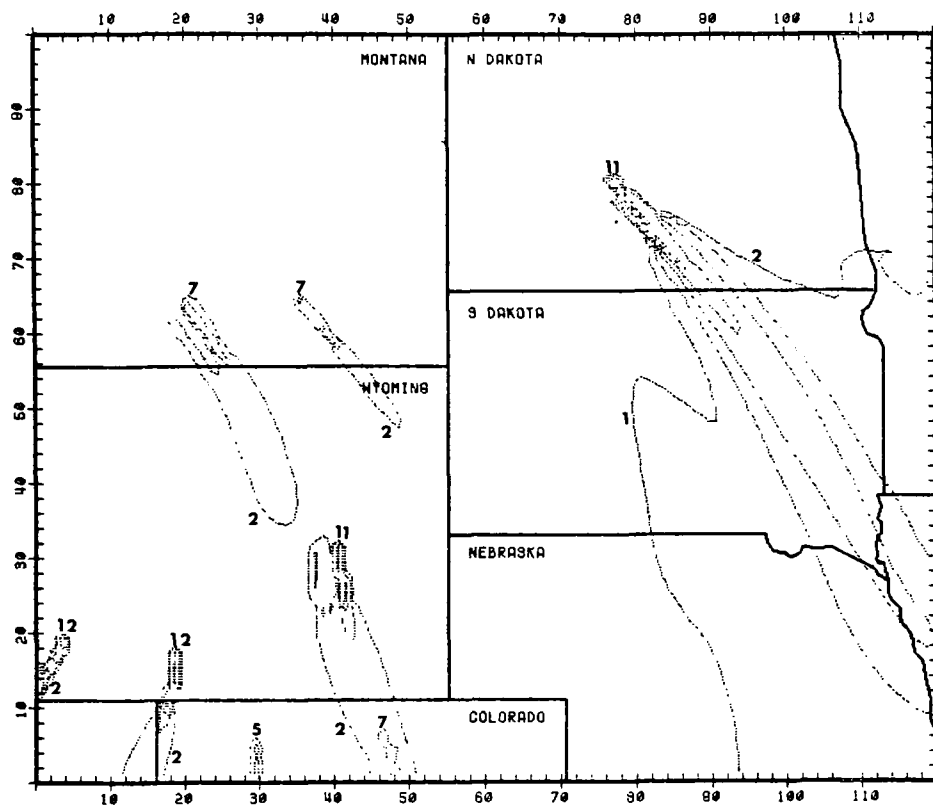
SO2 CONCENTRATIONS IN UG/M3 FOR THE HOUR 1400-1700 MST ON 760130



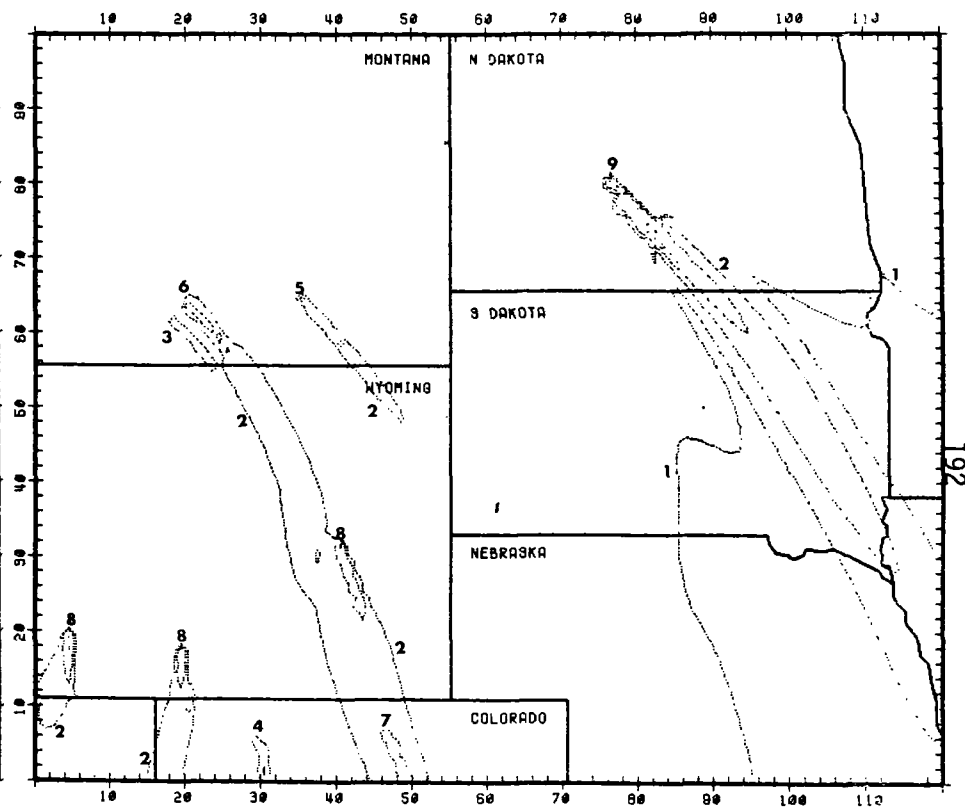
SO2 CONCENTRATIONS IN $\mu\text{G}/\text{M}^3$ FOR THE HOUR 1700-2000 MST ON 7/6/13



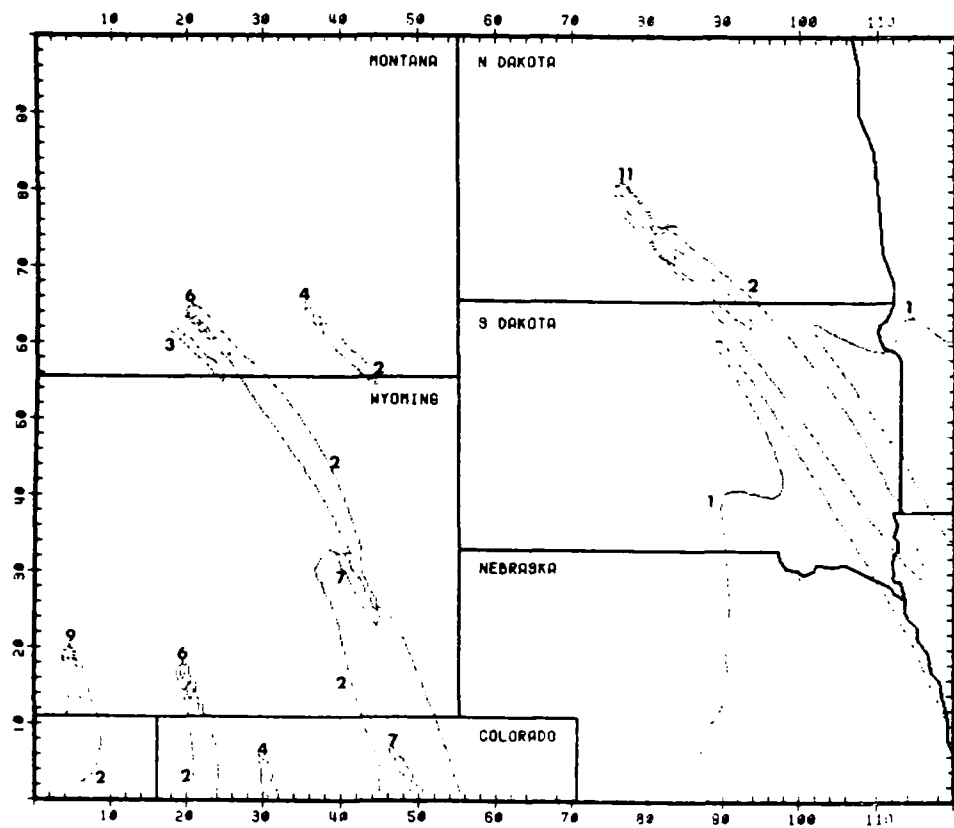
SO2 CONCENTRATIONS IN $\mu\text{G}/\text{M}^3$ FOR THE HOUR 2000-2300 MST ON 7/7/13



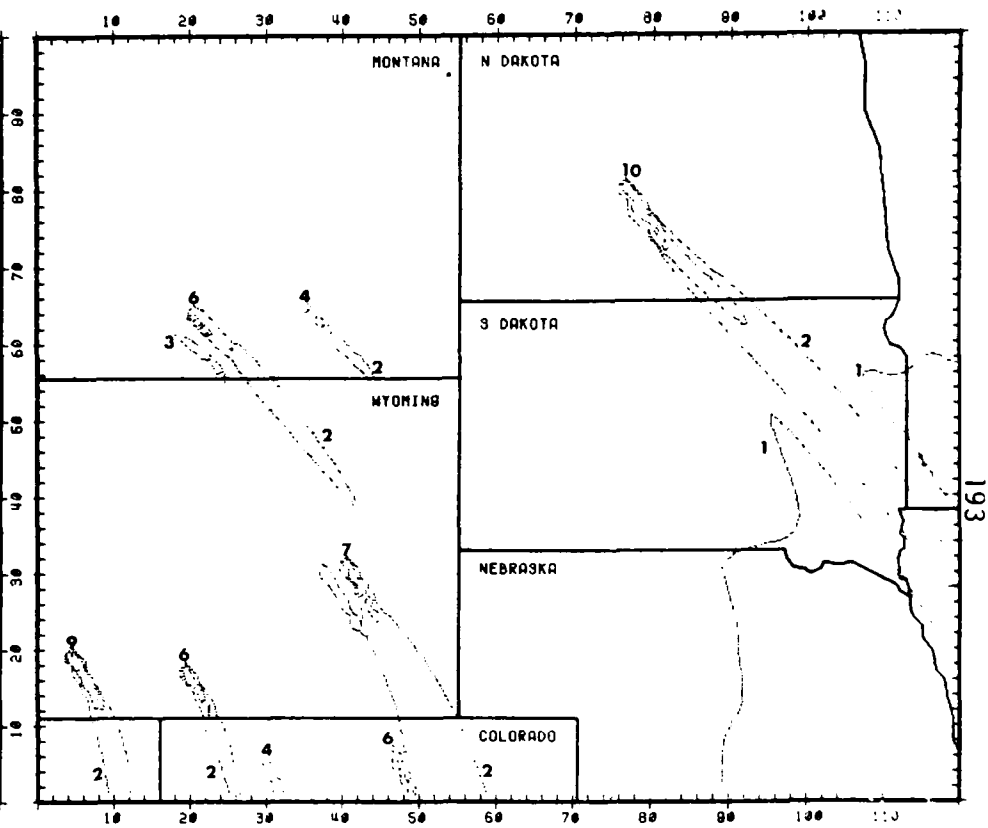
SO₂ CONCENTRATIONS IN UG/M3 FOR THE HOUR -100-200 MST ON 760131



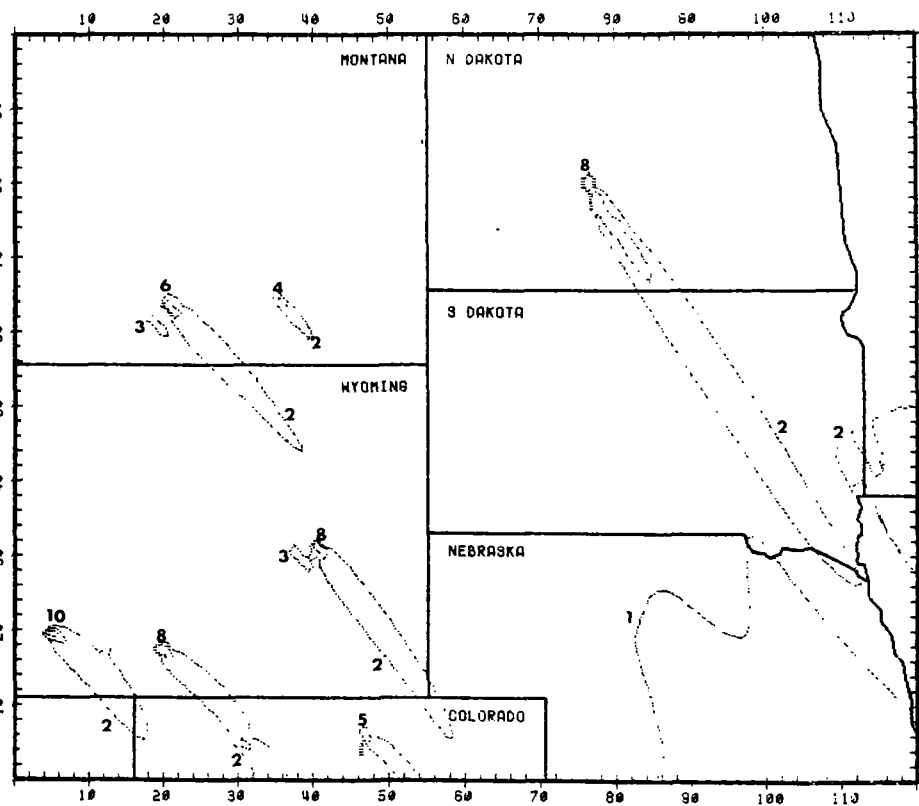
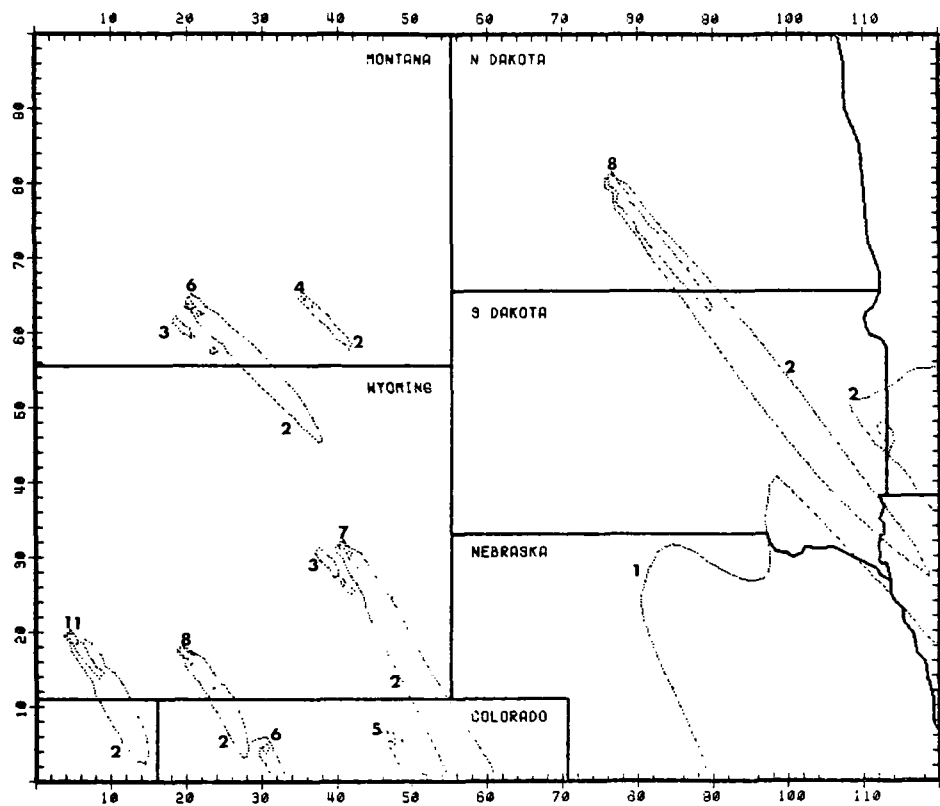
SO₂ CONCENTRATIONS IN UG/M3 FOR THE HOUR 200-500 MST ON 760131



SO2 CONCENTRATIONS IN UG/M3 FOR THE HOUR 500-800 MST ON 7/6/13.

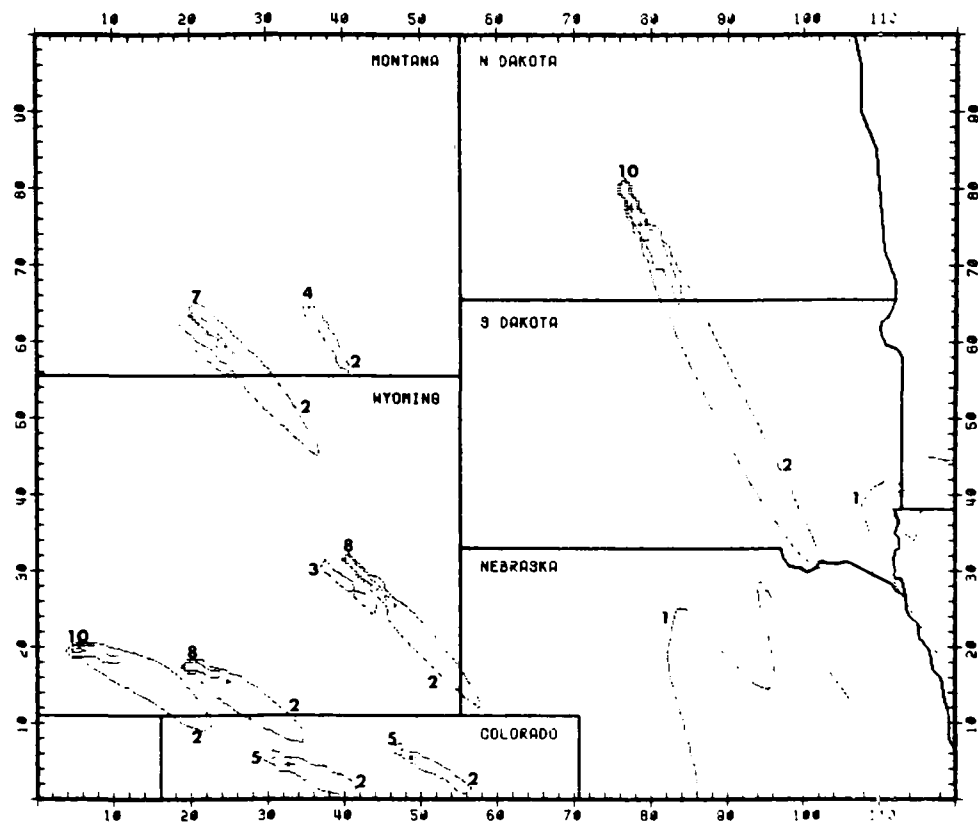


SO2 CONCENTRATIONS IN UG/M3 FOR THE HOUR 800-1100 MST ON 7/6/13.



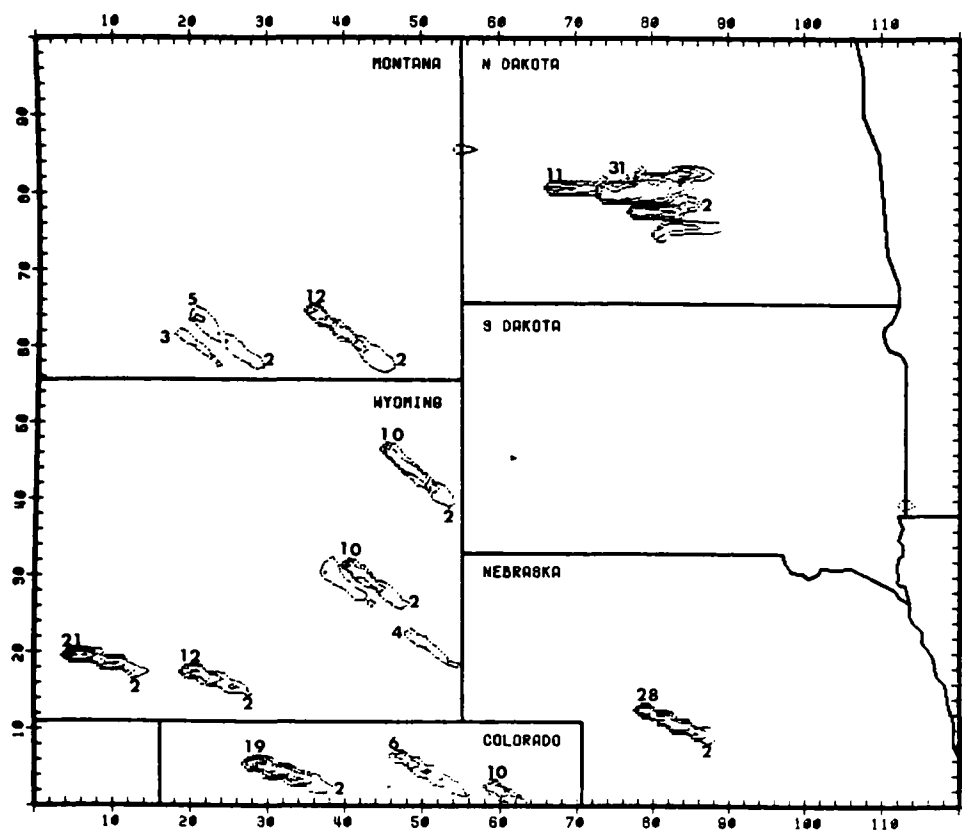
SO2 CONCENTRATIONS IN $\mu\text{G}/\text{M}^3$ FOR THE HOUR 1100-1400 MST ON 760131

SO2 CONCENTRATIONS IN $\mu\text{G}/\text{M}^3$ FOR THE HOUR 1400-1700 MST ON 760131

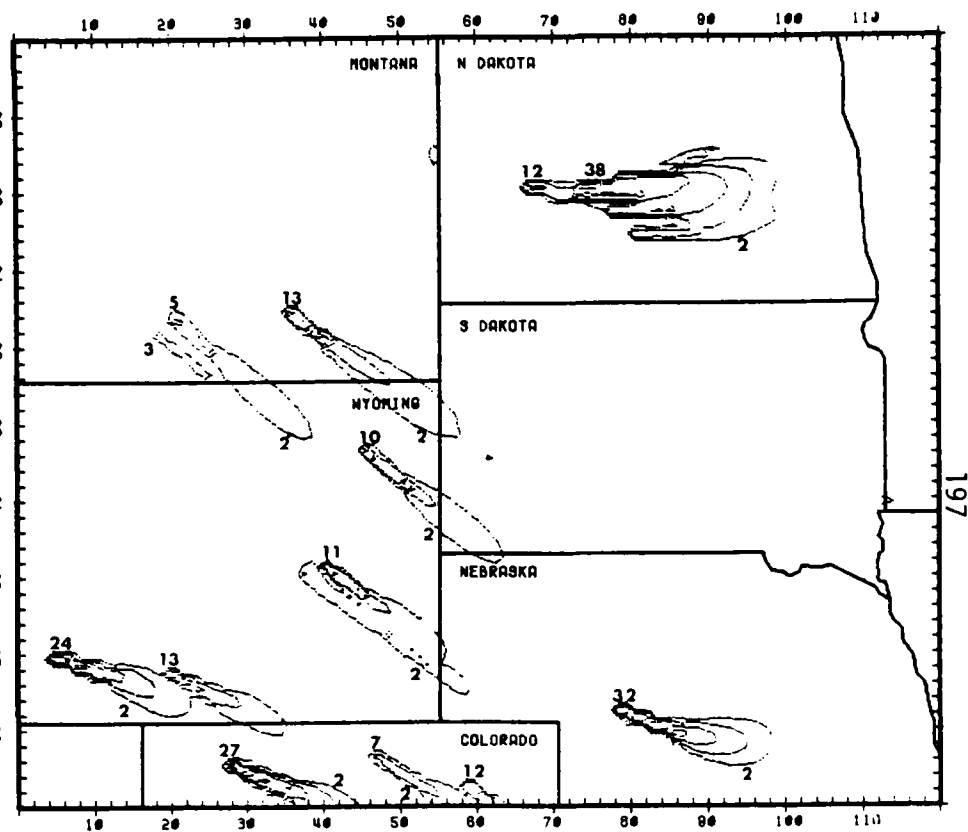


SO₂ CONCENTRATIONS IN UG/M³ FOR THE HOUR 1700-2000 MST ON 7/31/91

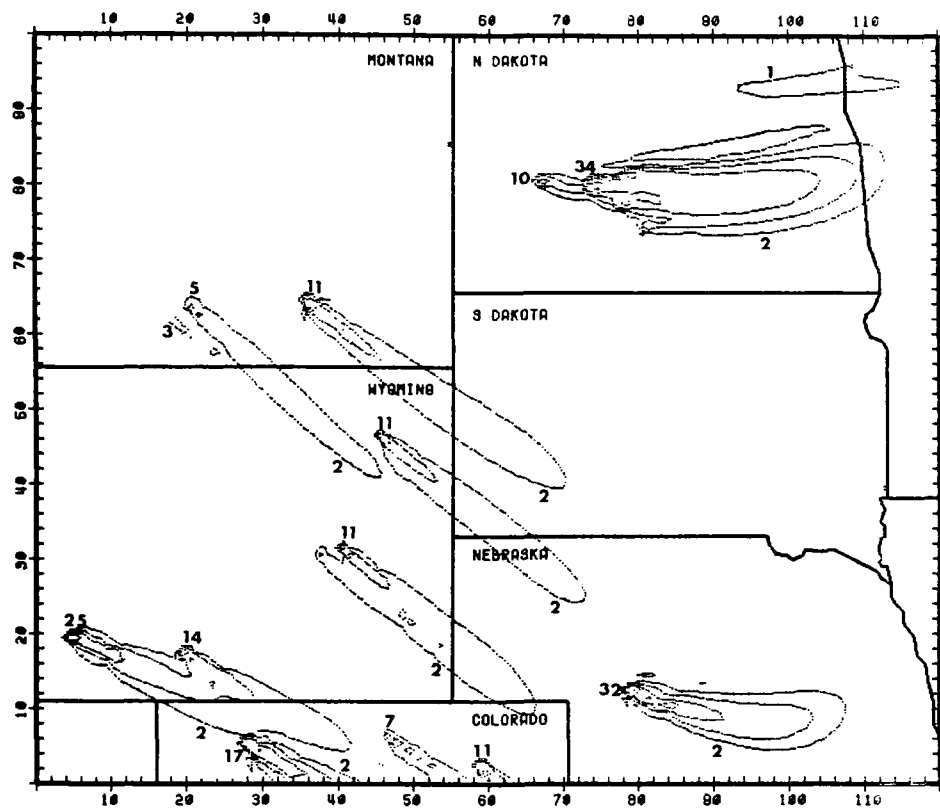
2. 27-31 JANUARY 1976 METEOROLOGY; 1986 EMISSIONS



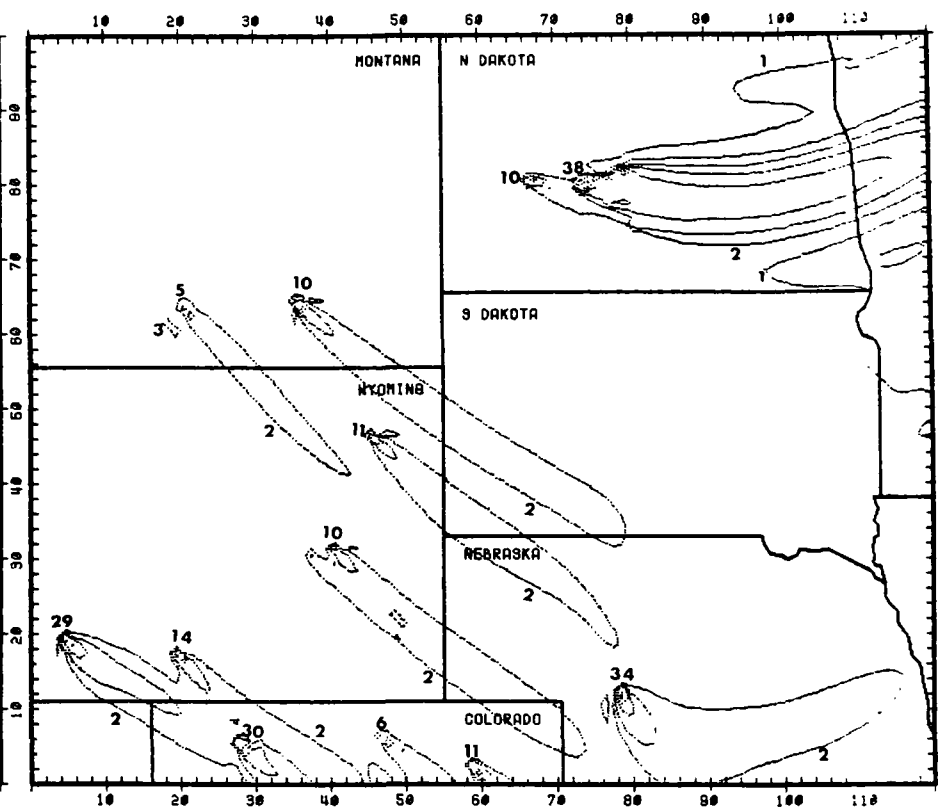
SO₂ CONCENTRATIONS IN UG/M3 FOR THE HOUR 500-800 MST ON 760127



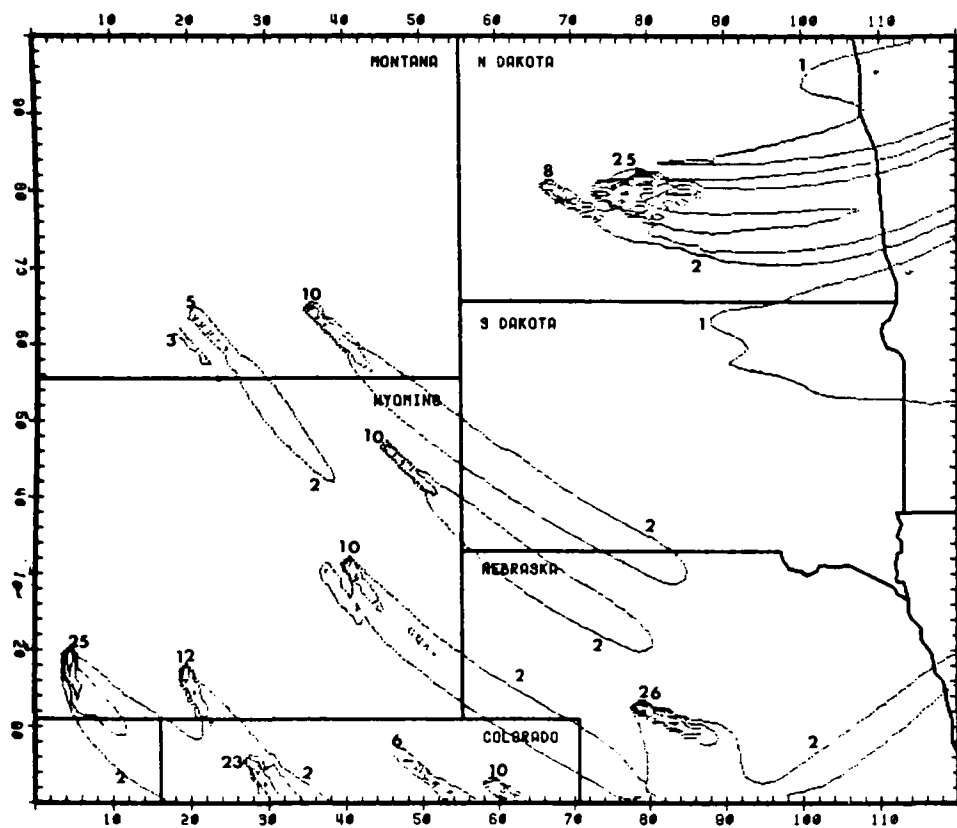
SO₂ CONCENTRATIONS IN UG/M3 FOR THE HOUR 800-1100 MST ON 760127



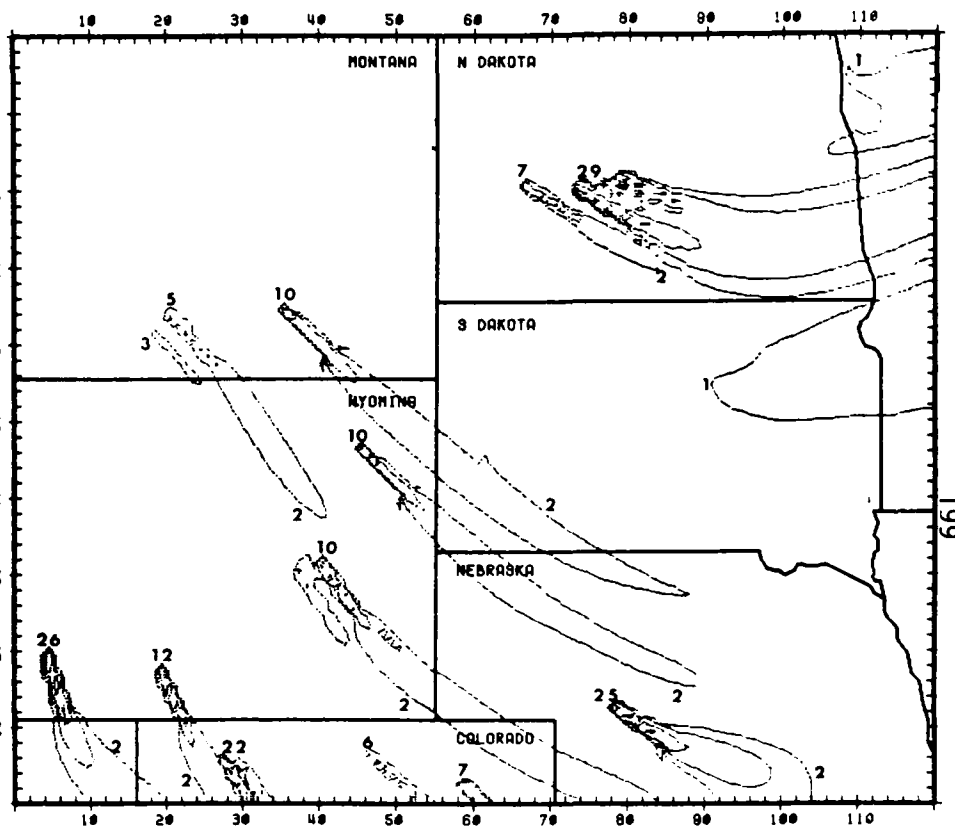
SO2 CONCENTRATIONS IN UG/M3 FOR THE HOUR 1100-1400 MST ON 760127



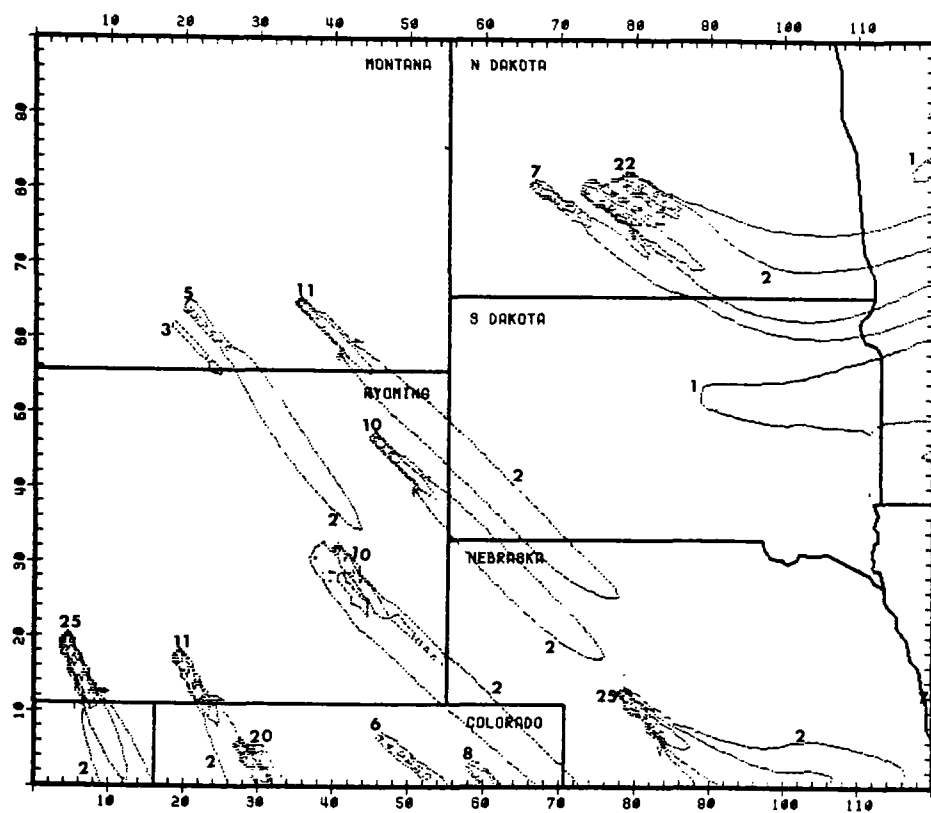
SO2 CONCENTRATIONS IN UG/M3 FOR THE HOUR 1400-1700 MST ON 760127



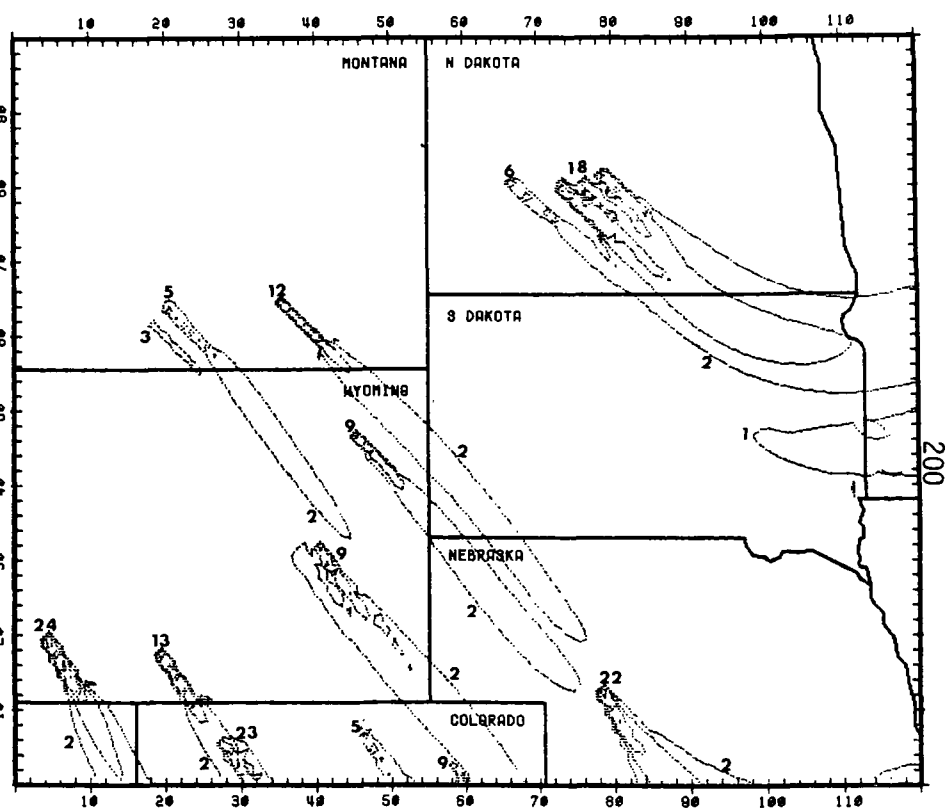
SO₂ CONCENTRATIONS IN UG/M3 FOR THE HOUR 1700-2000 MST ON 760127



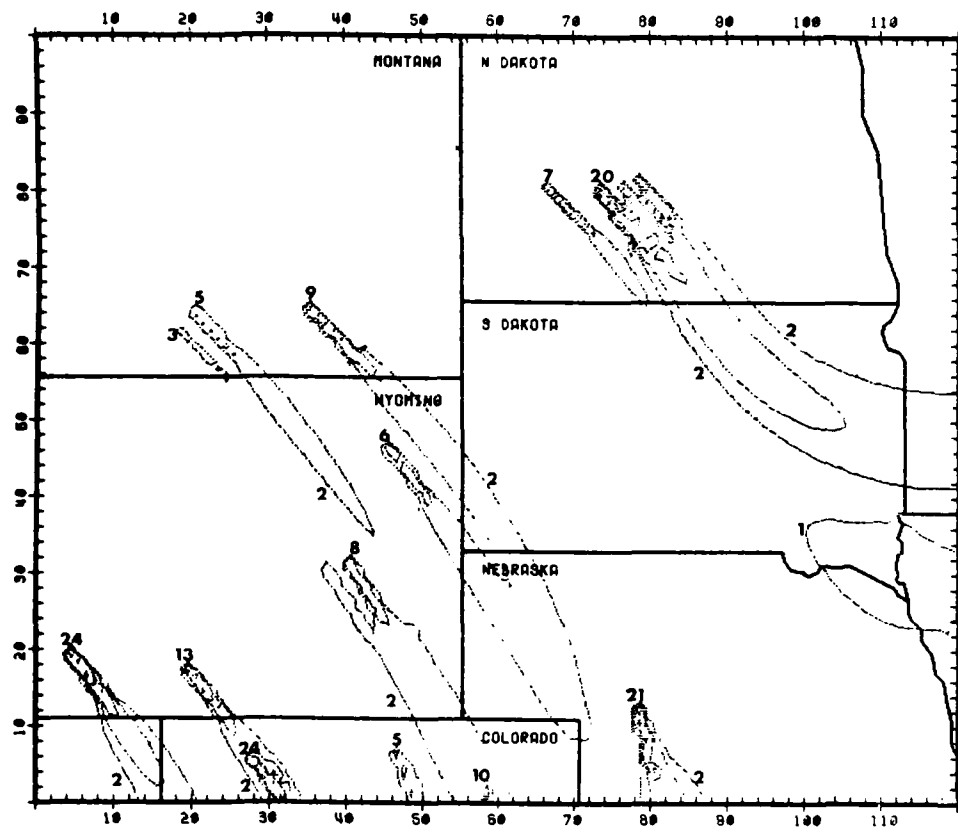
SO₂ CONCENTRATIONS IN UG/M3 FOR THE HOUR 2000-2300 MST ON 760127



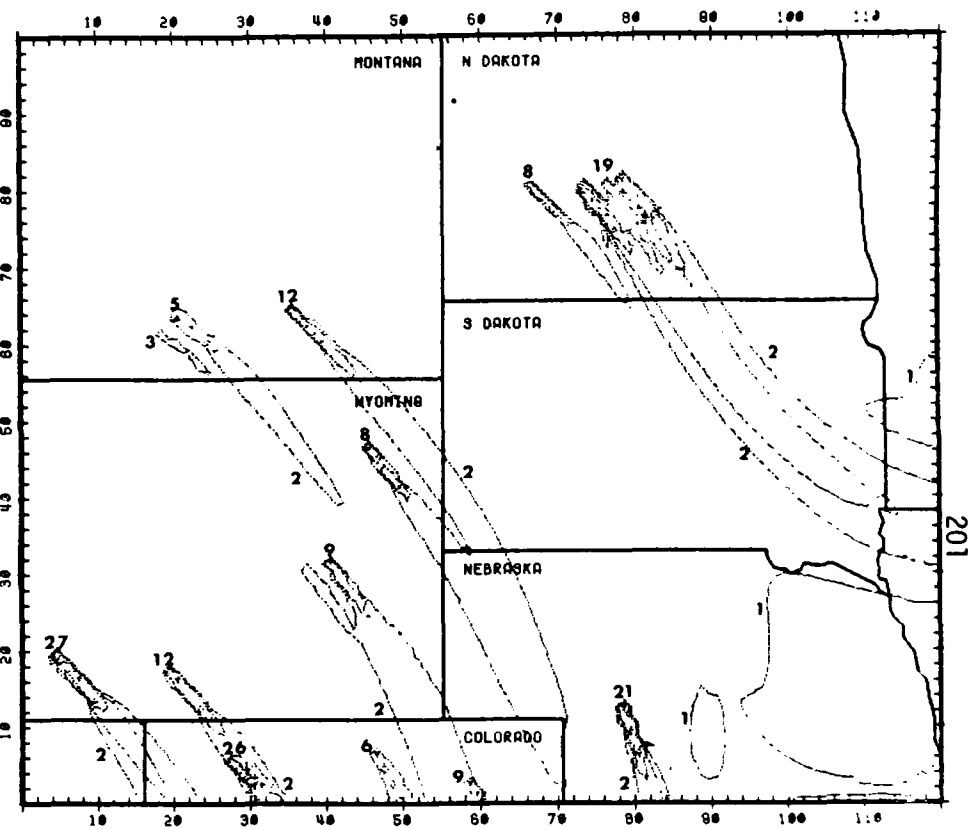
SO2 CONCENTRATIONS IN UG/M3 FOR THE HOUR -100-200 MST ON 760128



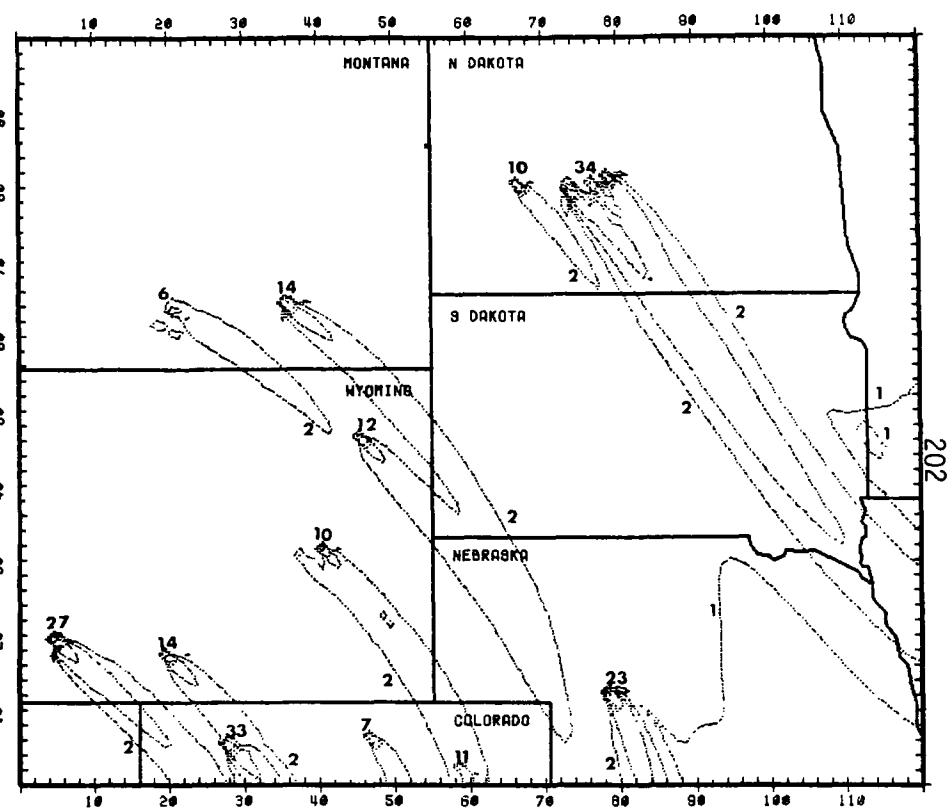
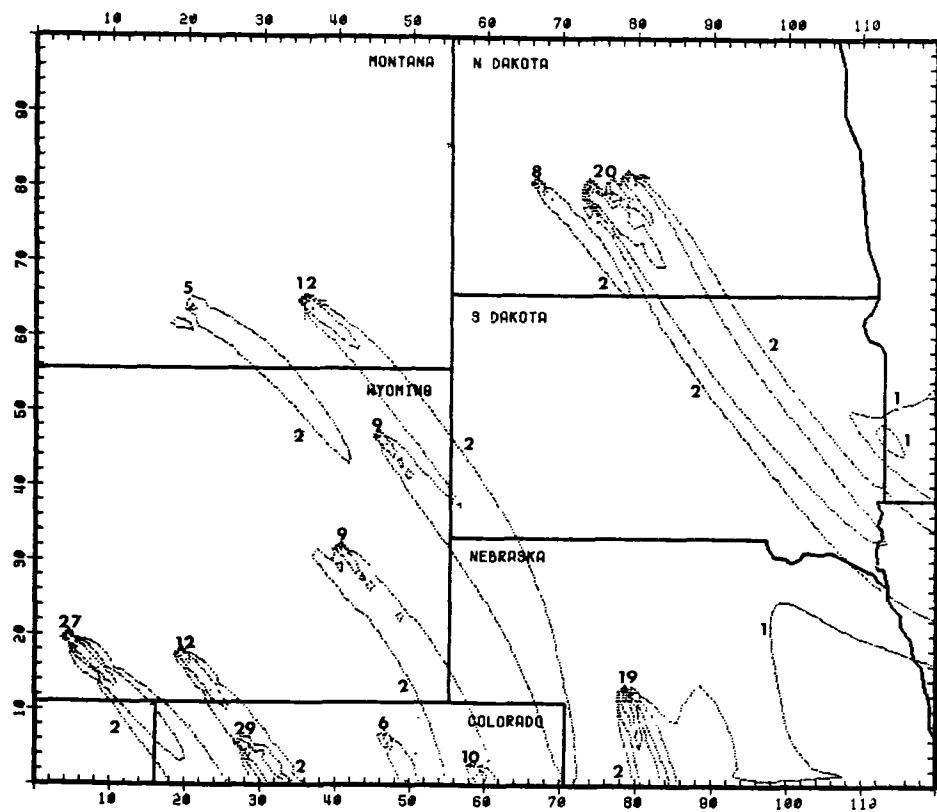
SO2 CONCENTRATIONS IN UG/M3 FOR THE HOUR 200-500 MST ON 760128



SO2 CONCENTRATIONS IN UG/M3 FOR THE HOUR 500-800 MST ON 760123

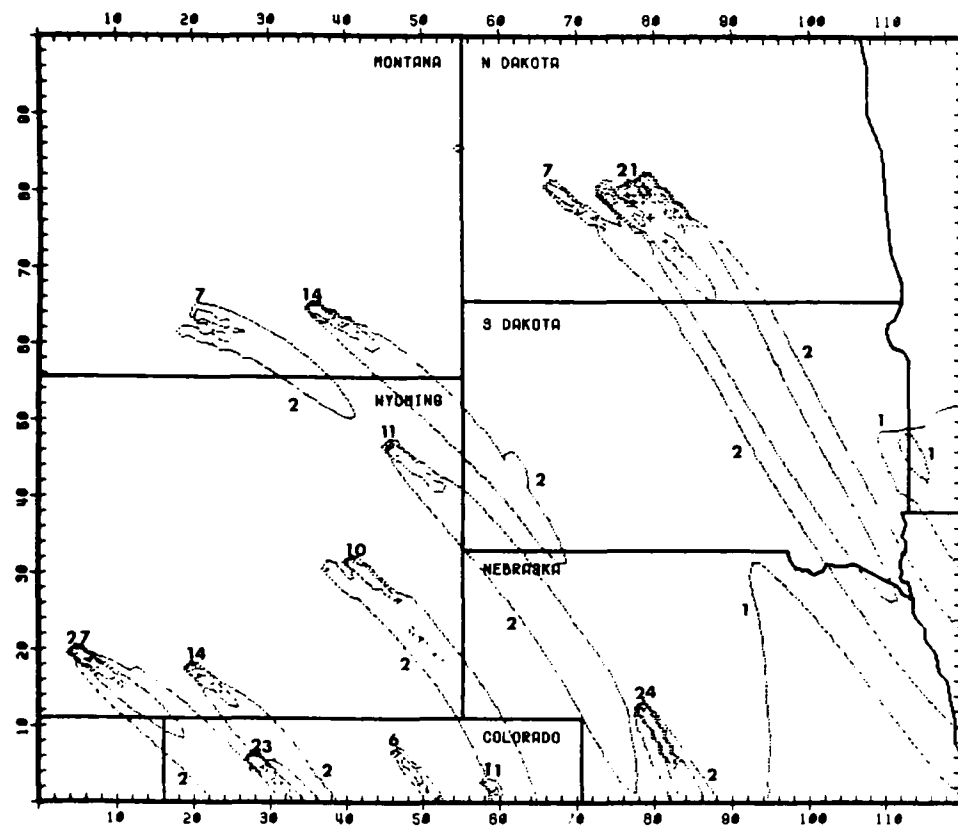


SO2 CONCENTRATIONS IN UG/M3 FOR THE HOUR 800-1100 MST ON 760123

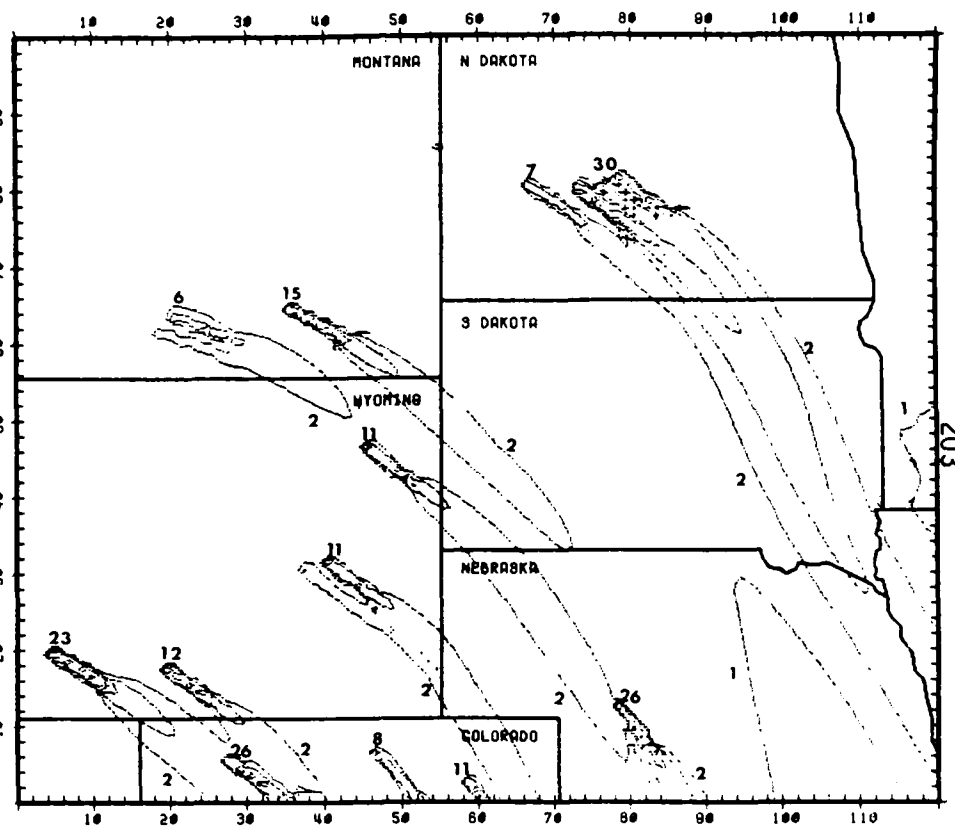


SO₂ CONCENTRATIONS IN UG/M³ FOR THE HOUR 1100-1400 MST ON 760128

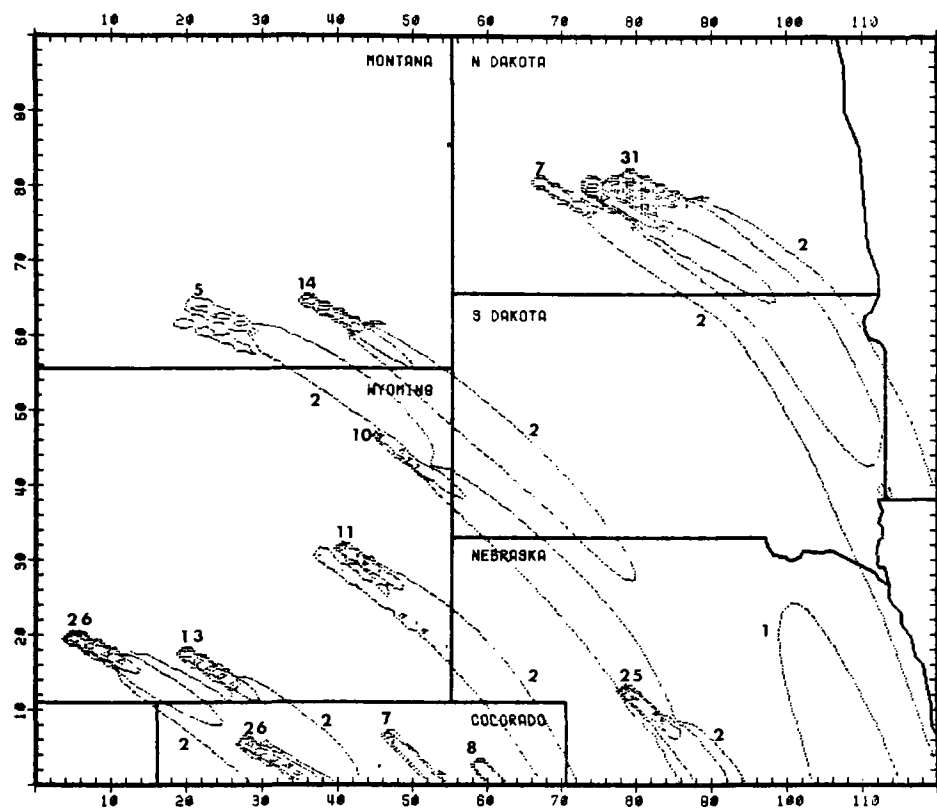
SO₂ CONCENTRATIONS IN UG/M³ FOR THE HOUR 1400-1700 MST ON 760128



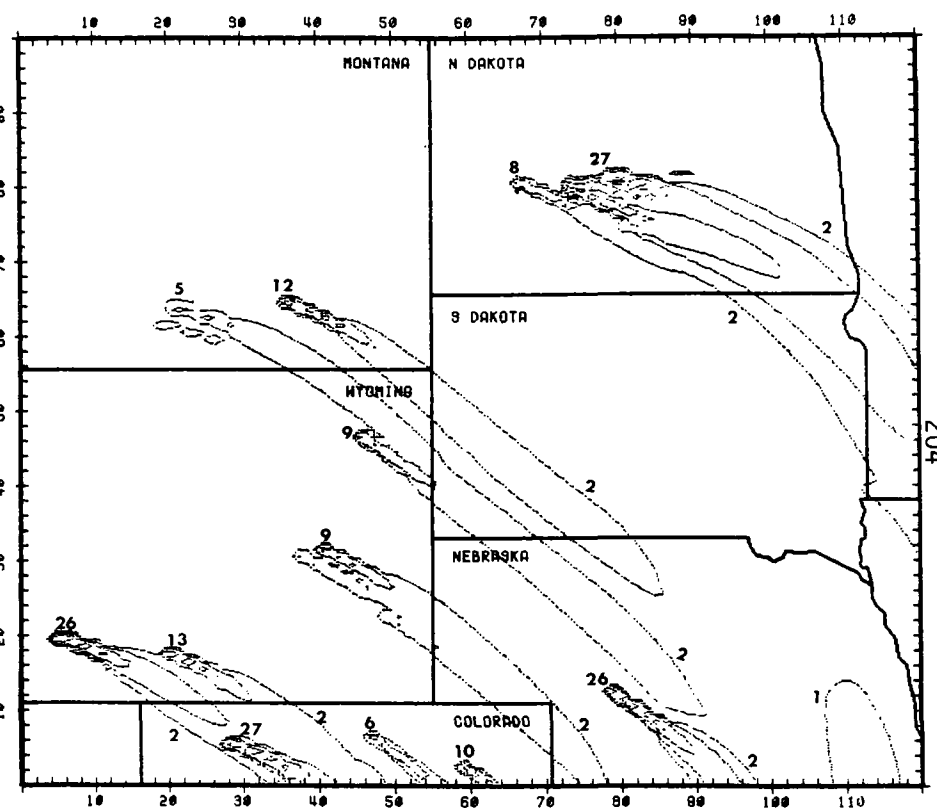
SO2 CONCENTRATIONS IN $\mu\text{g}/\text{m}^3$ FOR THE HOUR 1700-2000 MST ON 7/6/12



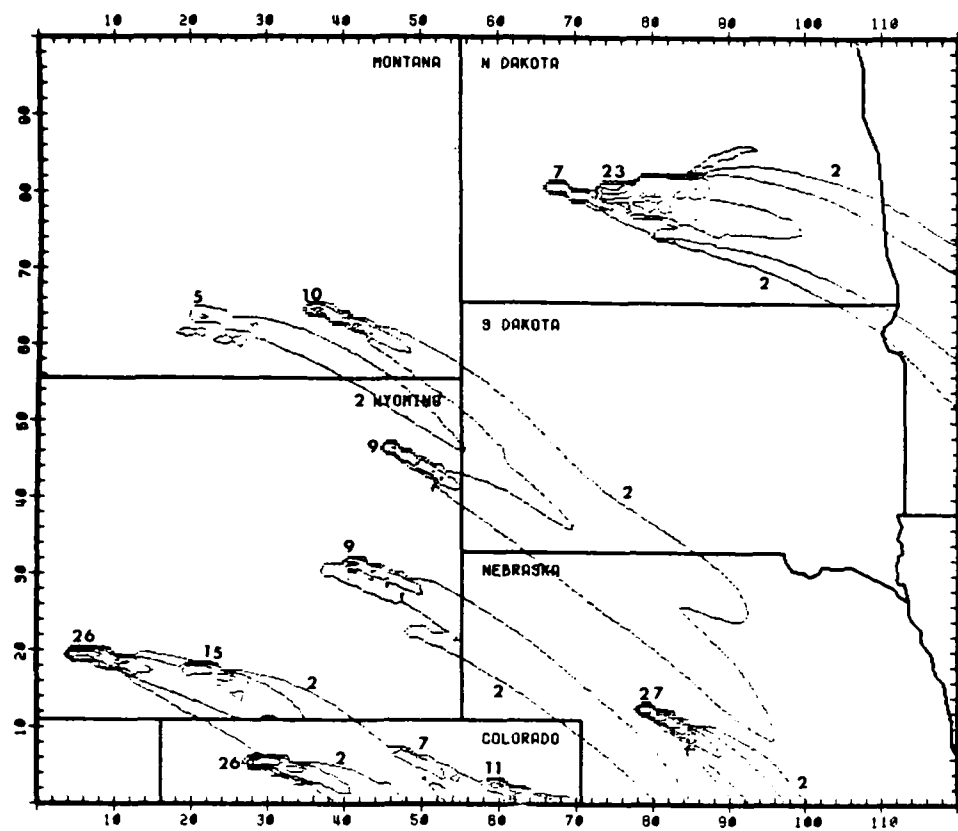
SO2 CONCENTRATIONS IN $\mu\text{g}/\text{m}^3$ FOR THE HOUR 2000-2300 MST ON 7/6/12



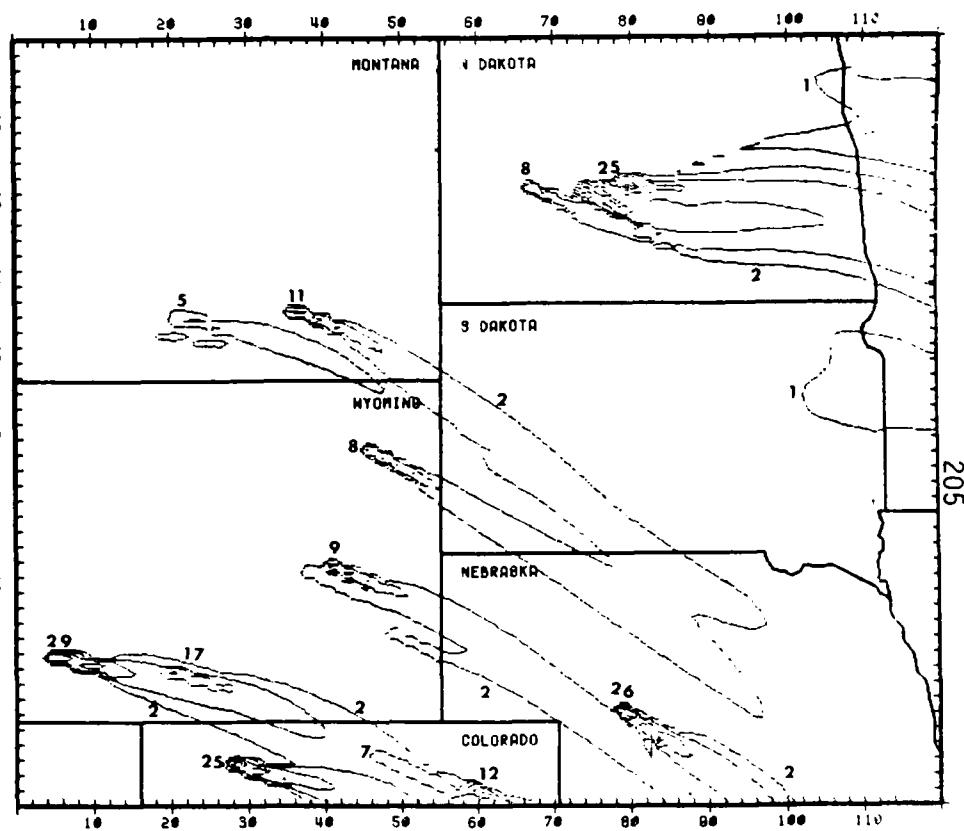
S02 CONCENTRATIONS IN UG/M3 FOR THE HOUR -100-200 MST ON 760129



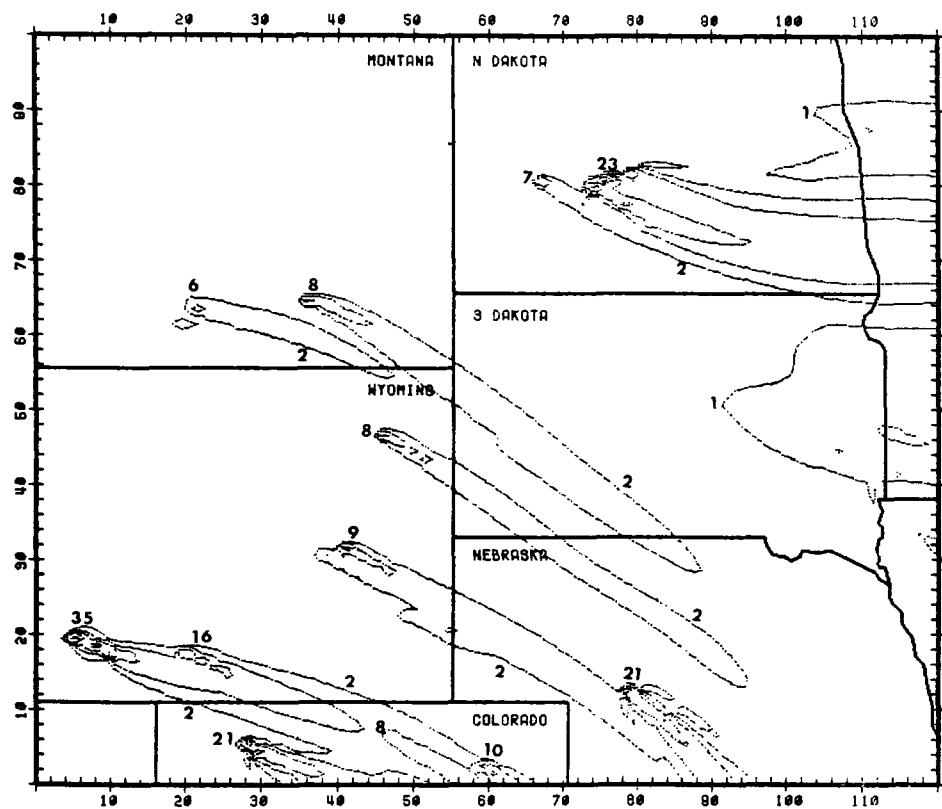
S02 CONCENTRATIONS IN UG/M3 FOR THE HOUR 200-500 MST ON 760129



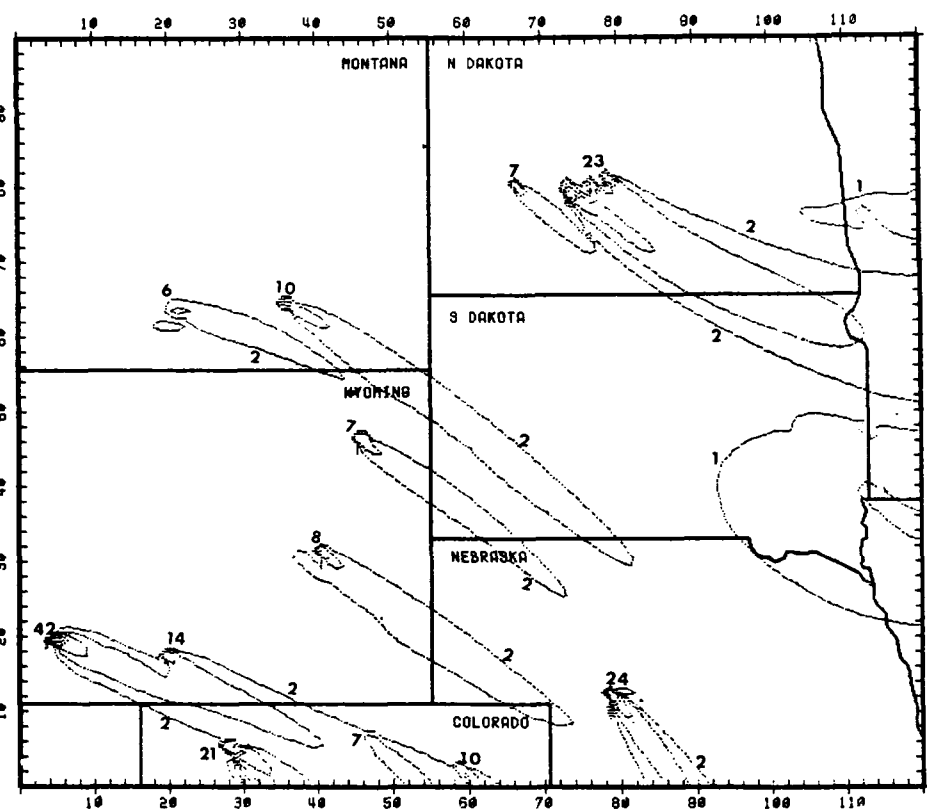
SO₂ CONCENTRATIONS IN UG/M3 FOR THE HOUR 500-800 MST ON 760129



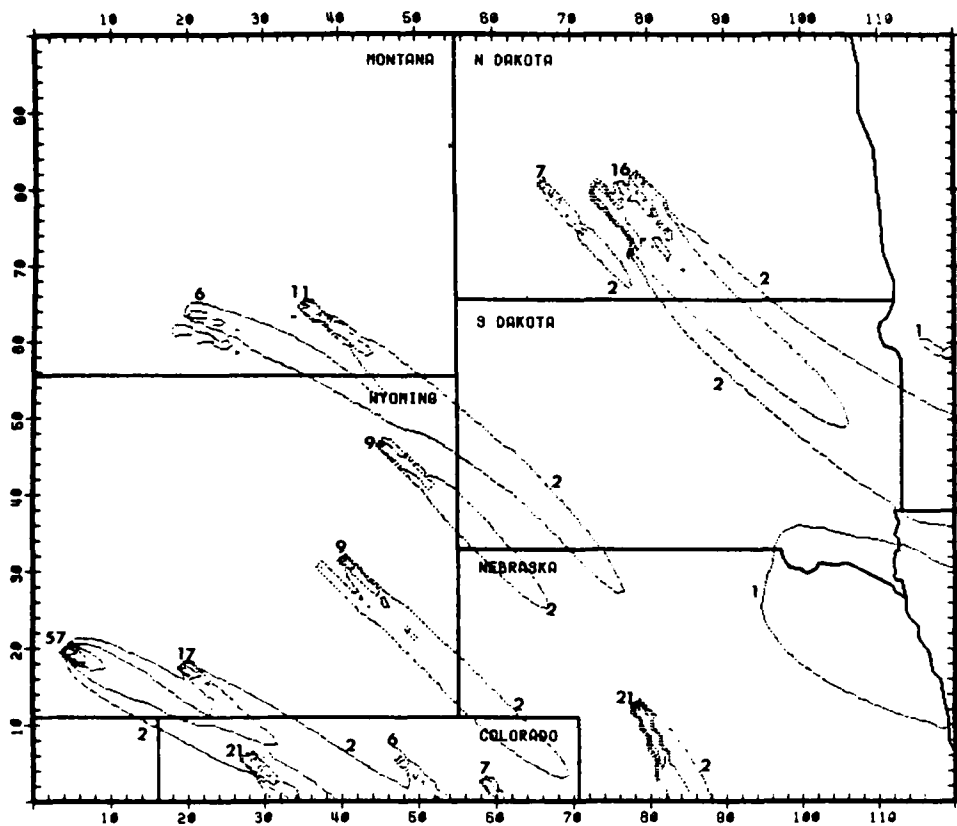
SO₂ CONCENTRATIONS IN UG/M3 FOR THE HOUR 800-1100 MST ON 760129



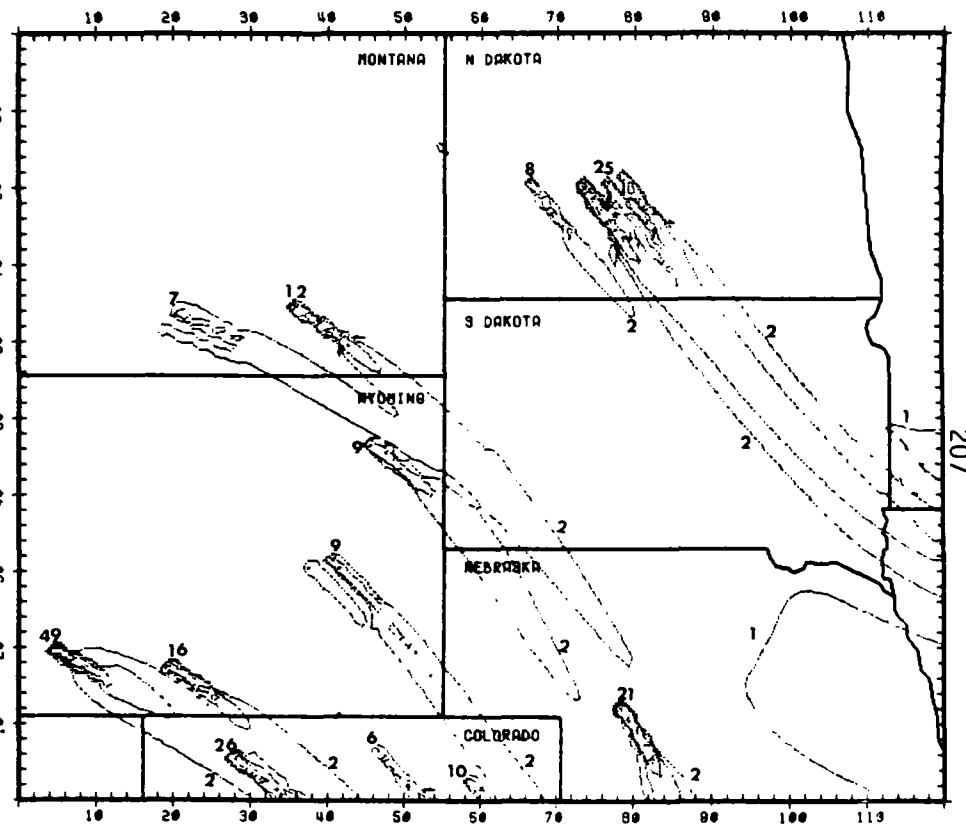
SO2 CONCENTRATIONS IN $\mu\text{G}/\text{M}^3$ FOR THE HOUR 1100-1400 MST ON 760129



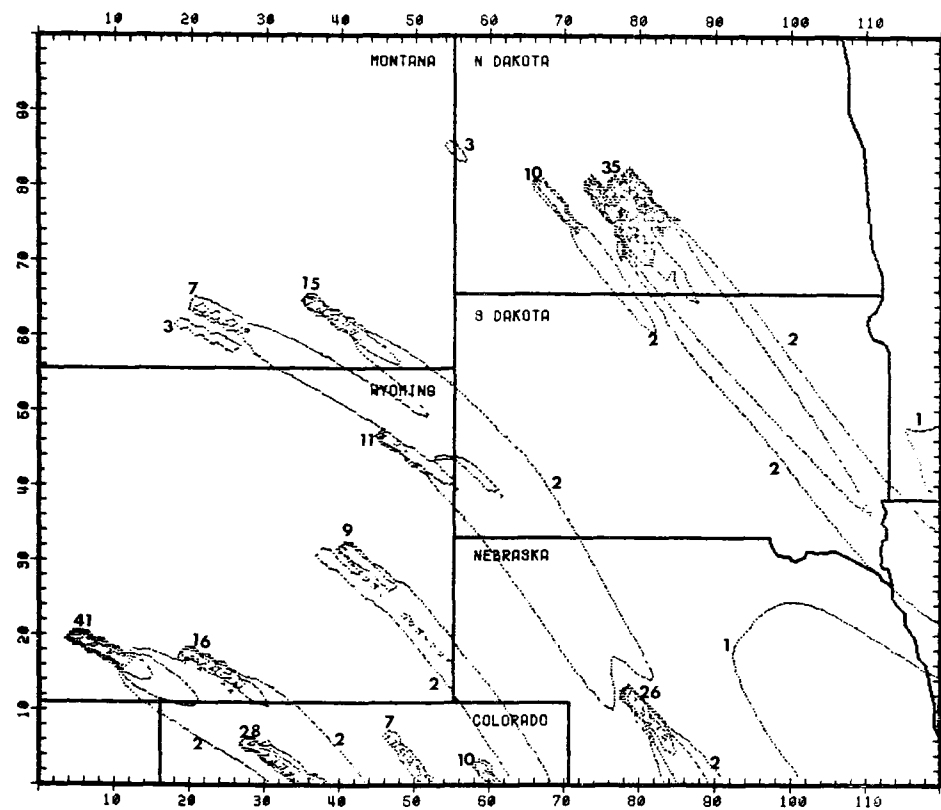
SO2 CONCENTRATIONS IN $\mu\text{G}/\text{M}^3$ FOR THE HOUR 1400-1700 MST ON 760129



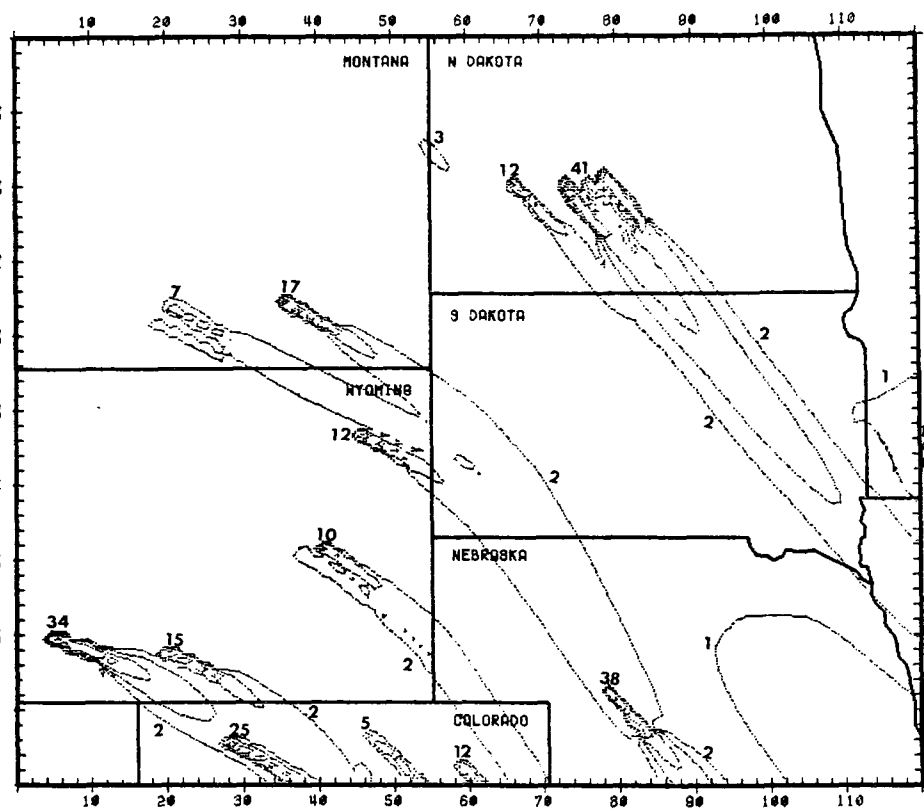
SO2 CONCENTRATIONS IN UG/M3 FOR THE HOUR 1700-2000 MST ON 760129



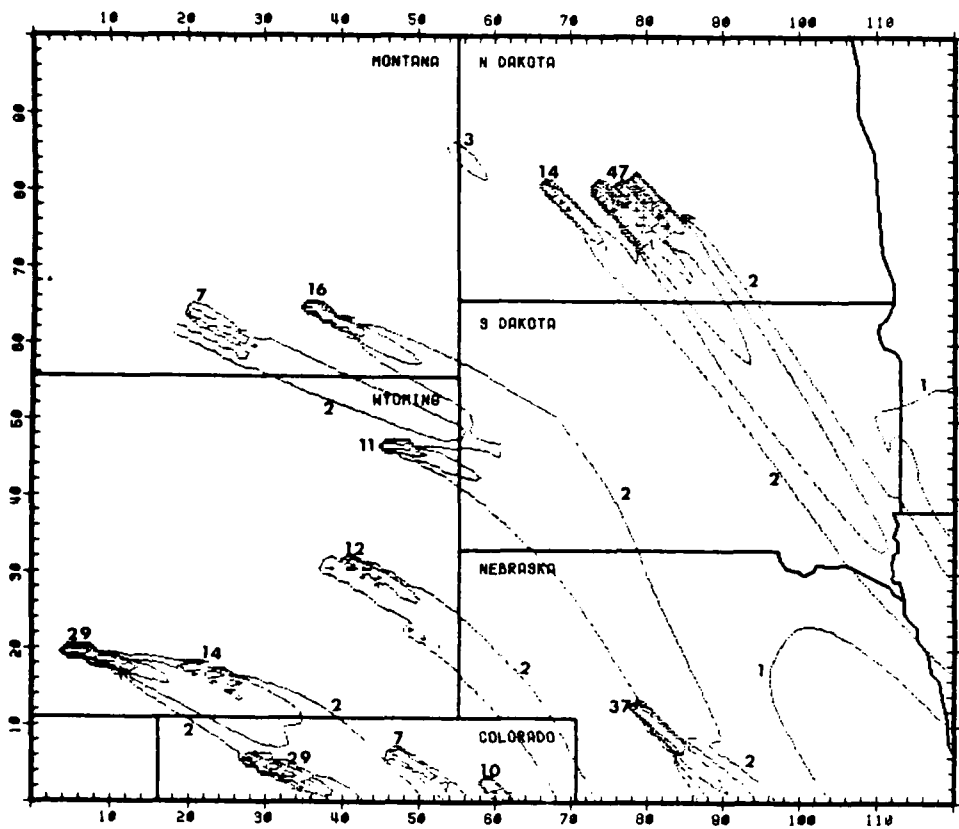
SO2 CONCENTRATIONS IN UG/M3 FOR THE HOUR 2000-2300 MST ON 760129



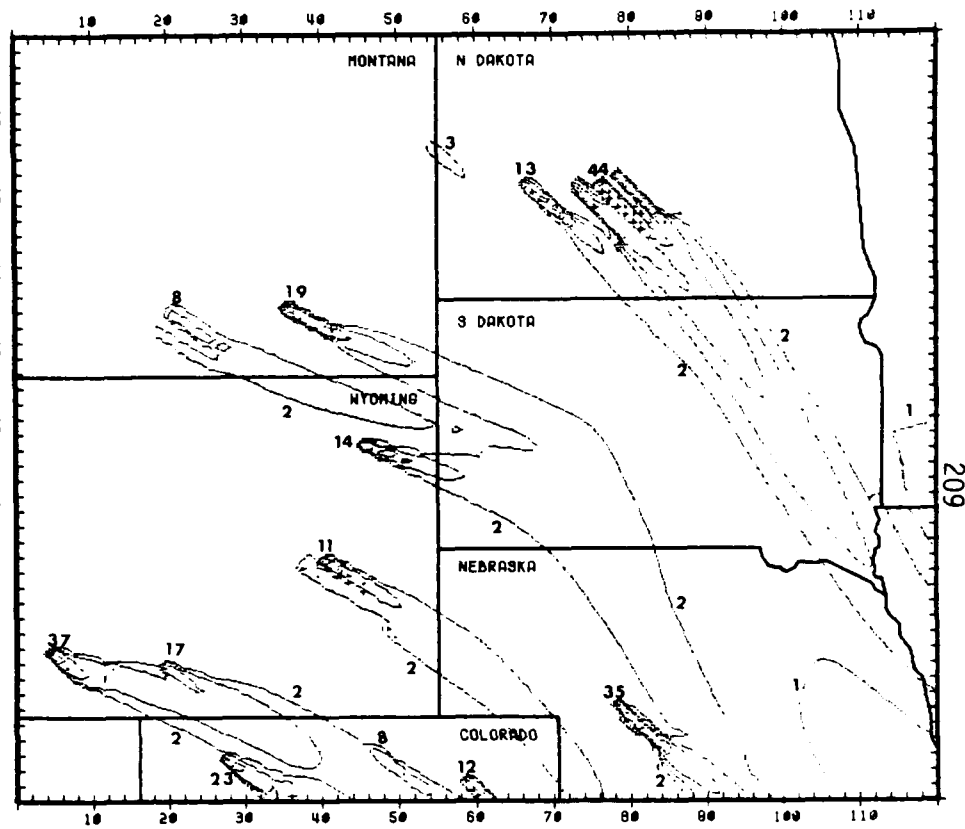
SO2 CONCENTRATIONS IN UG/M3 FOR THE HOUR -100-200 MST ON 760130



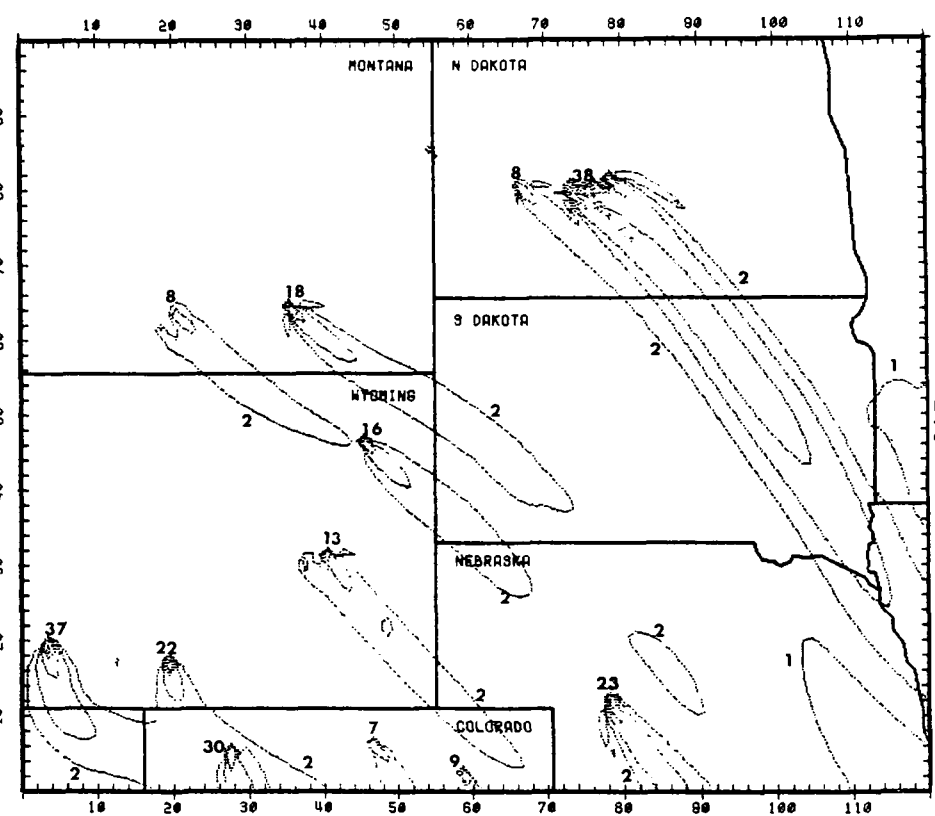
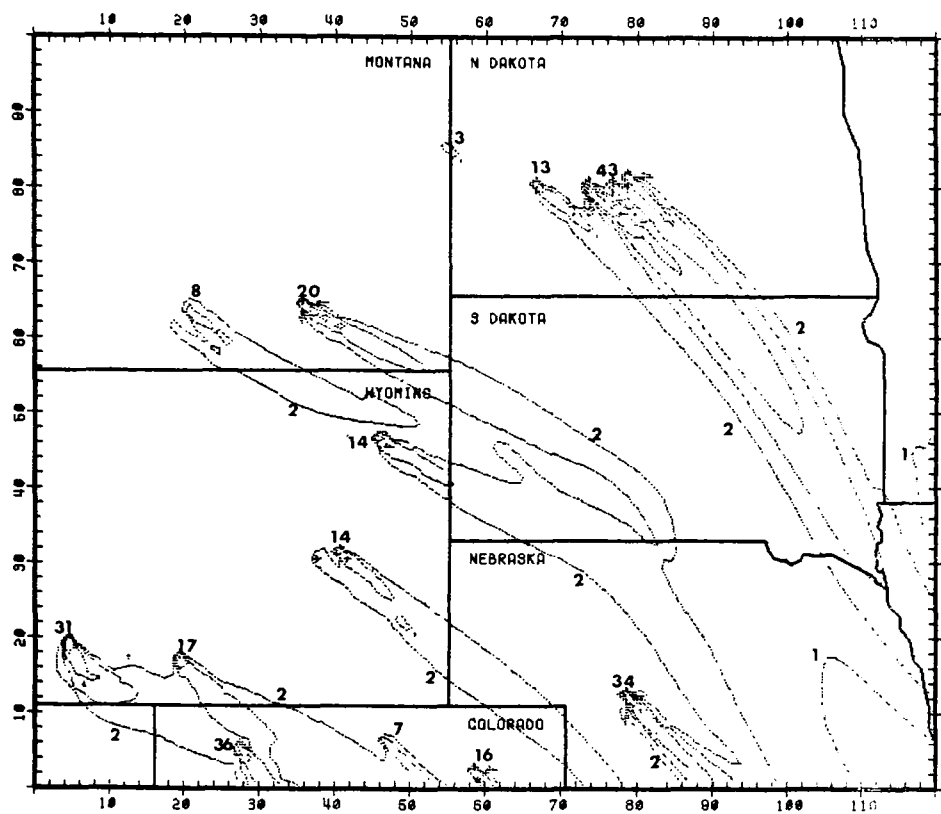
SO2 CONCENTRATIONS IN UG/M3 FOR THE HOUR 200-500 MST ON 760130



SO2 CONCENTRATIONS IN $\mu\text{g}/\text{m}^3$ FOR THE HOUR 500-800 MST ON 760130

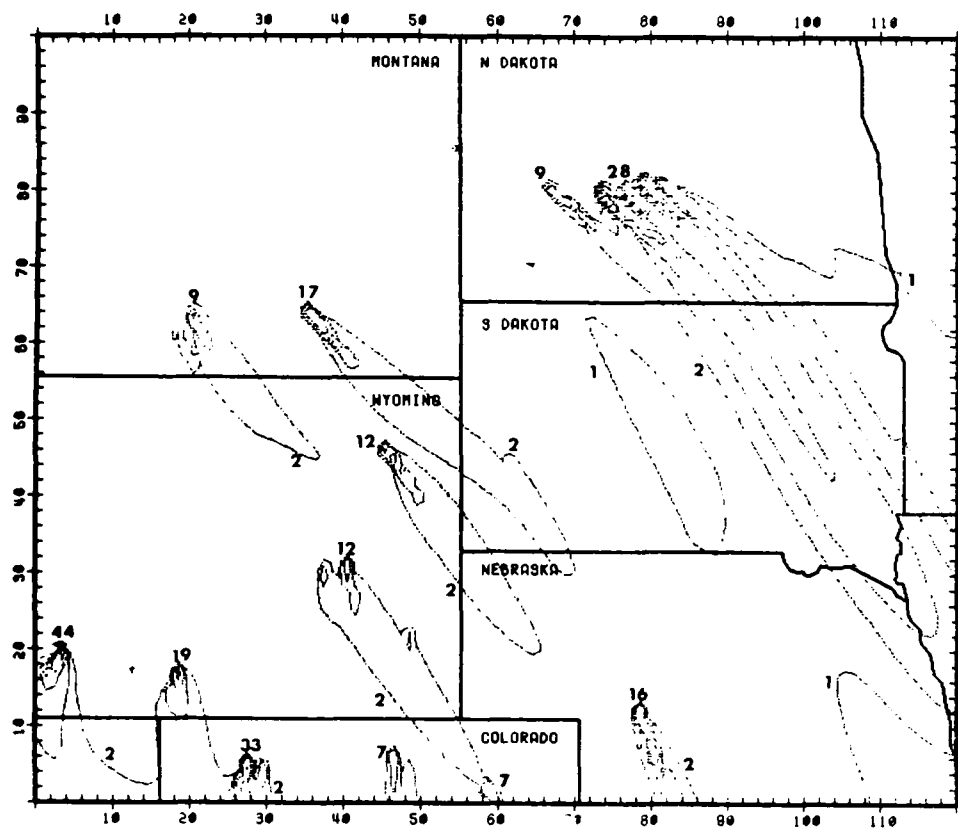


SO2 CONCENTRATIONS IN $\mu\text{g}/\text{m}^3$ FOR THE HOUR 800-1100 MST ON 760130

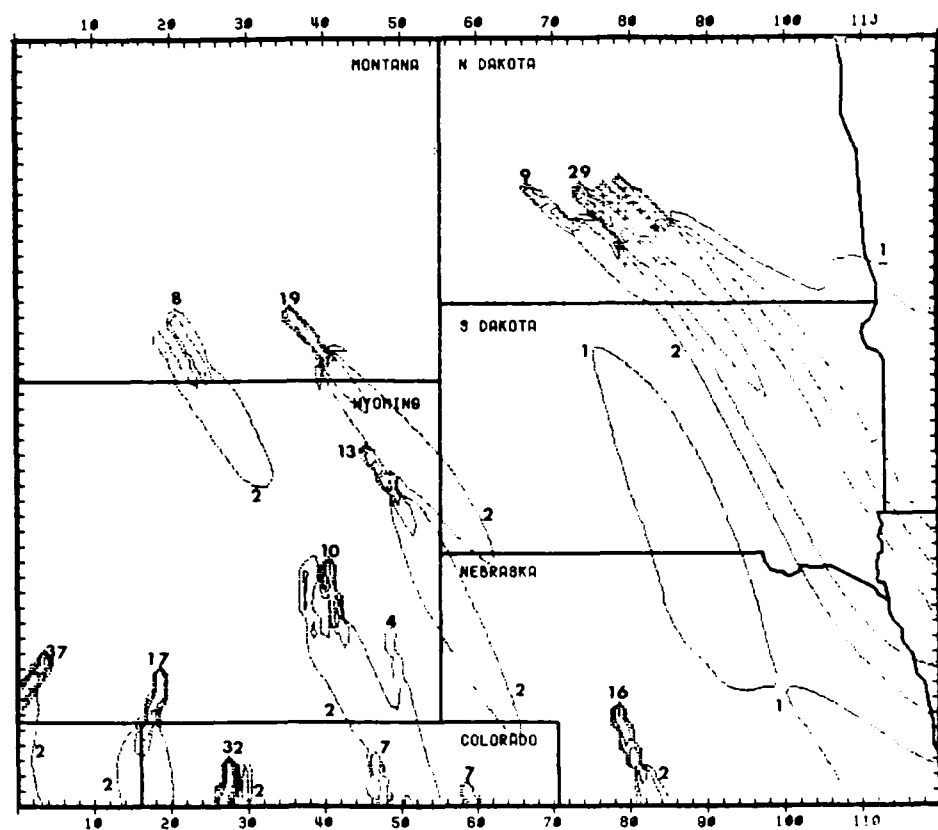


SO₂ CONCENTRATIONS IN UG/M3 FOR THE HOUR 1100-1400 MST ON 760130

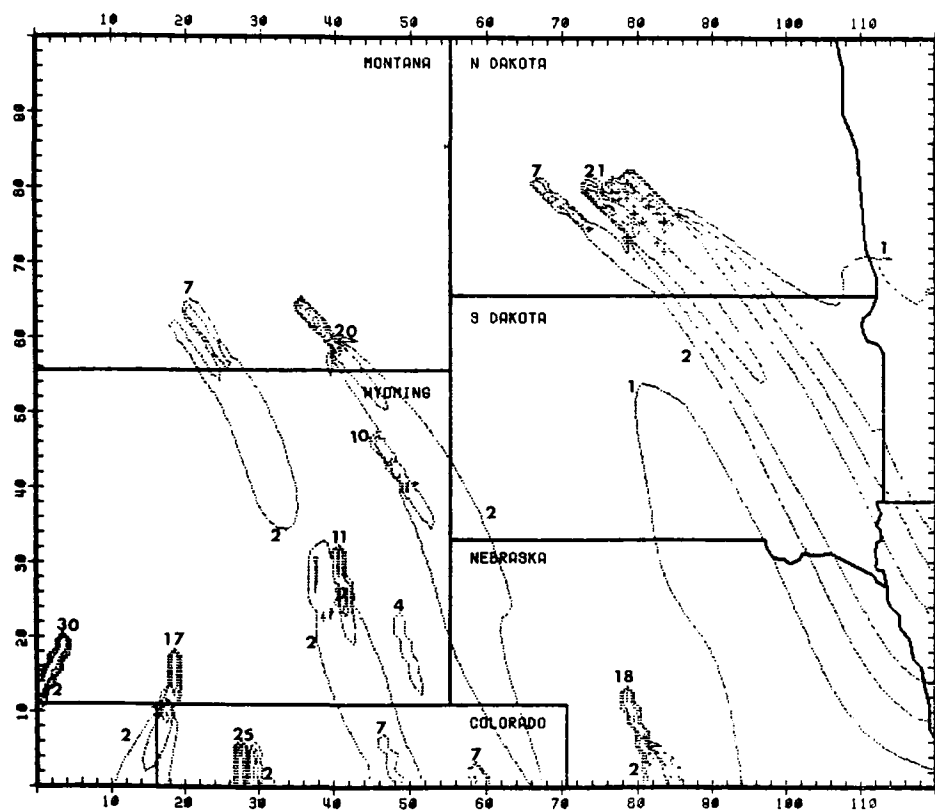
SO₂ CONCENTRATIONS IN UG/M3 FOR THE HOUR 1400-1700 MST ON 760130



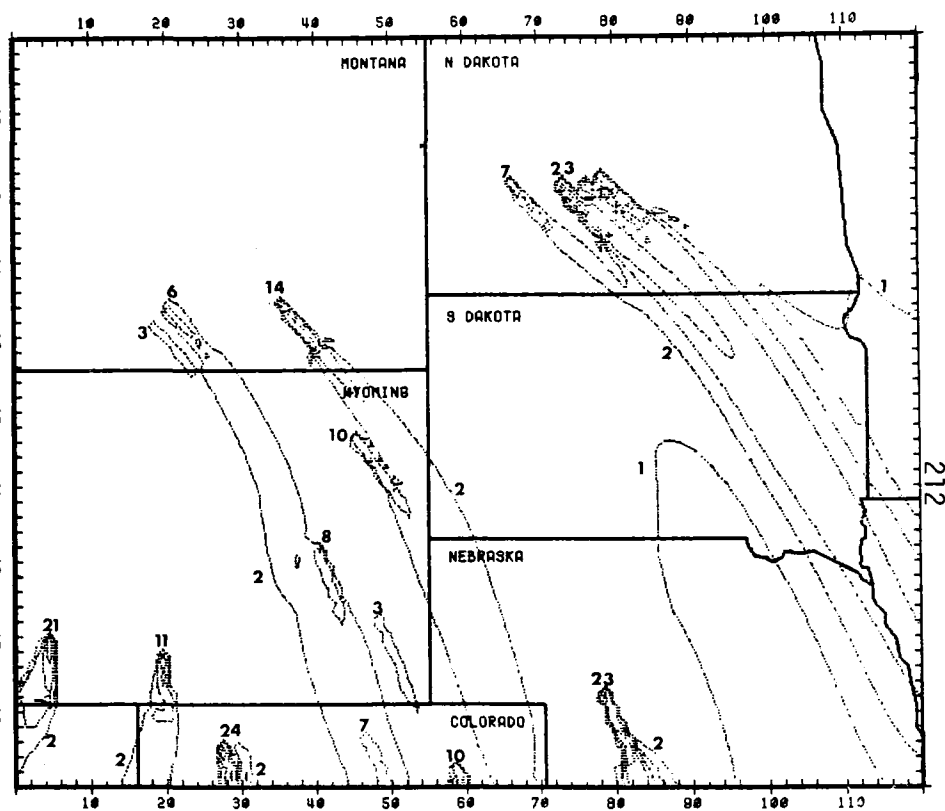
SO2 CONCENTRATIONS IN UG/M3 FOR THE HOUR 1700-2000 MST ON 760130



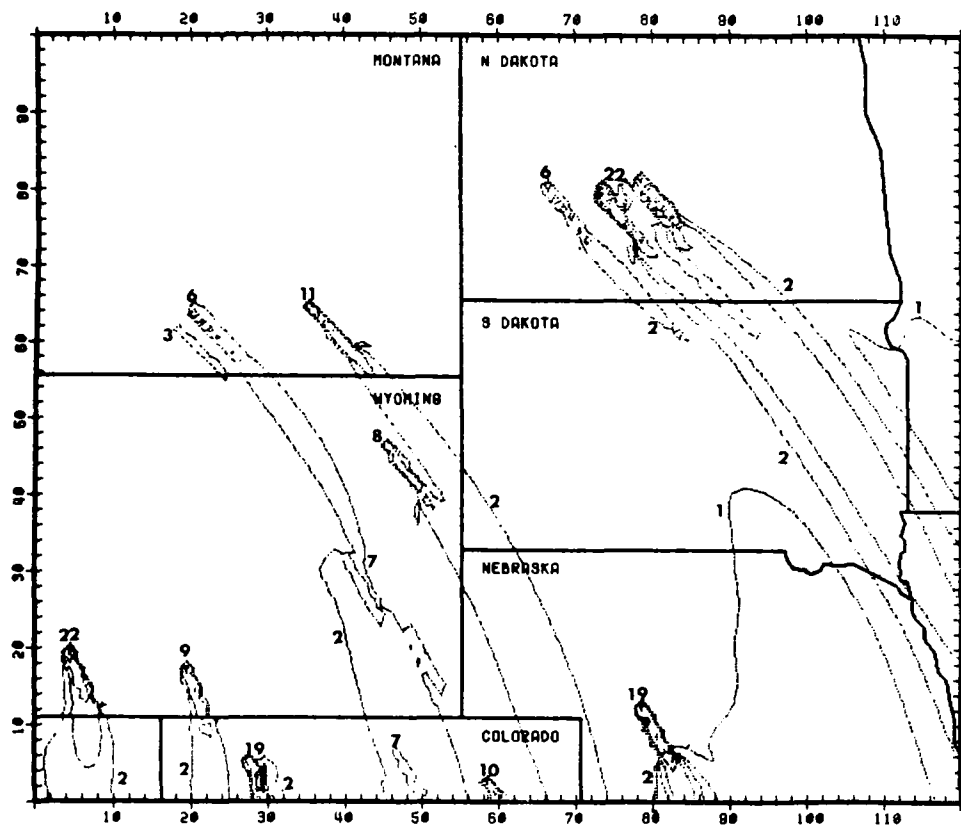
SO2 CONCENTRATIONS IN UG/M3 FOR THE HOUR 2000-2300 MST ON 760130



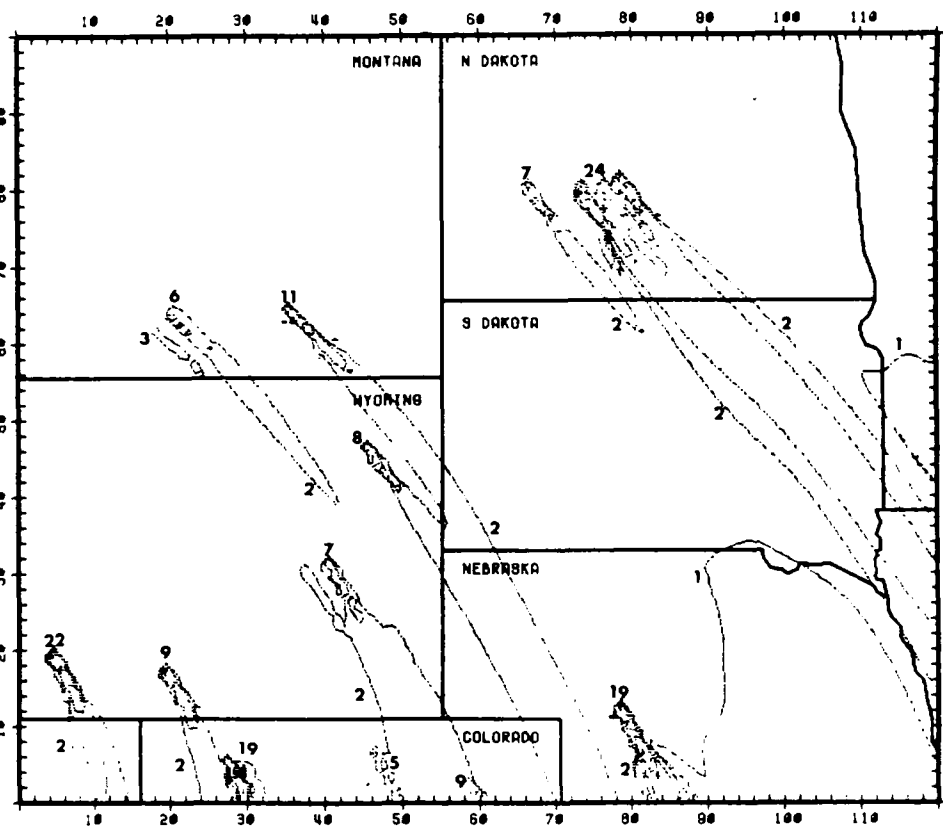
SO2 CONCENTRATIONS IN $\mu\text{g}/\text{m}^3$ FOR THE HOUR -100-200 MST ON 760131



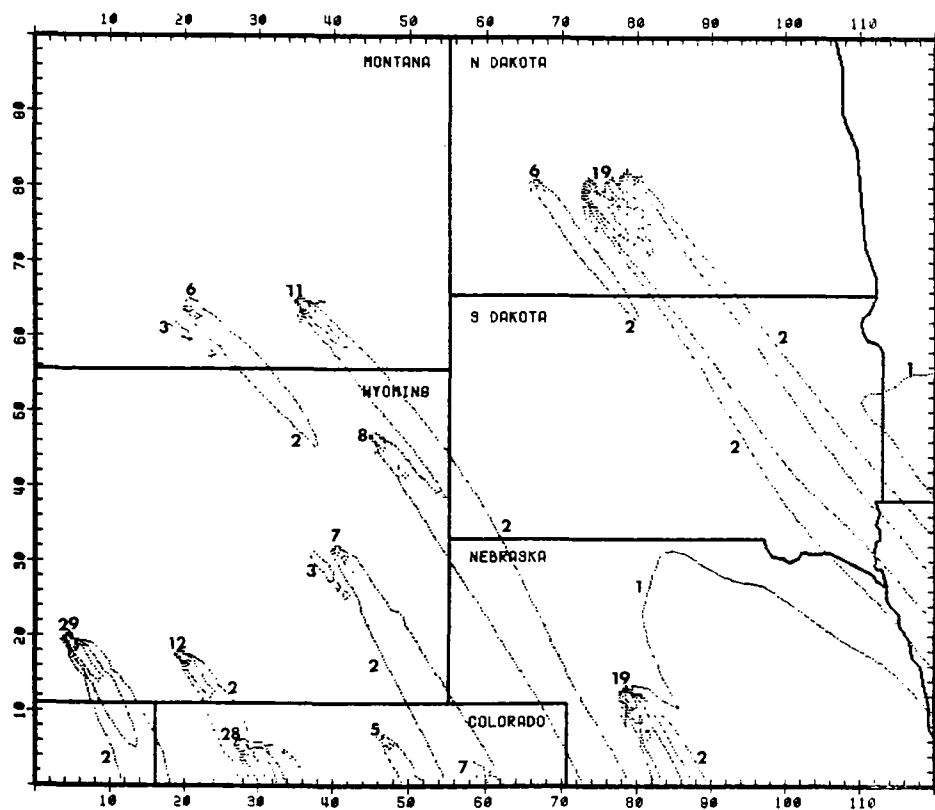
SO2 CONCENTRATIONS IN $\mu\text{g}/\text{m}^3$ FOR THE HOUR 200-500 MST ON 760131



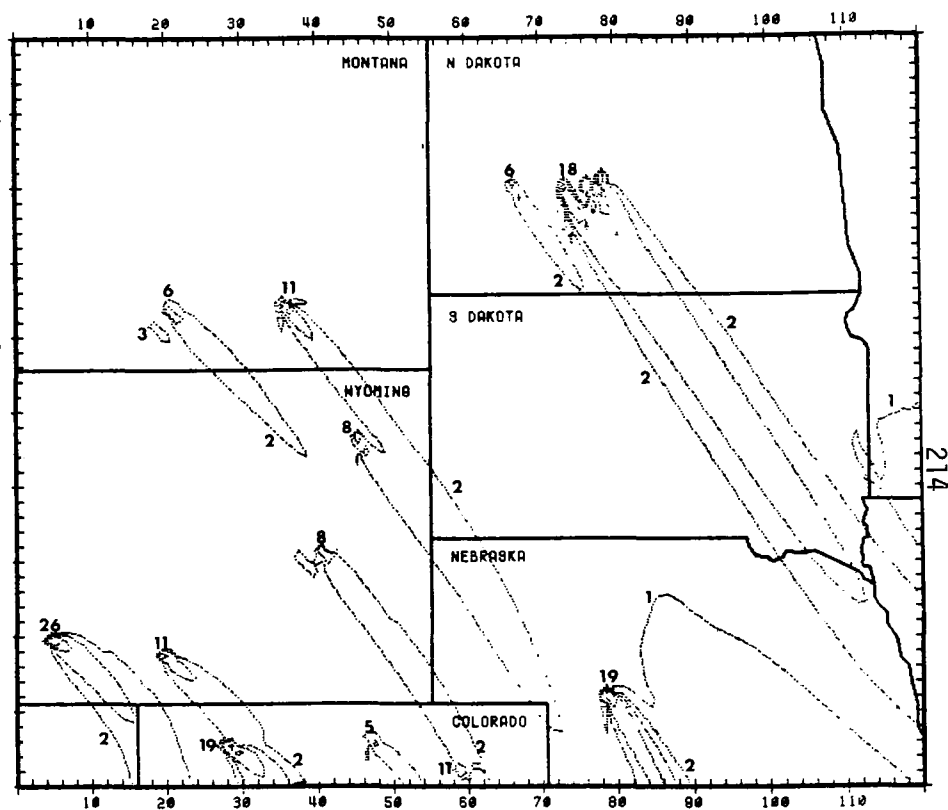
SO2 CONCENTRATIONS IN UG/M3 FOR THE HOUR 500-800 MST ON 760131



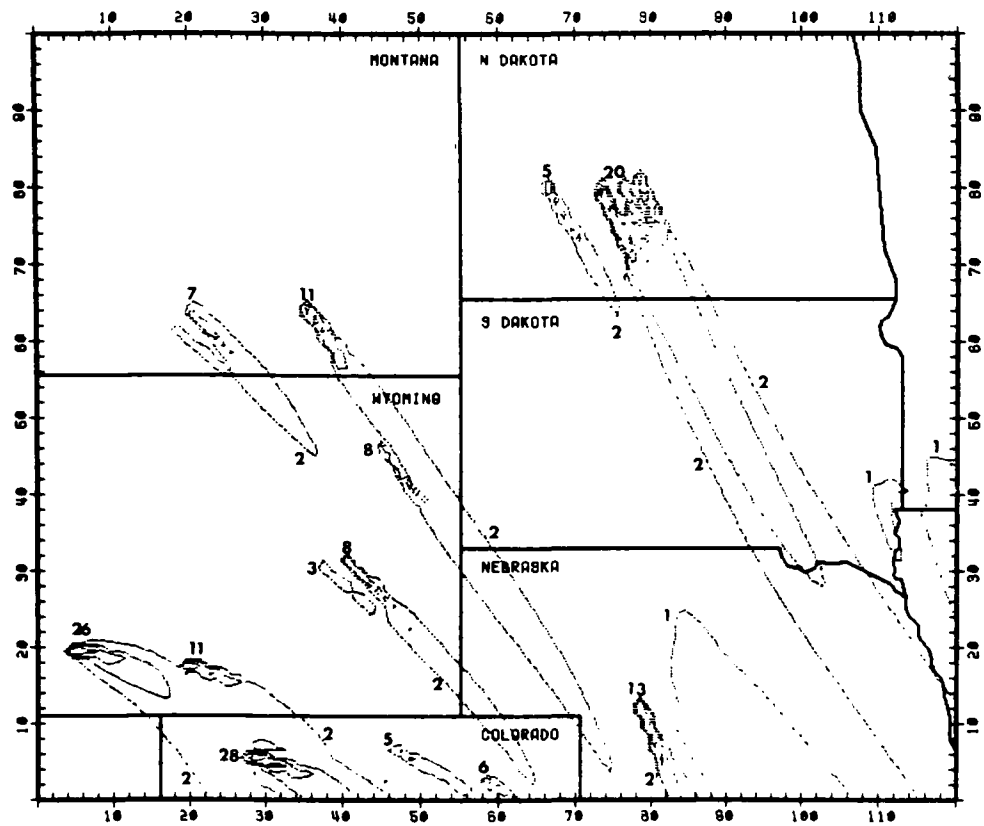
SO2 CONCENTRATIONS IN UG/M3 FOR THE HOUR 800-1100 MST ON 760131



SO₂ CONCENTRATIONS IN UG/M3 FOR THE HOUR 1100-1400 MST ON 760131

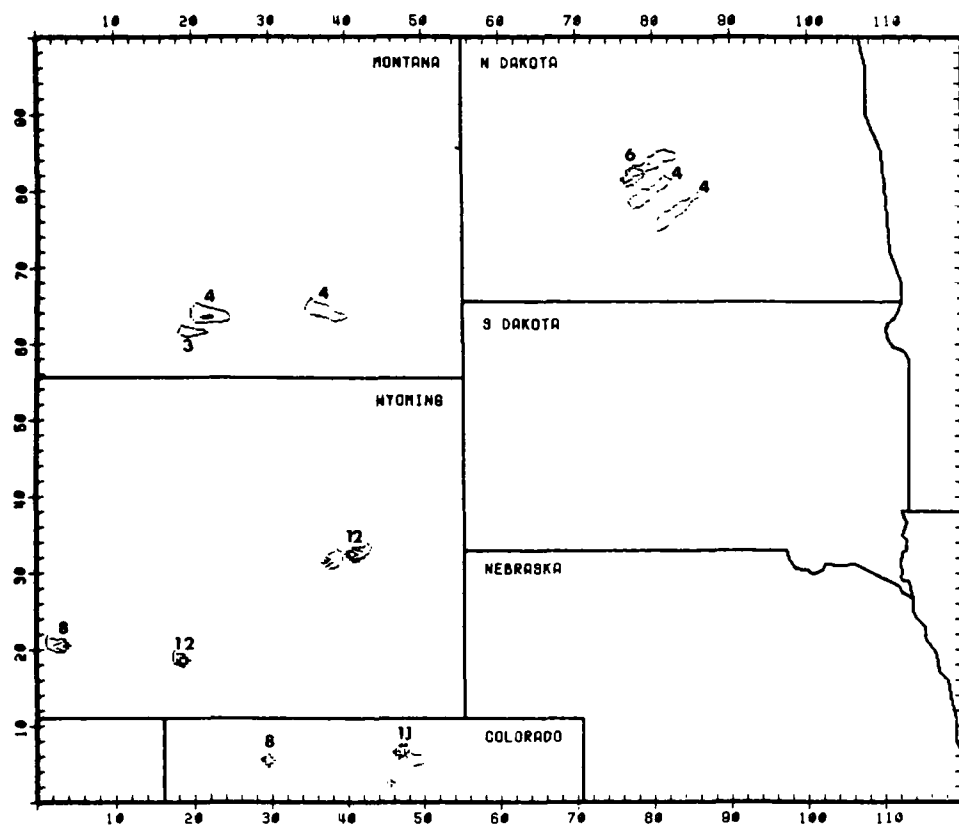


SO₂ CONCENTRATIONS IN UG/M3 FOR THE HOUR 1400-1700 MST ON 760131

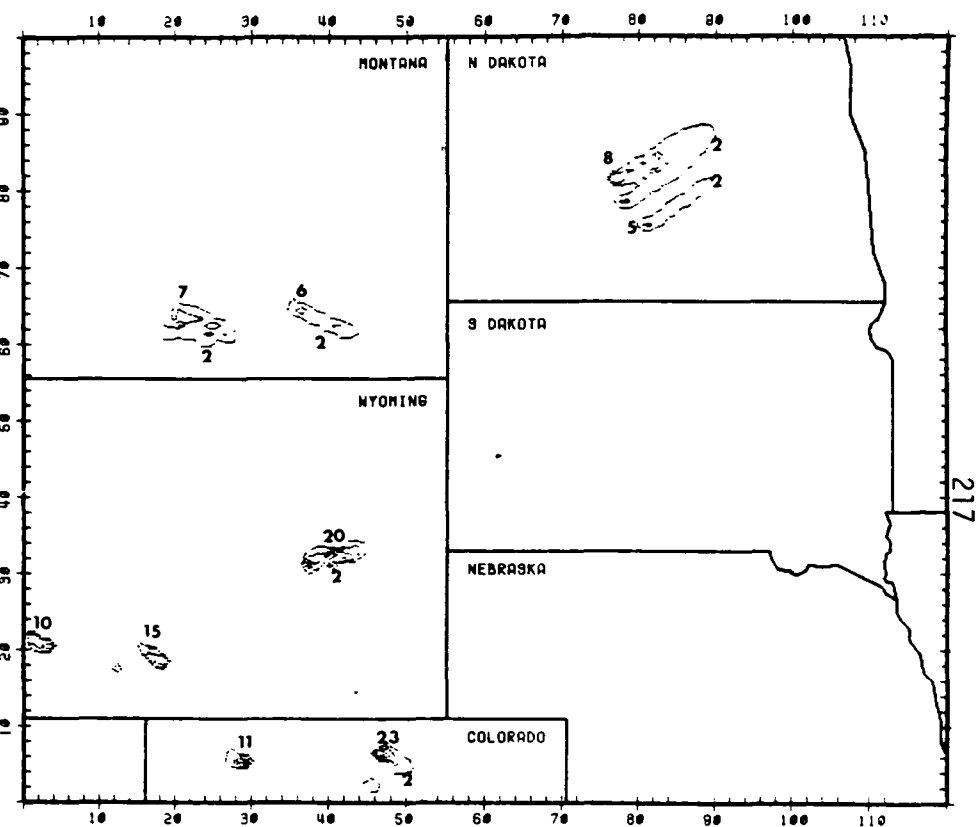


SO₂ CONCENTRATIONS IN UG/M³ FOR THE HOUR 1700-2000 MST ON 760131

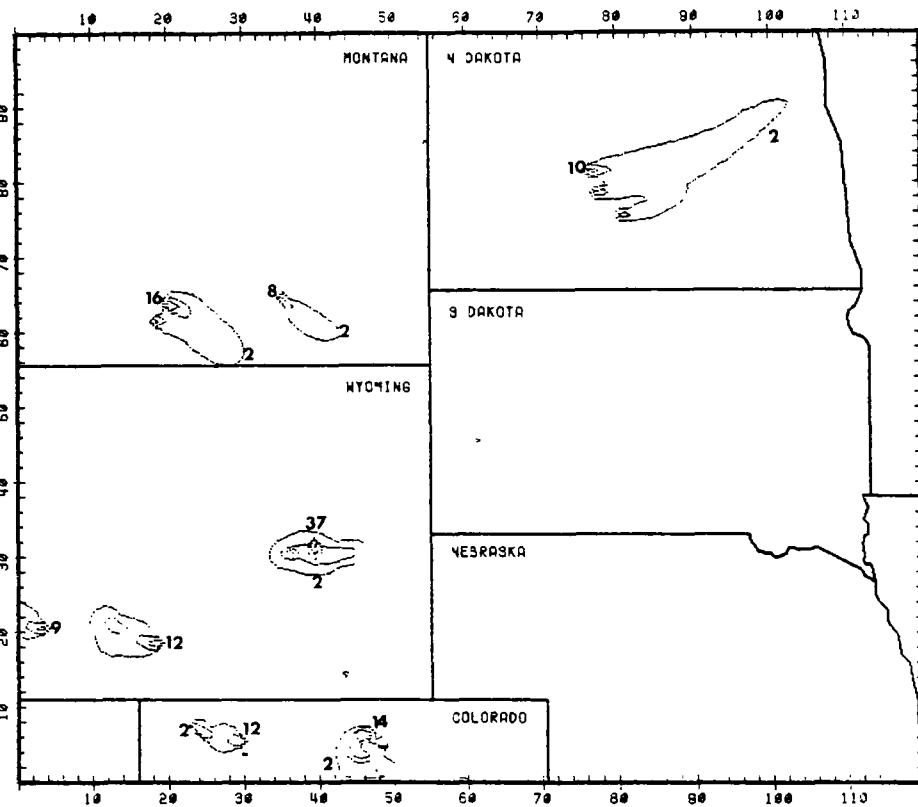
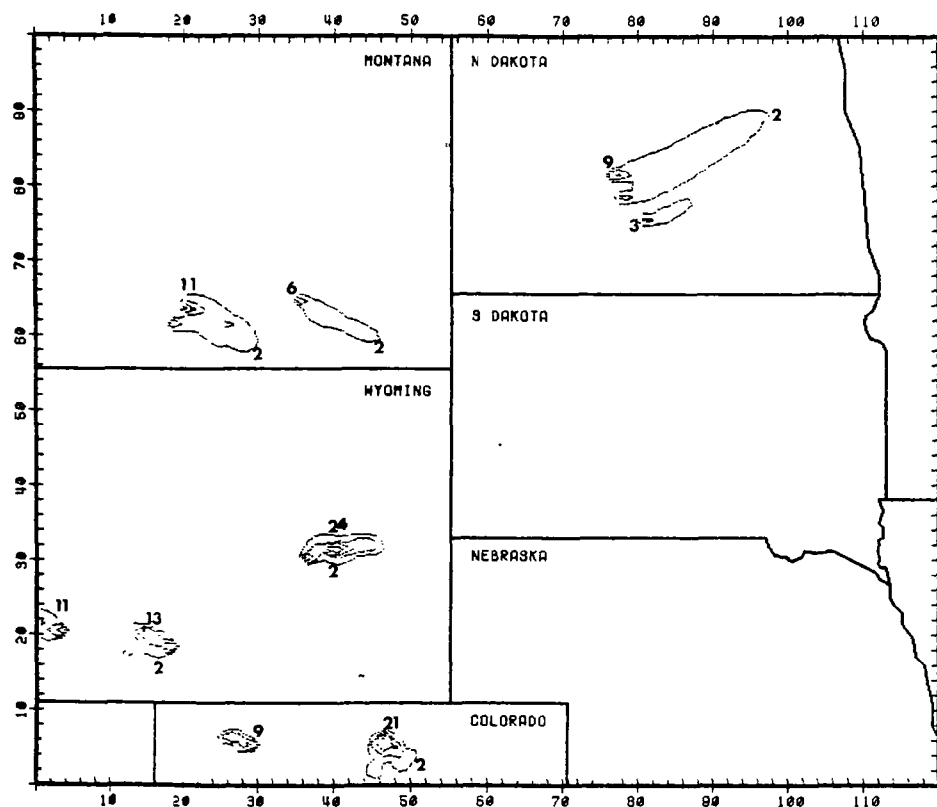
3. 4-7 APRIL 1976 METEOROLOGY; 1976 EMISSIONS



SO₂ CONCENTRATIONS IN UG/M3 FOR THE HOUR 500-800 MST ON 760404

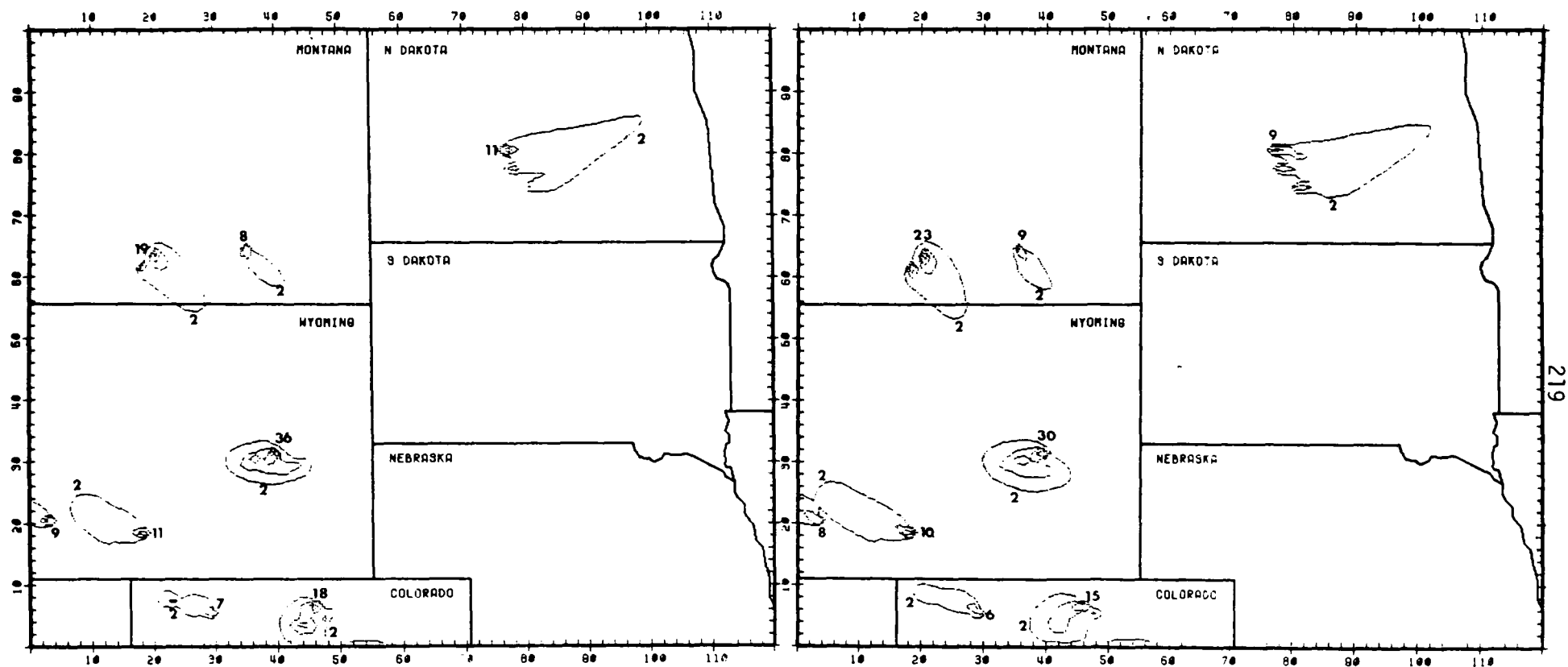


SO₂ CONCENTRATIONS IN UG/M3 FOR THE HOUR 800-1100 MST ON 760404



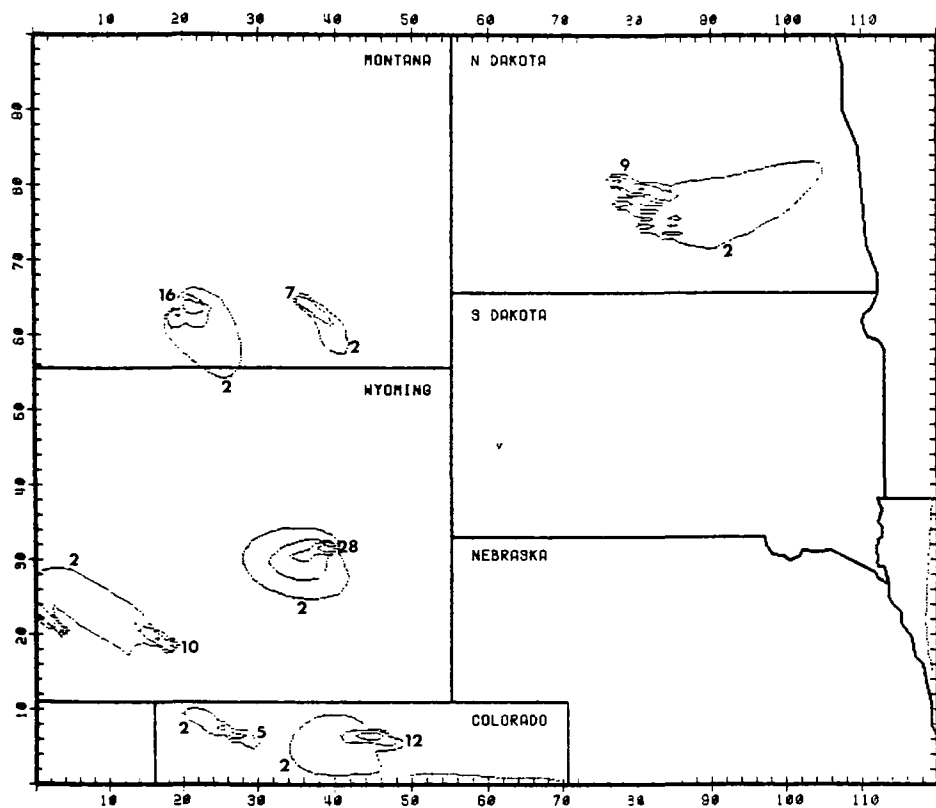
SO₂ CONCENTRATIONS IN UG/M³ FOR THE HOUR 1100-1400 MST ON 760404

SO₂ CONCENTRATIONS IN UG/M³ FOR THE HOUR 1400-1700 MST ON 760404

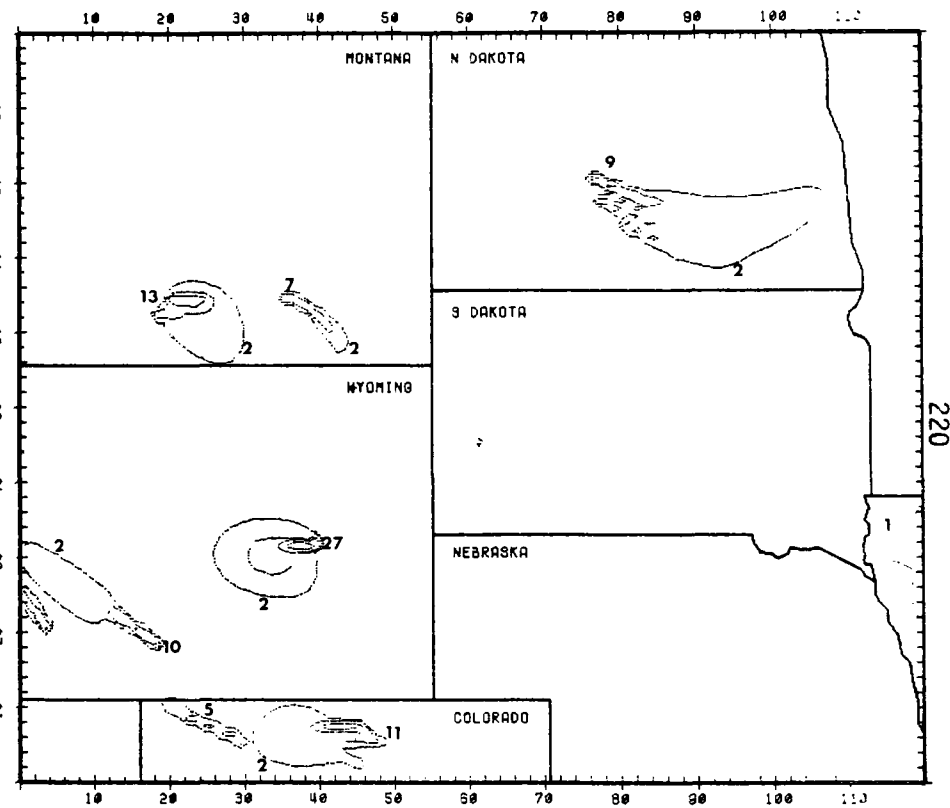


SO₂ CONCENTRATIONS IN UG/M³ FOR THE HOUR 1700-2000 MST ON 760404

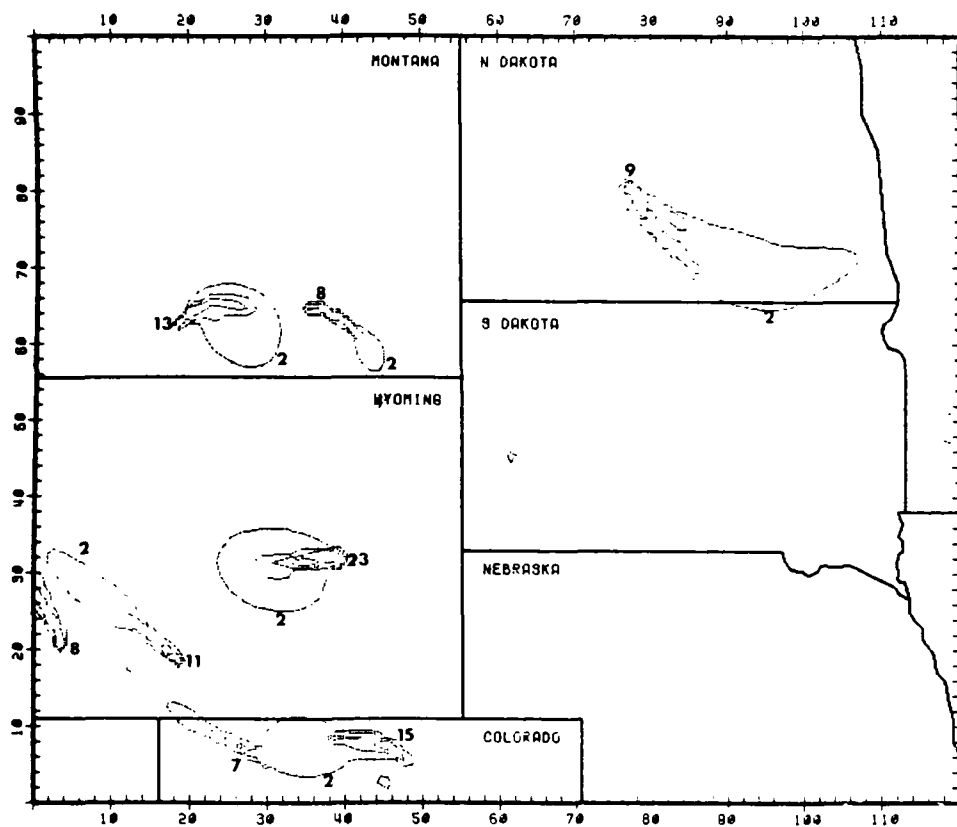
SO₂ CONCENTRATIONS IN UG/M³ FOR THE HOUR 2000-2300 MST ON 760404



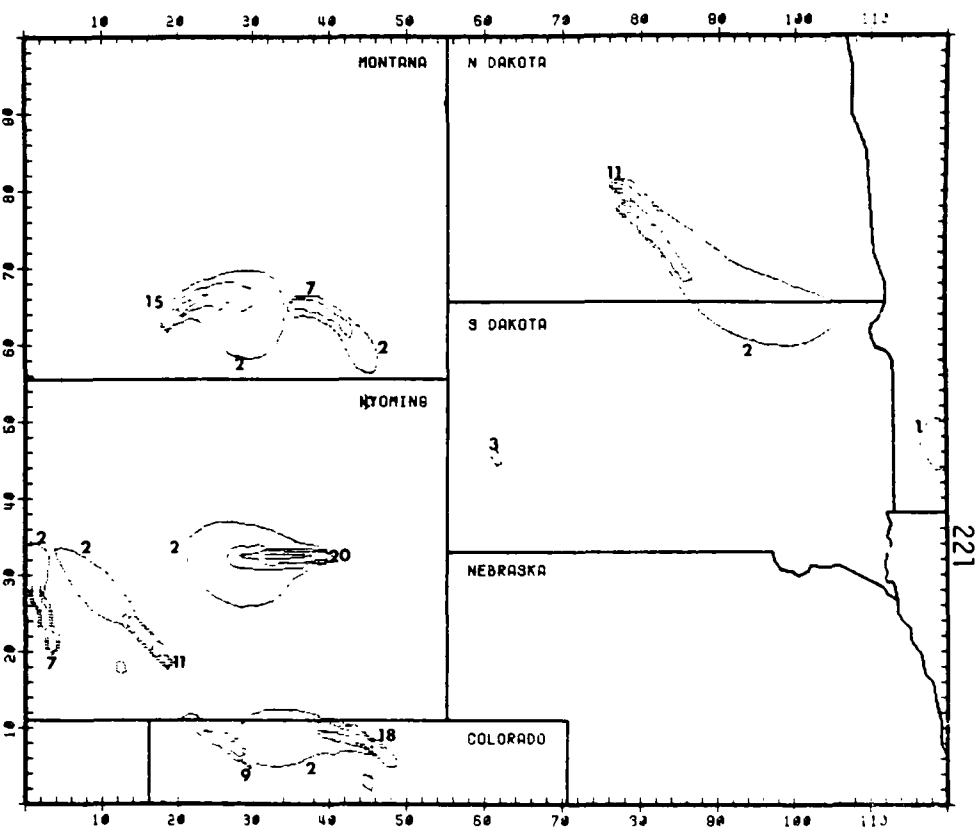
SO2 CONCENTRATIONS IN UG/M3 FOR THE HOUR -120-200 MST ON 760405



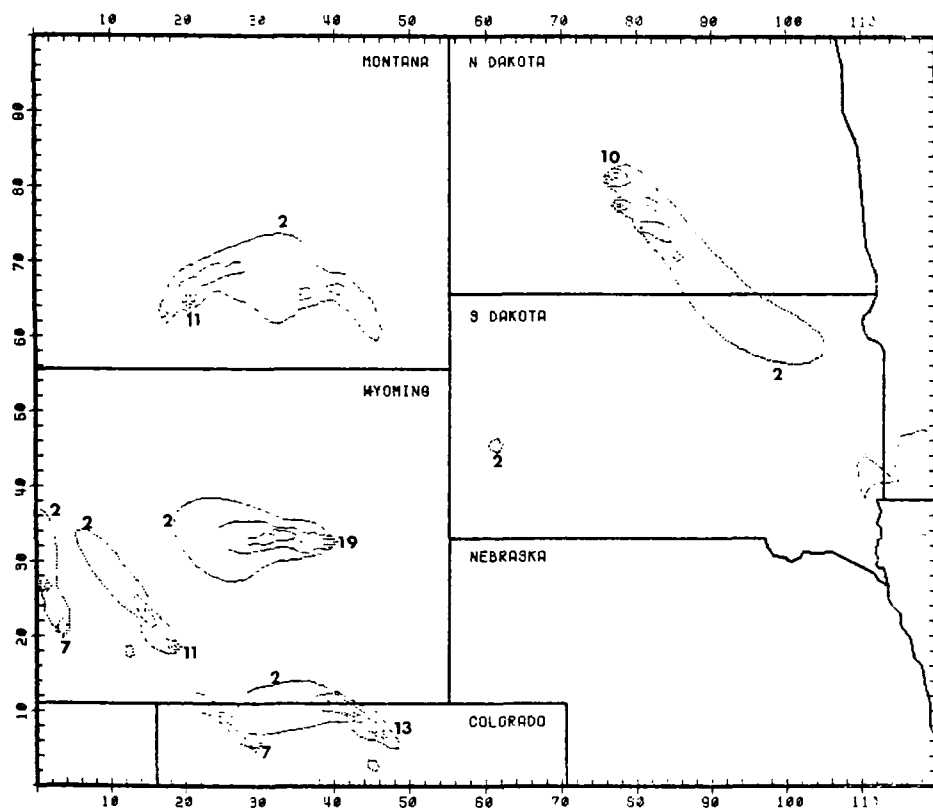
SO2 CONCENTRATIONS IN UG/M3 FOR THE HOUR 200-500 MST ON 760405



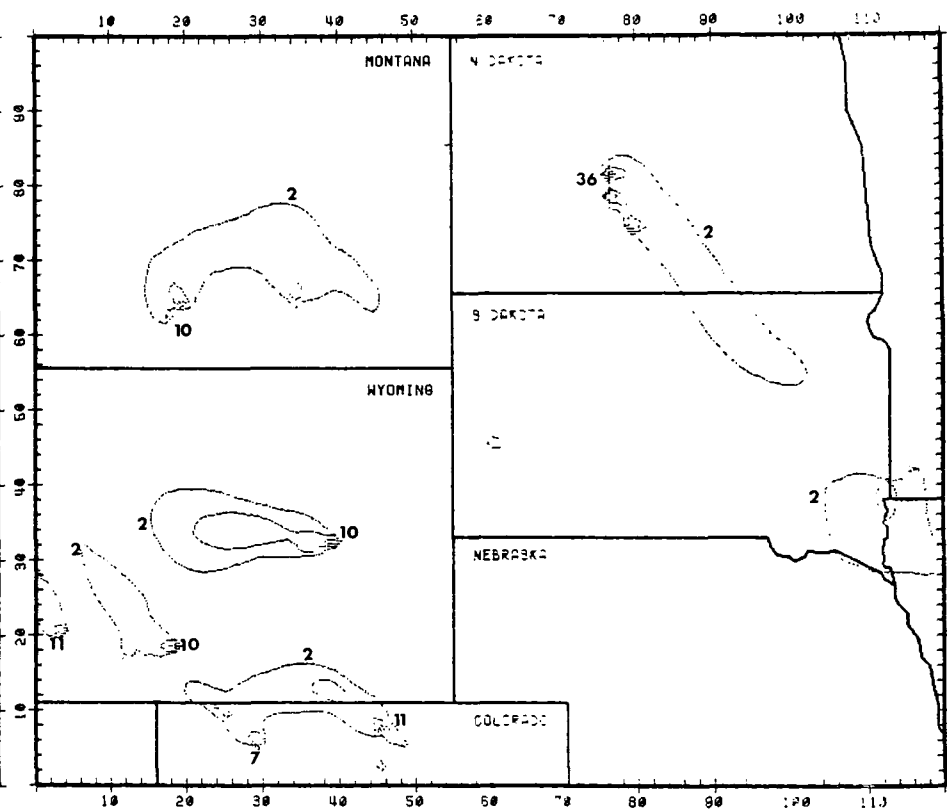
SO2 CONCENTRATIONS IN UG/M3 FOR THE HOUR 500-900 MST ON 7/24/05



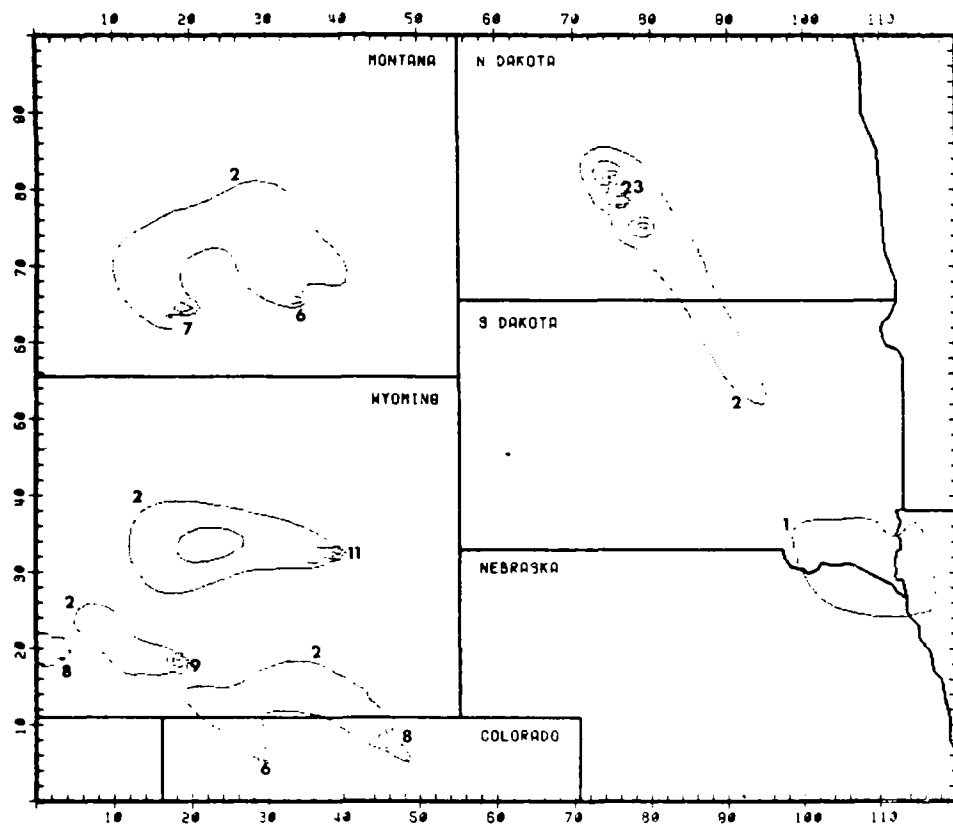
SO2 CONCENTRATIONS IN UG/M3 FOR THE HOUR 800-1100 MST ON 7/24/05



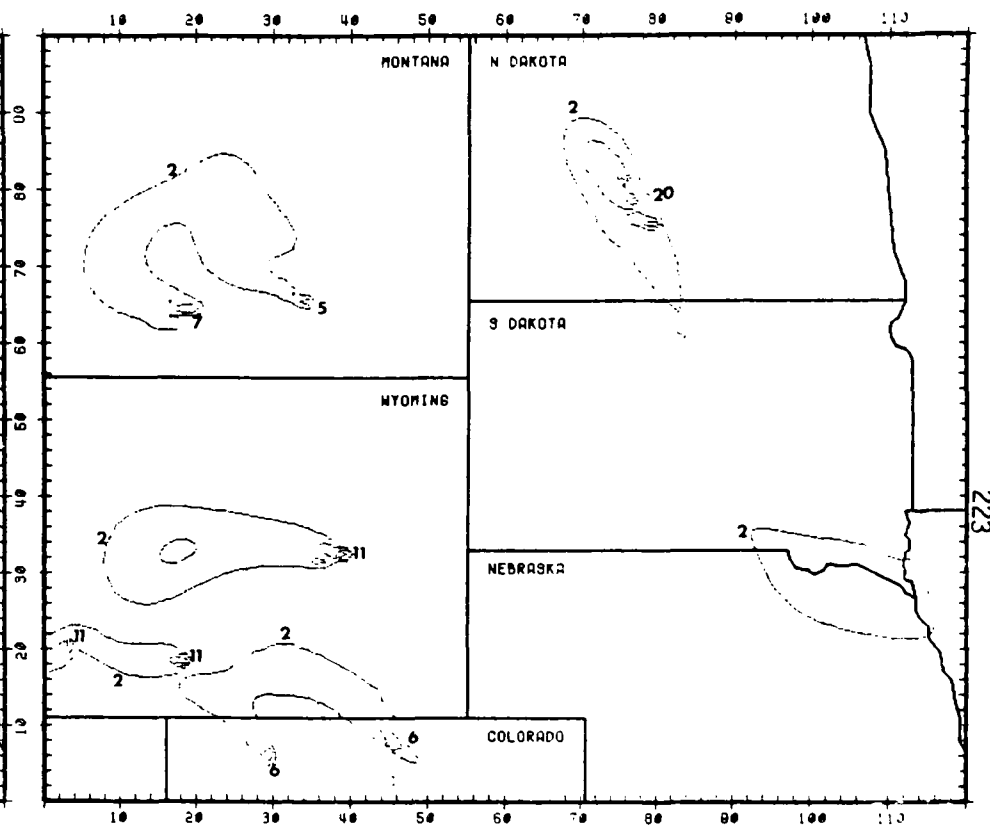
SO₂ CONCENTRATIONS IN UG/M³ FOR THE HOUR 1100-1400 MST ON 760405



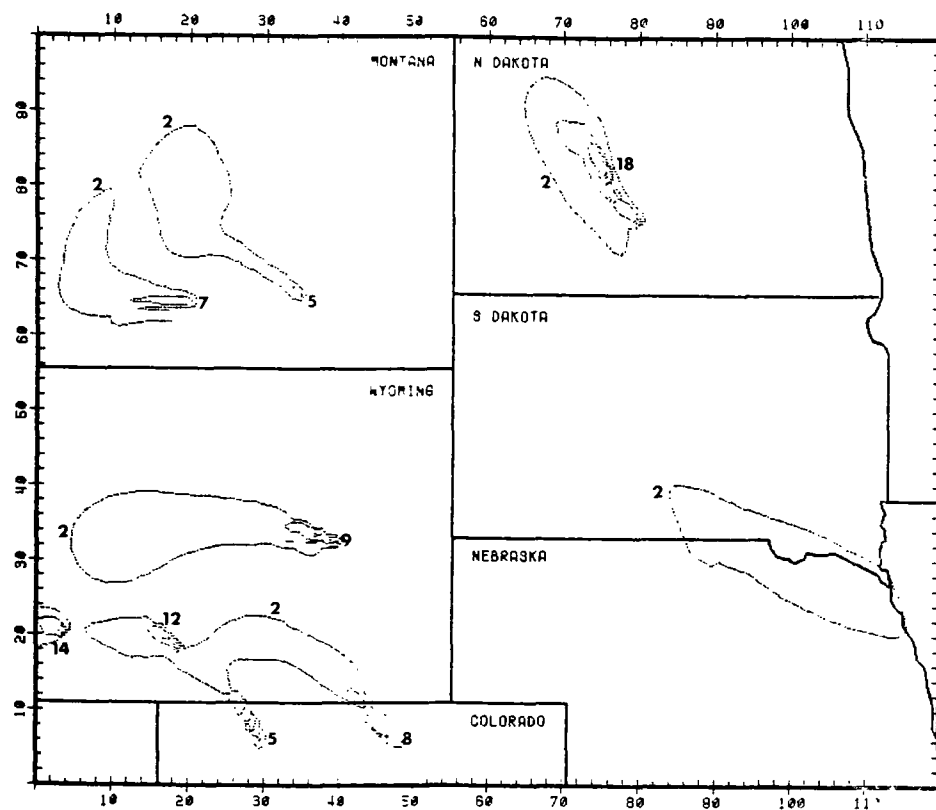
SO₂ CONCENTRATIONS IN UG/M³ FOR THE HOUR 1400-1700 MST ON 760405



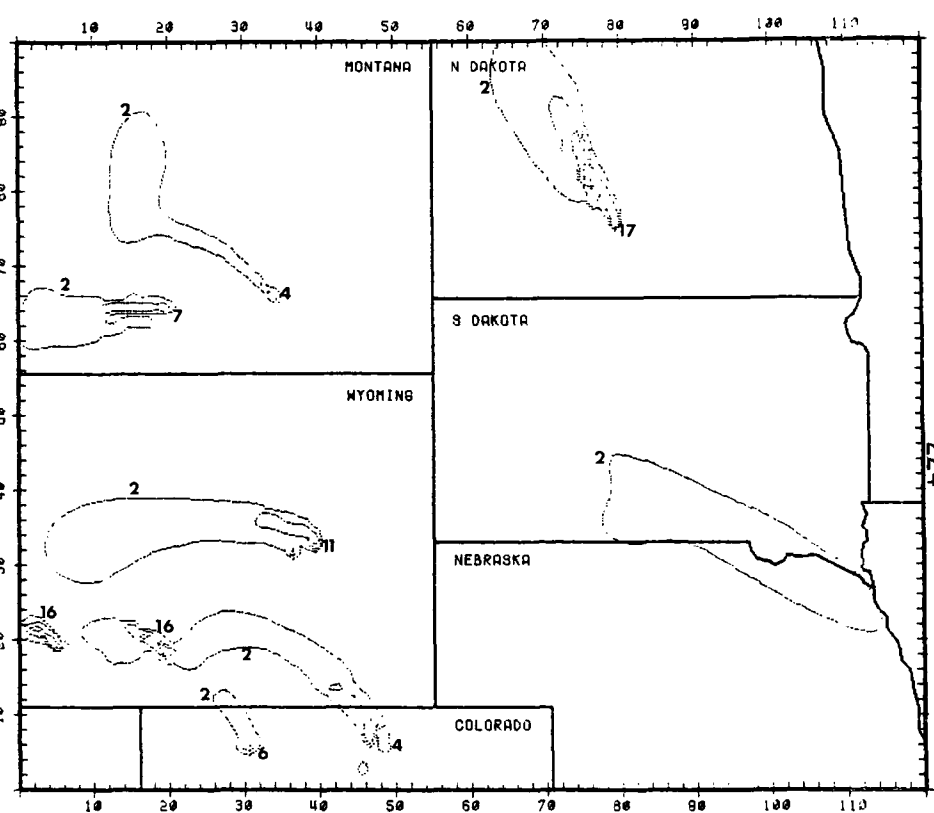
SO₂ CONCENTRATIONS IN UG/M³ FOR THE HOUR 1700-2000 MST ON FEB0485



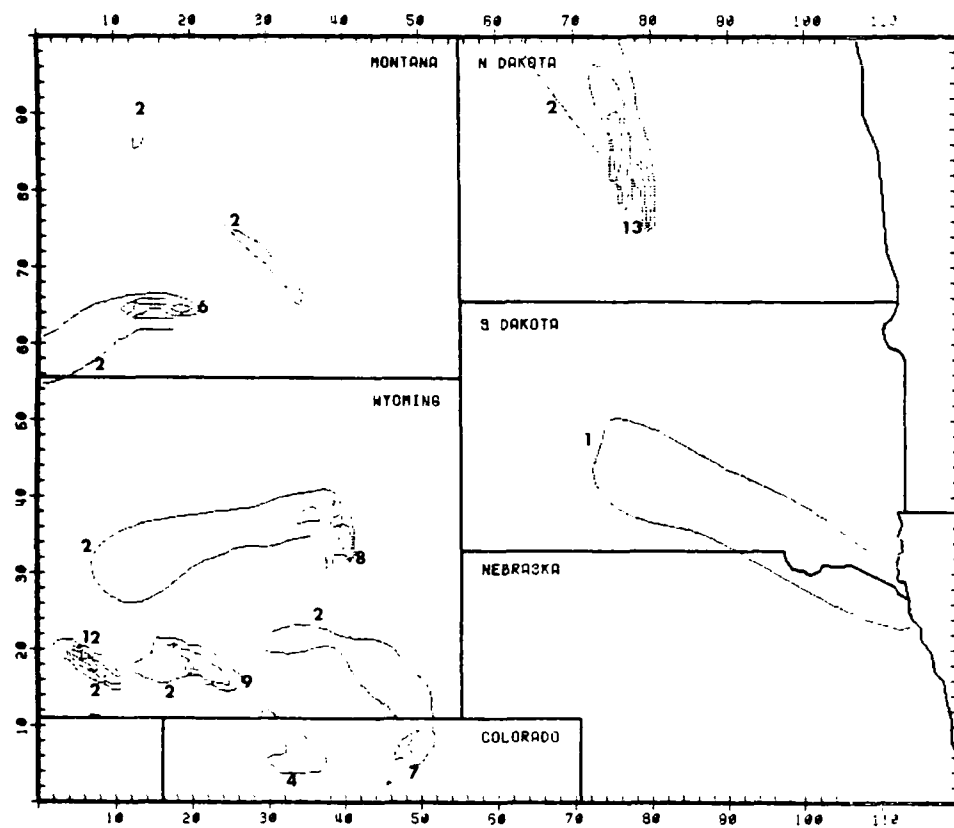
SO₂ CONCENTRATIONS IN UG/M³ FOR THE HOUR 2000-2300 MST ON FEB0485



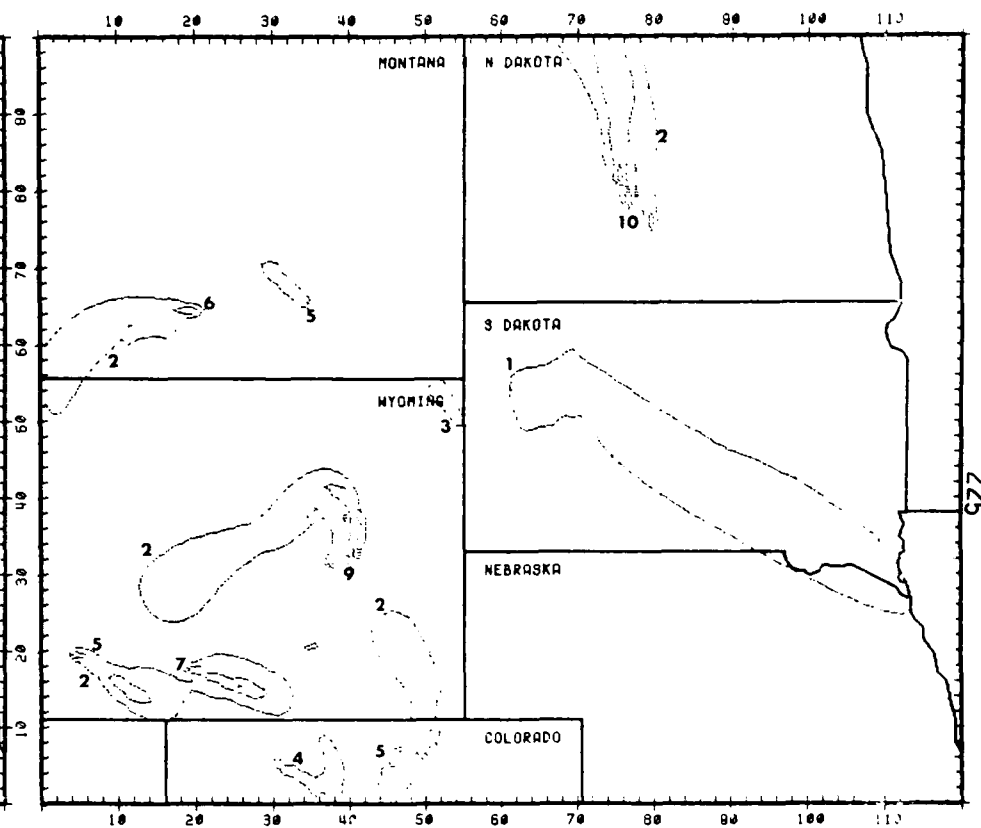
SO₂ CONCENTRATIONS IN UG/M3 FOR THE HOUR -100-200 MST ON 760406



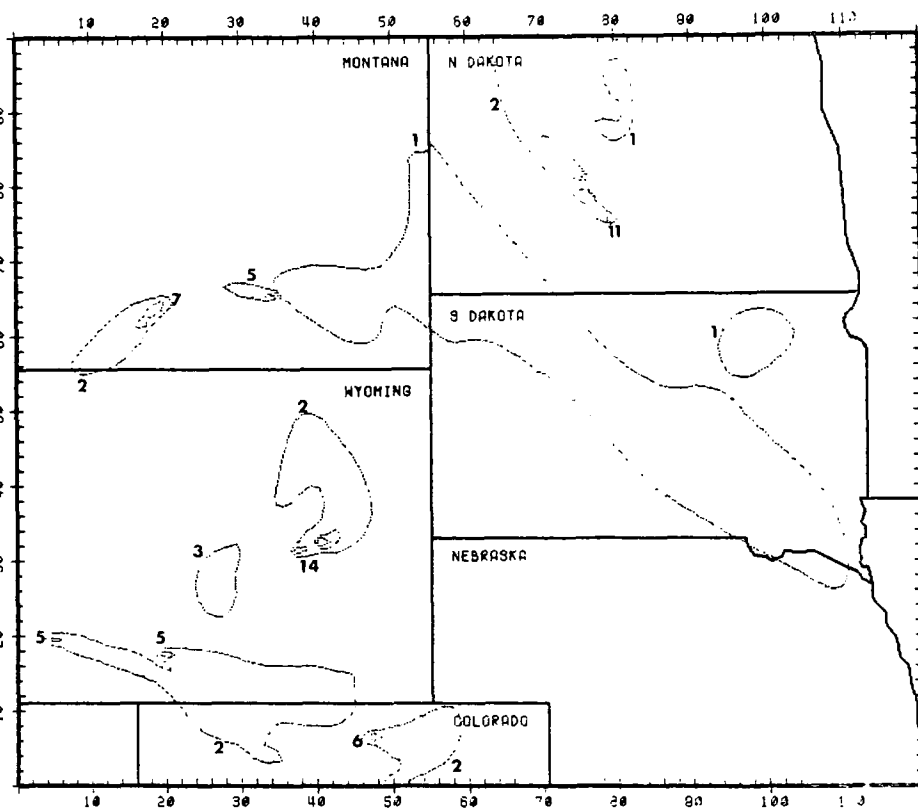
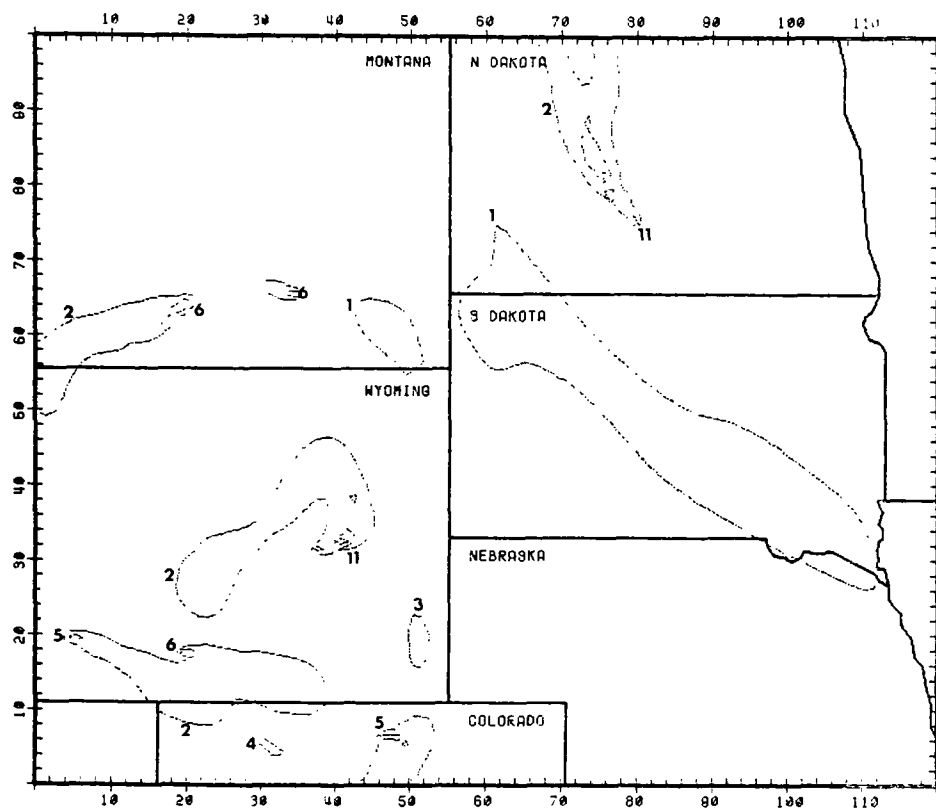
SO₂ CONCENTRATIONS IN UG/M3 FOR THE HOUR 200-500 MST ON 760406



SO2 CONCENTRATIONS IN $\mu\text{G}/\text{M}^3$ FOR THE HOUR 500-800 MST ON 7/20/99

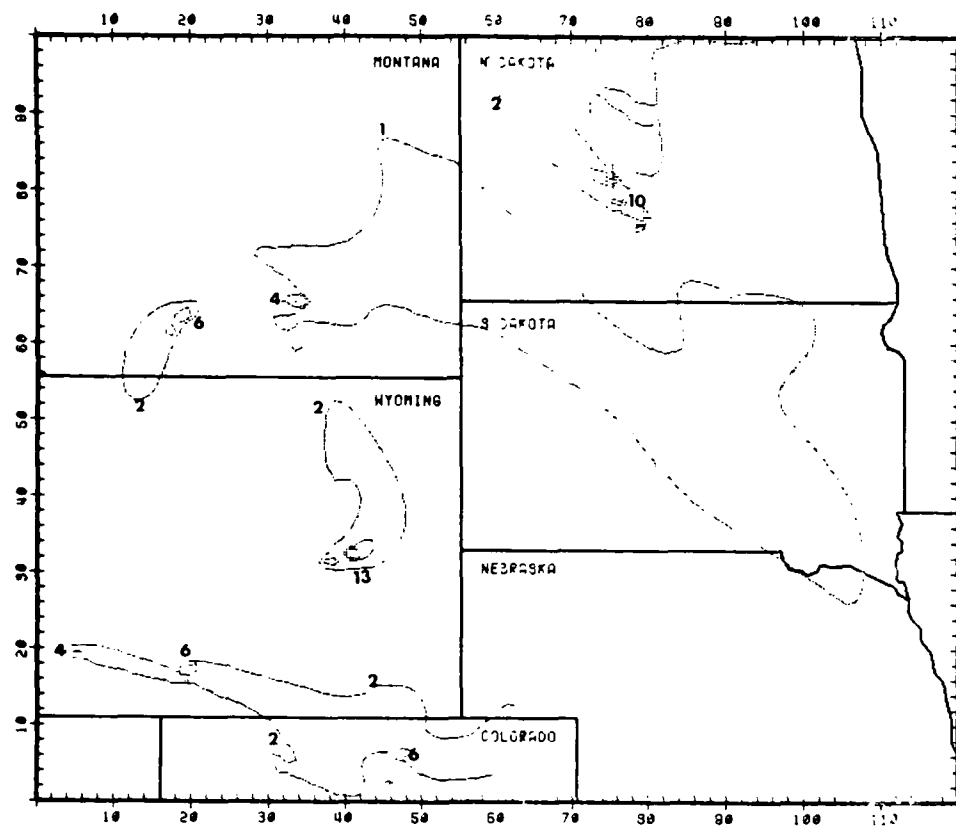


SO2 CONCENTRATIONS IN $\mu\text{G}/\text{M}^3$ FOR THE HOUR 800-1100 MST ON 7/20/99

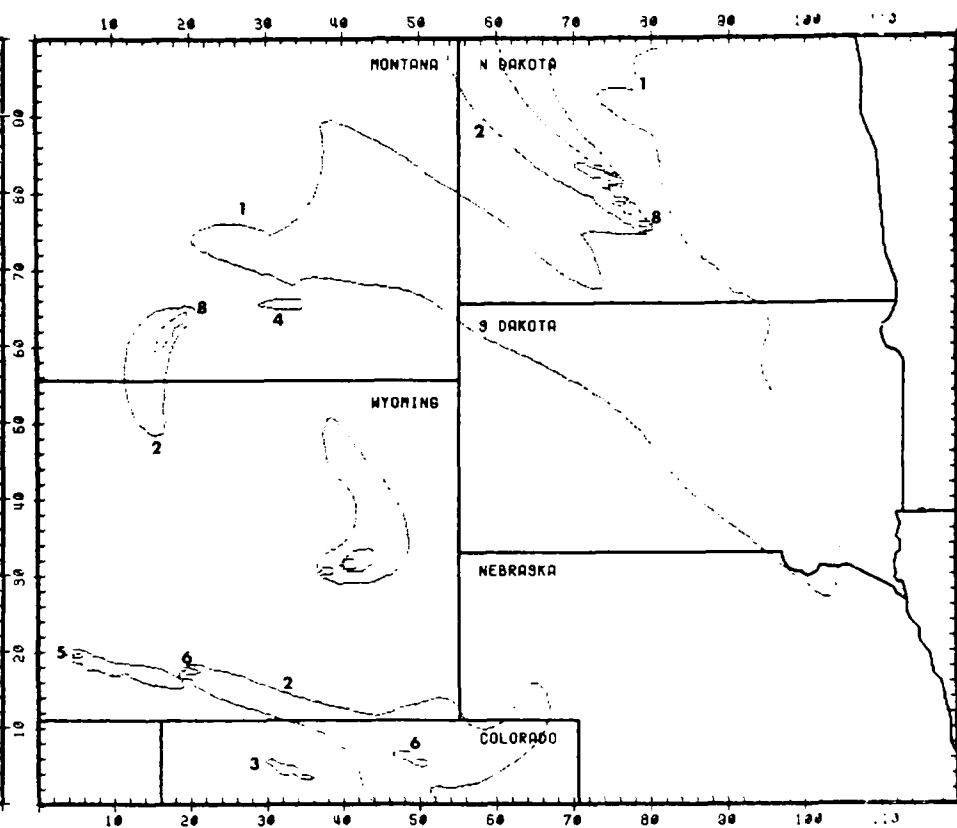


SO2 CONCENTRATIONS IN $\mu\text{G}/\text{M}^3$ FOR THE HOUR 1100-1400 MST ON 7/24/06

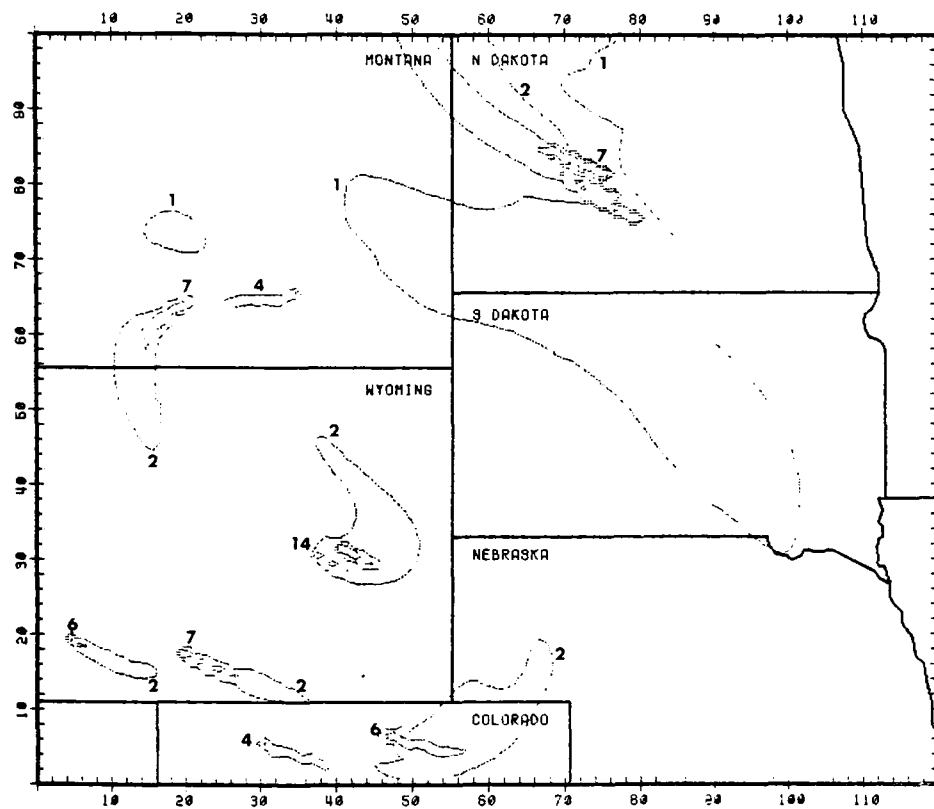
SO2 CONCENTRATIONS IN $\mu\text{G}/\text{M}^3$ FOR THE HOUR 1-30-1730 MST ON 7/24/06



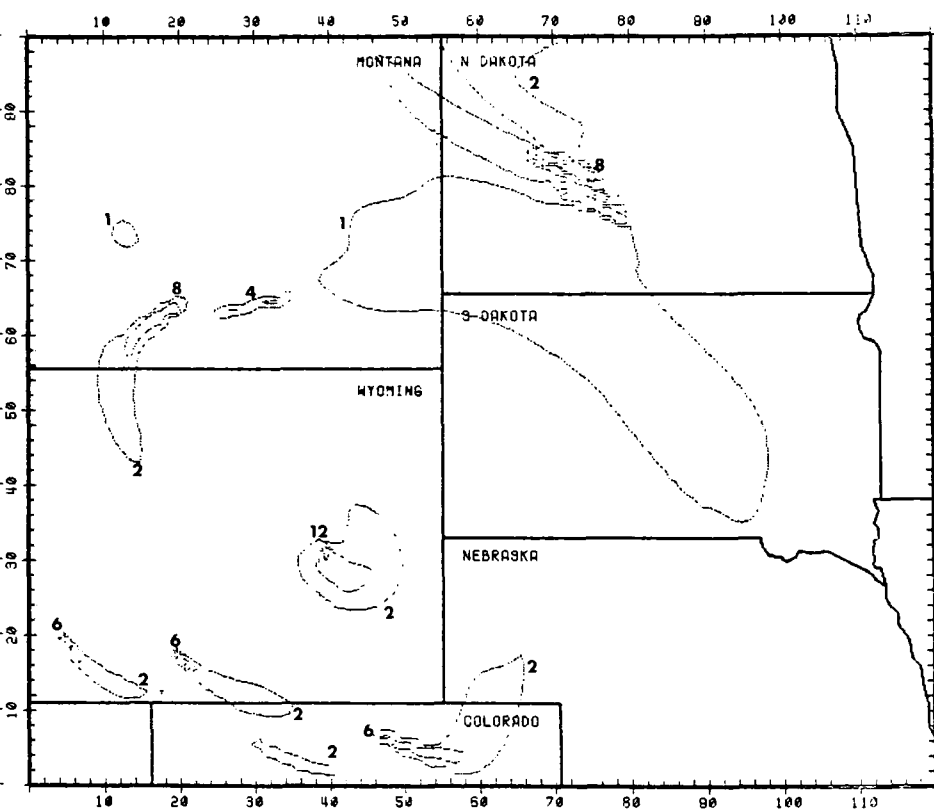
SO2 CONCENTRATIONS IN $\mu\text{G}/\text{M}^3$ FOR THE HOUR 1700-2000 MST ON 7/24/00



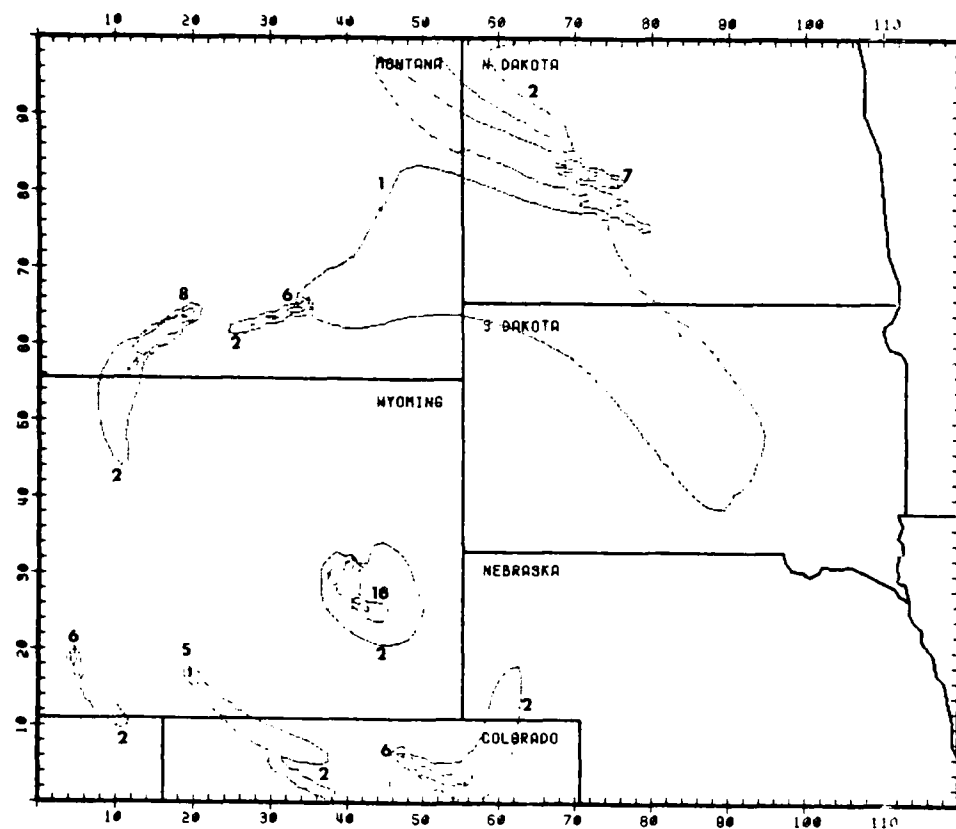
SO2 CONCENTRATIONS IN $\mu\text{G}/\text{M}^3$ FOR THE HOUR 2000-2300 MST ON 7/24/00



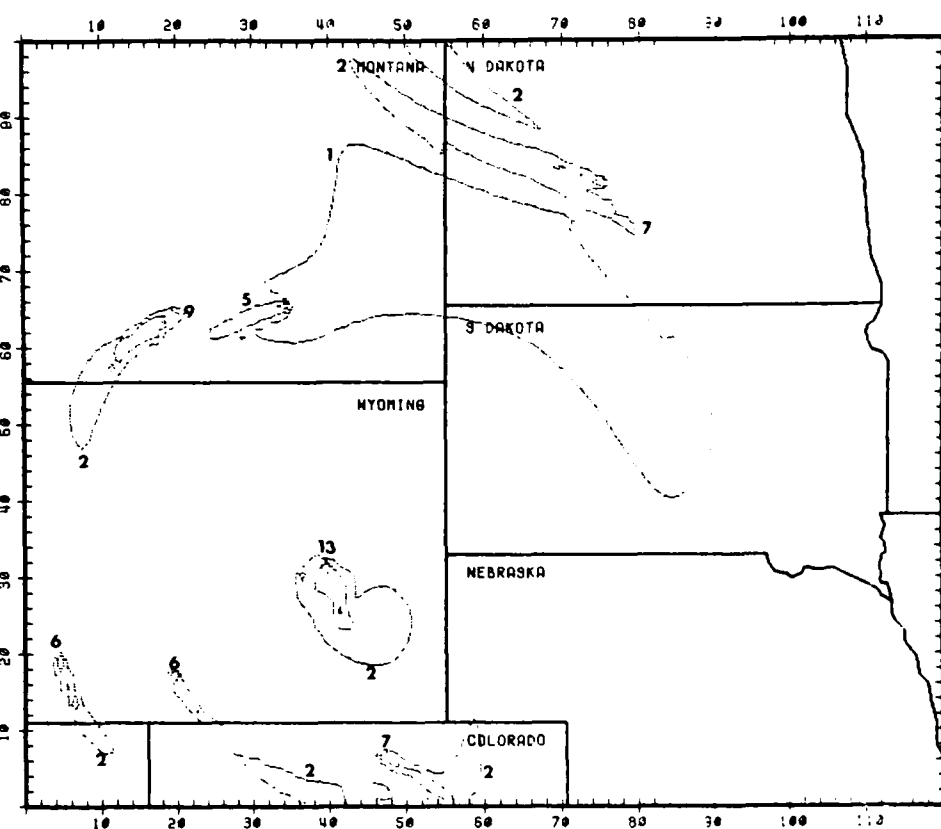
SO2 CONCENTRATIONS IN $\mu\text{G}/\text{M}^3$ FOR THE HOUR -100-200 MST ON 760407



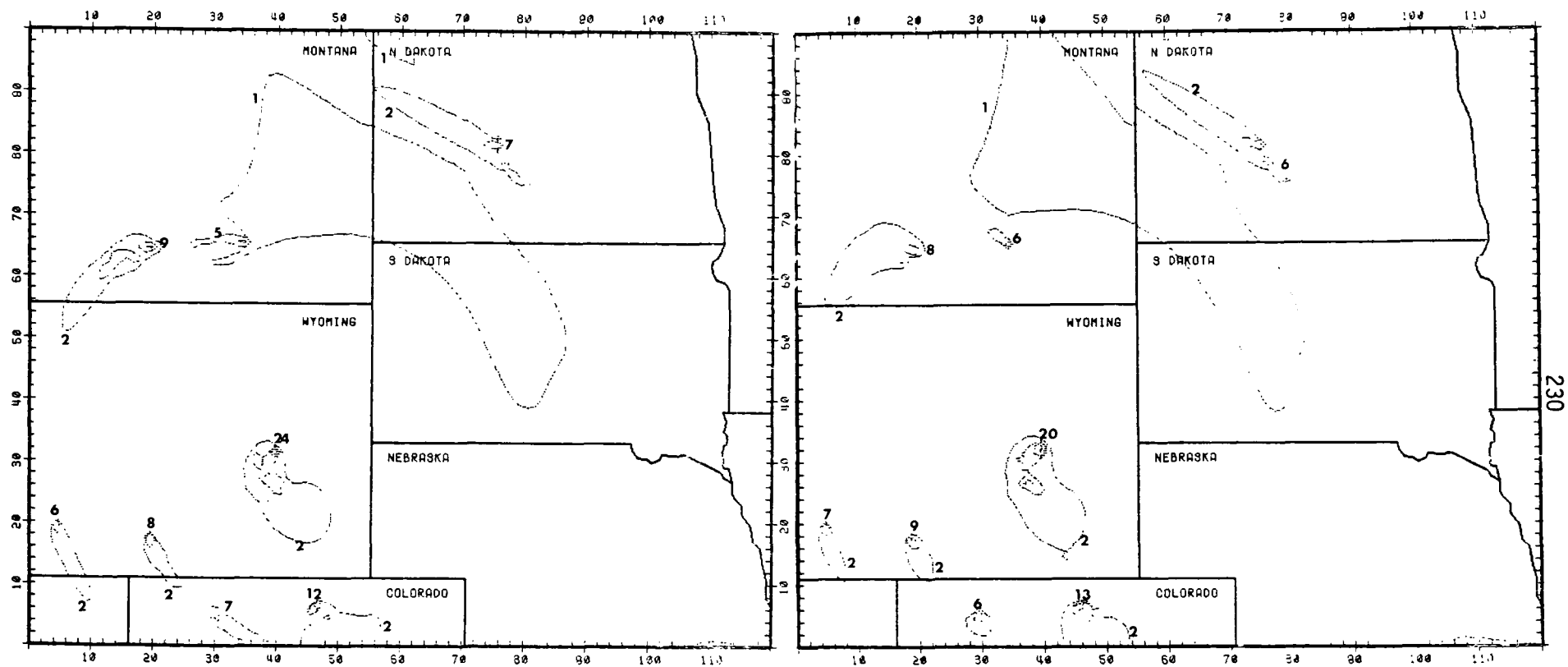
SO2 CONCENTRATIONS IN $\mu\text{G}/\text{M}^3$ FOR THE HOUR 200-500 MST ON 760407



SO₂ CONCENTRATIONS IN UG/M³ FOR THE HOUR 500-800 MST ON 7/6/407

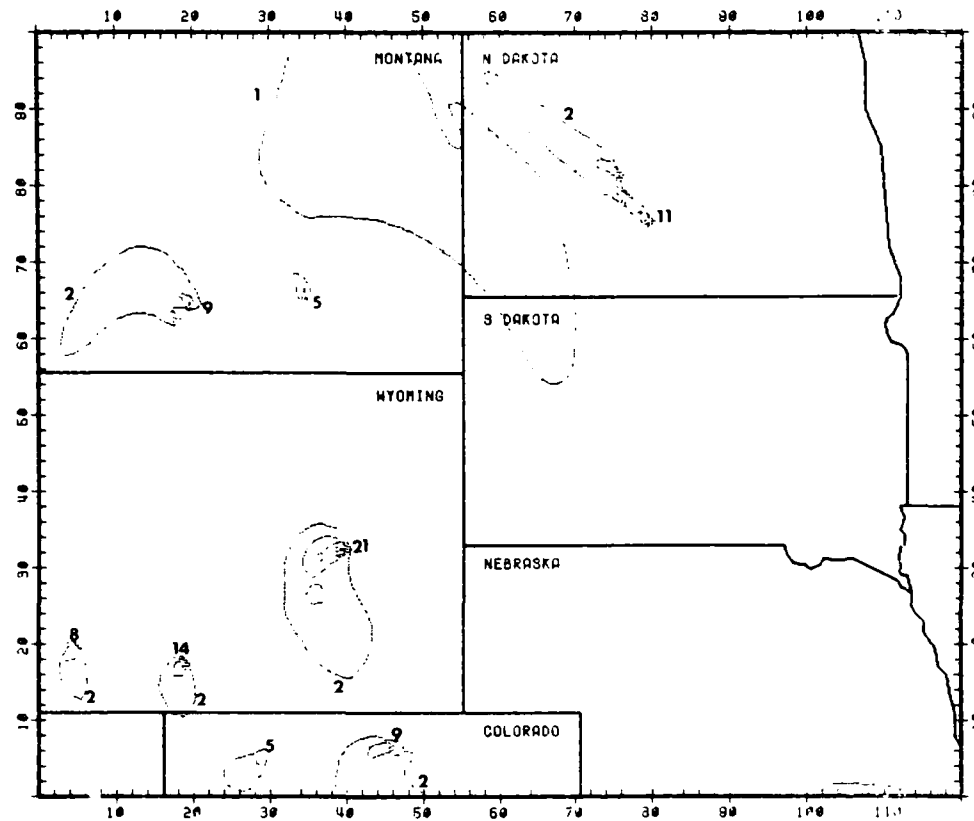


SO₂ CONCENTRATIONS IN UG/M³ FOR THE HOUR 800-1120 MST ON 7/6/407



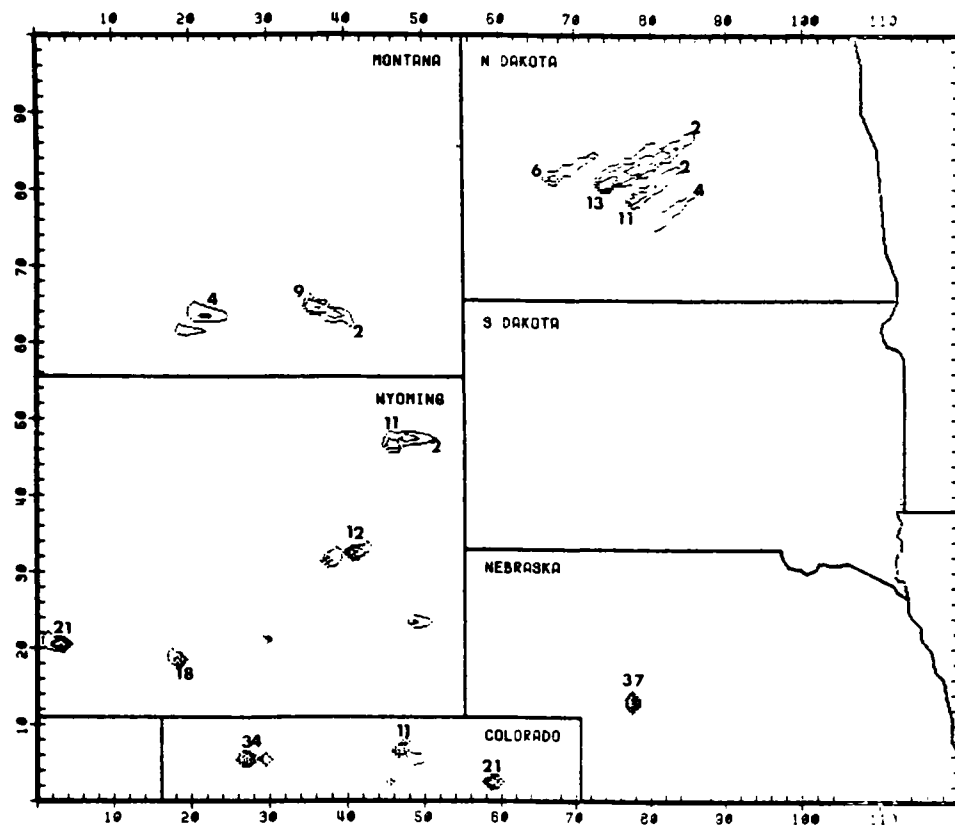
SO₂ CONCENTRATIONS IN UG/M³ FOR THE HOUR 1100-1400 MST ON 7/30/97

SO₂ CONCENTRATIONS IN UG/M³ FOR THE HOUR 1400-1700 MST ON 7/30/97

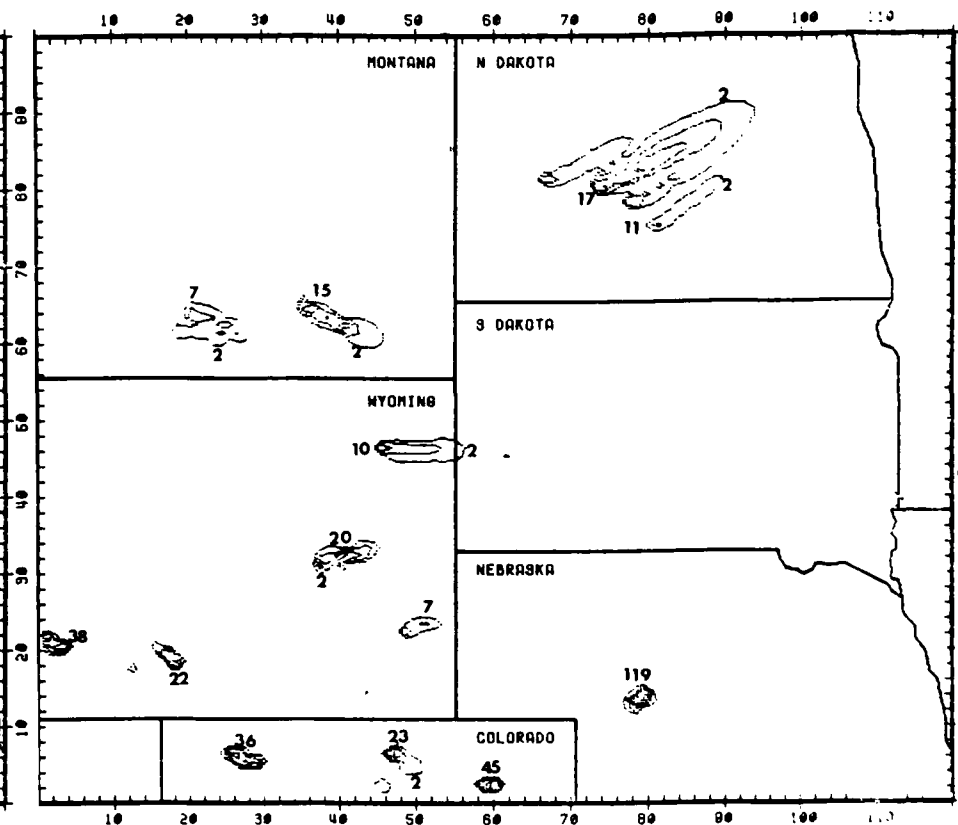


SO2 CONCENTRATIONS IN UG-M3 FOR THE HOUR 1700-2000 MST ON 10/4/97

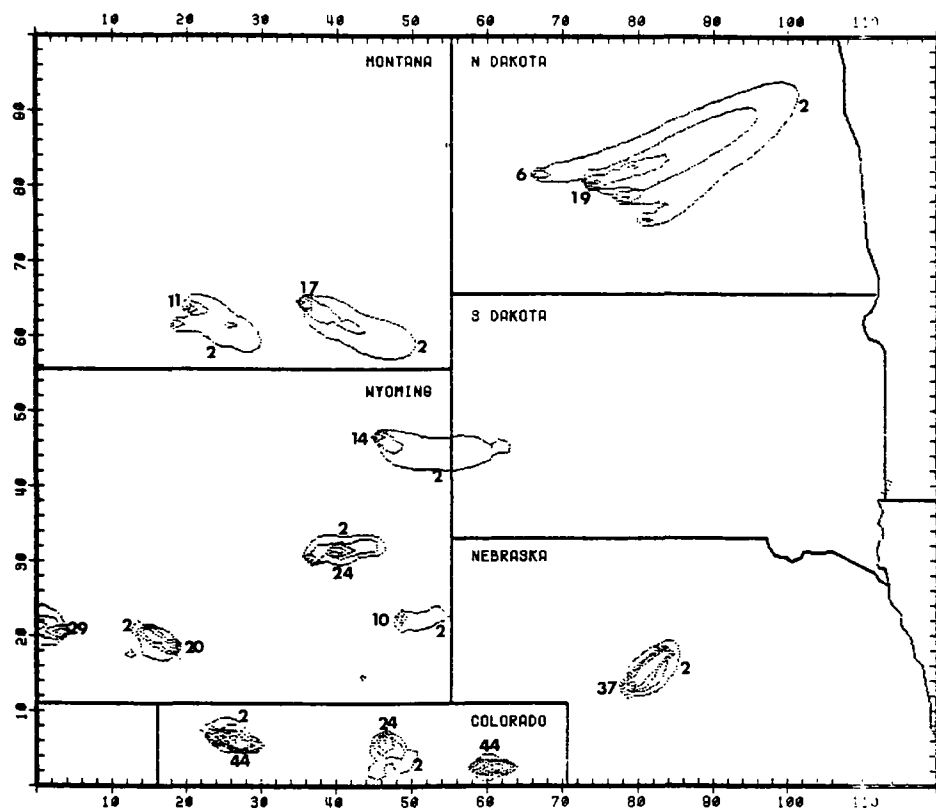
4. 4-7 APRIL 1976 METEOROLOGY; 1986 EMISSIONS



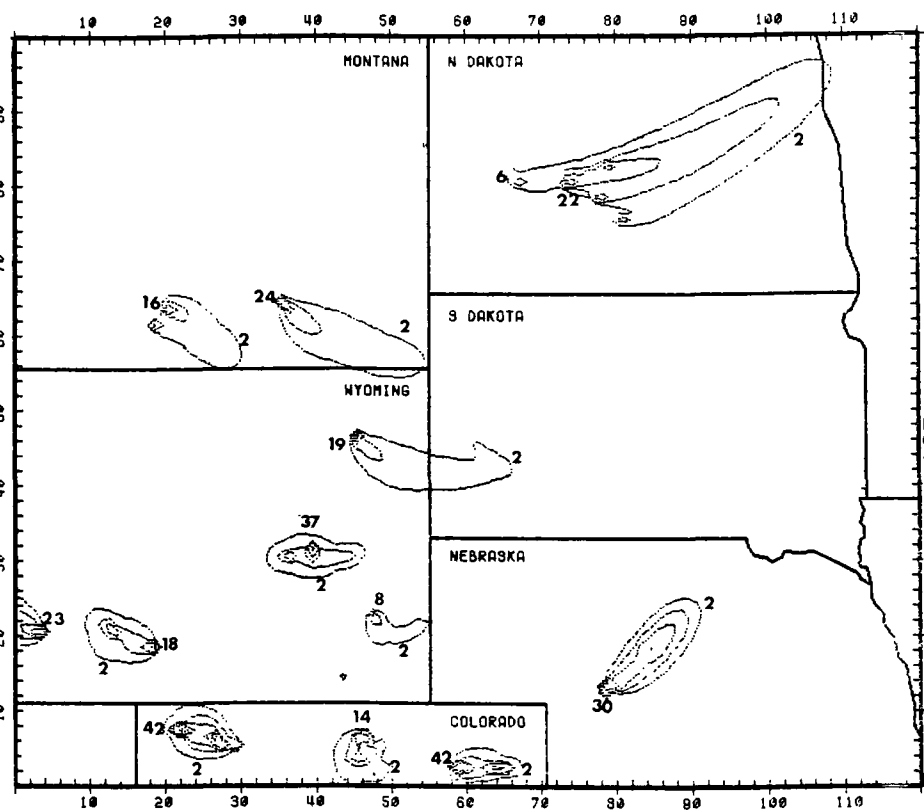
SO₂ CONCENTRATIONS IN UG/M³ FOR THE HOUR 500-800 MST ON 7/24/04



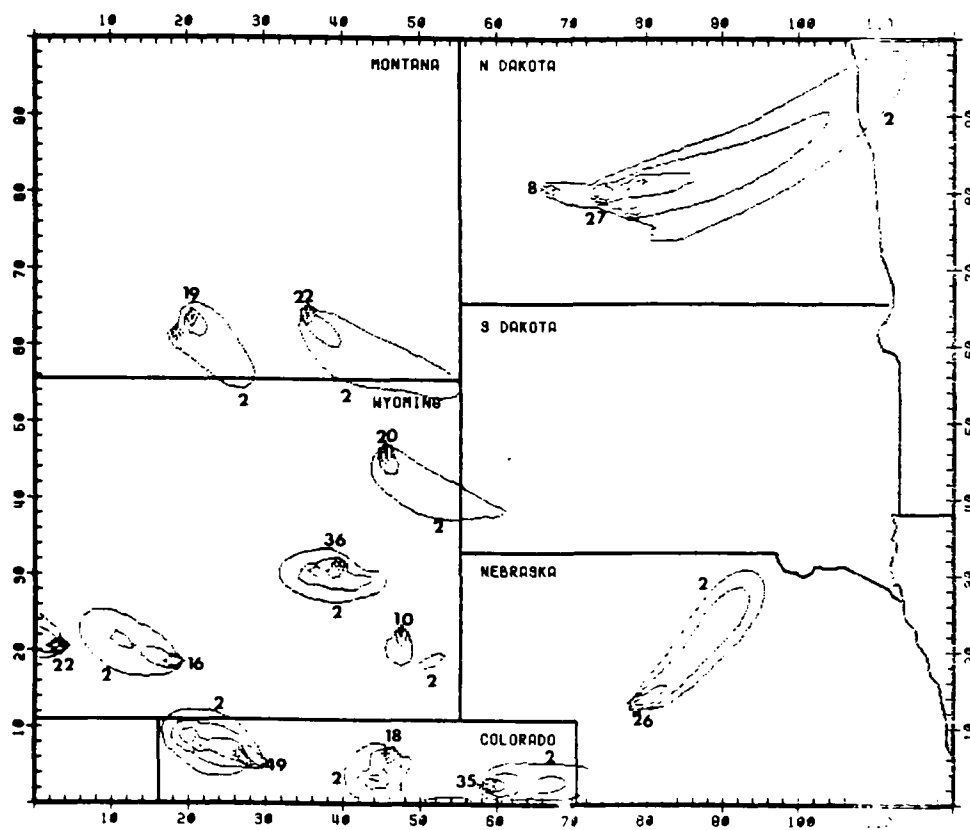
SO₂ CONCENTRATIONS IN UG/M³ FOR THE HOUR 800-1100 MST ON 7/24/04



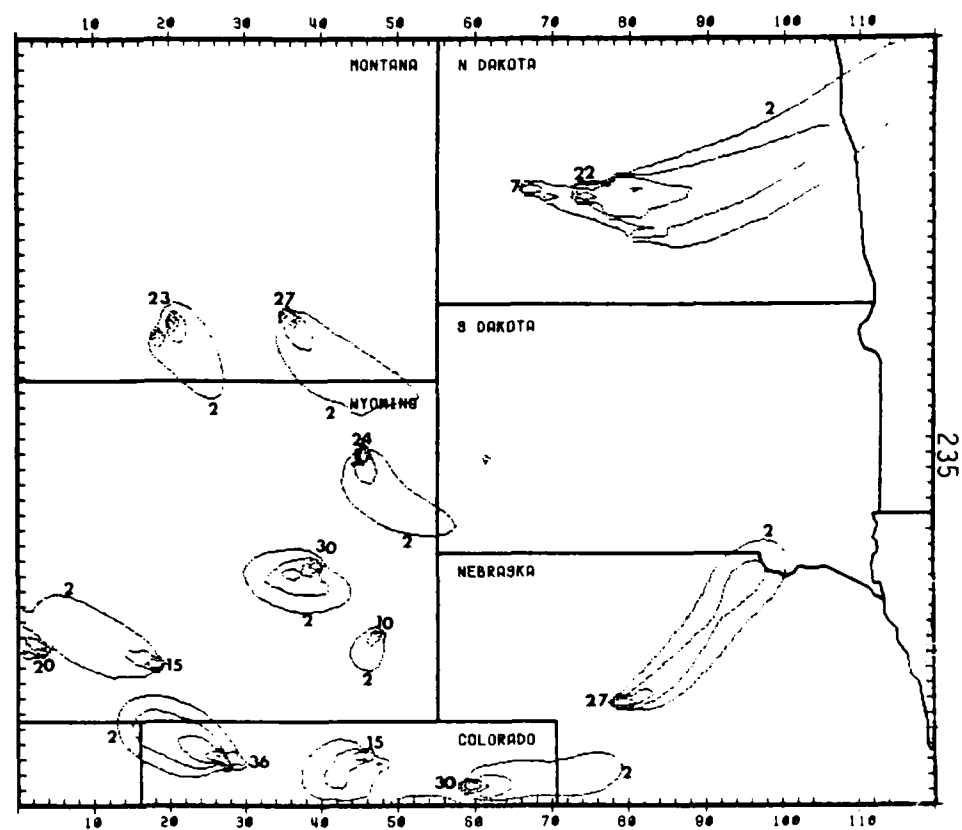
SO₂ CONCENTRATIONS IN UG/M3 FOR THE HOUR 1100-1400 MST ON 760404



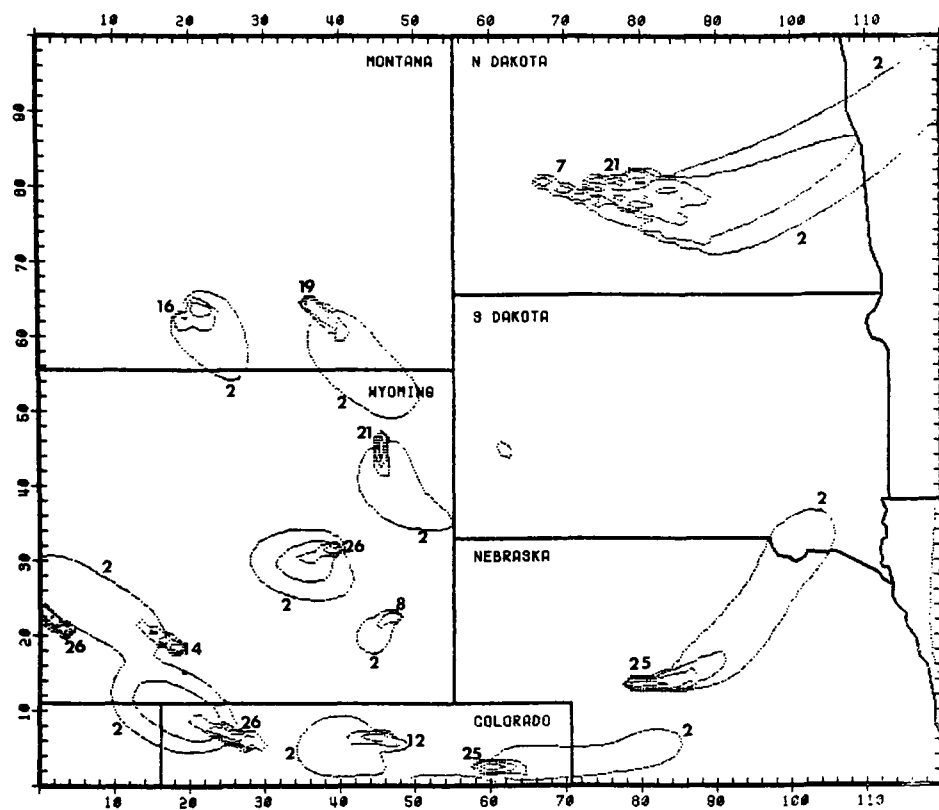
SO₂ CONCENTRATIONS IN UG/M3 FOR THE HOUR 1400-1700 MST ON 760404



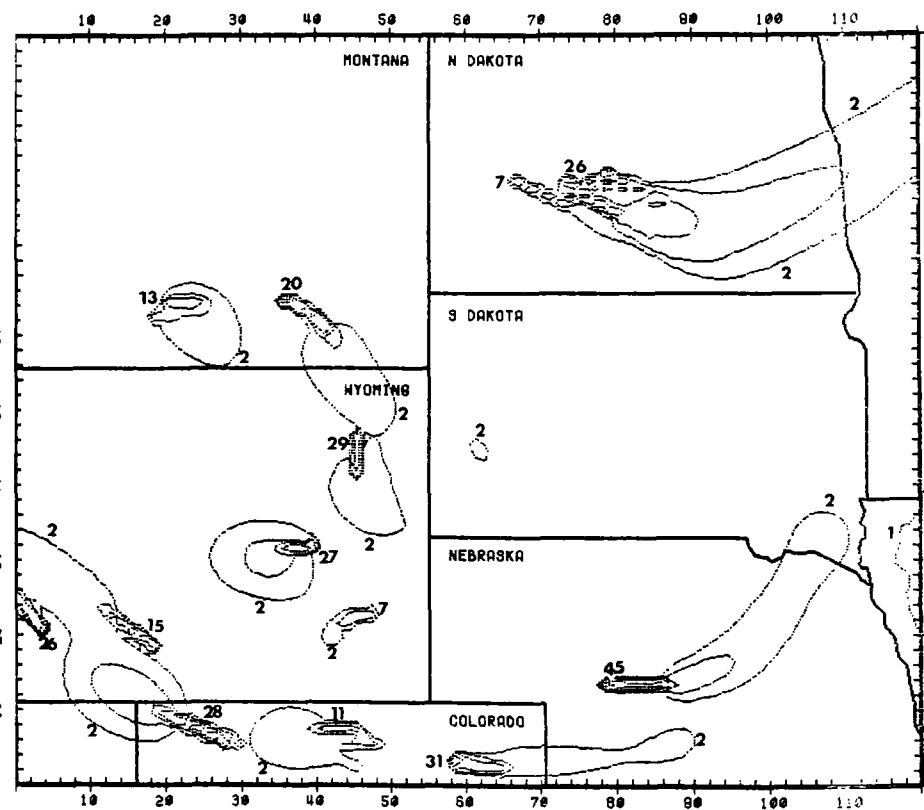
SO2 CONCENTRATIONS IN $\mu\text{g}/\text{m}^3$ FOR THE HOUR 1700-2000 MST ON 760404



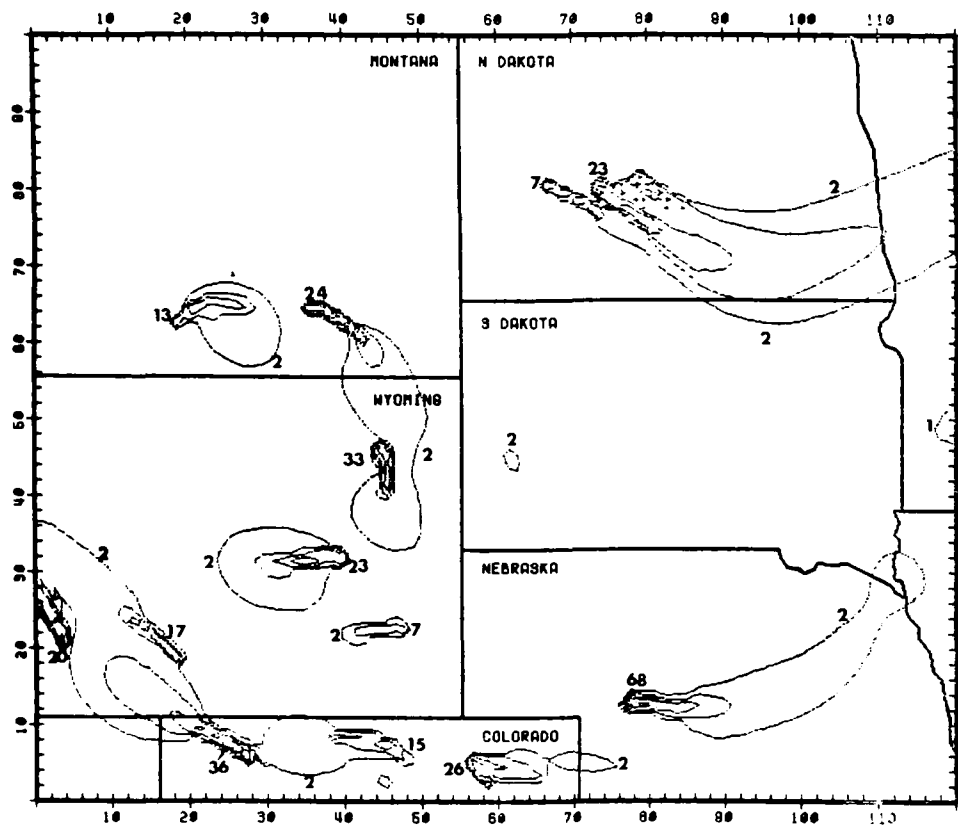
SO2 CONCENTRATIONS IN $\mu\text{g}/\text{m}^3$ FOR THE HOUR 2000-2300 MST ON 760404



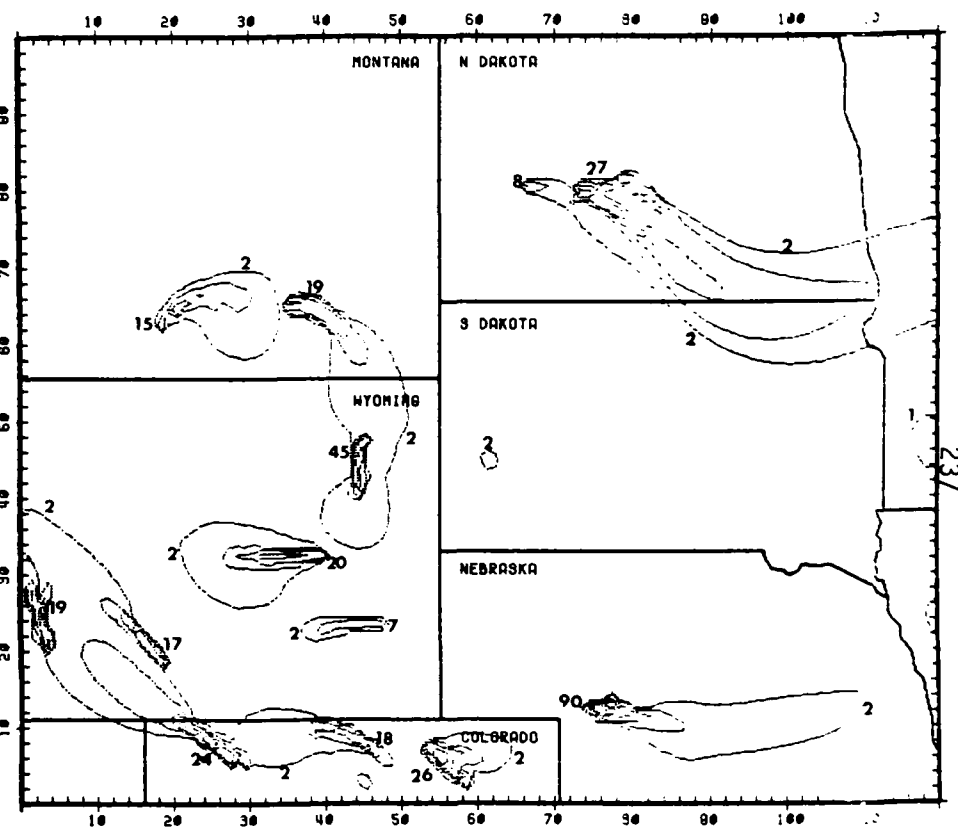
SO2 CONCENTRATIONS IN $\mu\text{G}/\text{M}^3$ FOR THE HOUR -100-200 MST ON 760405



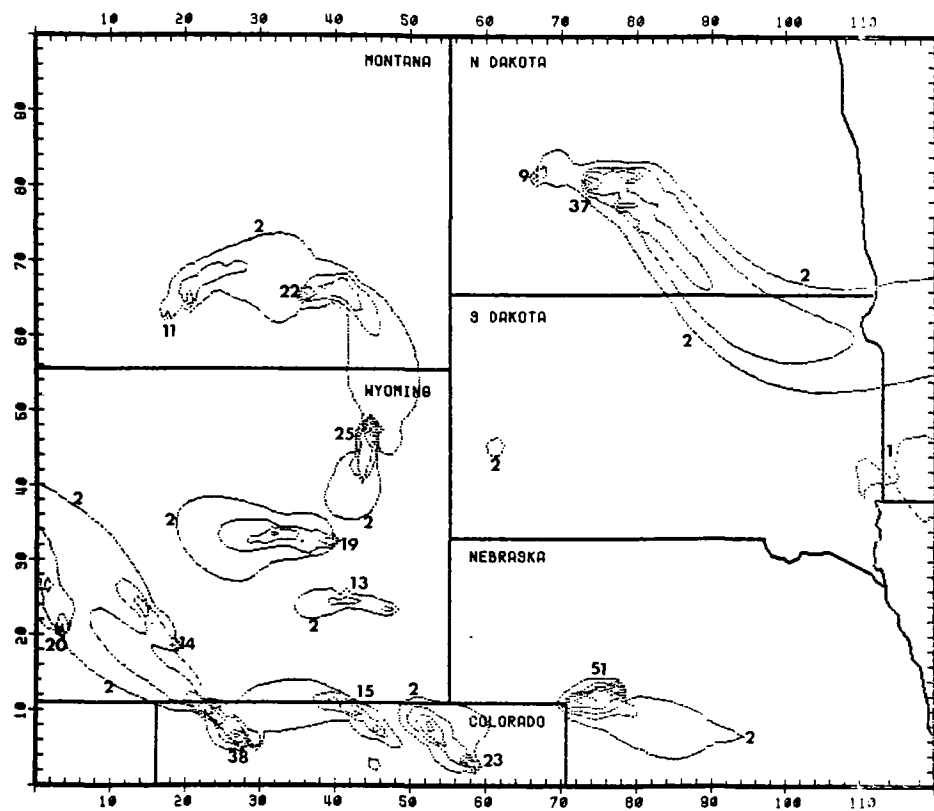
SO2 CONCENTRATIONS IN $\mu\text{G}/\text{M}^3$ FOR THE HOUR 200-500 MST ON 760405



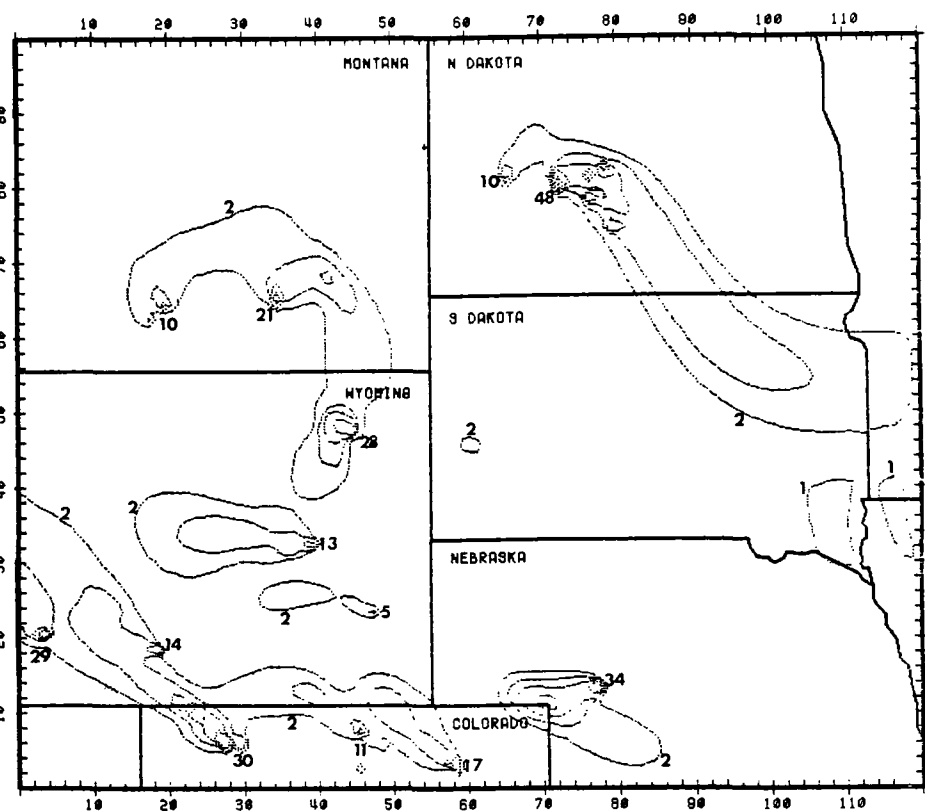
SO2 CONCENTRATIONS IN UG/M3 FOR THE HOUR 500-800 MST ON 7/20/05



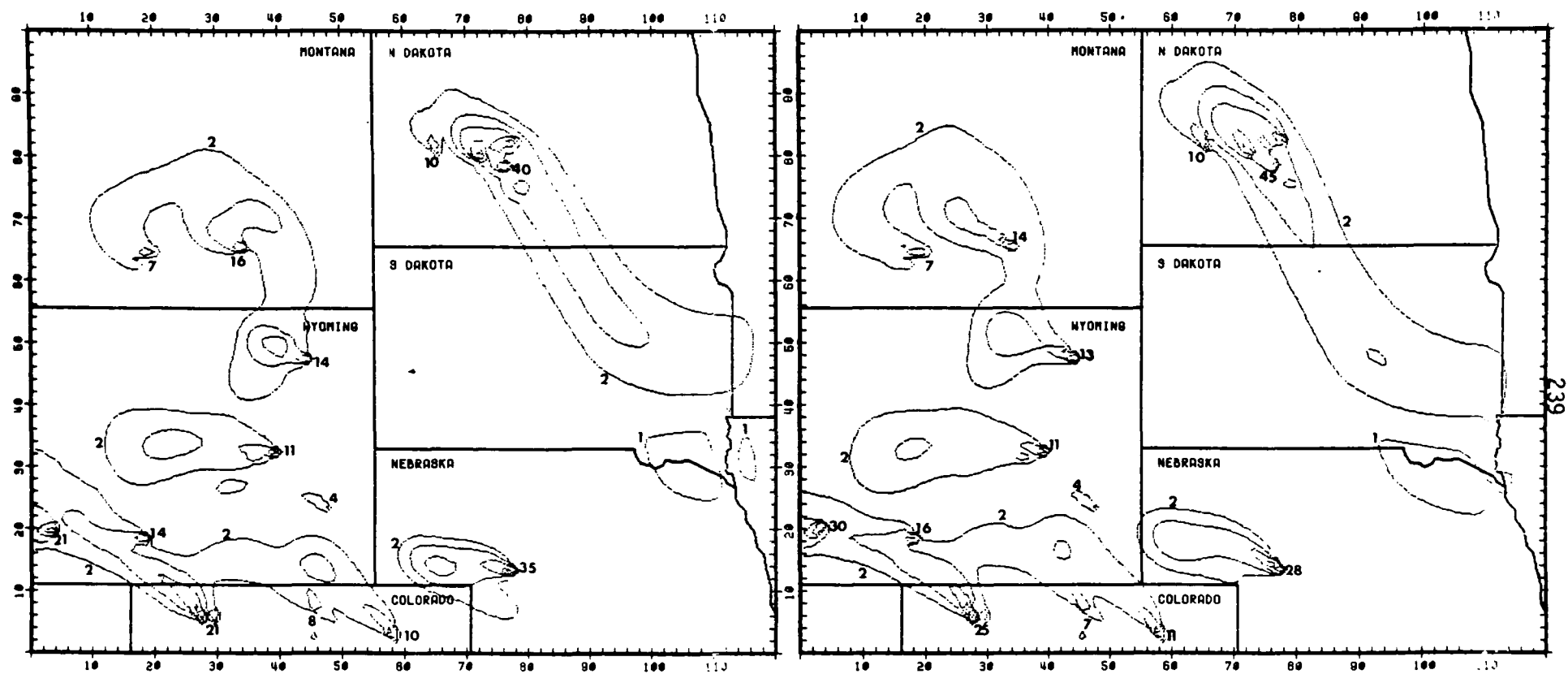
SO2 CONCENTRATIONS IN UG/M3 FOR THE HOUR 800-1100 MST ON 7/20/05



SO₂ CONCENTRATIONS IN UG/M3 FOR THE HOUR 1100-1400 MST ON 760405

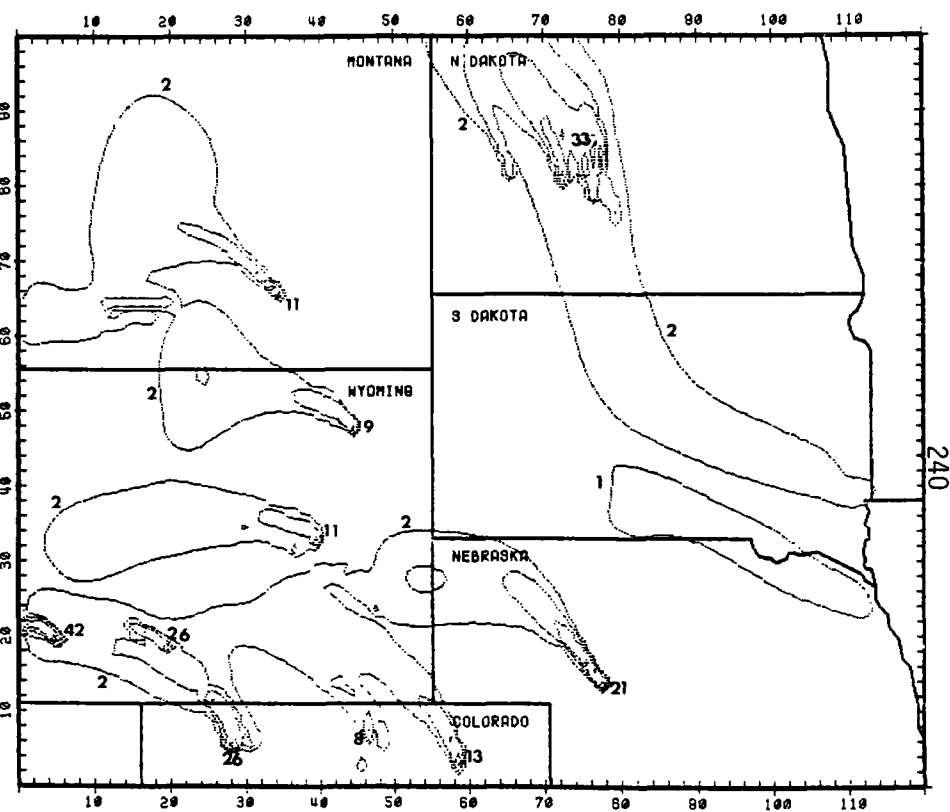
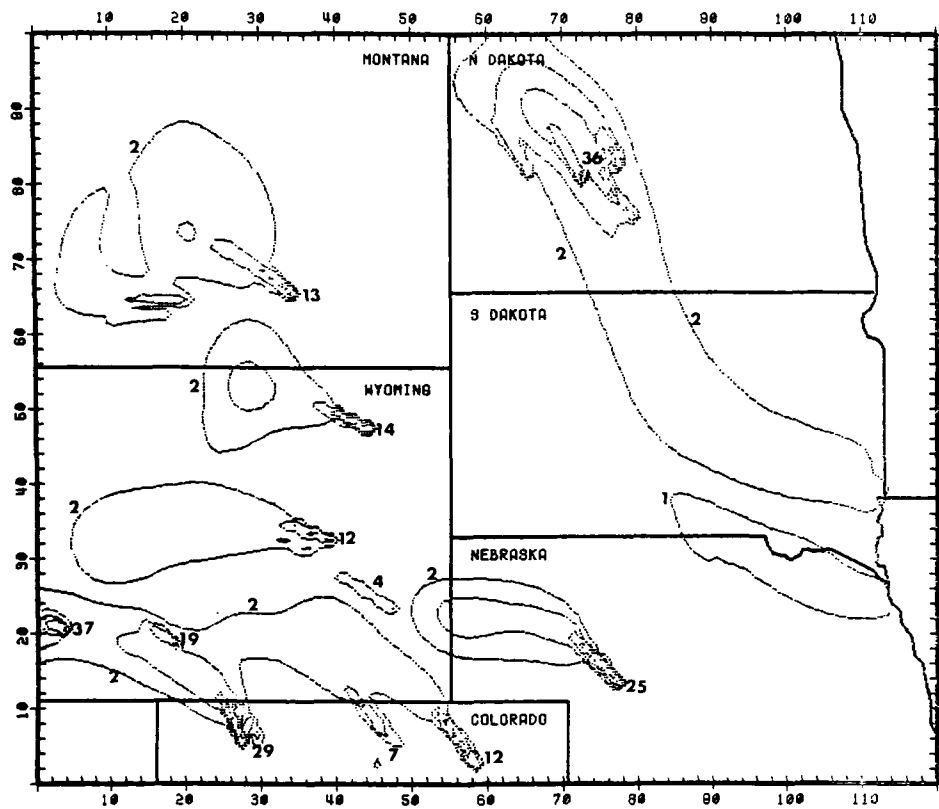


SO₂ CONCENTRATIONS IN UG/M3 FOR THE HOUR 1400-1700 MST ON 760405



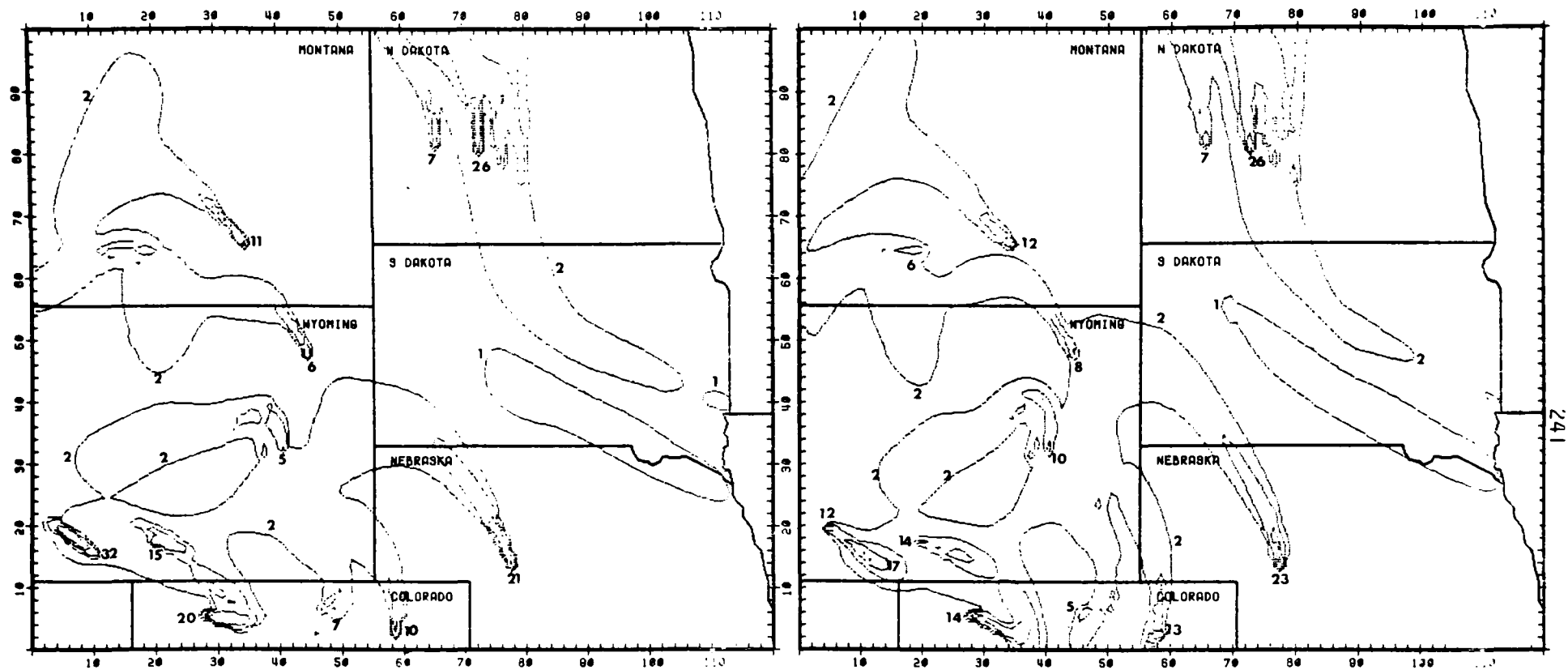
SO2 CONCENTRATIONS IN UG/M3 FOR THE HOUR 1700-2000 MST ON 760405

SO2 CONCENTRATIONS IN UG/M3 FOR THE HOUR 2000-2300 MST ON 760405



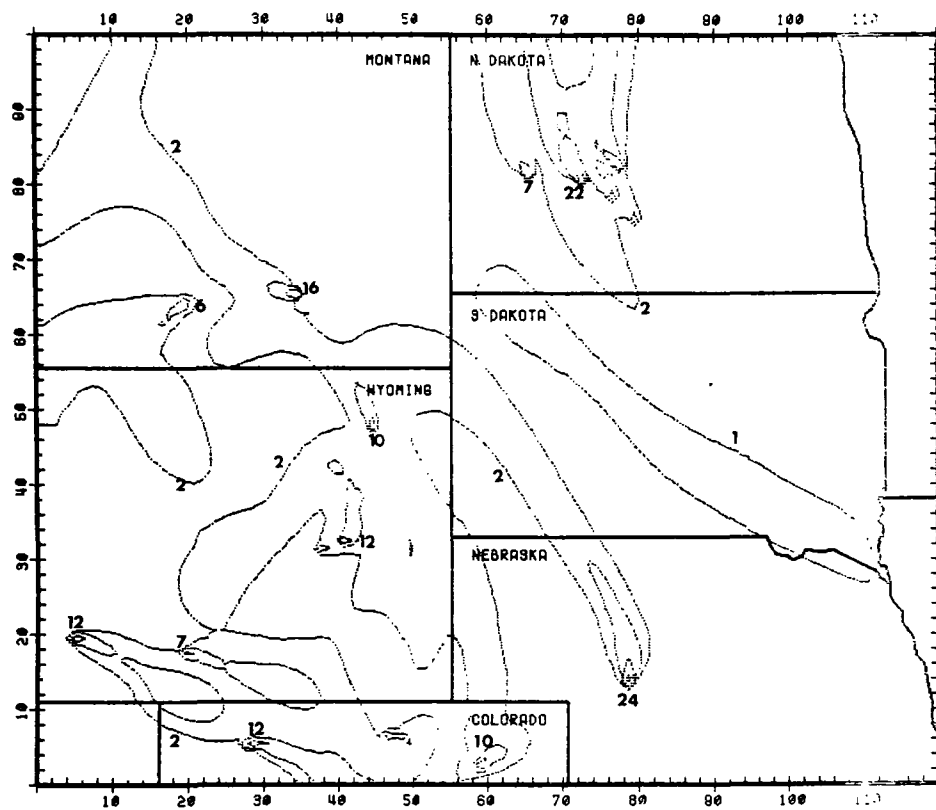
SO₂ CONCENTRATIONS IN UG/M3 FOR THE HOUR -100-200 MST ON 760406

SO₂ CONCENTRATIONS IN UG/M3 FOR THE HOUR 200-500 MST ON 760406

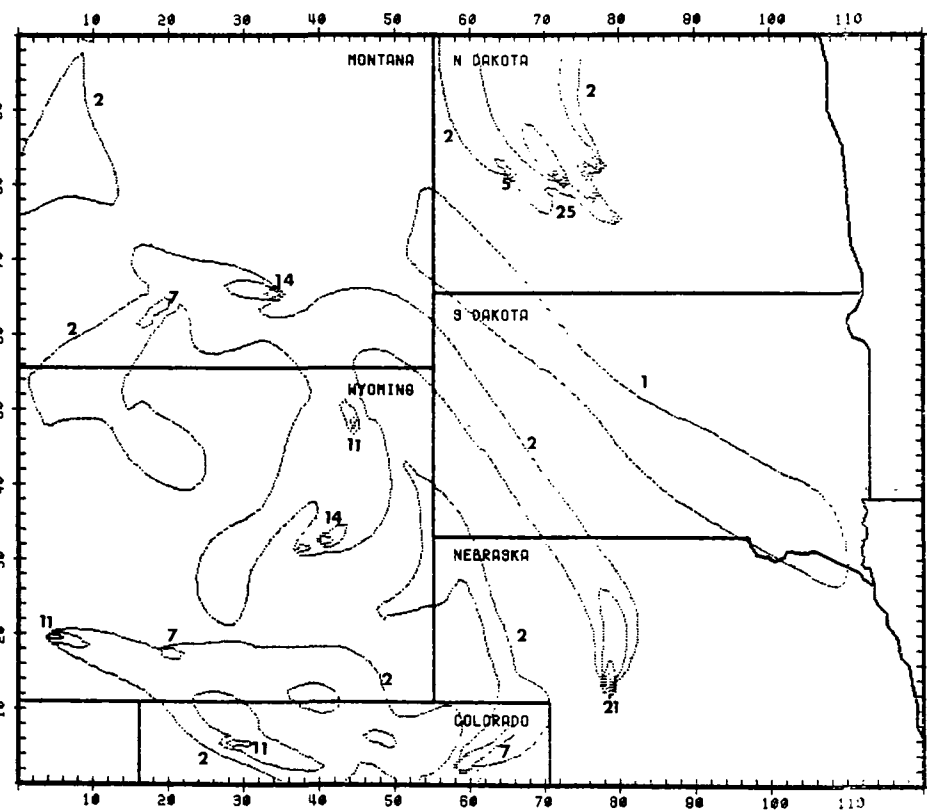


SO₂ CONCENTRATIONS IN UG/M³ FOR THE HOUR 500-800 MST ON 760406

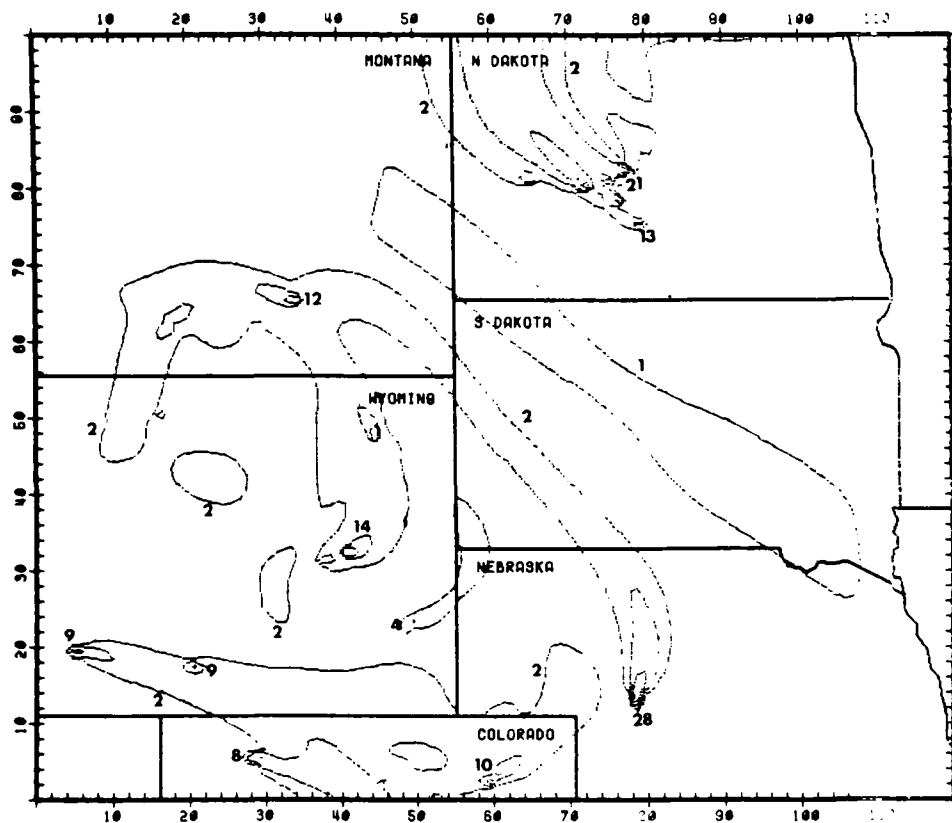
SO₂ CONCENTRATIONS IN UG/M³ FOR THE HOUR 800-1100 MST ON 760406



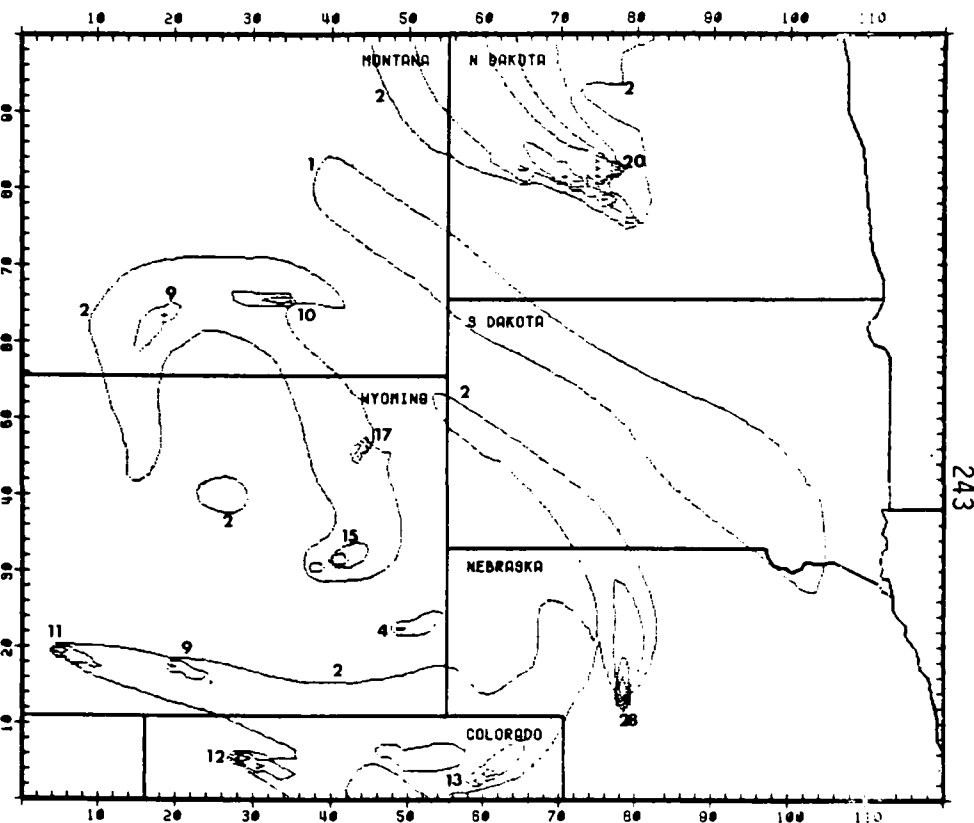
SO₂ CONCENTRATIONS IN UG/M3 FOR THE HOUR 1100-1400 MST ON 750406



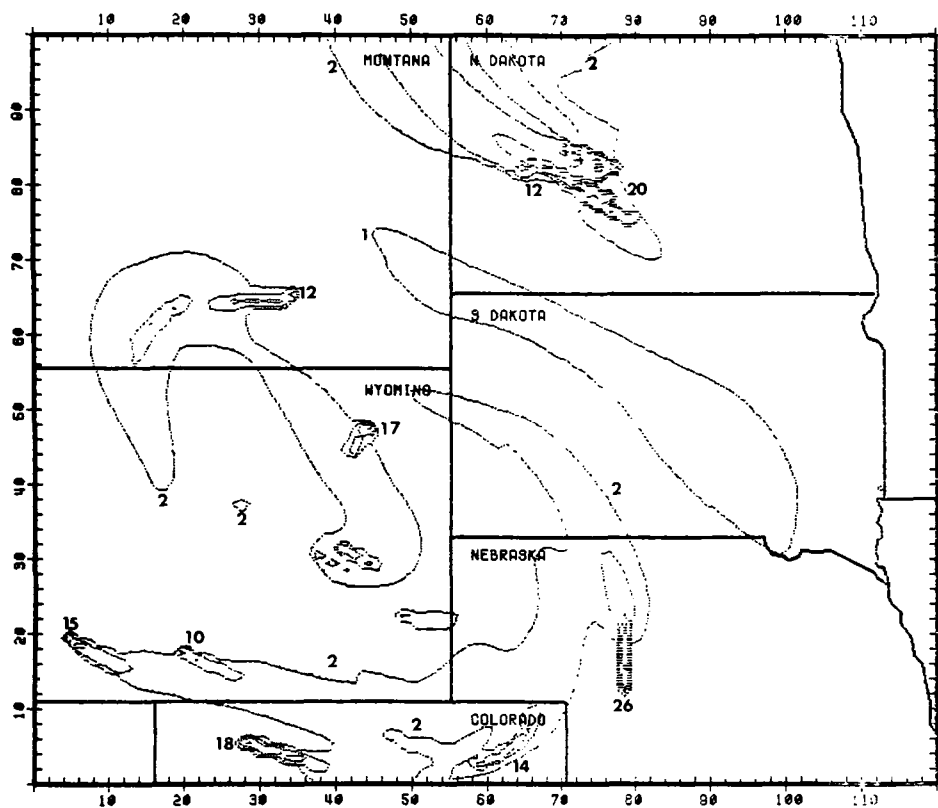
SO₂ CONCENTRATIONS IN UG/M3 FOR THE HOUR 1400-1700 MST ON 750406



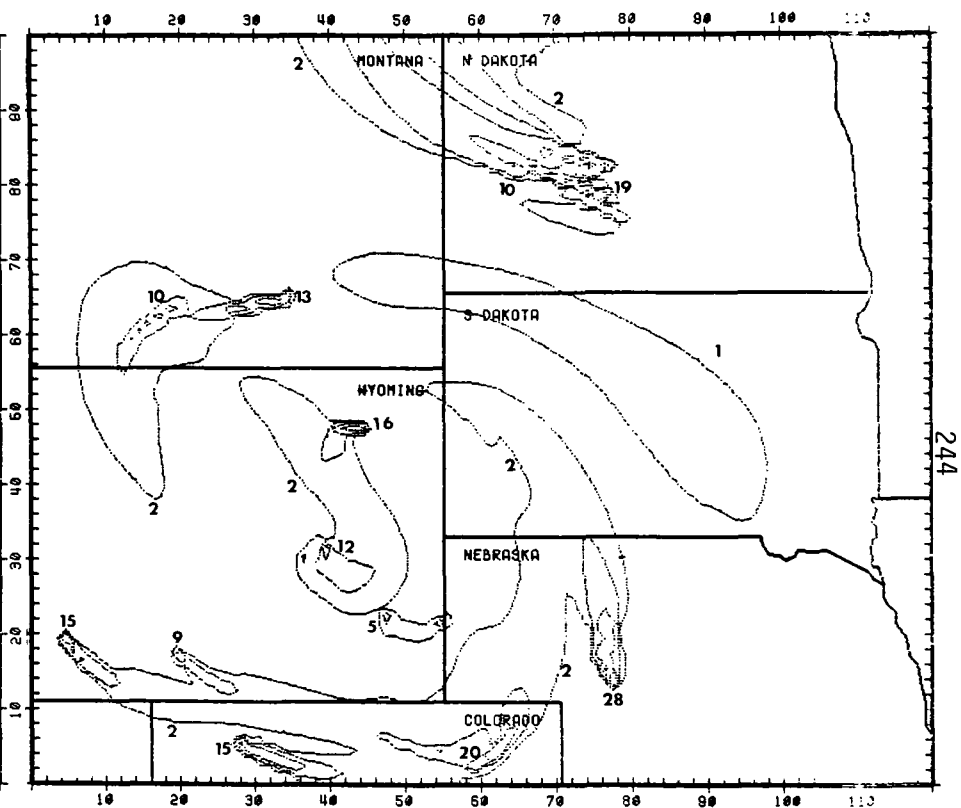
SO2 CONCENTRATIONS IN UG/M3 FOR THE HOUR 1700-2000 MST ON Feb-03



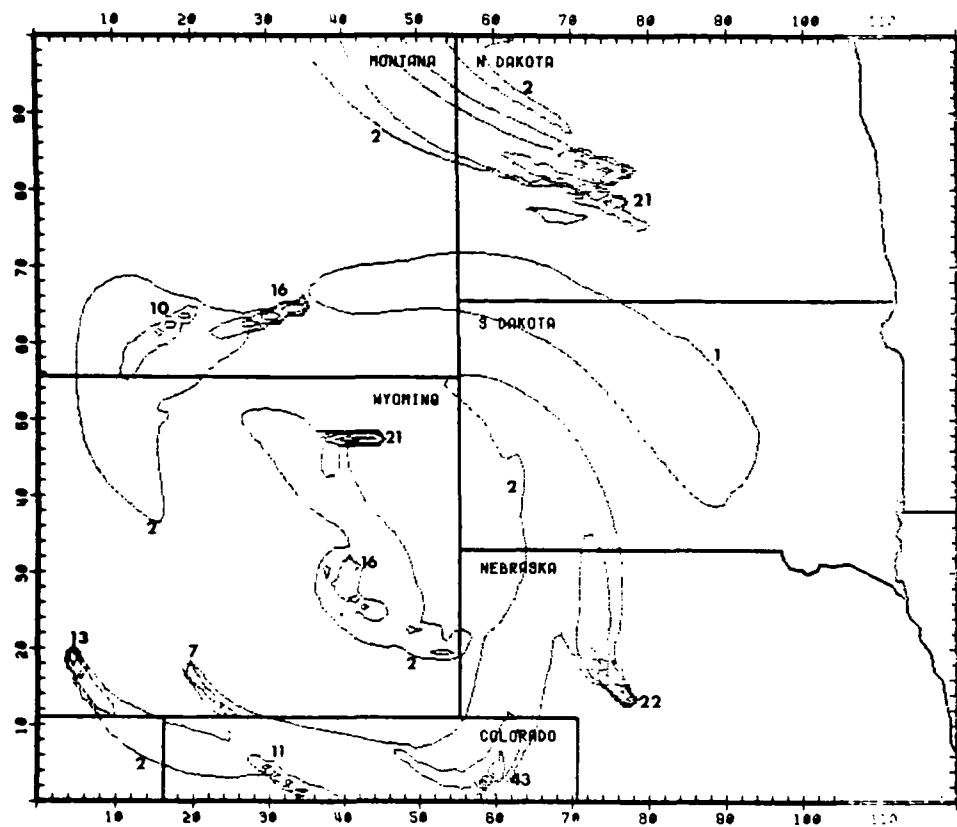
SO2 CONCENTRATIONS IN UG/M3 FOR THE HOUR 2000-2300 MST ON Feb-03



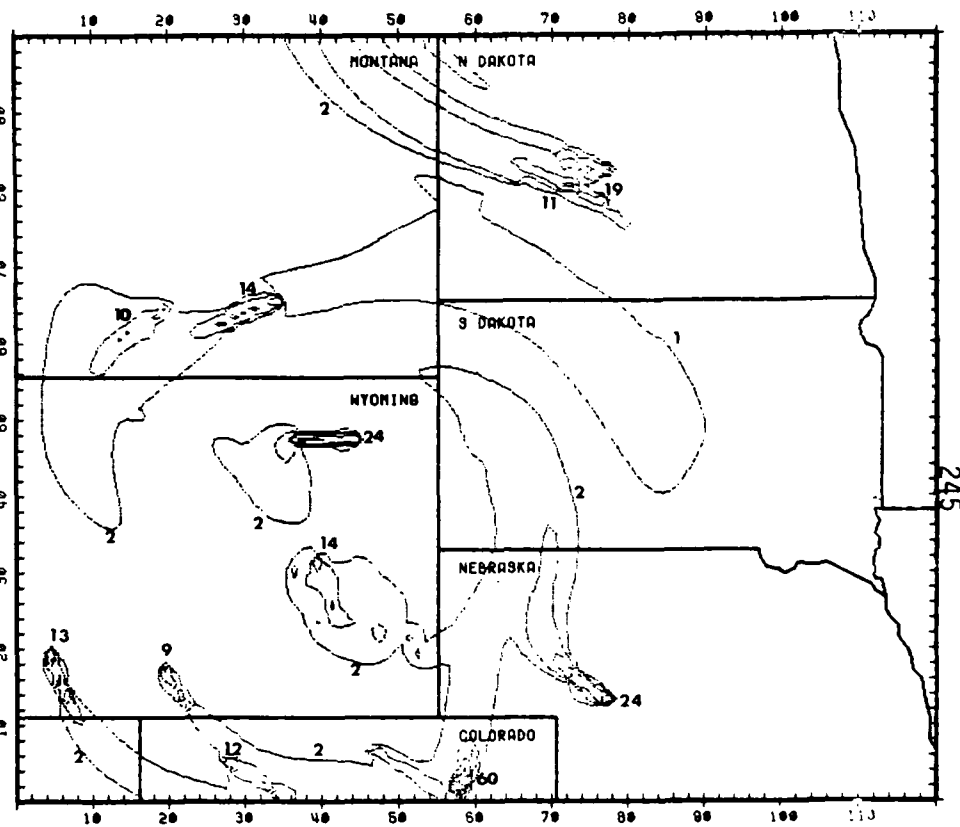
SO2 CONCENTRATIONS IN $\mu\text{G}/\text{M}^3$ FOR THE HOUR -100-200 MST ON 760407



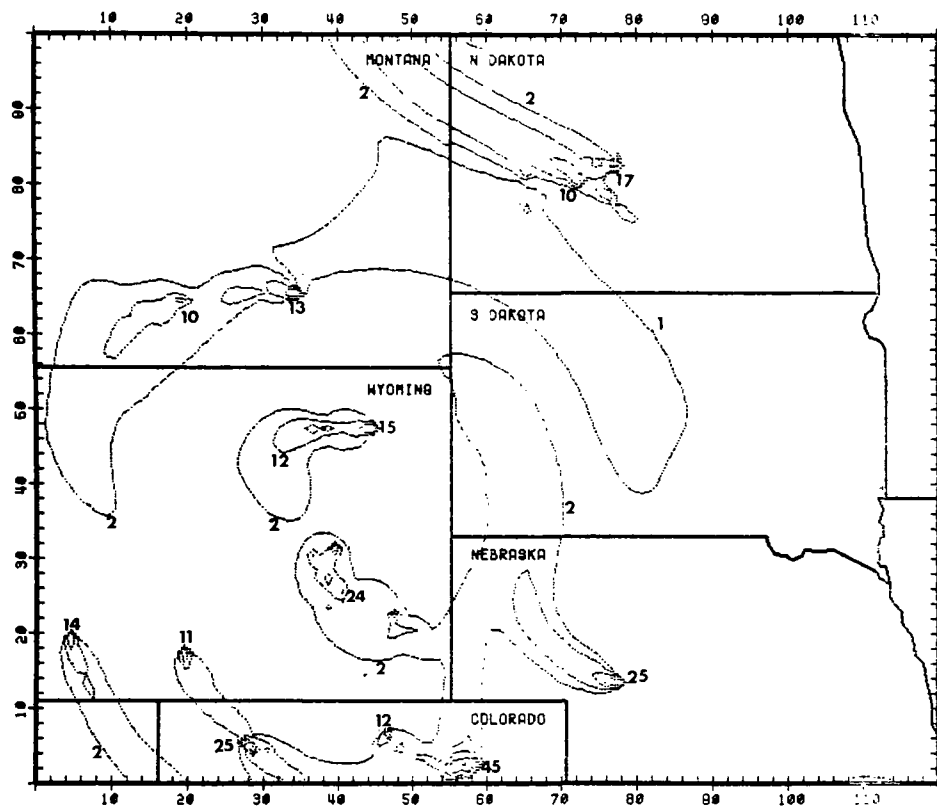
SO2 CONCENTRATIONS IN $\mu\text{G}/\text{M}^3$ FOR THE HOUR 200-500 MST ON 760407



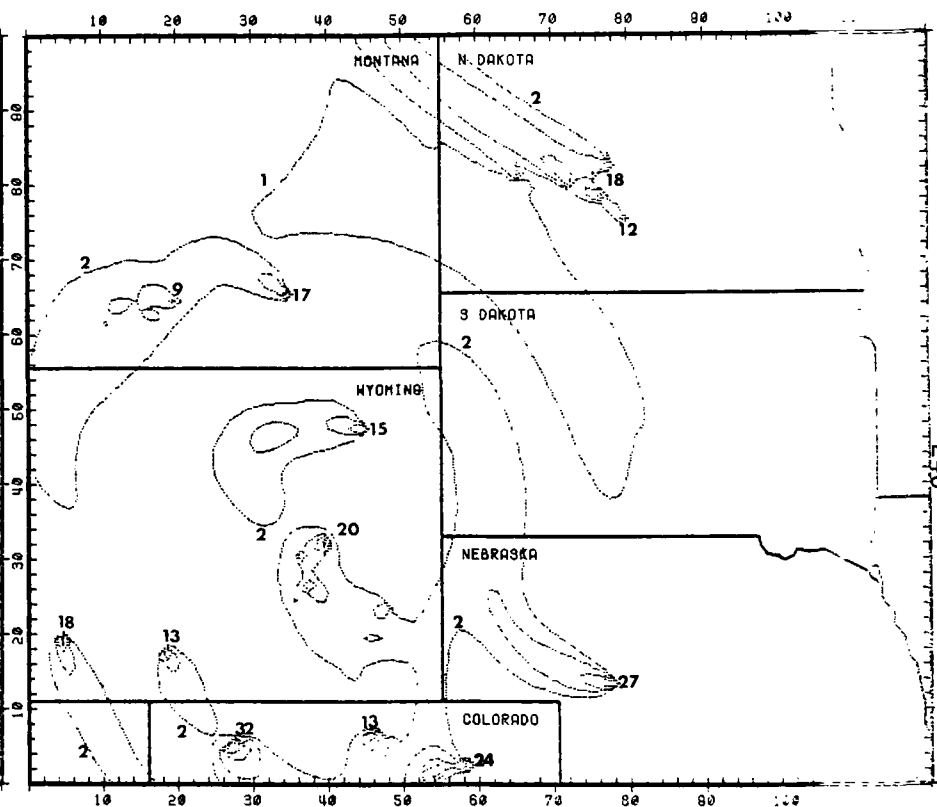
SO2 CONCENTRATIONS IN $\mu\text{g}/\text{m}^3$ FOR THE HOUR 500-800 MST ON 760407



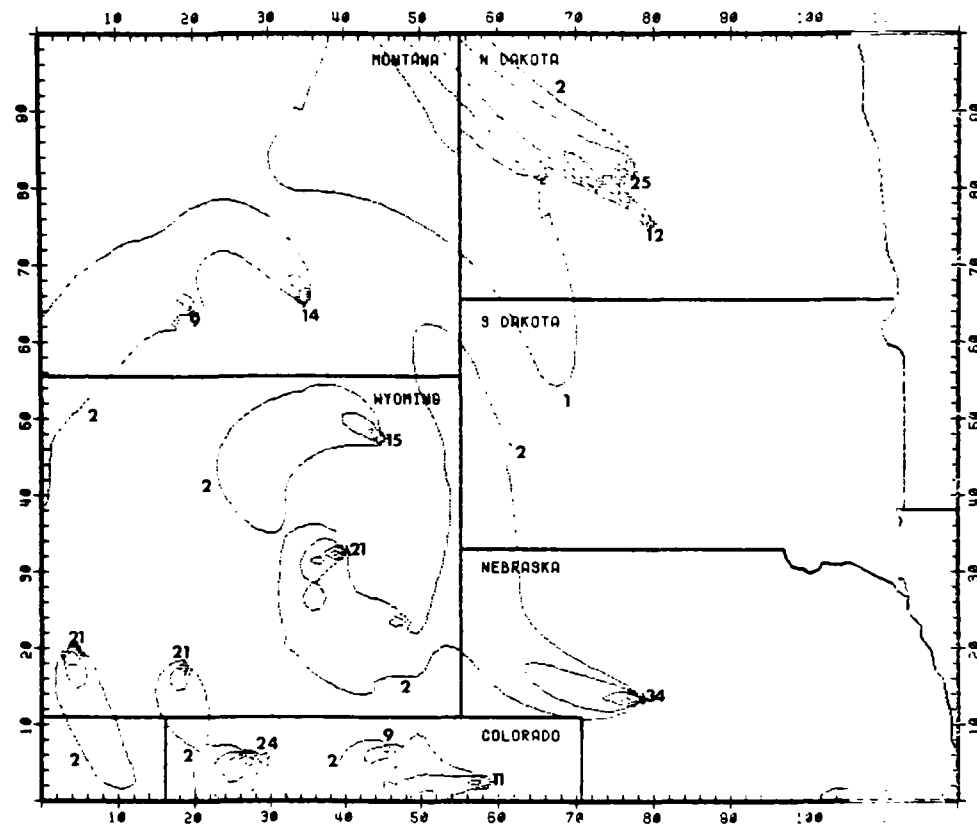
SO2 CONCENTRATIONS IN $\mu\text{g}/\text{m}^3$ FOR THE HOUR 800-1100 MST ON 760407



SO₂ CONCENTRATIONS IN UG/M3 FOR THE HOUR 1100-1400 MST ON 7/20/97

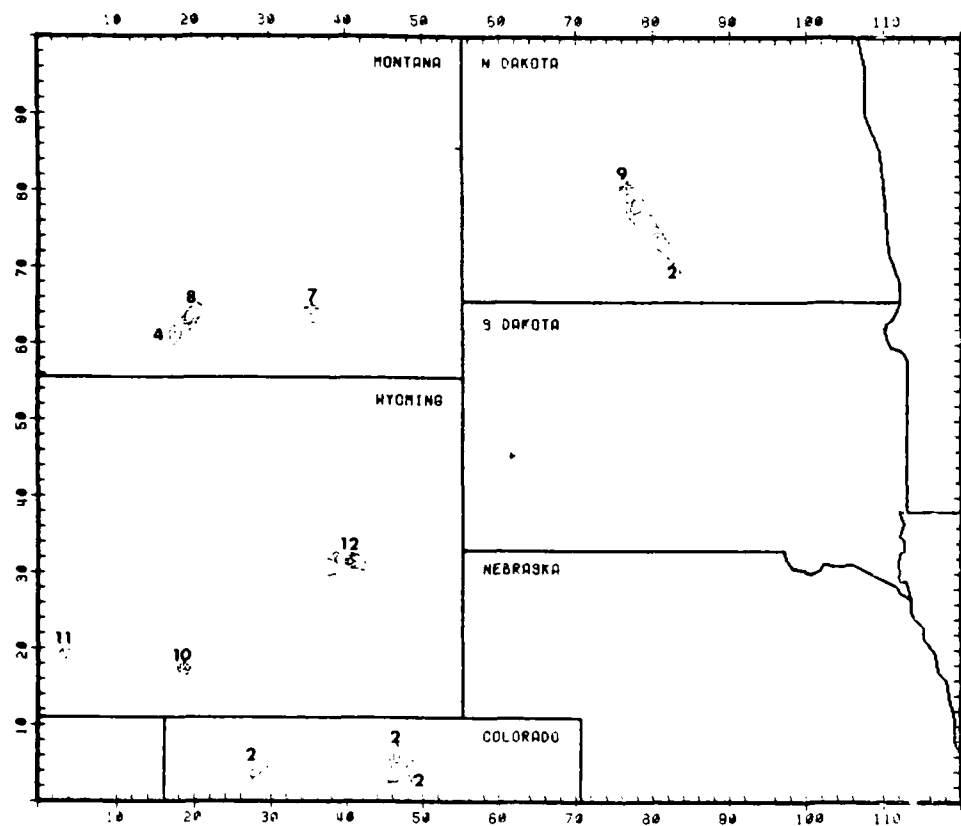


SO₂ CONCENTRATIONS IN UG/M3 FOR THE HOUR 1400-1700 MST ON 7/20/97

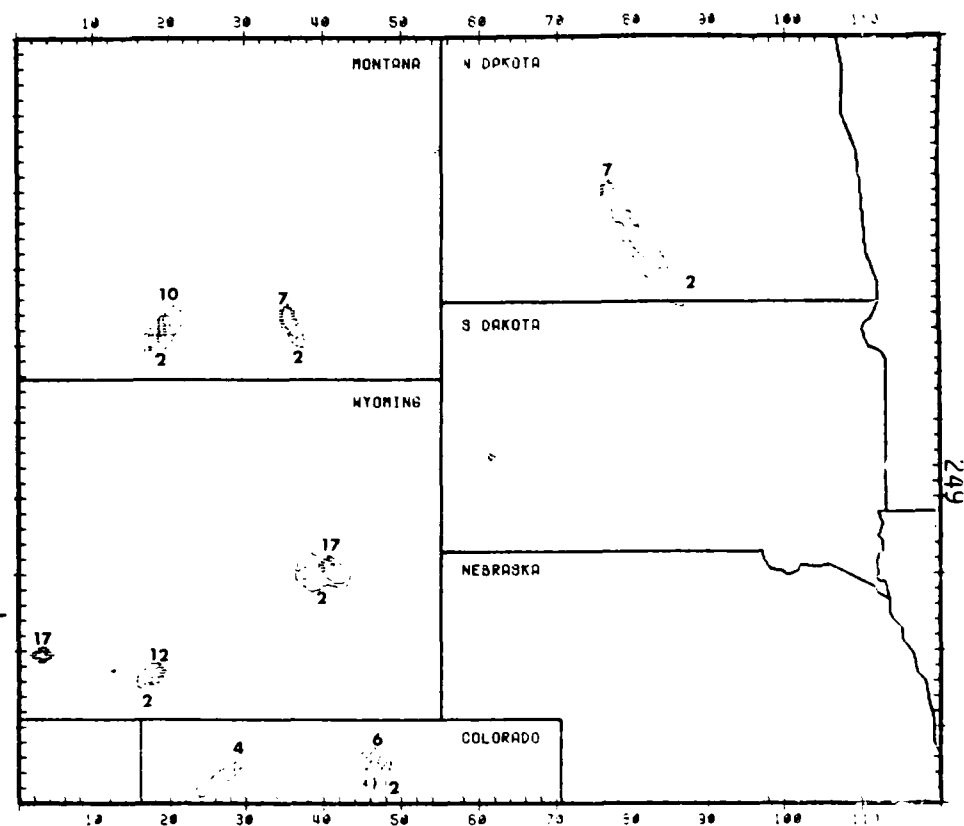


SO2 CONCENTRATIONS IN UG/M3 FOR THE HOUR 1700-2000 MST ON 11-10-87

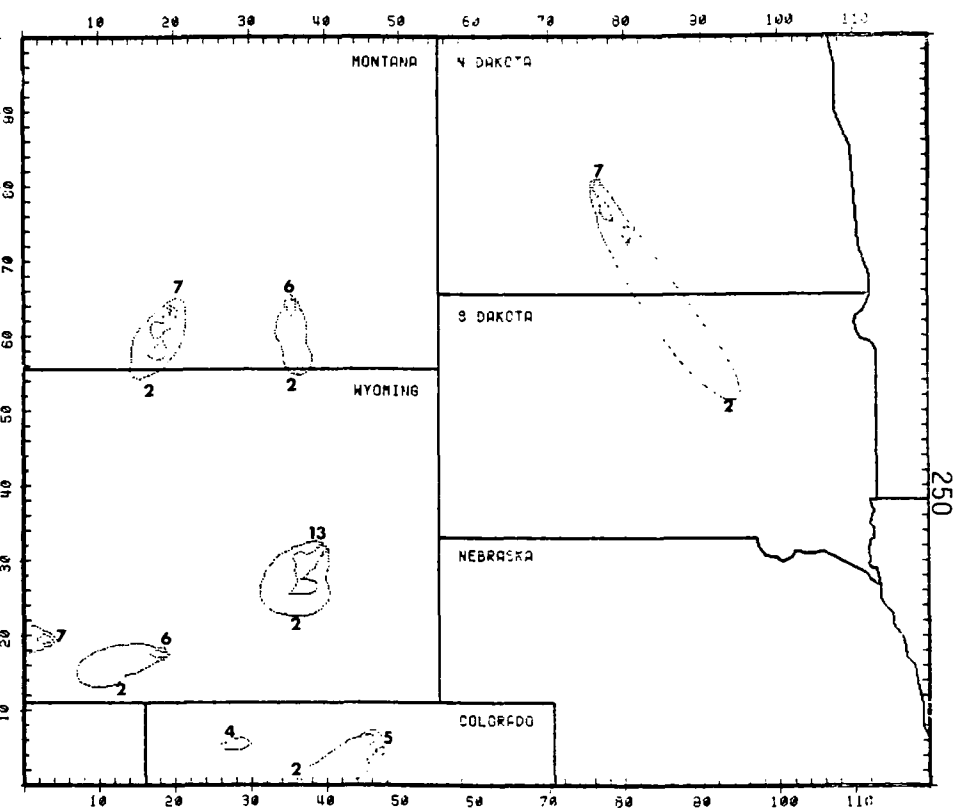
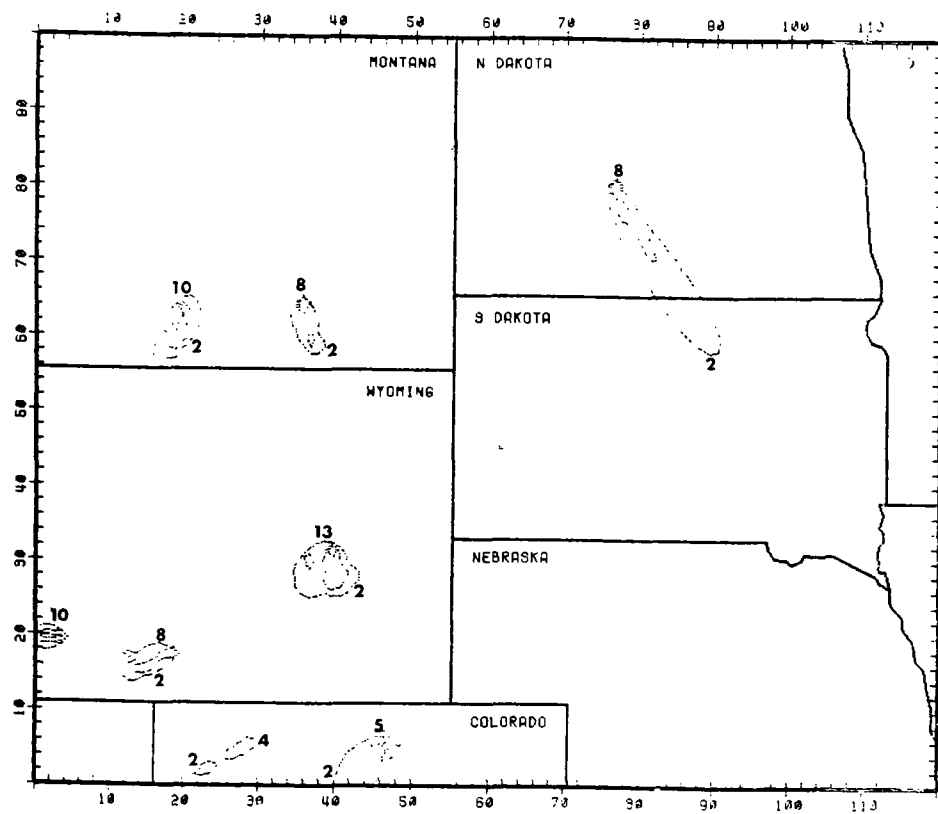
5. 9-11 JULY 1975 METEOROLOGY; 1976 EMISSIONS



SO₂ CONCENTRATIONS IN UG/M³ FOR THE HOUR 500-800 MST ON 7/20/77

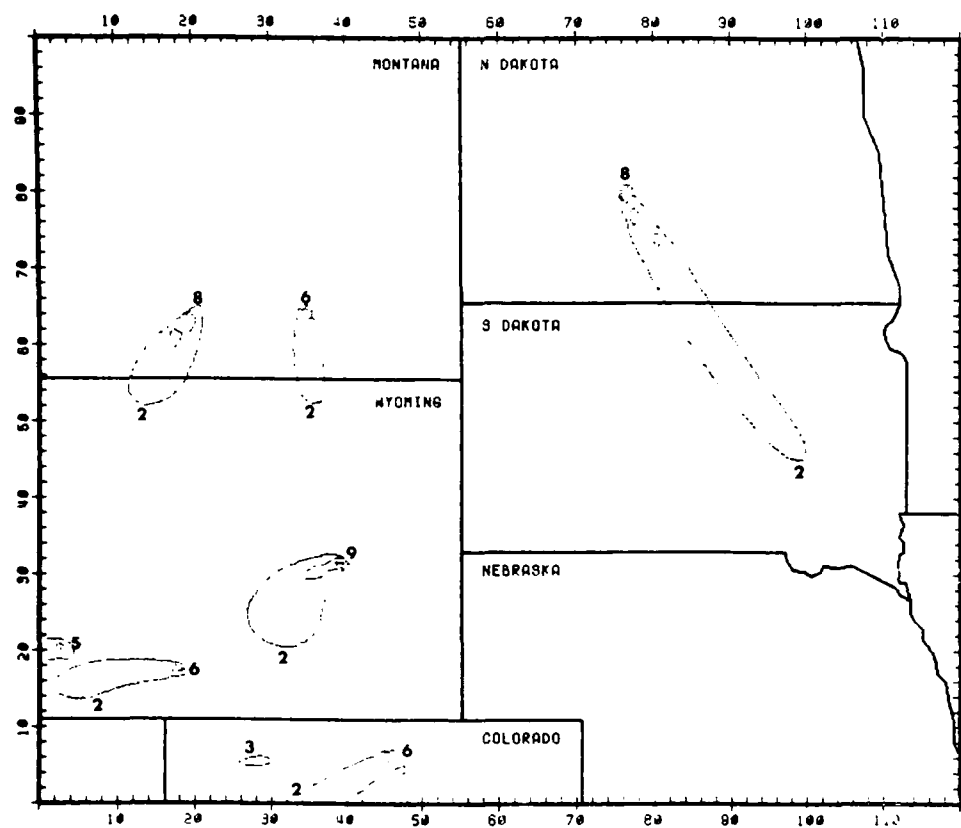


SO₂ CONCENTRATIONS IN UG/M³ FOR THE HOUR 800-1100 MST ON 7/20/77

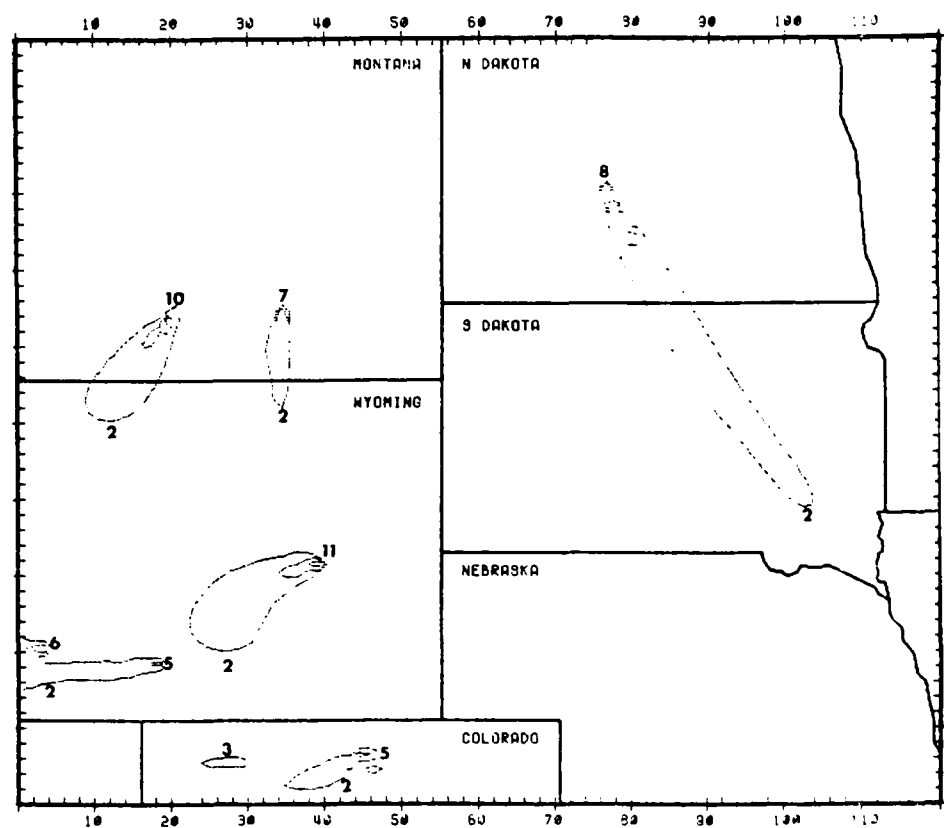


SO2 CONCENTRATIONS IN UG/M3 FOR THE HOUR 1100-1400 MST ON 750722

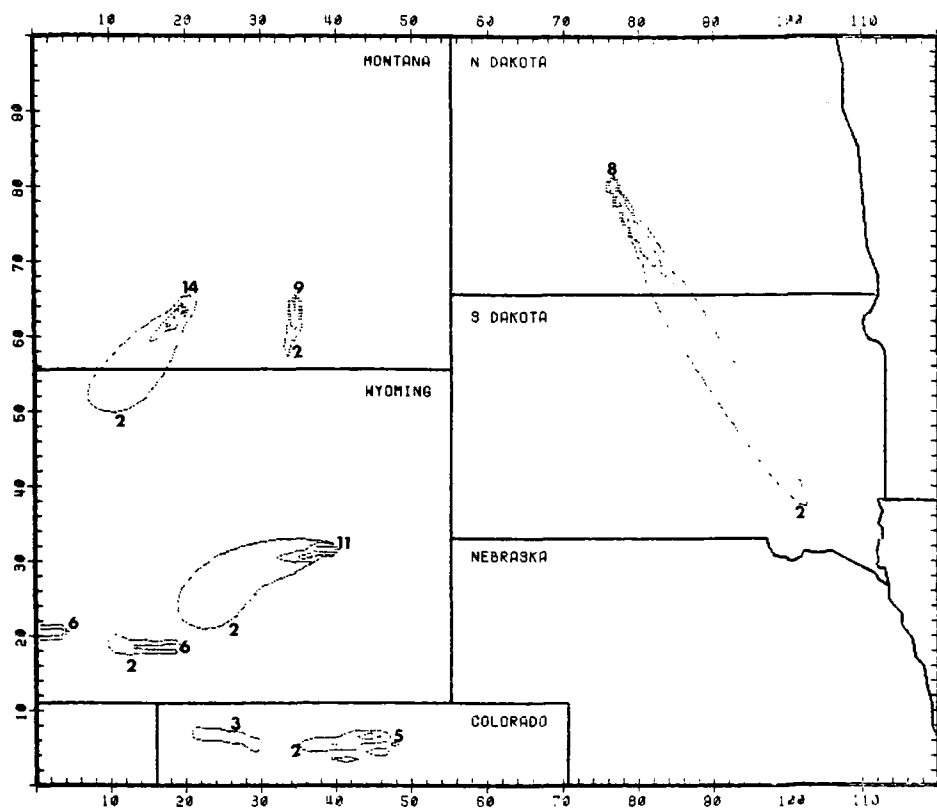
SO2 CONCENTRATIONS IN UG/M3 FOR THE HOUR 1400-1700 MST ON 750722



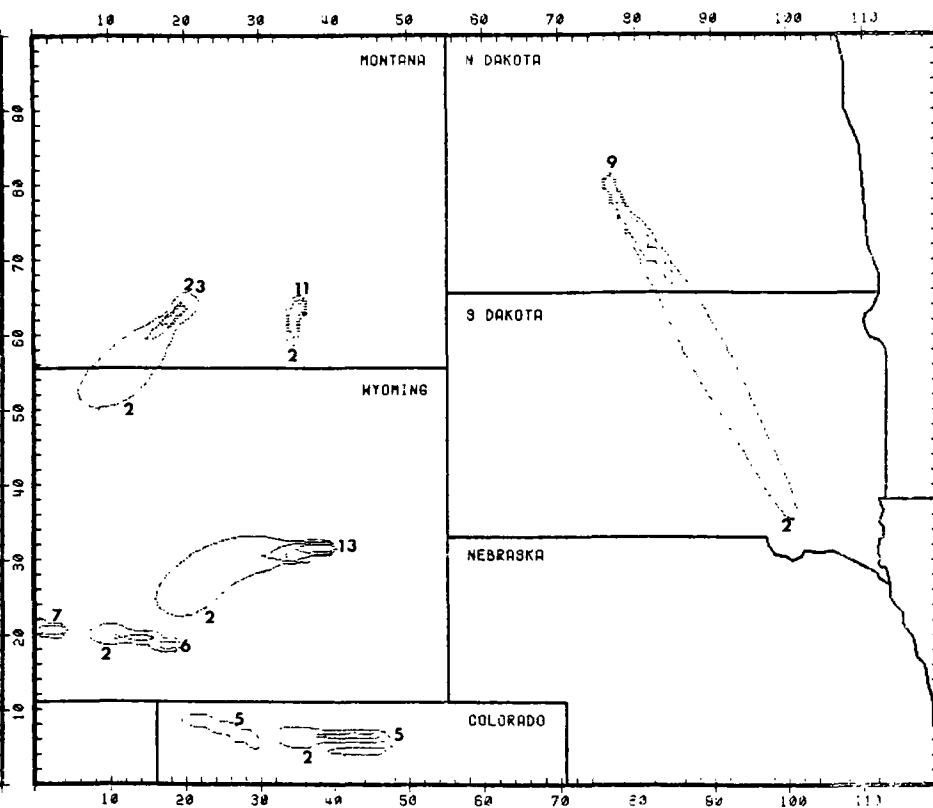
SO₂ CONCENTRATIONS IN UG/M³ FOR THE HOUR 1700-2000 MST ON 7/07/79



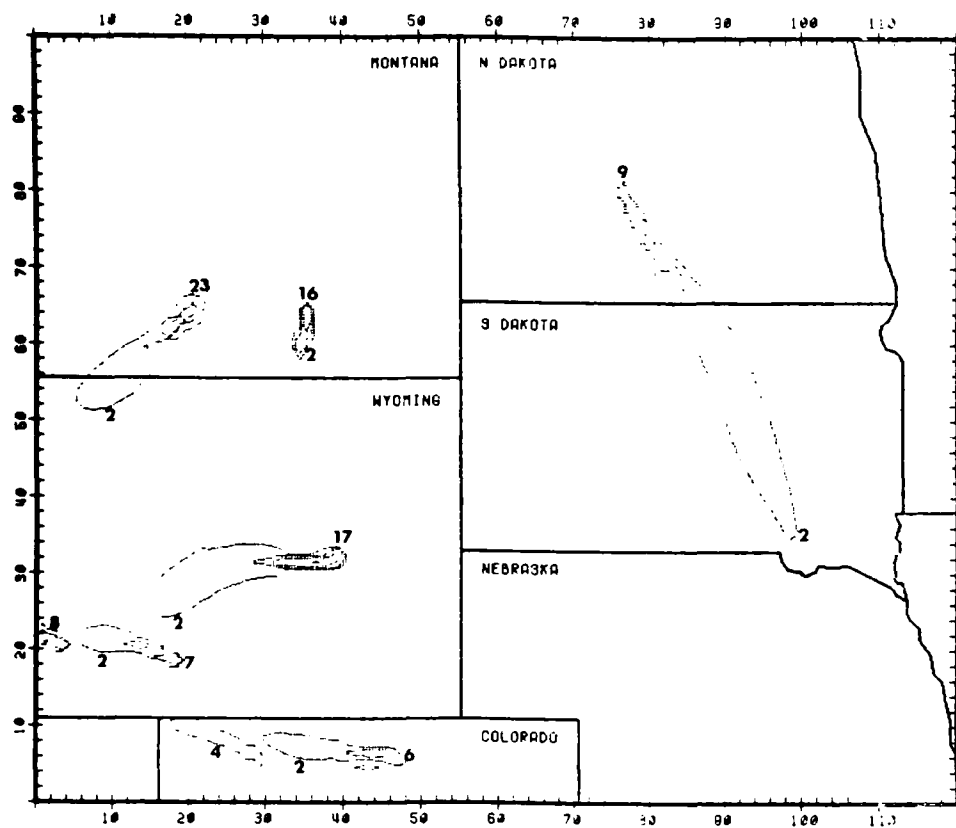
SO₂ CONCENTRATIONS IN UG/M³ FOR THE HOUR 2000-2300 MST ON 7/07/79



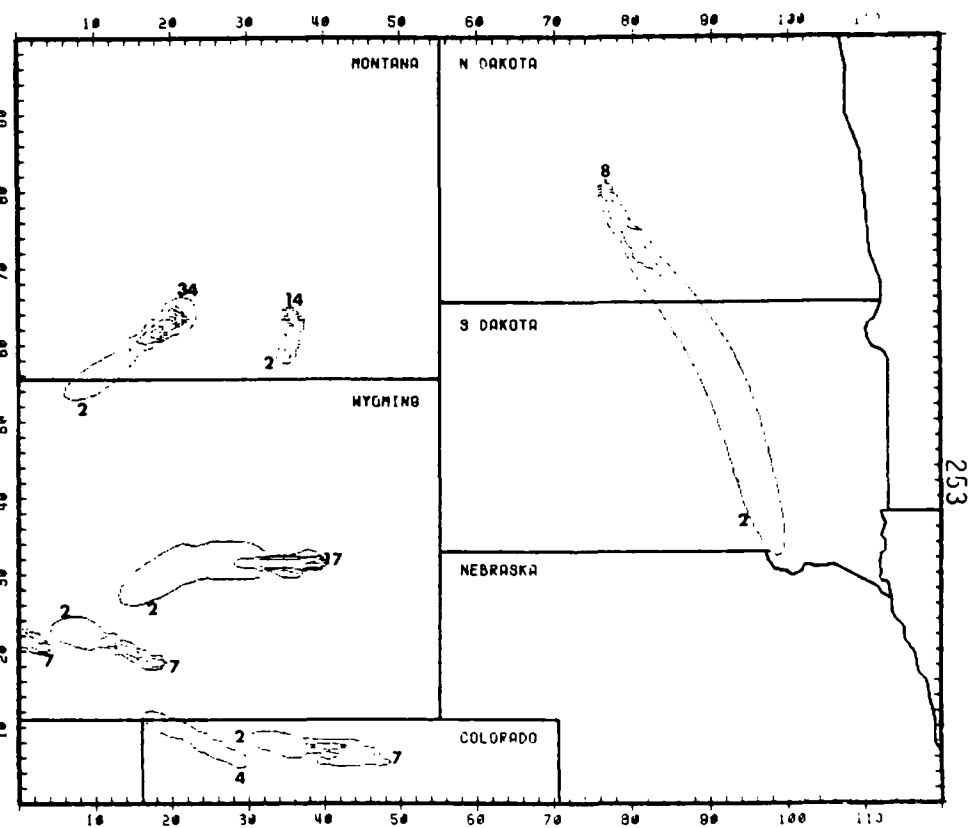
SO2 CONCENTRATIONS IN UG/M3 FOR THE HOUR -100-200 MST ON 750710



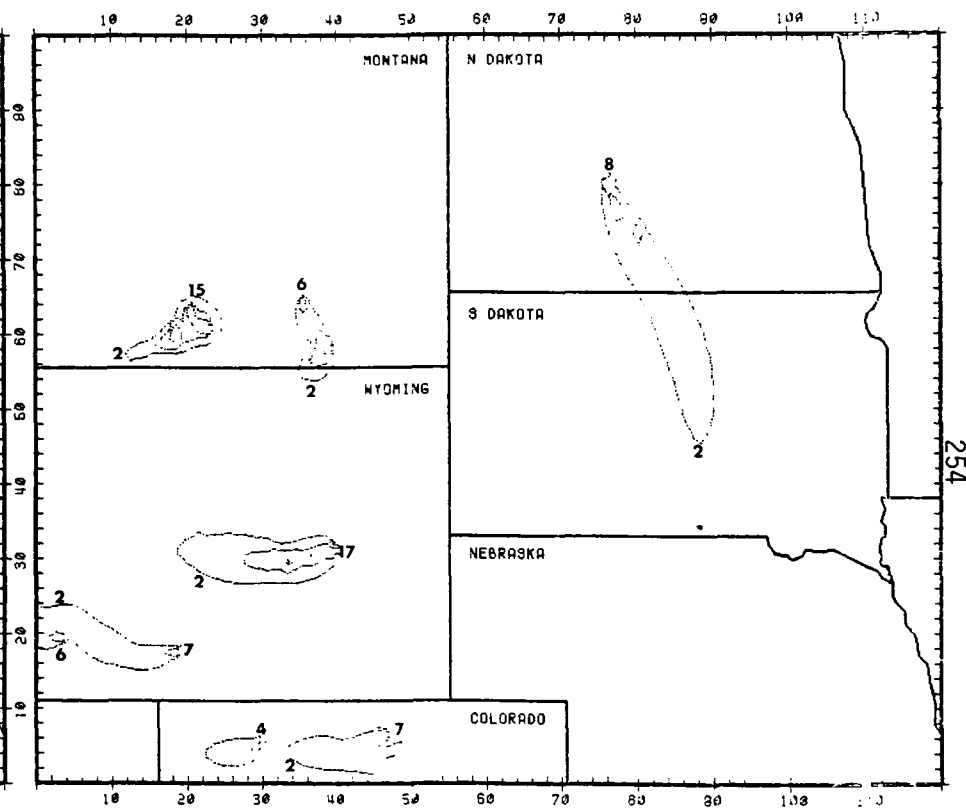
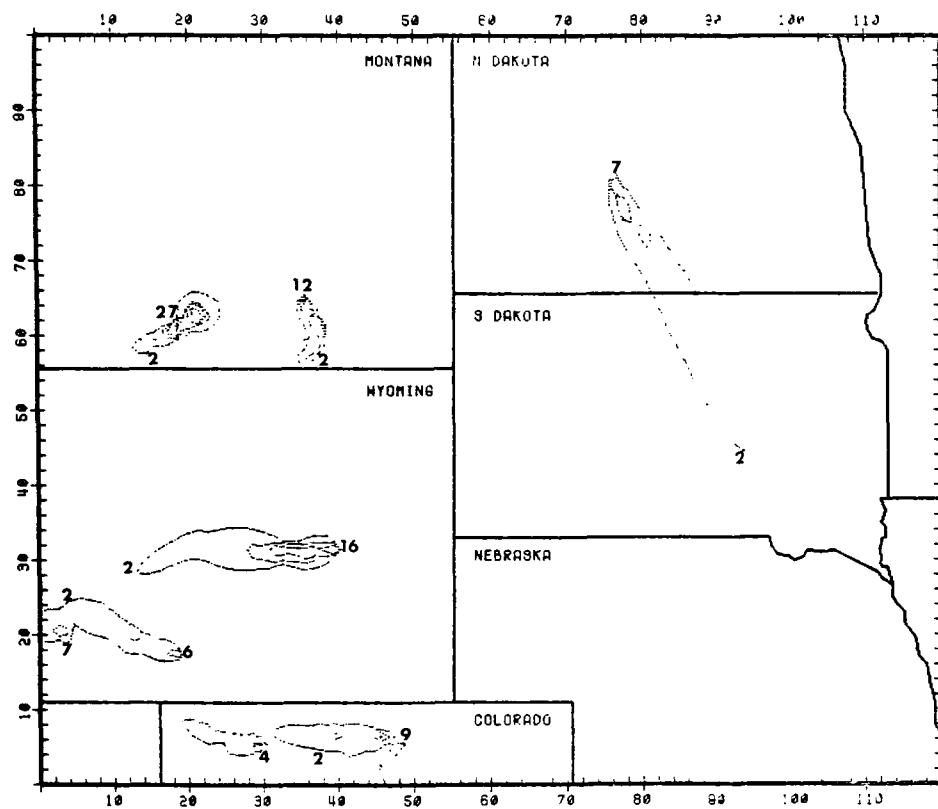
SO2 CONCENTRATIONS IN UG/M3 FOR THE HOUR 220-500 MST ON 750710



SO₂ CONCENTRATIONS IN UG/M³ FOR THE HOUR 500-599 MST ON 7/5/71

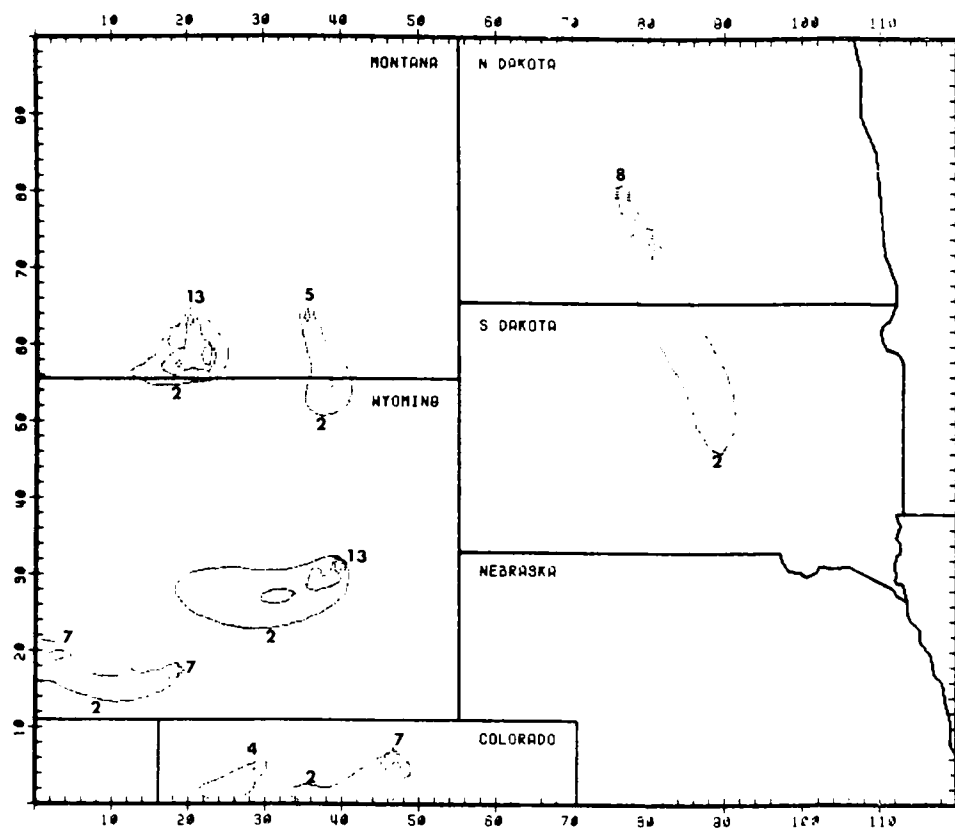


SO₂ CONCENTRATIONS IN UG/M³ FOR THE HOUR 600-699 MST ON 7/5/71

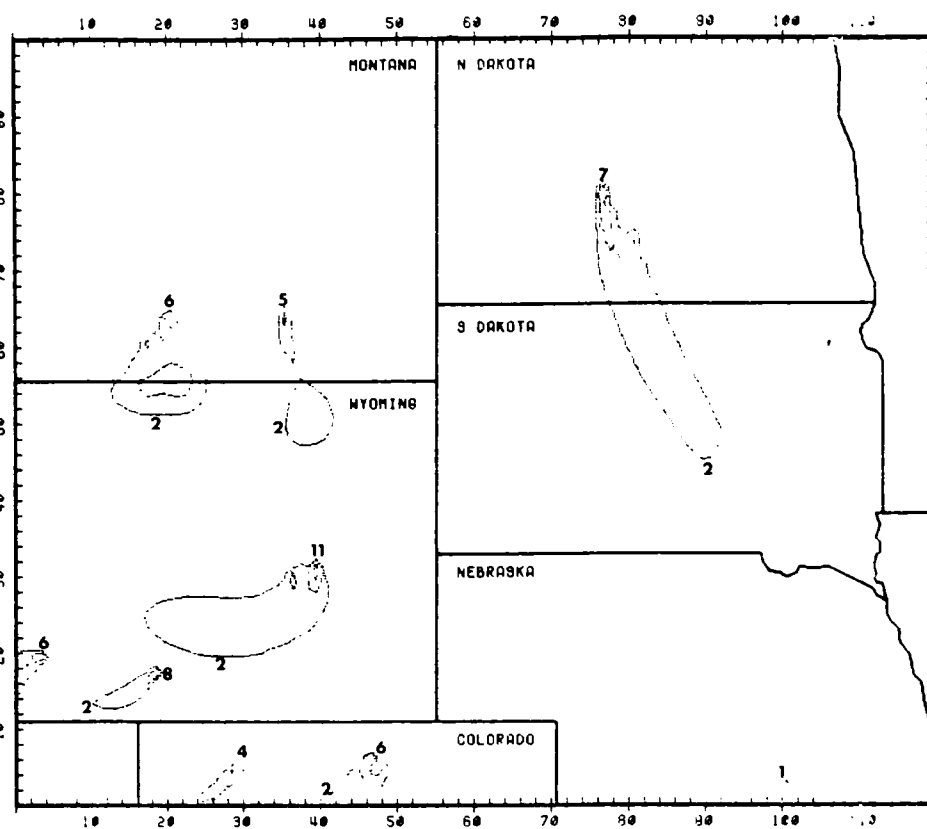


SO2 CONCENTRATIONS IN UG/M3 FOR THE HOUR 1100-1400 MST ON 11/07/10

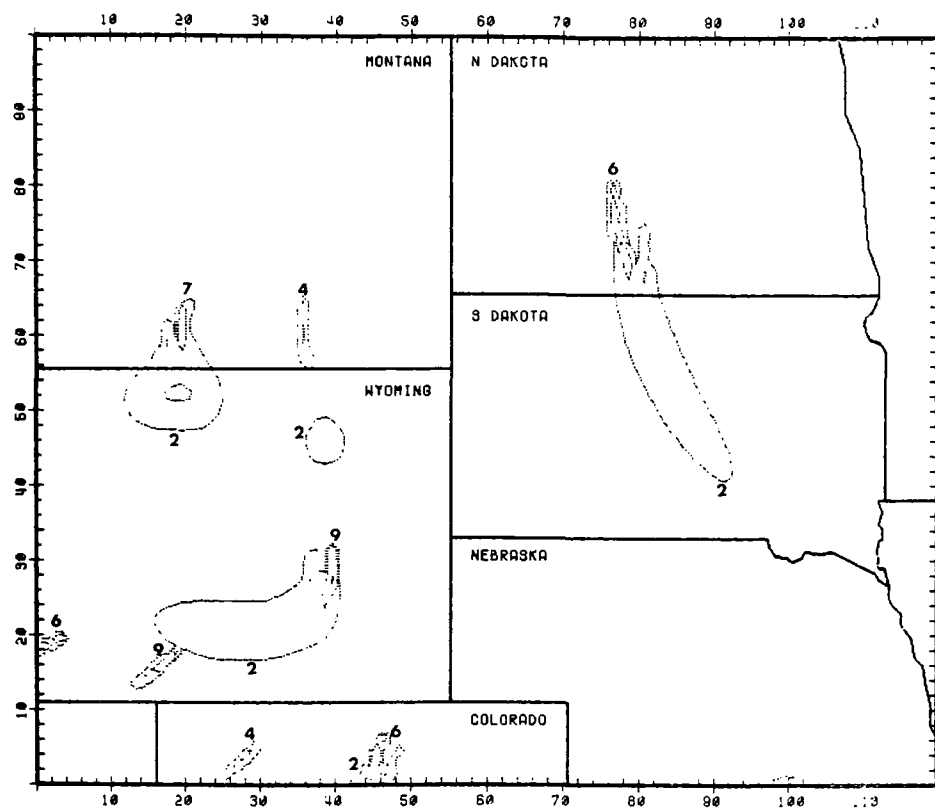
SO2 CONCENTRATIONS IN UG M3 FOR THE HOUR 1400-1700 MST ON 11/07/10



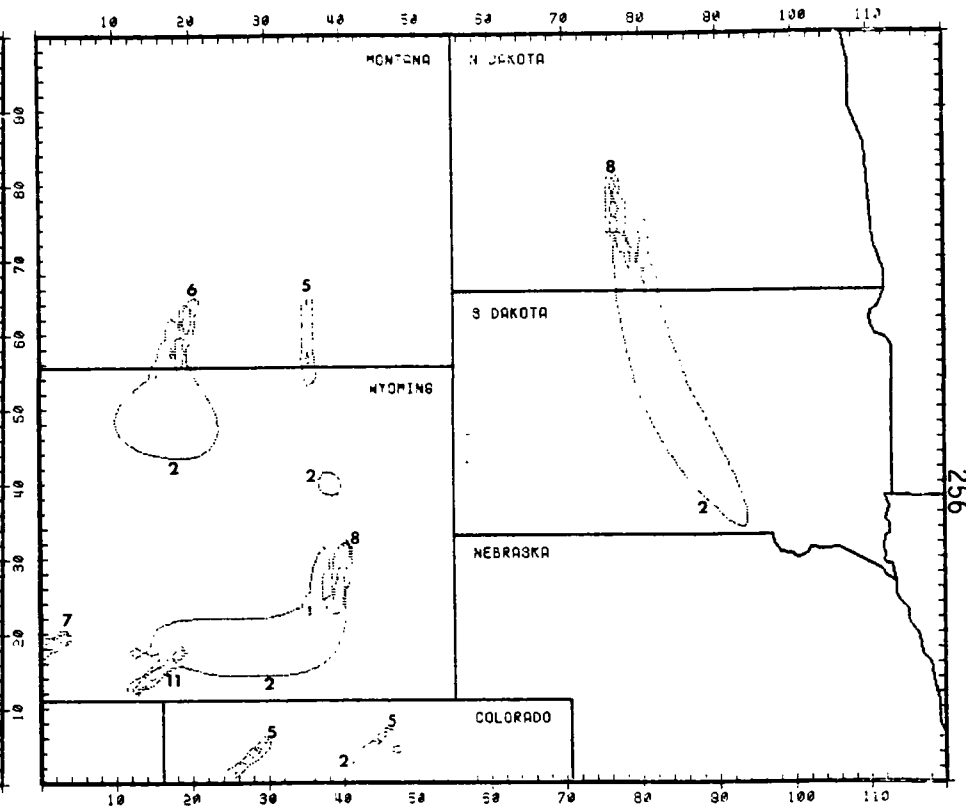
SO2 CONCENTRATIONS IN UG/M3 FOR THE HOUR 1700-2000 MST ON 750710



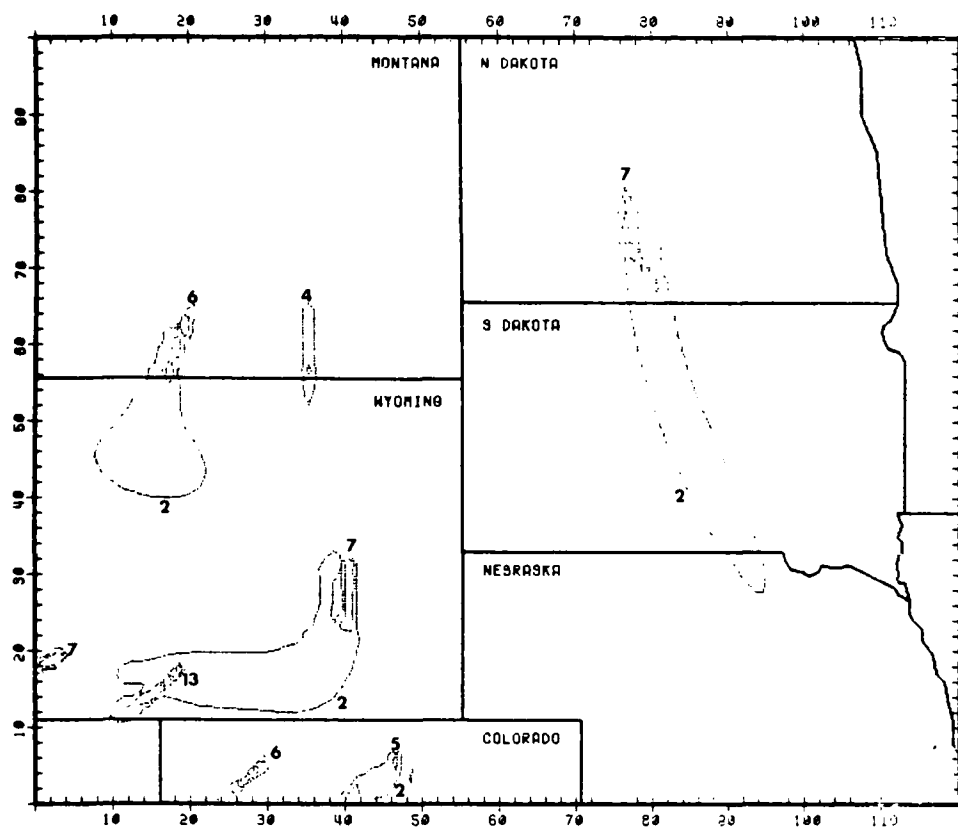
SO2 CONCENTRATIONS IN UG/M3 FOR THE HOUR 2000-2300 MST ON 750710



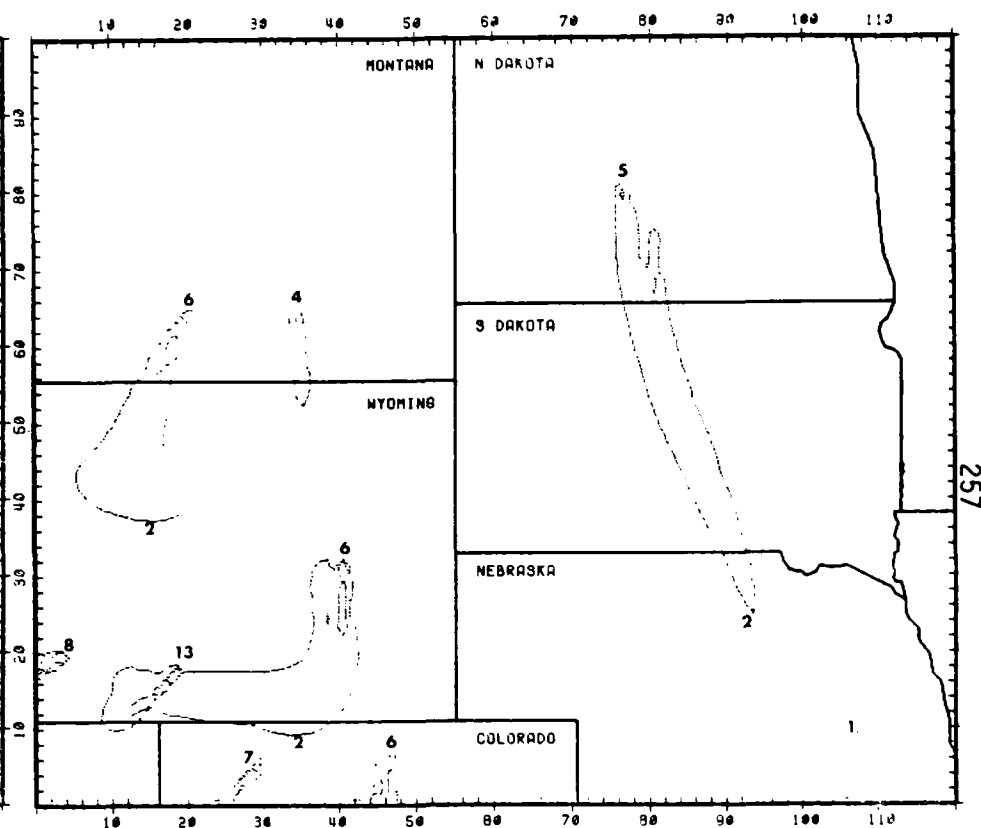
SO2 CONCENTRATIONS IN UG/M3 FOR THE HOUR -100-200 MST ON 750711



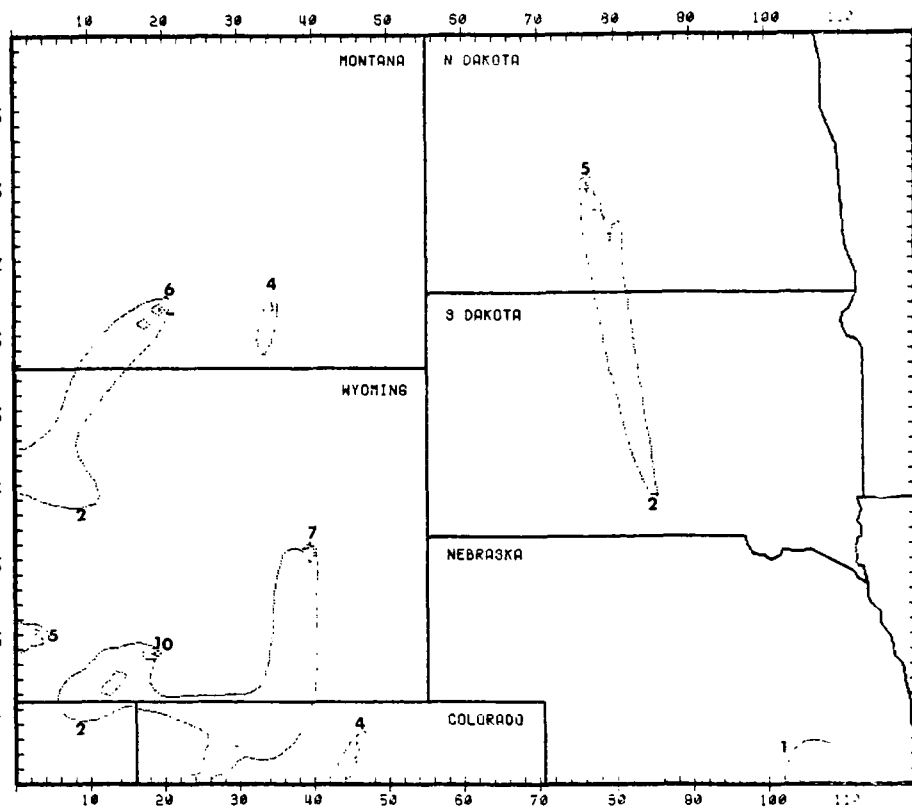
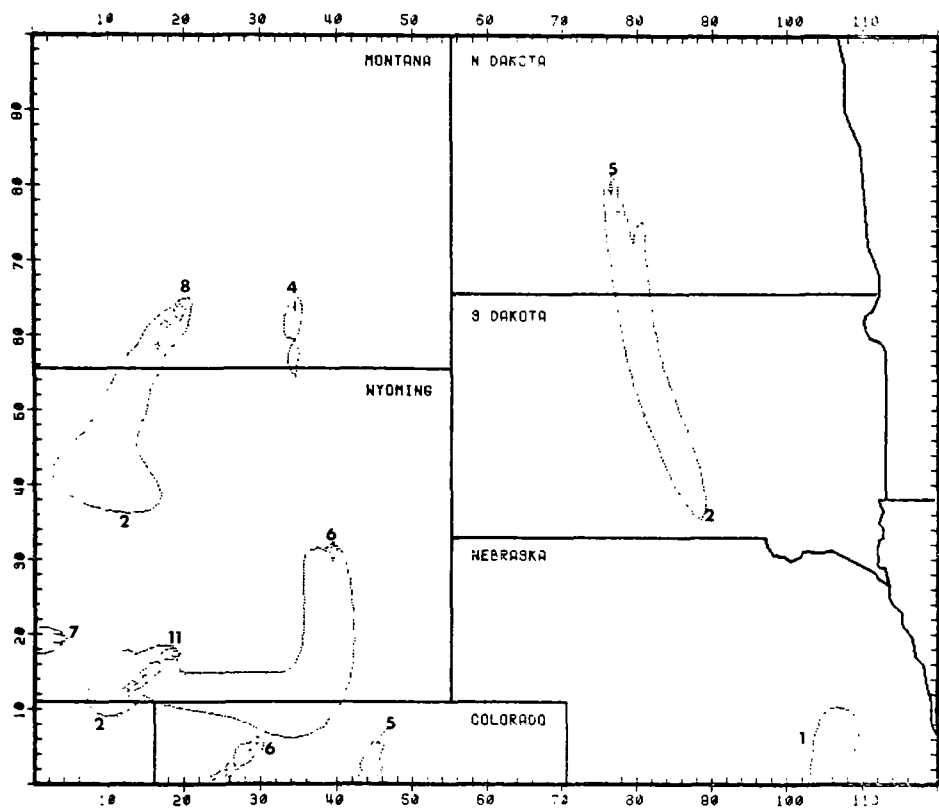
SO2 CONCENTRATIONS IN UG/M3 FOR THE HOUR 200-500 MST ON 750711



SO2 CONCENTRATIONS IN $\mu\text{G}/\text{M}^3$ FOR THE HOUR 500-800 MST ON 75JUN11

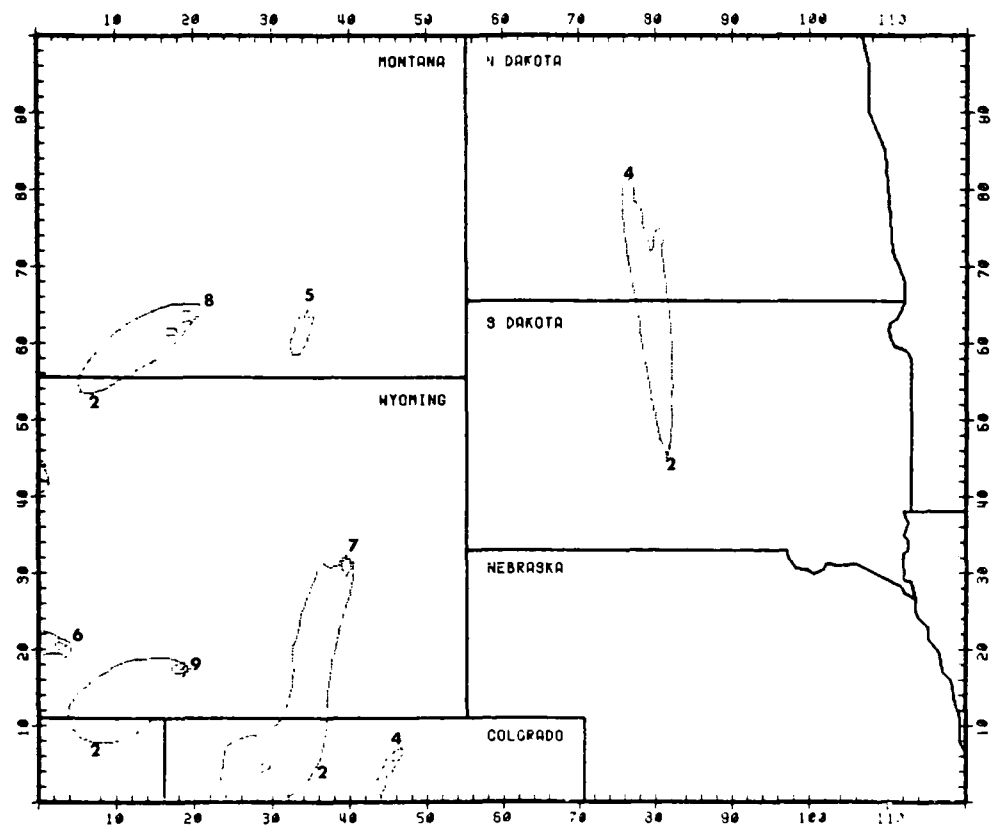


SO2 CONCENTRATIONS IN $\mu\text{G}/\text{M}^3$ FOR THE HOUR 900-1100 MST ON 75JUN11



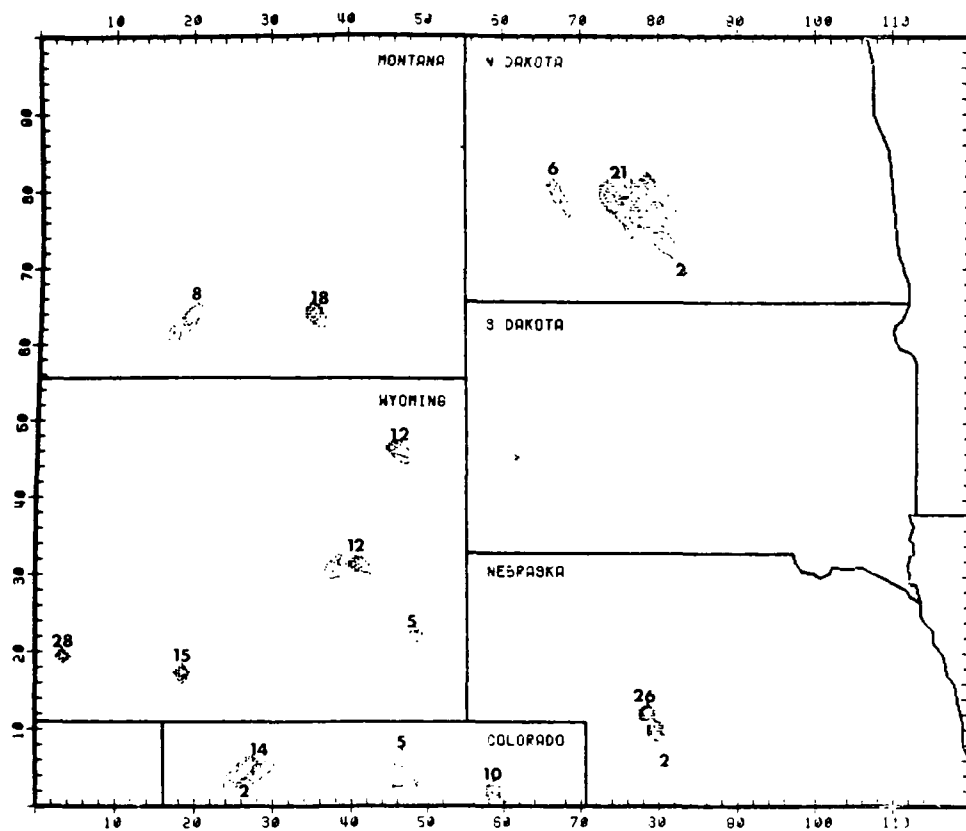
SO2 CONCENTRATIONS IN $\mu\text{g}/\text{m}^3$ FOR THE HOUR 1100-1400 MST ON 7/30/71

SO2 CONCENTRATIONS IN $\mu\text{g}/\text{m}^3$ FOR THE HOUR 1400-1700 MST ON 7/30/71

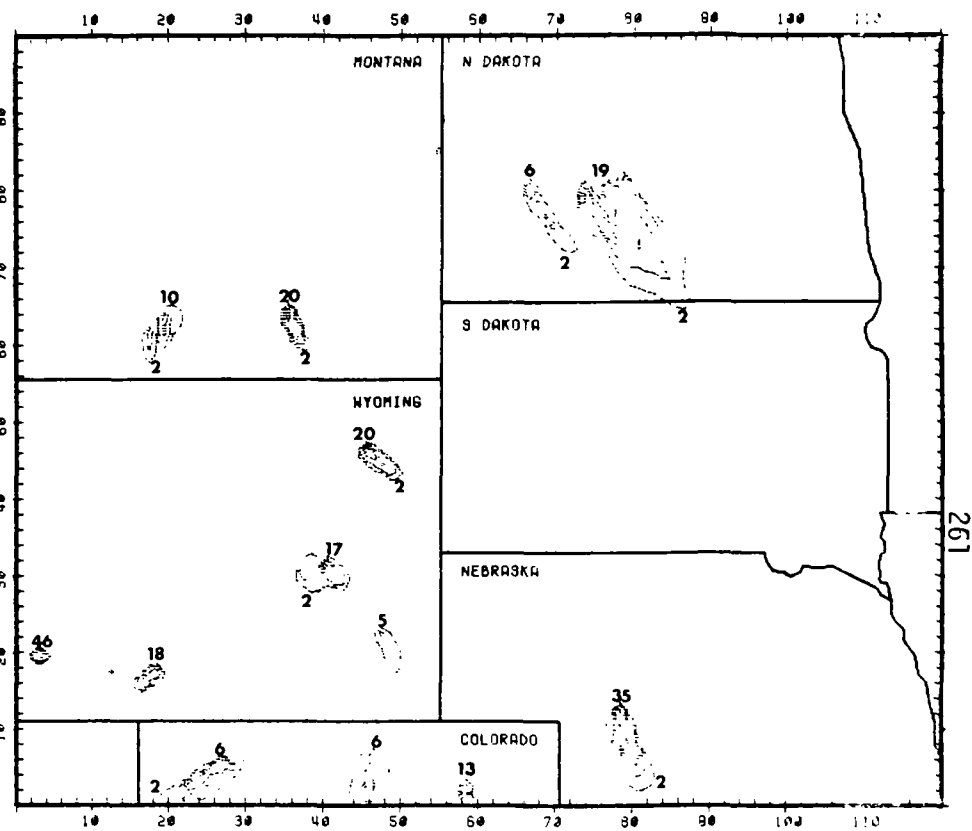


SO₂ CONCENTRATIONS IN UG/M³ FOR THE HOUR 1700-2000 MST ON JULY 11

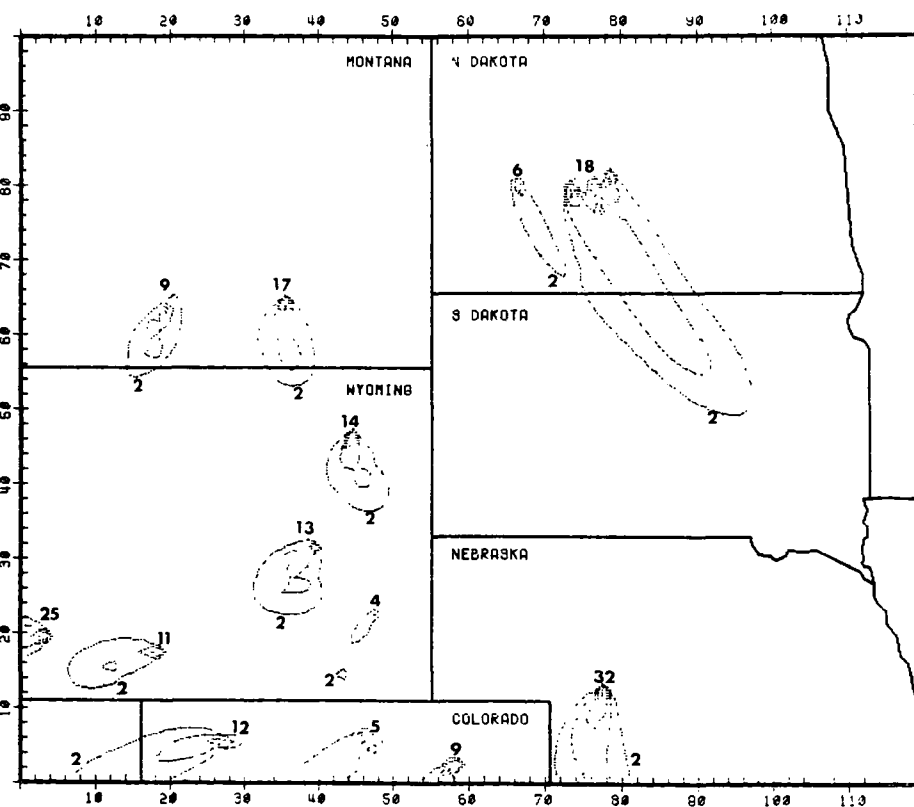
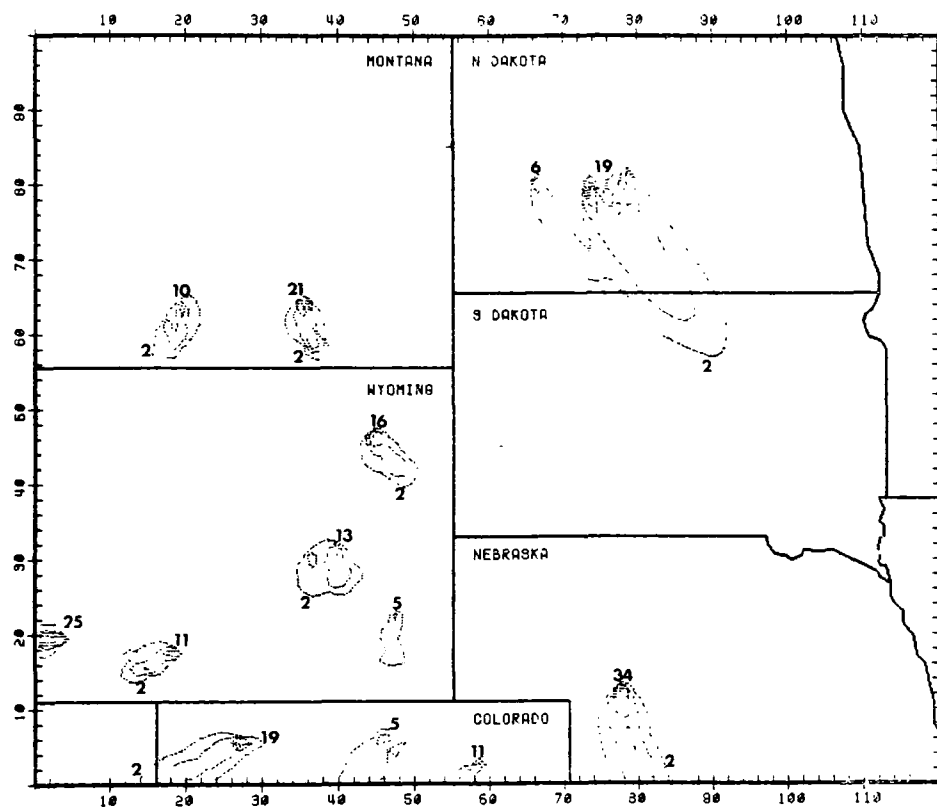
6. 9-11 JULY 1975 METEOROLOGY; 1986 EMISSIONS



SO2 CONCENTRATIONS IN $\mu\text{g}/\text{m}^3$ FOR THE HOUR 500-800 MST ON 750709

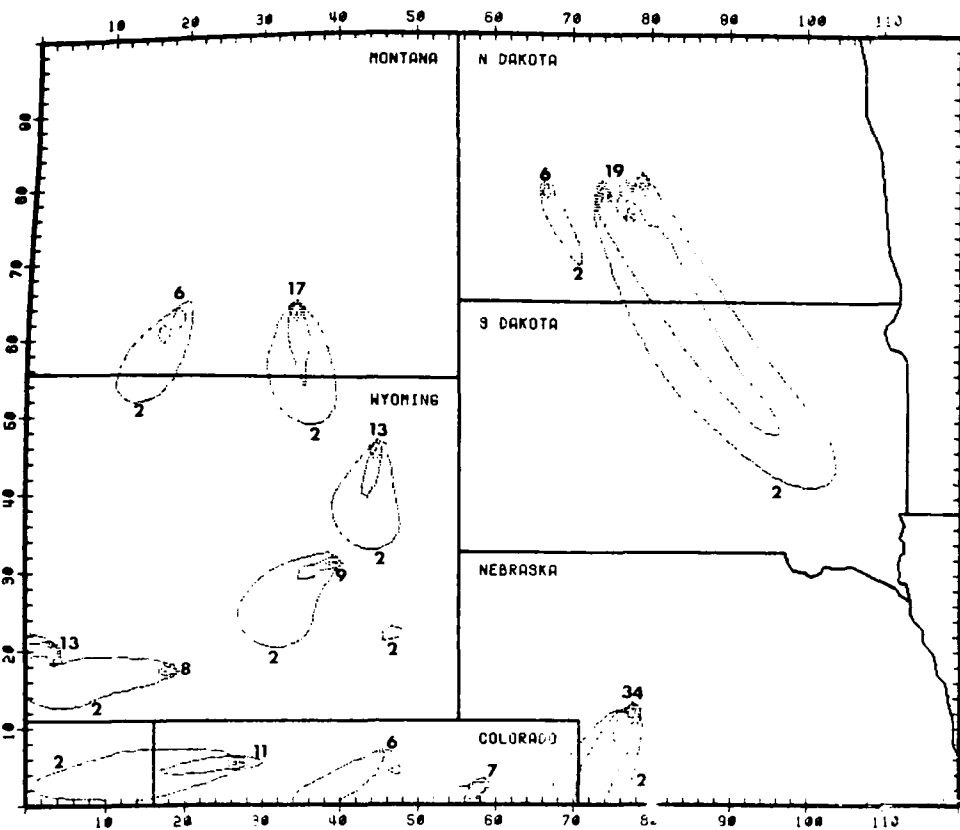


SO2 CONCENTRATIONS IN $\mu\text{g}/\text{m}^3$ FOR THE HOUR 800-1100 MST ON 750709

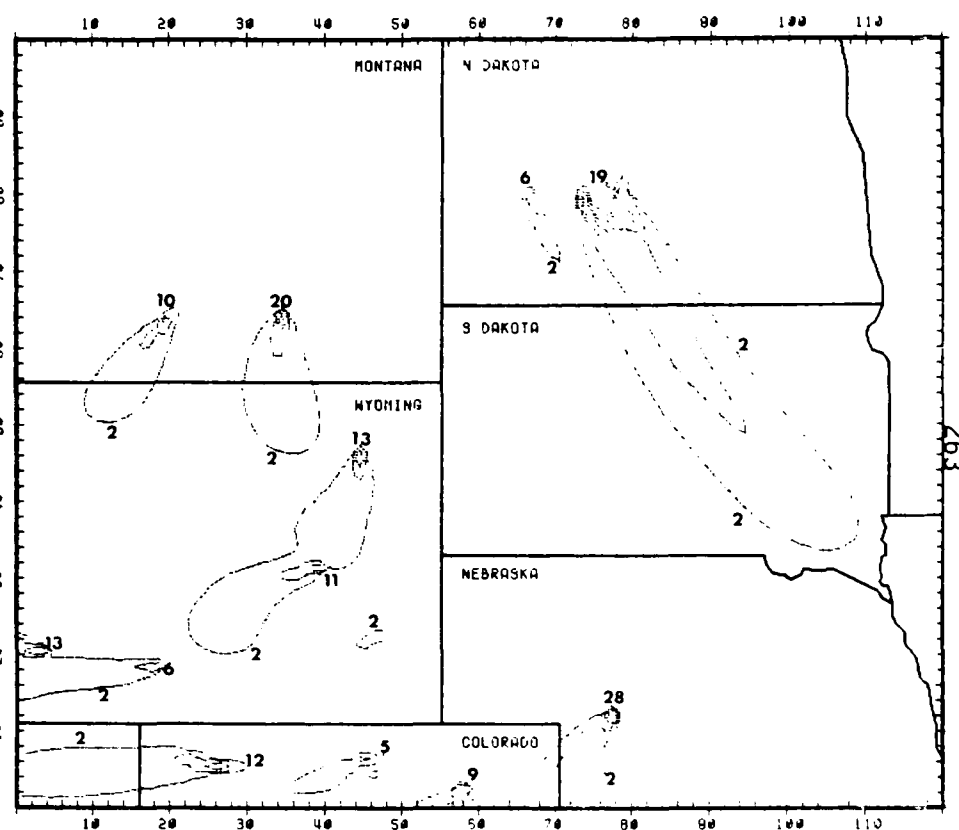


SO₂ CONCENTRATIONS IN UG/M³ FOR THE HOUR 1100-1400 MST ON 750709

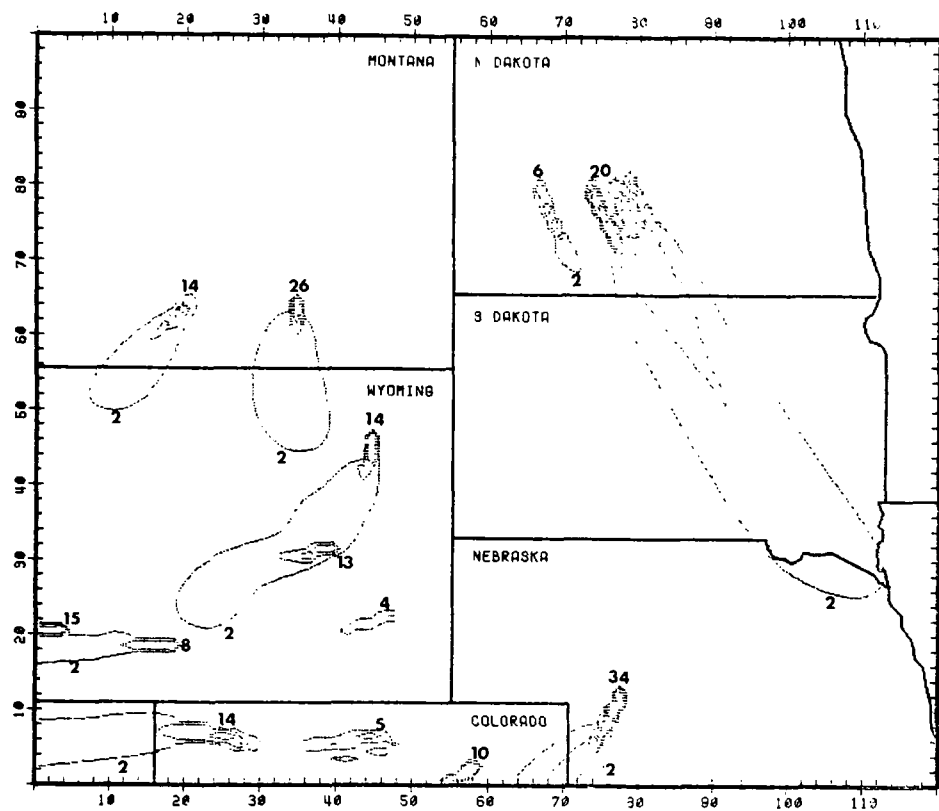
SO₂ CONCENTRATIONS IN UG/M³ FOR THE HOUR 1400-1700 MST ON 750709



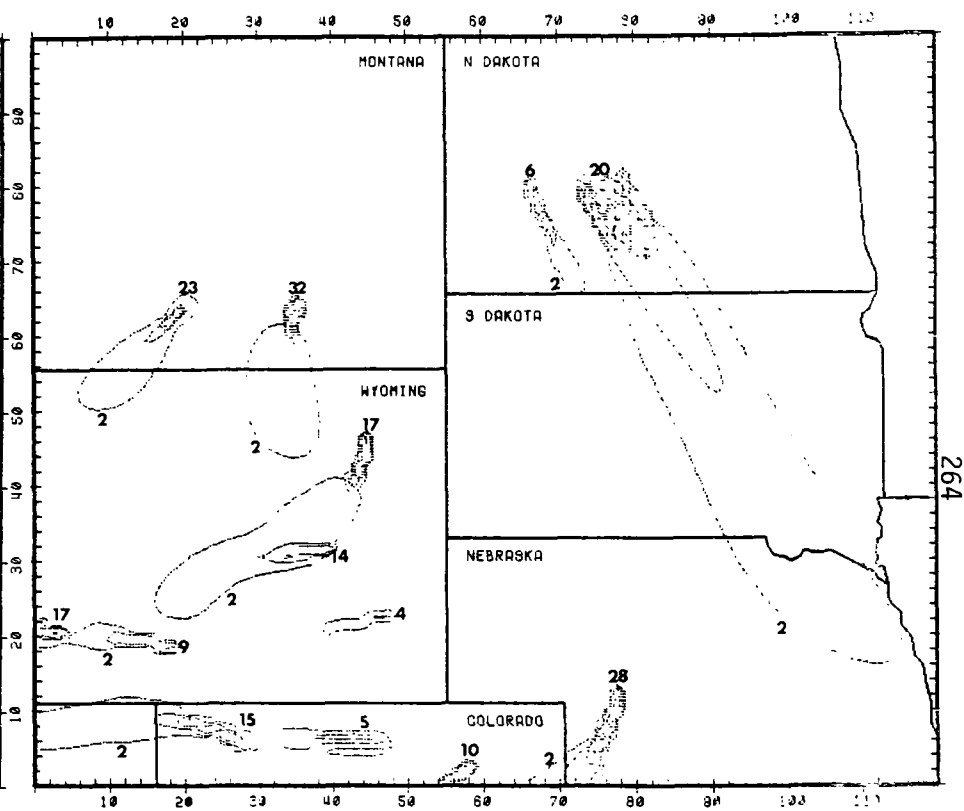
SO₂ CONCENTRATIONS IN UG/M³ FOR THE HOUR 1700-2000 MST ON 750701



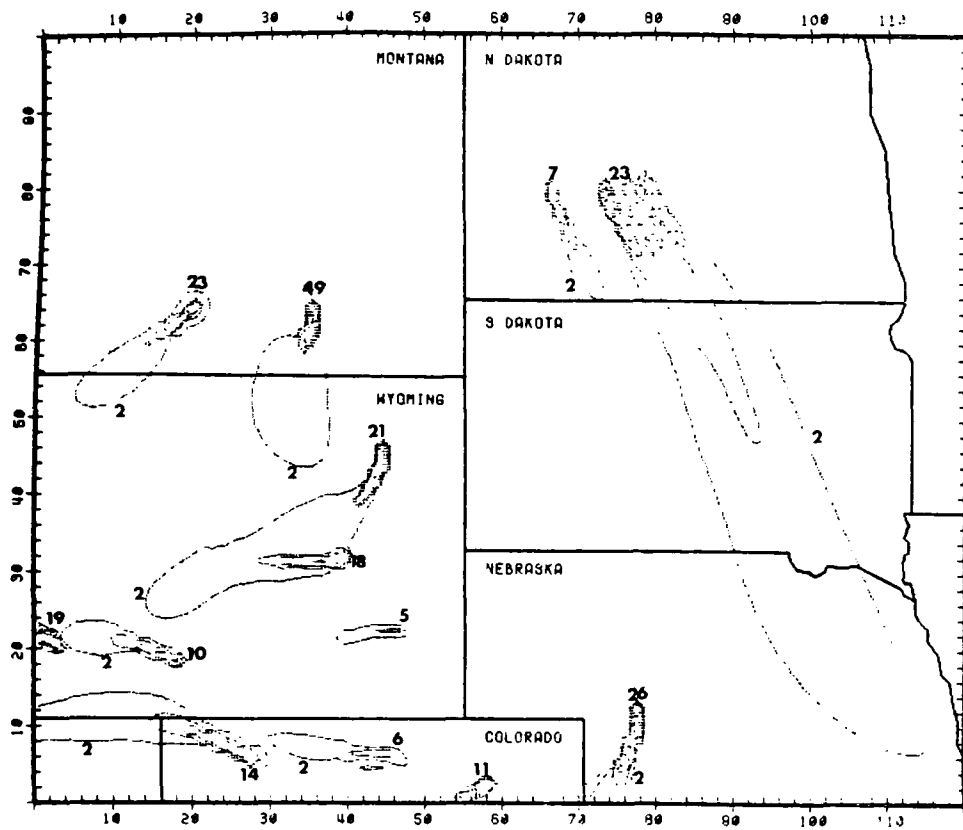
SO₂ CONCENTRATIONS IN UG/M³ FOR THE HOUR 2000-2300 MST ON 750701



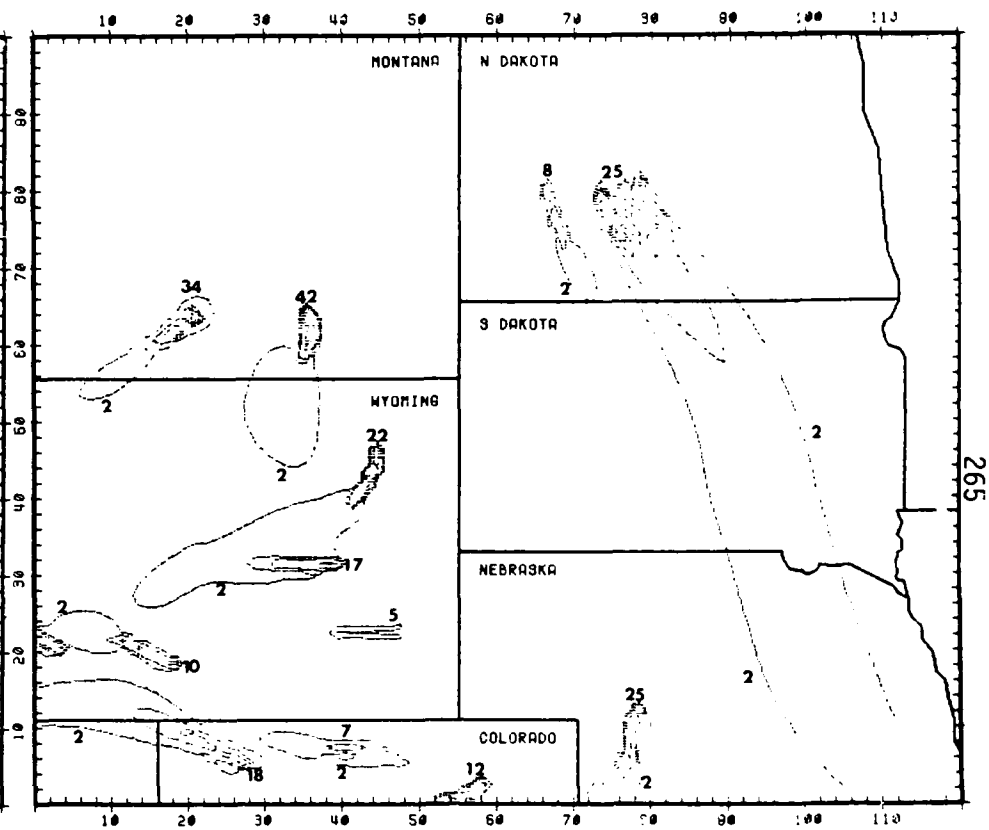
S02 CONCENTRATIONS IN UG/M3 FOR THE HOUR -100-200 MST ON 750710



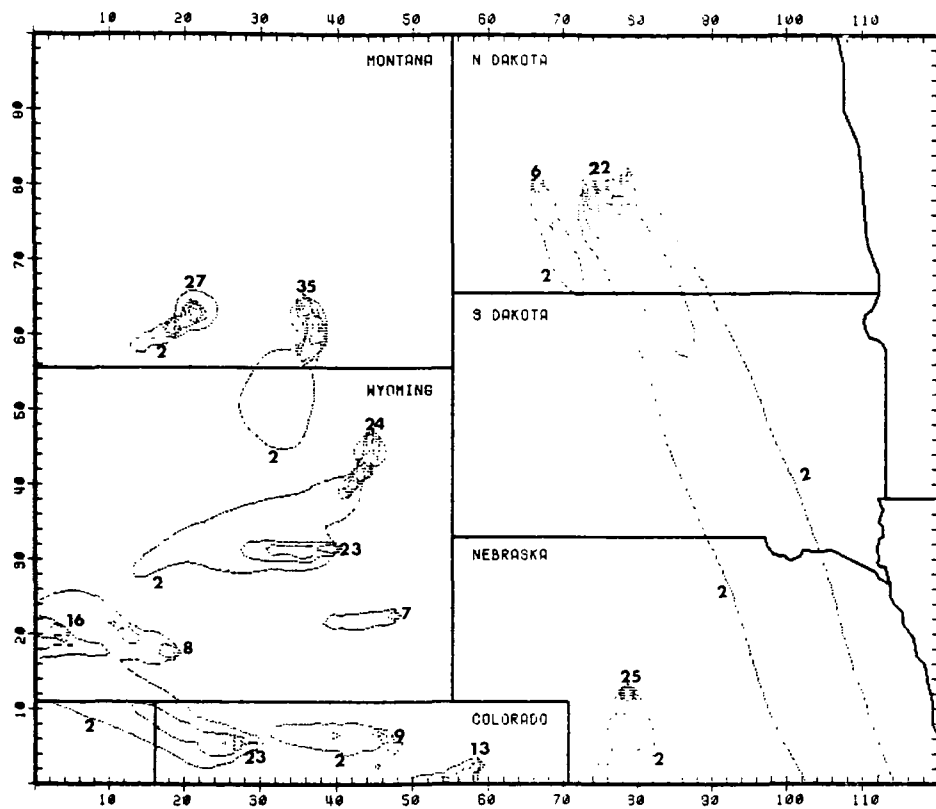
S02 CONCENTRATIONS IN UG/M3 FOR THE HOUR 200-500 MST ON 750710



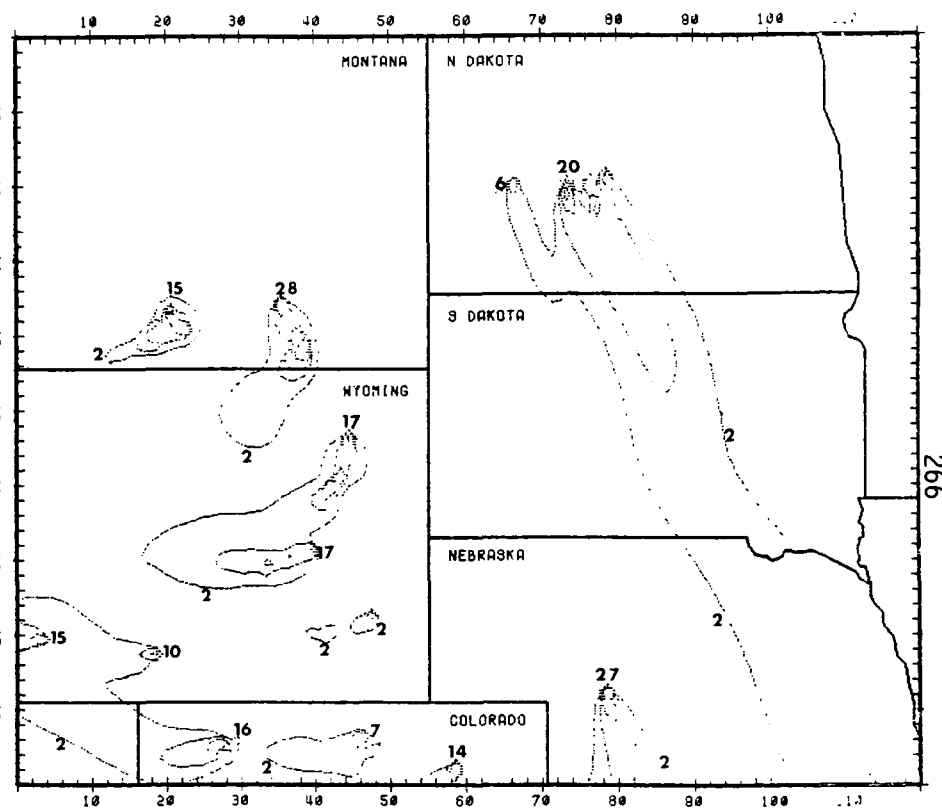
SO2 CONCENTRATIONS IN UG/M3 FOR THE HOUR 500-800 MST ON 750710



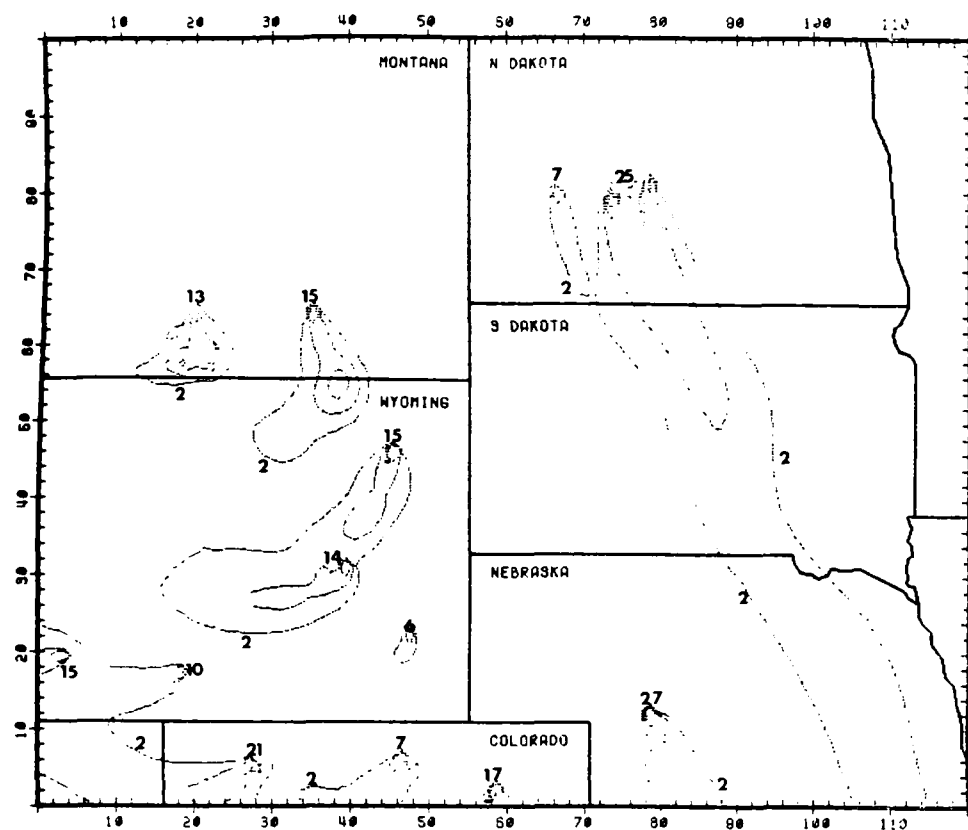
SO2 CONCENTRATIONS IN UG/M3 FOR THE HOUR 900-1100 MST ON 750710



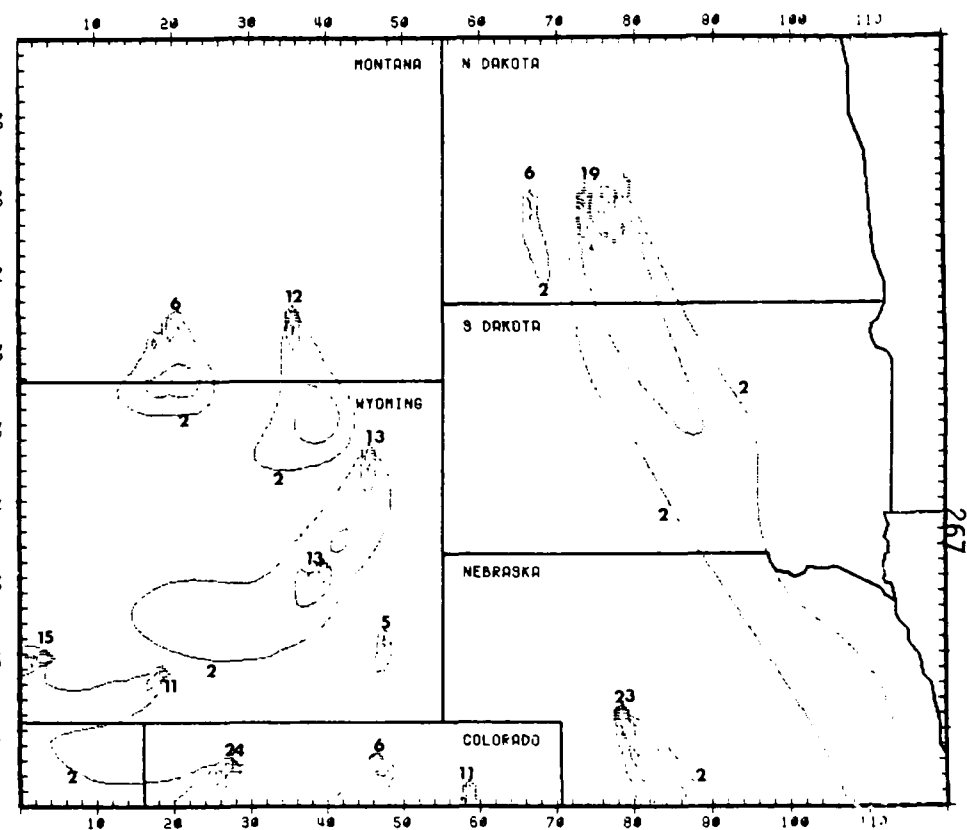
SO2 CONCENTRATIONS IN UG/M3 FOR THE HOUR 1100-1400 MST ON 750710



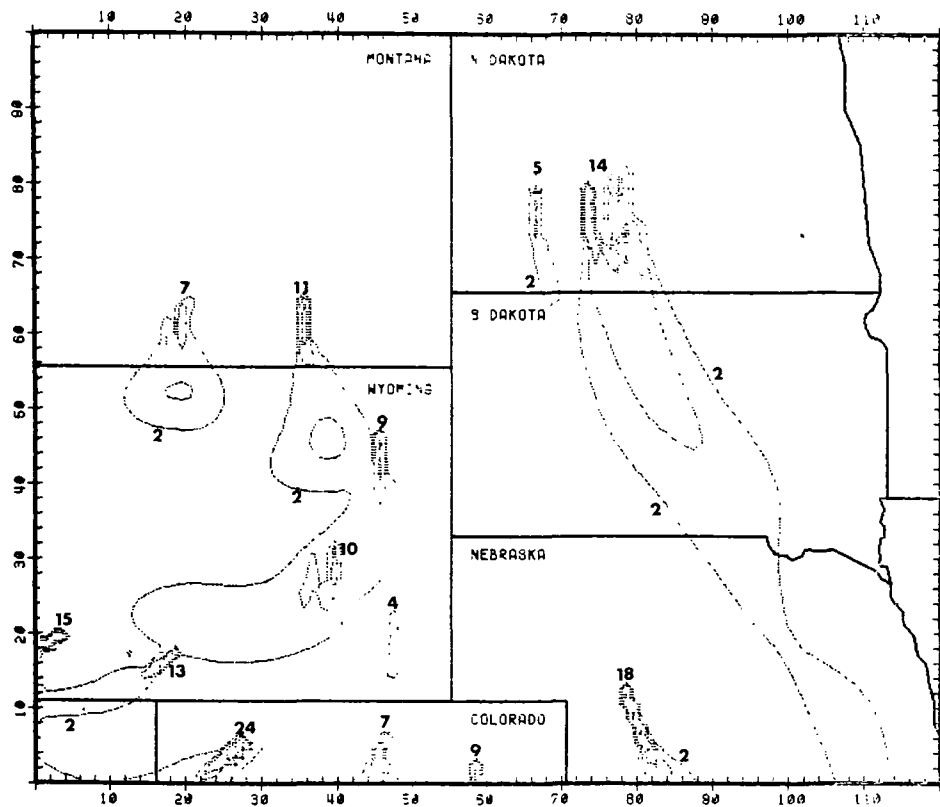
SO2 CONCENTRATIONS IN UG/M3 FOR THE HOUR 1400-1700 MST ON 750710



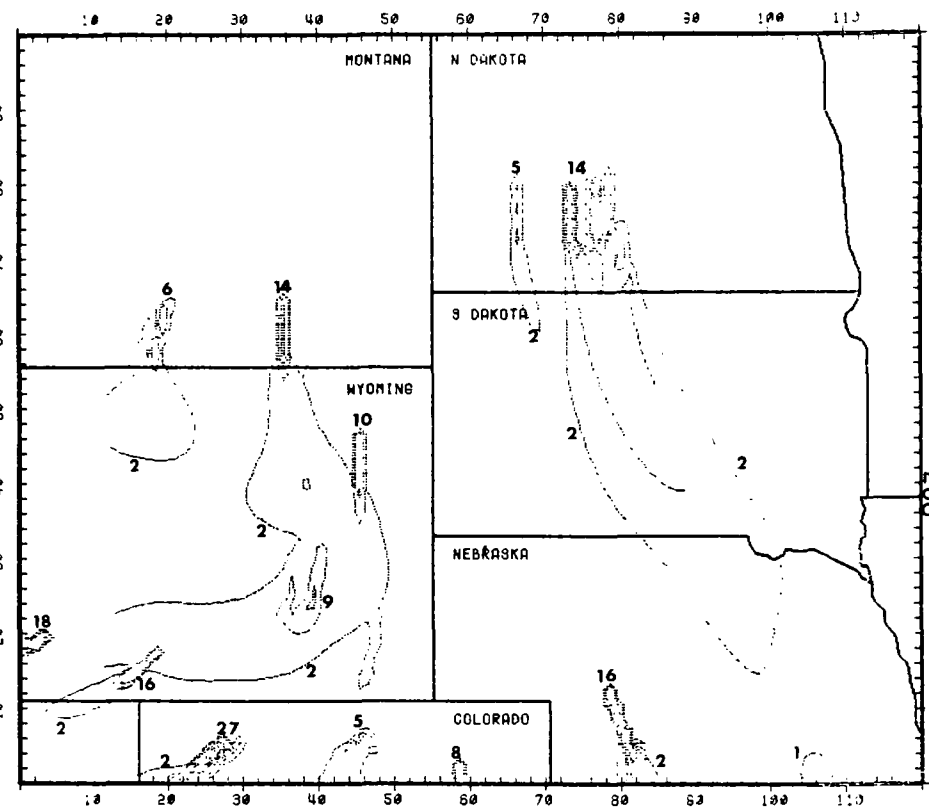
SO2 CONCENTRATIONS IN UG/M3 FOR THE HOUR 1700-2000 MST ON 750710



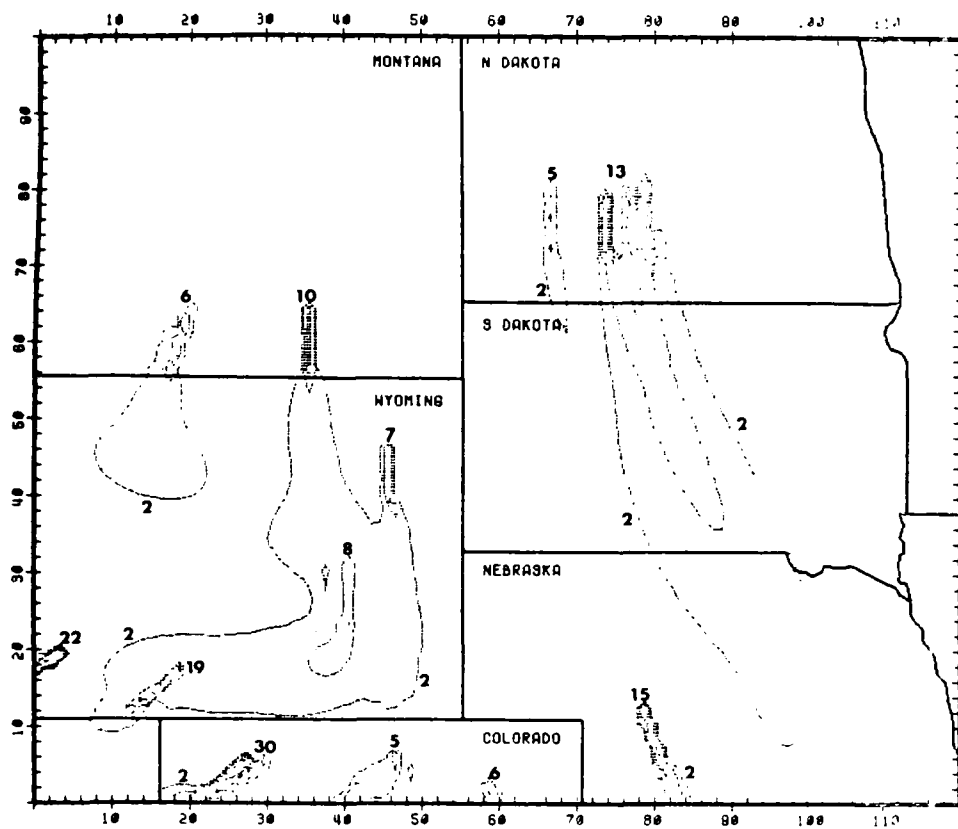
SO2 CONCENTRATIONS IN UG/M3 FOR THE HOUR 2000-2300 MST ON 750710



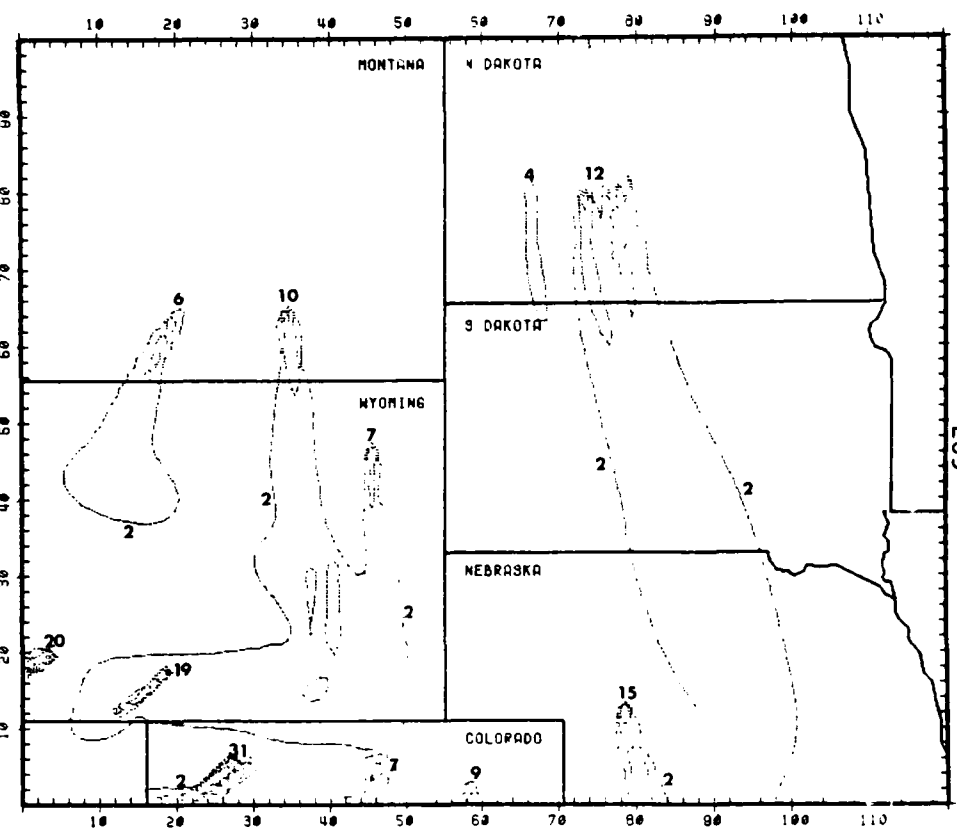
SO2 CONCENTRATIONS IN UG/M3 FOR THE HOUR -100-200 MST ON 750711



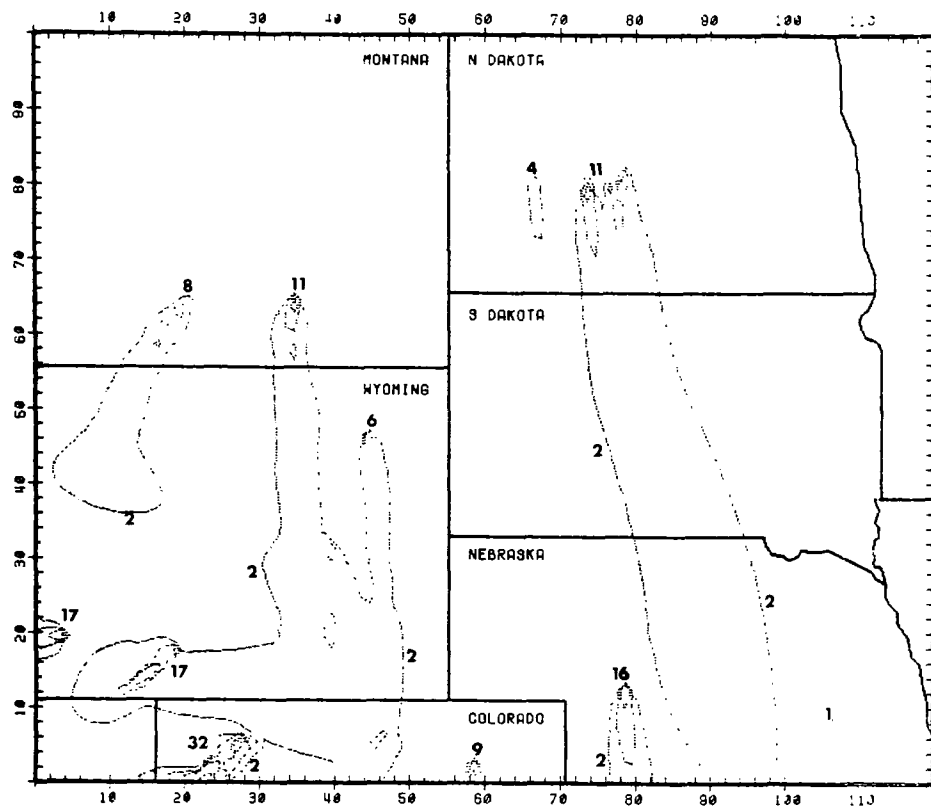
SO2 CONCENTRATIONS IN UG/M3 FOR THE HOUR 200-500 MST ON 750711



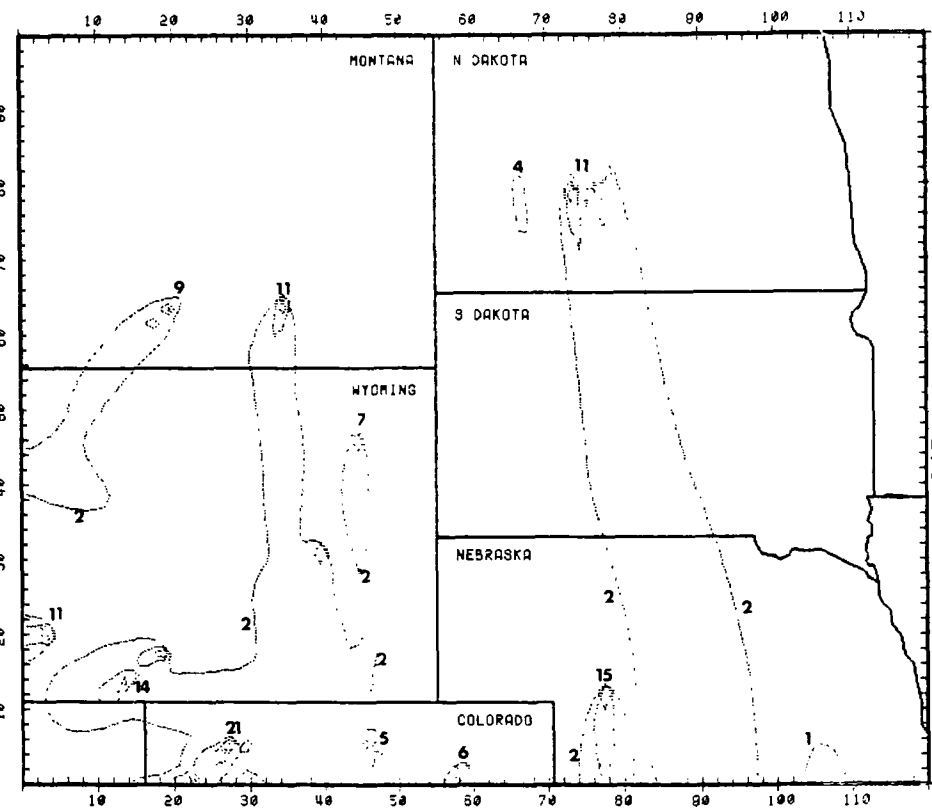
SO2 CONCENTRATIONS IN $\mu\text{G}/\text{M}^3$ FOR THE HOUR 500-800 MST ON 750711



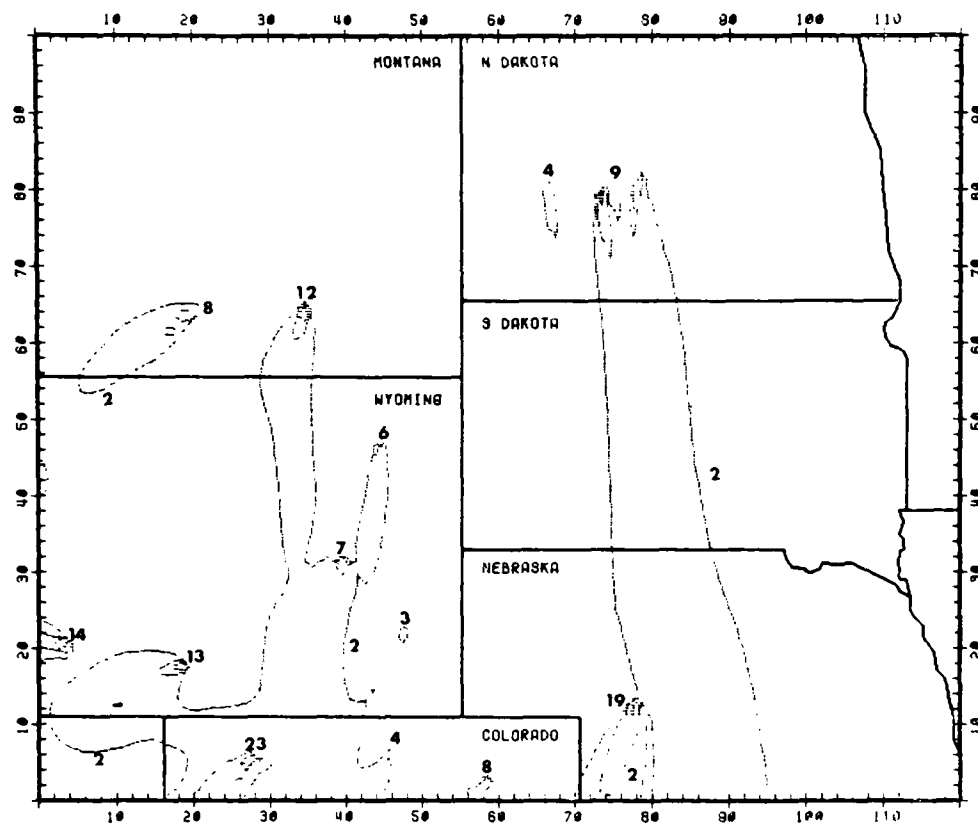
SO2 CONCENTRATIONS IN $\mu\text{G}/\text{M}^3$ FOR THE HOUR 800-1100 MST ON 750711



SO₂ CONCENTRATIONS IN UG/M³ FOR THE HOUR 1100-1400 MST ON 750711



SO₂ CONCENTRATIONS IN UG/M³ FOR THE HOUR 1400-1700 MST ON 750711



SO₂ CONCENTRATIONS IN UG/M³ FOR THE HOUR 1700-2000 MST ON 7/30/71

REFERENCES

- Averitt, Paul (1974), "Coal Resources of the United States," Bulletin 1412, U.S. Geological Survey, Washington, D.C.
- Benedict, Manson (1976), "U.S. Energy: The Plan That Can Work," Technol. Rev., May 1976, pp. 53-59.
- Benson, S. W. (1968), Thermochemical Kinetics (John Wiley & Sons, New York, New York).
- Bolin, B., and L. Granat (1973), "Local Fallout and Long Distance Transport of Sulfur," Ambio, Vol. 2, pp. 87-90.
- Bolin, B., and H. Rodhe (1973), "A Note on the Concepts of Age Distribution and Transit Time in Natural Reservoirs," Tellus, Vol. 25, pp. 58-62.
- Bolin, B., G. Aspling, and C. Persson (1974), "Residence Time of Atmospheric Pollutants as Dependent on Source Characteristics, Atmospheric Diffusion Processes, and Sink Mechanisms," Tellus, Vol. 26, pp. 185-194.
- Boris, J. P., and D. L. Book (1973), "Flux Corrected Transport--I. SHASTA, A Fluid Transport Algorithm That Works," J. Comput. Phys., Vol. 11, pp. 38-69.
- Brosset, C. (1973), "Airborne Acid," Ambio, Vol. 2, No. 1-2, pp. 1-9.
- Bufalini, J. J., and W. A. Lonneman (1977), "Proceedings of Symposium on the 1975 Northeast Oxidant Transport Study," EPA 600/3-77-017, Environmental Protection Agency, Research Triangle Park, North Carolina.
- Bureau of Mines (1975), "The Reserve Base of U.S. Coals by Sulfur Content," IC8680 (East of the Mississippi) and IC8683 (The Western States), Washington, D.C.
- Businger, J. A., et al. (1971), "Flux-Profile Relationships in the Atmospheric Surface Layer," J. Atmos. Sci., Vol. 28, pp. 181-189.
- Chamberlain, A. C. (1966), "Transport of Gases to and from Grass and Grass-Like Surfaces," Proc. Roy. Soc., A, 290, pp. 236-260.
- _____ (1960), "Aspects of the Deposition of Radioactive and Other Gases and Particles," Int. J. Air Poll., Vol. 3, pp. 63-88.

- Chemistry and Engineering News [C&EN](1977), "Outlook for Coal: Bright, but with Problems," pp. 24-31, 14 February 1977.
- Christensen, O., and L. P. Prahm (1976), "A Pseudospectral Model for Dispersion of Atmospheric Pollutants," J. Appl. Meteor., Vol. 15, pp. 1284-1294.
- Corrsin, S. (1974), "Limitations of Gradient Transport Models in Random Walks and in Turbulence," Adv. in Geophysics, Vol. 18A, pp. 25-60.
- Czeplak, G., and C. Junge (1974), "Studies of Interhemispheric Exchange in the Troposphere by a Diffusion Model," Adv. in Geophysics, Vol. 18B, pp. 57-72.
- Dana, M. T., J. M. Hales, and M. A. Wolf (1972), "Natural Precipitation Washout of Sulfur Dioxide," BNW-389, Atmospheric Sciences Dept., Battelle-Pacific Northwest Laboratories, Richland, Washington (NTIS PB-210 968).
- Davis, B. L., et al. (1976), "A Study of the Green Area Effect in the Black Hills of South Dakota," Atmos. Environ., Vol. 10, pp. 363-370.
- DeMarrais, G. A., and N. F. Islitzer (1960), "Diffusion Climatology of the National Reactor Testing Station," Report IDO-12015, Idaho Falls Operation Office, U.S. Atomic Energy Commission, Idaho Falls, Idaho.
- Dickerson, M. H., T. V. Crawford, and W. K. Crandall (1972), "Long-Range Transport, Diffusion, and Deposition from a Russian Nuclear Excavation Project," UCRL-51281, Lawrence Livermore Laboratory, Livermore, California.
- Draxler, R. R., and W. P. Elliott (1977), "Long-Range Travel of Airborne Material Subjected to Dry Deposition," Atmos. Environ., Vol. 11, pp. 35-40.
- Edwards, R. G., A. B. Broderson, and W. P. Hauser (1976), "Social, Economic, and Environmental Impacts of Coal Gasification and Liquefaction Plants," IMMR14-GR2-76, Institute for Mining and Minerals Research, University of Kentucky, Lexington, Kentucky.
- Egan, B. A., and J. R. Mahoney (1972a), "Numerical Modeling of Advection and Diffusion of Urban Area Source Pollutants," J. Appl. Meteor., Vol. 11, pp. 312-322.
- ____ (1972b), "Applications of a Numerical Air Pollution Transport Model to Dispersion in the Atmospheric Boundary Layer," J. Appl. Meteor., Vol. 11, pp. 1023-1039.
- Eliassen, A., and J. Saltbones (1975), "Decay and Transformation Rates of SO₂ as Estimated from Emission Data, Trajectories and Measured Air Concentrations," Atmos. Environ., Vol. 9, pp. 425-430.

Environmental Protection Agency [EPA](1977), unpublished data supplied by Mr. Terry Thoem, EPA Region VIII, Denver, Colorado.

____ (1976a), "Surface Coal Mining in the Northern Great Plains of the Western United States," OEA 76-1, EPA Region VIII, Denver, Colorado.

____ (1976b), "Monitoring and Air Quality Trends Report, 1974," EPA-450/1-76-001, Environmental Protection Agency, Washington, D.C.

____ (1976c), "Existing and Proposed Fuel Conversion Facilities Summary," TS-5, EPA Region VIII, Denver, Colorado.

____ (1975), "Standards of Performance for New Stationary Sources," Code of Federal Regulations, §40, Part 60.

____ (1973), "Emission Factors for Trace Substances," EPA-450/2-73-001, Research Triangle Park, North Carolina.

Environmental Science & Technology [ES&T](1976), "How To Make Coal Burn Cleaner," Vol. 10, pp. 16-17.

Eriksson, E. (1966), Handbuch de Pflanzenernahrung und Dungung, Vol. 2, No. 1, p. 774.

Federal Energy Administration [FEA](1975), "Coal Conversion Program--Final Environmental Statements," Washington, D.C. (also NTIS PB-250 104).

Federal Power Commission [FPC](1976), "FPC Form 67: Steam Electric Plant Air and Water Quality Control Data for the Year Ending December 31, 1975

Federal Register (1975), Vol. 40, No. 33, pp. 7042-7070, 18 February 1975.

____ (1974), "Air Quality Implementation Plans--Prevention of Significant Air Quality Deterioration," Vol. 39, No. 235, Part III, pp. 42510-42517, 5 December 1974.

Fisher, B.E.A. (1975), "The Long Range Transport of Sulphur Dioxide," Atmos. Environ., Vol. 9, pp. 1063-1070.

Forsythe, G. E., and W. R. Wasow (1960), Finite-Difference Methods for Partial Differential Equations (John Wiley & Sons, New York, New York).

Fortak, H. G. (1974), "Mathematical Modeling of Urban Pollution," Adv. in Geophysics, Vol. 18B, pp. 159-172.

Fox, D. G. (1975), "Modeling Atmospheric Effects--An Assessment of the Problems," Proc. of the First International Symposium on Acid Precipitation of the Forest Ecosystems, Ohio State University.

Fox, D. G., and S. A. Orszag (1973), "Pseudospectral Approximation to Two-Dimensional Turbulence," J. Comp. Phys., Vol. 11, pp. 612-619.

- Galbally, I. E. (1974), "Gas Transfer Near the Earth's Surface," Adv. in Geophysics, Vol. 18B, pp. 329-340.
- Garland, J. A., et al. (1974), "Deposition of Gaseous Sulphur Dioxide to the Ground," Atmos. Environ., Vol. 8, pp. 75-79.
- Georgii, H. W. (1970), "Contributions to the Atmospheric Sulfur Budget," J. Geophys. Res., Vol. 75, pp. 2365-2371.
- Hage, K. D., et al. (1966), "Particle Fallout and Dispersion in the Atmosphere," Final Report SC-CR-66-2031, Aerospace Nuclear Safety, Sandia Corporation, Los Alamos, New Mexico.
- Heffter, J. L. (1965), "The Variation of Horizontal Diffusion Parameters with Time for Travel Periods of One Hour or Longer," J. Appl. Meteor., Vol. 4, pp. 153-156.
- Heffter, J. L., A. D. Taylor, and G. J. Ferber (1975), "A Regional-Continental Scale Transport, Diffusion, and Deposition Model," Technical Memorandum ERL ARL-50, National Oceanic and Atmospheric Administration, Air Resources Laboratories, Silver Springs, Maryland.
- Heimbach, J. A., A. B. Super, and J. T. McPartland (1975), "Colstrip Diffusion Experiment," Dept. of Earth Sciences, Montana State University, Bozeman, Montana.
- Hidy, G. M., E. Y. Tong, and P. K. Mueller (1976), "Design of the Sulfate Regional Experiment (SURE)," EPRI-EC-125 Volume 1, Electric Power Research Institute, Palo Alto, California.
- Hill, A. C. (1971), "A Sink for Atmospheric Pollutants," J. Air Poll. Contr. Assoc., Vol. 21, pp. 341-346.
- Högström, U. (1975), "Further Comments on the Long Range Transport of Airborne Material and Its Removal by Deposition and Washout," Atmos. Environ., Vol. 9, pp. 946-947.
- Holzworth, G. C. (1972), "Mixing Heights, Wind Speeds, and Potential for Urban Air Pollution Throughout the Contiguous United States," AP-101, Office of Air Programs, Environmental Protection Agency, Research Triangle Park, North Carolina.
- Hubbert, M. K. (1971), "Energy Resources," in Environment: Resources, Pollution & Society, W. W. Murdoch, ed., pp. 89-116 (Sinauer Associates, Incorporated, Stamford, Connecticut).
- InterTechnology Corporation (1971), "The U.S. Energy Problem," Vol. II, Appendices--Part B, Appendix S, "Technology of Alternative Fuels," Warrenton, Virginia (also NTIS PB-207 519).

- Izrael, Yu. A. (1971). "Radiation Conditions in the Zone of Long-Range Fallout from Underground Nuclear Cratering Explosions," The State Committee for Uses of Atomic Energy, Moscow, U.S.S.R., presented at the Third Stage Soviet-American Technical Talks on the Peaceful Uses of Nuclear Explosions, Washington, D.C.
- Johnson, W. B., D. E. Wolf, and R. L. Mancuso (1975), "Feasibility of the Air Quality Budget Concept," Stanford Research Institute, Menlo Park, California.
- Junge, C. E. (1963), Air Chemistry and Radioactivity (Academic Press, New York, New York).
- Kaakinen, J. W., R. M. Jorden, and R. E. West (1974), "Trace Element Study in a Pulverized Coal-Fired Power Plant," Paper 74-8, 67th Annual Meeting of the Air Pollution Control Association, Denver, Colorado, June 1974.
- Kao, S. K. (1974), "Basic Characteristics of Global Scale Diffusion in the Troposphere," Adv. in Geophysics, Vol. 18B, pp. 15-32 (Academic Press, New York, New York).
- Kao, S. K., and D. Henderson (1970), "Large-Scale Dispersion of Clusters of Particles in Various Flow Patterns," J. Geophys. Res., Vol. 75, pp. 3104-3113.
- Katz, M. (1949), "Sulphur Dioxide in the Atmosphere and Its Relation to Plant Life," Ind. and Eng. Chem., Vol. 41, pp. 2450-2465.
- Knox, J. B. (1974), "Numerical Modeling of the Transport, Diffusion and Deposition of Pollutants for Regional and Extended Scales," J. Air Poll. Contr. Assoc., Vol. 24, pp. 660-664.
- Küchler, A. W. (1966), "Potential Natural Vegetation," Sheet #90 (map), U.S. Geological Survey, Washington, D.C.
- Lamb, R. G., and G. Z. Whitten (1975), "An Assessment of the Impact of Illinois Sulfur Emissions on the Air Quality of the Northeastern United States," EF75-63, Systems Applications, Incorporated, San Rafael, California.
- Li, T. Y., and H. E. Landsberg (1975), "Rainwater pH Close to a Major Power Plant," Atmos. Environ., Vol. 9, pp. 81-88.
- Liu, M. K., and D. R. Durran (1977), "On the Prescription of the Vertical Dispersion Coefficient over Complex Terrain," Joint Conf. on Applications of Air Pollution Meteorology, American Meteorological Society and Air Pollution Control Association, 28 November-2 December 1977, Salt Lake City, Utah.

- Liu, M. K., et al. (1976), "The Chemistry, Dispersion, and Transport of Air Pollutants Emitted from Fossil Fuel Power Plants in California," EF76-18, Systems Applications, Incorporated, San Rafael, California.
- Liu, M. K., and J. H. Seinfeld (1975), "On the Validity of Grid and Trajectory Models of Urban Air Pollution," Atmos. Environ., Vol. 9, pp. 555-574.
- Los Angeles Air Pollution Control District [LAAPCD](1974), "Profile of Air Pollution--1974," Los Angeles, California.
- MacCracken, M. C. (1976), "Multistate Atmospheric Power Production Pollution Study (MAP³S)," UASG 76-11, Lawrence Livermore Laboratory, Livermore, California.
- Machta, L. (1966), "Some Aspects of Simulating Large Scale Atmospheric Mixing," Tellus, Vol. 18, pp. 355-362.
- Magee, E. M., H. J. Hall, and G. M. Varga, Jr. (1973), "Potential Pollutants in Fossil Fuels," EPA-R2-73-249, Environmental Protection Agency, Research Triangle Park, North Carolina.
- Mansfield, T. A., and O.V.S. Heath (1963), "An Effect of 'Smog' on Stomatal Behavior," Nature, Vol. 200, p. 596.
- Marschner, F. (1950), "Major Land Uses in the U.S.," revised by J. R. Anderson (1967), U.S. Government Printing Office, Washington, D.C.
- Martin, A., and F. R. Barber (1971), "Some Measurements of Loss of Atmospheric Sulphur Dioxide Near Foliage," Atmos. Environ., Vol. 5, pp. 345-352.
- McMahon, T. A., P. J. Denison, and R. Fleming (1976), "A Long-Distance Air Pollution Transportation Model Incorporating Washout and Dry Deposition Components," Atmos. Environ., Vol. 10, pp. 751-761.
- McMullen, T. B., R. B. Faoro, and G. B. Morgan (1970), "Profile of Pollutant Fractions in Nonurban Suspended Particulate Matter," J. Air Poll. Contr. Assoc., Vol. 20, pp. 369-372.
- Miller, J. M., J. Galloway, and G. E. Likens (1975), Proc. of the First International Symposium on Acid Precipitation of the Forest Ecosystem, Ohio State University.
- Miller, J. M., and R. de Pena (1972), "Contribution of Scavenged Sulfur Dioxide to the Sulfate Content of Rain Water," J. Geophys. Res., Vol. 77, pp. 5905-5916.
- Monin, A. S., and A. M. Yaglom (1971), Statistical Fluid Mechanics: Mechanics of Turbulence, Vol. 1 (MIT Press, Cambridge, Massachusetts).

- Nehring, Richard, and Benjamin Zycher (1976), "Coal Development and Government Regulation in the Northern Great Plains: A Preliminary Report," R-1981-NSF/RC, The Rand Corporation, Santa Monica, California.
- Nephew, E. A. (1973), "The Challenge and Promise of Coal," Technol. Rev., December 1973, pp. 20-29.
- Nördlund, G. G. (1975), "A Quasi-Lagrangian Cell Method for Calculating Long-Distance Transport of Airborne Pollutants," J. Appl. Meteor., Vol. 14, pp. 1095-1104.
- ____ (1973), "A Particle-in-Cell Method for Calculating Long Range Transport of Airborne Pollutants," Technical Report No. 7, Finnish Meteorological Institute.
- Nordö, J. (1973), "Meso-Scale and Large-Scale Transport of Air Pollutants Proc. Third International Clean Air Congress, B105-B108, Dusseldorf, Federal Republic of Germany, VDI-Verlag.
- Nordö, J., A. Eliassen, and J. Saltbones (1974), "Large-Scale Transport of Air Pollutants," Adv. in Geophysics, Vol. 18B, pp. 137-150.
- Northern Great Plains Resource Program [NGPRP](1974), "Atmospheric Aspects Work Group Report," Denver, Colorado.
- Ottar, B. (1973), "The Long Range Transport of Air Pollutants," Proc. Third International Clean Air Congress, B102-B104, Dusseldorf, Federal Republic of Germany, VDI-Verlag.
- Owen, P. R., and W. R. Thompson (1963), "Heat Transfer Across Rough Surfaces," J. Fluid Mech., Vol. 15, pp. 321-324.
- Owers, M. J., and O. W. Powell (1974), "Deposition Velocity of Sulphur Dioxide on Land and Water Surfaces Using a ^{35}S Tracer Method," Atmos. Environ., Vol. 8, pp. 63-67.
- Parker, N. A., and B. C. Thompson (1976), "U.S. Coal Resources and Reserves," FEA/B-76/210, Federal Energy Administration, National Energy Information Center, Washington, D.C. (also NITS PB-252 752).
- Pasquill, F. (1974), "Limitations and Prospects in the Estimation of Dispersion of Pollution on a Regional Scale," Adv. in Geophysics, Vol. 18B, pp. 1-14.
- Pedersen, L. B., and L. P. Prahm (1974), "A Method for Numerical Solution of the Advection Equation," Tellus, Vol. 26, pp. 594-602.
- Petrov, V. N. (1971), "Effect of Atmospheric Parameters on the Diffusion and Fallout of Radioactive Products from Clouds Traveling Great Distances," State Committee for Uses of Atomic Energy U.S.S.R., Moscow, presented at the Third Stage Soviet-American Technical Talks on the Peaceful Uses of Nuclear Explosions, Washington, D.C.

- Prahm, L. P., H. S. Buch, and U. Torp (1974), "Long-Range Transport of Atmospheric Pollutants over the Atlantic," Symposium on Atmospheric Diffusion and Air Pollution, pp. 190-195 (American Meteorological Society, Boston, Massachusetts).
- Prahm, L. P., U. Torp, and R. M. Stern (1976), "Deposition and Transformation Rates of Sulphur Oxides during Atmospheric Transport over the Atlantic," Tellus, Vol. 28, pp. 355-372.
- Radian Corporation (1975), "A Western Regional Energy Development Study," "Executive Summary" and "Volume III: Appendices," RC# 100-064, Austin, Texas.
- Randerson, D. (1972), "Temporal Changes in Horizontal Diffusion Parameters of a Single Nuclear Debris Cloud," J. Appl. Meteor., Vol. 11, pp. 670-673.
- Rao, K. S., J. S. Lague, and B. A. Egan (1976), "An Air Trajectory Model for Regional Transport of Atmospheric Sulfates," Preprints, Third Symposium on Atmospheric Turbulence, Diffusion, and Air Quality, 19-22 October 1976, Raleigh, North Carolina (American Meteorological Society, Boston, Massachusetts).
- Rao, K. S., I. Thomson, and B. A. Egan (1976), "Regional Transport Model of Atmospheric Sulfates," 69th Annual Meeting of the Air Pollution Control Association, Portland, Oregon.
- Rasmussen, K. H., M. Taheri, and R. L. Kabel (1974), "Sources and Natural Removal Processes for Some Atmospheric Pollutants," EPA-650/4-74-032, Environmental Protection Agency, Washington, D.C.
- Reiquam, J. (1970), "Sulfur: Simulated Long-Range Transport in the Atmosphere," Science, Vol. 170, pp. 318-320.
- Rodhe, H. (1972), "A Study of the Sulphur Budget for the Atmosphere over Northern Europe," Tellus, Vol. 24, pp. 128-138.
- ____ (1971), "Measurements of Sulfur in the Free Atmosphere over Sweden, 1969-1970," Report AC-12, Institute of Meteorology, University of Stockholm, Stockholm, Sweden.
- Rodhe, H., and J. Grandell (1973), "On the Removal Time of Aerosol Particles from the Atmosphere by Precipitation Scavenging," Report AC-20, Institute of Meteorology, University of Stockholm, Sweden.
- Scott, W. D., and P. V. Hobbs (1967), "The Formation of Sulfate in Water Droplets," J. Atmos. Sci., Vol. 24, p. 54.
- Scriven, R. A., and B.E.A. Fisher (1975a), "The Long Range Transport of Airborne Material and Its Removal by Deposition and Washout--I. General Considerations," Atmos. Environ., Vol. 9, pp. 49-58.

- ____ (1975b), "The Long Range Transport of Airborne Material and Its Removal by Deposition and Washout--II. The Effect of Turbulent Diffusion," Atmos. Environ., Vol. 9, pp. 59-68.
- Sehmel, G. A., S. L. Sutter, and M. T. Dana (1973), "Dry Deposition Processes," in "Pacific Northwest Laboratory Annual Report for 1971, to the USAEC, Division of Biomedical and Environmental Research, Vol. II: Physical Sciences, Part I, Atmospheric Science," BNWL-1751, pp. 150-153, Battelle Northwest Laboratories, Richland, Washington.
- Sellers, W. D. (1965), Physical Climatology (University of Chicago Press, Chicago, Illinois).
- Shepherd, J. G. (1974), "Measurements of the Direct Deposition of Sulphur Dioxide Onto Grass and Water By the Profile Method," Atmos. Environ., Vol. 8, pp. 69-74.
- Slade, D. H. (1967), "Modeling Air Pollution in the Washington, D.C. to Boston Megalopolis," Science, Vol. 157, pp. 1304-1307.
- Smagorinsky, J. (1963), "General Circulation Experiments with the Primitive Equations: I. The Basic Experiment," Mon. Wea. Rev., Vol. 91, pp. 99-164.
- Smith, F. B. (1970), "A Contribution to the Estimation of Pollutant Dosages Arising from a U.K. Source Using a Simplified Trajectory Method," Internal Meteorological Office Memorandum.
- Smith, W. S. (1966), "Atmospheric Emissions from Coal Combustion," Publication AP-42, Public Health Service, U.S. Department of Health, Education, and Welfare, Washington, D.C.
- Spedding, D. J. (1969), "Uptake of Sulphur Dioxide by Barley Leaves at Low Sulphur Dioxide Concentration," Nature, Vol. 224, pp. 1229-1231.
- Thom, A. S. (1972), "Momentum, Mass and Heat Exchange of Vegetation," Quart. J. Roy. Meteor. Soc., Vol. 98, pp. 124-134.
- Tillman, D. A. (1976), "Status of Coal Gasification," Environ. Sci. Technol., Vol. 10, pp. 34-38.
- Trijonis, J. C., and K. W. Arledge (1975), "Impact of Reactivity Criteria on Organic Emission Control Strategies in the Metropolitan Los Angeles AQCR," TRW, Incorporated, El Segundo, California.
- Turner, D. B. (1969), "Workbook of Atmospheric Dispersion Estimates," 999-AP-26, U.S. Public Health Service, Cincinnati, Ohio.
- Turner, D. B., J. R. Zimmerman, and A. D. Busse (1973), "An Evaluation of Some Climatological Dispersion Models," Appendix E of "User's Guide for the Climatological Dispersion Model," EPA-R4-73-024, Environmental Protection Agency, Research Triangle Park, North Carolina.

- Van der Hoven, I. (1957), "Power Spectrum of Horizontal Wind Speed in the Frequency Range from 0.0007 to 900 Cycles per Hour," J. Meteor., Vol. 14, p. 160.
- Wendell, L. L. (1972), "Mesoscale Wind Fields and Transport Estimates Determined from a Network of Wind Towers," Mon. Wea. Rev., Vol. 100, pp. 565-578.
- Wendell, L. L., D. C. Powell, and R. L. Drake (1976), "A Regional Scale Model for Computing Deposition and Ground Level Air Concentration of SO₂ and Sulfates from Elevated and Ground Sources," pp. 318-324, Preprints, Third Symposium on Atmospheric Turbulence, Diffusion, and Air Quality, 19-22 October 1976, Raleigh, North Carolina (American Meteorological Society, Boston, Massachusetts).
- White, W. H., et al. (1976), "Midwest Interstate Sulfur Transformation and Transport Project: Aerial Measurements of Urban and Power Plant Plumes, Summer 1974," EPA-600/3-76-110, Environmental Protection Agency, Research Triangle Park, North Carolina.
- Yanenko, N. N. (1971), The Method of Fractional Steps (Springer-Verlag, Berlin, Germany).